# Harnessing the Potential of Sulfamidyl Radical in Photocatalytic Synthesis of Organosilanes and Organogermanes

**Ph.D. Thesis**

By

**KALU RAM BAJYA**

**DEPARTMENT OF CHEMISTRY**
**INDIAN INSTITUTE OF TECHNOLOGY INDORE**

**December 2025**

# Harnessing the Potential of Sulfamidyl Radical in Photocatalytic Synthesis of Organosilanes and Organogermanes

**A THESIS**

*Submitted in partial fulfilment of the*

*requirements for the award of the degree*

*of*

**DOCTOR OF PHILOSOPHY**

*By*

**KALU RAM BAJYA**

**DEPARTMENT OF CHEMISTRY**

**INDIAN INSTITUTE OF TECHNOLOGY INDORE**

**December 2025**

**INDIAN INSTITUTE OF TECHNOLOGY INDORE**

I hereby certify that the work which is being presented in the thesis entitled "**Harnessing the Potential of Sulfamidyl Radical in Photocatalytic Synthesis of Organosilanes and Organogermanes**" in the partial fulfillment of the requirements for the award of the degree of **DOCTOR OF PHILOSOPHY** and submitted in the **DEPARTMENT OF CHEMISTRY, Indian Institute of Technology Indore**, is an authentic record of my own work carried out during the time period from **August 2020** to **December 2025** under the supervision of **Dr. Selvakumar Sermadurai**, **Associate Professor**, **Department of Chemistry**, **Indian Institute of Technology Indore**.

The matter presented in this thesis has not been submitted by me for the award of any other degree of this or any other institute.

KaluRam
09.04.2026

**Signature of the student with date**
**(KALU RAM BAJYA)**

---

This is to certify that the above statement made by the candidate is correct to the best of my knowledge.

S. Selvakumar 09.04.2026

**Signature of Thesis Supervisor with date**
**(Dr. Selvakumar Sermadurai)**

---

**Mr. Kalu Ram Bajya** has successfully given his Ph.D. Oral Examination held on **09.04.2026**

S. Selvakumar 09.04.2026

**Signature of Thesis Supervisor with date**
**(Dr. Selvakumar Sermadurai)**

---

# ACKNOWLEDGEMENTS

The successful completion of my Ph.D. research is not merely the outcome of my individual efforts but the culmination of the constant encouragement, invaluable guidance, and generous support of many remarkable individuals. I take this opportunity to express my deepest gratitude to all those who contributed, directly and indirectly, to this achievement.

I would like to begin by expressing deepest gratitude and heartfelt respect to my revered supervisor, **Dr. Selvakumar Sermadurai**. I consider myself extremely fortunate to have been guided by a mentor who not only shaped my scientific thinking but also believed in me at every stage of my doctoral journey. He gave me the freedom to pursue ideas independently, instilling confidence in my abilities, while always offering patient guidance, encouragement, and unwavering support whenever I faced challenges or moments of doubt. His strength of character, resilience, and unshakeable commitment to scientific integrity have left an indelible mark on me, both as a researcher and as an individual. His inspiration, wisdom, and humanity will continue to guide me long after this journey, and I will always strive to carry forward his values, vision, and passion in all my future endeavors.

I am sincerely grateful to PSPC members, **Prof. Sanjay Kumar Singh** and **Prof. Chelvam Venkatesh**, for their valuable suggestions, insightful corrections, and constructive comments during Comprehensive Evaluation of Research Progress (CERP) and other progress-related activities, which greatly contributed to the refinement and advancement of my research.

I am deeply grateful to **Prof. Suhas S. Joshi** (Director, Indian Institute of Technology Indore) for providing the opportunity to pursue my doctoral studies and for the necessary research facilities.

I would like to express my gratitude to **Prof. Tushar Kanti Mukherjee** (Head of the Department of Chemistry, Indian Institute of Technology Indore) as well as to all faculty members for their guidance and support.

I extend my gratitude to Dr. Azaj Ansari, Central University of Haryana, for his valuable contributions for theoretical studies.

I am grateful to Mr. Kinny Pandey, Mr. Ghanashyam Bhavsar, Mr. Manish Kushwaha, Mr. Parthiban P. K., Mr. Rameshwar, and Ms. Vinita Kothari for their valuable technical assistance and support.

I would like to thank CSIR-HRDG, New Delhi, for providing financial support (JRF and SRF fellowships) for my research at IIT Indore.

I wish to express my profound gratitude to my cousin's brother, **Dr. Surendra** (MBBS, MS, Ortho), whose unwavering presence has been a constant source of strength throughout my Ph.D. journey. His emotional, moral, and financial support sustained me during some of the most challenging phases of my academic and personal life. In moments of uncertainty and self-doubt, he consistently encouraged me to remain focused and resilient, inspiring me to make difficult decisions with confidence and clarity. During my toughest personal times, he stood beside me without hesitation, offering reassurance, perspective, and hope. His belief in my abilities and his unconditional support played a pivotal role in helping me persevere through setbacks and achieve this milestone. I will always remain deeply grateful for his generosity, guidance, and the quiet strength he imparted during this journey.

I sincerely thank Dr. Rajesh Kumar, Dr. Chandra Prakash Barala, Dr. Ramakant Gavale and Mr. Vinod Swami for their encouragement and support throughout my Ph.D. journey. I would like to extend my sincere thanks to all my seniors, juniors and friends at IIT Indore, Dr. Faizal Khan, Dr. Indresh Kumar Yadav, Dr. Rahul Kumar Singh, Dr. Wazid, Dr. Dilip Pinjari, Dr. Pankaj Gupta, Dr. Dilip Pandey, Dr. Sanjeev Kushwaha, Dr. Nikhil ji Tiwari, Dr. Rajesh Bhawale, Dr. Laxman

Kharabe, Dr. Lalita, Dr. Zaheer, Mr. Ashu Singh, Mr. Naveen Kumar, Mr. Vishal Jaiswal, Mr. Tushar Kharde, and Mr. Khanindra Kalita.

My special thanks go to the members cum close friends of our laboratory, Mr. Ravikumar, Mr. Akshay Pathare, Mr. Shivam Maurya, Mr. Vitthal Paighan, and Ms. Gladys J., for fostering a positive, collaborative, and encouraging laboratory environment.

I would like to express my deepest gratitude and heartfelt respect to my loving families. I express my deep sense of gratitude to my father, Late Shri Gulla Ram Bajya and my mother, Smt. Prem Devi, for the love and faith they kept in my dreams. My special thanks go to my loving sisters, Ms. Asha and, Ms. Manju, and my wife, Ms. Nirmala, for all their constant help, love and support. I am also grateful to all my other family members and friends for their support throughout my life and for their encouragement in my dreams.

Words are short to express my gratitude, but at the end of this journey, it is my great pleasure to thank all of them who supported in many ways to my success and made it an unforgettable experience for me.

Thank You!!!!! Kalu Ram Bajya

IIT Indore

DEDICATED

TO

MY PARENTS

AND

MY PH.D.

SUPERVISOR

# SYNOPSIS

Organosilicon compounds represent a diverse class of molecules that possess a silicon-carbon bond. Silicon has a larger covalent radius, which provides the unique characteristics to organosilicon compounds, such as longer bond length, different bond angle and ring conformation compared to their carbon analogues. The low polarity of the Si-C bond enhances the lipophilicity of organosilicon compounds, which often improves cell and tissue penetration that in turn alters the potency and selectivity of the silicon structure relative to carbon. The electropositive nature of silicon contributes an electron-deficient center in the molecule and reverse bond polarization, which makes them susceptible to nucleophilic attack, as well as this characteristic of silicon stabilizes the carbocation at the $\beta$-position with respect to silicon. Generally, organosilicon compounds are considered non-toxic because no element-specific toxicity associated with silicon. Silicon is a classical isostere of carbon and is often used as a bioisostere *via* the "silicon-switch" strategy in bioactive molecules. All these characteristics make organosilicon compounds an ideal candidate for organic synthesis, material science, agrochemicals, pharmaceuticals, and everyday care products. Similar to organosilicon compounds, organogermanium compounds possess a germanium-carbon bond, have a larger atomic size, and are more electropositive than carbon with reverse bond polarization. These characteristics make organogermanium compounds suitable for its use in optoelectronics and semiconductors. Generally acknowledged that germanium is an essential trace element, particularly crucial for the regular functioning of the immune system and plays a significant role in the prevention of cancer. Some organogermanium compounds exhibit medicinal applications, such as Ge-132 shows immunomodulatory, antioxidant, and anti-inflammatory properties.

Organosilicon compounds are generally synthesized using organometallic reagents, metal catalysts, or Brønsted and Lewis acid-catalyzed reactions. However, these methods often require harsh reaction conditions and rely on precious metals, highlighting the need for the development of novel and sustainable methodologies for the synthesis of organosilicon and organogermanium compounds. In this context, we envision to develop a metal-free, visible light-mediated and organophotocatalyzed protocol for the synthesis of organosilicon and organogermanium compounds.

This thesis aims to develop novel methodologies for the synthesis of organosilicon and organogermanium compounds *via* hydrogen atom transfer process, enabled under metal-free visible light photoredox conditions, using simple hydrosilanes and hydrogermane as radical precursors.

***Objective***

We intended to use the Si-H and Ge-H bond functionalization strategy for the synthesis of organosilicon and organogermanium compounds using simple hydrosilanes and hydrogermanes. The electropositive nature of silicon and germanium relative to carbon results in a high hydridic character in Si-H and Ge-H bonds of hydrosilanes and hydrogermanes, making them ideal candidates for functionalization through hydrogen atom transfer (HAT) by electrophilic radical, a process that is polarity-matched. The electrophilic radical can be generated *via* thermal or photochemical methods, and we intended to use the latter due to the ease of handling and mild reaction conditions. The photochemical generation of an electrophilic radical can be realized using a transition metal photocatalyst or an organophotocatalyst, with the latter attracting our attention because it avoids the usage of hazardous and precious metals.

In our search for an ideal electrophilic radical to initiate the hydrogen atom transfer, sulfamidyl radical was recognized to be suitable for this process. Appropriate precursors were employed to generate sulfamidyl radical through oxidative and reductive quenching pathways of a visible-light-assisted excited photocatalyst, enabling the functionalization of Si-H and Ge-H bond of hydrosilanes and hydrogermanes.

***Chapter 1: Introduction***

In this chapter, we begin with a brief discussion on silicon and germanium, their physicochemical properties, and continue with a general introduction to organosilicon compounds. Next, the historical background for the synthesis of organosilicon compounds is discussed, along with modern protocols using different sources of silicon, such as halosilanes, oligosilanes, silicon-boron reagents, organosilicon precursors (e.g., silylcarboxylic acid) and lastly hydrosilanes in metal-catalyzed and metal-free protocols. Organosilicon compounds have diverse applications in pharmaceuticals, agrochemicals, and materials research. Some of these applications are further discussed in this chapter, such as daily life (e.g., Polydimethylsiloxanes and Simeticone), agriculture (e.g., Sylgard 309 and Silthiofam), and medicinal applications (e.g., anticancer, antiviral, antibacterial, etc.). After the discussion on organosilicons, this chapter provides a brief introduction to organogermanium compounds and their detailed synthesis from various germanium sources, including halogermanes, oligogermanes, organogermanium precursors (e.g., germylcarboxylic acid), and hydrogermanes. Furthermore, we discussed daily life and medicinal applications of organogermanium compounds. Since our effort to synthesize organosilicon and organogermanium compounds *via* Si-H and Ge-H bond functionalization is under photochemical conditions, we provided a brief overview of photoredox catalysis and its significance. Moreover, we discussed the detailed description of the photophysical process of the photocatalyst. Furthermore, the detailed operating mechanism of the photocatalyst through oxidative and reductive quenching pathways is discussed, and the table of photocatalysts, along with their ground-state and excited-state redox potentials, is provided. Lastly, we discussed our approach to the functionalization of the Si-H and Ge-H bond of hydrosilanes and hydrogermanes using an electrophilic radical.

*Chapter 2: Development of Sulfonamide as Photoinduced Hydrogen Atom Transfer Catalyst for Organophotoredox Hydrosilylation and Hydrogermylation of Activated Alkenes*

In this chapter, we describes the development of an easily synthesizable, inexpensive, sterically and electronically tunable sulfonamide as a hydrogen atom transfer catalyst for the selective functionalization of Si-H/Ge-H bond of hydrosilanes and hydrogermanes using an organophotocatalyst under visible light irradiation.

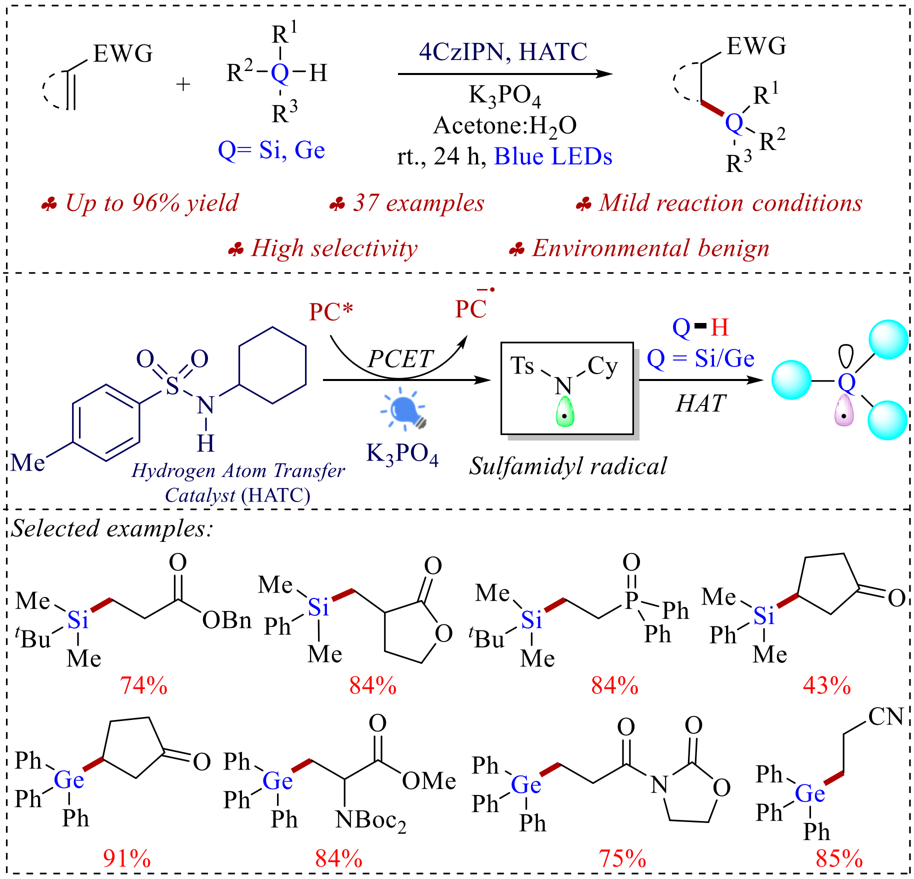


**Scheme 1** *N*-cyclohexyl-4-methylbenzenesulfonamide as a hydrogen atom transfer catalyst for photocatalytic hydrosilylation and hydrogermylation of activated alkenes

The screening of different sulfonamides possessing electron-withdrawing/donating groups, as well as different steric groups, revealed that *N*-cyclohexyl-4-methylbenzenesulfonamide outperformed other tested sulfonamides and selectively functionalize the Si-H bond over the C-H bond of hydrosilanes, despite their comparable bond dissociation energies, and theoretical studies further confirmed the selective functionalization of the Si-H bond. Optimization studies revealed 4CzIPN as the optimal photocatalyst, $K_3PO_4$ as the best base, and with acetone-water mixture as the ideal solvent, using *N*-cyclohexyl-4-methylbenzenesulfonamide as the hydrogen atom transfer catalyst for hydrosilylation of activated alkenes. Different activated alkenes, such as acrylic esters, maleate esters, *α*-methylene-*γ*-butyrolactone, cyclopentenones, acrylamides, vinyl phosphine oxides, and vinyl sulfone, tolerate the reaction conditions and undergo hydrosilylation smoothly, affords the corresponding product in moderate to good yields. Within the scope of hydrosilanes, we found that the developed protocol is suitable for both linear and branched alkyl silanes. Also, aryl silanes undergo efficient hydrosilylation with activated alkenes. Next, we extended this protocol to the selective functionalization of the Ge-H bond and achieved the hydrogermylation of activated alkenes in excellent yields. Both alkyl and aryl hydrogermanes are compatible under the developed reaction conditions. We performed different control experiments to investigate the reaction mechanism. Radical inhibition experiments confirmed the involvement of the radical in the mechanism, quantum yield measurements ruled out a radical chain mechanism, and deuterium-labelling studies indicated water as the proton source. The Stern-Volmer quenching revealed that the potassium salt of *N*-cyclohexyl-4-methylbenzenesulfonamide is an actual quencher of the excited photocatalyst. The oxidation potential of the potassium salt of sulfonamide was measured using cyclic voltammetry. A scale-up reaction further demonstrated the practical utility of this method.

***Chapter 3: Organophotocatalytic Regioselective Silylation/ Germylation and Cascade Cyclization of N-Alkenyl α-CF₃ Acrylamides: Access to Densely Functionalized 4-Pyrrolin-2-ones***

In this chapter, we describes the development of an alternative strategy for sulfamidyl radical generation and its utilization in the synthesis of silylated and germylated 4-pyrrolin-2-ones *via* functionalization of Si-H/Ge-H bond of hydrosilanes and hydrogermanes under photochemical conditions.

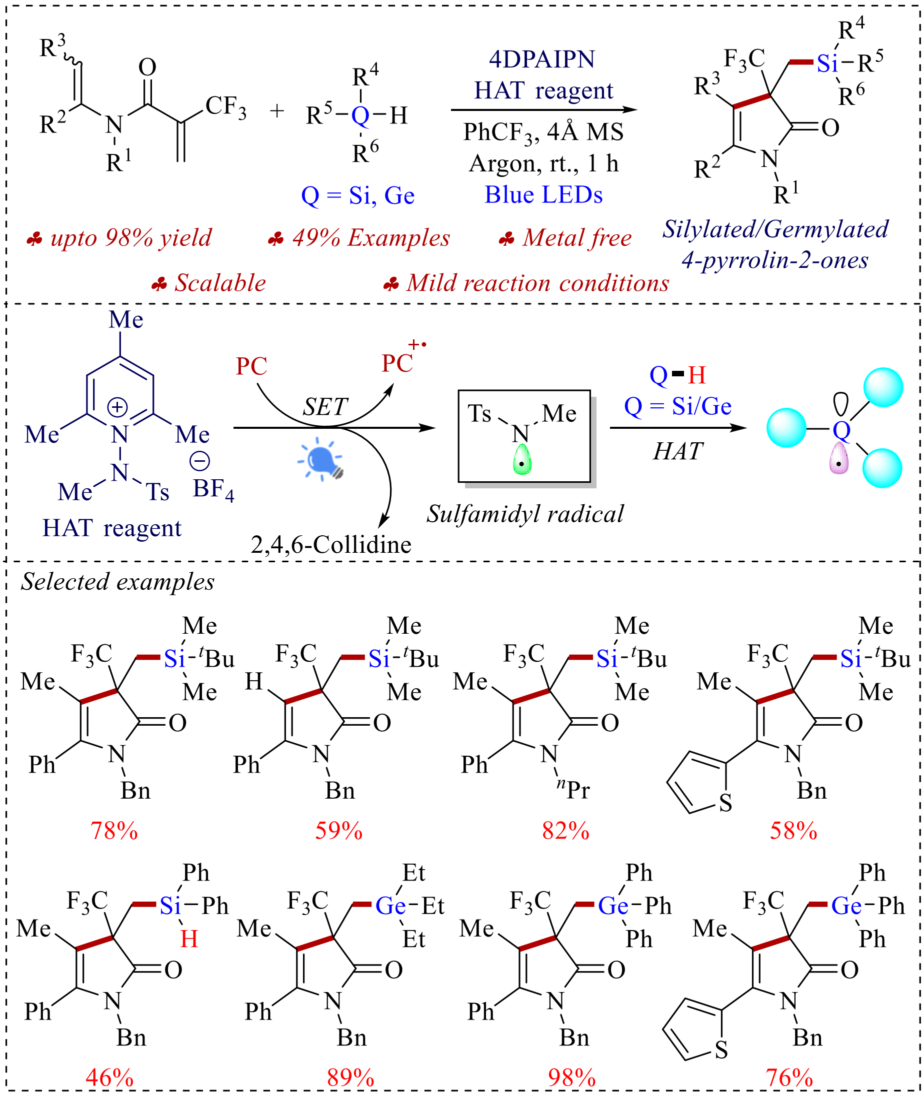


**Scheme 2** Photochemical synthesis of silylated/germylated 4-pyrrolin-2-ones *via* radical addition and cascade cyclization from *N*-Alkenyl *α*-$CF_3$ Acrylamides

To construct the 4-pyrrolin-2-one scaffold, we employed 3-aza-1,5-dienes as substrates, anticipating that silyl or germyl radical addition followed by cascade cyclization would deliver silylated or germylated 4-pyrrolin-2-ones. Our previously developed strategy for generating sulfamidyl radicals from sulfonamides could not be applied in this context because it proceeds *via* a reductive quenching pathway that generates a reduced photocatalyst, whereas the tentative mechanism suggest that the synthesis of 4-pyrrolin-2-ones from 3-aza-1,5-dienes requires an oxidized photocatalyst to complete the catalytic cycle. In this context, an alternative strategy was developed for the simultaneous generation of the sulfamidyl radical and an oxidized photocatalyst and we realized that *N*-aminopyridinium salts would be well-suited to generate sulfamidyl radical while providing the oxidized photocatalyst through an oxidative quenching pathway.

Optimization identified 4DPAIPN as the best photocatalyst and trifluorotoluene as the ideal solvent, using an *N*-aminopyridinium salt as the hydrogen atom transfer reagent for the photochemical synthesis of silylated and germylated 4-pyrrolin-2-ones. In the scope of 3-aza-1,5-dienes, enamides bearing ethyl, propyl, or phenyl substituents at the 2-position smoothly afforded the corresponding silylated 4-pyrrolin-2-ones in excellent yields. Both aryl and alkyl *N*-substituents were well tolerated, giving moderate to excellent yields. Substituents at the *meta* and *para*-positions of aryl rings and heteroaromatic ring 2-thienyl at the $\alpha$-position of the enamide, afforded the corresponding silylated 4-pyrrolin-2-ones in good to excellent yields. The developed methodology was efficient for both linear and branched alkyl silanes, as well as for aryl silanes undergo efficient radical addition and cyclization for the synthesis of silylated 4-pyrrolin-2-ones. The protocol was successfully employed for the synthesis of germylated 4-pyrrolin-2-ones, both alkyl and aryl hydrogermanes were compatible under the developed reaction conditions. The synthetic and practical utility of this method was further demonstrated by the compatibility of natural products and drug scaffold-tethered to starting materials, as well as through the scale-up reaction.

The proposed mechanism was supported by control experiments, including radical inhibition studies, which confirmed the involvement of a radical in product formation, trapping of the sulfamidyl radical with 1,1-diphenylethylene and quantum yield measurements indicating the involvement of a short radical chain mechanism. The fluorescence quenching of the excited photocatalyst by *N*-aminopyridinium salt was further confirmed through Stern-Volmer quenching studies.

***Chapter 4: Organophotocatalytic Regioselective Silylation/ Germylation and Cascade Cyclization of 1,7-Dienes: Access to Silylated/Germylated Benzazepines***

This chapter describes the synthesis of silylated and germylated seven-membered heterocycles, benzazepines, *via* regioselective radical addition and cascade cyclization of silyl and germyl radical to 1,7-dienes under photochemical conditions using our previously developed *N*-aminopyridinium salt as the hydrogen atom transfer reagent through Si-H/Ge-H bond functionalization of hydrosilanes and hydrogermanes.

The systematic reaction condition optimization revealed 4DPAIPN as the most efficient photocatalyst and acetonitrile as the ideal solvent, facilitating the synthesis of silylated benzazepine in 30 minutes. In the scope of 1,7-dienes, substituents at the *ortho*, *meta*, and *para*-positions of the benzene ring, as well as replacement of the benzene ring with a 2-thiophene tethered to the alkene, were tolerated under the optimized reaction conditions, affording silylated benzazepines in good to moderate yields. Further screening of substituents at different positions of the aryl ring of arylamine affords the desired product. Methyl substitution at the terminal position of the tethered alkene, as well as $\alpha$-methacryloyl-derived substrates, underwent radical addition and cyclization to afford the corresponding products. The protocol is also applicable to linear and branched alkyl silanes as well as aryl silanes, affording a variety of silylated benzazepine derivatives. We extended this protocol for the synthesis of germylated benzazepines, alkyl and aryl hydrogermanes smoothly underwent radical addition and cyclization to give the corresponding product. The drug febuxostat and natural product (+)-$\alpha$-tocopherol tethered 1,7-diene affords the desired silylated/germylated benzazepine in moderate to good yields. The further transformation of the photoproduct silylated benzazepine was achieved by converting it to the corresponding thioamide and bromo-substituted benzazepine.

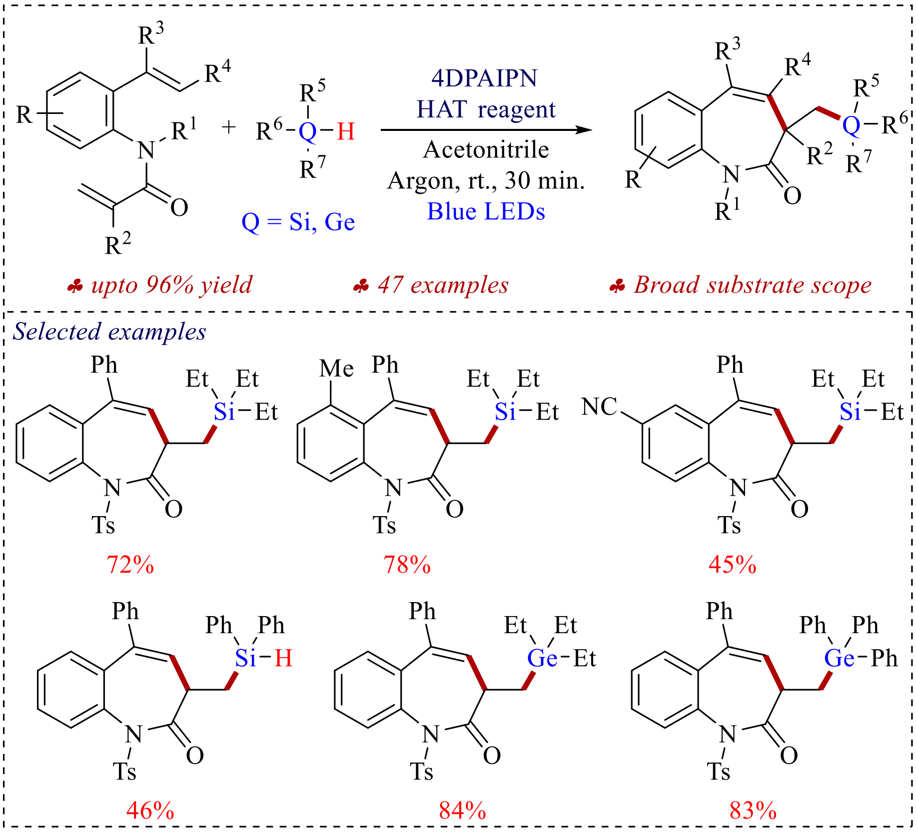


**Scheme 3** The photochemical synthesis of silylated/germylated benzazepines from 1,7-dienes *via* silyl/germyl radical addition and cascade cyclization

To gain insight into the reaction mechanism, various control experiments and intermediate trapping experiments were conducted. The product formation was not detected when the reaction was performed in the presence of the radical quencher TEMPO, indicating the involvement of a radical pathway in the reaction mechanism. The possibility of short radical chain involvement was determined by the quantum yield and the kinetic isotope effect revealed no role of C-H bond cleavage in the rate-determining step.

Furthermore, the formation of the carbocation intermediate during the synthesis of silylated and germylated benzazepines was confirmed through the detection of hydroxyl-trapped benzazepine derivative by HRMS. The practicality of this protocol was tested by performing a 2 mmol scale reaction.

***Summary***

In summary, we developed the first method to use sulfamidyl radical for the selective functionalization of the Si-H and Ge-H bonds of hydrosilanes and hydrogermanes and made efforts to advance the synthesis of organosilicon and organogermanium compounds. **Chapter 1** deals with the general introduction of organosilicon and organogermanium compounds and their physicochemical properties. Next, we discussed a detailed synthesis of these compounds from various available sources and their applications in daily life, medicine and agriculture. Furthermore, we discussed photoredox catalysis, along with the photophysical and electrochemical properties of photocatalysts and their operating mechanism. Finishing this chapter on our approach to the synthesis of organosilicon and organogermanium compounds. **Chapter 2** deals with the development of sulfamidyl radical from easily synthesizable, inexpensive, sterically and electronically tunable sulfonamide as a HAT precursor and employed in the hydrosilylation of activated alkenes *via* selective functionalization of Si-H/Ge-H bond of hydrosilanes and hydrogermanes. **Chapter 3** deals with the development of an alternative protocol for the generation of sulfamidyl radical from *N*-aminopyridinium salt *via* the oxidative quenching pathway and employed in the synthesis of silylated/germylated 4-pyrrolin-2-ones. **Chapter 4** describes the synthesis of silylated and germylated benzazepines from 1,7-dienes *via* silyl and germyl radical addition followed by cascade cyclization. The silyl and germyl radicals were generated from hydrosilanes and hydrogermanes through a hydrogen atom transfer process mediated by *N*-aminopyridinium salts derived sulfamidyl radical under an oxidative quenching cycle.

## Outcomes from Ph.D. thesis work:

1. **Bajya, K. R.**, Selvakumar, S. (2025). Organophotocatalytic Regioselective Silylation/Germylation and Cascade Cyclization of 1,7-dienes: Access to Silylated/Germylated Benzazepine Derivatives. *J. Org. Chem. 90*, 16131. (DOI:10.1021/acs.joc.5c02091).

2. **Bajya, K. R.**, Maurya, S. K., Selvakumar, S. (2024). Organophotocatalytic Regioselective Silylation/Germylation and Cascade Cyclization of *N*-Alkenyl $\alpha$-$CF_3$ Acrylamides: Access to Densely Functionalized 4-Pyrrolin-2-ones. *Org. Lett. 26*, 9269. (DOI: 10.1021/acs.orglett.4c03427).

3. **Bajya, K. R.**, Kumar, M., Ansari, A., Selvakumar, S. (2023). Sulfonamide as Photoinduced Hydrogen Atom Transfer Catalyst for Organophotoredox Hydrosilylation and Hydrogermylation of Activated Alkenes. *Adv. Synth. Catal. 365,* 976. (DOI:10.1002/adsc.202300040).

## Additional Work:

4. **Bajya, K. R.**, Selvakumar, S. (2022). Dual Photoredox and Cobalt Catalysis Enabled Transformations. *Eur. J. Org. Chem.* e202200229. (DOI: 10.1002/ejoc.202200229).

5. Jangir, P., **Bajya, K. R.**, Pathare, A. S., Sodoor, M., Saini, R., Purohit, M., Selvakumar, S. (2024). Metal-Free *ipso*-Halocyclization of *N*-Arylpropynamides Using Hypervalent Iodine(III) Reagents under Aqueous Condition. *Eur. J. Org. Chem. 27,* e202400203. (DOI: 10.1002/ejoc.202400203).

6. Monika, **Bajya, K. R.**, Gupta M. K., Selvakumar S. (2023). Visible-Light Mediated Metal-free Synthesis of 3-Bromo Coumarins Using In situ Generated Transient Non-Symmetric Bromoiodanes. *Chemistry Select 8*, e202300496. (DOI: 10.1002/slct.202300496).

**Conferences: Oral/Poster Presentation**

1. Poster presentation at "**ACS Publication Symposium: Catalysis for Organic Synthesis**", August 2024 at the University of Vienna, Austria.
2. Poster presentation at "**Emerging Trends in Catalysis and Synthesis (ETCS)**", March 2024 at the Indian Institute of Technology Kharagpur, India.
3. Poster presentation at "**Indo-German Partnership Sustainability Conference (IGP)**", February 2023, at the Indian Institute of Technology Indore, India.
4. Oral presentation at "**In-house symposium**", March 2023, Department of Chemistry, Indian Institute of Technology Indore, India.

## Table of Contents

**Chapter 2 Development of Sulfonamide as Photoinduced Hydrogen Atom Transfer Catalyst for Organophotoredox Hydrosilylation and Hydrogermylation of Activated Alkenes**

**Chapter 3 Organophotocatalytic Regioselective Silylation/ Germylation and Cascade Cyclization of *N*-Alkenyl $\alpha$-$CF_3$ Acrylamides: Access to Densely Functionalized 4-Pyrrolin-2-ones**



**Chapter 4 Organophotocatalytic Regioselective Silylation/ Germylation and Cascade Cyclization of 1,7-Dienes: Access to Silylated/Germylated Benzazepine Derivatives**

## List of Figures

### Chapter 1 Introduction

**Chapter 2 Development of Sulfonamide as Photoinduced Hydrogen Atom Transfer Catalyst for Organophotoredox Hydrosilylation and Hydrogermylation of Activated Alkenes**



**Chapter 3 Organophotocatalytic Regioselective Silylation/ Germylation and Cascade Cyclization of *N*-Alkenyl $\alpha$-$CF_3$ Acrylamides: Access to Densely Functionalized 4-Pyrrolin-2-ones**

## List of Schemes

## List of Tables

### Chapter 1 Introduction



### Chapter 2 Development of Sulfonamide as Photoinduced Hydrogen Atom Transfer Catalyst for Organophotoredox Hydrosilylation and Hydrogermylation of Activated Alkenes

## List of Symbols, Units and Acronyms

| | |
|---|---|
| • | radical |
| $e^-$ | electron |
| α | alpha |
| β | beta |
| γ | gamma |
| δ | delta NMR scale |
| Δ | delta |
| η | eta |
| ϕ | phi (quantum yield) |
| λ | wavelength |
| *h* | Planck's constant |
| *v* | frequency |
| Å | angstrom |
| ε | molar absorptivity |
| σ | sigma |
| π | pi |

| | |
|---|---|
| $f$ | fraction of light absorbed |
| ° | degree |
| °C | degree centigrade |
| J | coupling constant |
| W | Watt |
| V | Volt |
| $A$ | absorbance |
| $V$ | volume |
| $l$ | length |
| s | singlet in NMR |
| d | doublet in NMR |
| t | triplet in NMR |
| q | quartet in NMR |
| dd | doublet of doublet in NMR |
| m | multiple in NMR |
| $\Delta G$ | change in Gibbs free energy |
| $\Delta G^{\neq}$ | active Gibbs free energy |
| cm | centimeter |
| nm | nonometer |
| pm | picometer |
| μL | microlitre |
| mL | millilitre |
| g | gram |
| mg | milligram |
| mmol | millimole |
| kcal | kilocalorie |
| Hz | hertz |
| MHz | mega hertz |
| M.P. | melting point |
| $^{13}C$ | carbon-13 |
| $^{19}F$ | fluorine-19 |
| $^{1}H$ | proton |
| $^{31}P$ | phosphorous-31 |

| | |
|---|---|
| APCI | atmospheric pressure chemical ionization |
| BDE | bond dissociation energy |
| CV | cyclic voltammetry |
| DFT | density functional theory |
| EDA | electron donor acceptor complex |
| ET | electron transfer |
| $EC_{50}$ | half-maximal effective concentration |
| EI | elemental analysis |
| ESI | electron spray ionization |
| $E_{ox}$ | oxidation potential |
| $E_{red}$ | reduction potential |
| GCMS | gas chromatography mass spectrometry |
| HAT | hydrogen atom transfer |
| HATC | hydrogen atom transfer catalyst |
| HATR | hydrogen atom transfer reagent |
| HRMS | high resolution mass spectrometry |
| HOMO | highest occupied molecular orbital |
| IR | infrared spectroscopy |
| KIE | kinetic isotope effect |
| LED | light emitting diode |
| LMCT | ligand to metal charge transfer |
| LCMS | liquid chromatography mass spectrometry |
| LUMO | lowest unoccupied molecular orbital |
| m/z | mass to charge ratio |
| NMR | nuclear magnetic resonance |
| PCET | proto-coupled electron transfer |
| rt | room temperature |
| SCE | standard calomel electrode |
| SET | single electron transfer |
| UV/Vis | ultraviolet-visible absorption spectroscopy |

## List of Chemical Abbreviations

| | |
|---|---|
| ACN | acetonitrile |
| AIBN | azobisisobutyronitrile |
| BHT | butylated hydroxytoluene |
| DCE | dichloroethane |
| DCM | dichloromethane |
| DMF | dimethylformamide |
| DMSO | dimethylsulfoxide |
| DMA | dimethylacetamide |
| DIPEA | *N*,*N*-diisopropylethylamine |
| $Et_2O$ | diethylether |
| Fc | ferrocene |
| HFIP | 1,1,1,3,3,3-hexafluoroisopropanol |
| NBS | *N*-bromosuccinimide |
| $^t$Bu | *tert*-butyl |
| THF | tetrahydrofuran |
| TMS | trimethylsilyl |
| Ts | *para*-toluenesulfonyl or Tosyl |
| TEMPO | 2,2,6,6-tetramethylpiperidine-1-oxyl |
| $TBAPF_6$ | tetra-*n*-butylammonium hexafluorophosphate |
| $PhCF_3$ | trifluorotoluene |
| ppy | 2-phenylpyridine |
| bpy | 2,2'-bipyridine |
| dtbbpy | 4,4'-di-*tert*-butyl-2,2'-bipyridine |
| 4CzIPN | 2,4,5,6-tetra(9*H*-carbazol-9-yl)isophthalonitrile |
| 4DPAIPN | 2,4,5,6-tetrakis(diphenylamino)isophthalonitrile |
| 3DPAFIPN | 2,4,6-tris(diphenylamino)-5-fluoroisophthalonitrile |

## Materials and Experimental Techniques

Commercial reagents and solvents were purchased from commercially available sources and used without further purification. Organic solutions were concentrated under reduced pressure on Heidolph rotary evaporator. Thin layer chromatography was carried out on Merck silica gel 60F254 pre-coated aluminium sheets and were visualized using UV light (254 nm). Silica gel column chromatographic purification of products was performed with 100-200 and 240-400 mesh silica gel. $^{1}$H and $^{13}$C, $^{19}$F and $^{31}$P spectra were recorded on a Fourier transform nuclear magnetic resonance spectrometer, model Bruker Avance 400 or 500 MHz spectrometer. All chemical shift values are mentioned in δ scale in parts per million (ppm). The residual solvent peaks of $CDCl_3$ and DMSO-$d_6$ were recorded at 7.26 and 2.54 ppm for $^{1}$H NMR and at 77.16 and 40.45 for $^{13}$C NMR respectively. High-resolution mass spectra were recorded on WATERS-XEVO G2-XS-QToS mass spectrometer in positive/negative ion mode. GC-MS analysis was performed with GCMS QP 2010 Ultra mass spectrometer (EI mode) from Shimadzu analytical. Absorption spectra were recorded on Perkin Elmer Lambda 750 model spectrophotometer. Fluorescence quenching experiments were performed using Fluoromax_PLUS_C Spectrofluorometer (HORIBA Jobin Yvon, model FM100). FT-IR analysis was performed on Fourier Transform Infrared Spectrometer (FT-IR), Bruker Tensor27. Cyclic voltammetry was recorded on C-H instruments model CHI1103C with the three-electrode cell (beaker type cell) at room temperature. The melting point was measured using Analab Thermocal melting point apparatus.

# Chapter 1

# Introduction

## 1.1 General introduction

Silicon lies in the third row of the periodic table, below carbon. It is the second most abundant element in the earth's crust.[1] Both carbon and silicon shows a valency of 4 and form tetrahedral compounds, but there are certain differences in their properties. Carbon forms stable $\pi$ bonds, but not in the case of silicon.[2] Silicon exists in nature as silicate and silica, as it forms a stable $\sigma$-bond with oxygen.[3,4] The compounds that possess a "silicon-carbon bond" referred to organosilicon compounds, which are not readily available in nature.[2] As a result, elemental silicon is used to synthesize organosilicon compounds. Based on the nature of bonds, organosilicon compounds are classified into various categories, such as organosilanes, siloxanes, silazanes, silylethers, and halosilanes. Additionally, they also bonded with other elements such as sulfur, phosphorus, and various metals to give different types of silicon containing compounds.

Germanium also lies in the same fourth row of the periodic table, below silicon. It was separated from mineral argyrodite ($Ag_8GeS_6$, containing 5-7% Ge) in 1886 by the German chemist Clemens Winkler.[5,6] The physical and chemical characteristics of germanium are similar to non-metal silicon and, to a lesser extent with tin, and usually classified it as a semi-metal. Germanium is generally found in the +4 oxidation state as oxides or in solution as Germanic acid ($Ge(OH)_4$).[7]

## 1.2 Silicon and germanium versus carbon

The covalent radii of both silicon and germanium are larger than that of carbon, while their electronegativities are lower.[8] The Si-C and Ge-C bonds are longer than the C-C bonds. Silicon's higher covalent radius results in approximately 20% longer bond lengths, different bond angles, and distinct ring conformations compared to its carbon analogues. The increased size and covalent radius can have a significant impact on the conformation and reactivity of ring structures with a silicon center. Silicon's electropositive character (relative to C, N, O, and H) results in an electron-deficient centre in a molecule and reversed bond polarization when compared to analogous carbon bonds.[8]Organosilicon molecule exhibits high lipophilic characteristics[9,10] and the incorporation of a silyl group into an organic compound can alter its chemical and physical properties that makes the resulting products with distinct characteristics. These characteristics make silicon an ideal candidate for medicinal studies.

**Table 1.1** Covalent radius, electronegativity, and bond length comparison of C, Si and Ge

| | **Carbon** | **Silicon** | **Germanium** |
|---|---|---|---|
| Covalent radius | 77 pm | 117 pm | 122 pm |
| Electronegativity | 2.50 | 1.90 | 2.01 |
| Bond length | C-C is 1.54 Å | Si-C is 1.87 Å | Ge-C is 1.95 Å |
| (*p*-*d*) $\pi$-bond | Absent | Strong | Weaker than Si |

On comparing germanium with silicon and carbon, it exhibits similar physicochemical properties with silicon rather than carbon. Although silicon and germanium are much closer to one another, there can be some quantitative differences in potency due to the difference in rate of Si-C and Ge-C bond cleavage. This is because germanium has a reduced capacity to form (p-d) $\pi$ bonds, and triorganylgermanyl derivatives are somewhat more lipophilic.[7]

### 1.3 Organosilicon compounds

The compounds that possess a "silicon-carbon bond" refer to organosilicon compounds. Silicon has become a key element in research and applications, since the late 1800s demonstrating a substantial advancement in organosilicon chemistry.[11] Organosilicons are integral in both academic research and industrial applications.[12,13] Their flexibility covers multiple scientific disciplines, including materials science,[14-17] medicines,[1,9,18] chemosensors,[19] catalysis,[20,21] and polymer chemistry.[22] These organosilicon compounds are also crucial for drug discovery and biomedical engineering, as well as in the synthesis of complex molecules.[23]

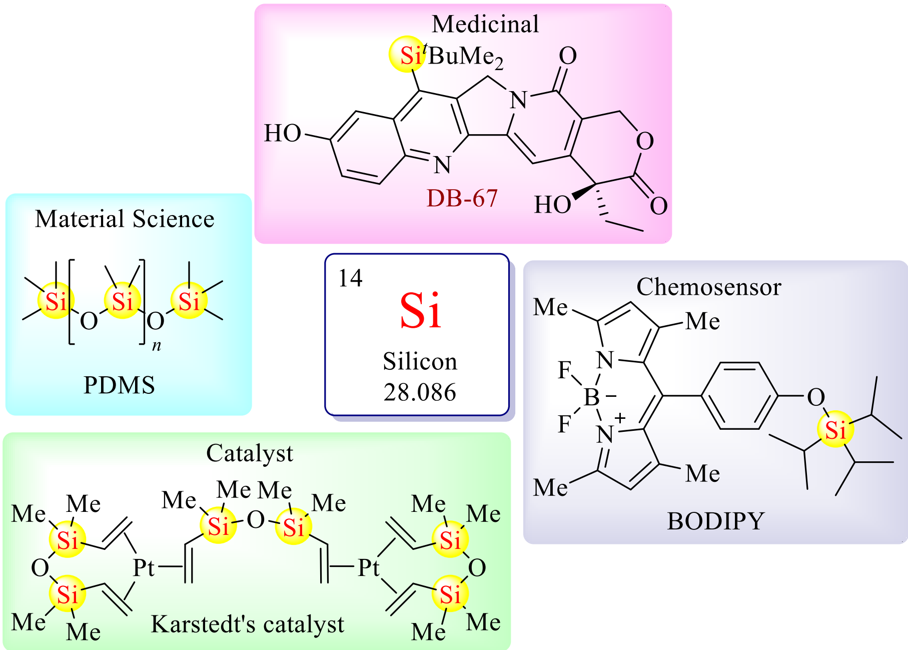


**Figure 1.1** Representative examples of silicon-containing functional molecules

### 1.3.1 Historical background for the synthesis of organosilicon compounds

In the early days of silicon chemistry, the practical utility of organosilicon compounds was not immediately evident. The scientific curiosity motivated early researchers to explore their synthesis and investigate its chemical behaviour. A pivotal advancement occurred in the early 1820s, when J. J. Berzelius first isolated a volatile silicon compound from its oxygen-rich mineral. He synthesized tetrachlorosilane ($SiCl_4$) by reacting sodium hexafluorosilicate with potassium in chlorine gas.[24] This milestone laid the groundwork for the modern field of organosilicon chemistry. The progress of organosilicon chemistry closely tracks that of organometallic chemistry. However, in 1849, Sir Edward Frankland reported the first use of ethyl zinc iodide and diethyl zinc as organometallic reagents.[25] It was not until 1863 that Friedel and Crafts synthesized the first organosilicon compound (**Scheme 1.1a**). This was achieved by heating diethyl zinc with tetrachlorosilane ($SiCl_4$) in a sealed tube at 140-160 °C.[26,27] Furthermore, In 1873 Ladenburg reported the first synthesis of an aryl silane derivative by reacting diphenyl mercury with tetrachlorosilane (**Scheme 1.1b**).[28-30] In 1884, by adopting the Wurtz-Fittig condition Polis synthesized tetraphenyl silane (**Scheme 1.1c**).[31]

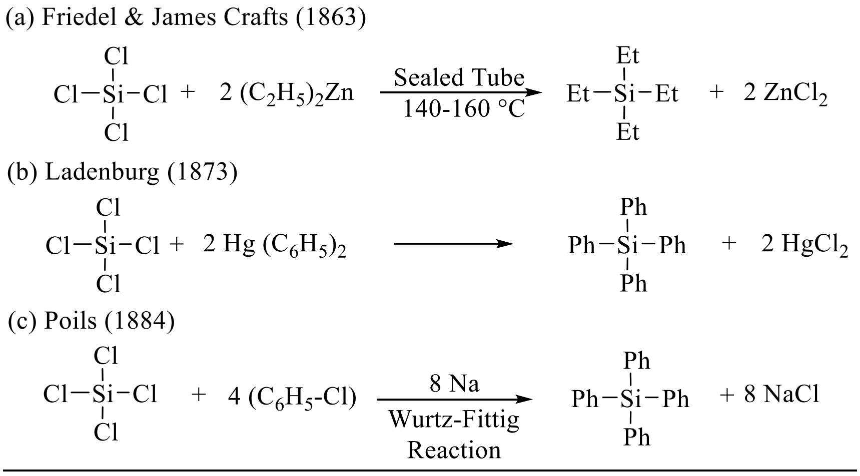


**Scheme 1.1** Early synthesis of the organosilicon compounds

Invention of the Grignard reagent[32] by Victor Grignard in 1900 drew the attention of Kipping, who performed the reaction of tetrachlorosilane with ethylmagnesium iodide and obtained a mixture of ethyl trichlorosilane, diethyl dichlorosilane, triethyl chlorosilane and tetraethylsilane (**Scheme 1.2a**).[33] Although Si-C bond formation was attractive in the early 19$^{th}$ century, it was cumbersome due to the intensive energy requirement and difficulty in the removal of by-products. Almost four decades later, Rochow developed the direct process for synthesizing organosilicon compounds. In the direct process, the reaction of chloromethane with silicon using copper as a catalyst at 300 °C yields dichlorodimethylsilane as the major product (**Scheme 1.2b**).[34] In the late 1950s, chloroplatinic acid (Speier's catalyst) was successfully used to hydrosilylate olefins (**Scheme 1.3a**)[35]. In 1989, Rich group developed a new synthetic method on an industrial scale. This procedure rely on the reaction between chlorodimethylsilane and substituted acid chloride (**Scheme 1.3b**).[36]

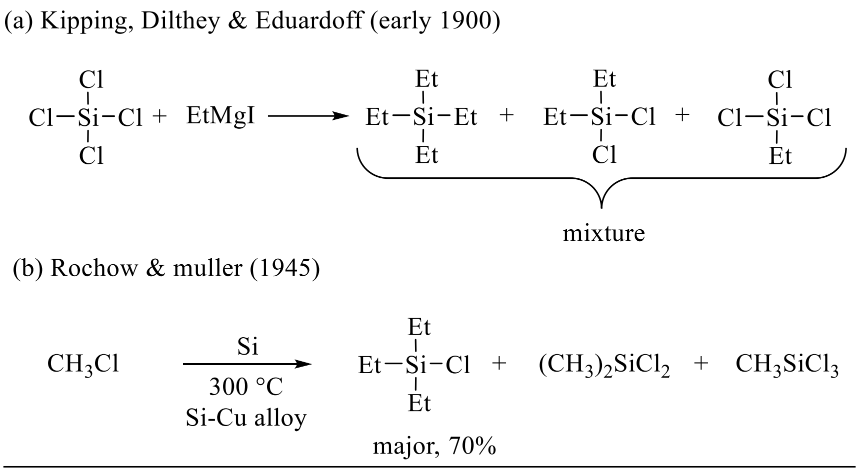


**Scheme 1.2** Organosilicon synthesis *via* Grignard reagent and direct process

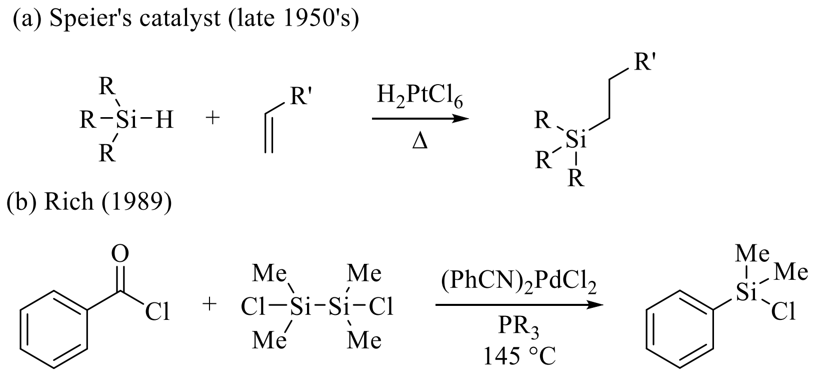


**Scheme 1.3** Speier's and Rich method for the synthesis of organosilicon compounds

### 1.3.2 Synthesis of organosilicon compounds from different silicon sources

Organosilicon compounds can be synthesized using a variety of silicon sources, including halosilanes, silylboronates, hydrosilanes, disilanes, and silylcarboxylates. Elemental silicon was used as a source by Müller and Rochow in the direct process.[34] In the early stages on developing methods to access organosilicon compounds, tetrachlorosilane was used as the primary source of silicon with various metals.[22-31] Disilanes were widely utilized in the synthesis of oligosilane backbone in material chemistry due to their unique properties as $\sigma$-$\pi$ hybrid architectures.[37] In this regard, oligosilanyl hydride was used to introduce the oligosilane unit.[38-41]

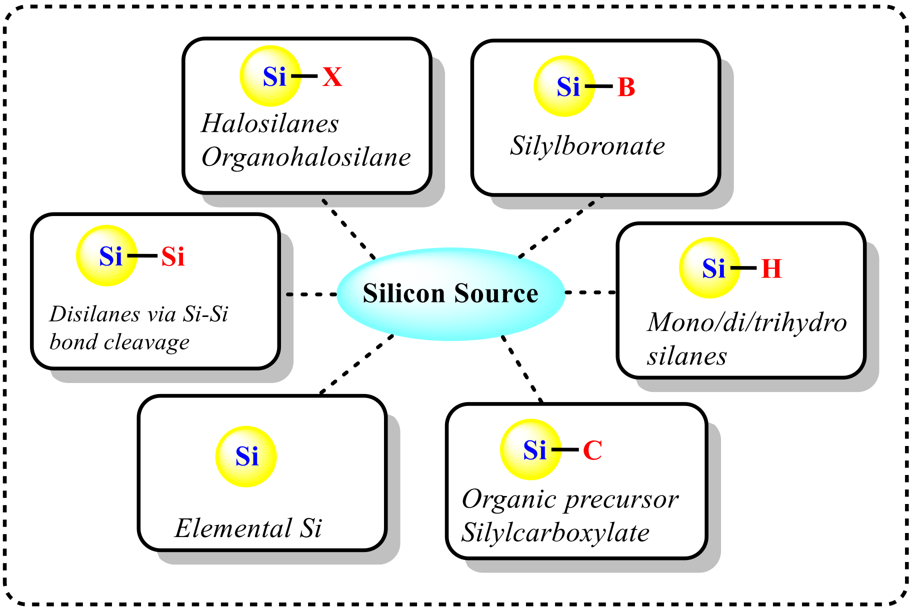


**Figure 1.2** Source of silicon in the synthesis of organosilicon compounds

However, over the past few decades, tris(trimethylsilyl)silanes, a unique class of oligosilanes, have drawn a lot of attention as a commercially accessible reagent.[42,43] The $(TMS)_3SiR$ (R= aryl, alkyl) such as organotris(trimethylsilyl)-silanes and others make oligosilanes into greatly enriched available silanyl precursors *via* cleavage of the Si-Si bond **(Scheme 1.4)**.[44-46] The silicon-boron reagents are also versatile intermediates to synthesize organosilicon compounds. There are several ways to activate the Si-B bond using different transition metal catalysts (**Scheme 1.5**).[47-50] The Muller-Rochow “direct process” yields halosilanes (especially chlorosilanes) as a product[51] which is frequently used as a silicon source on a commodity scale due to its availability. The organometallic reactions, transition metal-catalyzed reactions, and photo/electrochemical reactions emphasize the scope of chlorosilane as a silicon source, in addition few reports are also available for the use of iodosilane.[52-55] Here, we describe some recent studies for the synthesis of organosilicon compounds using different metal catalysts. The Oshima group disclose the silver-catalyzed transmetallation reaction between chlorosilanes using alkyl and alkenyl Grignard reagents for the synthesis of tetraorganosilanes (**Scheme 1.6a**).[55] Palladium-catalyzed cross-coupling between monochlorosilanes and Grignard reagents also provides tetra-alkyl-substituted organosilicon compounds (S**cheme 1.6b**). [56]

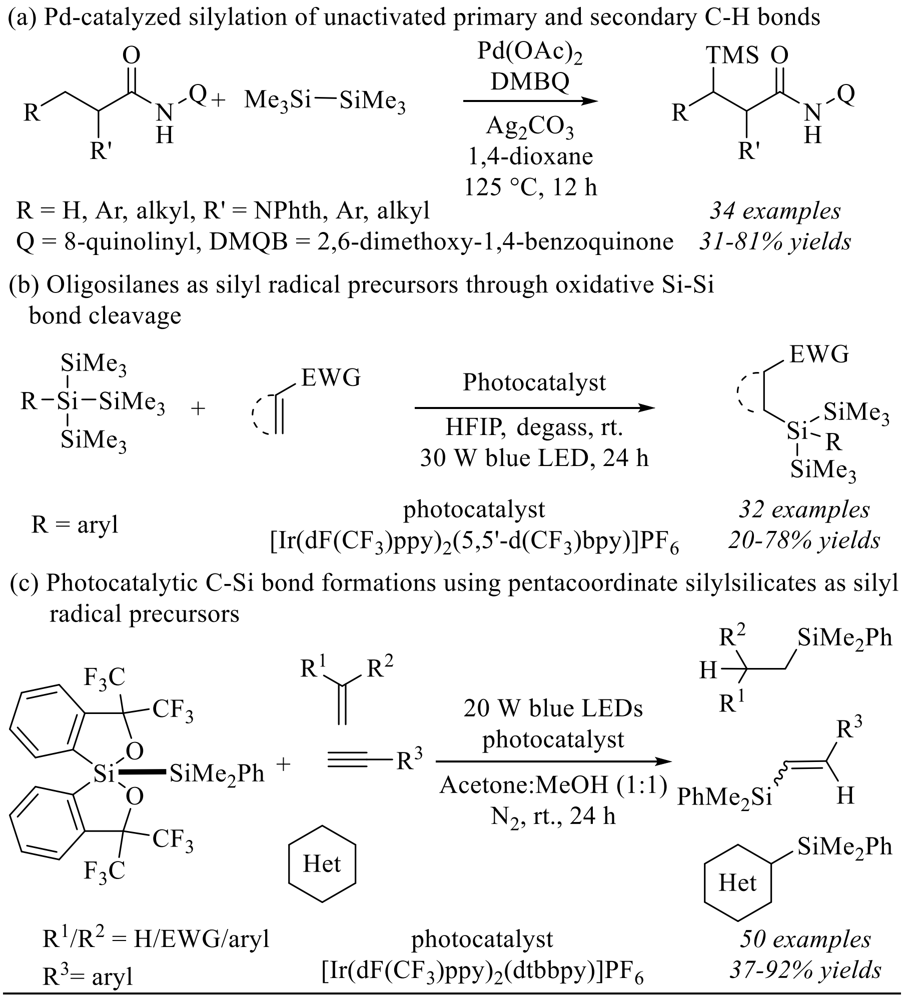


**Scheme 1.4** Representative reports for the synthesis of organosilicon compounds using oligosilanes as a silyl source

A three-component Ni-catalyzed regioselective silylation of acrylonitrile was reported by Zhang using unactivated alkyl bromide and chlorosilanes (**Scheme 1.6c**).[57] Recently, Xie's group disclosed the copper-catalyzed cross-coupling reaction of aryl halides with chlorosilanes under reductive conditions (**Scheme 1.6d**).[58] In the process of developing organosilicon chemistry, silylcarboxylic acid[59] and other carbon-based silylating reagents[60-64] were also used as a silicon source by the group of Studer, Oestreich, and Uchiyama.

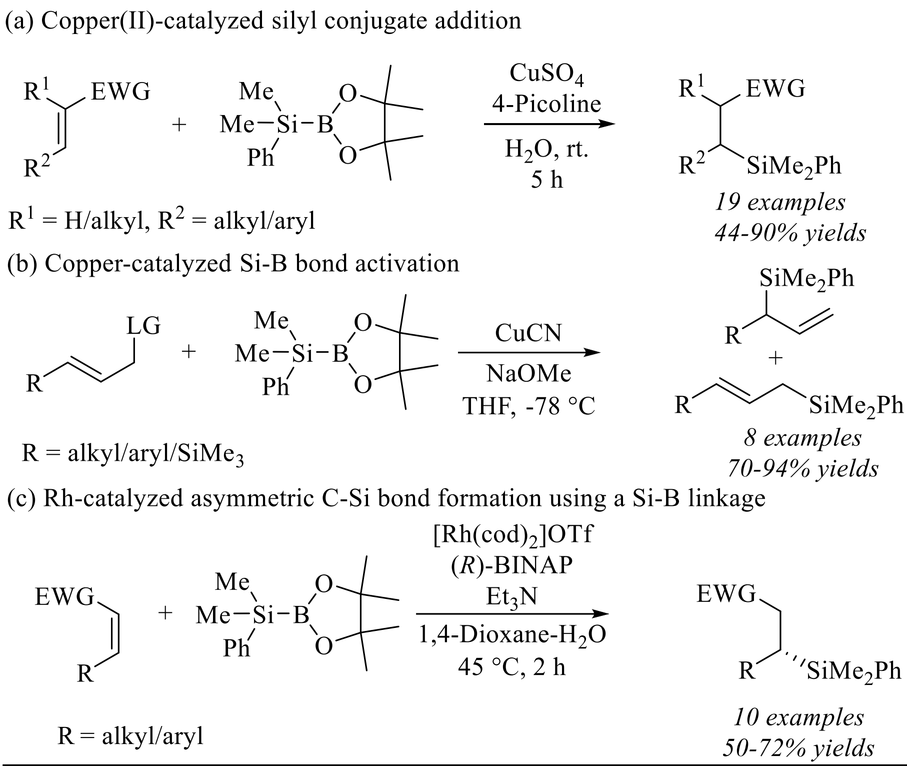


**Scheme 1.5** Selected reports for the synthesis of organosilicon compounds using silyl-boron reagents as a silyl source

In 2001, Studer group reported the radical transfer hydrosilylation-cyclization of alkenes using silylated cyclohexadienes and reaction was initiated by AIBN under thermal condition (**Scheme 1.7a**).[65] Subsequently, in 2013 Oestreich developed the $B(C_6F_5)_3$-catalyzed transfer hydrosilylation of alkenes using 3-silylated cyclohexa-1,4-dienes as a silyl precursor at room temperature (**Scheme 1.7b**).[61] Recently, Uchiyama group utilized silylcarboxylic acids (**Scheme 1.7c**) and 3-silyl-1,4-cyclohexadiene as a silylating agent in the hydrosilylation of alkenes under visible light-mediated photocatalytic conditions.[59,63] Hydrosilanes are a versatile silicon precursor for the synthesis of organosilicon compounds through addition to C-C multiple bonds, C-H activation of arenes and heteroarenes (Minisci type addition), and cross-coupling reactions with aryl halides under both metal-free and transition metal-catalyzed conditions.[66-75] Here, we discussed some selected reports for the synthesis of organosilicon compounds under metal-free and metal-catalyzed conditions using hydrosilanes as a silyl source.

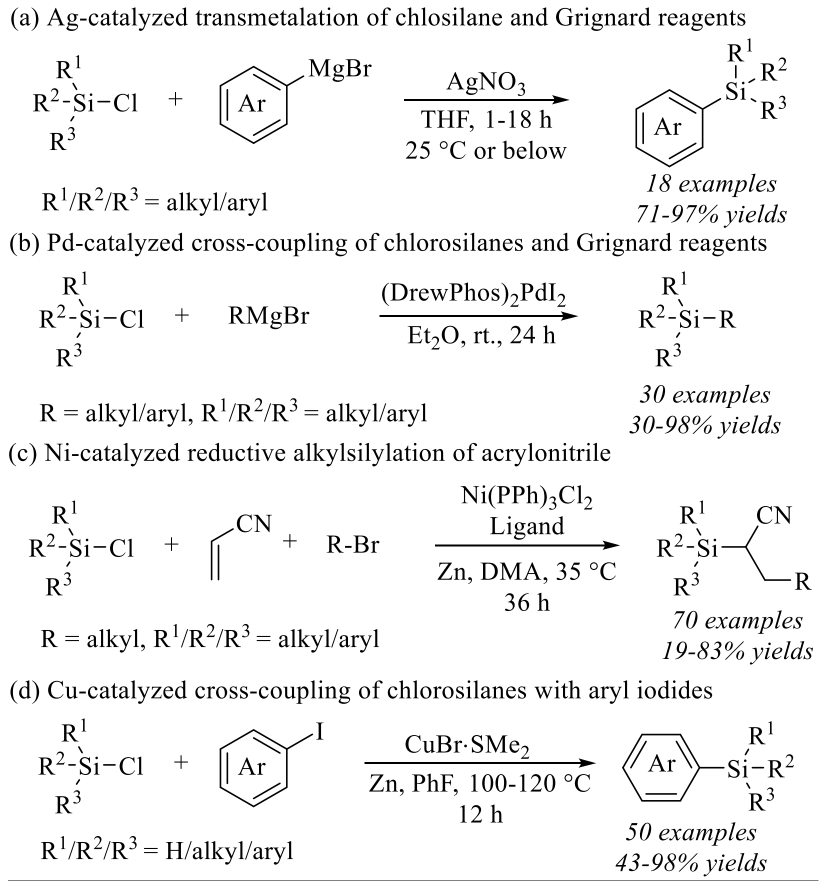


**Scheme 1.6** Selected reports for the synthesis of organosilicon compounds using chlorosilane reagents as a silyl source

The Grubbs and Stoltz reported transition metal-free C-H bond functionalization of heteroarenes using potassium *tert*-butoxide as a catalyst (**Scheme 1.8a**)[76] as well as C-H bond functionalization of terminal alkynes using alkali metal hydroxides (**Scheme 1.8c**).[78] Subsequently, the Hou's group reports the electron-deficient boron-catalyzed C-H bond functionalization of arenes using hydrosilanes (**Scheme 1.8b**).[77]

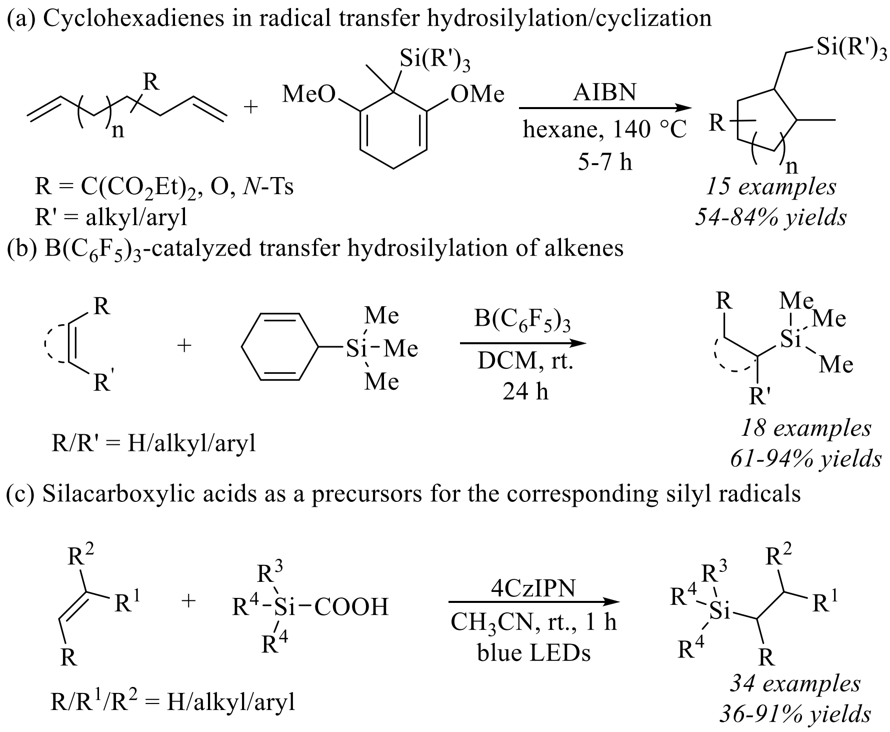


**Scheme 1.7** Silylated cyclohexadienes and silylcarboxylic acids as a silyl source

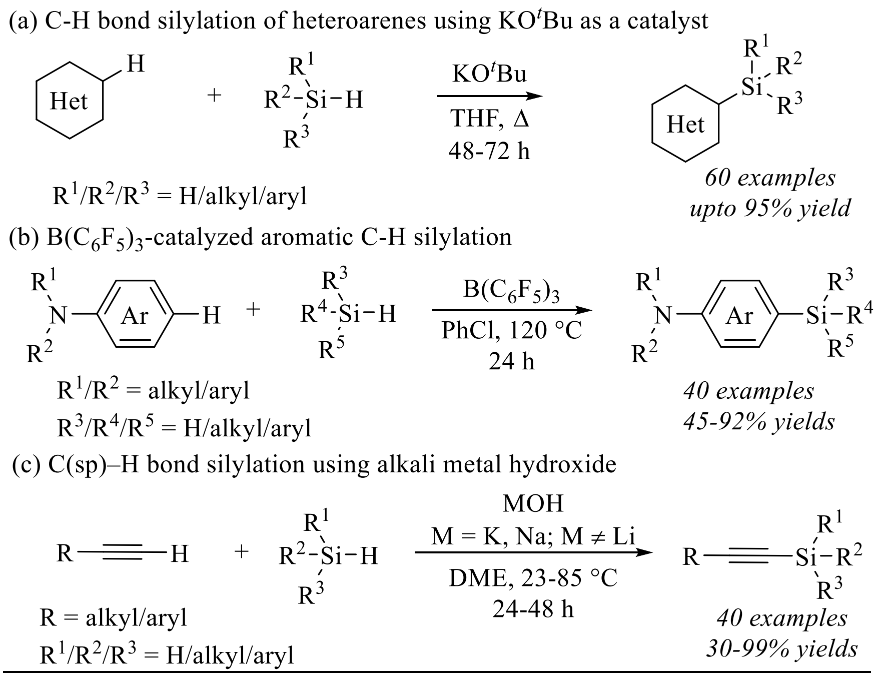


**Scheme 1.8** Representative reports for transition metal-free synthesis of organosilanes using hydrosilanes as silicon source

Transition metal-catalyzed organosilicon compounds synthesis were developed using Pt, Pd, Rh, Ru, Fe, Ir, Ni, and Cu, among others.[66-75]

Here, we have shown some of the selected reports for transition metal-catalyzed organosilicon compound synthesis using hydrosilanes as silyl source. In 1965, Chalk and Harrod utilized $Co_2(CO)_8$ as a catalyst for the hydrosilylation of olefins using hydrosilanes (**Scheme 1.9a**).[79] Yamanoi disclosed the silylation of aryl halides using palladium as a transition metal catalyst with a bulky alkyl phosphine as the ligand (**Scheme 1.9b**).[80] An Ir-catalyzed silylation of the heteroarenes using hydrosilanes under thermal conditions was reported by the Falck group (**Scheme 1.9c**).[81] Very recently, the Zhang group disclosed the Ni-catalyzed Markovnikov hydrosilylation of vinylarenes *via* hydrogen atom transfer process (**Scheme 1.9d**).[82]

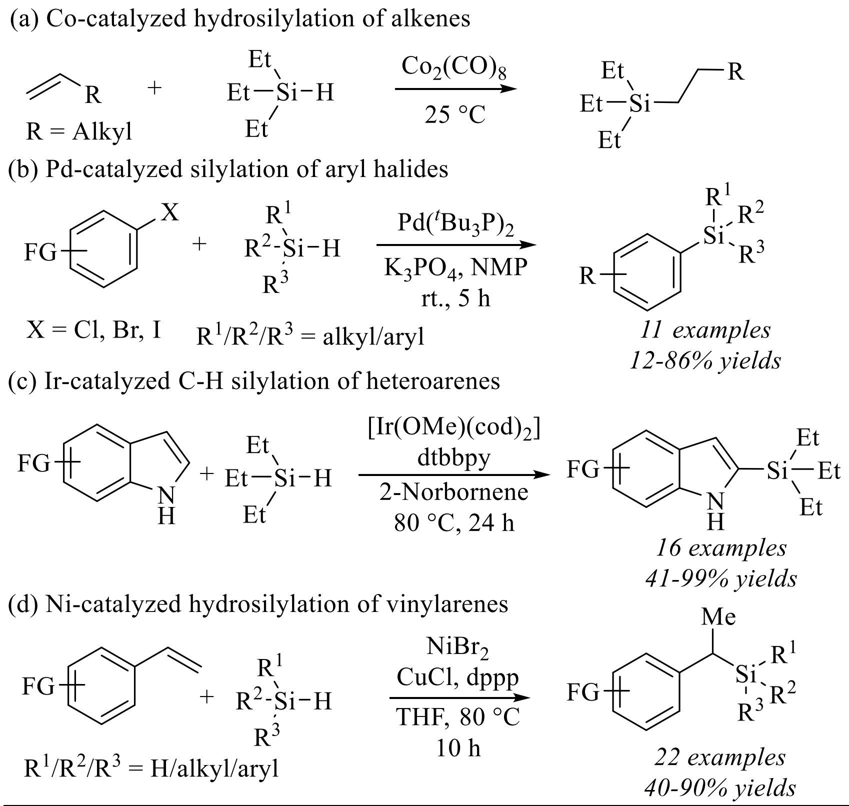


**Scheme 1.9** Selected examples for the transition metal-catalyzed catalyzed organosilicon compounds synthesis from hydrosilanes

### 1.3.3 Applications of organosilicon compounds

Organosilicon compounds have extensive and widespread applications in synthetic chemistry, pharmaceuticals, agrochemicals, and materials research.[9,83,84] Selected applications are discussed below.

**<u>Daily life applications</u>:** Organosilicon compounds have been widely used in daily life for example, polydimethylsiloxanes (PDMS) (**Figure 1.3**) a silicon polymer used as a food additive under the European Food Safety Authority (EFSA)[85] and also used in medicine, cosmetics, foam deforming agents,[86] superhydrophobic coating agents for advanced surfaces,[97] lubricants, and in heat-resistant tiles.

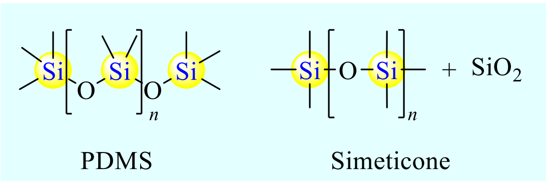


**Figure 1.3** Organosilicon compounds PDMS and Simeticone

Simeticone (**Figure 1.3**) is an FDA-approved over-the-counter medicine based on silicone that is used as a gastrointestinal surfactant to treat infant colic.[88]

**<u>Agricultural applications</u>:** In the field of agriculture, organosilicon compounds are used as an adjuvant or additive with herbicides/pesticides as a spray improver, leaf absorption additive or activator. For instance, silicone polyether copolymer and silicon surfactant Sylgard 309[89] enhances the efficacy of agricultural agents, including fungicides, insecticides, herbicides, and as a plant growth regulators.

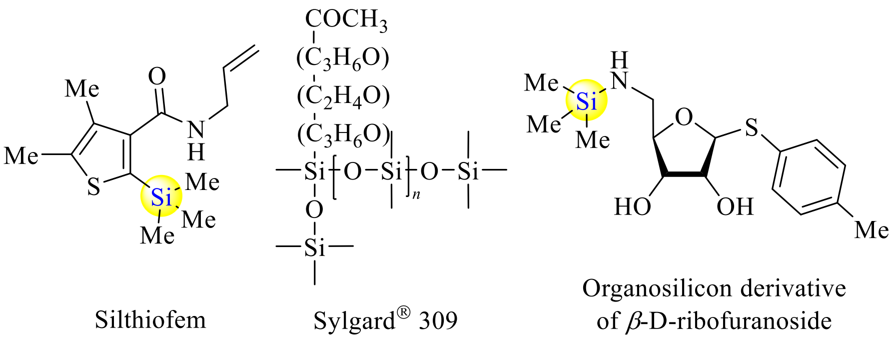


**Figure 1.4** Organosilicon compounds Silthiofem, Sylgard 309, and *β*-D-ribofuranoside

Organosilicon derivatives of $\beta$-D-ribofuranoside exhibit insecticidal activity with low toxicity.[90] Silthiofam is used as a fungicide to control fungal diseases in wheat and vegetables (**Figure 1.4**).[91]

**<u>Medicinal applications</u>:** Due to the unique physicochemical properties of silicon, organosilicon compounds are ideal candidates for its use in medicinal chemistry.[9] Some medicinal applications are discussed here, including anticancer, antiviral, and antibacterial properties.

*<u>Anticancer</u>*: DB-67, also known as Silatecan or AR-67 is a highly potent silicon-containing anticancer drug. DB-67 is a silicon derivative of plant derived alkaloid camptothecin known for its stability in the bloodstream and strong cytotoxicity towards a wide range of cancer cells.[9] Amsilarotene, a silyl derivative of retinoid benzoic acid, exhibit potential antineoplastic properties by inhibiting retinoblastoma phosphorylation. The silylated bisfurans shows cytotoxic activity towards human fibrosarcoma, and murine hepatocellular carcinoma, it also shows cytotoxic activity towards normal 3T3 cells.[84] Silicon-containing clinically proven platinum complex (Silaplatin) *cis*-dichlorodiamineplatinum (*cis*-Platin) is well known for its antitumor activity (**Figure 1.5**).[92]

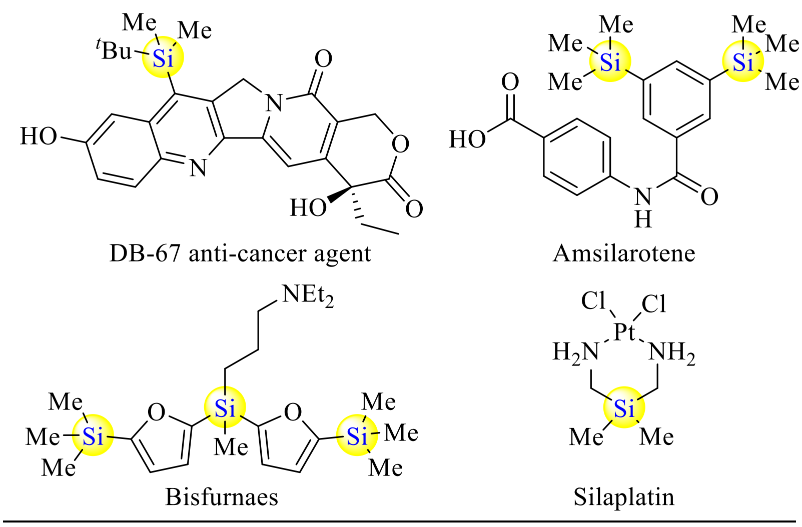


**Figure 1.5** Selected examples of silicon-containing anticancer agents

*<u>Antiviral</u>:* Organosilicon derivatives of some bioactive carbon analogous were found to show potent antiviral activity against multidrug-resistant influenza A.

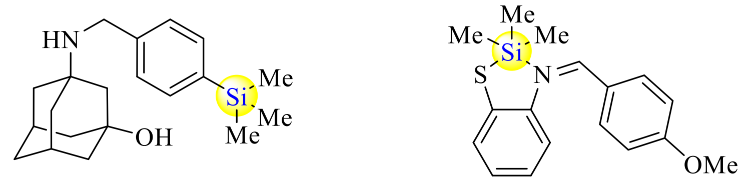

Organosilianes against multi-drug resistant influenza-A
$EC_{50}$ 0.4 µM (Si) *vs* 2.5 µM (C)

Organosilicon compound exhibits anti-bacterial activity

**Figure 1.6** Organosilicon as antiviral and antibacterial agents

From the study, silyl analogues were found to exhibit better activity than the carbon analogue in response to increasing resistance to oseltamivir (Tamiflu), and effectively combated both oseltamivir-sensitive and oseltamivir-resistant influenza A viruses (**Figure 1.6**).[93]
*Antibacterial:* Organosilicon compounds exhibit antibacterial properties against both gram-positive and gram-negative bacteria. Generally, they are more active and surpass the activity of streptomycin against staphylococcus aureus (**Figure 1.6**).[94]

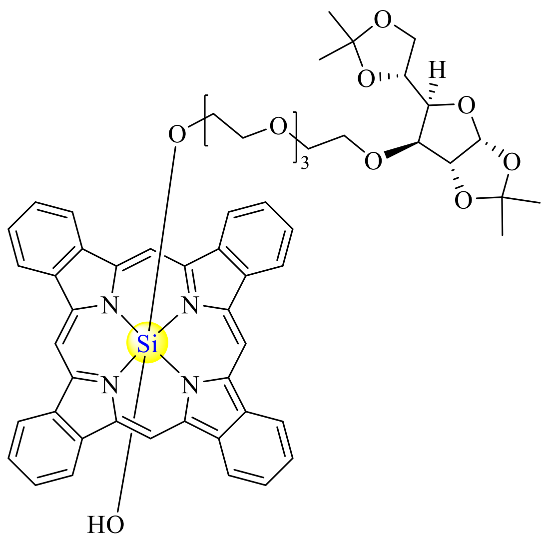

Novel glucoconjugated silicon(IV) phthalocyanines

**Figure 1.7** Organosilicon in photodynamic therapy

*Organosilicon in photodynamic therapy:* Silicon is considered to be the best choice for photodynamic therapy (PDT) because it provides macrocycles with the desired photophysical properties and permits the axial introduction of ligands to modify the macrocyclic properties, including aggregation, solubility, and other targeted characteristics. A novel glucoconjugated silicon(IV) phthalocyanine was found to have high photocytotoxic activity towards human colorectal carcinoma and human hepatocarcinoma (**Figure 1.7**).[95] Apart from these activities, researchers have also synthesized silicon-containing drug molecules, either independently or as carbon analogues, that exhibit neurotropic, anti-diarrheal, active against cardiovascular disease, anti-inflammatory, anti-parasitic, anti-diabetic, and antifungal activities.[87]

### 1.3.4 Silicon as a bioisostere of carbon

Silicon is a classical isostere of carbon (in the context of several biologically active molecules). Several "silicon-switched" biomolecules of carbon analogues have been advanced into clinical studies. At the same time, some silicon-containing molecules, such as the antifungal Flusilazole and the insecticide Silafluofen, with broad commercial applications in the agricultural field, are available in the market (**Figure 1.8**).[1,8,9]

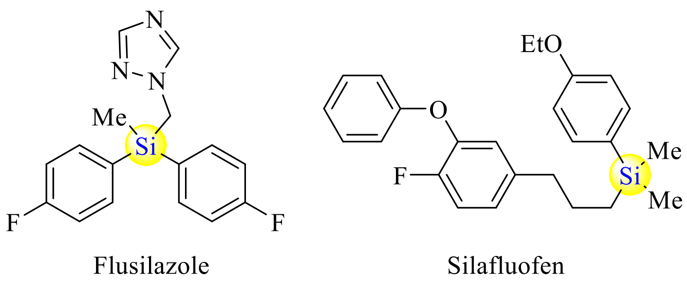


**Figure 1.8** Organosilicon compound Flusilazole and Silafluofen

The potential of utilizing silicon as a bioisostere stems from the intrinsic differences between silicon and carbon, which can result in significant changes to the physicochemical and biological characteristics of silicon-containing analogues, thereby offering several advantages in drug design. Some of the key properties of carbon and silicon are given in **Table 1.2**.[8,9]

**Table 1.2** Comparison of key physical parameters associated with carbon and silicon

| | **Carbon** | **Silicon** |
|---|---|---|
| Covalent radius | 77 pm | 117 pm |
| Electronegativity | 2.50 | 1.90 more electropositive than C, N, O & H |
| Bond length | C-C is 1.54 Å | Si-C is 1.87 Å |
| Lipophilicity | Ph-$^t$Bu; cLogP = 3.97 | Ph-Si($CH_3$)$_3$; cLogP = 4.72 |
| Bond stability | C-H stable, C-O-C stable | Si-H is labile, particularly under basic conditions, Si-O-C hydrolytically sensitive |

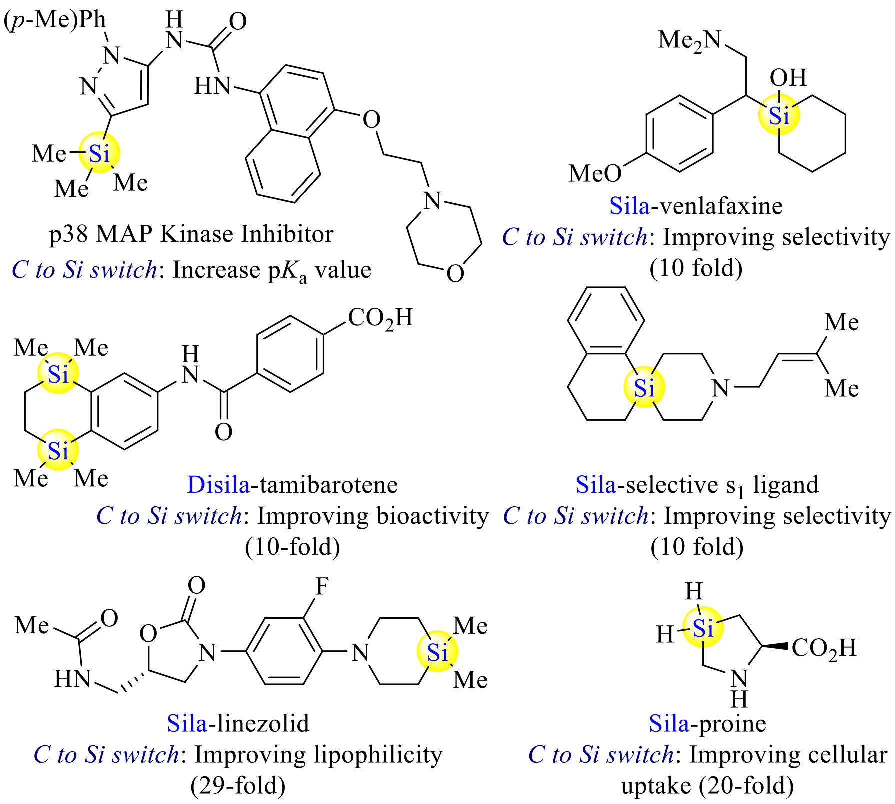


**Figure 1.9** Selected examples of silicon switch organosilicon compounds

The transition state mimics and metabolic pathways of silicon-containing compounds appear to be as predictable as those of carbon analogs. The C/Si switch in p38 MAP kinase inhibitor, featuring a *tert*-

butyl moiety, is a powerful example of simple bioisosteric substitution. The Si for C switch slightly increases the p*Ka* value of the morpholine *N*-atom with similar efficacy to the progenitor.[96] The silicon switch in various bioactive carbon analogues, such as linezolid, venlafaxine, and tamibarotene leads to an improvement in lipophilicity, selectivity, bioactivity, and cellular uptake.[8,96-100] Some selected examples are depicted in **Figure 1.9**.

<u>Other applications</u>: Additionally, because of their unique semiconducting and photophysical properties, organosilicon compounds are utilized in molecular electronics and photonics.[101,102] For example, silicon derivative of fluoranthene exhibits higher thermal stability than fluoranthene. An anthracene derivative exhibits efficient blue shift with a higher quantum yield than the progenitor.[103]

## 1.4 Organogermanium compounds

The compounds featuring "the Ge-C bond" are known as organogermanium compounds. The first organogermanium compound, "Tetraethylgermane" was synthesized by Winkler in 1887 through the reaction of germanium tetrachloride and diethylzinc.[104] Organogermanium compounds have emerged as useful building blocks for the synthesis of highly functionalized molecules.[105-107] Germanium and its derivatives have several industrial applications, including semiconductors, infrared optics, optical fibers, ceramics, polymers.[114,117,129,139-141] The biological actions include fungicide, bactericide, anticancer, psychotropic, and radioprotective properties.[108-109]

### 1.4.1 Synthesis of organogermanium compounds

Organogermanium compounds are synthesized using halogermanes and hydrogermanes as the most accessible sources, although reports are available with the cleavage of the Ge-C and Ge-Ge bonds.[59,65, 110-113]

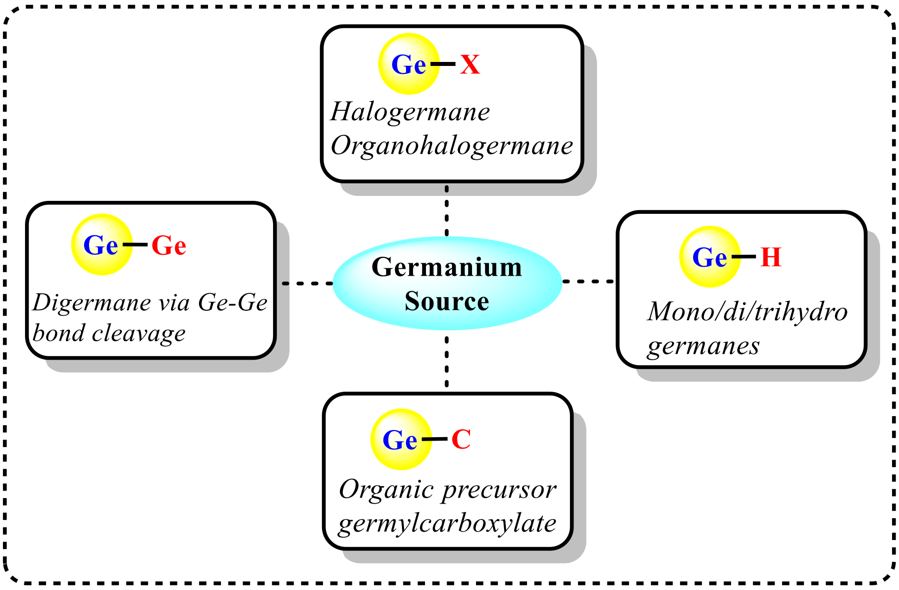


**Figure 1.10** Source of germanium in the synthesis of organogermanium compounds

Traditionally, compounds with Ge-C bonds are synthesized by combining alkyl or arylmetal nucleophiles (lithium, potassium, magnesium; mono and bimetallic derivatives) with germanium electrophiles (typically halides).*[114]*

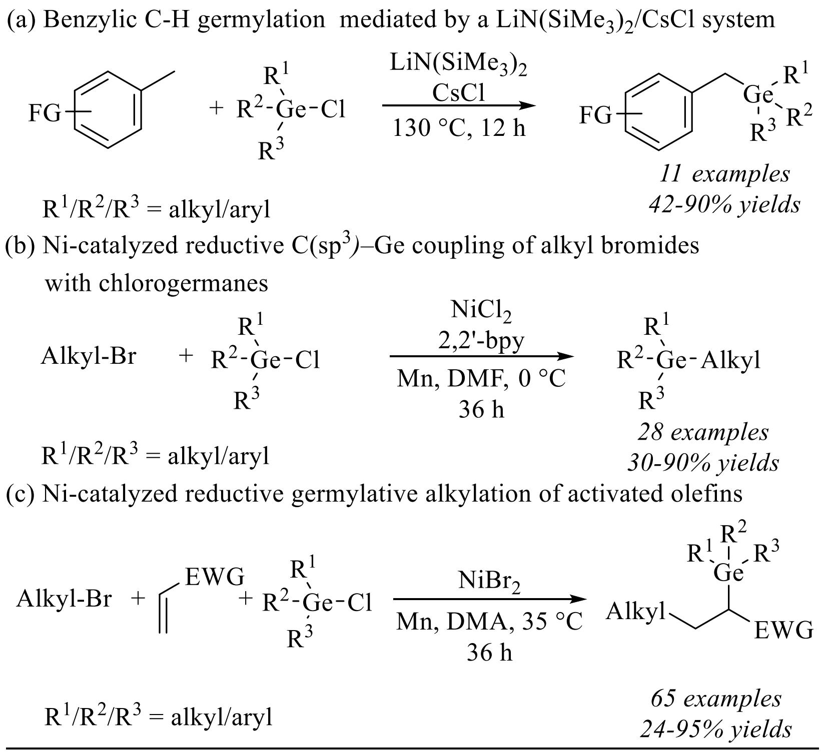


**Scheme 1.10** Selected reports for the synthesis of organogermanium compounds using chlorogermanes

Halogermanes are a primary source for the construction of Ge-C bond under transition metal-catalyzed reactions, electrochemical reactions, and visible light photocatalyzed reactions.[115-120] Some recent reports are discussed, In 2021 the Mao group disclosed $LiN(SiMe_3)_2$ and CsCl mediated germylation of toluene C(sp$^3$)-H bond (**Scheme 1.10a**).[121] Nickel-catalyzed reductive coupling of alkyl bromide with chlorogermanes for the synthesis of organogermane was reported by Shu's group (**Scheme 1.10b**).[122]

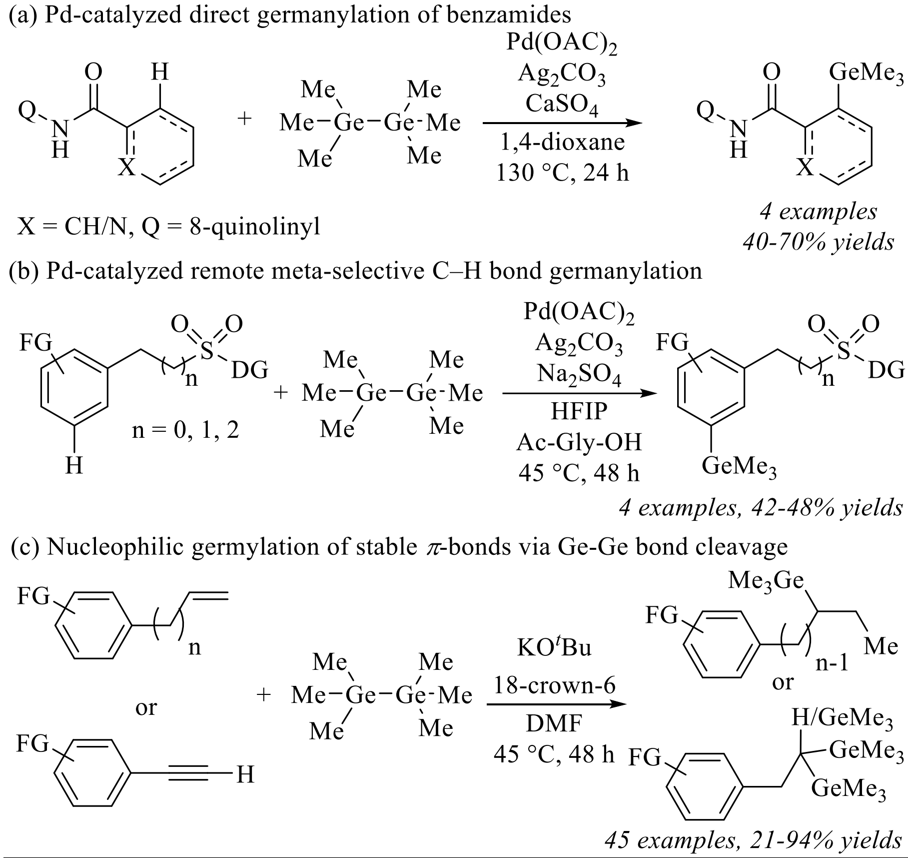


**Scheme 1.11** Synthesis of organogermanium compounds *via* Ge-Ge bond cleavage of hexamethyldigermane

Recently, Zhang and coworkers reported access to alkylgermanes *via* nickel-catalyzed reductive germylative alkylation of activated olefins (**Scheme 1.10c**).[123] Similarly, Ge-Ge bond cleavage approaches have also been employed in the synthesis of organogermanium compounds. For example, Kanai reports the palladium-catalyzed germylation of benzamides using hexamethyldigermane under thermal conditions

(**Scheme 1.11a**).[124] Soon later, Maiti group reported palladium-catalyzed *meta*-selective germylation at relatively low temperatures (**Scheme 1.11b**).[125] Recently, Uchiyama achieved the germylation and multigermylation of alkenes and alkynes using potassium *tert*-butoxide and 18-crown-6 ether at room temperature under thermal conditions (**Scheme 1.11c**).[113] Different germanium precursors were also utilized for the synthesis of organogermanium compounds, such as germylcarboxylic acids and germyl cyclohexadiene derivatives. Oestrich group reports the Lewis acid-catalyzed hydrogermylation of alkenes and alkynes using germyl cyclohexadiene (**Scheme 1.12a**).[126] Subsequently, Uchiyama disclosed the visible light-mediated hydrogermylation of alkenes *via* Ge-C bond cleavage of germacarboxylic acid and derivatives of germyl cyclohexadiene (**Scheme 1.12-b,c**).[59,63] Hydrogermanes are the most reliable source of germanium in the synthesis of modern organogermanium compounds.

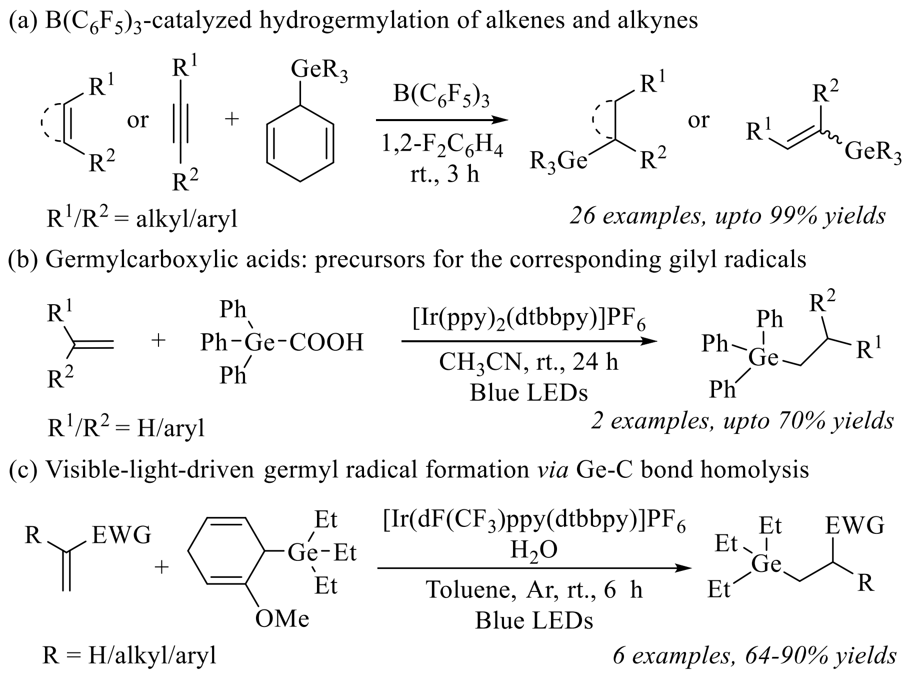


**Scheme 1.12** Synthesis of organosilicon compounds by Ge-C bond cleavage

Hydrogermanes are utilized in the hydrogermylation of alkenes and alkynes to obtain organogermanium compounds under metal-free, metal-catalyzed reactions, photo/electrochemical catalysis and other methods .[117,127-136] In 2001 Oshima group reported palladium-catalyzed hydrogermylation of alkenes and dienes using hydrogermanes as a source of germanium to access organogermanium compounds (**Scheme 1.13a**).[136] Subsequently, In 2010 Yamanoi and Nishihara disclosed an elegant method for the synthesis of organogermanium compounds using mono, di- and trihydrogermanes. The reaction between different hydrogermanes and aryl iodides was catalyzed by a palladium catalyst (**Scheme 1.13b**).[137] Very recently, He and coworkers reported the copper-catalyzed enantioselective hydrogermylation of alkenes utilizing mono-, di-, and trihydrogermanes (**Scheme 1.13c**).[132] Hydrogermanes are also used in transition metal-free hydrogermylation reactions. In 2022 Schoenebeck group reported the germylation of alkynes using $B(C_6F5)_3$ as a catalyst (**Scheme 1.14a**)[138] and very recently, the base-catalyzed remote hydrogermylation of alkenes was also reported (**Scheme 1.14b**).[120]

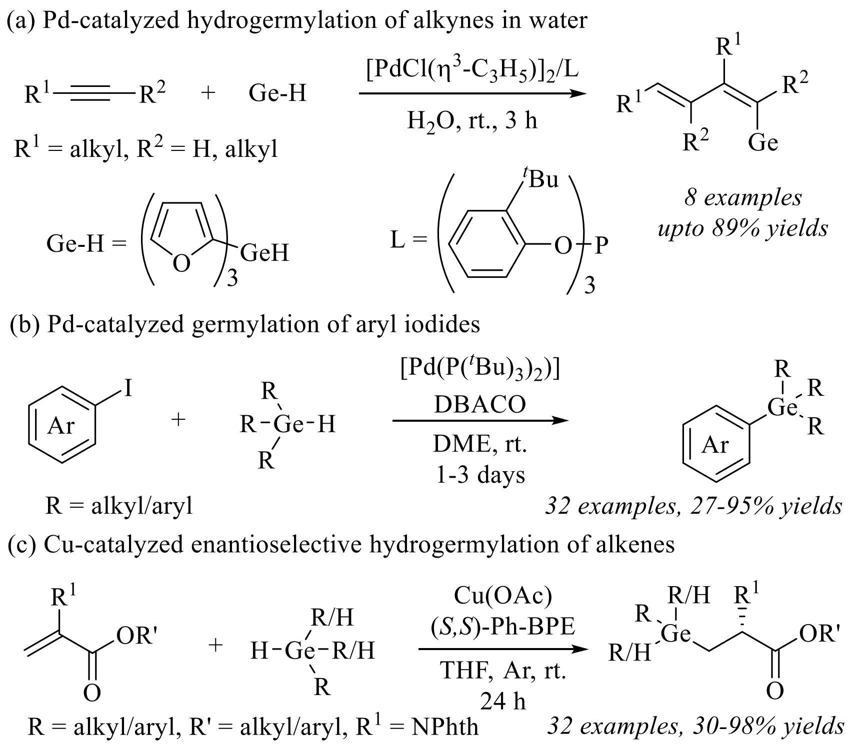


**Scheme 1.13** Selected examples of the metal-catalyzed organogermanium compound synthesis using hydrogermanes

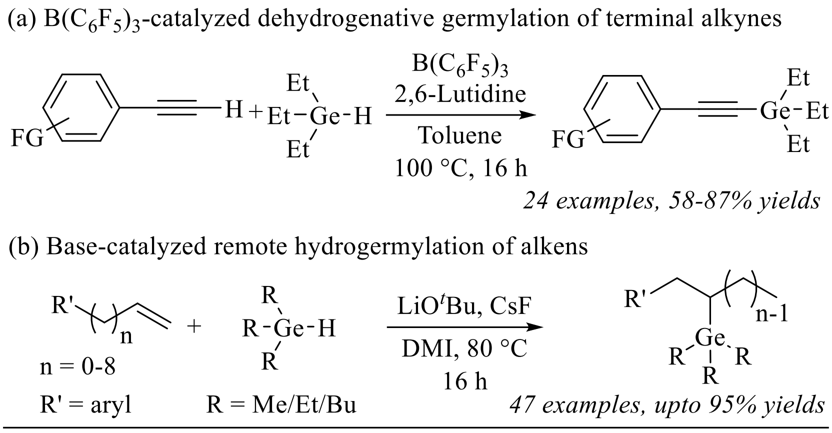

**Scheme 1.14** Representative examples of metal-free germylation using hydrogermanes

### 1.4.2 Applications of organogermanium compounds

Organogermanium compounds have a wide range of applications in medicinal chemistry, organic synthesis, semiconductor industries, and fiber optics.[109,117, 129, 139-144]

**Daily life application**: Nowadays, it is generally acknowledged that germanium is an essential trace element, particularly crucial for the regular functioning of the immune system and plays a significant role in the prevention of cancer.[142-149] Thymus contains the highest concentration of germanium, which is found in all mammalian organs and tissues. Several physiological processes, particularly those related to blood, such as pH, glucose, uric acid, minerals, cholesterol, hemoglobin, and leukocytes are regulated by germanium.[150,151]

**Medicinal applications**: Natural sources of germanium compounds have long been considered as medicinally active agent with antiviral, antitumor, anticancer, and anti-inflammatory properties.[153] Germanium is found in garlic, aloe, echinacea, ginseng, and saprophyte mushrooms, especially lacquered polypore (Ganoderma lucidum) and chaga. It has also been demonstrated that germanium compounds normalize oxidative phosphorylation, or oxygen respiration in cells, which can also slow down the growth of tumors.[153] Bis(carboxyethylgermanium) sesquioxide (Ge-132) (**Figure 1.11**), an organogermanium compound, exhibits a variety of biological activities, including anticancer, immunomodulatory, antiviral, and anti-inflammatory properties.[154]

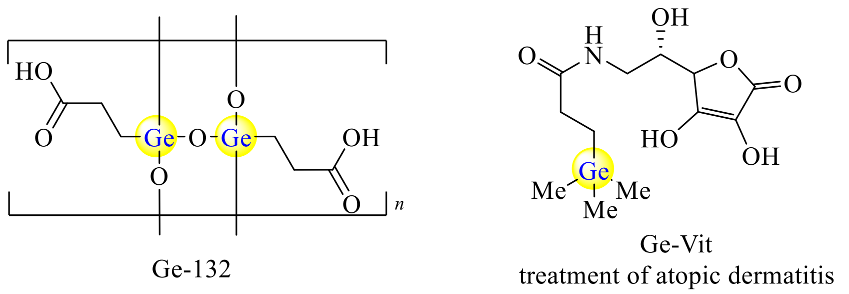


**Figure 1.11** Organogermanium compound Ge-132 and Ge-Vit

The germanium derivative of ascorbic acid (Ge-Vit) exhibits high antioxidant properties and is proposed for the treatment of atopic dermatitis (**Figure 1.11**).[155] The germatranes are another class of organogermanium compounds that exhibit biological activities i.e. 3-germatranyl-3-(4-hydroxy-3-methoxyphenyl) propionic acid (germatranes), which is based on caffeic acid, demonstrated potent efficacy against cervical tumor.[156] 6-O-[3-(trimethylgermyl)propyl]-*β*-D-glucopyranoside is another trimethylgermyl group-containing molecule that promotes the synthesis of interferon (**Figure 1.12**). Owing to its high water solubility, it exhibited greater activity than Ge-132 and was significantly less toxic.[157] Spirogermane compounds have also been found to be biologically active in clinical trials.[129]

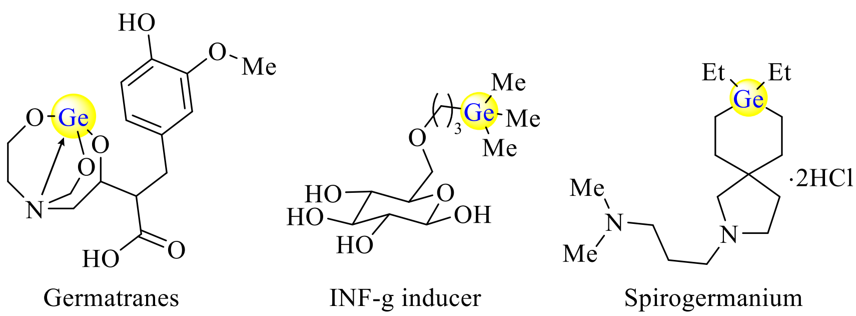


**Figure 1.12** Medicinally active organogermanium compounds

## 1.5 Si-H and Ge-H bond functionalization in the synthesis of organosilicon and organogermanium compounds

Even though the silyl/germyl functionalities can be added to organic molecules from a variety of silicon/germanium sources, due to the inherent reactivity of the Si-H/Ge-H bond, its functionalization can be harnessed under milder conditions, with high atom economy, minimal and harmless waste generation, high functional group tolerance, and catalyst-driven excellent regio- and stereoselective control.

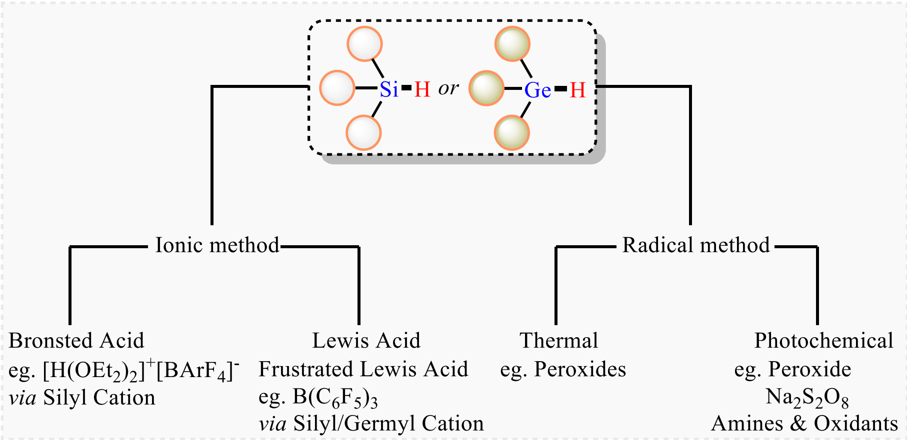


**Figure 1.13** Flow chart for functionalization of the Si-H and Ge-H bonds of hydrosilanes and hydrogermanes using ionic and radical methods

In this context, we envisioned the use of hydrosilanes and hydrogermanes for synthesizing organosilicon and organogermanium compounds (formation of Si-C/Ge-C bond) *via* Si-H and Ge-H bond functionalization. To functionalize the Si-H/Ge-H bond of the hydrosilane and hydrogermane, various ionic (Brønsted acid/Lewis acid) as well as free radical (Thermal/photochemical) methods are available. We intend to use photochemical (radical) method for the functionalization of Si-H and Ge-H bonds in hydrosilanes and hydrogermanes.

## 1.6 Photoredox catalysis

The increasing need for sustainable processes and more efficient synthetic methods are one of the primary drivers of new discoveries. Additionally, this requirement stimulates creative rethinking of established concepts, which will eventually lead to the development of new chemistry. The concept of “the light as a renewable energy source in a chemical reaction” was given by Giacomo Ciamician in 1908.[158] With the application of plentiful metals and organophotocatalysts, artificial photosynthesis, photo-biocatalysis, and photoredox catalysis are just a few of the many applications in the broad and quickly evolving field of photochemistry. As early as the 20th century, photochemistry already drew the attention of (organic) chemists, because of its use in unconventional chemical transformations and its requirement for mild conditions. So, there has been a surge in pursuing these processes in recent years.

The early examples of photochemical transformations typically involve the direct irradiation of substrates. Currently, photoredox catalysis is one of the most widely used and rapidly developing area of synthetic chemistry. Unquestionably, visible-light photoredox catalysis has proven to be an effective method for activating small molecules and functionalization to enable formerly challenging or unattainable chemical transformations. When exposed to visible light, typical photocatalysts (PCs), which can be transition metal-based complexes, or organic dyes, or an material which can harvests light, can reach electronically excited states, allowing for photoinduced electron transfer (PET), single-electron transfer (SET), proton-coupled electron transfer (PCET), energy transfer (ET), or hydrogen atom transfer (HAT) reactions with organic substrates.[159-180]

### 1.6.1 Photophysical process of photoredox catalyst

The diverse photochemistry associated with molecules and materials, exhibits a range of excited state energies and the rates associated with their photophysical processes. Typical photophysical processes are depicted in **Figure 1.14**.[159-171]

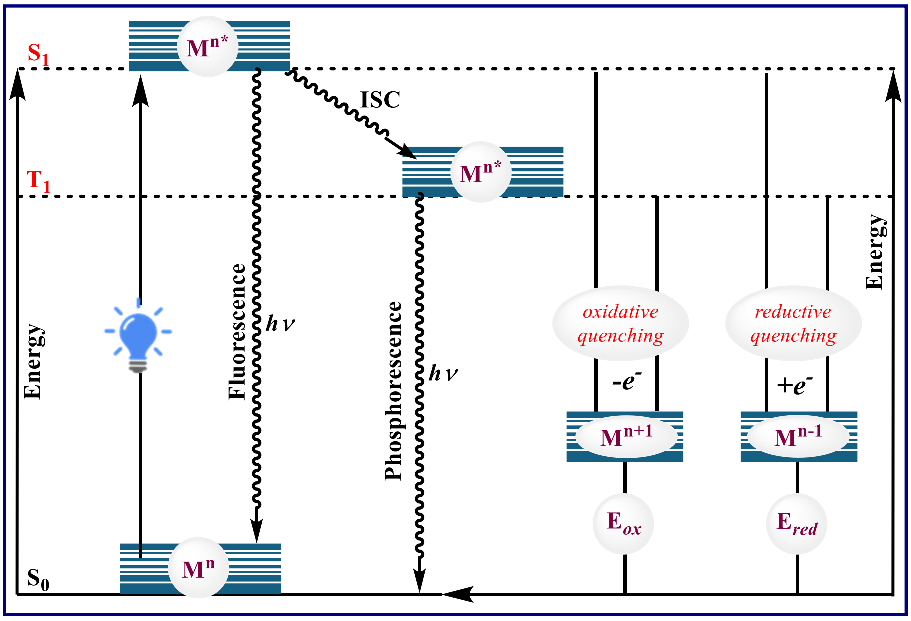


**Figure 1.14** Photophysical processes of photoredox catalysts

The absorption of light (+*hv*) by a molecule results in an electronically excited molecule, typically by promoting an electron from the ground state singlet ($S_0$) to the singlet excited state ($S_1$). The fate of singlet excited state ($S_1$) depends on both radiative and nonradiative pathways (when only the photophysical pathways of an electronically excited molecule in isolation are considered). Radiative pathways are transitions to lower energy states by emitting light (−*hv*), whereas the energy dissipated in a nonradiative transition is lost as heat. $S_1$ can proceed to $T_1$ *via* spin-forbidden intersystem crossover (ISC, nonradiative process), or it can return to ground state $S_0$ *via* fluorescence (radiative transition) or internal conversion (IC, nonradiative transition). The transition from $T_1$ to $S_0$ is also spin-forbidden; therefore, the $T_1$ states are often the longest-lived and can perform both radiative (phosphorescence) and nonradiative processes. Usually, the nonradiative process of $T_1$ to $S_0$ dominates under standard conditions. $S_1$ and $T_1$ are the most likely excited states involved in the bimolecular reaction (i.e., the substrate) and can perform energy transfer or electron transfer, with lifetimes ranging from nanoseconds to milliseconds. The process of electron transfer between an excited-state molecule and an electron donor or an electron acceptor is known as "*photoinduced electron transfer*" and is a redox process.

### 1.6.2 Oxidative and reductive quenching pathways of photoredox catalyst

Most of the photoredox catalytic reactions follow either oxidative quenching pathways or reductive quenching pathways, as illustrated in **Figure 1.15**. [159-171] Classically, the photoinduced electron transfer (PET) process, in which an excited molecule acts as a reductant and is subsequently oxidized, is known as "*oxidative quenching*." On the other hand, in "*reductive quenching*" the excited-state molecule is reduced.

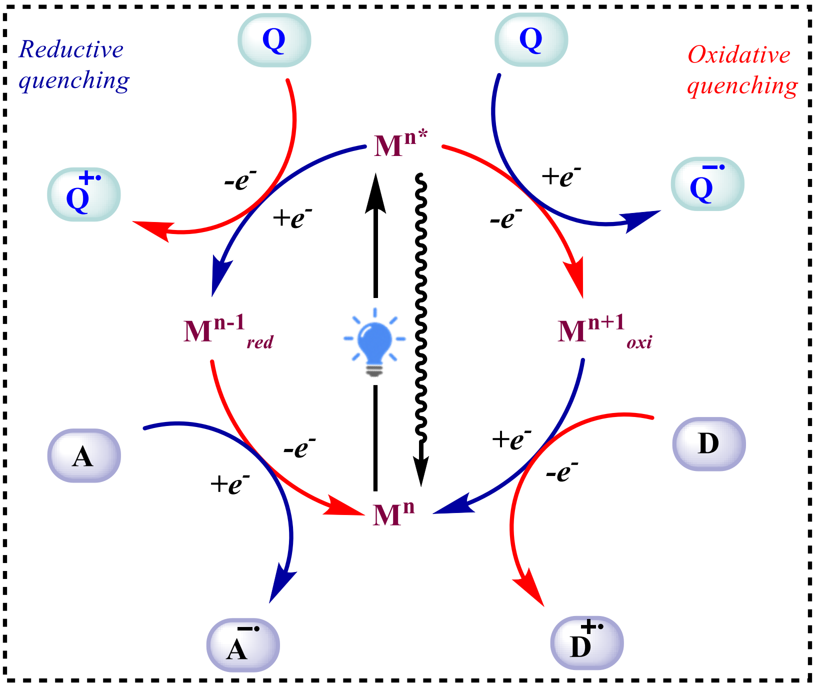


**Figure 1.15** Oxidative and reductive quenching cycles of photoredox catalysis

<u>Oxidative quenching pathway of photoredox catalyst</u>: This cycle starts with the excitation of ground state catalyst $\mathbf{M^n}$ upon absorption of light (+*hν*) and produces excited state catalyst $\mathbf{M^{n*}}$. The excited-state catalyst $\mathbf{M^{n*}}$ gets oxidized by donating an electron to the quencher **[Q]**. The catalytic turnover step involves the reduction of **[$\mathbf{M^{n+1}}$]** by donor **[D]**.

<u>Reductive quenching pathway of photoredox catalyst</u>: This cycle commences with the excitation of ground state catalyst $\mathbf{M^n}$ upon absorption of light (+*hv*) and produces excited state catalyst $\mathbf{M^{n*}}$. The excited state catalyst $\mathbf{M^{n*}}$ gets reduced by accepting an electron from the quencher **[Q]**. The catalytic turnover step involves the oxidation of $\mathbf{[M^{n-1}]}$ by donating an electron to the acceptor **[A]**.

Here, we provide the structure of selected photocatalysts, along with their excited-state and ground-state redox potentials, which were used to conduct the research throughout our work (**Figure 1.16**).

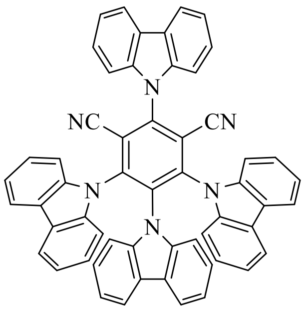

4CzIPN

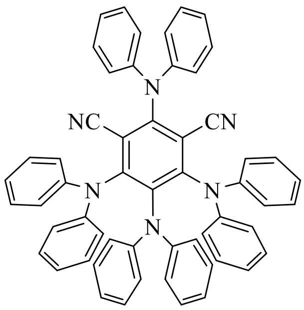

4DPAIPN

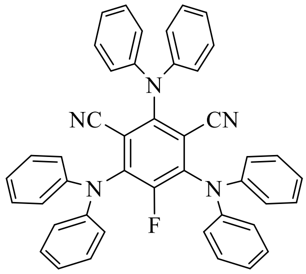

3DPAFIPN

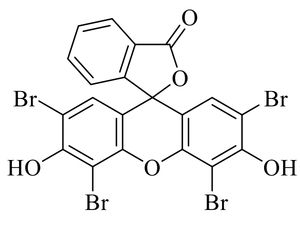

Eosin Y

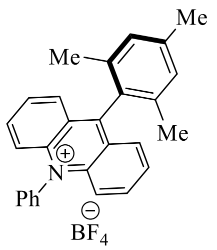

Mes-Acr-Ph$^+$ $BF_4^-$

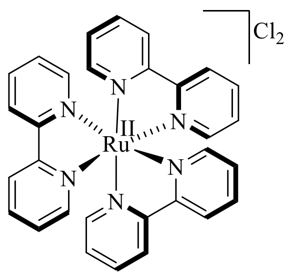

$[Ru(bpy)_3]Cl_2.H_2O$

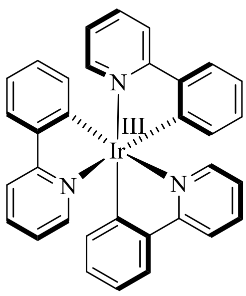

$Ir(ppy)_3$

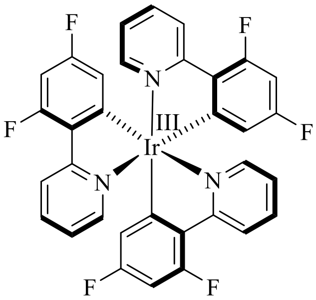

$Ir(dFppy)_3$

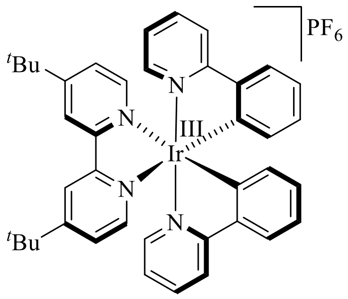

$Ir(ppy)_2(dtbbpy)]PF_6$

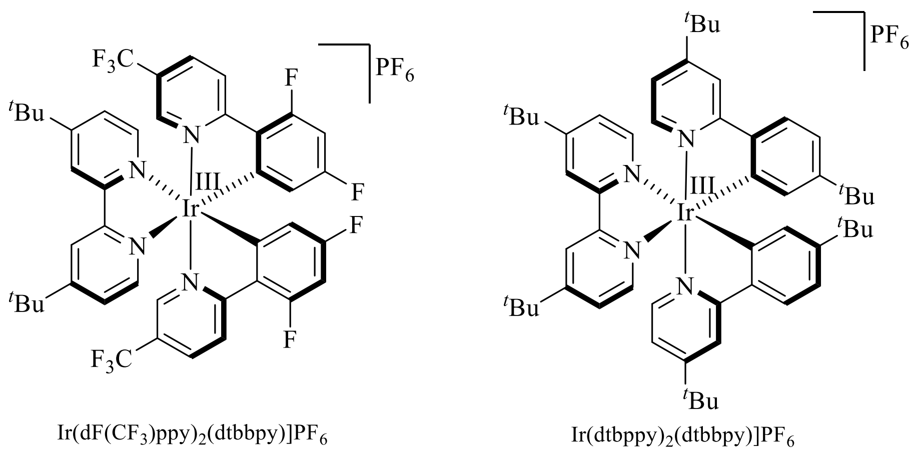

**Figure 1.16** Photocatalyst used to carry out our research work

**Table 1.3** Ground-state and excited-state redox potentials for photocatalysts[178-189]

| Photocatalyst | ground-state redox potentials | | excited-state redox potentials | |
|---|---|---|---|---|
| | $E°_{ox}$ $(PC^+/PC)^a$ | $E°_{red}$ $(PC/PC^-)^a$ | $E°_{ox}$ $(PC^+/PC^*)^a$ | $E°_{red}$ $(PC^*/PC^-)^a$ |
| 4CzIPN | $+1.11^b$ | $-1.59^b$ | $-1.56^b$ | $+0.97^b$ |
| 4DPAIPN | $+0.65^b$ | $-2.03^b$ | $-1.90^b$ | $+0.52^b$ |
| 3DPAFIPN | $+0.92^b$ | $-1.97^b$ | $-1.76^b$ | $+0.72^b$ |
| Eosin Y | - | $-1.44^{b,c}$ | $-1.49^{b,c}$ | $+0.45^{b,c}$ |
| Mes-Acr-$Ph^+$ $BF_4^-$ | - | - | - | +2.20 |
| $[Ru(bpy)_3]Cl_2.6H_2O$ | $+0.88^b$ | $-1.71^b$ | $-1.19^b$ | $+0.39^b$ |
| $Ir(ppy)_3$ | $+0.39^b$ | $-2.57^b$ | $-2.11^b$ | $-0.07^b$ |
| $Ir(dFppy)_3$ | +0.69 | -2.51 | -1.82 | 0.00 |
| $Ir(ppy)_2(dtbbpy)]PF_6$ | $+0.83^b$ | $-1.89^b$ | $-1.34^b$ | $+0.28^b$ |
| $Ir(dF(CF_3)ppy)_2(dtbbpy)]PF_6$ | $+1.31^b$ | $-1.75^b$ | $-1.59^b$ | $+0.51^b$ |

[a]Potentials measured in V vs $Fc^+/Fc$ and measured in MeCN unless indicated. [b]converted to $Fc^+/Fc$ from the reference electrode used in the original report[189] . [c]measured in 1:1 $MeCN:H_2O$.

## 1.7 Our effort in the synthesis of organosilicon and organogermanium compounds

We envisioned using hydrosilanes and hydrogermanes as sources of silicon and germanium for the synthesis of organosilicon and organogermanium compounds *via* Si-H and Ge-H bond functionalization. Our interest narrows down to radical method for functionalizing Si-H and Ge-H bonds. The electropositive nature of silicon and germanium results in a high hydridic character for Si-H and Ge-H bonds of hydrosilanes and hydrogermanes, making them ideal candidates for functionalization using an electrophilic radical center. The electrophilic radical can be generated using thermal or photochemical methods, and we intended to use the latter owing to the ease of handling and mild reaction conditions. The photochemical generation of an electrophilic radical can be accomplished using a transition metal photocatalyst or an organophotocatalyst.

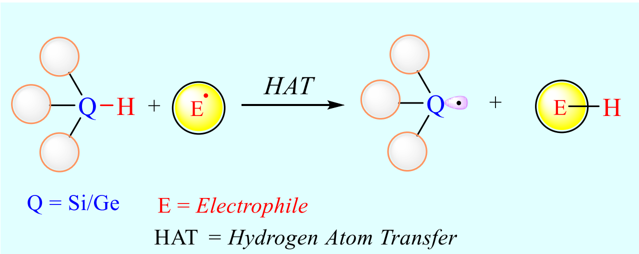


**Scheme 1.15** Functionalization of Si-H/Ge-H bond using an electrophilic reaction

### 1.8 Conclusion

In this chapter, begin with a brief discussion of silicon and germanium, and their physicochemical properties. Furthermore, we discussed the synthesis of organosilicon and organogermanium compounds by different silyl/germyl sources and their applications. Since our efforts in synthesizing organosilicon and organogermanium compounds align with photoredox catalysis, we provide a general introduction to photoredox catalysis, the photophysical process of photocatalysts, and their working mechanisms *via* oxidative and reductive pathways. Lastly, concluded with our approach in the synthesis of organosilicon and organogermanium compounds.

### 1.9 References


1. Ramesh, R., Reddy, D. S. (2018). Quest for novel chemical entities through incorporation of silicon in drug scaffolds. *J. Med. Chem. 61*, 3779-3798. (DOI:10.1021/acs.jmedchem.7b00718).

2. Thames, S.F., Panjnani, K.G. (1996). Organosilane polymer chemistry: A review. *J. Inorg. Organomet. Polym.* 6, 59-94. (DOI: 10.1007/BF01098320).

3. Clayden, J., Greeves, N., Warren, S. (2012). Organic Chemistry, 2nd ed.; Oxford University Press: Oxford, U.K. pages: 668-677.

4. Bertrand, G. (2004). The modest undressing of a silicon center. *Science 305*, 783-785. (DOI:10.1126/science.1102270).

5. Winkler, C. A. (1886). *Ber. Dtsch. Chem. Ges*. *19*, 210-211.

6. Winkler, C. A. (1886). *J. Prakt. Chem. 34*, 177-229.

7. Lukevics, E., Ignatovich, L. (1992). Comparative study of the biological activity of organosilicon and organogermanium compounds. *Appl. Organometal. Chem*. *6*, 113-126. (DOI:10.1002/aoc.590060204).

8. Meanwell, N. A. (2011). Synopsis of some recent tactical application of bioisosteres in drug design. *J. Med. Chem. 54*, 2529-2591. (DOI: 10.1021/jm1013693).

9. Franz, A. K., Wilson, S. O. (2013). Organosilicon molecules with medicinal applications. *J. Med. Chem. 56*, 388-405. (DOI: 10.1021/jm3010114).

10. Brook, M. A. (2000). Silicon in organic, organometallic, and polymer Chemistry. John Wiley & Sons, New York.

11. K.M. Lewis, S. Couderc, (2022). 1946 and the early history of hydrosilylation. *Molecules 27*, 4341. (DOI:10.3390/molecules27144341).

12. Mollabagher, H., Mojtahedi, M.M., Mousavi, S. A. H. S. (2024). Recent progress of organosilicon compound: Synthesis and applications. *J. Iran Chem. Soc. 21*, 1795-1816. (DOI:10.1007/s13738-024-03041-7).

13. L. Jin, X. Zhang, C. Cui, Z. Xi, J. Sun, *et al*. (2021). Simultaneous process parameters and heat integration optimization for industrial

organosilicon production. *Sep. Purif. Technol. 265*, 118520. (DOI: 10.1016/j.seppur.2021.118520).

14.Y. Zuo, X. Liang, J. Yin, Z. Gou, W. Lin, (2021). Understanding the significant role of Si-O-Si bonds: organosilicon materials as powerful platforms for bioimaging. *Coord. Chem. Rev. 447*, 214166. (DOI: 10.1016/j.ccr.2021.214166).

15. Mougel, V., Chan, K.-W., Siddiqi, G., Kawakita, K., Nagae, H., Tsurugi, H., Mashima, K., Safonova, O., Coperet, C. (2016). Low temperature activation of supported metathesis catalysts by organosilicon reducing agents. *ACS Cent. Sci. 2*, 569-576. (DOI: 10.1021/acscentsci.6b00176).

16. Tong, C., McCarthy, S., Li, Z., Guo, J., Li, Q., Pacheco, C. N., Ren, Y., Allcock, H. R. (2019). Hybrid polyphosphazene-organosilicon polymers as useful elastomers. *ACS Appl. Polym. Mater. 1*, 1881-1886. (DOI:10.1021/acsapm.9b00381).

17. Danishefsky, S., Kitahara, T. et al. (1976). Reactions of silyl enol ethers and lactone enolates with dimethyl(methylene)ammonium iodide. The bis-$\alpha$-methylenation of pre-vernolepin and pre-vernomenin. *J. Am. Chem. Soc. 98*, 6715-6717. (DOI:10.1021/ja00437a058).

18. Showell, G. A., Mills, J. S. (2003). Chemistry challenges in lead optimization: Silicon isosteres in drug discovery. *Drug Discov. Today 8*, 551-556. (DOI:10.1016/S1359-6446(03)02726-0).

19. Gai, L., Mack, J., Lu, H., Nyokong, T., Li, Z., Kobayashi, N., Shen, Z. (2015). Organosilicon compounds as fluorescent chemosensors for fluoride anion recognition. *Coord. Chem. Rev. 285*, 24-51. (DOI: 10.1016/j.ccr.2014.10.009).

20. Troegel, D., Stohrer, J. (2011). Recent advances and actual challenges in late transition metal catalyzed hydrosilylation of olefins from an industrial point of view. *Coord. Chem. Rev. 255*, 1440-1459. (DOI: 10.1016/j.ccr.2010.12.025).

21. Shinde, P. S., Suryawanshi, P. S., Patil, K. K., Belekar, V. M., Sankpal, S. A., Delekar, S. D., Jadhav, S. A. (2021). A brief overview of recent progress in porous silica as catalyst supports. *J. Compos. Sci. 5*, 75. (DOI:10.3390/jcs5030075).

22. Prem, N., Sindersberger, D., Striegl, B., Böhm, V., & Monkman, G. J. (2020). Shape memory effects using magnetoactive boron-organo-silicon oxide polymers. *Macromol. Chem. Phys*. *221*, 2000149. (DOI: 10.1002/macp.202000149).

23. Francis, A. (2021). Biological evaluation of preceramic organosilicon polymers for various healthcare and biomedical engineering applications: A review. *J. Biomed. Mater. Res. Part B: Applied Biomaterials*, *109*, 744-764. (DOI: 10.1002/jbm.b.34740).

24. Berzelius, J. J. (1824). Investigation of hydrofluoric acid and its most remarkable compounds. *Ann. Physik. Chem. 1*, 169, 204.

25. Frankland, E. (1848-1849). *J. Chem. Soc*. 2, 263.

26. Friedel, C., Crafts, J. M. (1863). *Ann. Chem*. 127, 28.

27. Friedel, C., Crafts, J. M. (1863). On certain new organosilicon combinations. *Compt*. *Rend.* 56, 590.

28. Ladenburg, A. (1873). On aromatic compound containing silicon. *Ber. Deut. Chem. Ges.* 6, 379-381. (DOI: 10.1002/cber.187300601125).

29. Ladenburg, A. (1874). On aromatic silicon compounds. *Ber. Deut. Chem. Ges. 7*, 387-390. (DOI: 10.1002/cber.187400701123).

30. Ladenburg, A. (1874). On new silicon compounds. *Ann. Chem.* 173, 143-166. (DOI: 10.1002/jlac.18741730204).

31. Polis, A. (1885). On aromatic silicon compounds. *Reports of the German Chemical Society*, *18*, 1540-1544.

32. Grignard, V. (1900). Alkyl halides & aryl halides. *Synthesis*, *130*, 1322.

33. Kipping, F. S. (1904). *Proc. Chem. Soc*. *209*, 91.

34. Rochow, E. G. (1945). The direct synthesis of organosilicon compounds. *J. Am. Chem. Soc. 67*, 963-965. (DOI: 10.1021/ja01222a026).

35. Speier, J. L., Webster, J. A., Barnes, G. H. (1957). The addition of silicon hydrides to olefinic double bonds. Part II. The use of group VIII metal catalysts. *J. Am. Chem. Soc. 79*, 974-979. (DOI: 1021/ja01561a054).

36. Rich, J. (June 1987), *Abstracts of Papers*. VIIIth International symposium on organosilicon chemistry, abstract A 41. Washington University. St. Louis, MO.

37. Zhou, Z., Gai, L., Xu, Li-W., Guo, Z., Lu, H. (2023). Disilane-bridged architectures: an emerging class of molecular materials. *Chem. Sci. 14*, 10385–10402. ( DOI: 10.1039/d3sc02690f).

38. Marschner, C., Scheschkewitz, D. (2014). Functional molecular silicon compounds I: Regular oxidation States. Ed. D. Scheschkewitz, *Springer*, *Cham.*, page: 163.

39. Chatgilialoglu, C. Structural and chemical properties of silyl radicals. (1995). *Chem. Rev. 95,* 1229-1251. (DOI: 10.1021/cr00037a005).

40. Rivard, E. (2016). Group 14 inorganic hydrocarbon analogues. *Chem. Soc. Rev. 45,* 989-1003. (DOI: 10.1039/C5CS00365B).

41. Kanno, Ken-I., Aikawa, Y., Niwayama, Y., Ino, M., Kawamura, K., Kyushin, S. *(2018).* Stepwise introduction of different substituents to *α*-chloro-*ω*-hydrooligosilanes: Convenient synthesis of unsymmetrically substituted oligosilanes. *Inorganics 6*, 99.

(DOI: 10.3390/inorganics6030099).

42. Chatgilialoglu, C., Lalevee, J. (2012). Recent applications of the $(TMS)_3SiH$ radical-based reagent. *Molecules 17*, 527-555. (DOI: 10.3390/molecules17010527).

43. Chatgilialoglu, C., Ferreri, C., Landais, Y., Timokhin, V. I. (2018). Thirty Years of $(TMS)_3SiH$: A milestone in radical-based synthetic chemistry. *Chem. Rev. 118*, 6516-6572. (DOI: 10.1021/acs.chemrev.8b00109).

44. Liu, Y.-J., Liu, Y.-H., Zhang, Z.-Z., Yan, S.-Y., Chen, K., Shi, B.-F. (2016). Divergent and stereoselective synthesis of *β*-Silyl-*α*-amino acids through palladium-catalyzed intermolecular silylation of unactivated primary and secondary C-H bonds. *Angew. Chem. Int. Ed. 55*, 13859-13862. (DOI: 10.1002/anie.201607766).

45. Yu, X., Lubbesmeyer, M., Studer, A. (2021). Oligosilanes as silyl radical precursors through oxidative Si-Si bond cleavage using redox catalysis. *Angew. Chem. Int. Ed. 60*, 675-679. (DOI: 10.1002/anie.202011738).

46. Zhao, Y., Wan, Y., Yuan, Q., Wei, J., Zhang, Y. (2023). Photocatalytic C-Si bond formation using pentacoordinate silylsilicates as silyl radical precursors: Synthetic tricks using old reagents. *Org. Lett. 25*, 1386-1391. (DOI: 10.1021/acs.orglett.3c00096).

47. Oestreich, M., Hartmann, E., Mewald, M. (2013). Activation of the Si-B interelement bond: mechanism, catalysis, and synthesis. *Chem. Rev. 113*, 402-441. (DOI: 10.1021/cr3003517).

48. Walter, C., Oestreich, M. (2008). Catalytic Asymmetric C-Si bond formation to acyclic *α,β*-unsaturated acceptors by Rh(I)-catalyzed conjugate silyl transfer using a Si-B linkage. *Angew. Chem. Int. Ed. 47*, 3818-3820. (DOI: 10.1002/anie.200800361).

49. Vyas, D.J., Oestreich, M. (2010). Copper-catalyzed Si-B bond activation in branched-selective allylic substitution of linear allylic chlorides. *Angew. Chem. Int. Ed. 49*, 8513-8515. (DOI:10.1002/anie.201004658).

50. Calderone, J. A., Santos, W. L. (2012). Copper(II)-catalyzed silyl conjugate addition to *α,β*-unsaturated conjugated compounds: Brønsted

base-assisted activation of Si-B bond in water. *Org. Lett. 14*, 2090-2093. (DOI:10.1021/ol300618j).

51. Kalchauer, W., Pachaly, B. (2008). Muller-Rochow synthesis: the direct process to methylchlorosilanes. In handbook of heterogeneous catalysis (*Wiley-VCH Verlag GmbH & Co. KGaA: Weinheim*, Germany). (DOI: 10.1002/9783527610044.hetcat0134).

52. Zlota, A. A., Felix Frolow, F., Milstein, D. (1989). Oxidative addition of Si-Cl bonds to electron-rich $Ir^{I}$ complexes. *J. Chem. Soc. Chem. Commun.* 1826-1827. (DOI: 10.1039/C39890001826).

53. Lu, L., Siu, J. C., Lai, Y., Lin, S. (2020). An electroreductive approach to radical silylation *via* the activation of strong Si-Cl bond. *J. Am. Chem. Soc. 142*, 21272−21278. (DOI:10.1021/jacs.0c10899).

54. Cinderella, A. P., Vulovic, B., Watson, D. A. (2017). Palladium-catalyzed cross-coupling of silyl electrophiles with alkylzinc halides: A Silyl-Negishi reaction. *J. Am. Chem. Soc. 139*, 7741-7744. (DOI: 10.1021/jacs.7b04364).

55. Murakami, K., Hirano, K., Yorimitsu, H., Oshima, K. (2008), Silver-catalyzed transmetalation between chlorosilanes and aryl and alkenyl Grignard reagents for the synthesis of tetraorganosilanes. *Angew. Chem. Int. Ed. 47*, 5833-5835. (DOI: 10.1002/anie.200801949).

56. Vulovic, B., Cinderella, A. P., Watson, D. A. (2017). Palladium-catalyzed cross-coupling of monochlorosilanes and grignard reagents. *ACS Catal. 7*, 8113-8117. (DOI: 10.1021/acscatal.7b03465).

57. Sun, J., Zhou, Y., Gu, R. *et al.* (2022). Regioselective Ni-catalyzed reductive alkylsilylation of acrylonitrile with unactivated alkyl bromides and chlorosilanes. *Nat Commun* 7093. (DOI:10.1038/s41467-022-34901-6).

58. Qiu, L., Liu, Y., Chen, H., Song, L., Xie, W. (2025). A general copper catalytic system for cross-coupling of aryl iodides with

chlorosilanes under reductive conditions. *Chem. Sci. 16*, 9454-9461. (DOI:10.1039/d5sc01304f).

59. Xu, N.-X., Li, B.-X., Wang, C., Uchiyama, M. (2020). Sila- and Germacarboxylic acids: Precursors for the corresponding silyl and germyl radicals. *Angew. Chem. Int. Ed. 59*, 10639-10644. (DOI:10.1002/anie.202003070).

60. Studer, A., Amrein, S. (2000). Silylated cyclohexadienes: New Alternatives to Tributyltin Hydride in Free Radical Chemistry. *Angew. Chem. Int. Ed. 39*, 3080-3082. (DOI:10.1002/1521-3773(20000901)39:17<3080::AID-ANIE3080>3.0.CO;2-E).

61. Simonneau, A., Oestreich, M. (2013), 3-Silylated Cyclohexa-1,4-dienes as Precursors for Gaseous Hydrosilanes: The $B(C_6F_5)_3$-Catalyzed Transfer Hydrosilylation of Alkenes. *Angew. Chem. Int. Ed. 52*, 11905-11907. (DOI:10.1002/anie.201305584).

62. Keess, S. Oestreich, M. (2017). Cyclohexa-1,4-dienes in transition-metal-free ionic transfer processes. *Chem. Sci. 8*, 4688-4695. (DOI: 10.1039/C7SC01657C).

63. Li, B.-X., Ishida, H., Wang, C., Uchiyama, M. (2023). Visible-light-driven silyl or germyl radical generation *via* Si-C or Ge-C bond homolysis. *Org. Lett. 25*, 1765-1770. (DOI:10.1021/acs.orglett.3c00503).

64. Keess, S., Simonneau, A., Oestreich, M. (2015). Direct and transfer hydrosilylation reactions catalyzed by fully or partially fluorinated triarylboranes: A systematic study. *Organometallics 34*, 790-799. (DOI:10.1021/om501284a).

65. Amrein, S., Timmermann, A., Studer, A. (2001). Radical transfer hydrosilylation/cyclization using silylated cyclohexadienes. *Org. Lett. 3*, 2357-2360. (DOI:10.1021/ol016160c).

66. Jose, J., Mathew, T. V. (2024). Cobalt-catalyzed hydrosilylation across carbon-carbon, carbon-oxygen, and carbon-nitrogen multiple

bonds- a comprehensive review. *ChemCatChem 16*, e202301626. (DOI:10.1002/cctc.202301626).

67. Sun, J., Deng, L. (2016). Cobalt complex-catalyzed hydrosilylation of alkenes and alkynes. *ACS Catal. 6*, 290-300. (DOI:10.1021/acscatal.5b02308).

68. Nakajima, Y., Shimada, S. (2015). Hydrosilylation reaction of olefins: recent advances and perspectives. *RSC Adv. 5*, 20603-20616. (DOI:10.1039/c4ra17281g).

69. Xiaoyong Du, X., Huang, Z. (2017). Advances in base-metal-catalyzed alkene hydrosilylation. *ACS Catal. 7*, 1227-1243. (DOI:10.1021/acscatal.6b02990).

70. Almeida, L. D. de, Wang, H., Junge, K., Cui, X., Beller, M. (2021). Recent advances in catalytic hydrosilylations: Developments beyond traditional platinum catalysts. *Angew. Chem. Int. Ed. 60*, 550-565. (DOI:10.1002/anie.202008729).

71. Xu, Z., Xu, L.-W. (2015), Silylations of arenes with hydrosilanes: From transition-metal-catalyzed C-X bond cleavage to environmentally benign transition-metal-free C-H bond activation. *ChemSusChem*, *8*, 2176-2179. (DOI:10.1002/cssc.201500467).

72. Saptal, V. B., Wang, R., Park, S. (2010). Recent advances in transition metal-free catalytic hydroelementation (E = B, Si, Ge, and Sn) of Alkynes. *RSC Adv. 10*, 43539-43565. (DOI:10.1039/D0RA07768B).

73. Xu, Z., Huang, W. S., Zhang, J., Xu, L. W. (2015). Recent advances in transition-metal-catalyzed silylations of arenes with hydrosilanes: C-X bond cleavage or C-H bond activation synchronized with Si-H bond activation. *Synthesis 47*, 3645-3668. (DOI:10.1055/s-0035-1560646)

74. Cheng, C., Hartwig, J. F. ( 2015). Catalytic silylation of unactivated C-H bonds. *Chem. Rev. 115*, 8946-8975. (DOI:10.1021/cr5006414).

75. Li, B., Dixneuf, P. H. (2021). Metal-catalyzed silylation of $sp^3$ C-H bonds. *Chem. Soc. Rev. 50*, 5062-5085. (DOI:10.1039/D0CS01392G).

76. Toutov, A., Liu, WB., Betz, K. *et al.* (2015). Silylation of C-H bonds in aromatic heterocycles by an Earth-abundant metal catalyst. *Nature 518*, 80-84. (DOI:10.1038/nature14126).

77. Ma, Y., Wang, B., Zhang, L., Hou, Z. (2016). Boron-catalyzed aromatic C-H bond silylation with hydrosilanes. *J. Am. Chem. Soc. 138*, 3663-3666. (DOI:10.1021/jacs.6b01349).

78. Toutov, A. A., Betz, K. N., Schuman, D. P., Liu, W.-B., Fedorov, A., Stoltz, B. M., Grubbs, R. H. (2017). Alkali metal-hydroxide-catalyzed C(sp)-H bond silylation. *J. Am. Chem. Soc. 139*, 1668-1674. (DOI:10.1021/jacs.6b12114).

79. Harrod, J. F., Chalk, A. J. (1965). Dicobalt octacarbonyl as a catalyst for hydrosilation of olefins. *J. Am. Chem. Soc. 87*, 1133-1135. (DOI:10.1021/ja01083a034).

80. Yamanoi, Y. (2005). Palladium-catalyzed silylations of hydrosilanes with aryl halides using bulky alkyl phosphine. *J. Org. Chem. 70*, 9607-9609. (DOI:10.1021/jo051131r).

81. Biao Lu, B., Falck, J. R. (2008) Efficient iridium-catalyzed C-H functionalization/silylation of heteroarenes. *Angew. Chem. Int. Ed.* 120, 7618-7620. (DOI:10.1002/ange.200802456).

82. Lu, W., Ni, H., Bao, Z., Wu, J., *et al*. (2025) Nickel-catalyzed regioselective Markovnikov hydrosilylation of vinylarenes *via* hydrogen atom transfer. *Org. Lett.* 27, 12264-12269. (DOI: 10.1021/acs.orglett.5c03797).

83. Gao, J., Ge, Y., He, C. ( 2024). X-Type silyl ligands for transition-metal catalysis. *Chem. Soc. Rev. 53*, 4648-4673. (DOI: 10.1039/D3CS00893B).

84. Panayides, J. L., Riley, D. L., Hasenmaile, F., Otterlo, W. A. L. V. (2024). The role of silicon in drug discovery: A review. *RSC Med. Chem. 15,* 3286-3344. (DOI: 10.1039/D4MD00169A).

85. Joint FAO/WHO Expert Committee on Food Additives (JECFA) (2011). WHO Technical Report Series 966: Evaluation of certain food additives and contaminants. World Health Organ. (DOI:10.1016/S0140-6736(02)11326-2).

86. Prentice, W. E., Voight, M. L. (2001). Techniques in musculoskeletal rehabilitation. McGraw-Hill Professional. Page: 369. (ISBN 978-0-07-135498-1).

87. Pradhan, R., Grewal, H. S. (2024). Towards sustainability: An eco-friendly approach for durable anti-icing superhydrophobic surfaces. *Small Methods 8*, 2400459. (DOI: 10.1002/smtd.202400459).

88. Metcalf, T. J., Irons, T. G., Sher, L. D., Young, P. C. (1994). Simethicone in the treatment of infant colic: A randomized, placebo-controlled, multicenter trial. *Pediatrics 94,* 29-34. (DOI: 10.1542/peds.94.1.29).

89. Roggenbuck, F.C., Penner, D., Burow, R.F., Thomas, B. (1993). Study of the enhancement of herbicide activity and rainfastness by an organosilicone adjuvant utilizing radiolabelled herbicide and adjuvant. *Pestic. Sci. 37*, 121-125. (DOI: 10.1002/ps.2780370203).

90. Belakhov, V. V., Krasnobaeva, I. L. (2023). Organosilicon derivatives of $\beta$-D-ribofuranoside: Synthesis, pharmacological study, and insecticidal activity. *Russ. J. Gen. Chem. 93*, 3464-3473. (DOI: 10.1134/S1070363223130297).

91. Phillips, Fevig, T. L., Lau, P. H., Klemm, G. H., Mao, M. K., Ma, C., Gloeckner, J. A., Clark, A. S. (2002). Process research on the synthesis of Silthiofam: A novel fungicide for wheat. *Org. Proc. Res. Dev. 6*, 357-366. (DOI: 10.1021/op020206f).

92. Anderson, W. K., Kasliwal, R., Houston, D. M., Wang, Y. S., Narayanan, V. L., Haugwitz, R. D., Plowman, J. (1995). Synthesis, antitumor activity, and chemical properties of silaplatin and related platinum(II) and platinum(IV) complexes derived from *b*-silyl amines. *J. med. Chem. 38*, 3789-3797. (DOI: 10.1021/jm00019a008).

93. Hu, Y., Wang, Y., Li, F., Ma, C., Wang, J. (2017). Design and expeditious synthesis of organosilanes as potent antivirals targeting multidrug-resistant influenza A viruses. *Eur. J. med. Chem. 135*, 70-76. (DOI: 10.1016/j.ejmech.2017.04.038).

94. Dhingra, N., Singh, J. B., Singh, H. L. (2022). Synthesis, spectroscopy, and density functional theory of organotin and organosilicon complexes of bioactive ligands containing nitrogen, sulfur donor atoms as antimicrobial agents: In vitro and in silico studies. *Dalton Transactions*, *51*, 8821-8831. (DOI: 10.1039/D2DT01051H).

95. Lo, P. C., Chan, C. M. H., Liu, J. Y., Fong, W. P., Ng, D. K. P. (2007). Highly photocytotoxic glucosylated Silicon(IV) phthalocyanines. Effects of peripheral chloro substitution on the photophysical and photodynamic properties. *J. Med. Chem*. *50,* 2100-2107. (DOI: 10.1021/jm061415j).

96. Barnes, M. J., Conroy, R., Miller, D. J., Mills, J. S., Montana, J. G., Pooni, P. K., Showell, G. A., Walsh, L. M., Warneck, J. B. H. ( 2007). Trimethylsilylpyrazoles as novel inhibitors of p38 MAP kinase: A new use of silicon bioisosteres in medicinal chemistry. *Bioorg. Med. Chem. Lett. 17*, 354-357. (DOI: 10.1016/j.bmcl.2006.10.044).

97. Showell, G. A., Barnes, M. J., Daiss, J. O., Mills, J. S., Montana, J. G., Tacke, R., Warnecka, J. B. H. (2006). (*R*)-Sila-Venlafaxine: A selective noradrenaline reuptake inhibitor for the treatment of emesis. *Bioorg. Med. Chem. Lett. 16*, 2555-2558. (DOI:10.1016/j.bmcl.2005.12.062).

98. Daiss, J. O., Burschka, C., Mills, J. S., Montana, J. G., Showell, G. A., Warneck, J. B. H., Tacke, R. (2006). Sila-venlafaxine, a sila-analogue of the serotonin/noradrenaline reuptake inhibitor venlafaxine: Synthesis, crystal structure analysis, and pharmacological characterization. *Organometallics* *25*, 1188-1198. (DOI:10.1021/om058051y)

99. Daiss, J. O., Burschka, C., Mills, J. S., Montana, J. G., Showell, G. A., Warneck, J. B. H., Tacke, R. (2006). Synthesis, crystal structure analysis, and pharmacological characterization of desmethoxy-Sila-Venlafaxine, a derivative of the serotonin/noradrenaline reuptake inhibitor Sila-Venlafaxine. *J. Organomet. Chem*. *691*, 3589-3595. (DOI:10.1016/j.jorganchem.2006.04.015).

100. Guo, Z., Ye, J., Zang, Y., Wang, D., Yu, X., Li, C., Wu, Y., Liu, Ze-S. (2025). Modular and regioselective synthesis of eight-membered benzosilacycles enable by ring expansion of silacyclobutanes with aryl halides and alkynes. *ACS Catal. 15*, 7066-7078. (DOI: 10.1021/acscatal.5c01177).

101. Ponomarenko, S. A., Kirchmeyer, S. (2010). Conjugated organosilicon materials for organic electronics and photonics. *Adv. Polym. Sci.* 235, 33-110. (DOI:10.1007/12_2009_48).

102. Su, T. A., Li, H., Klausen, R. S., Kim, N. T., Neupane, M., Leighton, J. L., Steigerwald, M. L., Venkataraman, L., Nuckolls, C. (2017). Silane and germane molecular electronics. *Acc. Chem. Res. 50*, 1088-1095. (DOI: 10.1021/acs.accounts.7b00059).

103. Karatsu, T., Hazuku, R., Asuke, M., Nishigaki, A., Yagai, S., Suzuri, Y., Kita, H., Kitamura, A. (2007). Blue electroluminescence of silyl substituted anthracene derivatives. *Org. Electron. 8*, 357-366. (DOI: 10.1016/J.ORGEL.2006.12.009).

104. Winkler, C. (1887). Communications on Germanium. *J. Pract. Chem. 36*, 177-209. (DOI:10.1002/prac.18870360119).

105. Weinert, C. S. (2007). Germanium organometallics. *In Comprehensive Organometallic Chemistry III*, Mingos, M. P., Crabtree, R. H., Ed.; Elsevier, *3*, 699-808. (DOI:10.1016/B0-08-045047-4/00053-4).

106. Wang, H., Yuan, Y., Zhang, Y., Franke, R., Wu, X.-F. (2020). Ruthenium-catalyzed *ortho*-alkenylation of aroylgermanes. *Eur. J. Org. Chem. 19*, 2842-2845. (DOI:10.1002/ejoc.202000062).

107. Kawashima, T. (2000). Small ring compounds containing highly coordinate group 14 elements. *J. Organomet. Chem. 611*, 256-263. (DOI:10.1016/S0022-328X(00)00491-5).

108. Satge, J. (2004). Some applications of germanium and its derivatives. *Main Group Metal Chemistry 27,*301-307.

109. Nakamura, T., Shimada, Y. and Sato, K. (2023). Bioorganic and medicinal organogermanium chemistry. In organogermanium compounds, Lee, V. Y., Ed. 839-865. (DOI: 10.1002/9781119613466.ch19).

110. Deb, A., Singh, S., Seth, K., Pimparkar, S., Bhaskararao, B., Guin, S., Sunoj, R. B., Maiti, D. (2017). Experimental and computational studies on remote $\gamma$-C($sp^3$)-H silylation and germanylation of aliphatic carboxamides. *ACS Catal. 7*, 8171-8175. (DOI: 10.1021/acscatal.7b03056).

111. Zhou, Z. X., Rao, W. H., Zeng, M. H., & Liu, Y. J. (2018). Facile synthesis of unnatural $\beta$-germyl-$\alpha$-amino amides *via* Pd(II)-catalyzed primary and secondary C($sp^3$)-H bond germylation. *Chem. Commun. 54*, 14136-14139. (DOI:10.1039/C8CC08098D).

112. Lv, W., Yu, J., Ge, B., Wen, S., Cheng, G. (2018). Palladium-catalyzed catellani-type bis-silylation and bis-germanylation of aryl iodides and norbornenes. *J. Org. Chem. 83*, 12683-12693. (DOI:10.1021/acs.joc.8b02018).

113. Sakamoto, K., Nagashima, Y., Kamino, S., Uchiyama, M. (2025). Nucleophilic germylation of stable *π* bonds *via* Ge-Ge bond heterolysis. *Angew. Chem. Int. Ed. 64*, e202506106. (DOI: 10.1002/anie.202506106).

114. Zaitsev, K.V. (2023). Organogermanium compounds of the main group elements. In organogermanium compounds, Lee, V. Y., Ed. 103-193. (DOI:10.1002/9781119613466.ch2).

115. Qiao, Y.-W., Zhou, B.-Q., Huang, Y. (2023). Ni-catalyzed reductive alkylgermylation of activated alkenes: Modular access to polyfunctionalized alkyl germanes. *Chem Catalysis*, *3*, 100819. (DOI:10.1016/j.checat. 2023.100819).

116. Tu, J.-L., Huang, B. (2024). Catalytic construction of C($sp^3$)-Ge bonds: Recent advances and future perspectives. *Adv. Synth. Catal.* 366, 4618-4633. (DOI:10.1002/adsc.202401069).

117. Rogova, T., Ahrweiler, E., Schoetz, M. D., Schoenebeck, F. (2024). Recent developments with organogermanes: Their preparation and application in synthesis and catalysis. *Angew. Chem. Int. Ed. 63*, e202314709. (DOI:10.1002/anie.202314709).

118. Schoetz, M. D., Deckers, K., Singh, G., Ahrweiler, E., Hoeppner, A., Schoenebeck, F. (2024). Electrochemistry-enabled C-H heteroatom bond formation of alkyl germanes. *J. Am. Chem. Soc. 146*, 21257-21263. (DOI:10.1021/jacs.4c08008).

119. Chen, H., Zhai, C., Zhang, H., Zhu, C., Rueping, M. (2025). Switchable electrochemical pathways for the selective C($sp^3$)-Ge bond formation. *Nat. Commun.* 16, 7247. (DOI:10.1038/s41467-025-62141-x).

120. Ahrweiler, E., Selmani, A., Schoenebeck, F. (2025). Base-catalyzed remote hydrogermylation of olefins. *Angew. Chem. Int. Ed. 64*, e202503573. (DOI:10.1002/anie.202503573).

121. Yuan, Y., Gu, Y., Wang, Y.-E., Zheng, J., Ji, J., Xiong, D., Xue, F., Mao, J. (2022). One-pot rapid access to benzyl silanes, germanes, and stannanes from toluenes mediated by a $LiN(SiMe_3)_2$/CsCl System. *J. Org. Chem. 87*, 13907-13918.

(DOI: 10.1021/acs.joc.2c01612).

122. Guo, P., Pang, X., Wang, K., Su, P.-F., Pan, Q.-Q., Han, G.-Y., Shen, Q., Zhao, Z.-Z., Zhang, W., Shu, X.-Z. (2022). Nickel-catalyzed reductive $Csp^3$-Ge coupling of alkyl bromides with chlorogermanes. *Org. Lett. 24*, 1802-1806.

(DOI: 10.1021/acs.orglett.2c00207).

123. Gu, R., Feng, X., Bao, M. *et al.* (2023). Modular access to alkylgermanes *via* reductive germylative alkylation of activated olefins under nickel catalysis. *Nat Commun 14*, 7669. (DOI:10.1038/s41467-023-43561-z).

124. Kanyiva, K. S., Kuninobu, Y., Kanai, M. (2014). Palladium-catalyzed direct C-H silylation and germanylation of benzamides and carboxamides. *Org. Lett. 16*, 1968-1971. (DOI:10.1021/ol500519y).

125. Modak, A., Patra, T., Chowdhury, R., Raul, S., Maiti, D. (2017). Palladium-catalyzed remote meta-Selective C-H Bond silylation and germanylation. *Organometallic 36*, 2418-2423. (DOI:10.1021/acs.organomet.7b00309).

126. Keess, S., Oestreich, M. (2017). Access to fully alkylated germanes by $B(C_6F_5)_3$-catalyzed transfer hydrogermylation of alkenes. *Org. Lett. 19*, 1898-1901. (DOI: 10.1021/acs.orglett.7b00672).

127. Zhao, Z., Zhang, F., Wang, D. and Deng, L. (2023), Advances in transition-metal-catalyzed hydrogermylation of alkenes and alkynes. *Chin. J. Chem. 41*, 3063-3081. (DOI:10.1002/cjoc.202300276).

128. Tu, J.-L., Huang, B. (2024). Catalytic construction of C($sp^3$)-Ge bonds: Recent advances and future perspectives. *Adv. Synth. Catal. 366*, 4618-4633. (DOI:10.1002/adsc.202401069).

129. Xu, M. Y., Li, N. Xiao, B. (2025). Recently developed organogermanium(IV) compounds as drug candidates and synthetic tools in drug discovery. Org. Biomol. Chem. 23, 7852-7871. (DOI:10.1039/D5OB00716J).

130. Zhao, Z., Zhang, F., Wang, D. and Deng, L. (2023), Advances in transition-metal-catalyzed hydrogermylation of alkenes and alkynes. *Chin. J. Chem. 41*, 3063-3081. (DOI:10.1002/cjoc.202300276).

131. Wang, P., Wang, D., Deng, L. (2025). Cobalt-catalyzed hydrogermylation of nonactivated alkenes enabled by photoirradiation. *Organometallics 44*, 1648-1652.

(DOI:10.1021/acs.organomet.5c00237).

132. Lin, W., You, L., Yuan, W., He, C. (2022). Cu-catalyzed enantioselective hydrogermylation: Asymmetric synthesis of unnatural *β*-germyl *α*-amino acids. *ACS Catal. 12*, 14592-14600.

(DOI:10.1021/acscatal.2c04571).

133. Stachowiak-Dluzynska, H., Gruszczynski, M., Kubicki, M., Hreczycho, G. (2024). Pt(II) complexes bearing P, N-donor ligands as catalysts in chemoselective hydrosilylation, hydrogermylation, and hydroboration of terminal alkenes. *J. Catal. 433*, 115494. (DOI:10.1016/j.jcat.2024.115494).

134. Prima, D. O., Vatsadze, S. Z. (2025). Cocktail-type catalysis: An emerging concept in metal-mediated transformations. *Organometallics 44*, 1337-1357. (DOI:10.1021/acs.organomet.5c00117).

135. Queen, A. E., Selmani, A., Schoenebeck, F. (2022). Hydrogermylation of alkenes *via* organophotoredox-initiated HAT catalysis. *Org. Lett*. 24, 406-409. (DOI:10.1021/acs.orglett.1c04088).

136. Kinoshita, H., Nakamura, T., Kakiya, H., Shinokubo, H., Matsubara, S., Oshima, K. (2001). Remarkable rate acceleration of Pd(0)-catalyzed hydrogermylation of alkynes and dienes in water. *Org. Lett. 3*, 2521-2524. (DOI:10.1021/ol0161817).

137. Lesbani, A., Kondo, H. *et al*. (2010). Integrated palladium-catalyzed arylation of heavier group 14 hydrides. *Chem. Eur. J. 16*, 13519-13527. (DOI:10.1002/chem.201001437).

138. Dahiya, A., Schoenebeck, F. (2022). Direct C-H dehydrogenative germylation of terminal alkynes with hydrogermanes. *Org. Lett. 24*, 2728-2732. (DOI:10.1021/acs.orglett.2c00840).

139. Aizawa, K., Nakamura, T., Shimada, Y., Takeda, T., Azumi, J., Shore, A. C. (2025). Organogermanium: Potential beneficial effects on the cardiovascular system. *Physiological Reports 13*, e70234. (DOI: 10.14814/phy2.70234).

140. Srivastava, R., R., Ilyas, S. (2025). Harnessing germanium from industrial residues and electronic waste for a sustainable energy future. *Green Chem. 27*, 14744-14768. (DOI:10.1039/D5GC03018H).

141. Slavich, A.S., Ermolaev, G.A., Zavidovskiy, I.A. *et al.* (2025). Germanium disulfide as an alternative high refractive index and transparent material for UV-visible nanophotonics. *Light Sci Appl 14*, 213. (DOI:10.1038/s41377-025-01886-y).

142. Lukevics, E., Gar, T.K., Ignatovich, L.M., Mironov, V.F. (1990). Biological Activity of Germanium Compounds; Zinatne: Riga, Latvia, page-191.

143. Lukevics, E., Ignatovich, L. (2002). Biological activity of organogermanium compounds. In the chemistry of organic germanium, tin and lead compounds. *JohnWiley & Sons Ltd.*: Chichester, UK, *2*, 1653-1683. (DOI:10.1002/0470857188.ch23).

144. Wang, Y.-S., Teng, G.-Q., Zhou, H., Dong, C.-L. (2002). Germanium reduces inflammatory damage in mammary glands during

lipopolysaccharide-induced mastitis in mice. *Biol. Trace Elem. Res. 198*, 617-626. (DOI:10.1007/s12011-020-02106-x).

145. Kaplan, B.J., Parish, W.W., Andrus, G.M., Simpson, J. S. A., Field, C.J. (2004). Germane facts about germanium sesquioxide: I. Chemistry and anticancer properties. *J. Altern. Complement. Med. 10*, 337–344. (DOI:10.1089/107555304323062329).

146. World Health Organization. WHO Drug Information (2014). *WHO Drug Inf. 28*, 125-210.

147. Li, L., Ruan, T., Lyu, Y., Wu, B. (2017). Advances in effect of germanium or germanium compounds on animals- A review. *J. Biosci. Med. 5*, 56-73. (DOI:10.4236/jbm.2017.57006).

148. Kadomtseva, A.V., Mochalov, G.M., Kuzina, O.V. (2021). Biologically active coordination compounds of germanium. Synthesis and physicochemical properties. *Russ. J. Org. Chem. 57*, 879-888. (DOI:10.1134/S1070428021060026).

149. Rosenberg, E. (2013). Germanium-containing compounds, current knowledge and applications. In *Encyclopedia of Metalloproteins*. Kretsinger, R., Uversky, V., Permyakov, E., Eds., Springer: New York, NY, USA, 847-855. (DOI: 10.1007/978-1-4614-1533-6_582).

150. Ali, M.M. (2013). Germanium L-Cysteine *a*-Tocopherol complex as stimulator to antioxidant defense system. *In Encyclopedia of Metalloproteins.* Kretsinger, R., Uversky, V., Permyakov, E., Eds., Springer: New York, NY, USA, 836-841. (DOI: 10.1007/978-1-4614-1533-6_125).

151. Cho, J.M., Chae, J., Jeong, S.R., Moon, M.J., Shin, D.Y., Lee, J.H. (2020). Immune activation of bio-germanium in a randomized, double-blind, placebo-controlled clinical trial with 130 human subjects: Therapeutic opportunities from new insights. *PLoS ONE 15*, e0240358. (DOI:10.1371/journal.pone.0240358).

152. Chen, X.-C., Zhu, Y.-G., Zhu, L.-A., Huang, C., Chen, Y., Chen, L.-M., Fang, F., Zhou, Y.-C., Zhao, C.-H. (2003). Ginsenoside Rg1 attenuates dopamine-induced apoptosis in PC12 cells by suppressing oxidative stress. *Eur. J. Pharmacol. 473*, 1-7. (DOI: 10.1016/S0014-2999(03)01945-9).

153. Menchikov, L.G., Shestov, A.A., Popov, A.V. (2023). Warburg effect revisited: Embodiment of classical biochemistry and organic chemistry. Current state and prospects. *Biochemistry 88*, S1-S20. (DOI: 10.1134/S0006297923140018).

154. Menchikov, L. G., Popov, A. V. (2023). Physiological activity of trace element germanium including anticancer properties. *Biomedicines*, *11*, 1535. (DOI:10.3390/biomedicines11061535).

155. Lim, D.H., Li, M., Seo, J.-A., Lim, K.-M., Ham, S.W. (2010). A novel organogermanium protected atopic dermatitis induced by oxazolone. *Bioorg. Med. Chem. Lett. 20*, 4032-4034. (DOI:10.1016/j.bmcl.2010.05.097).

156. Ye, L., Ou, X., Peng, X., Luo, Y. (2012). Synthesis of 3-(2,8,9-trioxa-5-aza-1-germatricyclo [3.3.3.0] Undecane-1-yl)-3-(4-hydroxyl-3-methoxyphenyl)propionic acid and its inhibitory effect on the cervical tumour U14 in vitro and in vivo. *Med. Chem. 8*, 595-598. (DOI: 10.2174/157340612801216157).

157. Choi, S., Oh, S., Han, J., Park, J., Choi, J.-H., Min, N. Y., Lee, K.-H., Park, A. J., Kim, Y. J., Jang, S. J., Seung, D.-H., Ham, W. (2010). Synthesis and biological evaluation of water-soluble organogermanium. *Eur. J. Med. Chem.,* *45*, 1654-1656. (DOI:10.1016/j.ejmech.2009.12.069).

158. Albini, A., Fagnoni, M. (2008). 1908: Giacomo Ciamician and the concept of green chemistry. *ChemSusChem, 1*, 63-66. (DOI:10.1002/cssc.200700015).

159. Turro, N. J. Principles of molecular photochemistry: An introduction; University Science Books: Sausalito, California, 2009.

160. Zeitler, K. (2009), Photoredox catalysis with visible light. *Angew. Chem. Int. Ed. 48*, 9785-9789. (DOI:10.1002/anie.200904056).

161. Narayanam, J. M. R., Stephenson, C. R. J. (2011). Visible light photocatalysis: Applications in organic synthesis. *Chem. Soc. Rev. 40*, 102-113. (DOI:10.1039/B913880N).

162. Fukuzumi, S., Ohkubo, K. (2012). Selective photocatalytic reactions with organic photocatalysts. *Chem. Sci. 4*, 561-574. (DOI: 10.1039/C2SC21449K).

163. Prier, C. K., Rankic, D. A., Macmillan, D. W. C. (2013). Visible light photoredox catalysis with transition metal complexes: Applications in organic synthesis. *Chem. Rev.* 113, 5322-5363. (DOI:10.1021/cr300503r).

164. Romero, N. A., Nicewicz, D. A. (2016). Organic photoredox catalysis. *Chem. Rev. 116*, 10075-10166.

(DOI:10.1021/acs.chemrev.6b00057).

165. Shaw, M. H., Twilton, J., Macmillan, D. W. C. (2016). Photoredox catalysis in organic chemistry. *J. Org. Chem. 81*, 6898-6926. (DOI:10.1021/acs.joc.6b01449).

166. Ravelli, D., Protti, S., Fagnoni, M. (2016). Carbon-Carbon bond forming reactions *via* photogenerated intermediates. *Chem. Rev. 116*, 9850-9913. (DOI:10.1021/acs.chemrev.5b00662).

167. Bortolato, T., Cuadros, S., Simionato, G., Dell'Amico, L. (2021). The advent and development of organic photoredox catalysis. *Chem. Commun. 58*, 1263-1283. (DOI: 10.1039/D1CC05850A).

168. Rehm, D. and Weller, A. (1970). Kinetics of fluorescence quenching by electron and H-atom transfer. *Isr. J. Chem. 8*, 259-271. (DOI:10.1002/ijch.197000029).

169. Buzzetti, L., Crisenza, G. E. M., Melchiorre, P. (2019). Mechanistic studies in photocatalysis. *Angew. Chem., Int. Ed. 58*, 3730-3747. (DOI:10.1002/anie.201809984).

170. Knowles, R. R. *et al.* (2022). Photochemical and electrochemical applications of proton-coupled electron transfer in organic synthesis. *Chem. Rev. 122*, 2017-2291. (DOI:10.1021/acs.chemrev.1c00374).

171. Speckmeier, E., Fischer, T. G., Zeitler, K. (2018). A toolbox approach to construct broadly applicable metal-free catalysts for photoredox chemistry: Deliberate tuning of redox potentials and importance of halogens in donor-acceptor cyanoarenes. *J. Am. Chem. Soc. 140*, 15353-15365. (DOI:10.1021/jacs.8b08933).

172. Luo, J., Zhang, J. (2016) Donor-acceptor fluorophores for visible light-promoted organic synthesis: Photoredox/Ni dual catalytic C($sp^3$)-C($sp^2$) cross-coupling. *ACS Catal. 6*, 873-877. (DOI: 10.1021/acscatal.5b02204).

173. Garreau, M., Le Vaillant, F., Waser, J. (2019). C-Terminal bioconjugation of peptides through photoredox catalyzed decarboxylative alkynylation. *Angew. Chem. Int. Ed. 58*, 8182-8186. (DOI:10.1002/anie.201901922).

174. Neumann, M., Fuldner, S., Konig, B., Zeitler, K. (2011). Metal-free, cooperative asymmetric organophotoredox catalysis with visible light. *Angew. Chem. Int. Ed. 50*, 951-954. (DOI:10.1002/anie.201002992).

175. Lazarides, T., Mc-cormick, T., Du, P., Luo, G., Lindley, B., Eisenberg, R. (2009). Making hydrogen from water using a homogeneous system without noble metals. *J. Am. Chem. Soc. 131*, 9192-9194. (DOI:10.1021/ja903044n).

176. Kalyanasundaram, K. (1982). Photophysics, photochemistry and solar energy conversion with tris(bipyridyl)ruthenium(II) and its analogues. *Coord. Chem. Rev. 46*, 159-244. (DOI:10.1016/0010-8545(82)85003-0).

177. Flamigni, L., Barbieri, A., Sabatini, C., Ventura, B., Barigelletti, F. (2007). Photochemistry and photophysics of coordination compounds: Iridium. In Photochemistry and Photophysics of Coordination Compounds II; Springer, page: 143-203. (DOI:10.1007/128_2007_131).

178. Doeven, E. H., Zammit, E. M., Barbante, G. J., Francis, P. S., Barnett, N. W., Hogan, C. F. (2013). A potential-controlled switch on/off mechanism for selective excitation in mixed electrochemiluminescent systems. *Chem. Sci*. *4*, 977-982. (DOI: /10.1039/C2SC21707D).

179. Lowry, M. S., Goldsmith, J. I., Slinker, J. D., Rohl, R., Pascal, R. A., Malliaras, G. G., Bernhard, S. (2005). Single-layer electroluminescent devices and photoinduced hydrogen production from an ionic iridium(III) complex. *Chem. Mater*. *17*, 5712-5719. (DOI: 10.1021/cm051312+).

180. Pavlishchuk, V. V., Addison, A. W. (2000). Conversion constants for redox potentials measured versus different reference electrodes in acetonitrile solutions at 25 °C. *Inorg. Chim. Acta 298*, 97-102. (DOI: 10.1016/S0020-1693(99)00407-7).

# Chapter 2

# Development of Sulfonamide as Photoinduced Hydrogen Atom Transfer Catalyst for Organophotoredox Hydrosilylation and Hydrogermylation of Activated Alkenes

## 2.1 Introduction

One of the most valuable synthetic transformation in organosilicon chemistry is the hydrosilylation reaction. Which proceed through the addition of silicon hydride across C-C multiple bonds and give rise to range of organosilicon compounds. This method is more frequently used in the industries to produce silicone polymers, including oils, rubbers, and resins.[1] In addition, several other organosilicon reagents, which are utilized in fine chemical synthesis for the oxidation, cross-coupling reactions, and other applications can also be accessed through the hydrosilylation process.[2-6] In 1947, Sommer reported the first hydrosilylation reaction by treating trichlorosilane with 1-octene in the presence of peroxide under thermal condition.[7] In the late 1950s, a homogeneous transition metal catalyst derived from platinum, also known as “Speier’s catalyst”, was found to be effective with improved selectivity in the hydrosilylation reaction.[8] A notable improvement was observed in 1973 with the introduction of the Karstedt’s catalyst, which displayed enhanced activity and selectivity.[9] However, despite their high industrial utility, platinum catalysts are found to show a number of disadvantages. For instance, side reactions such as dehydrogenative silylation, hydrogenation, isomerization, olefin oligomerization, and redistribution of hydrosilanes. To overcome these disadvantages, researchers have developed numerous transition metal catalysts[10-18] for the hydrosilylation of C-C multiple bonds.

## 2.2 Literature reports for hydrosilylation and hydrogermylation of alkenes

The discovery of different metal complexes based on iridium, ruthenium, rhodium, nickel, cobalt, iron, and manganese, among others, as efficient hydrosilylation catalysts is the clear indication of intensive research in this area (**Scheme 2.1**).[14-20] Similarly, the hydrogermylation of alkenes also received great attention and was achieved using different transition metal catalysts.[21-25]

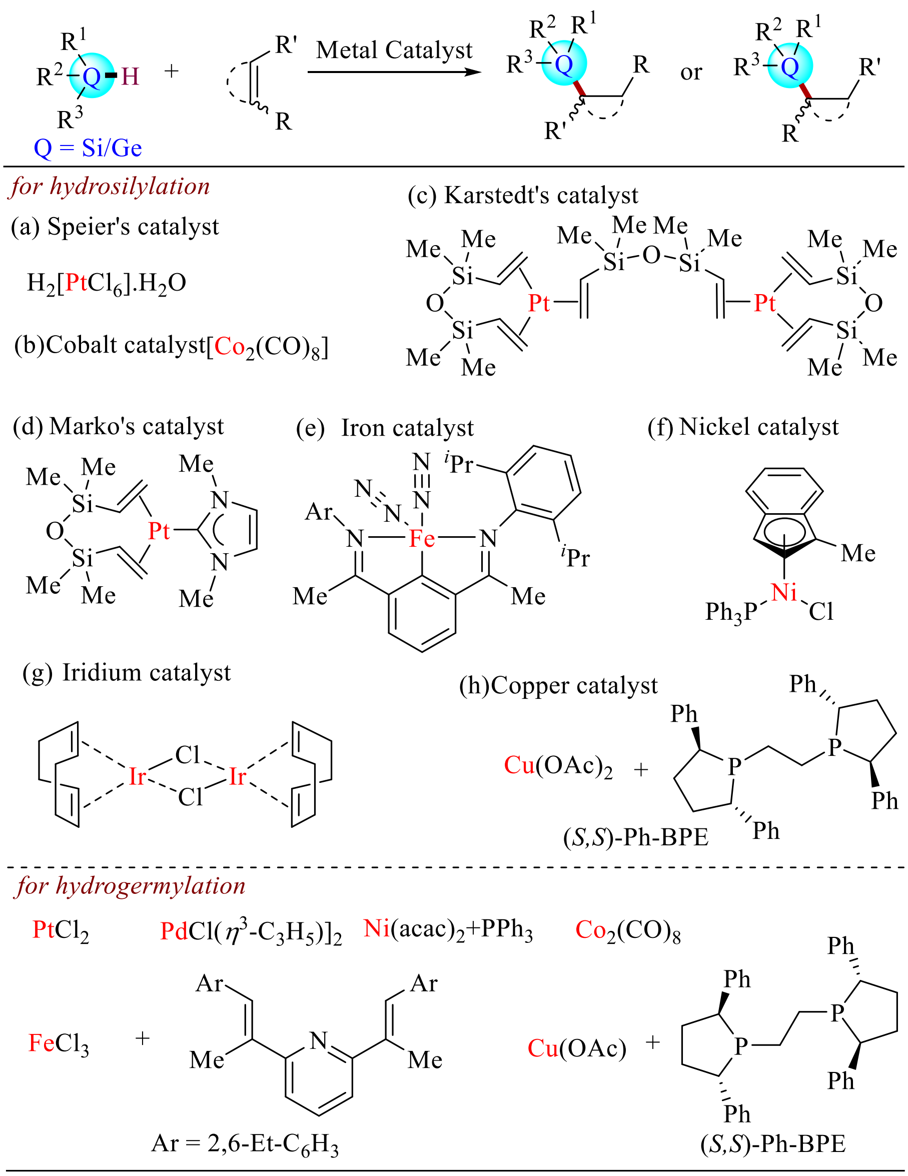


**Scheme 2.1** Selected examples of metal catalysts used for the hydrosilylation and hydrogermylation of alkenes

In addition, Lewis acid-catalyzed reactions has also been developed using catalysts such as $AlCl_3$,[26] electron-deficient boranes,[27-29] organoboron-phosphonium salts[30] in the hydrosilylation of alkenes (**Scheme 2.2**).

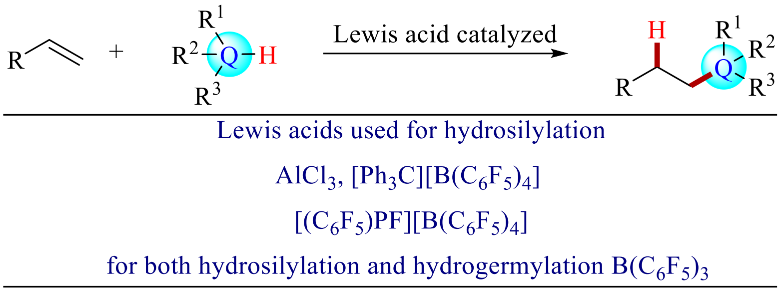


**Scheme 2.2** Lewis acid-catalyzed hydrosilylation and hydrogermylation of alkenes

The Schoenebeck group developed $[B(C_6F_5)_3]$ catalyzed hydrogermylation of alkenes.[31] Even though the above-mentioned methods worked very well with a variety of alkenes, an efficient catalytic system is still required, particularly for electron-deficient alkenes, especially under transition metal-free and environmental benign conditions.[32-34]

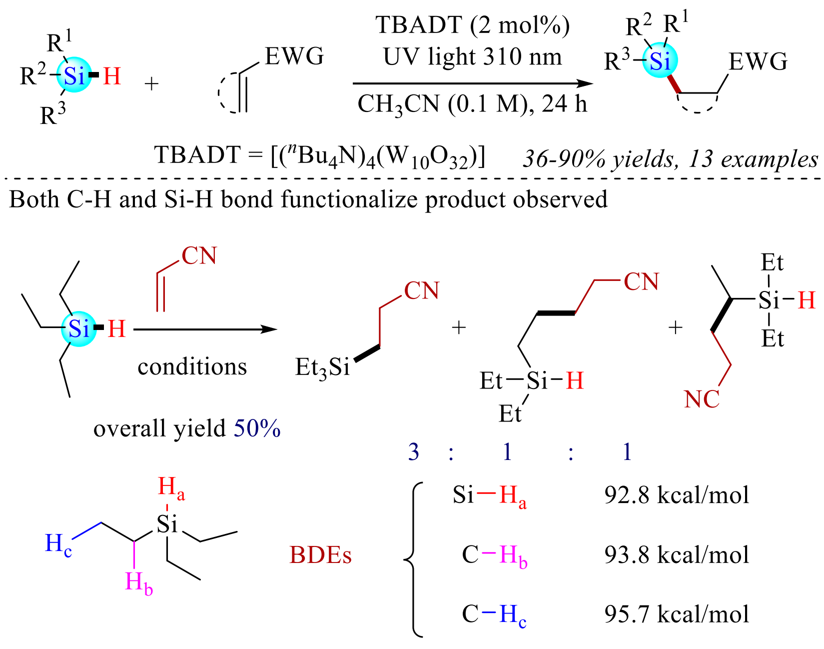


**Scheme 2.3** TBADT-mediated hydrosilylation of electron-poor alkenes

On the other hand, the synthesis of organosilanes *via* generation silyl radical from hydrosilanes has garnered significant interest. The hydrogen atom transfer (HAT) process is a classical route for generating a silyl radical with the help of radicals derived from peroxides under thermal condition.[35] Over the last decade, significant developments in photocatalysis have enabled the previously unattainable transformations.[36-45] In 2015, Fagnoni and co-workers achieved hydrosilylation of electron-deficient alkenes using tetrabutylammonium decatungstate (TBADT) as a direct hydrogen atom transfer catalyst to functionalize hydrosilanes under 310 nm ultraviolet light irradiation (**Scheme 2.3**).[46]

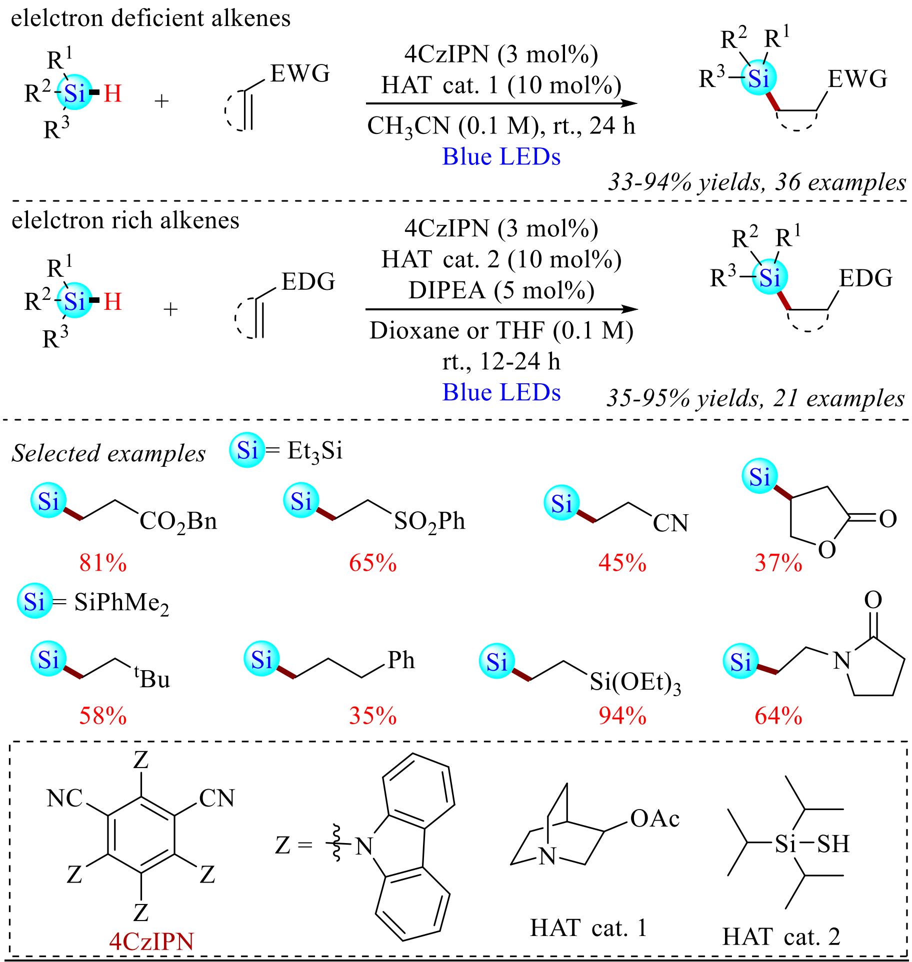


**Scheme 2.4** Hydrosilylation of alkenes using quinuclidin-3-yl-acetate and $^{i}Pr_3SiSH$ as HAT catalyst

However, this method was associated with poor chemoselectivity, both Si-H and C-H bond functionalized products of hydrosilanes were obtained, this is likely due to the similarities in bond dissociation energies. Soon after, inspired by Macmillan's work[47] on selective functionalization of hydridic C-H bond using quinuclidine as a HAT catalyst, the team led by Wu developed an elegant method for the hydrosilylation of electron-deficient alkenes under photocatalytic, metal-free conditions using modified quinuclidin-3-yl-acetate as the HAT catalyst (**Scheme 2.4**).[48] Under the developed conditions, the hydrosilylation of electron-rich alkenes with quinuclidine failed to provide the hydrosilylated product. Combining a photoredox catalyst with a polarity reversal catalyst ($^i$Pr$_3$SiSH) allowed the hydrosilylation of electron-rich alkenes. In this approach, the range of alkenes and hydrosilanes were investigated.

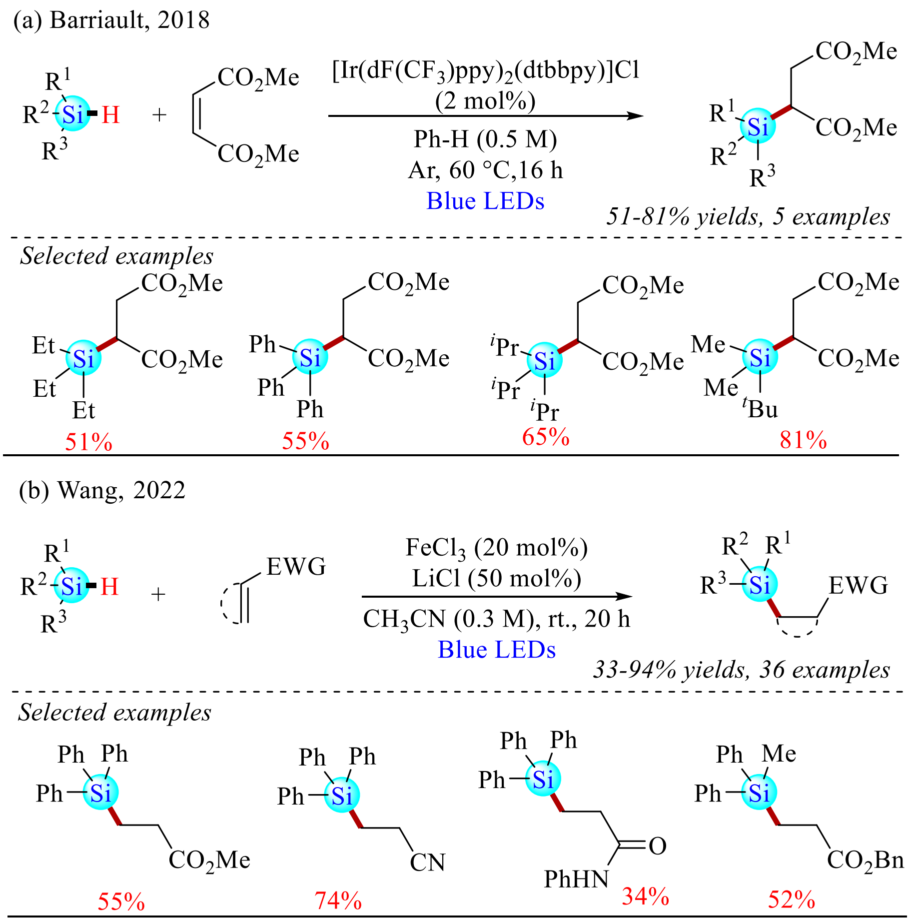


**Scheme 2.5** Chlorine radical-mediated hydrosilylation of activated alkenes

In 2018, Barriault and coworkers uncovered thermal and visible light irradiated, photoredox mediated catalytic generation of the chlorine radical for the functionalization of a variety of substrates such as alkanes, alcohols, ethers, esters, amides, aldehydes, and silanes (**Scheme 2.5a**). The scope of this method has been widely explored for the C-H bond activation of substrates, with a few examples of the Si-H bond of hydrosilanes.[49] In addition, the generation of chlorine radicals through ligand-to-metal charge transfer (LMCT) between the iron catalyst and lithium chloride, under visible light irradiation, promotes silyl radical formation *via* the HAT process from hydrosilanes, which eventually leads to the hydrosilylation of electron-deficient alkenes (**Scheme 2.5b**).[52] However, this method is only limited to arylsilanes and requires high loading of silanes. Reports on the synthesis of $\beta$-silyl-$\alpha$-amino acids were disclosed by Zhang (**Scheme 2.6**)[50] and others.[51] The reaction conditions were similar to the Wu's method (**Scheme 2.4**).

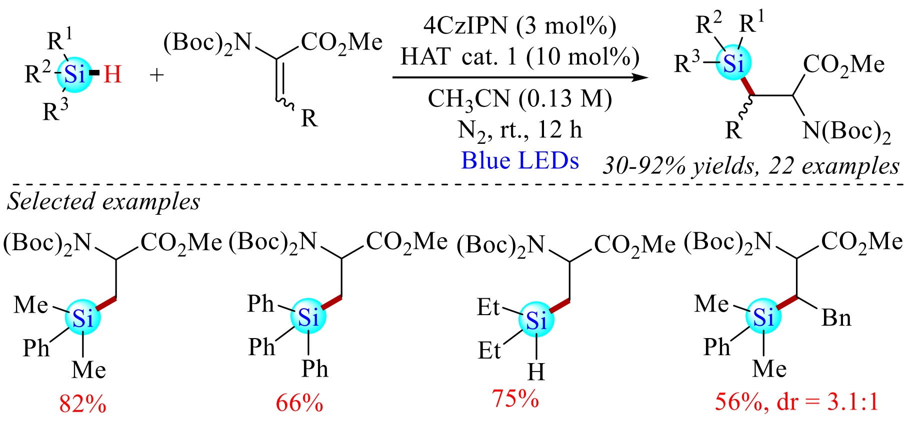


**Scheme 2.6** Synthesis of $\beta$-silyl-$\alpha$-amino acid derivatives through hydrosilylation of activated alkenes

In 2025, the Zhu group achieved hydrosilylation of alkenes using a uranyl(IV)-catalyst. However, this method is limited to tris(trimethylsilyl)silane as a silyl source (**Scheme 2.7**). Under blue LED irradiation, the excited uranyl catalyst undergoes LMCT and generates the silyl radical through hydrogen atom transfer. In this method, the overreactive product were also observed.[53] Concurrently, the Cao group developed a substrate-designed chiral Lewis acid-controlled enantioselective hydrosilylation and hydrogermylation of electron-deficient alkenes by combining anthraquinone as a photocatalyst along with Lewis acid $Zn(OTf)_2$ under blue LED irradiation (**Scheme 2.8**).

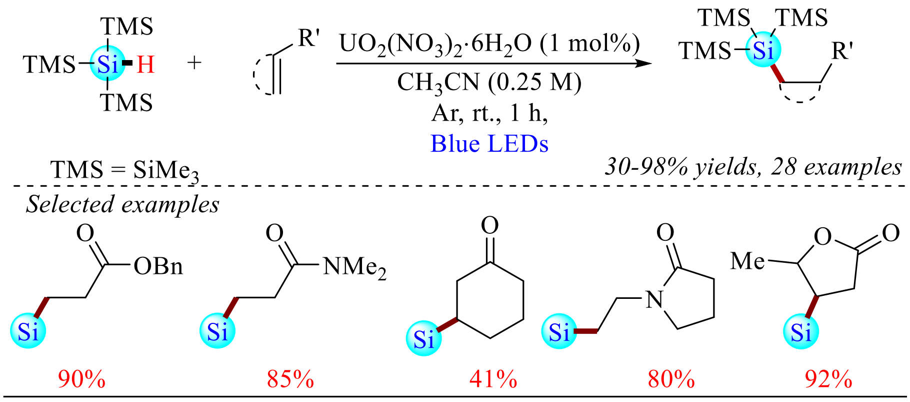


**Scheme 2.7** Uranyl-catalyst-catalyzed hydrosilylation of alkenes

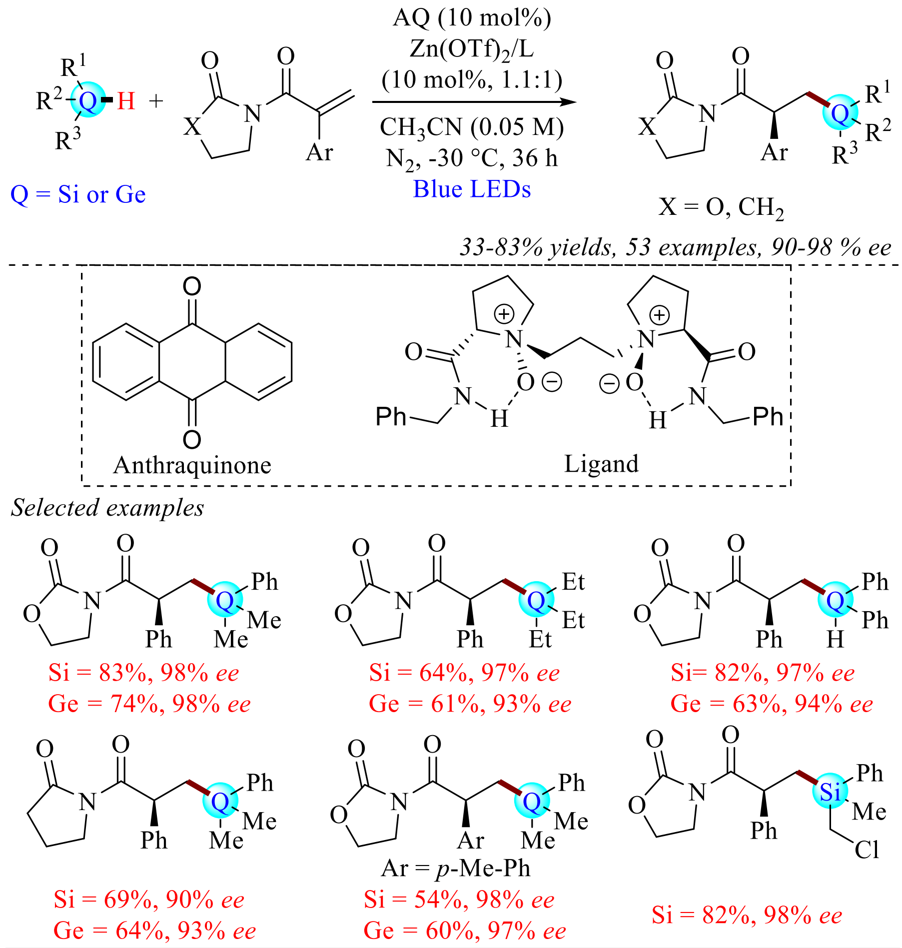


**Scheme 2.8** Dual chiral Lewis acid and photocatalytic merged enantioselective hydrosilylation/hydrogermylation of activated alkenes

Here, the chiral Lewis acid controls the enantioselectivity, while the silyl/germyl radical was generated *via* hydrogen atom transfer from hydrosilane/hydrogermanes at low temperature by anthraquinone, and a wide range of silyl and germyl groups were tolerated under the reaction conditions.[54] Subsequently, hydrogermylation of alkenes *via* HAT also drew attention. In 2022 the Schoenebeck group disclosed a hydrogermylation protocol for the electron-rich alkenes (**Scheme 2.9a**). In this method, 4CzIPN is used as an organophocatalyst along with $^{i}Pr_3SiSH$ as a hydrogen atom transfer catalyst under blue LED irradiation.[55]

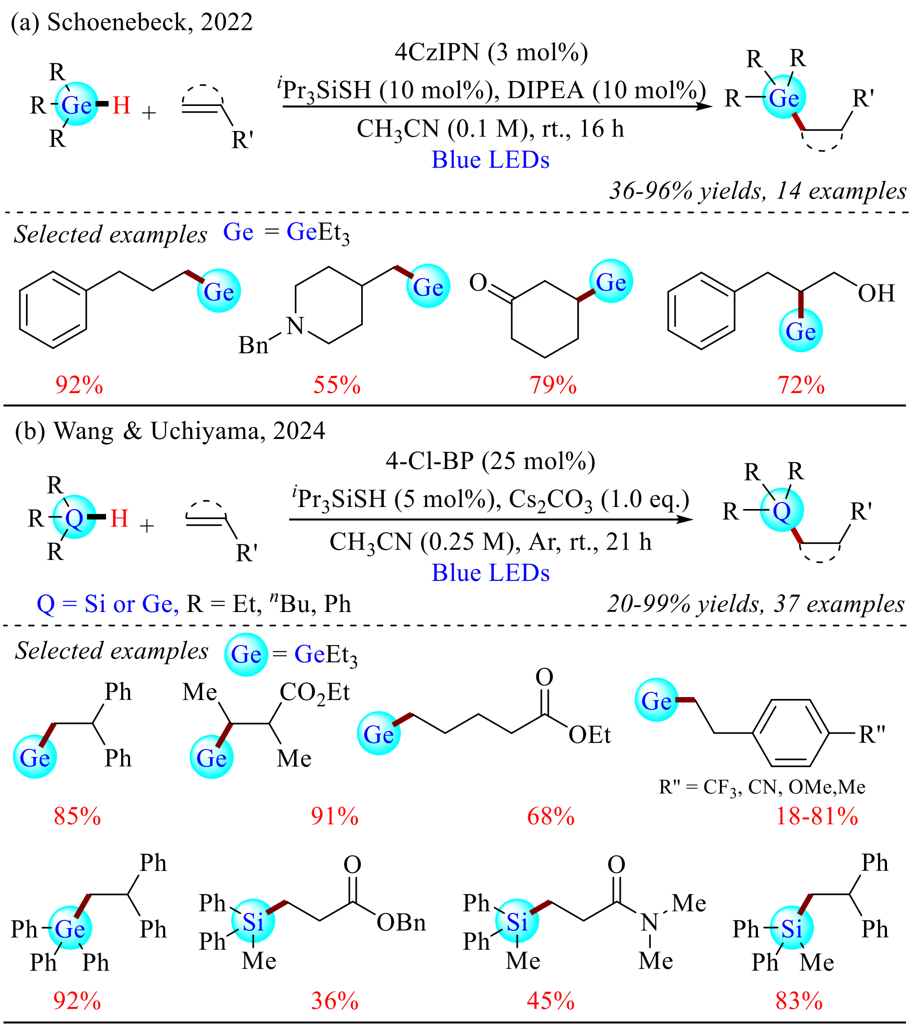


**Scheme 2.9** Hydrogermylation of alkenes using $^{i}Pr_3SiSH$ as HAT catalyst

Recently, Uchiyama group unveiled the visible light-assisted generation of germyl radical from hydrogermanes *via* electron-donor acceptor

(EDA)-catalyzed electron transfer-hydrogen atom transfer process (**Scheme 2.9b**). They utilized $^{i}Pr_3SiSH$ as the HAT catalyst, which also acts as an electron donor *via in situ* formation of $^{i}Pr_3SiS^-$ and electron-deficient 4-chlorobenzophenone (4-Cl-BP) as the acceptor. The EDA complex formation occurs *in situ* under the reaction condition. Upon irradiation with light, electron transfer from thiol anion to electron-deficient 4-chlorobenzophenone leads to the formation of thiol radical, which provides germyl radical through functionalization of the Ge-H bond of hydrogermanes.[56] Also, this strategy was extended for the hydrosilylation of alkenes, with only a few examples.

Despite all these advancements, the development of new, mild and practical methods for the synthesis of organosilanes and organogermanes remains highly desirable.

## 2.3 Objective

In the synthesis of organosilicon and organogermanium compounds from hydrosilanes and hydrogermanes through the functionalization of Si-H and Ge-H bonds, the use of electrophilic radical is crucial.

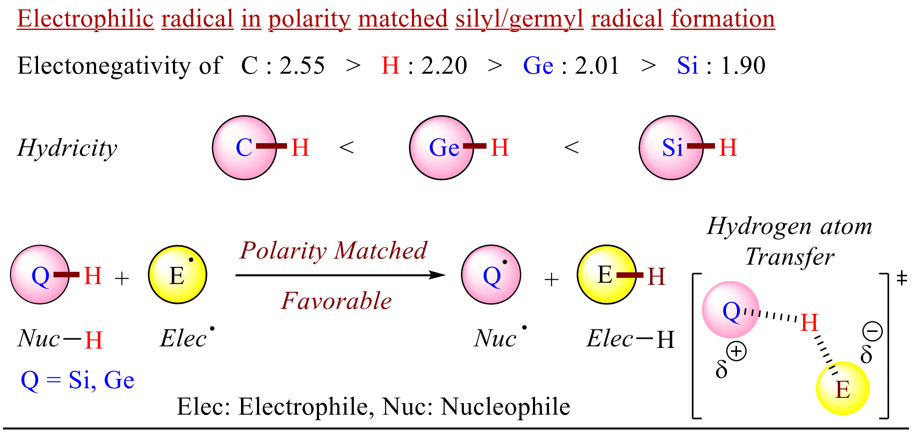


**Scheme 2.10** Electrophilic radical in Si-H and Ge-H bond functionalization

The electropositive nature of silicon and germanium relative to carbon leads to a more hydridic character for Si-H and Ge-H bonds of hydrosilanes and hydrogermanes, making them ideal candidates for functionalization through hydrogen atom transfer by electrophilic radical, and the process is polarity matched (**Scheme 2.10**). The nature of electrophilic radical is also crucial for the chemoselective functionalization of more hydridic Si-H and Ge-H bond. Although, the existing HAT catalyst has been successfully employed in hydrosilylation/hydrogermylation reactions, they are not structurally and electronically tunable to match with the variable bond dissociation energies (BDEs)[57-59] (**Scheme 2.11**) and polar effects[60] associated with different hydrosilanes and hydrogermanes.

Bond dissociation energies of hydrosilanes/hydrogermanes and hydrocarbons

| $Me_3Si-H$ | $Et_3Si-H$ | $PhMe_2Si-H$ | $Ph_2MeSi-H$ | $Ph_3Si-H$ | $(Me_3Si)_3Si-H$ |
|---|---|---|---|---|---|
| 93.2 | 92.8 | 91.3 | 90 | 88.6 | 82.3 (kcal/mol) |

| $Me_3Ge-H$ | $Et_3Ge-H$ | $Bu_3Ge-H$ | $Ph_3Ge-H$ | $Ph_2HGe-H$ |
|---|---|---|---|---|
| 81.6 | 82.3 | 82.6 | 80.2 | 79.5 (kcal/mol) |

| $CH_3-H$ | $CH_3CH_2-H$ | $(CH_3)_2CH-H$ | $(CH_3)_3C-H$ | $PhCH_2-H$ | $Ph_3C-H$ |
|---|---|---|---|---|---|
| 105 | 100.5 | 98.1 | 95.7 | 89.7 | 81.0 (kcal/mol) |

**Scheme 2.11** Bond dissociation energies of hydrosilanes, hydrogermanes and hydrocarbons

In our search for an ideal electrophilic radical to initiate hydrogen atom transfer process, the sulfamidyl radical was recognized to be suitable, as the process is thermodynamically favourable due to the difference in bond dissociation energies between the Si-H/Ge-H bonds of hydrosilanes/hydrogermanes and the corresponding N-H bond of sulfonamide[61,63] (**Scheme 2.12**). In this context, we envisioned utilizing sulfonamide as precursor for electrophilic *N*-centered sulfamidyl radical. Because sulfonamides are readily synthesizable, inexpensive, and can be tuned sterically and electronically to match the variable BDEs of different hydrosilanes and hydrogermanes.

The generation of electrophilic *N*-centered radical pioneered by Knowles[62-64] under visible-light-driven photochemical conditions through proton-coupled electron transfer (PCET) process and further utilized by others in C-H bond functionalization.[65-66] In 2017, the Kanai group utilized sulfonamide as a potent HAT catalyst for allylic and benzylic C-H arylation under visible light photoredox catalysis.[67] Soon after, the Duan group explored the utility of sulfonamide in C(sp$^3$)-H alkylation under metal-free photoredox catalysis.[68]

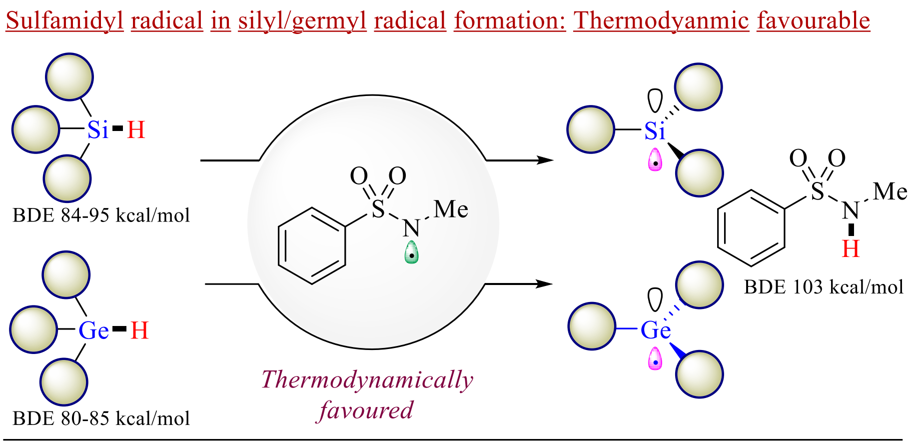


**Scheme 2.12** Sulfamidyl radical in functionalization of Si-H/Ge-H bond

Herein, we developed the first method to utilize sulfonamides as a photoinduced hydrogen atom transfer catalyst for the hydrosilylation/hydrogermylation of electron-deficient alkenes under metal-free visible light irradiation for the synthesis of functionalized organosilanes/organogermanes.

## 2.4 Present work

### 2.4.1 Selection of model reaction

The hydrosilylation of benzyl acrylate (**1a**) with *tert*-butyldimethylsilane (**2a**) was selected as a model reaction to systematically evaluate the reaction parameters and establish optimal conditions for assessing the feasibility of sulfonamide as a hydrogen atom transfer catalyst for the generation of silyl radical (**Scheme 2.13**).

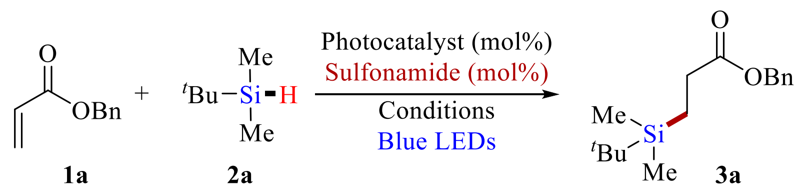


**Scheme 2.13** Model reaction to screen the reaction conditions

### 2.4.2 Screening of sulfonamides as a hydrogen atom transfer catalyst

To evaluate series of sulfonamides as HAT catalysts in the hydrosilylation of alkenes, 4CzIPN was selected as an organic photocatalyst owing to its broad redox potential window, $K_3PO_4$ was employed as the base for deprotonation, and an acetone-water mixture as the reaction medium under 450 nm blue LED irradiation at room temperature.

**Table 2.1** Screening of sulfonamides

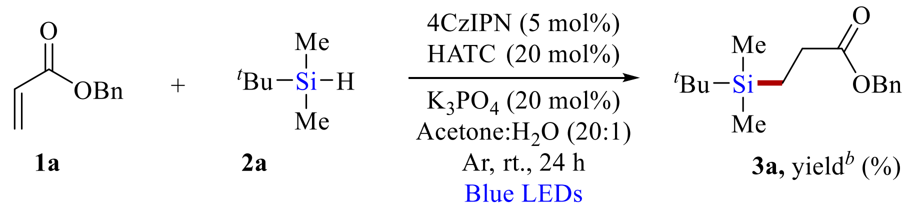


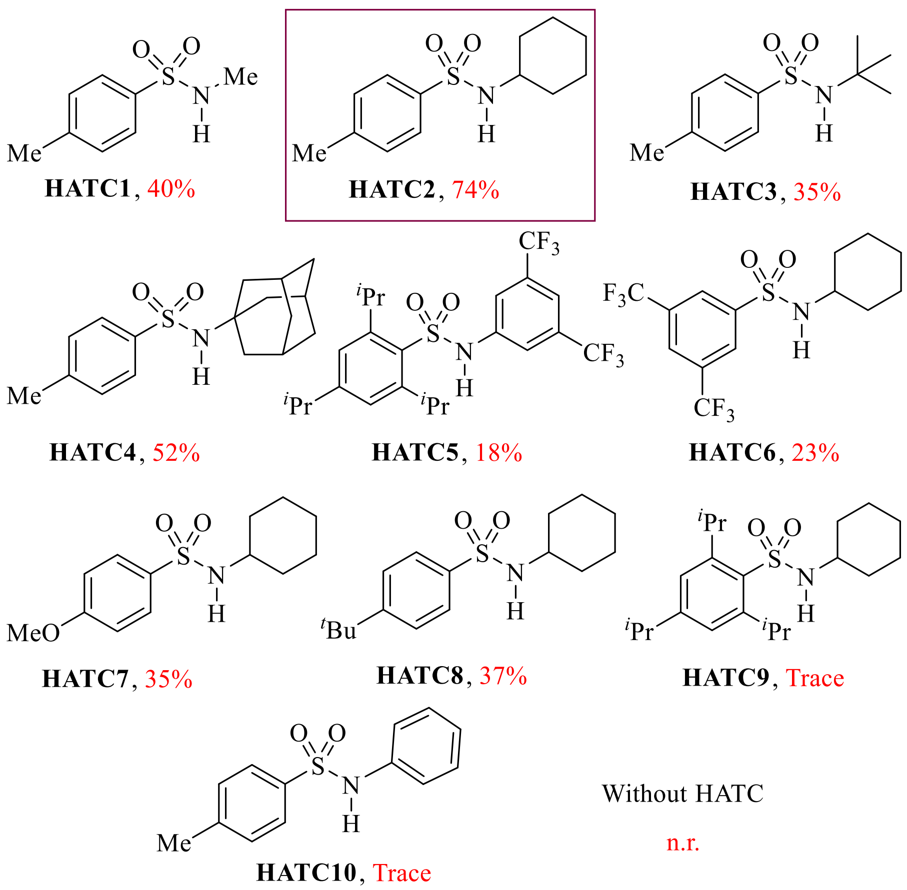


[a]Reaction conditions: **1a** (0.2 mmol), **2a** (0.6 mmol), 4CzIPN (0.01 mmol), HATC (0.04 mmol), $K_3PO_4$ (0.04 mmol) and 2 mL of Acetone:$H_2O$ (20:1) were irradiated under blue LEDs. [b]Isolated yield. n.r. = no reaction

Firstly, we evaluate effect of the sulfonamide as HAT catalyst (**Table 2.1**) using *N*,4-dimethylbenzenesulfonamide (HATC1), which provides 40% of desired hydrosilylated product **3a**. This result encouraged us to further examining the conditions. Notably, the replacement of the methyl group with a cyclohexyl group (HATC2) resulted in a significant increase and in the yield of the desired product to 74%. On the other hand, the yield drastically decreased when the *N*-cyclohexyl substituent was replaced with more sterically hindered *tert*-butyl (HATC3, 35%) and 1-adamantyl groups (HATC4, 52%). These results indicate that the cyclohexyl group provides the optimal steric and electronic environment for functionalization of the Si-H bond of hydrosilanes. Further screening with diaryl sulfonamide (HATC5), which was effective in the case of activated C($sp^3$)-H bond functionalization,[67] yielded the desired product only in 18%. Tuning of electronics and sterics of the HATC2 aryl ring with different electron-withdrawing and electron-donating groups provided inferior results. For example, replacement of the *p*-tolylsulfonyl group with 3,5-bistrifluoromethylphenylsulfonyl (HATC6) *p*-methoxyphenylsulfonyl (HATC7), or *p*-*tert*-butylphenylsulfonyl (HATC8) yielded 23%, 35% and 37% of the desired product respectively. Whereas only a trace amount of desired product formation was observed using *N*-cyclohexyl-2,4,6-triisopropylbenzenesulfonamide (HATC9) and 4-methyl-*N*-phenylbenzenesulfonamide (HATC10). However, no hydrosilylated product was observed in the absence of sulfonamide as a hydrogen atom transfer catalyst.

### 2.4.3 Screening of photocatalysts

In our effort to develop an efficient hydrosilylation protocol using sulfonamides as HAT catalyst, 4CzIPN proved to be effective during the screening of HAT catalysts. To achieve a better yield, we further screened different metal-based photocatalysts and organophotocatalysts (**Table 2.2**). Ir(dF($CF_3$)ppy)$_2$(dtbbpy)]$PF_6$ (entry 1) was able to provide the desired product in only 10% yield, whereas using Ru(bpy)$_3Cl_2\cdot 6H_2O$

(entry 2), product formation was not observed. On the other hand, organophotocatalysts such as Eosin-Y (entry 3) and Mes-Acr-Ph$^+$BF$_4^-$ (entry 4) were unable to provide the desired product. However, 4CzIPN (entry 5) outperformed other photocatalysts, yielding 74% of desired product with a 5 mol% photocatalyst loading. Furthermore, lowering the loading of 4CzIPN to 3 mol% (entry 6) and 1 mol% (entry 7) results in a slight decrease in yield. In the absence of a photocatalyst, product formation was not observed.

**Table 2.2** Screening of photocatalysts

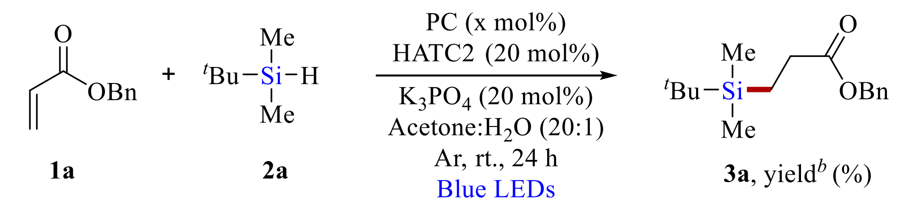


| Entry | Photocatalyst | mol% | Yield$^b$ (%) |
|---|---|---|---|
| 1. | [Ir(dF(CF$_3$)ppy)$_2$(dtbbpy)] PF$_6$ | 5 | 10 |
| 2. | Ru(bpy)$_3$Cl$_2$.6H$_2$O | 5 | n.r. |
| 3. | Eosin-Y | 5 | n.r. |
| 4. | Mes-Acr-Ph$^+$BF$_4^-$ | 5 | n.r. |
| **5.** | **4CzIPN** | **5** | **74** |
| 6. | 4CzIPN | 3 | 69 |
| 7. | 4CzIPN | 1 | 69 |
| 8. | none | - | n.r. |

$^a$Reaction conditions: **1a** (0.2 mmol), **2a** (0.6 mmol), Photocatalyst (x mol%), HATC2 (0.04 mmol), $K_3PO_4$ (0.04 mmol) and 2 mL of Acetone:$H_2O$ (20:1) were irradiated under blue LEDs. $^b$Isolated yield. n.r. = no reaction.

### 2.4.4 Screening of bases

The screening of base (**Table 2.3**) was started with 2.0 equivalents of carbonate base $K_2CO_3$, which establishes the compatibility of inorganic bases with 40% yield of hydrosilylated product **3a** (entry 1). Other carbonate bases, such as $Na_2CO_3$ (entry 2) and $Cs_2CO_3$ (entry 3), show inferior results. Furthermore, phosphate bases $K_3PO_4$ (entry 4) and

$K_2HPO_4$ (entry 5) were tested, and to our surprise $K_3PO_4$-assisted conditions yielded 65% hydrosilylated product.

**Table 2.3** Screening of different bases

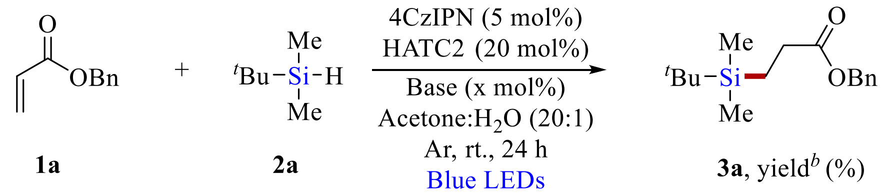


| Entry | Base | equivalent | Yield[b] (%) |
|---|---|---|---|
| 1. | $K_2CO_3$ | 2 | 40 |
| 2. | $Na_2CO_3$ | 2 | 24 |
| 3. | $Cs_2CO_3$ | 2 | 42 |
| 4. | $K_3PO_4$ | 2 | 65 |
| 5. | $K_2HPO_4$ | 2 | 05 |
| 6.[c] | $^iPr_2EtN$ | 2 | n.r. |
| 7.[c] | 2,6-Lutidine | 2 | n.r. |
| 8. | $K_3PO_4$ | 1 | 69 |
| 9. | $K_3PO_4$ | 0.5 | 71 |
| **10.** | $\mathbf{K_3PO_4}$ | **0.2** | **74** |
| 11. | $K_2CO_3$ | 0.2 | 45 |
| 12. | none | 0 | Trace |

[a]Reaction conditions: **1a** (0.2 mmol), **2a** (0.6 mmol), 4CzIPN (0.01 mmol), HATC2 (0.04 mmol), base (x equiv.) and 2 mL of Acetone:$H_2O$ (20:1) were irradiated under blue LEDs. [b]Isolated yield.[c]without water. n.r. = no reaction.

On the other hand, no reaction was observed while using organic bases $^iPr_2EtN$ (entry 6) and 2,6-lutidine (entry 7). Since $K_3PO_4$ outperformed the other tested bases, we sought to reduce the loading of $K_3PO_4$, and with 1 equivalent of $K_3PO_4$, the yield of the hydrosilylated product slightly increased (entry 8). Furthermore, lowering the loading of $K_3PO_4$ resulted in a slight increase in yield, and 20 mol% of $K_3PO_4$ is sufficient to produce the desired hydrosilylated product in 74% yield (entry 10). We also screened $K_2CO_3$ with a 20 mol% loading, but it provided inferior results (entry 11). The product formation was not observed in the absence of a base, which indicates the necessity of the base for the reaction (entry 12).

### 2.4.5 Screening of solvents

After successfully establishing the screening of the HAT catalyst, photocatalyst, and base, we move towards the screening of different solvents (**Table 2.4**).

**Table 2.4** Screening of solvents

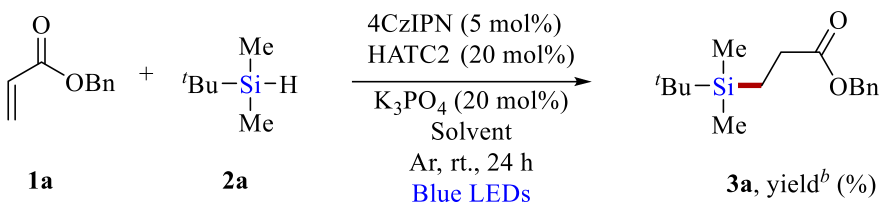


**1a** **2a** **3a**, yield[b] (%)

| Entry | Solvent | Yield[b] (%) |
|---|---|---|
| 1. | $CH_3CN$ | 23 |
| 2. | DMSO | 10 |
| 3. | Acetone | 35 |
| 4. | DMF | n.r. |
| 5. | $PhCF_3$ | 12 |
| 6. | DCM | n.r. |
| 7. | $CH_3CN$:$H_2O$ (20:1) | 69 |
| **8.** | **Acetone:$H_2O$ (20:1)** | **74** |

[a]Reaction conditions: **1a** (0.2 mmol), **2a** (0.6 mmol), 4CzIPN (0.01 mmol), HATC2 (0.04 mmol), $K_3PO_4$ (0.04 mmol) and 2 mL solvent were irradiated blue LEDs. [b]Isolated yield. n.r. = not detected

Begin the screening with polar aprotic solvent acetonitrile (entry 1), which gives 23% hydrosilylated product. The more polar and amphiphilic solvent dimethylsulfoxide yielded only 10% of the desired product (entry 2). Acetone was able to produce 35% of the desired product (entry 3), while in the case of dimethylformamide, the desired product formation was not observed (entry 4). Using a non-polar aprotic trifluorotoluene as a solvent yielded 12% of hydrosilylated product (entry 5). While using dichloromethane, product formation was not observed (entry 6). The mixture of acetonitrile and water (20:1) shows a significant increase in yield, from 23% to 69% (entry 1 *vs* entry 7), indicating that a small amount of water is crucial for the transformation, likely facilitating the dissolution of the inorganic base and accelerating the reaction. Using a mixture of acetone and water (20:1), the yield of the desired product further increases to 74% (entry 8). Thus, a mixture of acetone and water (20:1) serves as an ideal solvent system for the hydrosilylation of activated alkenes using sulfonamide (HATC2) as a HAT catalyst under visible light-assisted organophotocatalytic conditions.

### 2.4.6 Scope of electron-deficient alkenes

After successfully establishing the optimal conditions using sulfonamide (HATC2) as the HAT catalyst, we sought to screen the scope of different activated alkenes (**Scheme 2.14**), using $^t$BuMe$_2$SiH (**2a**) and PhMe$_2$SiH (**2b**) as silane precursors. As with benzyl acrylate, the reaction works with *n*-butyl acrylate **1b** to afford the corresponding product **3b** in 64% yield. Furthermore, it was found that *α*-methylene-*γ*-butyrolactone **1c** was an effective acceptor and yielded the desired product **3c** in 84% yield. Methyl and benzyl maleate smoothly underwent hydrosilylation with $^t$BuMe$_2$SiH (**2a**) to produce **3d** and **3e** in 61% and 58% yield respectively. Cyclopent-2-en-1-one **1f**, a cyclic internal activated alkene, was successfully hydrosilylated to produce the *β*-silylated cyclopentanone **3f** in 43% yield. The *N*,*N*-diphenyl acrylamide, **1g**, affords the desired product **3g** in 67% yield. On the other hand, acrylamides derived from pyrrolidinone (**1h**) and oxazolidinone (**1i**) also reacted smoothly to give 73% (**3h**) and 40% (**3i**) of desired product, respectively. Fortunately, *β*-silyl-*α*-amino acid ester derivatives were also synthesized from *N*-phthaloyl (**1j**) and bis-*N*-Boc-protected (**1k**) dehydroalanine ester, provided the corresponding hydrosilylated product in 39% (**3j**) and 96% (**3k**) yield respectively. Scope of the electron-deficient alkenes was also extended to diphenyl vinylphosphine oxide (**1l**) and phenyl vinyl sulfone (**1m**), which affords hydrosilylated products in good to excellent yield (**3l-3n**).

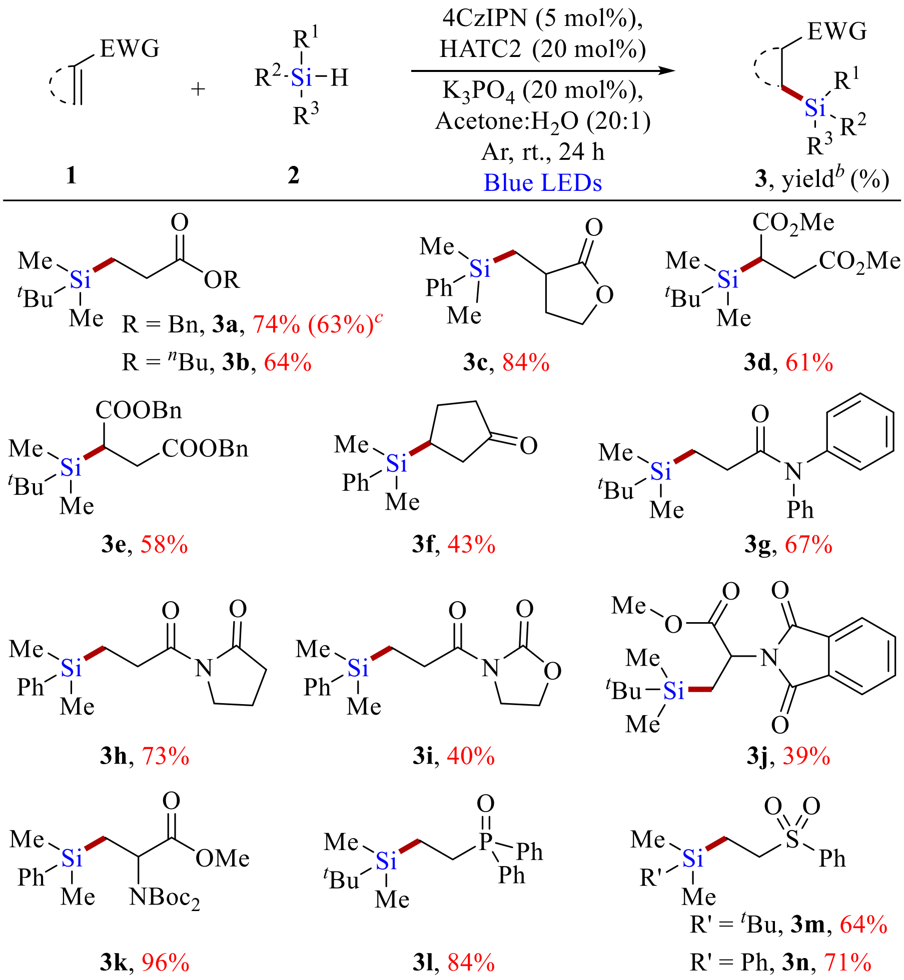

$^{a}$Reaction conditions: **1** (0.2 mmol), **2** (0.6 mmol), 4CzIPN (0.01 mmol), HATC2 (0.04 mmol), $K_3PO_4$ (0.04 mmol) and 2 mL of Acetone:$H_2O$ (20:1) were irradiated under blue LEDs. $^{b}$isolated yield. $^{c}$yield of 1.5 mmol reaction after 36 h.

**Scheme 2.14** Scope of electron-deficient alkenes in hydrosilylation

Nevertheless, when diethyl vinylphosphonate was used as an electron-deficient alkene, the intended product was not observed. The practicality of the developed protocol was further established through a 1.5 mmol scale reaction, which provided 63% yield of the hydrosilylated product **3a**.

### 2.4.7 Scope of hydrosilanes

After successfully testing series of activated alkenes, we turned our attention towards the scope of hydrosilanes (**Scheme 2.15**). For screening of different hydrosilanes, benzyl acrylate (**1a**) was utilized as an activated alkene. The desired product **3o-s** was obtained effectively *via* hydrosilylation of benzyl acrylate (**1a**) with both linear and branched hydrosilanes, such as triethylsilane (**2c**), tri-*n*-propyl silane (**2d**), tri-*n*-butyl silane (**2e**), tri-*iso*-propylsilane (**2f**) and benzyl dimethyl silane (**2g**) in good to excellent yield (64-88%).

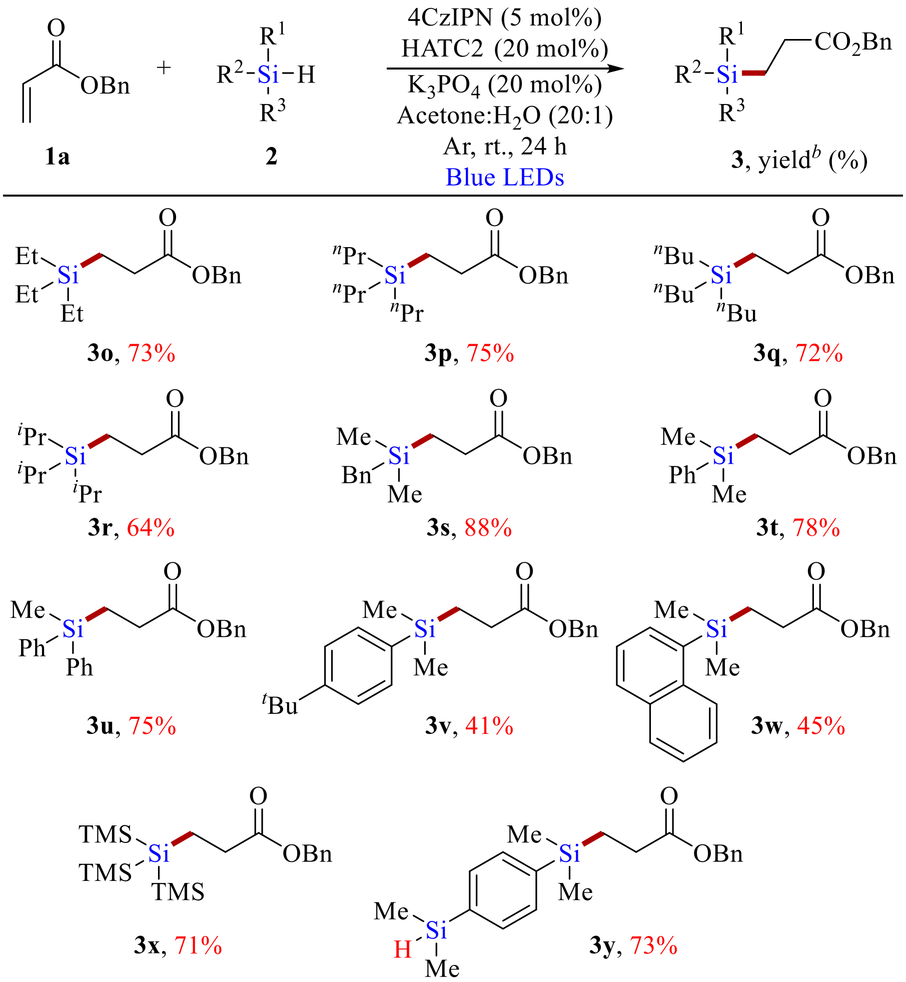


[a]Reaction conditions: **1a** (0.2 mmol), **2** (0.6 mmol), 4CzIPN (0.01 mmol), HATC2 (0.04 mmol), $K_3PO_4$ (0.04 mmol) and 2 mL of Acetone:$H_2O$ (20:1) were irradiated under blue LEDs. [b]isolated yield.

**Scheme 2.15** Scope of hydrosilanes in hydrosilylation of activated alkenes

It is worth to mention here that, where Fagnoni[46] observed both Si-H and C-H bond functionalized products using $Et_3SiH$ (**2c**) under TBADT-mediated hydrosilylation of alkenes, however, we only observed the Si-H bond functionalized product and the C-H functionalized product was not detected. Furthermore, different aromatic hydrosilanes, such as dimethylphenylsilane (**2b**) and diphenylmethylsilane (**2h**), underwent hydrosilylation smoothly to afford the desired products **3t** (78%) and **3u** (75%) respectively. Arylsilane with *tert*-butyl substituent on the aryl ring (**2i**) gives **3v** in slightly lower yield. The dimethyl(naphthalen-1-yl)silane (**2j**) affords the hydrosilylated product in 45% yield, whereas $(TMS)_3SiH$ (**2k**) provided the corresponding product in 71% yield. In addition, only mono-hydrosilylated product **3y** was observed in 73% yield on reaction with *para*-phenylenebis(dimethylsilane). The anticipated bis-hydrosilylated product was not detected by the subsequent reaction of **3y** as silane with benzyl acrylate **1a** under standard reaction conditions. The $Ph_3SiH$ was found to be inefficient under the developed reaction conditions.

### 2.4.8 Hydrogermylation of activated alkenes

The successful development of sulfonamide as a hydrogen atom transfer catalyst for the hydrosilylation of activated alkenes inspired us to extend the scope of this method to hydrogermylation of activated alkenes (**Scheme 2.16**). Notably, condition that are ideal for hydrosilylation was also found to be effective in the hydrogermylation of activated alkenes. As representative germylating agents, $^{n}Bu_3GeH$ (**4a**) and $Ph_3GeH$ (**4b**) were used to gain the scope of the activated alkenes. To our surprise, treating benzyl acrylate **1a** with tri-*n*-butyl germane **4a** under the conditions optimized for hydrosilylation provided the desired hydrogermylation product **5a** in 93% yield, validating the effectiveness of this protocol for hydrogermylation of activated alkenes. Dimethyl maleate and *α*-methylene-*γ*-butyrolactone are effective acceptors in hydrogermylation reactions with triphenyl germane (**4b**), yielding the desired products **5b** and **5c** in 94% and 90% yield respectively. Notably, bis-*N*-Boc-protected dehydroalanine ester **1k** was also a suitable substrate for the hydrogermylation reaction that produced the interesting *β*-germyl-*α*-amino acid derivative **5d** in an 84% yield. Additionally, other acrylate derivatives, like *α*-methyl acrylate **1n** and phenyl acrylate **1o**, were also effective reactants that produced hydrogermylation product **5e** and **5f** in good yield.

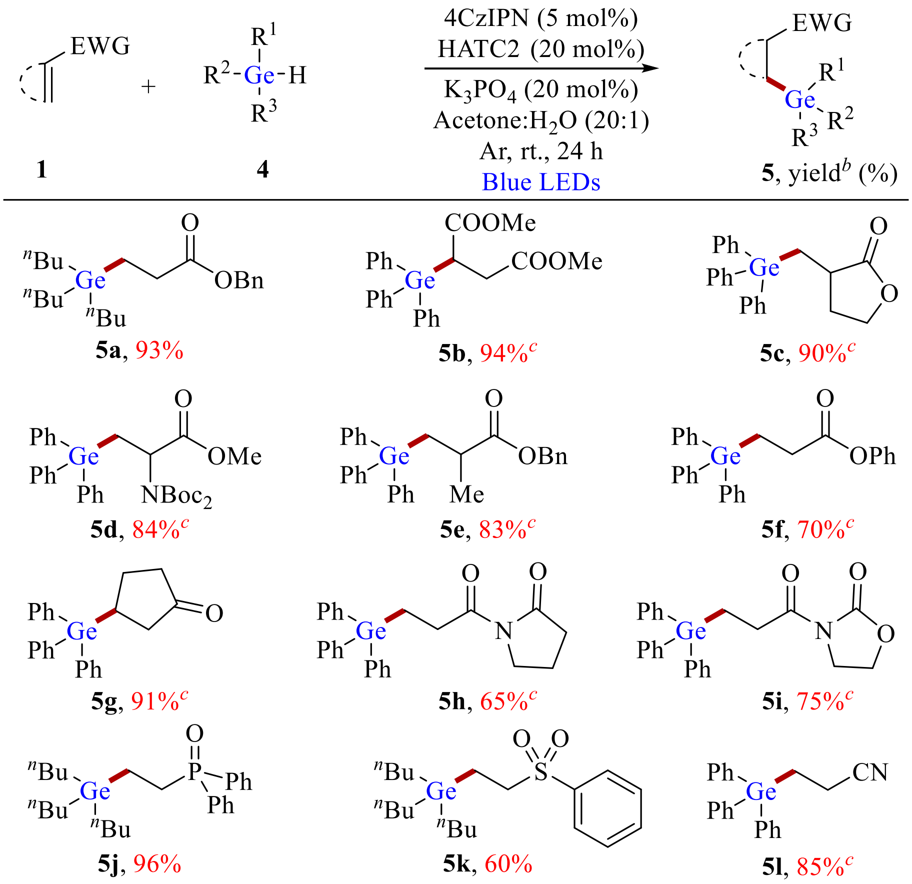


[a]Reaction conditions: **1** (0.2 mmol), **4** (0.6 mmol), 4CzIPN (0.01 mmol), HATC2 (0.04 mmol), $K_3PO_4$ (0.04 mmol) and 2 mL of Acetone:$H_2O$ (20:1) were irradiated under blue LEDs. [b]isolated yield. [c]using 0.4 mmol of $Ph_3GeH$.

**Scheme 2.16** Scope of hydrogermylation of activated alkenes

Further, the cyclopentenone gave the desired product **5g** in 91% yield. Other activated alkenes, such as *N*-acryloyl pyrrolidinone (**1h**) and *N*-acryloyl oxazolidinone (**1i**), smoothly underwent hydrogermylation to give **5h** and **5i** in good yield. Furthermore, screening the scope of activated alkenes such as diphenyl vinylphosphine oxide **1l**, phenylvinylsulfone **1m**, and acrylonitrile **1p** provided the desired organogermanes **5j-5l** in good to excellent yield (60-96%).

### 2.5 Mechanistic investigation

To gain mechanistic insight into the reaction, a series of control experiments was performed, including radical inhibition experiments, deuterium-labelling studies, fluorescence quenching, cyclic voltammetry measurement, quantum yield determination, and light on-off experiment.

### 2.5.1 Radical inhibition studies

To identify the involvement of radical in the mechanism, the radical-inhibiting experiment was performed using 3.0 equivalents of radical scavenger TEMPO, under the standard reaction conditions with **1a** and **2a** for hydrosilylation reaction, **1d** and **4b** for hydrogermylation reaction (**Scheme 2.17**). In both cases, the formation of the desired photoproduct was fully suppressed. These results support the involvement of radical in this reaction.

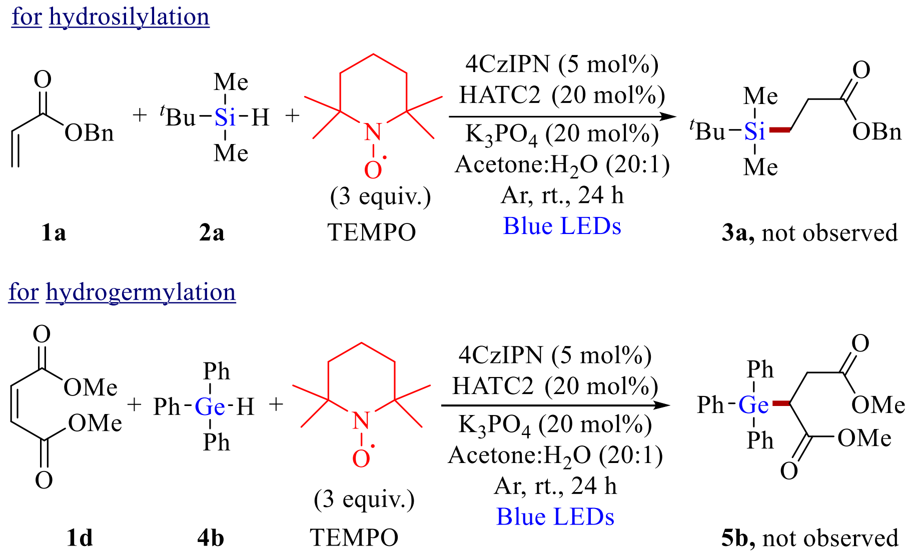


**Scheme 2.17** Radical inhibition studies

### 2.5.2 Deuterium labelling experiment

The deuterium labelling studies were performed to identify the source of the proton and keto-enol isomerization of the hydrosilylated product (**Scheme 2.18**). To identify the source of proton, the reaction of **1a** and **2a** was performed under the standard conditions with $D_2O$ instead of $H_2O$ and found 65% deuterium incorporation, which indicates that $H_2O$ could be a source of proton. On the other hand, replacement of acetone with acetone-$d_6$ doesn't provide any deuterium incorporation in the hydrosilylated product, revealing that acetone doesn't act as a proton donor.

When the photoproduct **3a** was treated in standard reaction conditions in the absence of **1a** and **2a** with $D_2O$ instead of $H_2O$, no deuterium incorporation in **3a** was observed. This clearly suggests that the $\alpha$-H of photoproduct **3a** is not involved in further keto-enol isomerization.

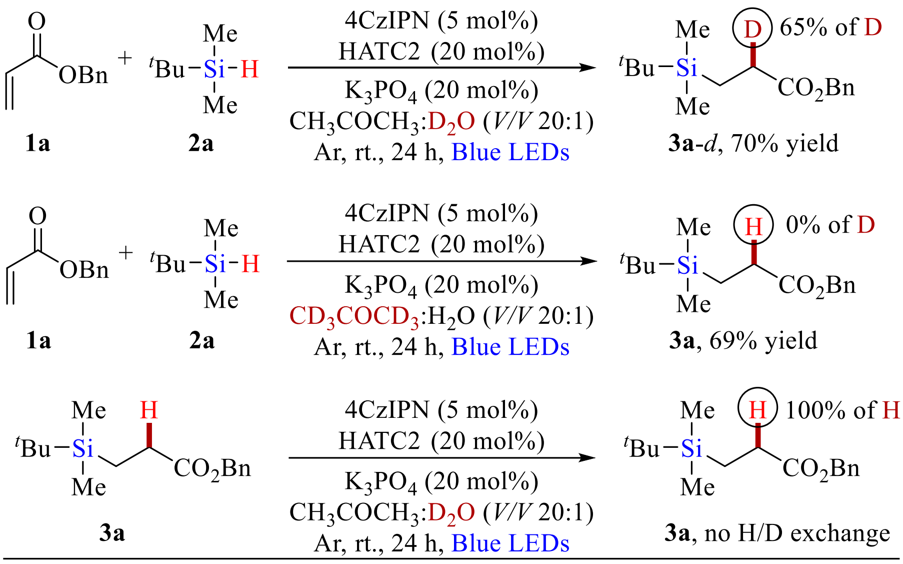


**Scheme 2.18** Deuterium labelling studies

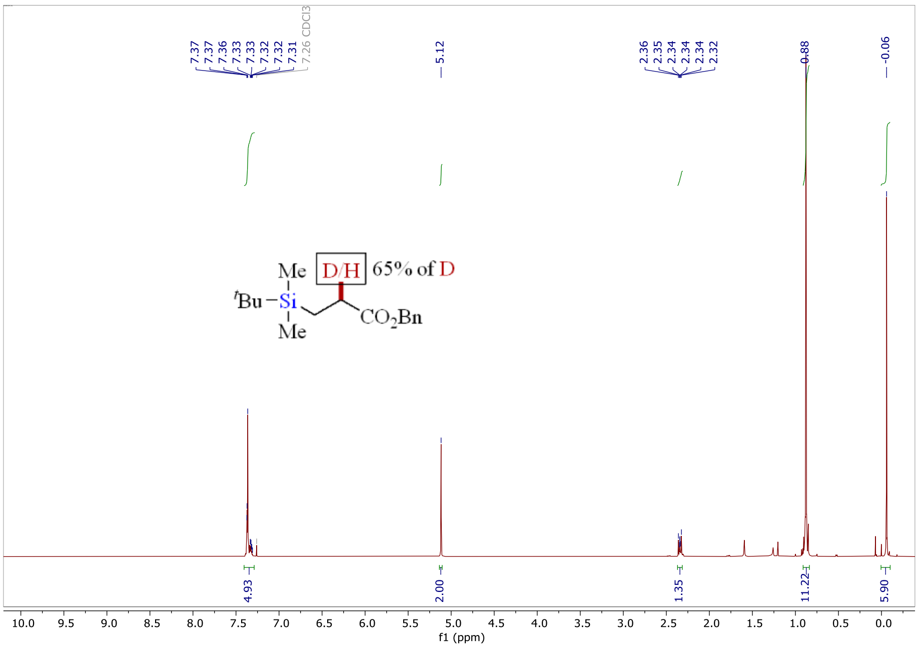


**Figure 2.1** $^1H$ NMR of deuterium studies

### 2.5.3 Stern-Volmer quenching

Stern-Volmer quenching studies were performed to identify the species that quenches the excited state photocatalyst during the course of the reaction. The quenching study was conducted between the photocatalyst 4CzIPN solution and other reaction components, including the activated alkene **1a**, hydrosilane **2a**, hydrogermane **4b**, and sulfonamide (HATC2). This study revealed that only deprotonated sulfonamide (potassium salt of HATC2) was the actual quencher of the excited photocatalyst (4CzIPN$^{*}$) (**Scheme 2.19**); neither HATC2, benzyl acrylate (**1a**) nor hydrosilane $^{t}BuMe_2SiH$ (**2a**)/hydrogermane $Ph_3GeH$ (**4b**) quenches the fluorescence of the excited organophotocatalyst.

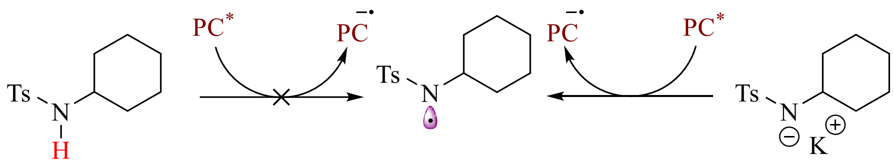


**Scheme 2.19** Representation for the generation of sulfamidyl radical

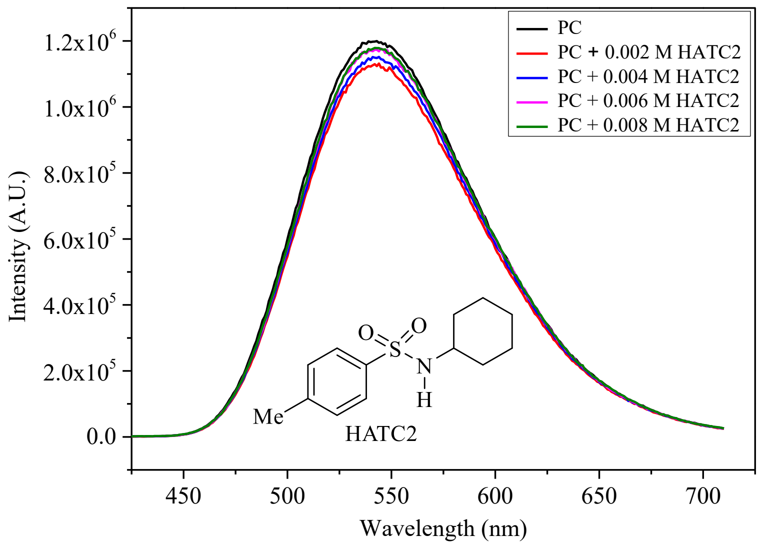


**Figure 2.2** Fluorescence quenching of 4CzIPN vs HATC2

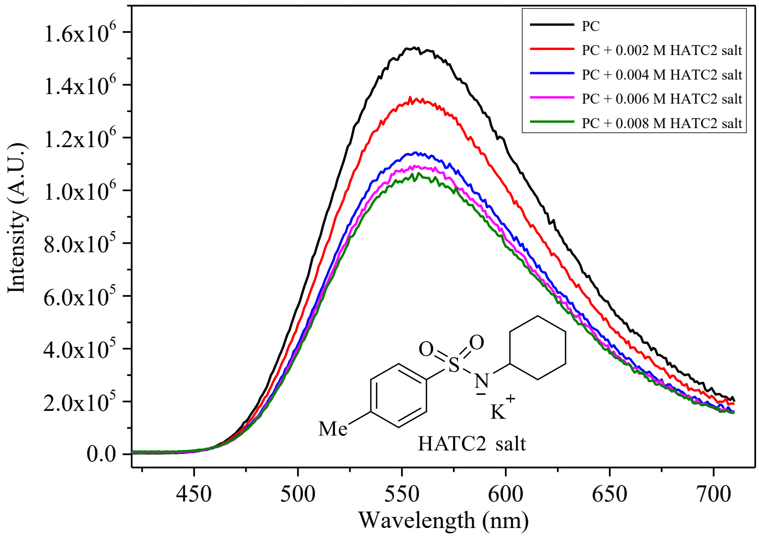


**Figure 2.3** Fluorescence quenching of 4CzIPN vs potassium salt of HATC2

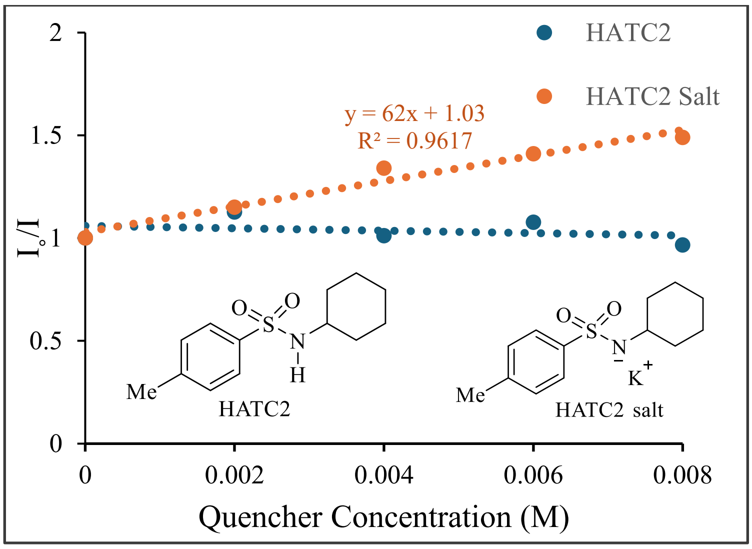


**Figure 2.4** Stern-Volmer plot for quenching of excited state 4CzIPN with HATC2 and the potassium salt of HATC2

### 2.5.4 Quantum yield

To identify the involvement of the radical chain mechanism in the reaction, we calculated the quantum yield by performing the standard reaction for 3 hours, and observed quantum yield was 0.181, which ruled out the possible involvement of a radical chain mechanism.

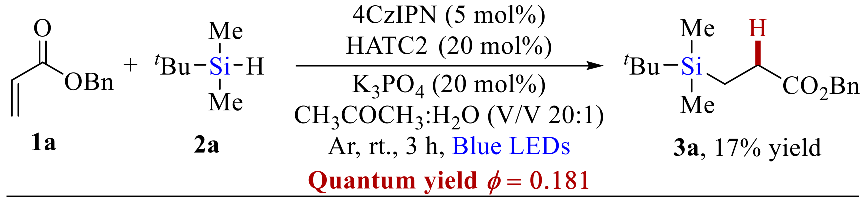


**Scheme 2.20** Quantum yield calculation

### 2.5.5 Cyclic-voltammetry study

A cyclic voltammogram was recorded for the potassium salt of *N*-cyclohexyl-4-methylbenzenesulfonamide, an oxidation peak was observed at +0.86 V vs SCE, which is significantly less than the oxidation potential of the excited state of 4CzIPN* (+1.35 V vs SCE)[76], allowing the oxidation of deprotonated sulfonamide and generation of sulfamidyl radical.

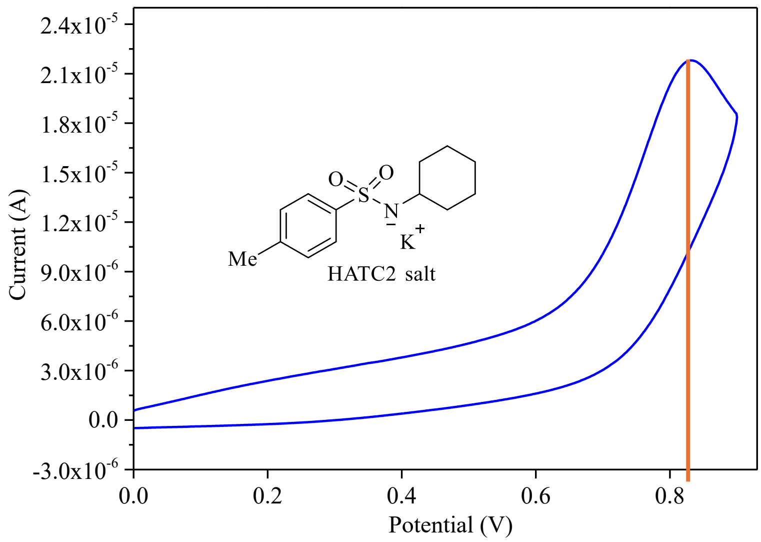


**Figure 2.5** Cyclic voltametric graph for potassium salt of *N*-cyclohexyl-4-methylbenzenesulfonamide (HATC2)

### 2.5.6 Theoretical Studies

The N-H bond dissociation energies of different HATC, Si-H, Ge-H, and C-H BDE of hydrosilanes and hydrogermanes, and the energy barrier for the abstraction of hydrogen from hydrosilanes and hydrogermanes by sulfamidyl radical were calculated. The calculations were carried out using Gaussian 16 software[69] and employing the M06-2X functional, which is considered a more suitable functional for computations involving organic and main group elements chemistry using B3LYP functional.[70-72] Here we have opted for two separate methods; M06-2X/6-31G(d,p) for silicon (Si), while M06-2X/6-311G(d,p) for the germanium (Ge) containing compounds.[73-74] Additionally, to verify the accuracy of the optimization we calculated frequencies and discovered that all of the frequencies for geometry optimizations were positive, while just one negative (imaginary) frequency was detected for the transition states. The active Gibbs free energy ($\Delta G^{\neq}$) and change in Gibbs free energy ($\Delta G$) were also evaluated using these frequency calculations. All energies are expressed in kcal/mol.

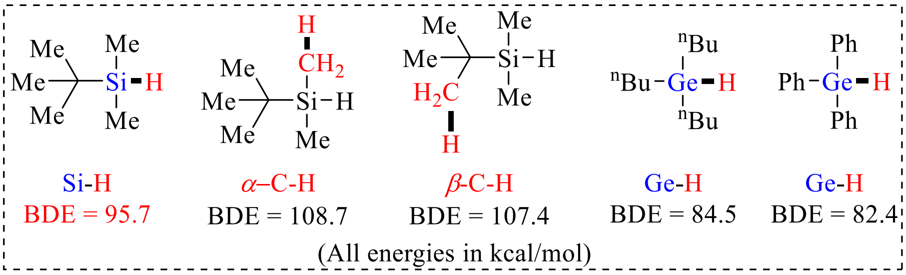


**Scheme 2.21** Bond dissociation energy of Si-H, C-H bond of hydrosilanes and Ge-H bond of corresponding hydrogermanes

**Table 2.5** Bond dissociation energy for the N-H bonds of the different sulfonamides (Hydrogen atom transfer catalyst)

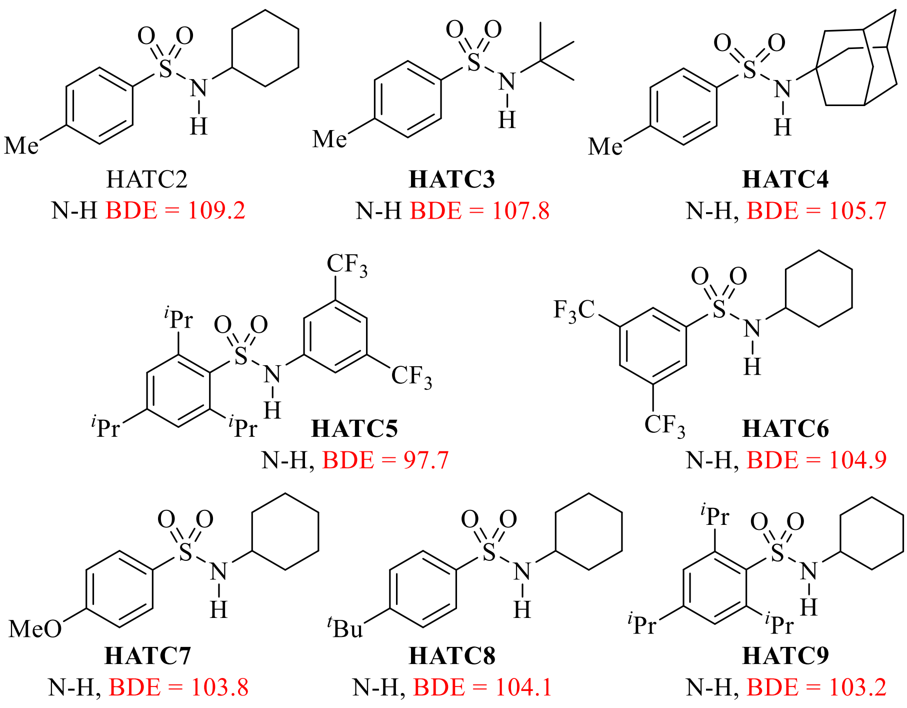


(All energies in kcal/mol)

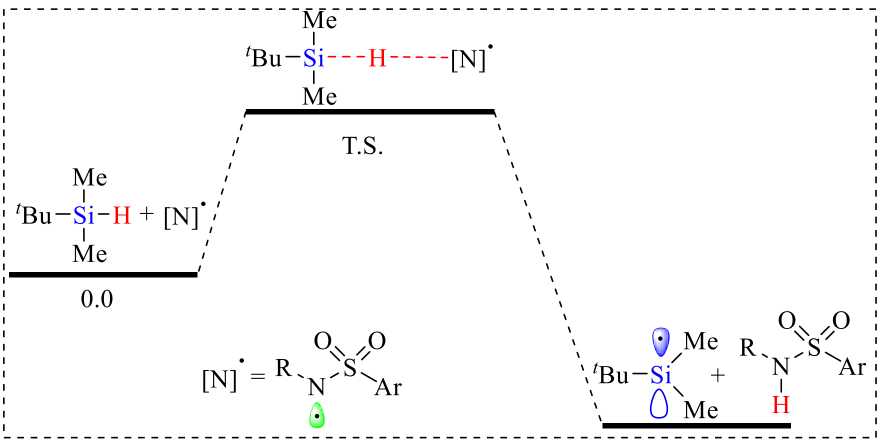


**Scheme 2.22** Energy barriers for the hydrogen atom transfer process between *tert*-butyldimethylsilane **2a** and different electrophilic sulfamidyl radicals

**Table 2.6** DFT calculated energy barriers for the hydrogen atom transfer process of *tert*-butyldimethylsilane **2a** with different sulfamidyl radicals (Thermal free energy corrections are considered)

| HATC | $\Delta G^{\neq}$ (kcal/mol) | $\Delta G$ (kcal/mol) |
|---|---|---|
| **HATC2** | **11.8** | **-9.3** |
| HATC3 | 13.9 | -6.9 |
| HATC4 | 16.2 | -6.4 |
| HATC5 | 14.7 | 2.3 |
| HATC6 | 14.4 | -3.8 |
| HATC7 | 16.2 | -4.1 |
| HATC8 | 14.3 | -4.4 |
| HATC9 | 14.8 | 3.3 |

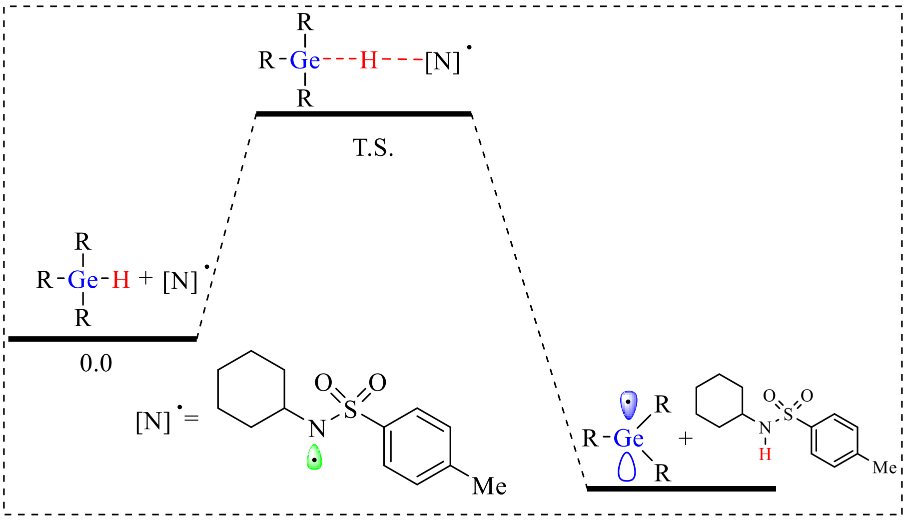


**Scheme 2.23** Energy barriers for the hydrogen atom transfer process between hydrogermanes with HATC2-derived electrophilic sulfamidyl radical (Thermal free energy corrections are considered)

**Table 2.7** DFT calculated energy barriers for the hydrogen atom transfer process of hydrogermanes with HATC2-derived electrophilic sulfamidyl radical (Thermal free energy corrections are considered)

| | $\Delta G^{\neq}$ (kcal/mol) | $\Delta G$ (kcal/mol) |
|---|---|---|
| $Ph_3GeH$ | 12.8 | -18.1 |
| $^nBu_3GeH$ | 11.1 | -17.5 |

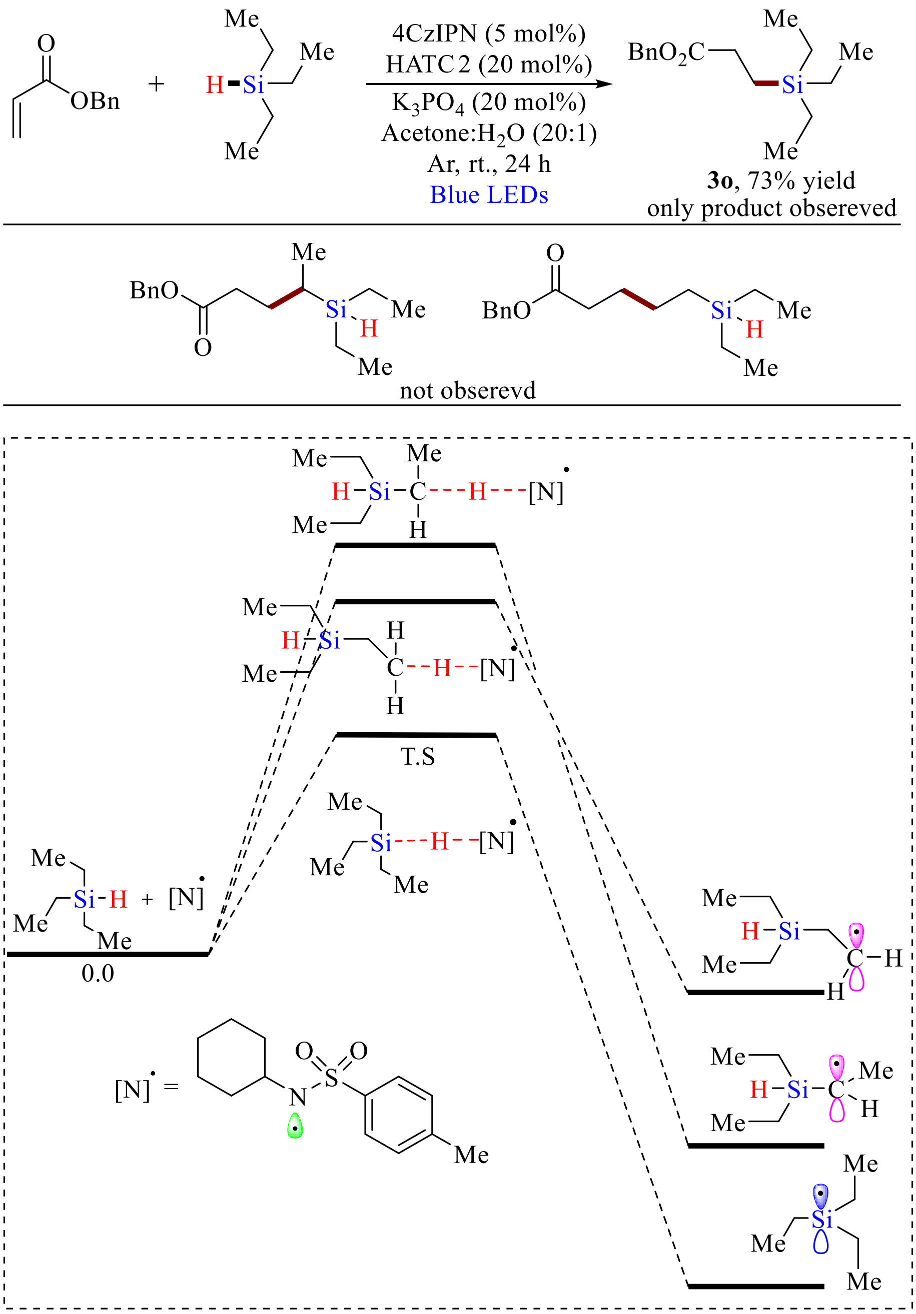


**Scheme 2.24** Chemoselective Si-H bond functionalization of $Et_3SiH$

**Table 2.8** DFT calculated energy barriers for the hydrogen atom transfer process for triethylsilane with HATC2 derived electrophilic sulfamidyl radical (Thermal free energy corrections are considered)

| Bond | $\Delta G^{\neq}$ (kcal/mol) | $\Delta G$ (kcal/mol) |
|---|---|---|
| Si-H | 9.4 | -11.4 |
| $\alpha$-C-H | 16.2 | -7.3 |
| $\beta$-C-H | 15.2 | -4.2 |

### 2.6 Possible mechanism

A possible mechanism is proposed (**Scheme 2.25**) based on the outcome of control experiments, theoretical studies and previous reports.[44, 75] The catalytic cycle commences with the ground-state photocatalyst 4CzIPN being excited by visible light to form the [4CzIPN]* species. This species has an oxidation potential [$PC^*/PC^-$ = +1.35 V vs SCE in $CH_3CN$][76] higher than that of deprotonated sulfonamide HATC2 [$N^\bullet/N^-$ = +0.86 V vs SCE in $CH_3CN$], which enables the generation of an active electrophilic *N*-centered sulfamidyl radical **I** and reduced photocatalyst $4CzIPN^{\bullet -}$ *via* proton-coupled electron transfer (PCET) from deprotonated sulfonamide HATC2. The *N*-centered sulfamidyl radical **I** initiates a selective hydrogen atom transfer (HAT) process with hydrosilane **2** or hydrogermane **4**, yielding nucleophilic radical **II** and regenerating HATC2. The addition of nucleophilic radical **II** to activated alkenes **1a** results in an electrophilic $\alpha$-carbonyl radical **III**. The reduction of **III** with a reduced photocatalyst [$PC/PC^-$ = -1.21 V *vs* SCE in $CH_3CN$], followed by protonation, provided the desired product **3** or **5**, and the photocatalyst is regenerated for the next photocatalytic cycle. The radical chain process *via* abstraction of N-H of HATC2 by enolate radical **III** is thermodynamically not favoured based on the difference in bond dissociation energy of HATC2 (N-H bond = 109.2

kcal mol$^{-1}$) and C-H bond $\alpha$ to the carbonyl carbon of photoproduct **3** ($\alpha$-C-H = 85.2 kcal mol$^{-1}$).[48] Additionally, the calculated quantum yield of the standard reaction ($\phi$ =0.181) and the light-on/off experiment also ruled out the possibility of a radical chain mechanism.

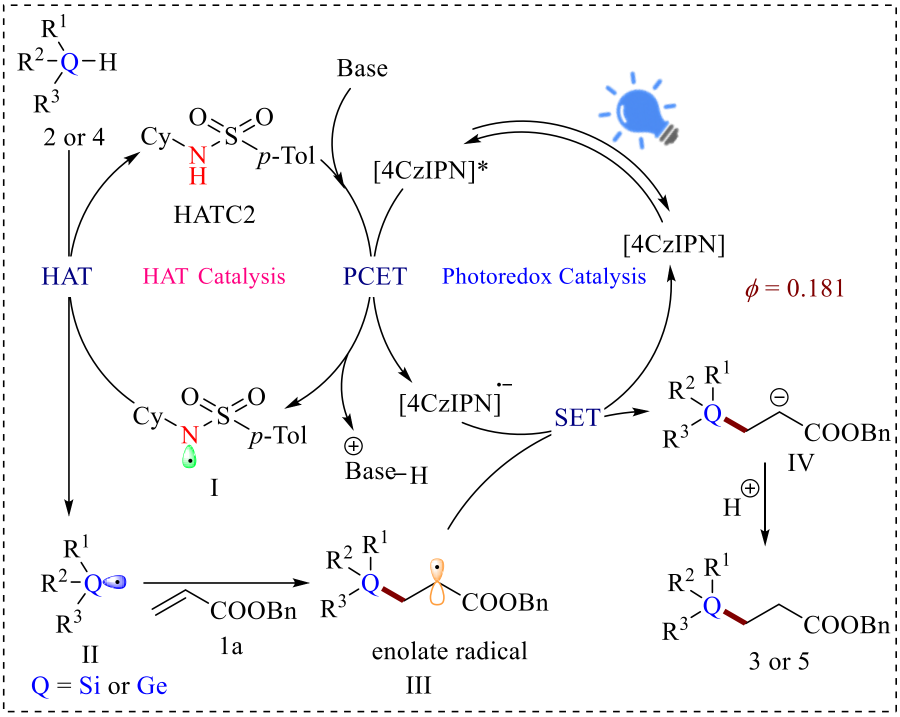


**Scheme 2.25** Possible mechanism

## 2.7 Conclusion

In conclusion, we developed a simple sulfonamide as a hydrogen atom transfer catalyst for the selective functionalization of Si-H/Ge-H bond over C-H bonds of hydrosilanes/hydrogermanes and achieved the hydrosilylation/hydrogermylation of activated alkenes under visible light-mediated organophotocatalyzed conditions. As a source of sulfamidyl radical, an easily synthesizable and inexpensive sulfonamide was utilized. A series of sulfonamides were tested with different sterically hindered groups on nitrogen and series of substituent of aryl ring (both electron withdrawing and electron donating), which revealed that the *N*-cyclohexyl-4-methylbenzenesulfonamide is the best hydrogen atom transfer catalyst for hydrosilylation/hydrogermylation of activated alkenes. Furthermore, optimized reaction conditions were established by screening of photocatalysts, base, and solvents. The scope of activated alkenes was evaluated using a diverse range of substrates, including acrylic esters, maleate esters, $\alpha$-methylene-$\gamma$-butyrolactone, cyclopentenones, acrylamides, vinyl phosphine oxides, and vinyl sulfones. All of these activated alkenes were well tolerated under the reaction conditions and underwent smooth hydrosilylation and hydrogermylation, affording the corresponding products in moderate to good yields. Both alkyl as well as aryl hydrosilanes and hydrogermanes were compatible under the optimized reaction conditions. Next, a series of control experiments were conducted to gain mechanistic insight, such as radical inhibition experiments, deuterium labelling studies, Stern-Volmer quenching studies, and quantum yield calculation. Theoretical studies were conducted to calculate transition energies associated with the hydrogen atom transfer (HAT) process between *tert*-butyldimethylsilane and different sulfamidyl radicals. On the basis of performed control experiments and literature precedents, a possible reaction mechanism was proposed.

## 2.8 Experimental section

### 2.8.1 Substrate synthesis

List of substrates

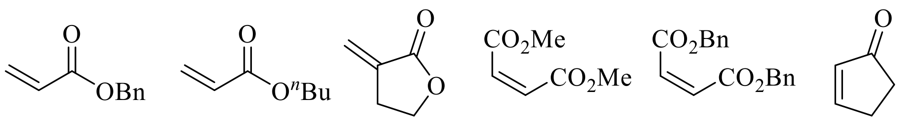


**1a** **1b** **1c** **1d** **1e** **1f**

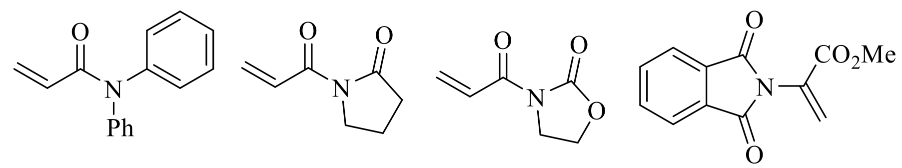


**1g** **1h** **1i** **1j**

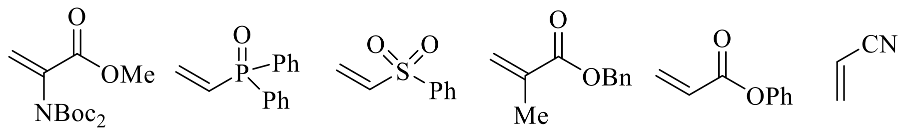


**1k** **1l** **1m** **1n** **1o** **1p**

Alkenes such as **1b, 1c, 1d, 1f, 1m, 1p** are commercially available and used as received. Other alkenes **(1a, 1e, 1g, 1h, 1i, 1j, 1k, 1l, 1n, 1o)** were prepared according to literature reports, and their spectral data were compared.[52, 77-84]

### 2.8.2 List of hydrosilanes and hydrogermanes

Hydrosilane such as **2a, 2b, 2c, 2d, 2e, 2f, 2h, 2k, 2l** and germanium hydride **4a, 4b** are commercially available and used as received. Other hydrosilanes such as **2g, 2i, 2j** were prepared according to the literature reports.[85-87]

$^{t}BuMe_2SiH$ **2a**   $PhMe_2SiH$ **2b**   $Et_3SiH$ **2c**   $^{n}Pr_3SiH$ **2d**   $^{n}Bu_3SiH$ **2e**   $^{i}Pr_3SiH$ **2f**   $BnMe_2SiH$ **2g**

$Ph_2MeSiH$ **2h**

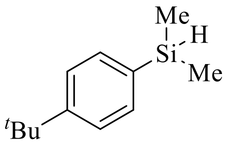

**2i**

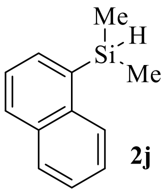

**2j**

$(TMS)_3SiH$ **2k**

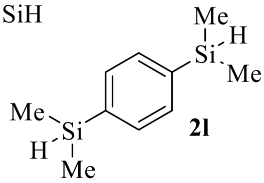

**2l**

$^{n}Bu_3GeH$ **4a**   $Ph_3GeH$ **4b**

### 2.8.3 General procedure for the synthesis of HATC

Hydrogen atom transfer catalysts HATC1, HATC2, HATC3, HATC4, HATC5, HATC7, and HATC10 were prepared according to literature reports, and their spectral data were compared.[69, 88-93]

To a stirred solution of cyclohexylamine (10 mmol) and triethylamine (12 mmol) in $CH_2Cl_2$ (20 ml) at 0 °C, the appropriate sulfonyl chloride (11 mmol) was added. The reaction mixture was then warmed to room temperature, and the progress of the reaction was monitored by TLC. Upon completion, the reaction mixture was diluted with water, and the combined layers were extracted three times with DCM. The combined organic extracts were washed with 1 M HCl, brine, and dried over $Na_2SO_4$. The solvent was removed in vacuo to afford the crude sulfonamide and was purified by column chromatography on silica gel (mesh 100-200) using hexane/ethyl acetate gradient eluent.

***N*-cyclohexyl-4-methylbenzenesulfonamide (HATC2)**:[69] The title compound was prepared from cyclohexylamine (1.14 mL, 10 mmol), triethylamine (1.66 mL, 12 mmol) and 4-methylbenzene sulfonyl chloride (2.1 g, 11 mmol) according to general procedure to give the desired product HATC2 (2.3 g) in 92% yield as white solid; **$^{1}$H NMR** (500 MHz, $CDCl_3$) δ 7.76 (d, *J* = 8.0 Hz, 2H), 7.29 (d, *J* = 8.0 Hz, 2H), 4.39 (d, *J* = 7.6 Hz, 1H), 3.18-3.07 (m, 1H), 2.42 (s, 3H), 1.79-1.71 (m, 2H), 1.66-1.60 (m, 2H), 1.54-1.47 (m, 1H), 1.27-1.05 (m, 5H). **$^{13}$C NMR** (126 MHz, $CDCl_3$) δ 143.2, 138.6, 129.7, 127.0, 52.7, 34.0, 25.2, 24.7, 21.6.

***N*-cyclohexyl-3,5-bistrifluoromethylbenzenesulfonamide (HATC6):** The title compound was prepared from cyclohexylamine (1.14 mL, 10 mmol), triethylamine (1.66 mL, 12 mmol) and 3,5-bistrifluoromethylbenzene sulfonyl chloride (3.4 g, 11 mmol) according to general procedure to give the desired product HATC6 (3.37 g) in 90% yield as white solid; **$^{1}$H NMR** (500 MHz, $CDCl_3$) δ 8.33 (d, *J* = 1.6 Hz, 2H), 8.06 (s, 1H), 4.71 (d, *J* = 7.9 Hz, 1H), 3.25 (m, 1H), 1.82-1.74 (m, 2H), 1.71-1.62 (m, 2H), 1.60-1.51 (m, 1H), 1.35 -1.07 (m, 5H); **$^{13}$C NMR** (126 MHz, $CDCl_3$) δ 144.7, 133.0 (q, *J* = 34.5 Hz), 127.3 (d, *J* = 3.7 Hz), 126.1 (t, *J* = 3.6 Hz), 122.6 (q, *J* = 273.3 Hz), 53.4, 34.1, 25.1, 24.7; **$^{19}$F NMR** (471 MHz, $CDCl_3$) δ -62.95; **IR** (neat): 3278, 2933, 2859, 1441, 1347, 1273, 1125, 1076 $cm^{-1}$.; **HRMS** (ESI-ve) m/z: [M-H] Calcd for $C_{14}H_{14}F_6NO_2S$ 374.0643, found 374.0679.

**4-(*tert*-butyl)-*N*-cyclohexylbenzenesulfonamide (HATC8):** [94] The title compound was prepared from cyclohexylamine (1.14 mL, 10 mmol), triethylamine (1.66 mL, 12 mmol) and 4-*tert*-butylbenzene sulfonyl chloride (2.6 g, 11 mmol) according to general procedure to give the desired product HATC8 (2.56 g) in 87% yield as white solid; **$^{1}$H NMR** (500 MHz, $CDCl_3$) δ 7.82-7.76 (m, 2H), 7.53-7.47 (m, 2H), 4.33 (d, *J* = 7.5 Hz, 1H), 3.16 (m, 1H), 1.83-1.74 (m, 2H), 1.68-1.58 (m, 2H), 1.56-1.47 (m, 1H), 1.34 (s, 9H), 1.30-1.06 (m, 5H); **$^{13}$C NMR** (126 MHz, $CDCl_3$) δ 156.3, 138.5, 126.9, 126.1, 52.7, 35.3, 34.2, 31.2, 25.3, 24.8. **IR** (neat): 3252, 2929, 2855, 1440, 1319, 1159, 1078 $cm^{-1}$.

***N*-cyclohexyl-2,4,6-triisopropylbenzenesulfonamide (HATC9):**[95] The title compound was prepared from cyclohexylamine (1.14 mL, 10 mmol), triethylamine (1.66 mL, 12 mmol) and 2,4,6-triisopropylbenzene sulfonyl chloride (3.3 g, 11 mmol) according to general procedure to give the desired product HATC9 (2.88 g) in 79% yield as white solid; **$^1$H NMR** (500 MHz, $CDCl_3$) δ 7.14 (s, 2H), 4.22 (dd, *J* = 8.1, 4.4 Hz, 1H), 4.16 (hept, *J* = 6.9 Hz, 2H), 3.23 (m, 1H), 2.89 (hept, *J* = 6.9 Hz, 1H), 1.85-1.78 (m, 2H), 1.69-1.61 (m, 2H), 1.60-1.50 (m, 1H), 1.34-1.04 (m, 23H); **$^{13}$C NMR** (126 MHz, $CDCl_3$) δ 152.6, 150.0, 134.0, 123.9, 52.5, 34.4, 34.2, 29.8, 25.3, 25.0 (2C), 23.7; **IR** (neat): 3302, 2931, 2860, 1433, 1368, 1307, 1143, 1092 $cm^{-1}$.

### 2.8.4 Synthesis of photocatalyst 4CzIPN

Sodium hydride (60% suspension in mineral oil, 0.936 g, 39 mmol) was added slowly at 0 °C to a stirred solution of carbazole (3.0 g, 18 mmol) in dry THF (60 mL) under nitrogen atmosphere. After the addition of NaH, the reaction mixture was warmed to room temperature and stirred for 30 minutes. Then, 2,4,5,6-tetrafluoroisophthalonitrile (1.2 g, 3 mmol) was added. After stirring at room temperature for 20 h, 2 mL of water was added to the reaction mixture to quench the excess NaH. The resulting mixture was extracted with 30 mL of DCM twice, and the organic layer was then concentrated under reduced pressure. The crude residue was purified by column chromatography on silica gel using DCM:hexane mixture, and 4CzIPN was obtained as a bright yellow solid. It was further purified by recrystallization from hexane:DCM mixture to yield a bright yellow crystalline solid in 65% yield (1.53 g). $^1$H and $^{13}$C NMR spectra in $CDCl_3$ are consistent with reported data.[96] **$^1$H NMR** (500 MHz, $CDCl_3$) δ 8.23 (d, *J* = 7.6 Hz, 2H), 7.76 -7.66 (m, 8H), 7.49 (ddd, *J* = 7.9, 6.7, 1.4 Hz, 2H), 7.33 (d, *J* = 7.6 Hz, 2H), 7.25-7.21 (m, 4H), 7.09 (m, 8H), 6.87-6.79 (m, 4H), 6.64 (td, *J* = 7.6, 1.2 Hz, 2H); **$^{13}$C NMR** (126 MHz, $CDCl_3$) δ 145.3, 144.7, 140.1, 138.3, 137.1, 134.8, 127.1, 125.9, 125.1, 124.9, 124.7, 124.0, 122.5, 122.1, 121.5, 121.1, 120.5, 119.7, 116.4, 111.7, 110.0, 109.6, 109.5.

### 2.8.5 Optimization of reaction conditions

All photochemical reactions were performed using Penn PhD Photoreactor m2 composed of cooling block and LED plate connected to AC/DC input 100 - 240 V AC, 50/60 Hz power supply with 450 nm LED. For more details about the instrument: https://www.pennphd.com/product/5

### 2.8.6 General procedure for screening of hydrogen atom transfer catalyst

To an oven-dried 10 mL reaction tube equipped with a magnetic stir bar were added benzyl acrylate **1a** (0.2 mmol, 32.4 mg), $^{t}BuMe_2SiH$ **2a** (0.6 mmol, 0.1 mL), 5 mol% 4CzIPN (7.9 mg, 0.010 mmol), 20 mol% HATC (0.04 mmol) and 20 mol% $K_3PO_4$ (8.5 mg, 0.04 mmol). The reaction tube was sealed and placed under an argon atmosphere, then 2 mL of 20:1 (*v/v*) acetone:water was added *via* syringe. The reaction mixture was then degassed *via* freeze-pump-thaw (three times) and refilled with argon. The sealed reaction tube was then placed inside the Penn photoreactor (Blue LEDs, $\lambda = 450$ nm) and irradiated for 24 hours. After the reaction was completed, acetone was evaporated under reduced pressure. The reaction mixture was diluted with water (5 mL) and extracted with ethyl acetate (3 x 10 mL). The combined organic layer was washed with brine (10 mL), dried over anhydrous sodium sulfate, and the solvent was removed using a rotary evaporator under reduced pressure. The crude product was then purified by column chromatography on silica gel (mesh 230-400) using a gradient elution with hexane/ethyl acetate (50:1 to 20:1) to yield the hydrosilylation product **3a**.

### 2.8.7 General procedure for the hydrosilylation of activated alkenes

To an oven-dried 10 mL reaction tube equipped with a magnetic stir bar were added substrate **1** (0.2 mmol, 32.4 mg), hydrosilanes **2** (0.6 mmol, 0.1 mL), 5 mol% 4CzIPN (7.9 mg, 0.010 mmol), 20 mol% HATC2 (0.04 mmol) and 20 mol% $K_3PO_4$ (8.5 mg, 0.04 mmol). The reaction tube was sealed and placed under an argon atmosphere. Then, 2 mL of a 20:1 (v/v) acetone:water mixture was added *via* syringe. The reaction mixture was then degassed *via* freeze-pump-thaw (three times) and refilled with argon. The sealed reaction tube was then placed inside the Penn photoreactor (Blue LEDs, $\lambda = 450$ nm) and irradiated for 24 hours. After completion of the reaction, acetone was evaporated under reduced pressure. The reaction mixture was diluted with water (5 mL) and extracted with ethyl acetate (3 x 10 mL). The combined organic layer was washed with brine (10 mL), dried over anhydrous $Na_2SO_4$, and the solvent was removed using a rotary evaporator under reduced pressure. The crude product was then purified by column chromatography on silica gel (mesh 230-400) using a gradient elution with hexane/ethyl acetate (50:1 to 20:1), which provided the hydrosilylation product **3**.

**Benzyl 3-(*tert*-butyldimethylsilyl)propanoate (3a):**[48] (41 mg) in 74% yield as colorless oil. **$^1$H NMR** (500 MHz, $CDCl_3$) δ 7.40-7.30 (m, 5H), 5.12 (s, 2H), 2.37- 2.30 (m, 2H), 0.92-0.84 (m, 11H), -0.06 (s, 6H); **$^{13}$C NMR** (126 MHz, $CDCl_3$) δ 175.2, 136.2, 128.7, 128.4, 128.3, 66.4, 29.4, 26.6, 16.6, 7.7, -6.4. **IR** (neat): 2940, 2859, 1737, 1460, 1134 $cm^{-1}$.

**Butyl 3-(*tert*-butyldimethylsilyl)propanoate (3b):** (33.8 mg) in 64% yield as colorless oil. **$^1$H NMR** (500 MHz, $CDCl_3$) δ 7.54-7.46 (m, 2H), 7.36 (m, 3H), 4.03 (t, $J$ = 6.7 Hz, 2H), 2.30-2.23 (m, 2H), 1.62-1.53 (m, 3H), 1.41-1.30 (m, 2H), 1.12-1.05 (m, 2H), 0.92 (t, $J$ = 7.4 Hz, 3H), 0.29 (s, 6H); **$^{13}$C NMR** (126 MHz, $CDCl_3$) δ 175.2, 138.4, 133.7, 129.2, 128.0, 64.5, 30.8, 29.0, 19.3, 13.9, 11.0, -3.2; **IR** (neat): 2953, 1734, 1424, 1243, 1201 $cm^{-1}$. **GC-MS** (EI) m/z: [M-$CH_3$] Calcd for $C_{14}H_{21}O_2Si$ 249, found 249.

**3-((dimethyl(phenyl)silyl)methyl)dihydrofuran-2(3*H*)-one (3c):** (39.3 mg) in 84% yield as colorless oil. **$^1$H NMR** (500 MHz, $CDCl_3$) δ 7.54-7.50 (m, 2H), 7.40-7.33 (m, 3H), 4.25 (td, $J$ = 8.7, 2.3 Hz, 1H), 4.09-4.02 (m, 1H), 2.48-2.39 (m, 1H), 2.24-2.16 (m, 1H), 1.78-1.69 (m, 1H), 1.53 (dd, $J$ = 15.0, 3.6 Hz, 1H), 0.85 (dd, $J$ = 15.0, 11.2 Hz, 1H), 0.35 (d, $J$ = 3.8 Hz, 6H); **$^{13}$C NMR** (126 MHz, $CDCl_3$) δ 180.9, 138.0, 133.7, 129.5, 128.1, 66.3, 35.9, 31.1, 17.4, -2.4, -2.7; **IR** (neat): 2953, 2914, 1765, 1419, 1374 cm$^{-1}$. **HRMS** (APCI) m/z: $[M+Na]^+$ Calcd for $C_{13}H_{18}O_2SiNa$ 257.0968, found 257.0989.

**Dimethyl 2-(*tert*-butyldimethylsilyl)succinate (3d):**[49] (17.7 mg) in 61% yield as colorless oil. **$^1$H NMR** (500 MHz, $CDCl_3$) δ 3.66 (d, *J* = 6.3 Hz, 6H), 2.91 (dd, *J* = 17.4, 12.3 Hz, 1H), 2.58 (dd, *J* = 12.3, 3.0 Hz, 1H), 2.41 (dd, *J* = 17.4, 3.0 Hz, 1H), 0.92 (s, 9H), 0.07 (s, 3H), 0.01 (s, 3H); **$^{13}$C NMR** (126 MHz, $CDCl_3$) δ 175.7, 173.7, 52.0, 51.4, 32.3, 30.1, 26.7, 17.7, -6.5, -6.6. **IR** (neat): 2934, 1739, 1724, 1248, 1143 cm$^{-1}$.

**Dibenzyl 2-(*tert*-butyldimethylsilyl)succinate (3e):** (47.8 mg) in 58% yield as colorless oil. **$^1$H NMR** (500 MHz, $CDCl_3$) δ 7.39-7.27 (m, 10H), 5.13-5.0 (m, 4H), 3.0 (dd, *J* = 17.4, 12.5 Hz, 1H), 2.65 (dd, *J* = 12.5, 3.0 Hz, 1H), 2.47 (dd, *J* = 17.4, 3.0 Hz, 1H), 0.90 (s, 9H), 0.05 (s, 3H), -0.03 (s, 3H); **$^{13}$C NMR** (126 MHz, $CDCl_3$) δ 175.0, 172.9, 136.2, 135.9, 128.7, 128.6, 128.5, 128.4, 128.4, 128.2, 66.8, 66.4, 32.7, 30.5, 26.7, 17.7, -6.4, -6.5; **IR** (neat): 2934, 2859, 1724, 1459, 1143 cm$^{-1}$. **HRMS** (APCI) m/z: $[M+Na]^+$ Calcd for $C_{24}H_{32}O_4SiNa$ 435.1962, found 435.2012.

**3-(dimethyl(phenyl)silyl)cyclopentane-1-one (3f):**[97] (18.8 mg) in 43% yield as colorless oil. **$^1$H NMR** (500 MHz, $CDCl_3$) δ 7.53-7.46 (m, 2H), 7.42-7.32 (m, 3H), 2.32- 2.18 (m, 2H), 2.15-2.05 (m, 2H), 1.89 (dd, *J* = 18.2, 13.0 Hz, 1H), 1.74- 1.62 (m, 1H), 1.60-1.49 (m, 1H), 0.32 (d, *J* = 1.4 Hz, 6H); **$^{13}$C NMR** (126 MHz, $CDCl_3$) δ 221.13, 137.1, 134.0, 129.9, 128.1, 40.3, 39.5, 25.1, 24.1, -4.7, -4.8; **IR** (neat): 2923, 1737, 1413, 1252, 1109 cm$^{-1}$.

**3-(*tert*-butyldimethylsilyl)-*N*,*N*-diphenylpropanamide (3g):** (45.4 mg) in 67% yield as colorless oil. **$^1$H NMR** (500 MHz, $CDCl_3$) δ 7.45-7.16 (br, m, 10H), 2.27-2.20 (m, 2H), 0.93-0.86 (m, 2H), 0.79 (s, 9H), -0.21 (s, 6H); **$^{13}$C NMR** (126 MHz, $CDCl_3$) δ 174.9, 143.2, 129.4 (br, 8C), 30.5, 26.6, 16.6, 8.5, -6.5; **IR** (neat): 2929, 2856, 1673, 1592, 1255

$cm^{-1}$. **HRMS** (ESI) m/z: $[M+Na]^+$ Calcd for $C_{21}H_{29}NOSiNa$ 362.1910, found 362.1924.

**1-(3-(dimethyl(phenyl)silyl)propanoyl)pyrrolidin-2-one (3h):** (40.2 mg) in 73% yield as colorless oil. **$^1$H NMR** (500 MHz, $CDCl_3$) δ 7.56-7.48 (m, 2H), 7.39-7.31 (m, 3H), 3.78-3.72 (m, 2H), 2.90-2.84 (m, 2H), 2.56 (t, $J$ = 8.1 Hz, 2H), 2.03-1.95 (m, 2H), 1.11-1.06 (m, 2H), 0.31 (s, 6H); **$^{13}$C NMR** (126 MHz, $CDCl_3$) δ 175.8, 175.4, 138.7, 133.8, 129.1, 127.9, 45.7, 33.8, 31.6, 17.4, 10.3, -3.1; **IR** (neat): 2943, 1735, 1690, 1421, 1243 $cm^{-1}$.; **HRMS** (ESI) m/z: $[M+Na]^+$ Calcd for $C_{15}H_{21}NO_2SiNa$ 298.1233, found 298.1262.

**3-(3-dimethyl(phenyl)silyl)propanoyl)oxazolidin-2-one (3i):***[48]* (22.2 mg) in 40% yield as colorless oil. **$^1$H NMR** (500 MHz, $CDCl_3$) δ 7.56-7.48 (m, 2H), 7.38-7.33 (m, 3H), 4.35 (dd, $J$ = 8.6, 7.6 Hz, 2H), 3.93 (dd, $J$ = 8.6, 7.6 Hz, 2H), 2.93-2.86 (m, 2H), 1.15-1.07 (m, 2H), 0.32 (s, 6H); **$^{13}$C NMR** (126 MHz, $CDCl_3$) δ 174.9, 153.6, 138.4, 133.8, 129.2, 127.9, 62.1, 42.7, 30.0, 10.4, -3.1; IR (neat): 2920, 1777, 1697, 1377, 1255 $cm^{-1}$.

**Methyl 3-(*tert*-butyldimethylsilyl)-2-(1,3-dioxoisoindolin-2-yl)propanoate (3j):** (27.1 mg) in 39% yield as colorless oil. **$^1$H NMR** (500 MHz, $CDCl_3$) δ 7.90-7.83 (m, 2H), 7.76-7.72 (m, 2H), 4.95 (dd, $J$ = 11.4, 4.7 Hz, 1H), 3.72 (s, 3H), 1.73-1.65 (m, 1H), 1.63-1.55 (m, 1H), 0.87 (s, 9H), 0.02 (s, 3H), -0.22 (s, 3H); **$^{13}$C NMR** (126 MHz, $CDCl_3$) δ 171.3, 167.8, 134.3, 132.0, 123.7, 53.0, 49.6, 26.5, 16.6, 12.7, -5.9, -6.4; **IR** (neat): 2956, 1713, 1610, 1463, 1247 $cm^{-1}$.; **HRMS** (ESI) m/z: $[M+Na]^+$ Calcd for $C_{18}H_{25}NO_4SiNa$ 370.1445, found 370.1432.

**Methyl 2-(bis(*tert*-butoxycarbonyl)amino)-3-(dimethyl(phenyl)silyl)propanoate (3k):***[50]* (84 mg) in 96% yield as colorless oil. **$^1$H NMR** (500 MHz, $CDCl_3$) δ 7.53-7.47 (m, 2H), 7.35-7.31 (m, 3H), 5.00 (dd, $J$ = 9.8, 5.7 Hz, 1H), 3.67 (s, 3H), 1.69 (dd, $J$ = 15.4, 5.7 Hz, 1H), 1.55-1.49 (m, 1H), 1.45 (s, 18H), 0.33 (s, 3H), 0.32 (s, 3H); **$^{13}$C NMR** (126 MHz, $CDCl_3$) δ 172.6, 152.2, 138.8, 133.7, 129.1, 127.9, 83.1, 55.7, 52.4, 28.2, 28.1, 17.6, -2.4, -2.5; **IR** (neat):

2965, 1744, 1703, 1362, 1256 $cm^{-1}$.; **HRMS** (ESI) m/z: $[M+Na]^+$ Calcd for $C_{22}H_{35}NO_6SiNa$ 460.2125; Found 460.2135.

**(2-(*tert*-butyldimethylsilyl)ethyl)diphenylphosphine oxide (3l):** (57.8 mg) in 84% yield as colorless oil. **$^1$H NMR** (500 MHz, $CDCl_3$) δ 7.77-7.68 (m, 4H), 7.56-7.44 (m, 6H), 2.23-2.14 (m, 2H), 0.83 (s, 9H), 0.81-0.73 (m, 2H), -0.04 (s, 6H); **$^{13}$C NMR** (126 MHz, $CDCl_3$) δ 133.0 (d, $J$ = 96.7 Hz), 131.8 (d, $J$ = 2.3 Hz), 131.0 (d, $J$ = 9.1 Hz), 128.8 (d, $J$ = 11.3 Hz), 26.6, 24.4 (d, $J$ = 69.3 Hz), 16.8, 2.9 (d, $J$ = 6.6 Hz), -6.5; **$^{31}$P NMR** (202 MHz, $CDCl_3$) δ 34.9; **IR** (neat): 2946, 2824, 1458, 1184, 1137 $cm^{-1}$.; **HRMS** (ESI) m/z: $[M+Na]^+$ Calcd for $C_{20}H_{29}OPSiNa$ 367.1617, found 367.1629.

***tert*-butyldimethyl(2-phenylsulfonyl)ethyl)silane (3m):** (36.4 mg) in 64% yield as colorless oil. **$^1$H NMR** (500 MHz, $CDCl_3$) δ 7.94-7.87 (m, 2H), 7.69-7.63 (m, 1H), 7.60-7.56 (m, 2H), 3.03-2.97 (m, 2H), 0.99-0.93 (m, 2H), 0.84 (s, 9H), -0.07 (s, 6H); **$^{13}$C NMR** (126 MHz, $CDCl_3$) δ 139.0, 133.7, 129.4, 128.3, 53.2, 26.5, 16.7, 5.0, -6.3; **IR** (neat): 2938, 2857, 1457, 1303, 1254 $cm^{-1}$.; **HRMS** (ESI) m/z: $[M+Na]^+$ Calcd for C14H24O2SSiNa 307.1158, found 307.1135.

**Dimethyl(phenyl)(2-phenylsulfonyl)ethyl)silane (3n):***[98]* (43.2 mg) in 71% yield as white solid. **$^1$H NMR** (500 MHz, $CDCl_3$) δ 7.90-7.84 (m, 2H), 7.68-7.62 (m, 1H), 7.58-7.53 (m, 2H), 7.42-7.31 (m, 5H), 3.00-2.92 (m, 2H), 1.19-1.14 (m, 2H), 0.28 (s, 6H); **$^{13}$C NMR** (126 MHz, $CDCl_3$) δ 138.8, 136.7, 133.7, 133.6, 129.7, 129.4, 128.4, 128.2, 52.6, 8.6, -3.3; **IR** (neat): 2921, 1433, 1309, 1260, 1148 $cm^{-1}$.

**Benzyl 3-(triethylsilyl)propanoate (3o):** *[48]* (40.6 mg) in 73% yield as colorless oil. **$^1$H NMR** (500 MHz, $CDCl_3$) δ 7.40-7.30 (m, 5H), 5.12 (s, 2H), 2.37-2.30 (m, 2H), 0.99-0.83 (m, 11H), 0.52 (q, $J$ = 8.0 Hz, 6H); **$^{13}$C NMR** (126 MHz, $CDCl_3$) δ 175.2, 136.3, 128.7, 128.4, 128.3, 66.4, 29.0, 7.5, 6.7, 3.1; **IR** (neat): 2923, 1737, 1457, 1338, 1199 $cm^{-1}$.

**Benzyl 3-(tripropylsilyl)propanoate (3p):***[48]* (48 mg) in 75% yield as colorless oil. **$^1$H NMR** (500 MHz, $CDCl_3$) δ 7.38-7.30 (m, 5H), 5.11 (s, 2H), 2.33-2.30 (m, 2H), 1.34-1.25 (m, 6H), 0.94 (t, $J$ = 7.2 Hz, 9H), 0.89-0.86 (m, 2H), 0.53-0.49 (m, 6H); **$^{13}$C NMR** (126 MHz, $CDCl_3$) δ 175.0, 136.2, 128.5, 128.2 (2C), 66.2, 29.0, 18.6, 17.4, 15.0, 7.7; **IR** (neat): 2926, 1737, 1455, 1201, 1134 cm$^{-1}$.

**Benzyl 3-(tributylsilyl)propanoate (3q):***[48]* (52.2 mg) in 72% yield as colorless oil. **$^1$H NMR** (500 MHz, $CDCl_3$) δ 7.37-7.31 (m, 5H), 5.11 (s, 2H), 2.34-2.06 (m, 2H), 1.33-1.23 (m, 12H), 0.90-0.86 (m, 11H), 0.51 (m, 6H); **$^{13}$C NMR** (126 MHz, $CDCl_3$) δ 175.1, 136.2, 128.5, 128.2, 128.1, 66.2, 29.0, 26.8, 26.0, 13.7, 11.9, 7.7; **IR** (neat): 2935, 1738, 1456, 1343, 1197 cm$^{-1}$.

**Benzyl 3-(triisopropylsilyl)propanoate (3r):***[48]* (41 mg) in 64% yield as colorless oil. **$^1$H NMR** (500 MHz, $CDCl_3$) δ 7.38-7.30 (m, 5H), 5.12 (s, 2H), 2.40-2.37 (m, 2H), 1.03 (s, 21H), 0.98-0.94 (m, 2H); **$^{13}$C NMR** (126 MHz, $CDCl_3$) δ 175.0, 136.2, 128.5, 128.2, 128.1, 66.3, 29.3, 18.7, 10.8, 4.3; **IR** (neat): 2934, 1738, 1459, 1202, 1139 cm$^{-1}$.

**Benzyl 3-(benzyldimethylsilyl)propanoate (3s):** *[48]* (54.9 mg) in 88% yield as colorless oil. **$^1$H NMR** (500 MHz, $CDCl_3$) δ 7.39-7.31 (m, 5H), 7.23-7.17 (m, 2H), 7.09-7.04 (m, 1H), 7.00-6.97 (m, 2H), 5.11 (s, 2H), 2.32-2.27 (m, 2H), 2.09 (s, 2H), 0.90-0.87 (m, 2H), -0.02 (s, 6H); **$^{13}$C NMR** (126 MHz, $CDCl_3$) δ 174.9, 139.9, 136.2, 128.7, 128.4, 128.4, 128.4, 128.2, 124.2, 66.4, 28.9, 25.4, 10.0, -3.7; **IR** (neat): 2919, 1735, 1452, 1201, 1148 cm$^{-1}$.

**Benzyl 3-(dimethyl(phenyl)silyl)propanoate (3t):** *[48]* (46.5 mg) in 78% yield as colorless oil. **$^1$H NMR** (500 MHz, $CDCl_3$) δ 7.51-7.49 (m, 2H), 7.36-7.33 (m, 8H), 5.07 (s, 2H), 2.33 (m, 2H), 1.12 (m, 2H), 0.29 (s, 6H); **$^{13}$C NMR** (126 MHz, $CDCl_3$) δ 174.7, 138.1, 136.1, 133.6, 129.1, 128.6, 128.3, 128.2, 127.9, 66.3, 28.9, 10.8, -3.3; **IR** (neat): 2915, 1734, 1423, 1199, 1119 cm$^{-1}$.

**Benzyl 3-(methyl(diphenyl)silyl)propanoate (3u):** *[48]* (54 mg) in 75% yield as colorless oil. **$^1$H NMR** (500 MHz, $CDCl_3$) δ 7.53-7.48 (m, 4H), 7.41-7.29 (m, 11H), 5.05 (s, 2H), 2.41-2.36 (m, 2H), 1.46-1.41 (m, 2H), 0.56 (s, 3H); **$^{13}$C NMR** (126 MHz, $CDCl_3$) δ 174.7, 136.2, 136.1, 134.6, 129.6, 128.7, 128.4, 128.3, 128.1, 66.5, 29.0, 9.4, -4.5; **IR** (neat): 2938, 1733, 1424, 1198, 1113 cm$^{-1}$.

**Benzyl 3-((4-(*tert*-butyl)phenyl)dimethylsilyl)propanoate (3v):** (29 mg) in 41% yield as colorless oil. **$^1$H NMR** (500 MHz, $CDCl_3$) δ 7.46-7.29 (m, 10H), 5.07 (s, 2H), 2.38-2.30 (m, 2H), 1.32 (s, 9H), 1.13-1.08 (m, 2H), 0.27 (s, 6H); **$^{13}$C NMR** (126 MHz, $CDCl_3$) δ 174.9, 152.2, 136.2, 134.6, 133.6, 128.7, 128.4, 128.3, 125.0, 66.4, 34.8, 31.4, 29.1, 11.1, -3.1; **IR** (neat): 2945, 1735, 1458, 1192, 1199 cm$^{-1}$.; **HRMS** (ESI) m/z: $[M+Na]^+$ Calcd for $C_{22}H_{30}O_2SiNa$ 377.1907, found 377.1916.

**Benzyl 3-(dimethyl(naphthalen-1-yl)silyl)propanoate (3w):** (31.3 mg) in 45% yield as colorless oil. **$^1$H NMR** (500 MHz, $CDCl_3$) δ 8.08-8.03 (m, 1H), 7.89-7.84 (m, 2H), 7.68-7.64 (m, 1H), 7.52-7.42 (m, 3H), 7.37-7.28 (m, 5H), 5.04 (s, 2H), 2.37-2.31 (m, 2H), 1.38- 1.32 (m, 2H), 0.48 (s, 5H); **$^{13}$C NMR** (126 MHz, $CDCl_3$) δ 174.8, 137.1, 136.1, 135.9, 133.9, 133.5, 130.2, 129.3, 128.7, 128.4, 128.3, 127.9, 126.0, 125.6, 125.2, 66.4, 29.2, 11.6, -1.6; **IR** (neat): 2935, 2869, 1732, 1453, 1248 cm$^{-1}$; **HRMS** (ESI) m/z: $[M+Na]^+$ Calcd for $C_{22}H_{24}O_2SiNa$ 371.1437, found 371.1445.

**Benzyl 3-(1,1,1,3,3,3-hexamethyl-2-(trimethylsilyl)trisilan-2-yl)propanoate (3x):**[48] (58.2 mg) in 71% yield as colorless oil. **$^1$H NMR** (500 MHz, $CDCl_3$) δ 7.37-7.31 (m, 5H), 5.11 (s, 2H), 2.39-2.36 (m, 2H), 1.14-1.11 (m, 2H), 0.17 (s, 27H); **$^{13}$C NMR** (126 MHz, $CDCl_3$) δ 174.5, 136.1, 128.5, 128.2 (2C), 66.3, 33.2, 2.8, 1.0; **IR** (neat): 2924, 1737, 1248, 1199, 1131 cm$^{-1}$.

**Benzyl 3-((4-(dimethylsilyl)phenyl)dimethylsilyl)propanoate (3y):** [48] (52.1 mg) in 73% yield as colorless oil. **$^1$H NMR** (500 MHz, $CDCl_3$) δ 7.53 (d, *J* = 7.8 Hz, 2H), 7.49 (d, *J* = 7.8 Hz, 2H), 7.38-7.30 (m, 5H), 5.07 (s, 2H), 4.46-4.38 (m, 1H), 2.36-2.31 (m, 2H), 1.14-1.09 (m, 2H), 0.34 (d, *J* = 3.8 Hz, 6H), 0.28 (s, 6H); **$^{13}$C NMR** (126 MHz, $CDCl_3$) δ 174.8, 139.3, 138.6, 136.8, 133.5, 133.1, 128.7, 128.4, 128.3, 66.4, 29.0, 10.9, -3.3, -3.7; **IR** (neat): 3047, 2955, 2117, 1736, 1378 cm$^{-1}$.

### 2.8.8 Scale-up reaction for hydrosilylation of activated alkenes

To an oven-dried 50 mL RB flask equipped with a magnetic stir bar were added alkene **1a** (223 mg, 1.5 mmol), $^{t}BuMe_2SiH$ **2a** (0.75 mL, 4.5 mmol), 5 mol% photocatalyst 4CzIPN (59.3 mg, 0.075 mmol), 20 mol% HATC2 (75.8 mg, 0.3 mmol), and 20 mol% $K_3PO_4$ (63.7 mg, 0.3 mmol). The reaction tube was sealed and placed under an argon atmosphere, then 15 ml of 20:1 (v/v) acetone:water was added *via* syringe, the reaction mixture was then degassed *via* freeze pump thaw (x 3 times) and refilled with argon. The sealed reaction tube was then placed inside the Penn photoreactor (Blue LEDs, $\lambda$ = 450 nm) and irradiated for 36 hours. After the completion of the reaction, acetone was evaporated under reduced pressure. The reaction mixture was diluted with water (20 mL) and extracted with ethyl acetate (three times, 50 mL each). The combined organic layer was washed with brine (25 mL) and dried over anhydrous $Na_2SO_4$, and the solvent was removed on a rotary evaporator under reduced pressure. The crude product was purified by column chromatography on silica gel (mesh 230-400) using hexane/ethyl acetate (50:1 to 5:1) as gradient eluent, giving the hydrosilylated product **3a** as colourless oil in 63% yield (263.2 mg).

### 2.9.9 General procedure for the hydrogermylation of activated alkenes

To an oven-dried 10 mL reaction tube equipped with a magnetic stir bar were added alkene 1 (0.2 mmol, 1 equiv.), hydrogermane **4a** (0.6 mmol, 3 equiv.) or **4b** (0.4 mmol, 2 equiv.), 5 mol% photocatalyst 4CzIPN (7.9 mg, 0.010 mmol), 20 mol% HATC2 (10.1 mg, 0.04 mmol) and 20 mol% $K_3PO_4$ (8.5 mg, 0.04 mmol). The reaction tube was sealed and placed under an argon atmosphere. Then, 2 mL of a 20:1 (v/v) acetone:water mixture was added *via* syringe. The reaction mixture was then degassed *via* freeze-pump-thaw (three times) and refilled with argon. The sealed reaction tube was then placed inside the Penn photoreactor (Blue LEDs, $\lambda$ = 450 nm) and irradiated for 24 hours. After completion of the reaction, the acetone was evaporated under reduced pressure. The reaction mixture was diluted with water (5 mL) and extracted with ethyl acetate (3 x 10 mL). The combined organic layer was washed with brine (10 mL), dried over anhydrous $Na_2SO_4$, and the solvent was removed using a rotary evaporator under reduced pressure. The crude product was purified by column chromatography on silica gel (mesh 230-400) using hexane/ethyl acetate (50:1 to 5:1) gradient eluent to give the hydrogermylated product **5**.

**Benzyl 3-(tributylgermyl)propanoate (5a):** (75.9 mg) in 93% yield as colorless oil. **$^1$H NMR** (500 MHz, $CDCl_3$) δ 7.40-7.30 (m, 5H), 5.12 (s, 2H), 2.41-2.34 (m, 2H), 1.32-1.23 (m, 12H), 1.06-0.99 (m, 2H), 0.92-0.84 (m, 9H), 0.76-0.66 (m, 6H); **$^{13}$C NMR** (126 MHz, $CDCl_3$) δ 175.2, 136.3, 128.7, 128.4, 128.3, 66.4, 30.3, 27.5, 26.7, 13.9, 12.4, 7.8; **IR** (neat): 2952, 2860, 1737, 1455, 1338 $cm^{-1}$; **HRMS** (ESI) m/z: $[M-C_4H_9]^+$ Calcd for $C_{18}H_{29}O_2Ge$ 351.1377, found 351.1385.

**Dimethyl 2-(triphenylgermyl)succinate (5b):** (84.6 mg) in 94% yield as white solid. **$^1$H NMR** (500 MHz, $CDCl_3$) δ 7.58-7.48 (m, 6H), 7.46-7.34 (m, 9H), 3.60 (s, 3H), 3.47 (dd, $J$ = 11.9, 3.5 Hz, 1H), 3.30 (s, 3H), 3.02 (dd, $J$ = 17.5, 11.9 Hz, 1H), 2.50 (dd, $J$ = 17.5, 3.5 Hz, 1H); **$^{13}$C NMR** (126 MHz, $CDCl_3$) δ 175.0, 173.4, 135.4, 134.2, 129.7, 128.5, 52.0, 51.4, 32.9, 31.7; **IR** (neat): 2954, 1742, 1717, 1428, $cm^{-1}$; **HRMS** (ESI) m/z: $[M+Na]^+$ Calcd for $C_{24}H_{24}O_4GeNa$ 473.0778, found 473.0783.

**3-((triphenylgermyl)methyl)dihydrofuran-2(3H)-one (5c):** (72.7 mg) in 90% yield as colorless oil. **$^1$H NMR** (500 MHz, $CDCl_3$) δ 7.56-7.48 (m, 6H), 7.45-7.34 (m, 9H), 4.19 (td, $J$ = 8.8, 2.4 Hz, 1H), 4.02-3.94 (m, 1H), 2.68-2.59 (m, 1H), 2.32 (dd, $J$ = 14.2, 3.1 Hz, 1H), 2.04-1.96 (m, 1H), 1.78-1.67 (m, 1H), 1.57-1.50 (m, 1H); **$^{13}$C NMR** (126 MHz, $CDCl_3$) δ 180.5, 136.1, 135.0, 129.4, 128.6, 66.2, 36.7, 31.2, 15.2; **IR** (neat): 2926, 2860, 1766, 1419, 1374 $cm^{-1}$; **HRMS** (ESI) m/z: $[M+Na]^+$ Calcd for $C_{23}H_{22}O_2GeNa$ 427.0723, found 427.0741.

**Methyl 2-(bis(*tert*-butoxycarbonyl)amino)-3-(triphenylgermyl)propanoate (5d):** (102 mg) in 84% yield as colorless oil. **$^1$H NMR** (500 MHz, $CDCl_3$) δ 7.54-7.46 (m, 6H), 7.40-7.31 (m, 9H), 5.12 (t, $J$ = 7.5 Hz, 1H), 3.51 (s, 3H), 2.55 (dd, $J$ = 14.2, 7.8 Hz, 1H), 2.05 (dd, $J$ = 14.1, 7.8 Hz, 1H), 1.39 (s, 18H); **$^{13}$C NMR** (126 MHz, $CDCl_3$) δ 171.8, 151.9, 136.9, 135.1, 129.0, 128.3, 83.1, 56.4, 52.3, 28.0, 16.0; **IR** (neat): 2979, 1741, 1703, 1435, 1363 $cm^{-1}$; **HRMS** (APCI) m/z: $[M+Na]^+$ Calcd for $C_{32}H_{39}GeNO_6Na$ 630.1881, found 630.1846.

**Benzyl 2-methyl-3-(triphenylgermyl)propanoate (5e):** (80 mg) in 83% yield as colorless oil. **$^1$H NMR** (500 MHz, $CDCl_3$) δ 7.55-7.45 (m, 6H), 7.42-7.27 (m, 12H), 7.23-7.17 (m, 2H), 4.87 (d, $J$ = 12.3 Hz, 1H), 4.64 (d, $J$ = 12.3 Hz, 1H), 2.79 (m, 1H), 2.07 (dd, $J$ = 14.0, 7.9 Hz, 1H), 1.69 (dd, $J$ = 14.0, 6.9 Hz, 1H), 1.21 (d, $J$ = 6.9 Hz, 1H); **$^{13}$C NMR** (126 MHz, $CDCl_3$) δ 176.9, 136.7, 136.1, 135.1, 129.1, 128.6, 128.4, 128.2, 128.2, 66.2, 36.5, 21.0, 18.8; **IR** (neat): 3056, 2927, 1729, 1437, 1258 $cm^{-1}$; **HRMS** (ESI) m/z: $[M+Na]^+$ Calcd for $C_{29}H_{28}O_2GeNa$ 505.1193, found 505.1209.

**Phenyl 3-(triphenylgermyl)propanoate (5f):** (63.6 mg) in 70% yield as colorless oil. **$^1$H NMR** (500 MHz, $CDCl_3$) δ 7.57-7.49 (m, 6H), 7.44-7.37 (m, 9H), 7.36-7.30 (m, 2H), 7.24-7.17 (m, 1H), 6.97-6.62 (m, 2H), 2.80-2.70 (m, 2H), 1.99-1.92 (m, 2H); **$^{13}$C NMR** (126 MHz, $CDCl_3$) δ 173.1, 150.9, 136.1, 135.1, 129.5, 129.3, 128.5, 125.8, 121.6, 30.3, 8.9; **IR** (neat): 3057, 2920, 1753, 1484, 1344 $cm^{-1}$; **HRMS** (ESI) m/z: $[M+Na]^+$ Calcd for $C_{27}H_{24}O_2GeNa$ 477.0880, found 477.0891.

**3-(triphenylgermyl)cyclopentan-1-one (5g):** (80 mg) in 83% yield as colorless oil. **$^1$H NMR** (500 MHz, $CDCl_3$) δ 7.53-7.46 (m, 6H), 7.45-7.34 (m, 9H), 2.61-2.52 (m, 1H), 2.52-2.34 (m, 2H), 2.26-2.09 (m, 3H), 2.00-1.88 (m, 1H); **$^{13}$C NMR** (126 MHz, $CDCl_3$) δ 220.1, 135.4, 135.3, 129.4, 128.6, 41.5, 39.0, 26.6, 23.9; **IR** (neat): 3055, 2921, 1729, 1477, 1393 $cm^{-1}$; **HRMS** (APCI) m/z: $[M+H]^+$ Calcd for $C_{23}H_{23}GeO$ 389.0955, found 389.0964.

**1-(3-(triphenylgermyl)propanoyl)pyrrolidin-2-one (5h):** (57 mg) in 64% yield as colorless oil. **$^1$H NMR** (500 MHz, $CDCl_3$) δ 7.57-7.49 (m, 6H), 7.37 (m, 9H), 3.63 (t, $J$ = 7.1 Hz, 2H), 3.15-3.08 (m, 2H), 2.49 (t, *J* = 8.2 Hz, 2H), 1.97- 1.90 (m, 2H), 1.90-1.84 (m, 2H); **$^{13}$C NMR** (126 MHz, $CDCl_3$) δ 175.8, 175.1, 136.6, 135.2, 129.1, 128.3, 45.6, 33.7, 32.7, 17.3, 8.2; **IR** (neat): 3049, 1732, 1694, 1407, 1365 cm$^{-1}$; **HRMS** (ESI) m/z: $[M+K]^+$ Calcd for $C_{25}H_{25}NO_2GeK$ 484.0728, found 484.0734.

**3-(3-(triphenylgermyl)propanoyl)oxazolidin-2-one (5i):** (35.8 mg) in 40% yield as colorless oil. **$^{1}$H NMR** (500 MHz, $CDCl_3$) δ 7.56-7.48 (m, 6H), 7.42-7.33 (m, 9H), 4.30-4.23 (m, 2H), 3.81-3.75 (m, 2H), 3.18-3.11 (m, 2H), 1.91-1.84 (m, 2H); **$^{13}$C NMR** (126 MHz, $CDCl_3$) δ 174.2, 153.4, 136.4, 135.1, 129.1, 128.4, 62.1, 42.5, 31.1, 8.3; **IR** (neat): 3056, 1776, 1695, 1427, 1376 cm$^{-1}$; **HRMS** (ESI) m/z: $[M+Na]^+$ Calcd for $C_{24}H_{23}NO_2GeNa$ 470.0781, found 470.0794.

**Diphenyl(2-(tributylgermyl)ethyl)phosphine oxide (5j):** (91 mg) in 96% yield as colorless oil. **$^{1}$H NMR** (500 MHz, $CDCl_3$) δ 7.77-7.69 (m, 4H), 7.55-7.43 (m, 6H), 2.26-2.17 (m, 2H), 1.35-1.20 (m, 12H), 0.94-0.81 (m, 11H), 0.75-0.68 (m, 6H); **$^{13}$C NMR** (126 MHz, $CDCl_3$) δ 133.10 (d, *J* = 96.1 Hz), 131.74 (d, *J* = 2.7 Hz), 131.06 (d, *J* = 8.9 Hz), 128.74 (d, *J* = 11.2 Hz), 27.45, 26.67, 25.28 (d, *J* = 68.0 Hz), 13.87, 12.27, 2.93 (d, *J* = 7.4 Hz); **$^{31}$P NMR** (202 MHz, $CDCl_3$) δ 34.2; **IR** (neat): 2917, 2857, 1448, 1177, 1114 cm$^{-1}$; **HRMS** (ESI) m/z: $[M+Na]^+$ Calcd for $C_{26}H_{41}OPGeNa$ 497.1999, found 497.2003.

**Tributyl(2-phenylsulfonyl)ethyl)germane (5k):** (49.7 mg) in 60% yield as colorless oil. **$^{1}$H NMR** (500 MHz, $CDCl_3$) δ 7.93-7.88 (m, 2H), 7.70-7.62 (m, 1H), 7.60-7.53 (m, 2H), 3.08-3.01 (m, 2H), 1.27-1.18 (m, 12H), 1.06-0.98 (m, 2H), 0.85 (t, *J* = 6.9 Hz, 9H), 0.73-0.66 (m, 6H); **$^{13}$C NMR** (126 MHz, $CDCl_3$) δ 138.8, 133.7, 129.3, 128.4, 54.0, 27.3, 26.5, 13.8, 12.4, 4.9; **IR** (neat): 2956, 2869, 1454, 1308, 1247 cm$^{-1}$; **HRMS** (ESI) m/z: $[M+Na]^+$ Calcd for $C_{20}H_{36}O_2SGeNa$ 437.1540, found 437.1552.

**3-(triphenylgermyl)propanenitrile (5l):** (61 mg) in 85% yield as white solid. **$^{1}$H NMR** (500 MHz, $CDCl_3$) δ 7.51-7.37 (m, 15H), 2.49-2.38 (m, 2H), 1.94-1.82 (m, 2H); **$^{13}$C NMR** (126 MHz, $CDCl_3$) δ 134.9, 129.7, 128.7, 121.0, 13.5, 10.3; **IR** (neat): 3058, 2920, 2244, 1480, 1310 $cm^{-1}$; **HRMS** (ESI) m/z: $[M+Na]^+$ Calcd for $C_{21}H_{19}NGeNa$ 382.0621, found 382.0632.

### 2.8.10 Stern-Volmer quenching

A $1.25\times10^{-4}$ M stock solution was prepared by dissolving 1.47 mg photocatalyst 4CzIPN in 15 mL of spectroscopic-grade acetonitrile and degassed with argon. The quenching experiment was performed by taking an appropriate volume of 4CzIPN from the stock solution, along with different concentrations of the quencher. The Emission intensity was observed at 556 nm with an excitation wavelength of 360 nm.

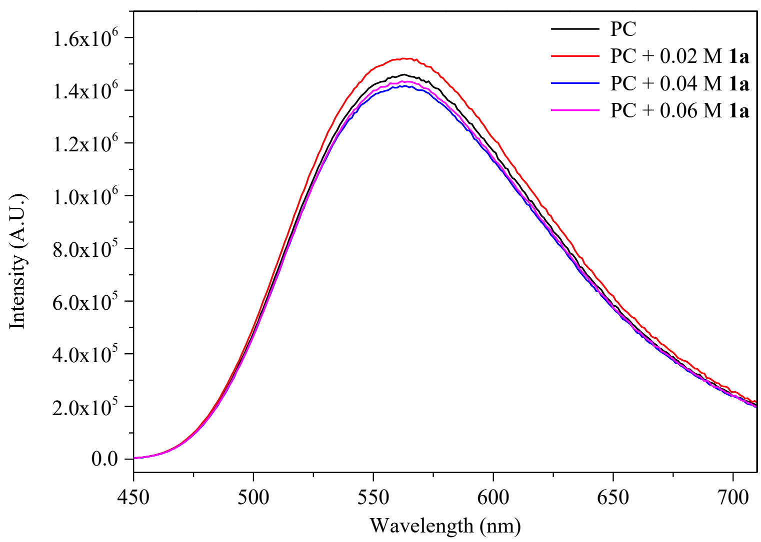

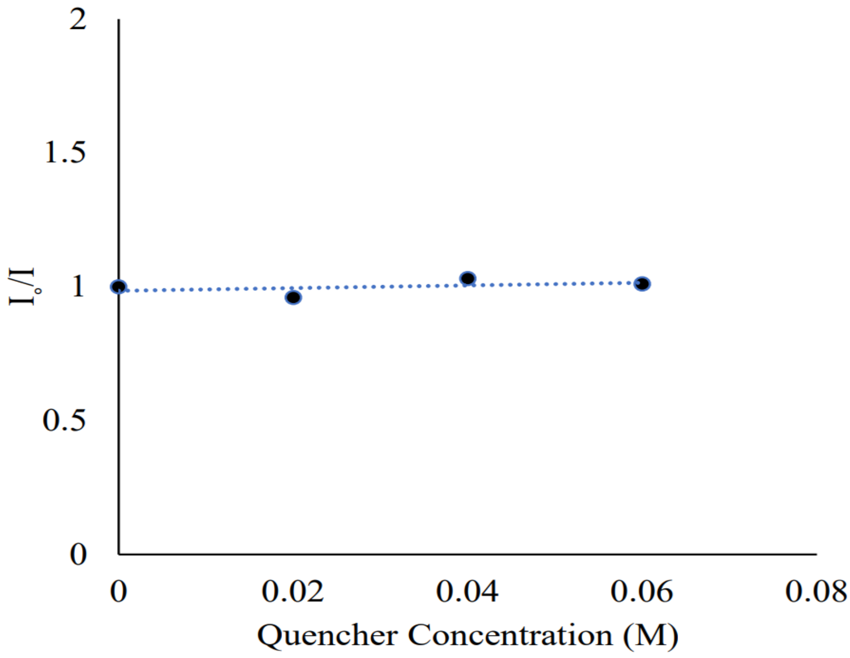


**Figure 2.6** Fluorescence quenching and Stern-Volmer plot of 4CzIPN *vs* **1a**

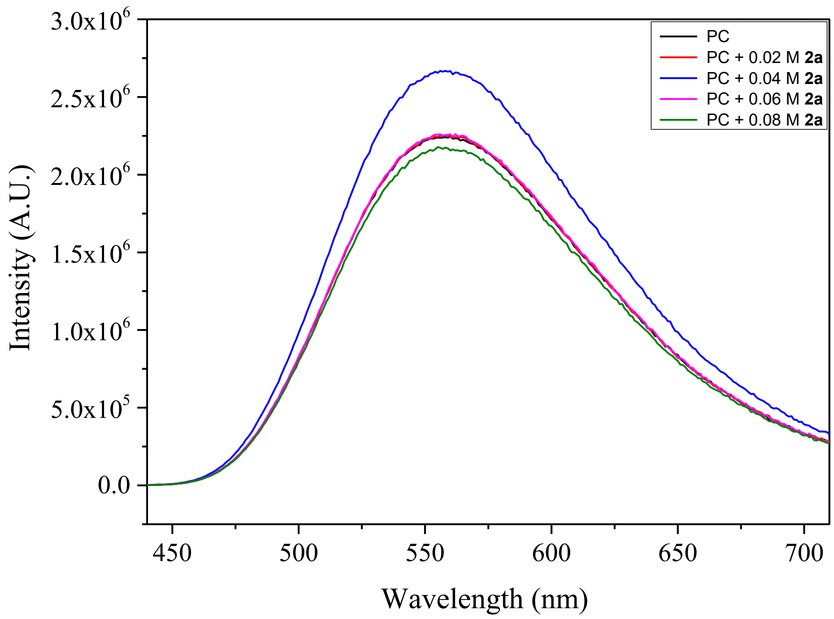

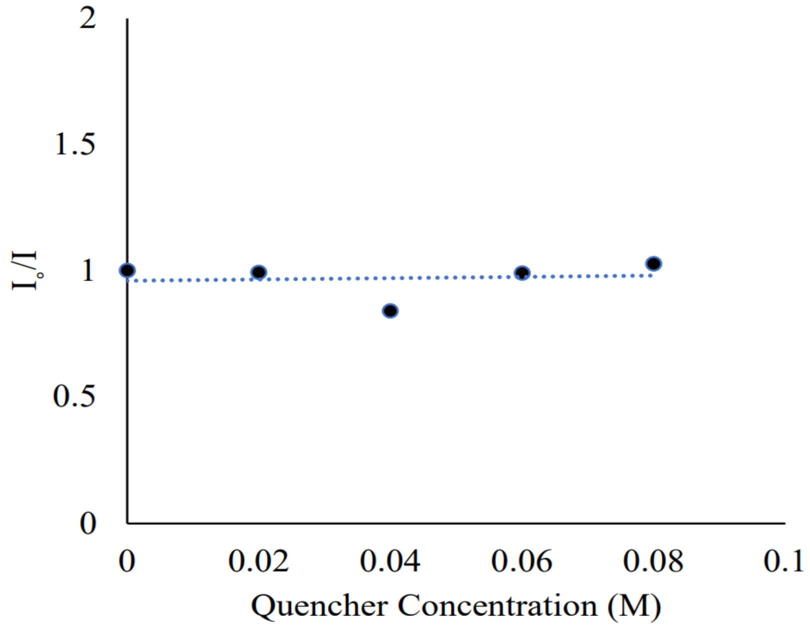


**Figure 2.7** Fluorescence quenching and Stern-Volmer plot of 4CzIPN *vs* **2a**

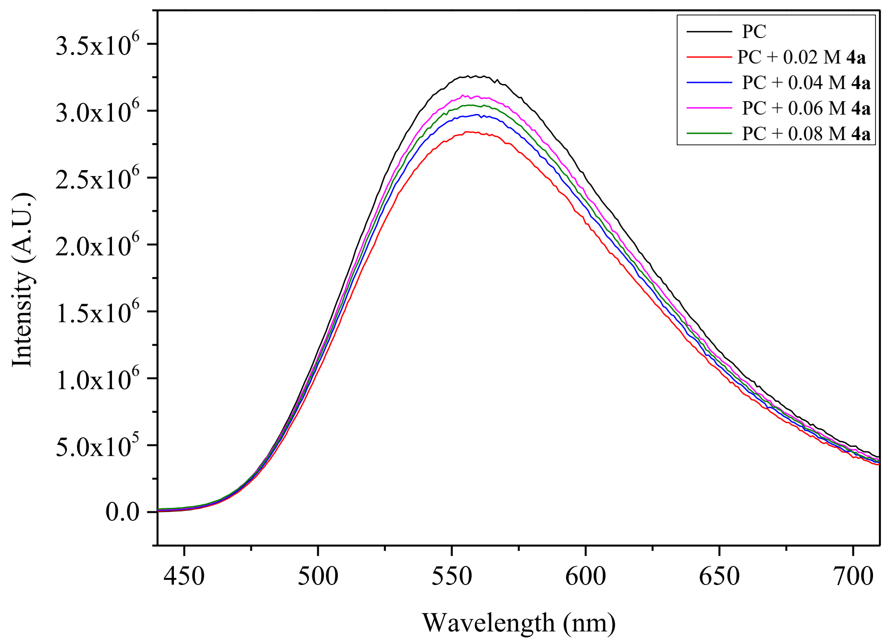

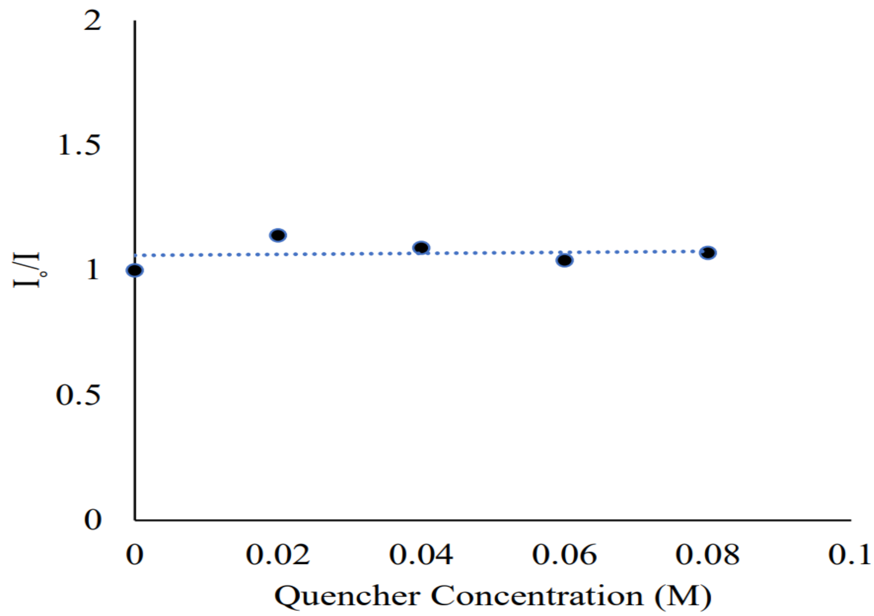


**Figure 2.8** Fluorescence quenching and Stern-Volmer plot of 4CzIPN *vs* **4a**

### 2.8.11 Determination of quantum yield[99,100]

Sample preparation: A potassium ferrioxalate solution (0.15 M) was prepared by dissolving 2.21 g of potassium ferrioxalate trihydrate in 30 mL $H_2SO_4$ (0.05 M). A buffer solution was prepared by dissolving 50 mg of phenanthroline and 11.25 g sodium acetate in 50 mL $H_2SO_4$ (0.5 M). Both solutions were stored in dark and wrapped with aluminium foil. A 10 mL reaction tube was covered with black electrical tape and wrapped in aluminium foil, except for a small window at the bottom for irradiation. Then, the reaction tube was charged with 5 mL of ferrioxalate solution and irradiated for 10 seconds. This solution was treated with 0.875 mL buffered phenanthroline solution. After irradiation, the reaction tube was covered completely with aluminium foil and stirred for 1 hour in a dark condition, allowing the ferrous ion to coordinate with phenanthroline completely. The absorbance of the resulting solutions was measured using a PerkinElmer Lambda 750 spectrometer at 510 nm. A non-irradiated solution was also prepared, and absorbance was measured at 510 nm.

The conversion of ferrioxalate was calculated as:

$$\text{Mol Fe}^{2+} = \frac{V \times \Delta A}{l \times \varepsilon}$$

$$= \frac{0.005875\ L \times (1.71615 - 1.04142)}{1\ cm \times 11100\ L\ mol^{-1} cm^{-1}} = 3.57120608 \times 10^{-7}\ mol$$

Where $V$ is the total volume (0.005875 L) of the solution after the addition of phenanthroline solution, $\Delta A$ is the difference in absorbance between irradiated and non-irradiated solutions at 510 nm, l is the path length (1.0 cm) and $\varepsilon$ is the molar absorptivity at 510 nm.

<u>The photo-flux was calculated as</u>:

$$\text{Photon flux} = \frac{molFe^{2+}}{\phi \times t \times f}$$

$$= \frac{3.51720608 \times 10^{-7}}{1.01 \times 10 \times 0.9968} = 3.49356165 \times 10^{-8}\ einstein\ sec^{-1}$$

Where $\phi$ is the quantum yield for the ferrioxalate actinometer (1.01 for 0.15 M solution), $t$ is the time, 10 seconds and $f$ is the fraction of light absorbed by the ferrioxalate actinometer solution at λ = 450 nm.

Absorbance at λ = 436 nm by ferrioxalate actinometer is A = 2.4762. So, the fraction of light absorbed ($f$) by the ferrioxalate actinometer at 436 nm is as:

$$f = 1 - 10^{-A} = 1 - 10^{-2.4762} = 0.9968$$

<u>Quantum yield calculation for standard reaction</u>:

The parent reaction was performed in a 10 mL reaction tube under optimal conditions at a 0.2 mmol scale for 3 hours. The $^{1}$H NMR yield was then calculated to be 17%, using triphenylmethane as the internal standard.

$$\phi = \frac{mol\ product}{flux \times t \times f} =$$

$$= \frac{0.2 \times 0.17}{3.49356165 \times 10^{-8} \times 10800 \times 0.496464609} = 0.181$$

Where $\phi$ is the quantum yield of the reaction, t is the reaction time (10800 seconds) and $f$ is the fraction of light absorbed by photocatalyst solution ($7.5\times10^{-6}$ M) at λ = 450nm.

Determination of fraction of light absorbed by photocatalyst at λ = 450 nm: A $7.5 \times 10^{-5}$ M solution was prepared by mixing 1.18 mg of 4CzIPN in 20 mL of spectroscopic-grade acetonitrile. From this solution, 3 mL was taken, and the UV-Visible spectra was recorded. The absorbance of the photocatalyst solution measured at 450 nm was 0.29797.

The fraction of light absorbed ($f$) by this solution was calculated as below, where A is absorbance at 450 nm.

$$f = 1 - 10^{-A} = 1 - 10^{-0.29797} = 0.496464609$$

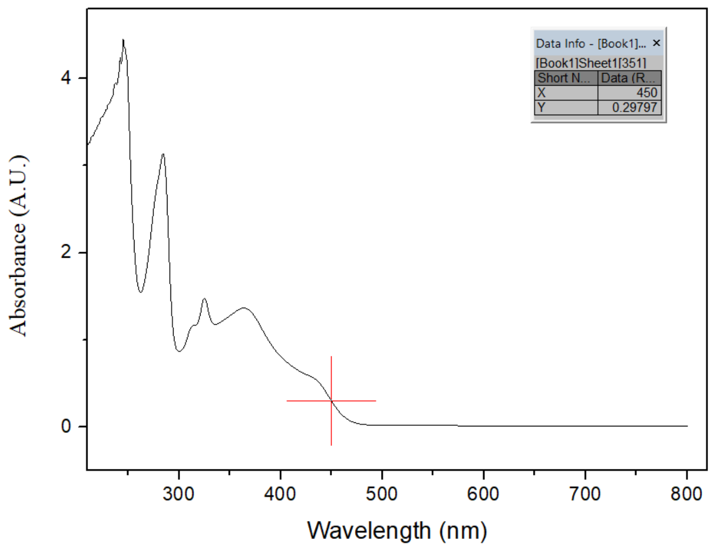


**Figure 2.9** Absorbance of photocatalyst solution ($7.5\times10^{-5}$ M)

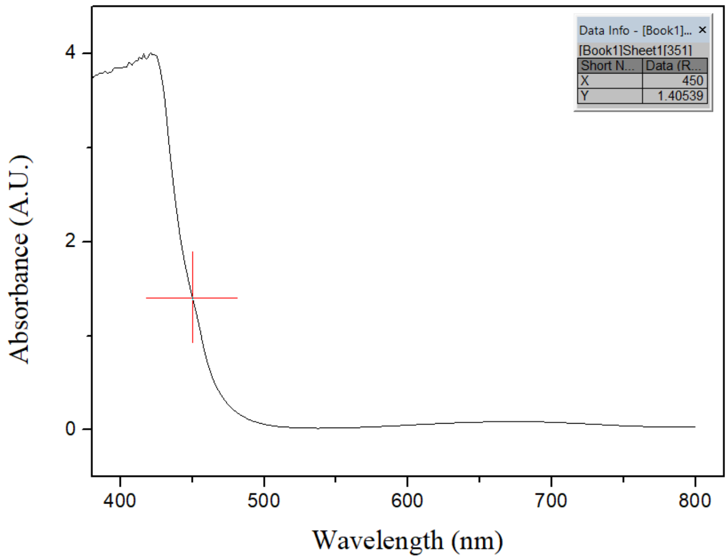


**Figure 2.10** Fraction of light absorbed by ferrioxalate solution without light irradiation and without adding 1,10 Phenanthroline solution

### 2.8.12 Cyclic voltammetry study

Cyclic voltammetry was measured using a C-H instrument model CHI1103C with a three-electrode cell (beaker-type cell) at room temperature. The experiment was performed in $CH_3CN$ (15 mL, degassed and spectroscopic grade solvent) with $TBAPF_6$ (0.1 M) using a glassy carbon working electrode, a Pt-wire counter electrode, and an Ag/AgCl (0.1 M KCl aqueous solution) reference electrode at a scan rate of 0.1 V/s.

To a solution of sulfonamide HATC2 (0.005 M) in acetonitrile, no oxidation peak was shown even the voltage rise up to 2.0 V. These results indicate that HATC2 cannot be oxidized by the excited 4CzIPN ($E_{1/2}^{red}$ [$4CzIPN^*$/$[4CzIPN]^{\bullet -}$ = +1.35 V vs saturated calomel electrode in MeCN).

Preparation of Potassium Salt of *N*-cyclohexyl-4-methylbenzenesulfonamide:*[67]* To a solution of (HATC2) *N*-cyclohexyl-4-methylbenzenesulfonamide (98.8mg, 0.39 mmol) in $CH_3CN$ (4 mL) was added potassium *tert*-butoxide (43.76mg, 0.39 mmol). The mixture was stirred for 3 hours at room temperature then the solvent was removed by rotary evaporation. After the salt was dried under high vacuum (10 mbar pressure) for 3 hours and obtained salt was white solid, which was used quickly in CV measurement. 15 mL of $CH_3CN$ containing 0.1 M $TBAPF_6$ (582 mg) and appropriate potassium sulfonamide salt was added and stirred for 10 minutes with $N_2$ gas purging in a beaker-type cell and then CV was recorded. The oxidation peak was noticed at +0.83 V vs $Ag/Ag^+$ (0.1 M KCl aq.) [+0.86 V vs. SCE]

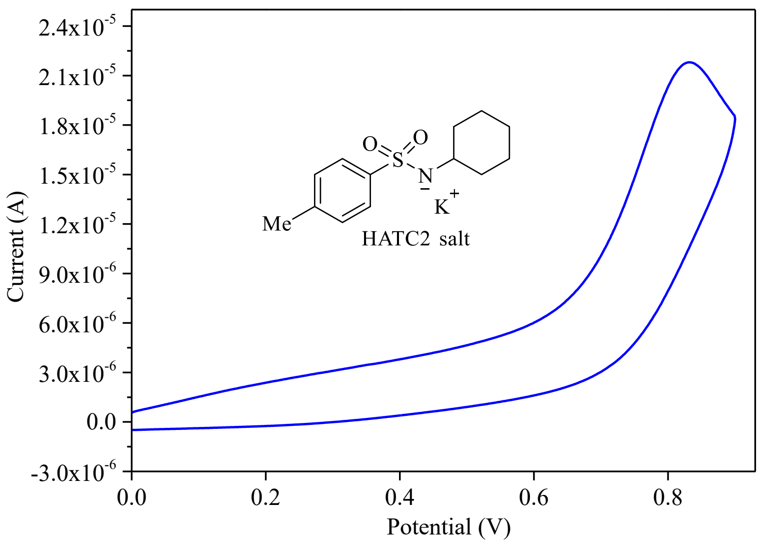


**Figure 2.5** Cyclic voltametric graph for Potassium Salt of *N*-cyclohexyl-4-methylbenzenesulfonamide

### 2.8.13 Light on-off experiment

To an oven-dried 20 mL reaction tube equipped with a magnetic stir bar were added benzyl acrylate **1a** (1 mmol, 1 equiv.), $^t$BuMe$_2$SiH **2a** (3 mmol, 3 equiv.), 5 mol% photocatalyst 4CzIPN (39.4 mg, 0.050 mmol), 20 mol% HATC-2 (50.6 mg, 0.2 mmol) and 20 mol% $K_3PO_4$ (42.4 mg, 0.2 mmol). Triphenylmethane (48.8 mg, 0.2 mmol) was added as an internal standard for $^1$H-NMR yield calculation. The reaction tube was sealed and placed under argon atmosphere, then 10 ml of 20:1 (*v*/*v*) acetone: water was added *via* syringe, the reaction mixture was degassed *via* freeze pump thaw (x 3 times) and refilled with argon. The sealed reaction tube was then placed inside the Penn photoreactor (Blue LEDs, λ = 450 nm) and irradiated under alternating light-dark conditions (light:dark, 3:3 hours) for up to 24 hours. After completing each 3 hours of light or dark conditions, 1 mL of the solution from the parent reaction was taken *via* syringes by applying an argon balloon, and the yield was analyzed using triphenylmethane as an internal standard. The result in the figure below shows the essential role of light, as the reaction proceeded in the presence of light and stopped in the dark condition. From these experiments, we concluded that a continuous supply of light is necessary for this reaction, confirming that the reaction does not proceed through a chain propagation mechanism.

**Table 2.9** Light On-Off experiment

| Entry | Time (Hours) | Light source | Yield (%) |
|---|---|---|---|
| 1. | 3 | ON | 17 |
| 2. | 6 | OFF | 17 |
| 3. | 9 | ON | 23 |
| 4. | 12 | OFF | 23 |
| 5. | 15 | ON | 28 |
| 6. | 18 | OFF | 28 |
| 7. | 21 | ON | 34 |
| 8. | 24 | OFF | 34 |

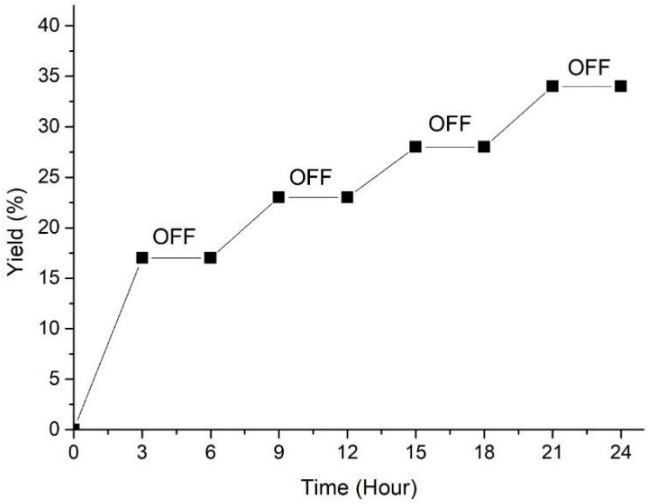


**Figure 2.11** Light On-Off experiment

## 2.9 Selected NMR spectra

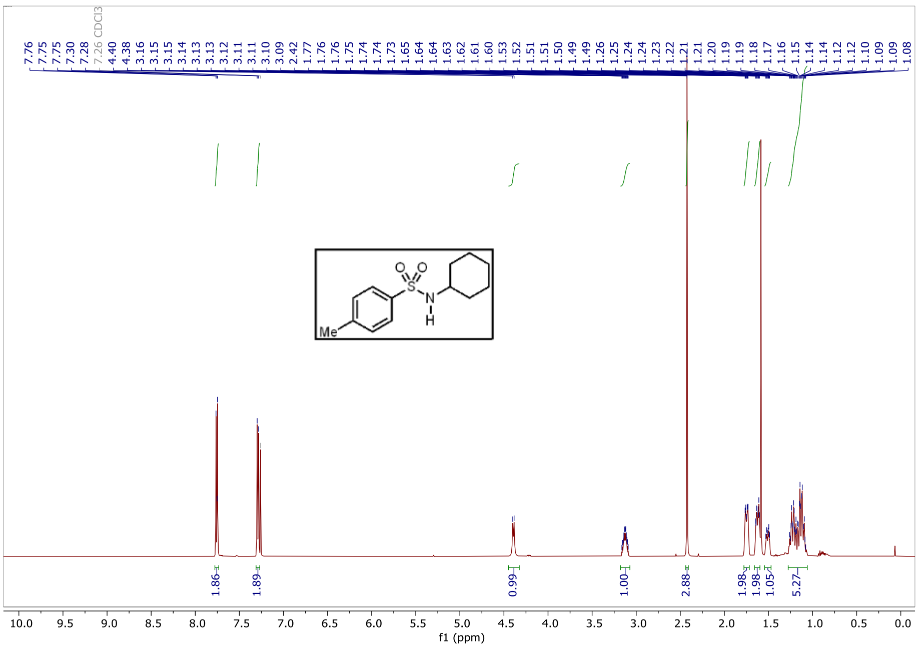

**Figure 2.9.1** $^{1}$H NMR spectra of **HATC2** [$CDCl_3$, 500 MHz]

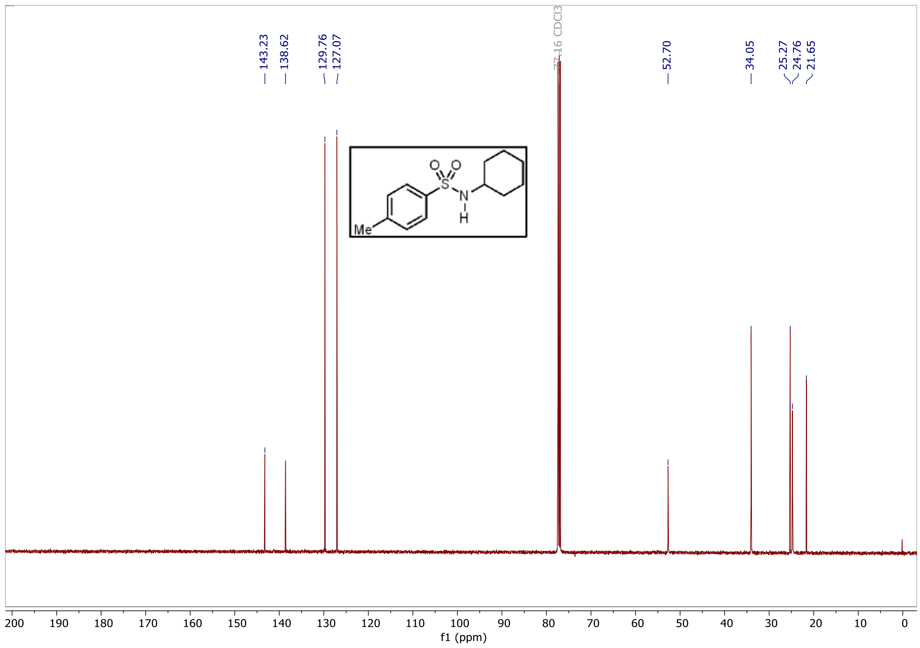

**Figure 2.9.2** $^{13}$C NMR spectra of **HATC2** [$CDCl_3$, 126 MHz]

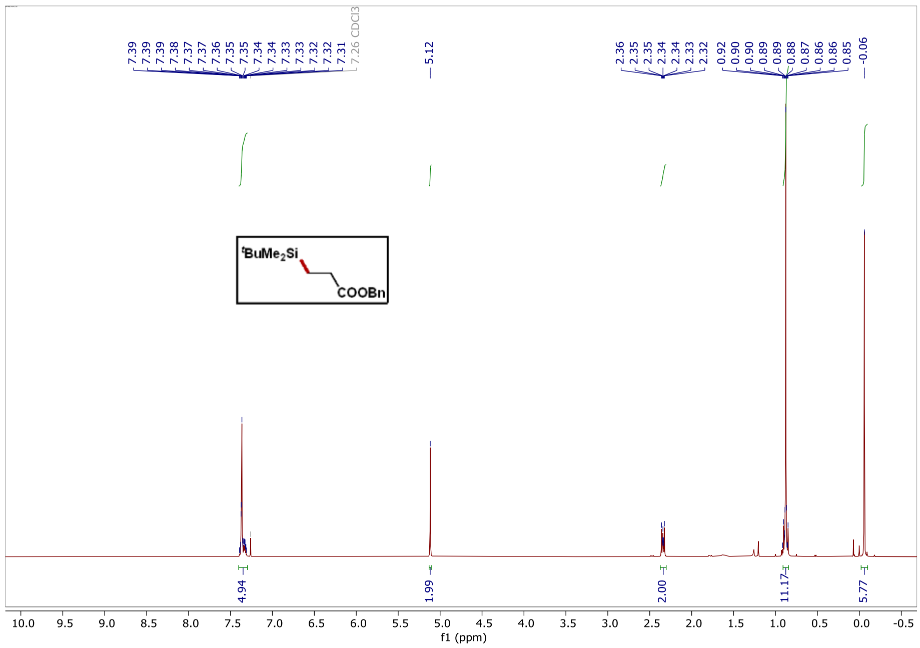

**Figure 2.9.3** $^{1}$H NMR spectra of **3a** [$CDCl_3$, 500 MHz]

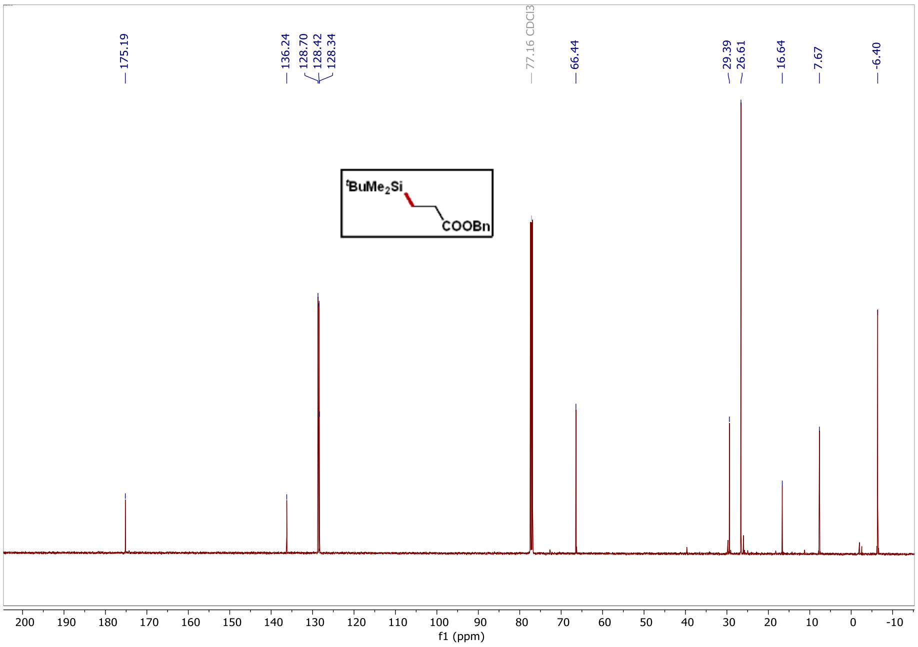


**Figure 2.9.4** $^{13}$C NMR spectra of **3a** [$CDCl_3$, 126 MHz]

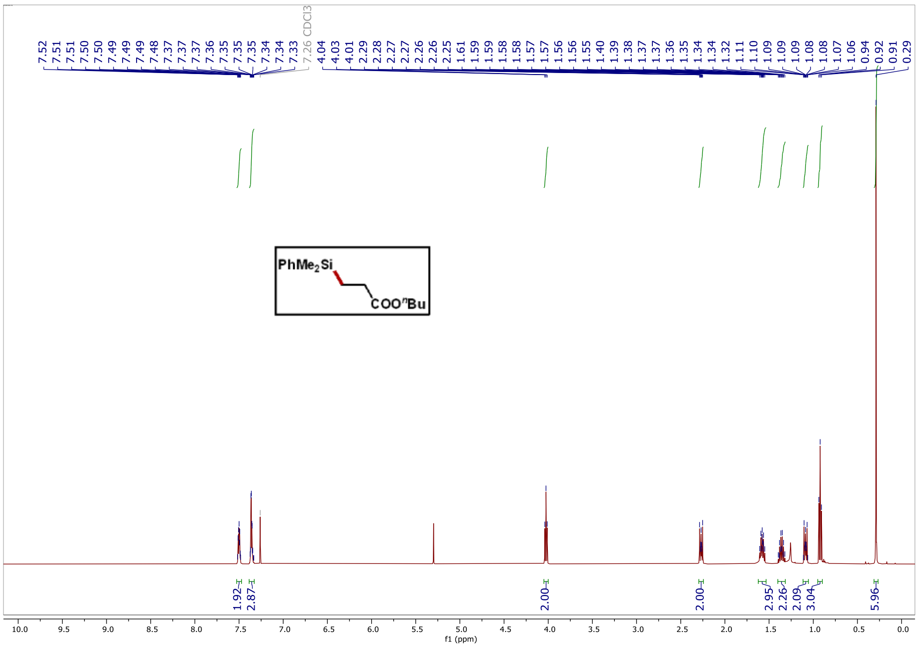


**Figure 2.9.5** $^{1}$H NMR spectra of **3b** [$CDCl_3$, 500 MHz]

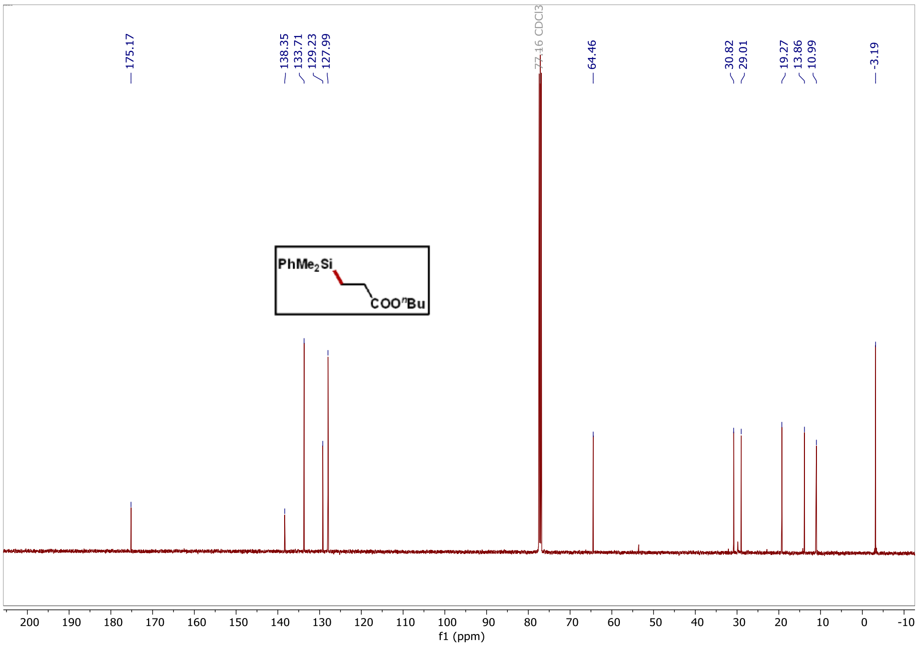


**Figure 2.9.6** $^{13}$C NMR spectra of **3b** [$CDCl_3$, 126 MHz]

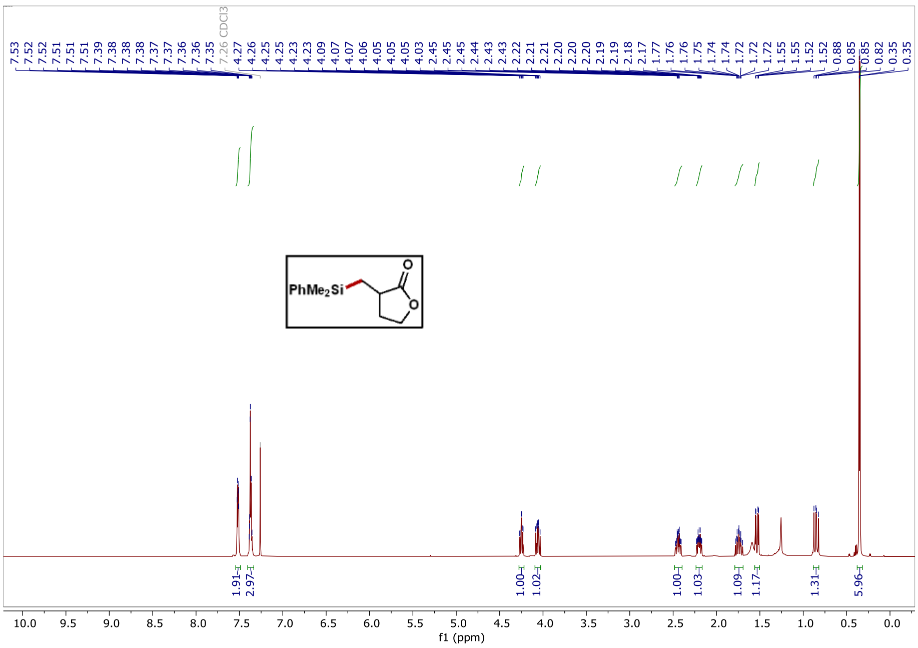


**Figure 2.9.7** $^{1}$H NMR spectra of **3c** [$CDCl_3$, 500 MHz]

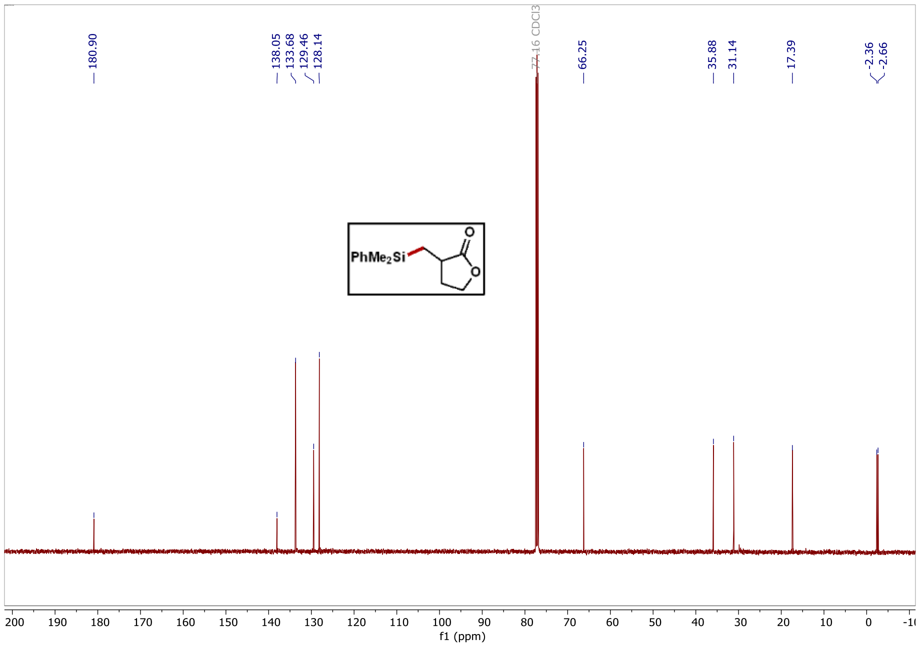

**Figure 2.9.8** $^{13}$C NMR spectra of **3c** [$CDCl_3$, 126 MHz]

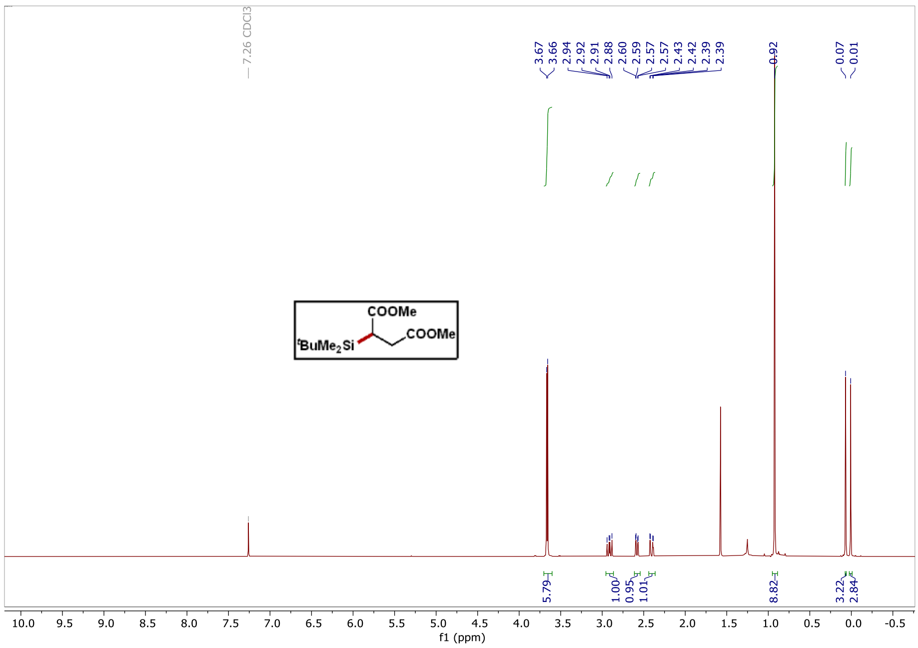

**Figure 2.9.9** $^{1}$H NMR spectra of **3d** [$CDCl_3$, 500 MHz]

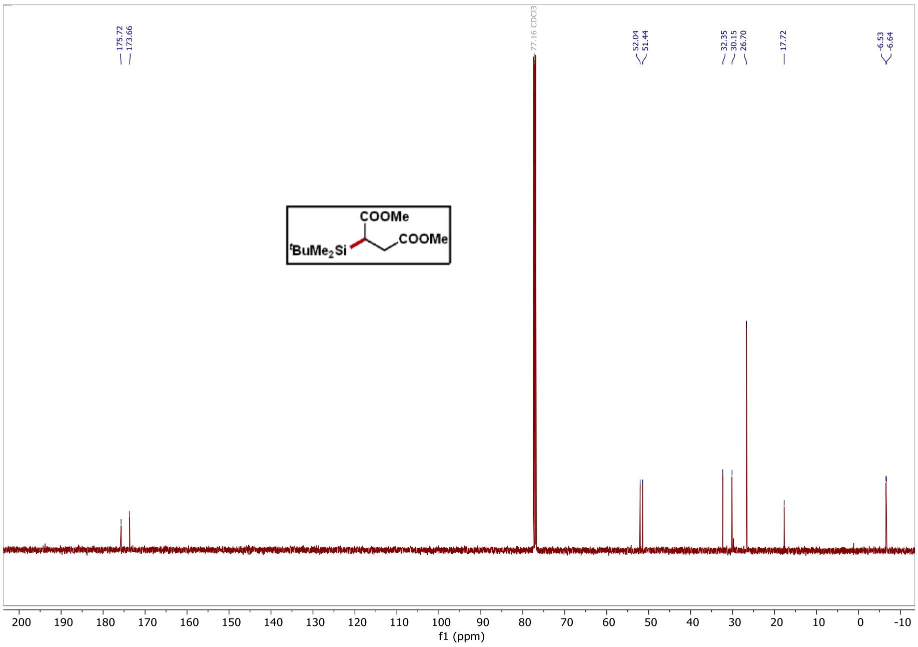

**Figure 2.9.10** $^{13}C$ NMR spectra of **3d** [$CDCl_3$, 126 MHz]

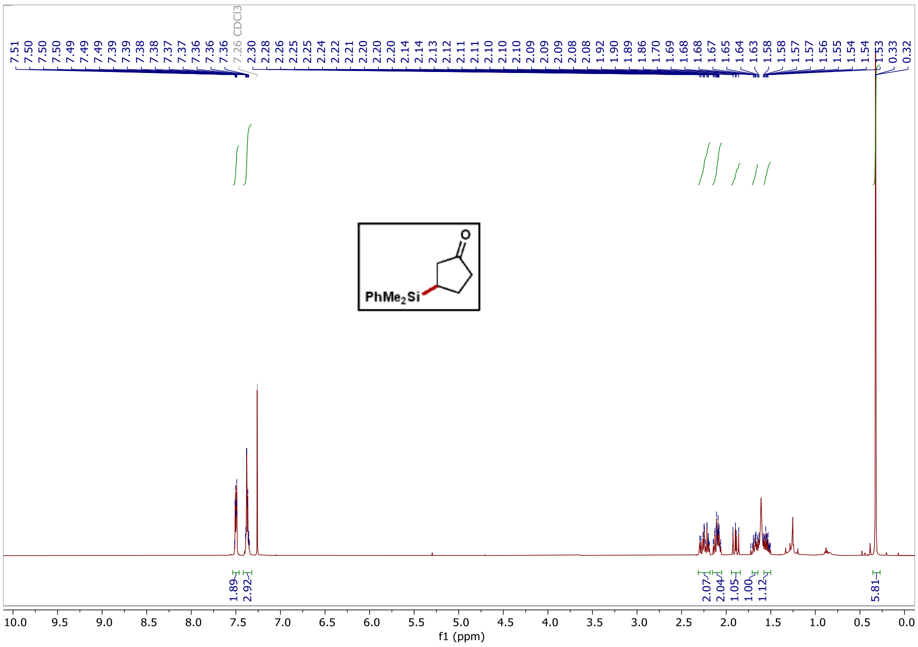

**Figure 2.9.11** $^{1}H$ NMR spectra of **3f** [$CDCl_3$, 500 MHz]

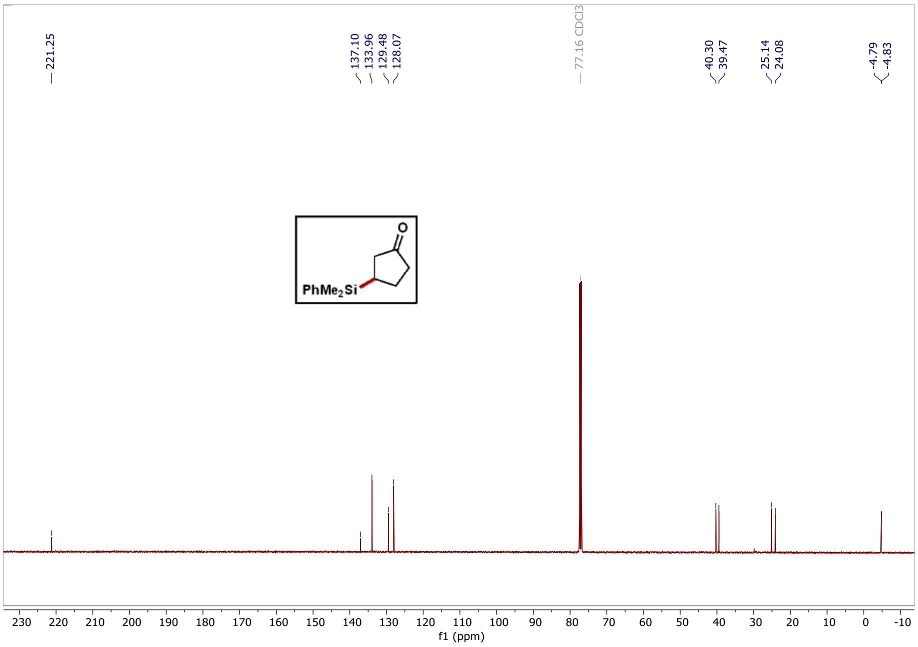

**Figure 2.9.12** $^{13}C$ NMR spectra of **3f** [$CDCl_3$, 126 MHz]

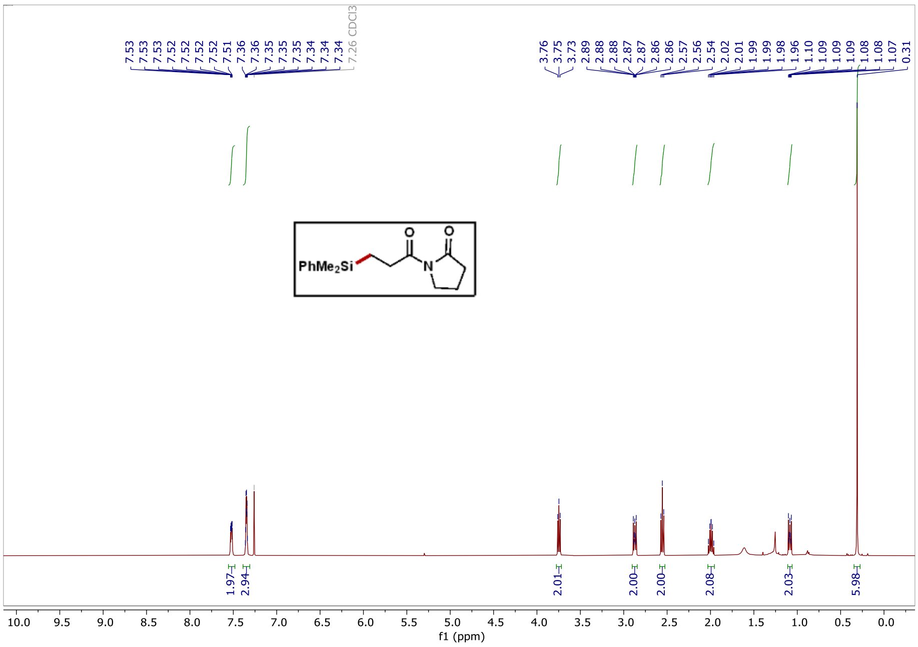

**Figure 2.9.13** $^{1}H$ NMR spectra of **3h** [$CDCl_3$, 500 MHz]

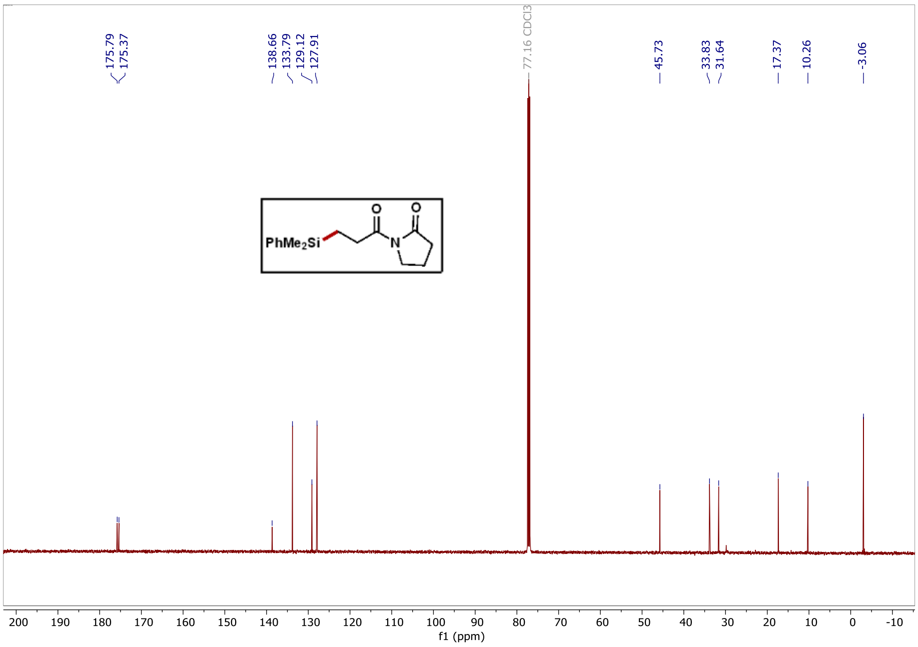


**Figure 2.9.14** $^{13}$C NMR spectra of **3h** [$CDCl_3$, 126 MHz]

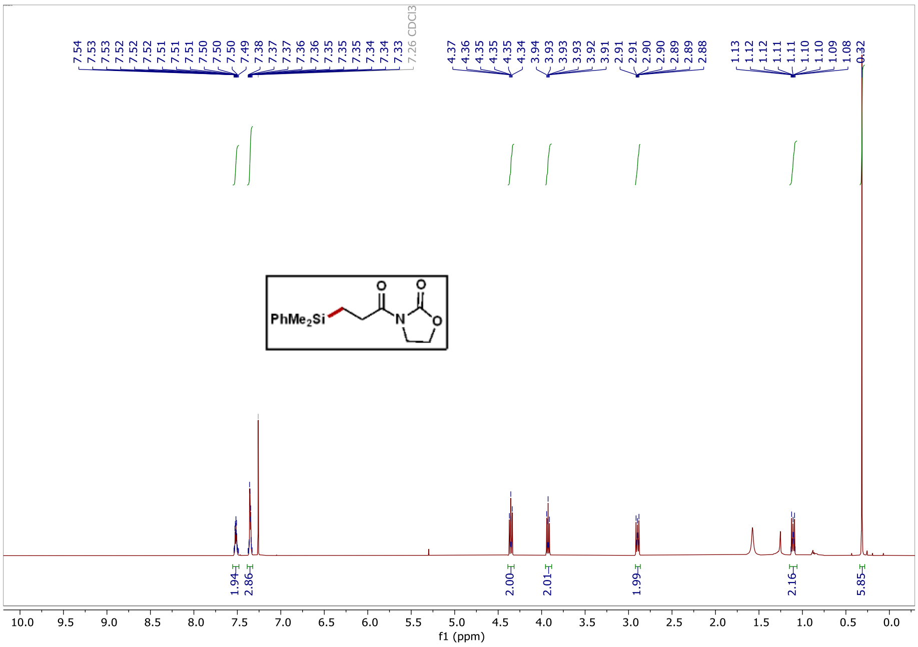


**Figure 2.9.15** $^{1}$H NMR spectra of **3i** [$CDCl_3$, 500 MHz]

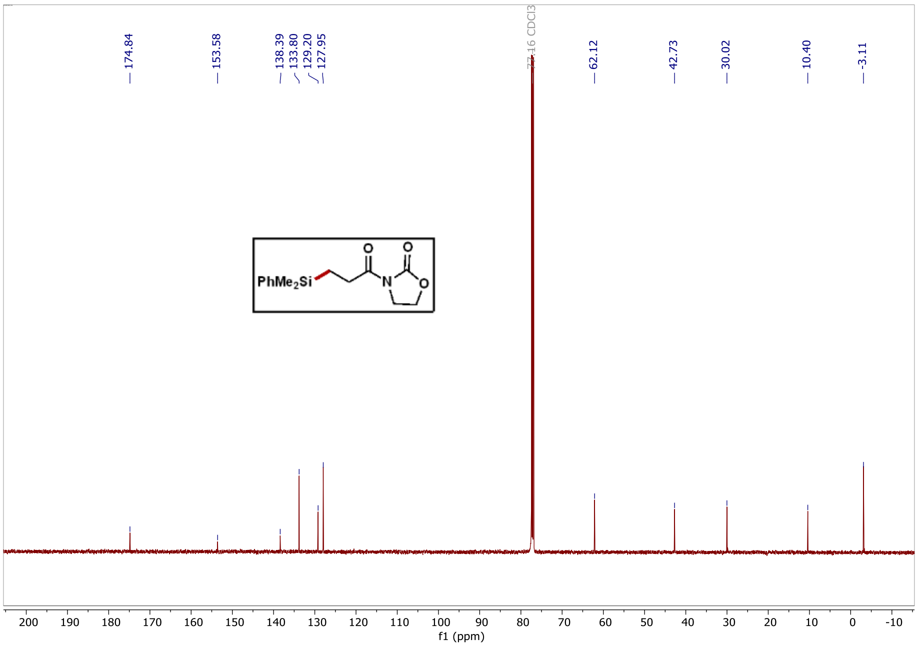

**Figure 2.9.16** $^{13}$C NMR spectra of **3i** [$CDCl_3$, 126 MHz]

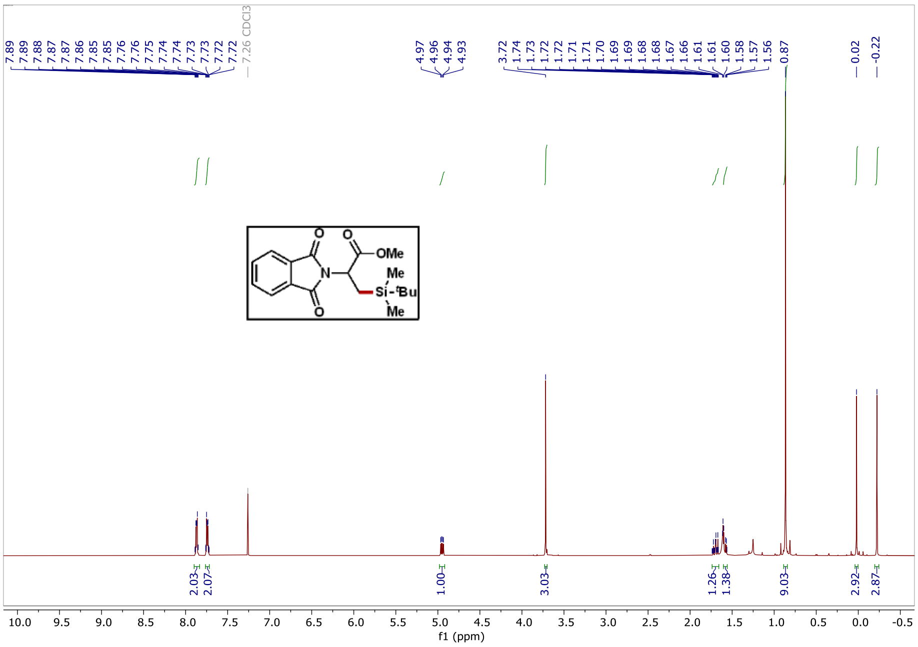

**Figure 2.9.17** $^{1}$H NMR spectra of **3j** [$CDCl_3$, 500 MHz]

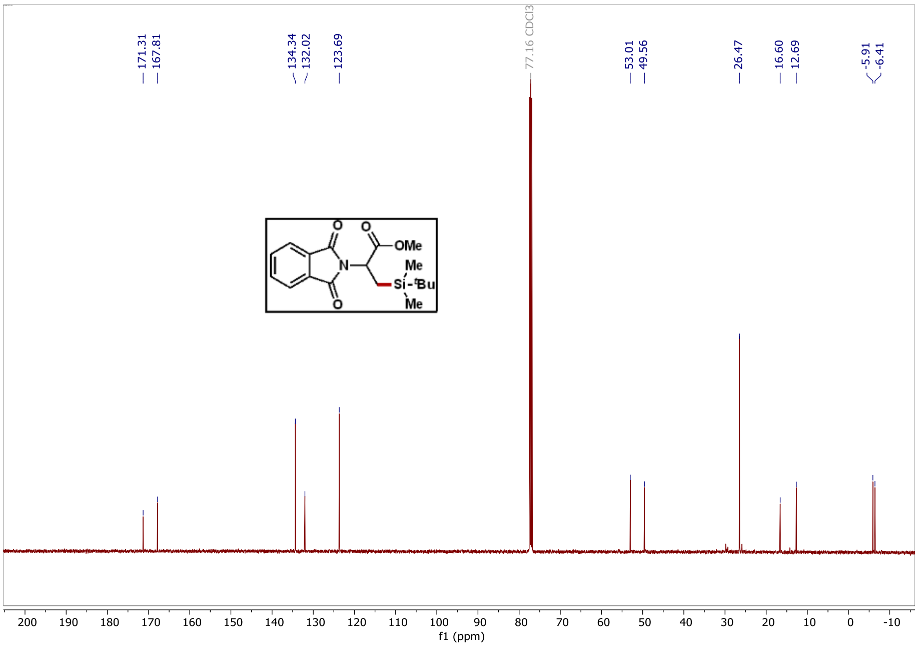

**Figure 2.9.18** $^{13}$C NMR spectra of **3j** [$CDCl_3$, 126 MHz]

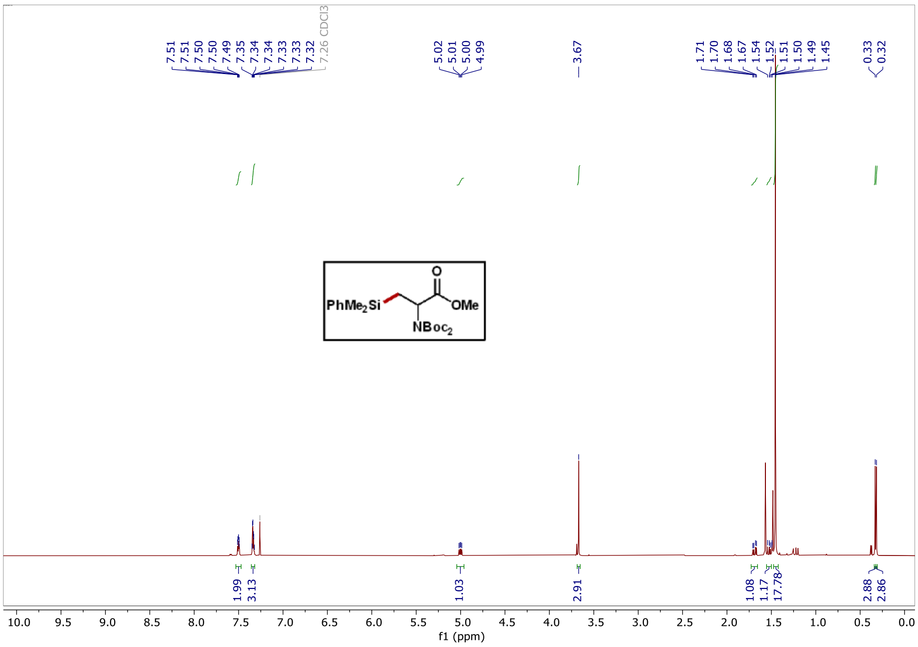

**Figure 2.9.19** $^{1}$H NMR spectra of **3k** [$CDCl_3$, 500 MHz]

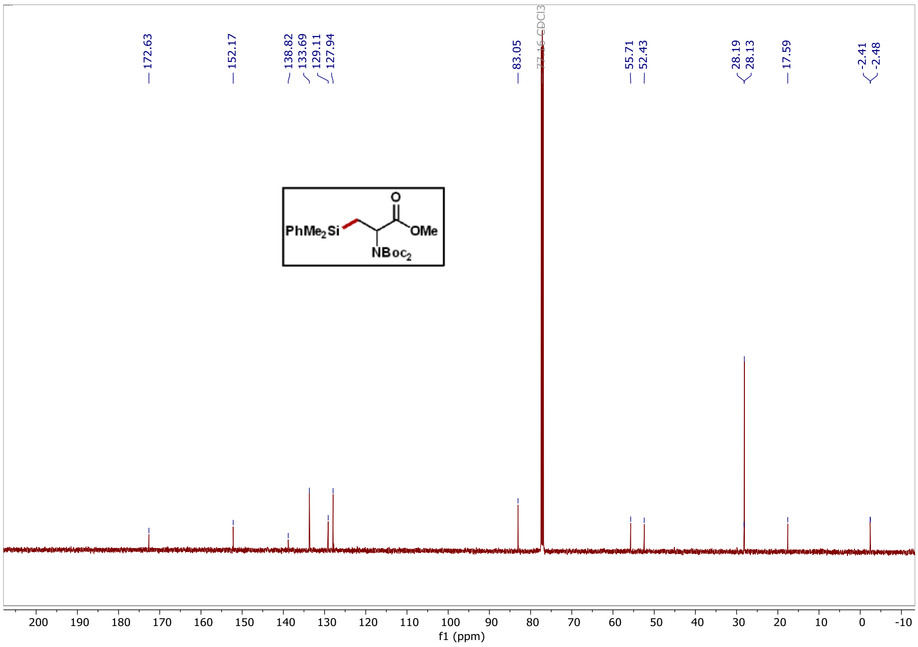

**Figure 2.9.20** $^{13}C$ NMR spectra of **3k** [$CDCl_3$, 126 MHz]

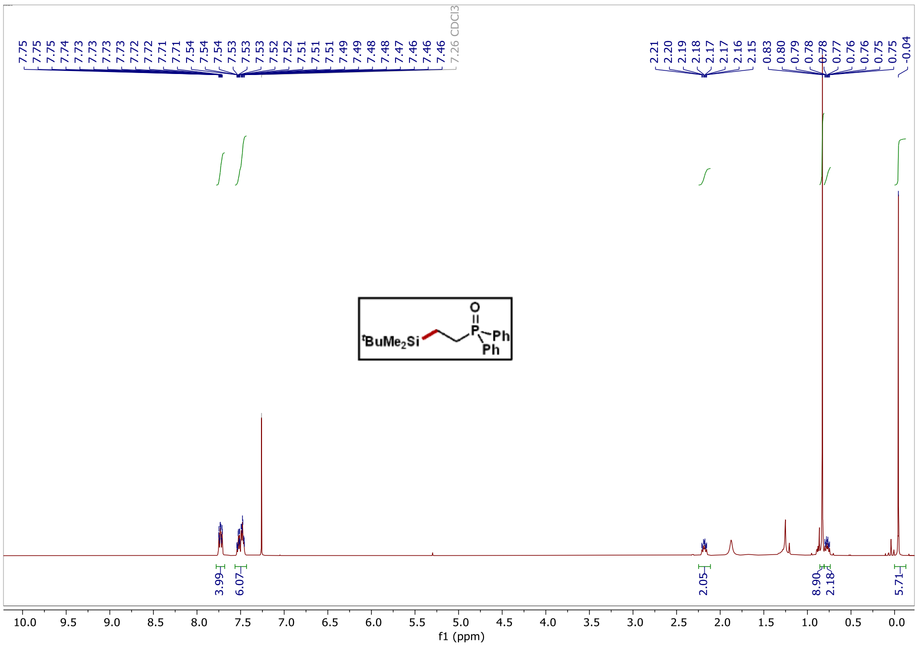

**Figure 2.9.21** $^{1}H$ NMR spectra of **3l** [$CDCl_3$, 500 MHz]

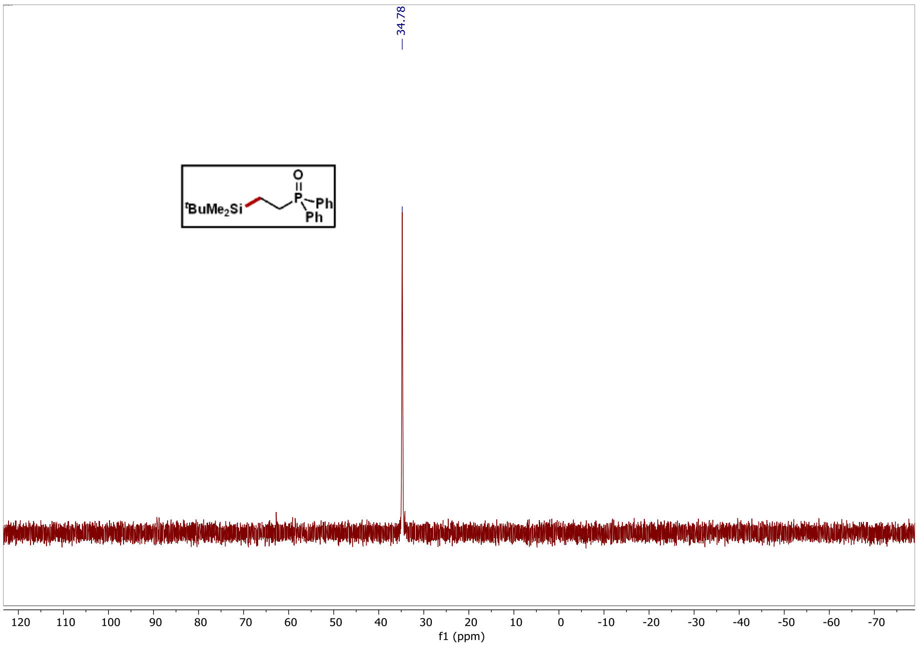


**Figure 2.9.22** $^{31}$P NMR spectra of **3l** [$CDCl_3$, 202 MHz]

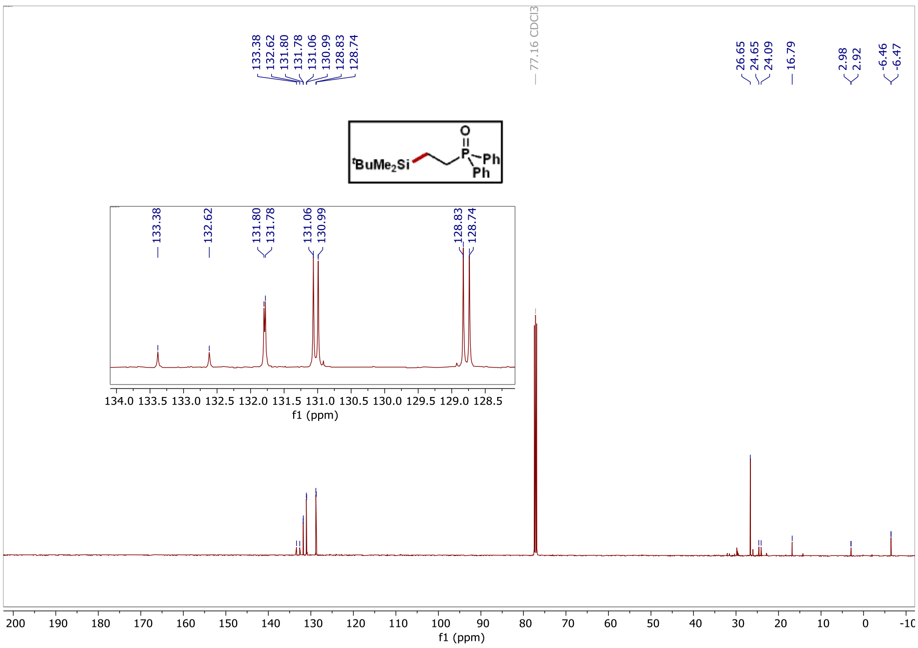


**Figure 2.9.23** $^{13}$C NMR spectra of **3l** [$CDCl_3$, 126 MHz]

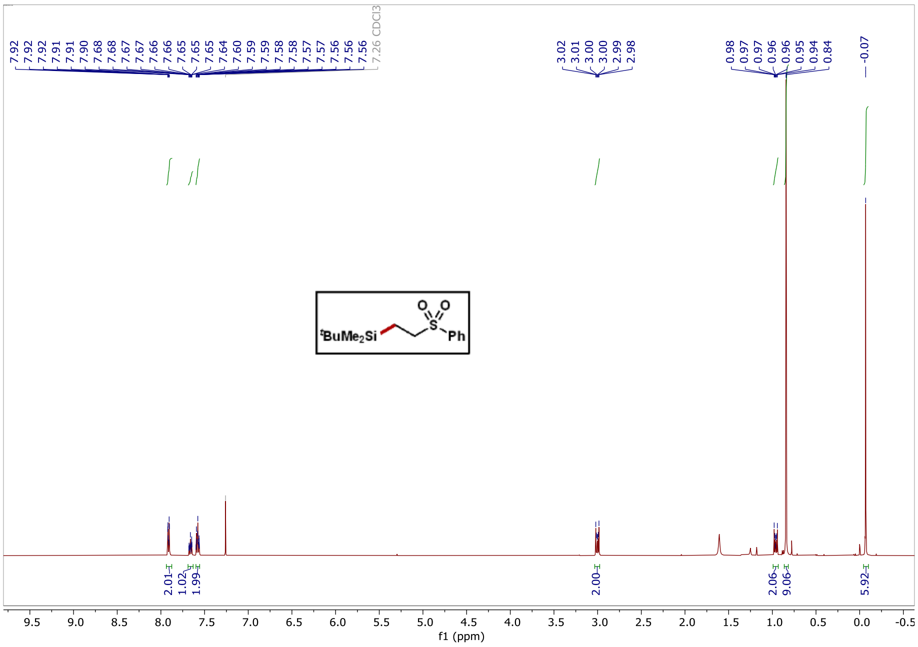

**Figure 2.9.24** $^{1}H$ NMR spectra of **3m** [$CDCl_3$, 500 MHz]

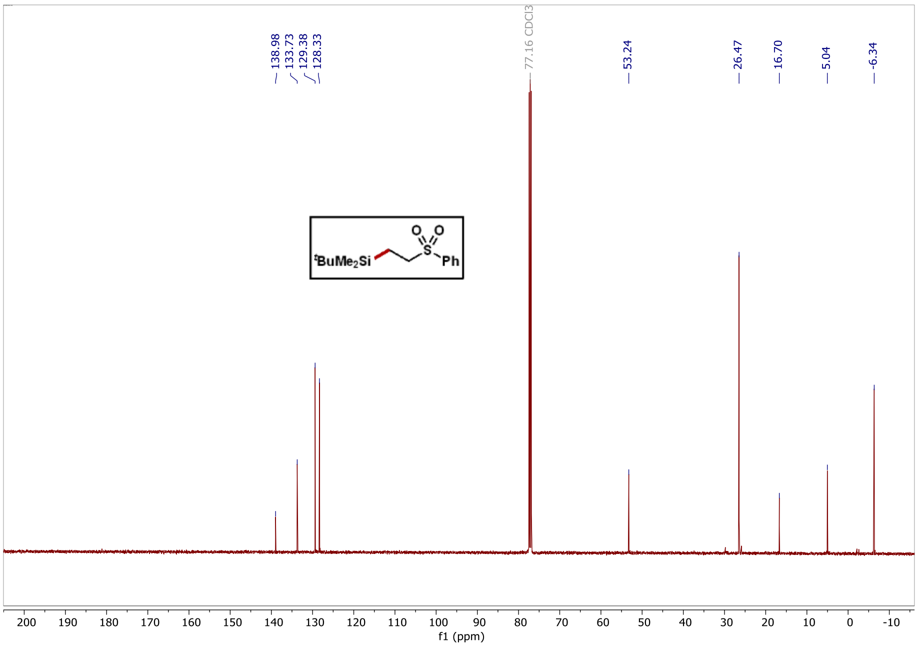

**Figure 2.9.25** $^{13}C$ NMR spectra of **3m** [$CDCl_3$, 126 MHz]

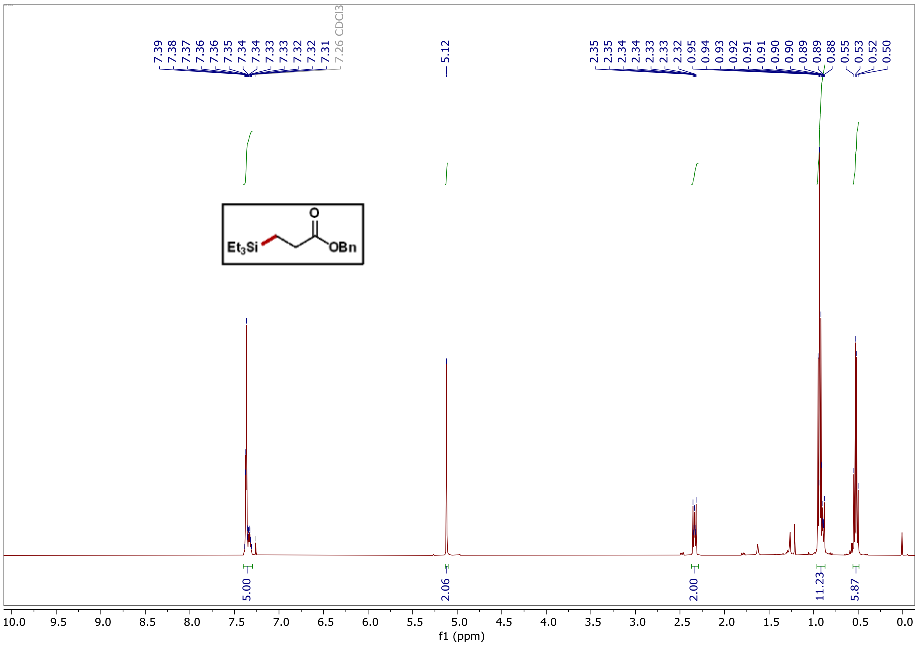

**Figure 2.9.26** $^{1}$H NMR spectra of **3o** [$CDCl_3$, 500 MHz]

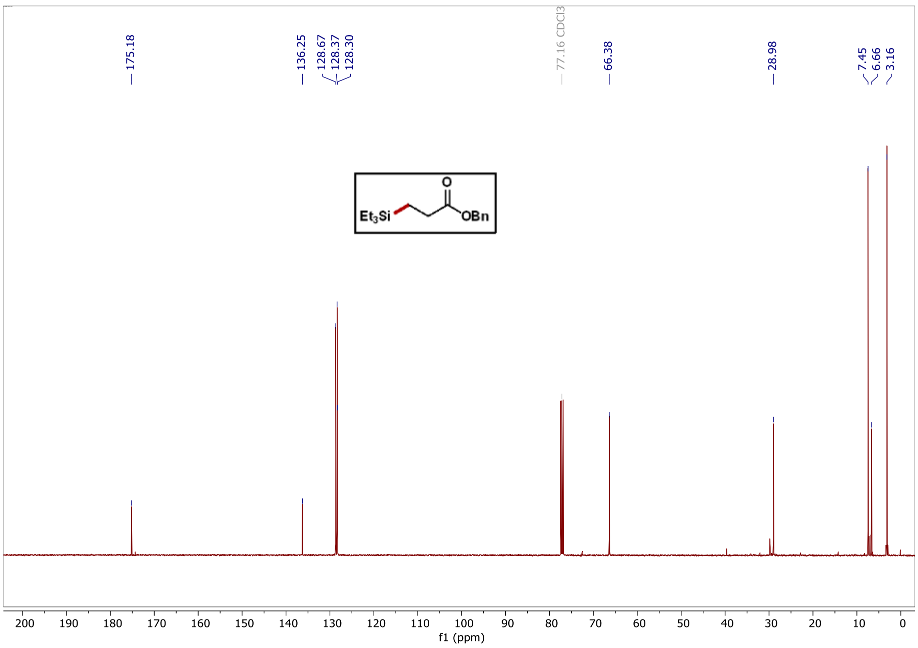

**Figure 2.9.27** $^{13}$C NMR spectra of **3o** [$CDCl_3$, 126 MHz]

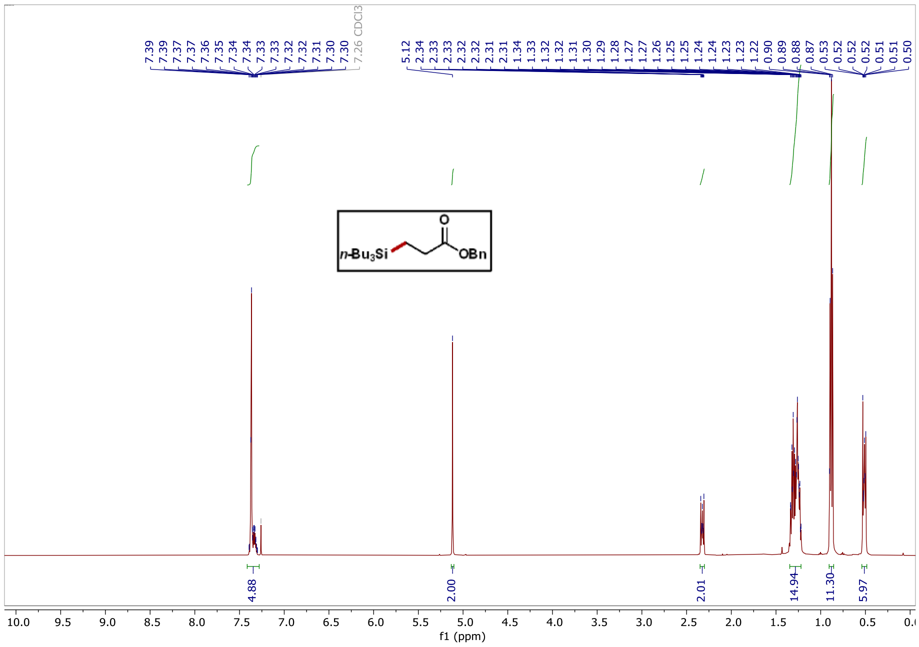

**Figure 2.9.28** $^1$H NMR spectra of **3q** [$CDCl_3$, 500 MHz]

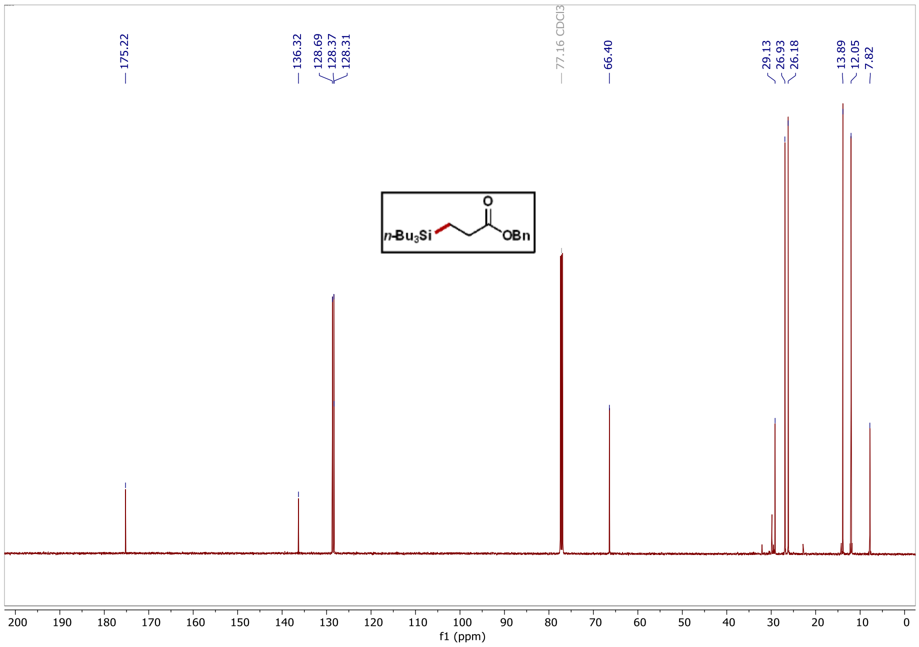

**Figure 2.9.29** $^{13}$C NMR spectra of **3q** [$CDCl_3$, 126 MHz]

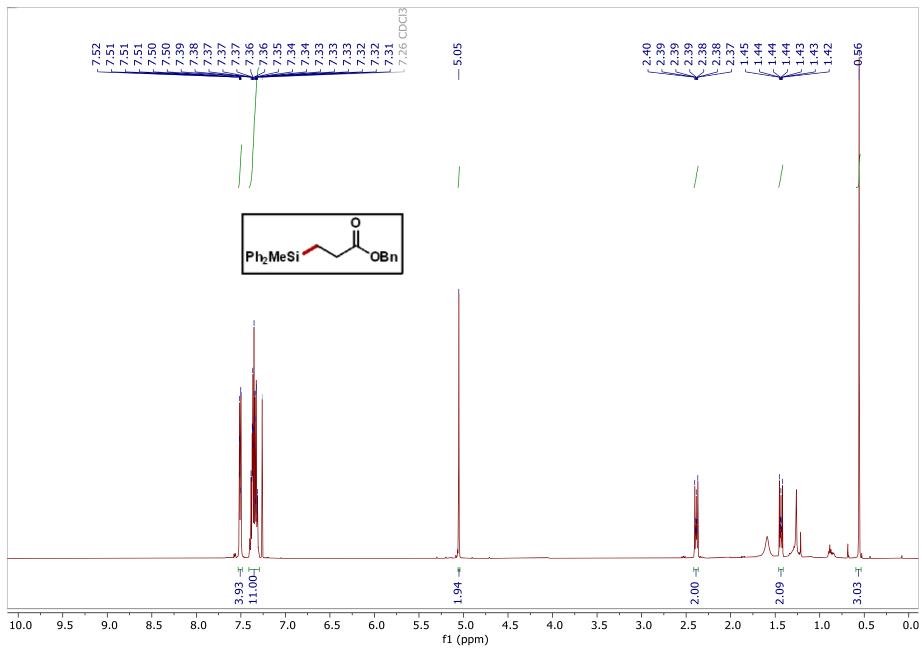

**Figure 2.9.30** $^{1}$H NMR spectra of **3u** [$CDCl_3$, 500 MHz]

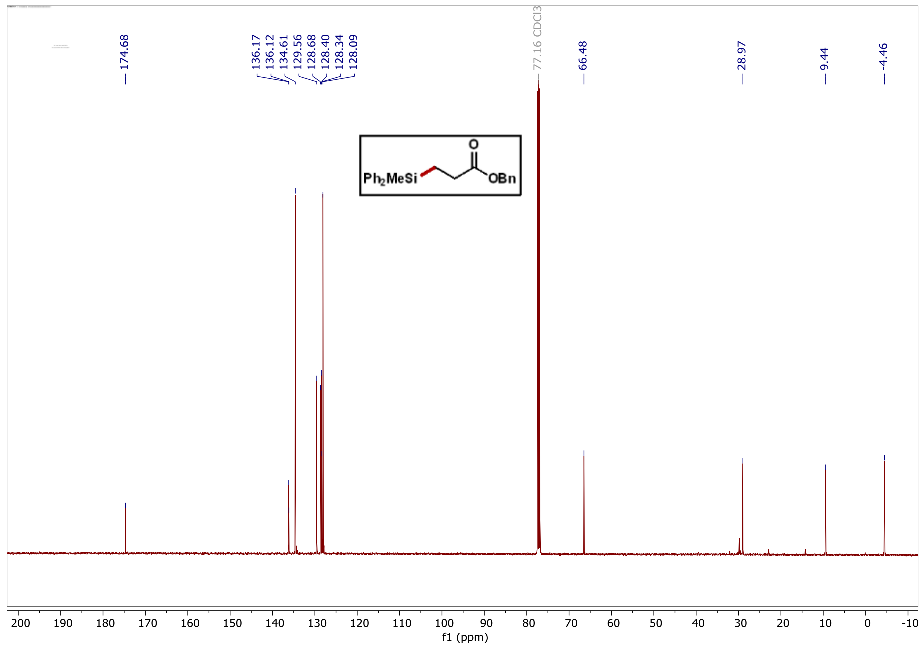

**Figure 2.9.31** $^{13}$C NMR spectra of **3u** [$CDCl_3$, 126 MHz]

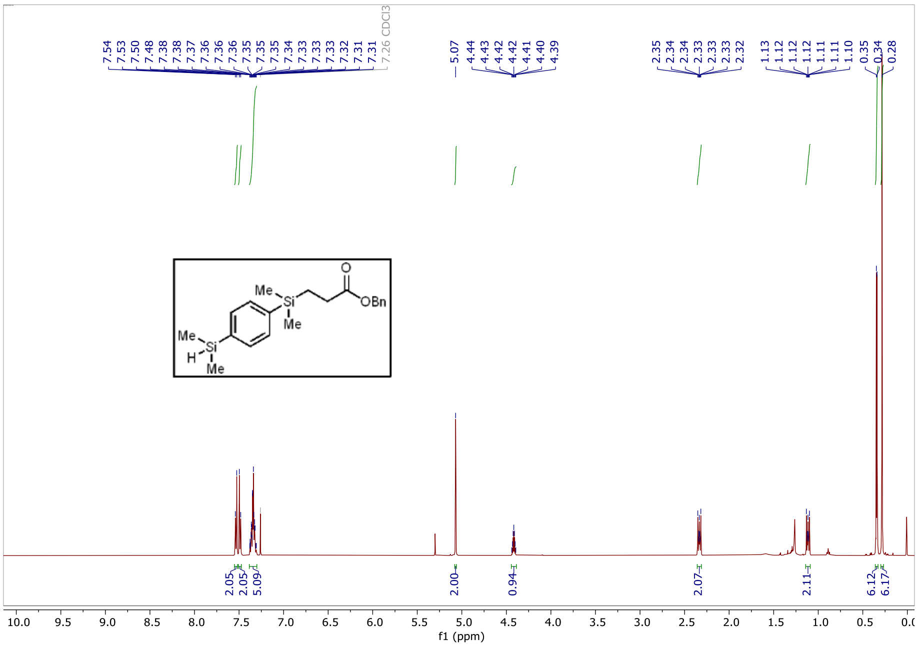

**Figure 2.9.32** $^{1}$H NMR spectra of **3y** [$CDCl_3$, 500 MHz]

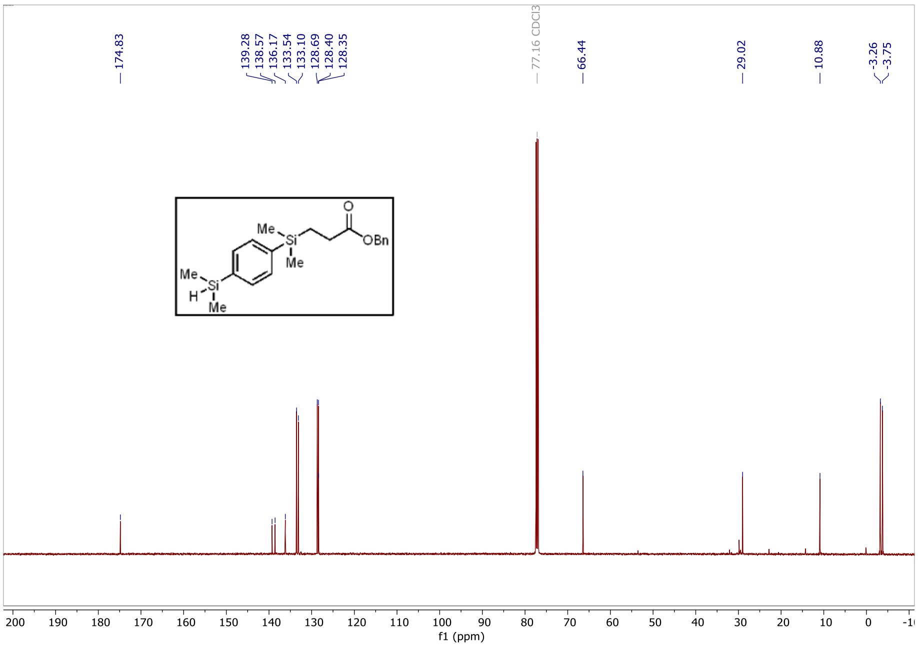

**Figure 2.9.33** $^{13}$C NMR spectra of **3y** [$CDCl_3$, 126 MHz]

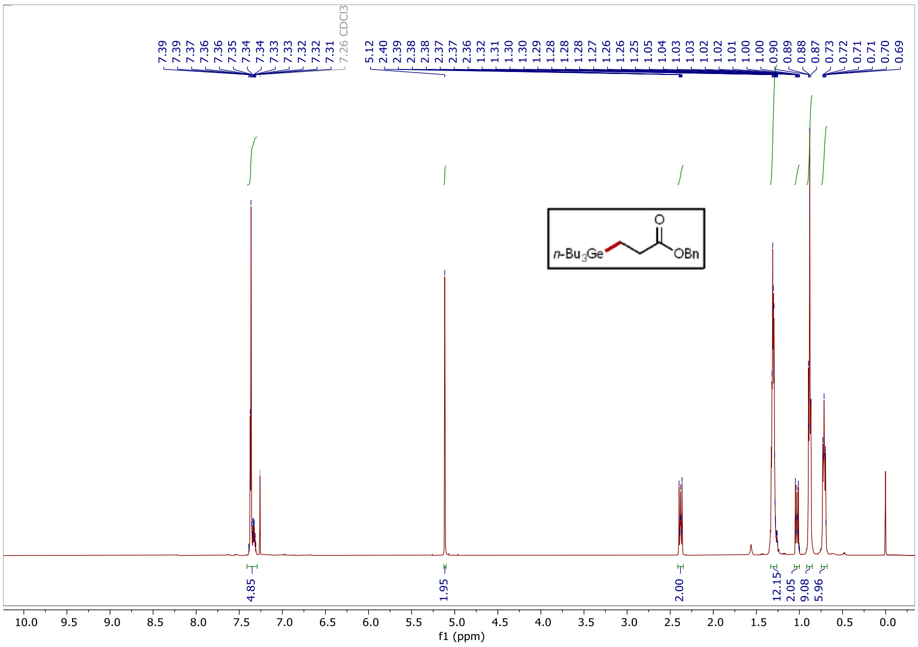

**Figure 2.9.34** $^{1}$H NMR spectra of **5a** [$CDCl_3$, 500 MHz]

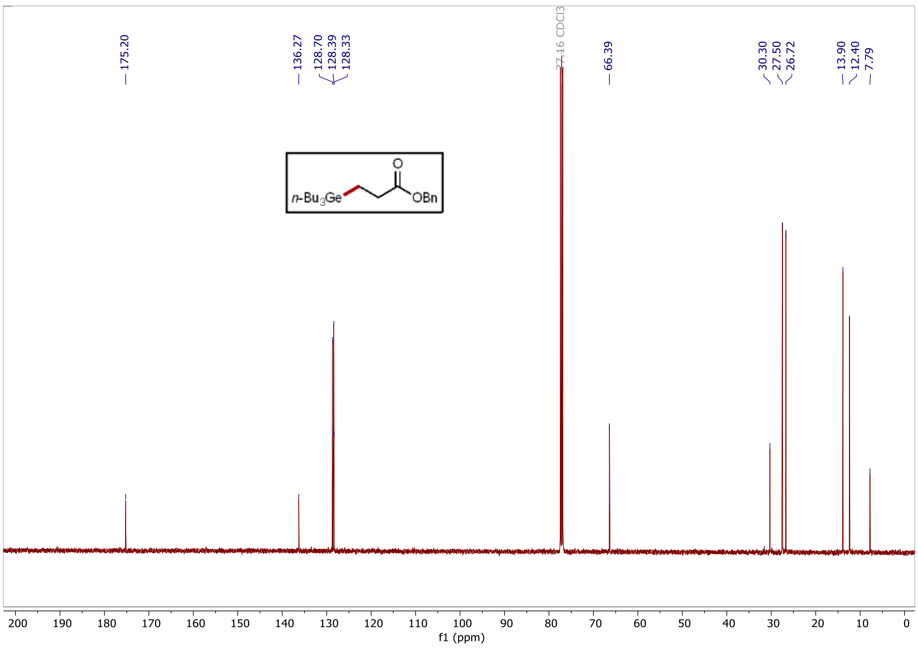

**Figure 2.9.35** $^{13}$C NMR spectra of **5a** [$CDCl_3$, 126 MHz]

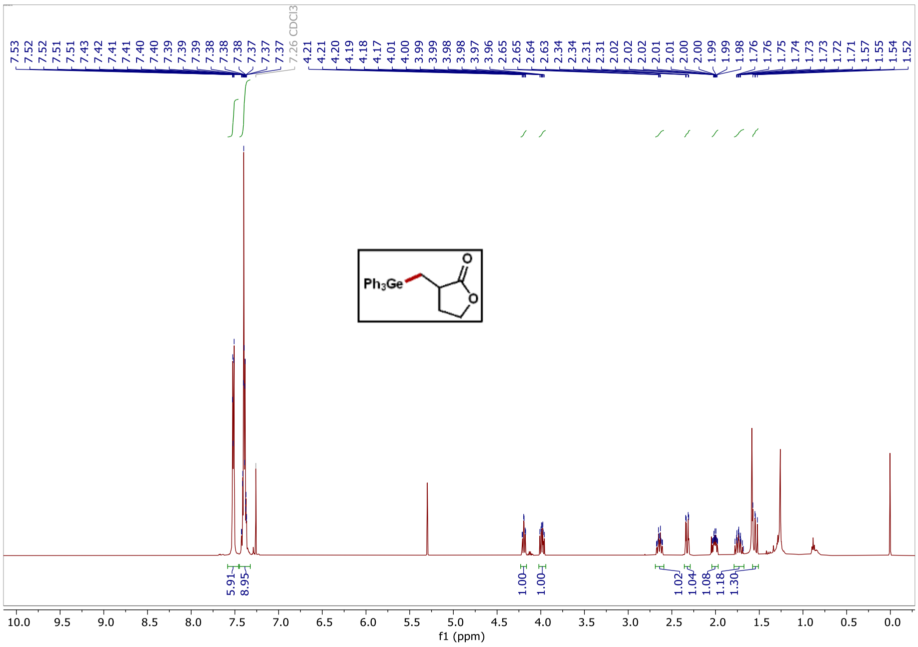

**Figure 2.9.36** $^{1}H$ NMR spectra of **5c** [$CDCl_3$, 500 MHz]

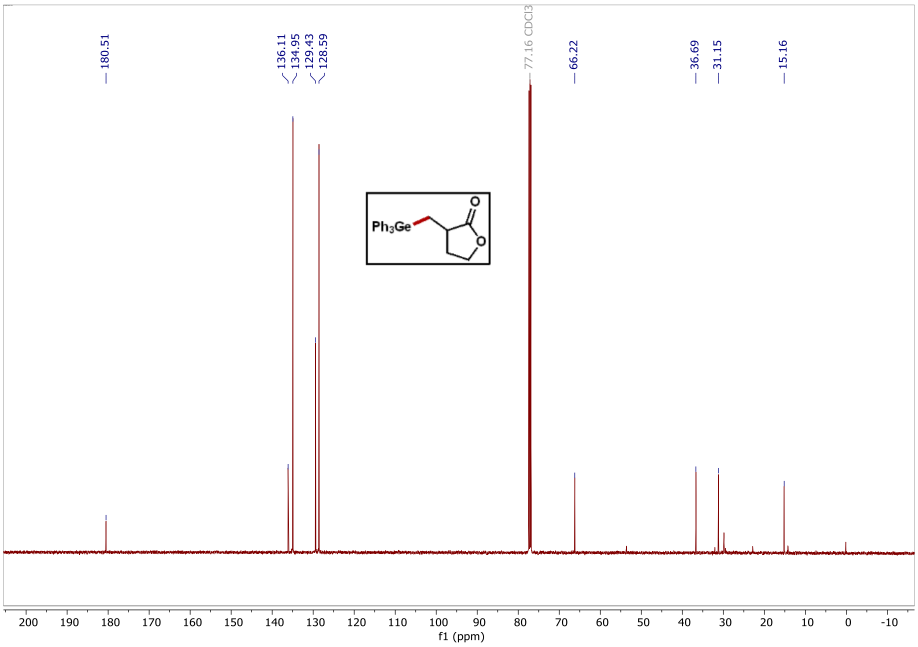

**Figure 2.9.37** $^{13}C$ NMR spectra of **5c** [$CDCl_3$, 126 MHz]

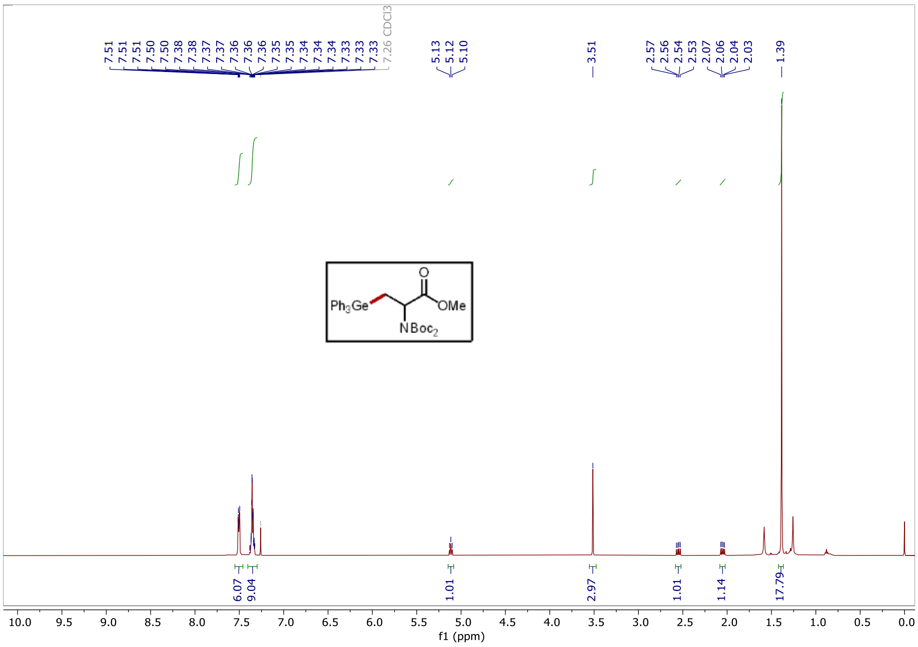

**Figure 2.9.38** $^{1}H$ NMR spectra of **5d** [$CDCl_3$, 500 MHz]

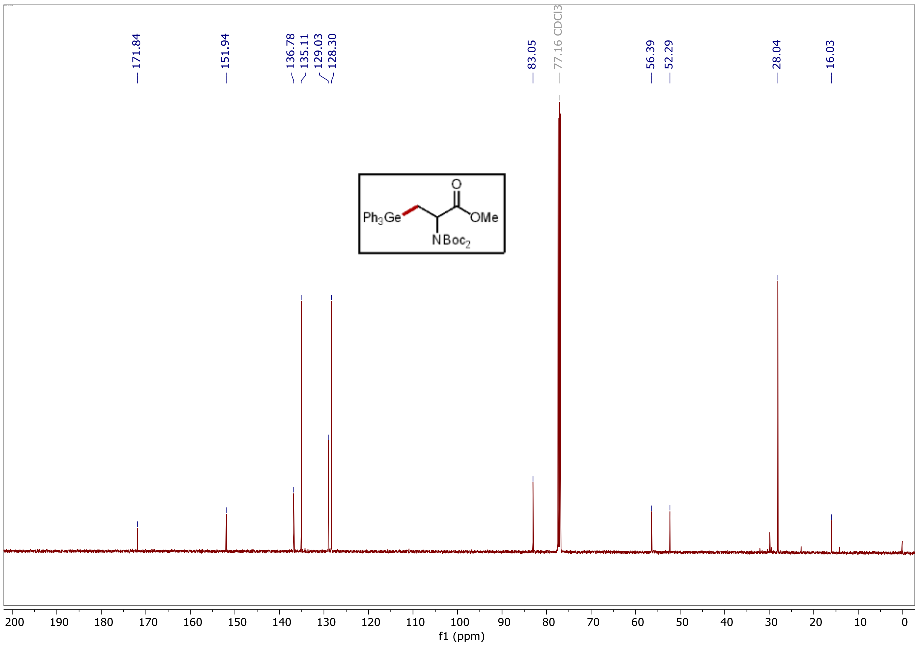

**Figure 2.9.39** $^{13}C$ NMR spectra of **5d** [$CDCl_3$, 126 MHz]

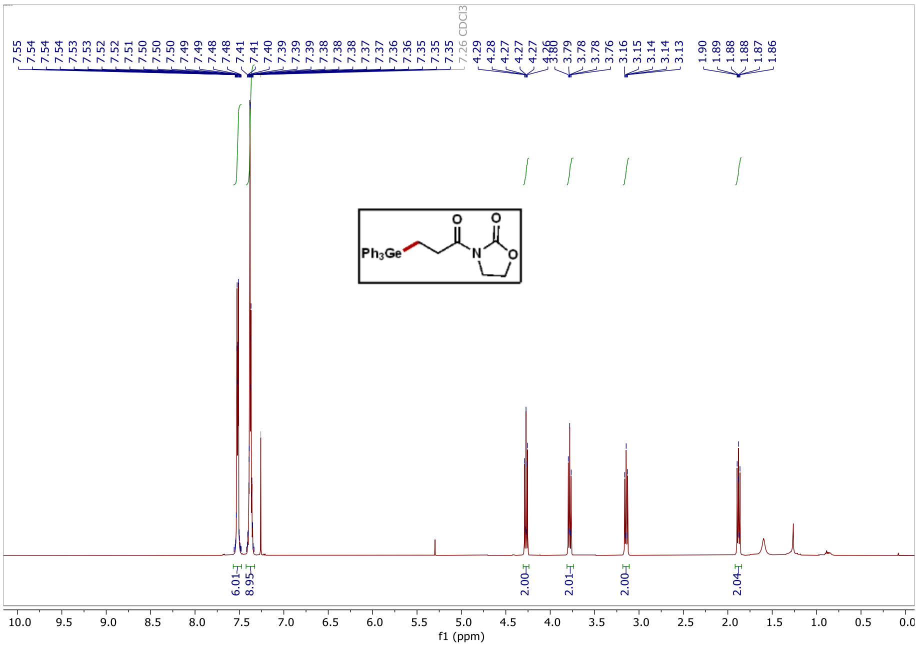


**Figure 2.9.40** $^{1}$H NMR spectra of **5i** [$CDCl_3$, 500 MHz]

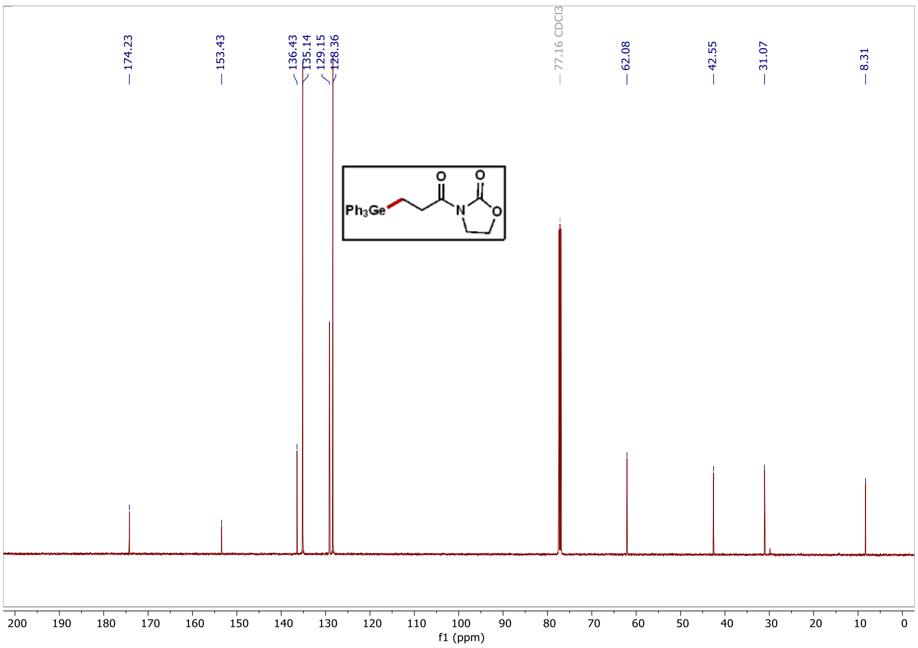


**Figure 2.9.41** $^{13}$C NMR spectra of **5i** [$CDCl_3$, 126 MHz]

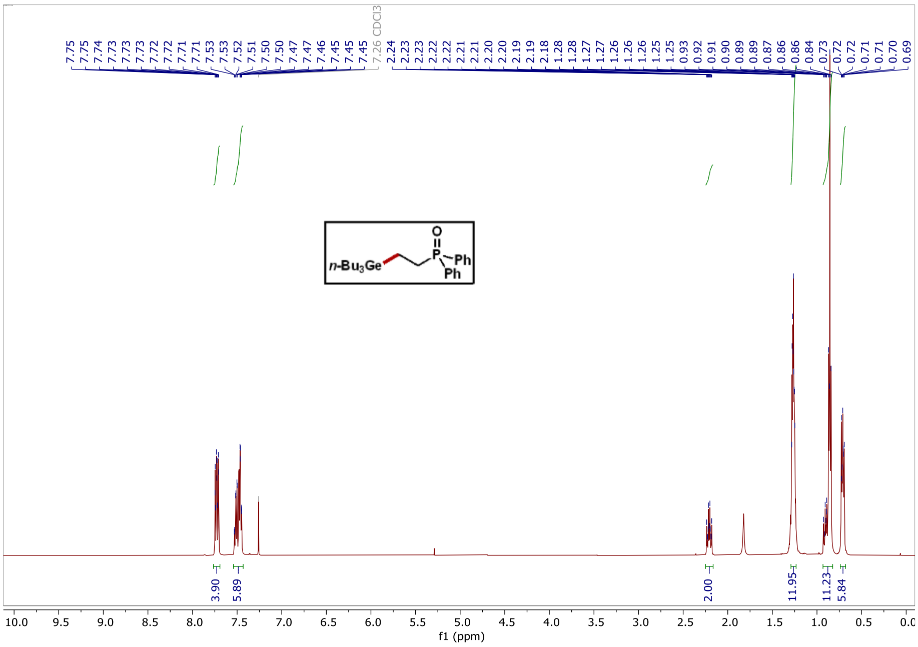

**Figure 2.9.42** $^{1}H$ NMR spectra of **5j** [$CDCl_3$, 500 MHz]

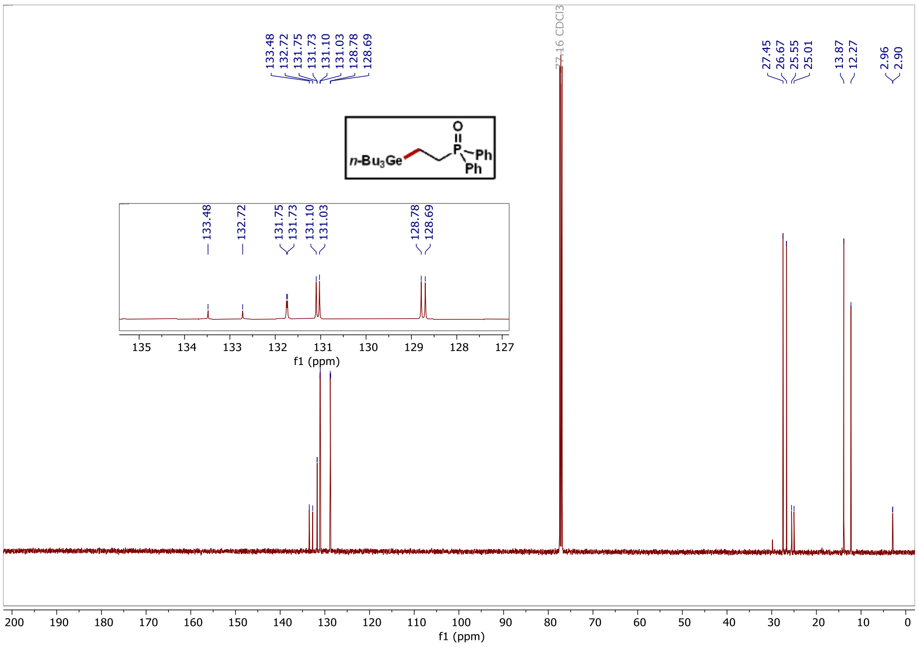

**Figure 2.9.43** $^{13}C$ NMR spectra of **5j** [$CDCl_3$, 126 MHz]

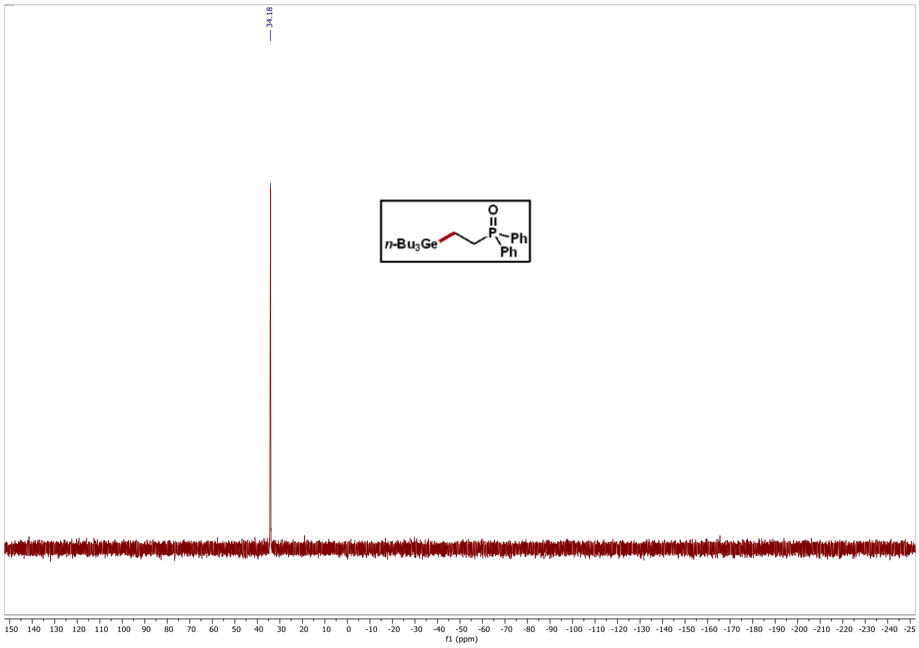

**Figure 2.9.44** $^{31}$P NMR spectra of **5j** [$CDCl_3$, 202 MHz]

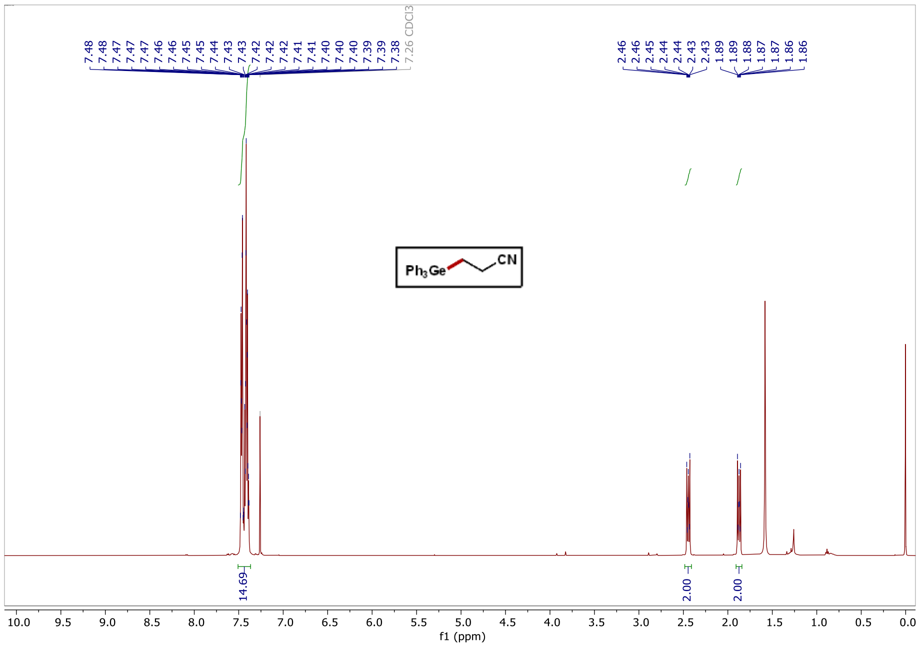

**Figure 2.9.45** $^{1}$H NMR spectra of **5l** [$CDCl_3$, 500 MHz]

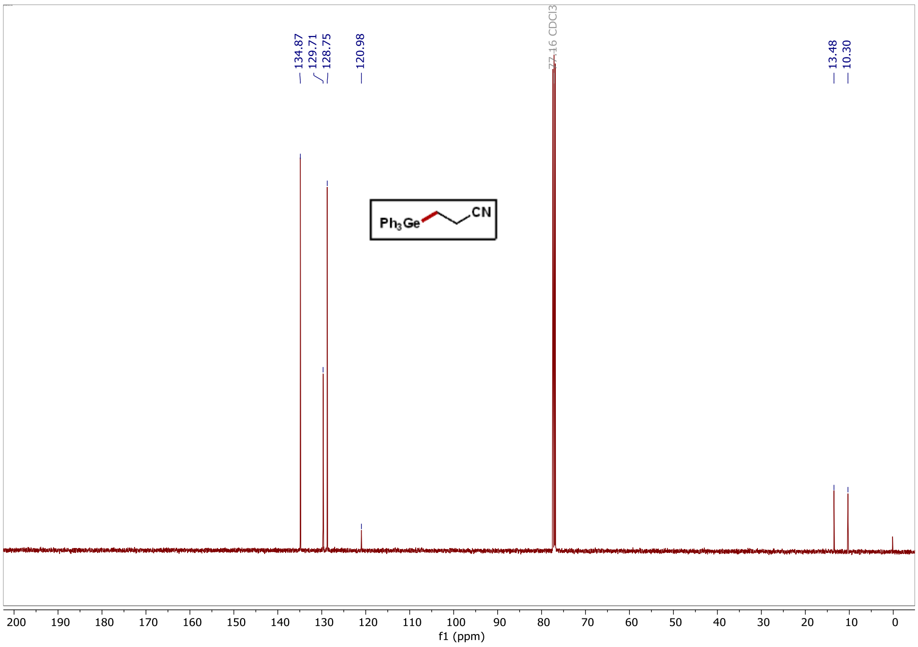


**Figure 2.9.46** $^{13}$C NMR spectra of **5l** [$CDCl_3$, 126 MHz]

## 2.10 References


1. Lewis, L. N., Stein, J., Gao, Y., Colborn, R. E., Hutchins, G. (1997). Platinum catalysts used in the silicon industry. *Platinum Met. Rev. 41*, 66-75. (DOI: 10.1595/003214097X4126675).
2. Tamao, K., Ishida, N., Tanaka, T., and Kumada, M. (1983). Silafunctional compounds in organic synthesis. Part 20. Hydrogen peroxide oxidation of the silicon-carbon bond in organoalkoxysilanes. *Organometallics 2*, 1694-1696. (DOI:10.1021/om50005a041).
3. Fleming, I., Henning, R., Plaut, H. (1984). The phenyldimethylsilyl group as a masked form of the hydroxy group. *J. Chem. Soc., Chem. Commun.* 29-31. (DOI:10.1039/C39840000029).
4. Hatanaka, H., Hiyama, T. (1988). Cross-coupling of organosilanes with organic halides mediated by a palladium catalyst and tris(diethylamino)sulfonium difluorotrimethylsilicate. *J. Org. Chem. 53*, 918-920. (DOI:10.1021/jo00239a056).
5. Fleming, I., Barbero, A., Walter, D. (1997). Stereochemical control in organic synthesis using silicon-containing

compounds. *Chem. Rev. 97*, 2063-2192. (DOI:10.1021/cr941074u).

6. Denmark, S. E. Regens, C. S. (2008). Palladium-catalyzed cross-coupling reactions of organosilanols and their salts: Practical alternatives to boron- and tin-based methods. *Acc. Chem. Res. 41*, 1486-1499. (DOI:10.1021/ar800037p).
7. Sommer, L. H., Pietrusza, E. W., Whitmore, F. C. (1947). The reaction of aminoacyl halides with diphenylacetonitrile: The structure of amidone. *J. Am. Chem. Soc. 69*, 188-189. (DOI:10.1021/ja01193a509)
8. Speier, J. L., Webster, J. A., Barnes, G. H. (1957). The addition of silicon hydrides to olefinic double bonds. Part II: The use of group VIII metal catalysts. *J. Am. Chem. Soc. 79*, 974-979. (DOI:10.1021/ja01561a054).
9. Karstedt, B. D. (1973). General electric company, platinum complexes of unsaturated siloxanes and platinum containing organopolysiloxanes. US3775452A.
10. Marciniec, B., Gulinski, J., Urbaniac, W., Kornetka, Z. W. (1992). Comprehensive handbook on hydrosilylation, Pergamon, Oxford, UK.
11. Marciniec, B. (2002). Catalysis of hydrosilylation of carbon-carbon multiple bonds: Recent progress. *Silicon Chemistry 1*, 155-174. (DOI:10.1023/A:1021235922742).
12. Marciniec, B. (2009). Hydrosilylation: A comprehensive review on recent advances, Springer, Berlin, *Silicon 1*, 57-58. (DOI:10.1007/s12633-009-9009-z).
13. Marciniec, B., Maciejewski, H., Pietraszuk, C., Pawluc, P. Gulinski, J. (2010). Hydrosilylation. *In Encyclopedia of Catalysis, I. Horvath (Ed.)*. (DOI:10.1002/0471227617.eoc117).
14. Sun, J., Deng, L. (2016). Cobalt complex-catalyzed hydrosilylation of alkenes and alkynes. *ACS Catal. 6*, 290-300. (DOI:10.1021/acscatal.5b02308).

15. Nakajima, Y., Shimada, S. (2015). Hydrosilylation reaction of olefins: Recent advances and perspectives. *RSC Adv. 5*, 20603-20616. ( DOI:10.1039/c4ra17281g).
16. Xiaoyong Du, X., Huang, Z. (2017). Advances in base-metal-catalyzed alkene hydrosilylation. *ACS Catal. 7*, 1227-1243. (DOI:10.1021/acscatal.6b02990).
17. Almeida, L. D. de, Wang, H., Junge, K., Cui, X., Beller, M. (2021). Recent advances in catalytic hydrosilylations: developments beyond traditional platinum catalysts. *Angew. Chem. Int. Ed. 60*, 550-565. (DOI:10.1002/anie.202008729).
18. Jose, J., Mathew, T. V. (2024). Cobalt-catalyzed hydrosilylation across carbon-carbon, carbon-oxygen, and carbon-nitrogen multiple bonds: A comprehensive review. *ChemCatChem 16*, e202301626. (DOI:10.1002/cctc.202301626).
19. Tondreau, A. M. *et al.* (2012). Iron catalysts for selective anti-Markovnikov alkene hydrosilylation using tertiary silanes. *Science 335*, 567-570. (DOI:10.1126/science.1214451).
20. Gribble, Jr. M. W., Prinot, M. T., Bandar, J. S., Liu, R. Y., Buchwald, S. L. (2017). Asymmetric copper hydride-catalyzed Markovnikov hydrosilylation of vinylarenes and vinyl heterocycles. *J. Am. Chem. Soc. 139*, 2192-2195. (DOI: 10.1021/jacs.6b13029).
21. Zhao, Z., Zhang, F., Wang, D. and Deng, L. (2023). Advances in transition-metal-catalyzed hydrogermylation of alkenes and alkynes. *Chin. J. Chem. 41*, 3063-3081. (DOI:10.1002/cjoc.202300276).
22. Wang, P., Wang, D., Deng, L. (2025). Cobalt-catalyzed hydrogermylation of nonactivated alkenes enabled by photoirradiation. *Organometallics 44*, 1648-1652. (DOI: 10.1021/acs.organomet.5c00237).

23. Lin, W., You, L., Yuan, W., He, C. (2022). Cu-catalyzed enantioselective hydrogermylation: asymmetric synthesis of unnatural $\beta$-germyl $\alpha$-amino acids. *ACS Catal. 12*, 14592-14600. (DOI:10.1021/acscatal.2c04571).

24. Stachowiak-Dluzynska, H., Gruszczynski, M., Kubicki, M., Hreczycho, G. (2024). Pt(II) complexes bearing P, N-donor ligands as catalysts in chemoselective hydrosilylation, hydrogermylation, and hydroboration of terminal alkenes. *J. Catal. 433*, 115494. (DOI:10.1016/j.jcat.2024.115494).

25. Prima, D. O., Vatsadze, S. Z. (2025). Cocktail-type catalysis: An emerging concept in metal-mediated transformations. *Organometallics 44*, 1337-1357. (DOI:10.1021/acs.organomet.5c00117).

26. Finke, U., Moretto, H.-H. (1978). Addition of dialkylhalogeno-hydridosilanes to unsaturated hydrocarbon compounds. US4254271A

27. Lambert, J. B., Zhao, Y., Wu, H. (1999). $\beta$-Silyl and $\beta$-germyl carbocations stable at room temperature. *J. Org. Chem. 64*, 2729-2736. (DOI:10.1021/jo982146a).

28. Rubin, M., Schwier, T., Gevorgyan, V. (2002). Highly efficient $B(C_6F_5)_3$-catalyzed hydrosilylation of olefins. *J. Org. Chem*. *67*, 1936-1940. (DOI:10.1021/jo016279z).

29. Long, P.-W., He, T., Oestreich, M. (2020). $B(C_6F_5)_3$-Catalyzed hydrosilylation of vinylcyclopropanes. *Org. Lett*. *22*, 7383-7386. (DOI:10.1021/acs.orglett.0c02751).

30. Perez, M., Hounjet, L. J., Caputo, C. B., Dobrovetsky, R., Stephan, D. W. (2013). Olefin isomerization and hydrosilylation catalysis by Lewis acidic organofluorophosphonium salts. *J. Am. Chem. Soc.* 135, 18308-18310. (DOI:10.1021/ja410379x).

31. Selmani, A., Schoenebeck, F. (2023). Anti-Markovnikov hydrogermylation of alkenes *via* Lewis acid catalysis. *Synthesis* 55, 1792-1798. (DOI: 10.1055/a-2036-3868).

32. Komine, N., Abe, M., Suda, R., Hirano, M. (2015). Markovnikov-selective hydrosilylation of electron-deficient alkenes with arylsilanes catalyzed by mono(phosphine)palladium(0). *Organometallics 34*, 432-437. (DOI:10.1021/om500964g).

33. Skrodzki, M., Patroniak, V., Pawluc, P. (2021). Schiff base cobalt(II) complex-catalyzed highly Markovnikov-selective hydrosilylation of alkynes. *Org. Lett. 23*, 663-667. (DOI: 10.1021/acs.orglett.0c03721).

34. Takeshita, K., Seki, Y., Kawamoto, K., Murai, S., Sonoda, N. (1987). The catalyzed reaction of *α,β*-unsaturated esters with various hydrosilanes. *J. Org. Chem. 52*, 4864-4868. (DOI: 10.1021/jo00231a008).

35. Chatgilialoglu, C. (1995). structural and chemical properties of silyl radicals. *Chem. Rev. 95*, 1229-1251. (DOI: 10.1021/cr00037a005).

36. Brimioulle, R., Lenhart, D., Maturi, M. M., Bach, T. (2015). Enantioselective catalysis of photochemical reactions. *Angew. Chem. Int. Ed. 54*, 3872-3890. (DOI:10.1002/anie.201411409).

37. Ravelli, D., Protti, S., Fagnoni, M. (2016). Carbon-carbon bond forming reactions *via* photogenerated intermediates. *Chem. rev. 116*, 9850-9913. (DOI:10.1021/acs.chemrev.5b00662).

38. Romero, N. A., Nicewicz, D. A. (2016). Organic photoredox catalysis. *Chem. rev. 116*, 10075-10166. (DOI: 10.1021/acs.chemrev.6b00057).

39. Fagnoni, M., Dondi, D., Ravelli, D., Albini, A. (2007). Photocatalysis for the Formation of the C-C Bond. *Chem. Rev. 107*, 2725-2756. (DOI:10.1021/cr068352x).

40. Ravelli, D., Dondi, D., Fagnoni, M., Albini, A. (2009). Photocatalysis: A multi-faceted concept for green chemistry. *Chem. Soc. Rev. 38*, 1999-2011. (DOI: 10.1039/B714786B).

41. Protti, S., Fagnoni, M., Ravelli, D. (2015). Photocatalytic C-H activation by hydrogen-atom transfer in synthesis. *ChemCatChem 7*, 1516-1523. (DOI: 10.1002/cctc.201500125).

42. Margrey, K. A., Nicewicz, D. A. (2016). A general approach to catalytic alkene anti-Markovnikov hydrofunctionalization reactions *via* acridinium photoredox catalysis. *Acc. Chem. Res. 49*, 1997-2006. (DOI:10.1021/acs.accounts.6b00304).

43. Capaldo, L., Ravelli, D. (2017). Hydrogen atom transfer (HAT): a versatile strategy for substrate activation in photocatalyzed organic synthesis. *Eur. J. Org. Chem. 15*, 2056-2071. (DOI:10.1002/ejoc.201601485).

44. Cao, H., Tang, X., Tang, H., Yuan, Y., Wu, J. (2021). Photoinduced intermolecular hydrogen atom transfer reactions in organic synthesis. *Chem Catalysis 1*, 523-598. (DOI: 10.1016/j.checat.2021.04.008).

45. Capaldo, L., Ravelli, D., Fagnoni, M. (2021). Direct photocatalyzed hydrogen atom transfer (HAT) for aliphatic C-H bonds elaboration. *Chem. rev. 122*, 1875-1924. (DOI: 10.1021/acs.chemrev.1c00263).

46. Qrareya, H., Dondi, D., Ravelli, D., Fagnoni, M. (2015). Decatungstate-photocatalyzed Si-H/C-H activation in silyl hydrides: Hydrosilylation of electron-poor alkenes. *ChemCatChem 7*, 3350. (DOI:10.1002/cctc.201500562).

47. Jeffery, J. L., Terrett, J. A., Macmillan, S. W. C. (2015). O-H hydrogen bonding promotes H-atom transfer from $\alpha$ C-H bonds for C-alkylation of alcohols. *Science* 349, 1532-1536. (DOI:10.1126/science.aac8555).

48. Zhou, R., Goh, Y. Y., Liu, H., Tao, H., Li, L., Wu, J. (2017). Visible-light-mediated metal-free hydrosilylation of alkenes through selective hydrogen atom transfer for Si-H activation. *Angew. Chem. Int. Ed. 56*, 16621-16625. (DOI: /10.1002/anie.201711250).

49. Rohe, S., Morris, A. O., McCallum, T., Barriault, L. (2018). Hydrogen atom transfer reactions *via* photoredox catalyzed chlorine atom generation. *Angew. Chem. Int. Ed. 57*, 15664-15669. (DOI:10.1002/anie.201810187).

50. Wan, Y., Zhu, J., Yuan, Q., Wang, W., Zhang, Y. (2021). Synthesis of $\beta$-silyl $\alpha$-amino acids *via* visible-light-mediated hydrosilylation. *Org. Lett. 23*, 1406-1410. (DOI: 10.1021/acs.orglett.1c00065).

51. Wang, G.-Q., Wang, T., Zhang, Y., Zhou, Y.-X., Yang, D., Han, P., Jing, L.-H. (2023). Photoredox metal-free synthesis of unnatural $\beta$-silyl-$\alpha$-amino acids *via* hydrosilylation. *Chem. Asian J.* 2023, 18, e202300805. (DOI:10.1002/asia.202300805).

52. Ding, L., Niu, K., Liu, Y., Wang, Q. (2022). Visible light-induced hydrosilylation of electron-deficient alkenes by iron catalysis. *ChemSusChem 15*, e202200367. (DOI: 10.1002/cssc.202200367).

53. Gong, X., Zhao, Q., Zhu, C. (2025). Visible-light-initiated uranyl-catalyzed hydrosilylation and hydrosulfonylation of alkenes and alkynes. *Adv. Synth. Catal. 367*, e202400745. (DOI:10.1002/adsc.202400745).

54. Chen, X., Zhou, Y., Yang, M., Yang, Y., Feng, X., Cao, W. (2025). Merging photocatalysis with chiral Lewis acid catalysis

for enantioselective hydrosilylation/hydrogermylation of electron-deficient alkenes. *Angew. Chem. Int. Ed.* 64, e202504676. (DOI:10.1002/anie.202504676).

55. Queen, A. E., Selmani, A., Schoenebeck, F. (2022). Hydrogermylation of alkenes *via* organophotoredox-initiated HAT catalysis. *Org. Lett. 24*, 406-409. (DOI: 10.1021/acs.orglett.1c04088).

56. Yoshizawa, K., Li, B.-X., Matsuyama, T., Wang, C., Uchiyama, M. (2024). Visible-light-driven germyl radical generation *via* EDA-catalyzed ET-HAT process. *Chem. Eur. J. 30*, e202401546. (DOI:10.1002/chem.202401546).

57. Wang, H.-J., Fu, Y. (2009). Designing new free-radical reducing reagents: Theoretical study on Si-H bond dissociation energies of organic silanes. *J. Mol. Struct.:THEOCHEM 893*, 67-72. (DOI:10.1016/j.theochem.2008.09.017).

58. Clark, K. B., Griller, D. (1991). The Ge-H bond-dissociation energies of organogermanes: A laser-induced photoacoustic study. *Organometallics*. *10*, 746-750. (DOI: 10.1021/om00049a039).

59. Becerra, R., Walsh, R. (2019). Thermochemistry of germanium and organogermanium compounds. *Phys. Chem. Chem. Phys. 21*, 988-1008. (DOI:10.1039/C8CP06208K).

60. Robert, B. P. (1999). Polarity-reversal catalysis of hydrogen atom abstraction reactions: concepts and applications in organic chemistry. *Chem. Soc. Rev. 28*, 25-35. (DOI: 10.1039/a804291h).

61. Sakic, D., Zipse, H. (2016). Radical stability as a guideline in C-H amination reactions. *Adv. Synth. Catal. 358*, 3983-3991. (DOI:10.1002/adsc.201600629).

62. Choi, G. J., Knowles, R. R. (2015). Catalytic alkene carboaminations enabled by oxidative proton-coupled electron transfer. *J. Am. Chem. Soc. 137*, 9226-9229. (DOI: 10.1021/jacs.5b05377).

63. Choi, G., Zhu, Q., Miller, D., Gu, C., J., Knowles, R. R. (2016). Catalytic alkylation of remote C-H bonds enabled by proton-coupled electron transfer. *Nature 539*, 268-271. (DOI: 10.1038/nature19811).

64. Gentry, E. C., Knowles, R. R. (2016). Synthetic applications of proton-coupled electron transfer. *Acc. Chem. Res. 49*, 1546-1556. (DOI: 10.1021/acs.accounts.6b00272).

65. Qin, Q., Yu, S. (2015). Visible-light-promoted remote C($sp^3$)-H amidation and chlorination. *Org. Lett. 17*, 1894-1897. (DOI:10.1021/acs.orglett.5b00582).

66. Martinez, C., Muniz, K. (2015). An iodine-catalyzed Hofmann-Loffler reaction. *Angew. Chem. Int. Ed. 54*, 8287-8291. (DOI:10.1002/anie.201501122).

67. Tanaka, H., Sakai, K., Kawamura, A., Oisaki, K., Kanai, M. (2018). Sulfonamides as new hydrogen atom transfer (HAT) catalysts for photoredox allylic and benzylic-C-H arylations. *Chem. Commun. 54*, 3215-3218. (DOI: 10.1039/C7CC09457D).

68. Ma, Z., Li, M., Guo, L., Liu, L., Wang, D., Duan, X. (2021). sulfonamide as photoinduced hydrogen-atom transfer catalyst for regioselective alkylation of C($sp^3$)-H bonds adjacent to heteroatoms. *Org. Lett. 23*, 474-479. (DOI: 10.1021/acs.orglett.0c03992).

69. Frisch, M. J. *et al*. Gaussian, Inc., Gaussian 16, Revision C.01; Wallingford CT, USA, 2016.

70. Zhao, Y., Truhlar, D.G. (2008). The M06 suite of density functionals for main group thermochemistry, thermochemical kinetics, noncovalent interactions, excited states, and transition elements: two new functionals and systematic testing of four M06-class functionals and 12 other functionals. *Theor Chem Account 120*, 215-241. (DOI:10.1007/s00214-007-0310-x).

71. Zhao, Y., Truhlar, D. G. (2008). Exploring the limit of accuracy of the global hybrid meta density functional for main-group thermochemistry, kinetics, and noncovalent interactions. *J. Chem. Theory Comput*. *4*, 1849-1868. (DOI: 10.1021/ct800246v).

72. Cheron, N., Jacquemin, D., Fleurat-Lessard, P. A. (2012). Qualitative failure of B3LYP for textbook organic reactions. *Phys. Chem. Chem. Phys. 14*, 7170-7175. (DOI:10.1039/C2CP40438A).

73. Hehre, W. J., Ditchfield, R., Pople, J. A. (1972). Self-consistent molecular orbital methods. XII. Further extensions of Gaussian-type basis sets for use in molecular orbital studies of organic molecules. *J. Chem. Phys.* 56, 2257-2261. (DOI:10.1063/1.1677527).

74. Cissell, J. A., Vaid, T. P., Yap, G. P. A. (2007). Reversible oxidation state change in germanium(tetraphenylporphyrin) induced by a dative ligand: Aromatic $Ge^{II}$(TPP) and antiaromatic $Ge^{IV}$(TPP)(pyridine)$_2$. *J. Am. Chem. Soc. 129*, 7841-7847. (DOI:10.1021/ja070794i).

75. Shao, X., Wu, X., Wu S., Zhu, C. (2020). Metal-free radical-mediated C($sp^3$)-H heteroarylation of alkanes. *Org. Lett.* 22, 7450-7454.(DOI:10.1021/acs.orglett.0c02475).

76. Luo, J., Zhang, J. (2016). Donor-acceptor fluorophores for visible-light-promoted organic synthesis: Photoredox/Ni dual catalytic C($sp^3$)-C($sp^2$) cross-coupling. *ACS Catal.* 6, 873-877. (DOI:10.1021/acscatal.5b02204).

77. Lan, Y., Chang, X.-H., Fan, P., Shan, C.-C., Liu, Z.-B., Loh, T.-P., Xu, Y.-H. (2017). Copper-catalyzed silylperoxidation reaction of $\alpha$, $\beta$-unsaturated ketones, esters, amides, and conjugated enynes. *ACS Catal. 7*, 7120-7125. (DOI:10.1021/acscatal.7b02754).

78. Kaplaneris, N., Bisticha, A., Papadopoulos, G. N., Limnios, D., Kokotos, C. G. (2017). Photoorganocatalytic synthesis of lactones *via* a selective C-H activation-alkylation of alcohols. *Green Chem. 19*, 4451-4456. (DOI: 10.1039/C7GC01903C).

79. Cai, L., Fu, L., Zhou, C., Gao, Y., Li, S., Li, G. (2020). Rh(I)-catalyzed regioselective arylcarboxylation of acrylamides with arylboronic acids and $CO_2$. *Green Chem. 22*, 7328-7332. (DOI:10.1039/D0GC02667K).

80. Svejstrup, T. D., Zawodny, W., Douglas, J. J., Bidgeli, D., Sheikh, N. S., Leonori, D. (2016). Visible-light-mediated generation of nitrile oxides for the photoredox synthesis of isoxazolines and isoxazoles. *Chem. Commun. 52*, 12302-12305. (DOI:10.1039/c6cc06029c).

81. Evans, D. A., Miller, S. J., Lectka, T., von Matt, P. ( 1999). Chiral bis(oxazoline)copper(II) complexes as Lewis acid catalysts for the enantioselective Diels-Alder reaction. *J. Am. Chem. Soc. 121*, 7559-7573. (DOI:10.1021/ja991190k).

82. Mikhailine, A. A., Maishan, M. I., Lough, A. J., Morris, R. H. (2012). The mechanism of efficient asymmetric transfer hydrogenation of acetophenone using an Iron(II) complex containing an (*S,S*)-$Ph_2PCH_2CH$=NCHPhCHPhN=$CHCH_2PPh_2$ ligand: Partial ligand reduction is the key. *J. Am. Chem. Soc. 134*, 12266-12280. (DOI:10.1021/ja304814s).

83. Dai, Z.-Y., Nong, Z.-S., Song, S., Wang, P.-S. (2021). Asymmetric photocatalytic C($sp^3$)-H bond addition to *α*-substituted acrylates. *Org. Lett. 23*, 3157-3161. (DOI:10.1021/acs.orglett.1c00801).

84. Zhou, B., Ma, P., Chen, H., Wang, C. (2014). Amine-accelerated manganese-catalyzed aromatic C-H conjugate addition to *α, β*-unsaturated carbonyls. *Chem. Commun. 50*, 14558-14561. (DOI:10.1039/C4CC07598F).

85. Omann, L., Pudasaini, B., Irran, E., Klare, H. F. T., Baik, M.-H., Oestreich, M. (2018). Thermodynamic versus kinetic control in substituent redistribution reactions of silylium ions steered by the counteranion *Chem. Sci. 9*, 5600-5607. (DOI:10.1039/C8SC01833B).

86. You, L., Yuan, W., He, C. (2021). Intermolecular dehydrogenative C-H/Si-H cross-coupling for the synthesis of arylbenzyl bis(silanes). *Eur. J. Org. Chem. 21*, 3079-3082. (DOI:10.1002/ejoc.202100474).

87. Wang, K., Zhou, J., Jiang, Y., Zhang, M., Wang, C., Xue, D., Tang, W., Sun, H., Xiao, J., Li, C. (2019). Selective manganese-catalyzed oxidation of hydrosilanes to silanols under neutral reaction conditions. *Angew. Chem. Int. Ed. 58*, 6380-6384. (DOI:10.1002/anie.201900342).

88. Zhang, Y., Lin, Z., Ackermann, L. (2021). Electrochemical C-H amidation of heteroarenes with *N*-Alkyl sulfonamides in aqueous medium. *Chem. Eur. J. 27*, 242-246. (DOI:10.1002/chem.202004229).

89. Tong, Z., Garry, O. L., Smith, P. J., Jiang, Y., Mansfield, S. J., Anderson, E. A. (2021). Au(I)-catalyzed oxidative functionalization of yndiamides. *Org. Lett. 23*, 4888-4892. (DOI:10.1021/acs.orglett.1c01625).

90. Yudasaka, M., Shimbo, D., Maruyama, T., Tada, T., Itoh, A. (2019). Synthesis, characterization, and reactivity of an ethynyl benziodoxolone (EBX)-acetonitrile complex. *Org. Lett. 21*, 1098-1102. (DOI:10.1021/acs.orglett.9b00005).

91. Pradhan, T. R., Kim, H. W., Park, J. K. (2018). Regiodivergent synthesis of 1,3- and 1,4-enynes through kinetically favored hydropalladation and ligand-enforced carbopalladation. *Angew. Chem. Int. Ed. 57*, 9930-9935. (DOI:10.1002/anie.201805408).

92. Xie, XQ., Yang, P., Zhang, Y. *et al.* (2015). Discovery of novel INK4C small-molecule inhibitors to promote human and murine hematopoietic stem cell *ex vivo* expansion. *Sci Rep 5*, 18115. (DOI:10.1038/srep18115).

93. Ramakrishana, K. K. G. *et al*. (2018). Identification of novel phenyl butenonyl *C*-glycosides with ureidyl and sulfonamidyl moieties as antimalarial. Agents. *ACS Med. Chem. Lett. 5*, 8, 878-883. (DOI:10.1021/ml500211c).

94. Chinn, A. J., Sedillo, K., Doyle, A. G. (2021). Phosphine/photoredox catalyzed anti-Markovnikov hydroamination of olefins with primary sulfonamides *via α*-scission from phosphoranyl radicals. *J. Am. Chem. Soc. 143*, 18331-18338. (DOI:10.1021/jacs.1c09484).

95. Li, C.-Y., Liu, Y.-C., Li, Y.-X., Reddy, D. M., Lee, F. A. (2019). Electrochemical dehydrogenative phosphorylation of thiols. *Org. Lett. 21*, 7833-7836. (DOI:10.1021/acs.orglett.9b02825).

96. Vaillant, F. Le., Garreau, M., Nicolai, S., Gryn'ova, G., Corminboeuf, C., Waser, J. (2018). Fine-tuned organic photoredox catalysts for fragmentation-alkynylation cascades of cyclic oxime ethers. *Chem. Sci. 9*, 5883-5889. (DOI:10.1039/C8SC01818A).

97. Dambacher, J., Bergdal, M. (2005). Conjugate additions of a simple monosilylcopper reagent with use of the CuI·DMS

complex: Stereoselectivities and a dramatic impact by DMS. *J. Org. Chem. 70*, 580-589. (DOI:10.1021/jo048269e).

98. Claderone, J. A., Santos, W. L. (2012). Copper(II)-catalyzed silyl conjugate addition to *α,β*-unsaturated conjugated compounds: Brønsted base-assisted activation of Si-B bond in water. *Org. Lett. 14*, 2090-2093. (DOI:10.1021/ol300618j).

99. Hatchard, C. G., Parker, C. A. (1956). A new sensitive chemical actinometer-II. Potassium ferrioxalate as a standard chemical actinometer. *Proc. Roy. Soc. (London) A235*, 518-536. (DOI:10.1098/rspa.1956.0102).

100. Cismesia, M.A., Yoon, T. P. (2015). Characterization chain processes in visible light photoredox catalysis. *Chem. Sci. 6*, 5426-5434. (DOI:10.1039/C5SC02185E).

# Chapter 3

## Organophotocatalytic Regioselective Silylation/Germylation and Cascade Cyclization of *N*-Alkenyl $\alpha$-$CF_3$ Acrylamides: Access to Densely Functionalized 4-Pyrrolin-2-ones

### 3.1 Introduction

In the previous chapter, we described the development of sulfonamide as an efficient hydrogen atom transfer catalyst for the selective functionalization of the Si-H/Ge-H bond of hydrosilanes and hydrogermanes and successfully employed it in the hydrosilylation and hydrogermylation *via* silyl/germyl radical addition to activated alkenes. Building on these findings, we sought to extend the "sulfamidyl radical-assisted Si-H and Ge-H bond functionalization of hydrosilanes and hydrogermanes *via* hydrogen atom transfer (HAT)" strategy to radical cascade cyclization reactions. The radical cascade cyclization reactions avoid multistep synthesis and deliver complex target molecules in an efficient and economical manner.[1-3] Also, these reactions arguably constitutes the most valuable tool in syntheses of numerous natural products,[2-3] carbocyclic and heterocyclic compounds.[4-5] We anticipated to synthesize a heterocyclic system *via* radical cascade cyclization that contains silyl and germyl functionalities, because integrating silyl and germyl functionalities with heterocycles may provide the final molecule with the benefit of their combined inherent properties. Heterocyclic compounds, being the most significant organic compounds often found in molecules pertinent to medicinal chemistry.[6] Among them, nitrogen-containing heterocycles are of great interest, as they are found in several natural products, such as vitamins, antibodies, and hormones, as well as synthetic derivatives of natural products with an *N*-containing backbone.[7-9] This perspective emphasizes the crucial function of nitrogen heterocycles as versatile and adjustable structural elements that are largely present among FDA-approved pharmaceuticals. [10-12] An analysis of a small dataset from January 2013 to December 2023 shows that almost 82% of U.S. FDA-approved small molecule drugs contain at least one nitrogen heterocycle.[10-12] As a result, the development of novel methodologies for the construction of small heterocyclic molecules is of great interest in modern organic synthesis and is being actively explored.

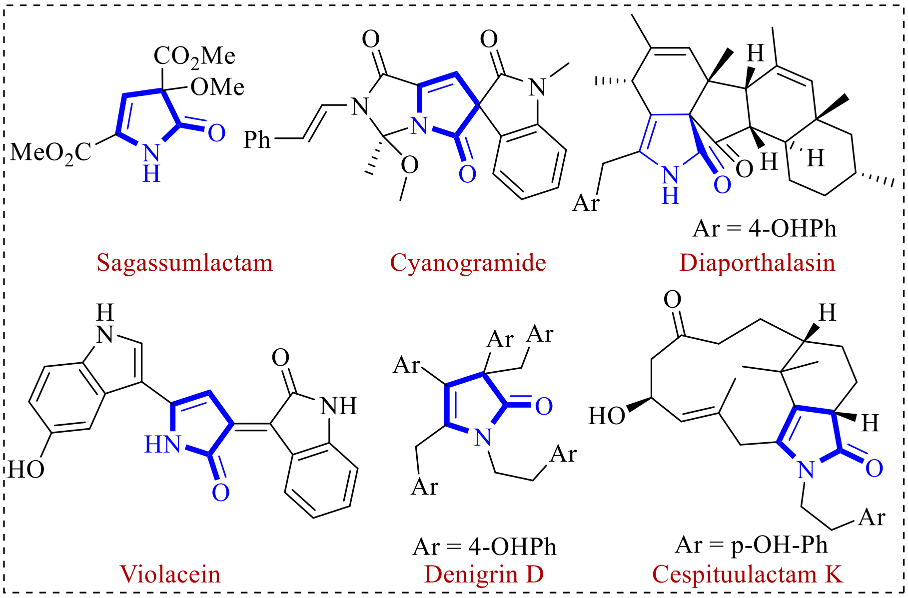


**Figure 3.1** Representative examples of bioactive molecules containing the 4-pyrrolin-2-one scaffold

4-Pyrrolin-2-ones are emblematic of nitrogen-containing heterocycles, as they are widely found in bioactive natural products and medicines, such as denigrin D, cyanogramide, sagassumlactam, and violacein.[13-16] Inevitably, a molecule containing both silyl group and a pyrrolin-2-one unit might profit from its combined inherent properties, which would provide an ideal design to study its therapeutic applications. Furthermore, the introduction of the $CF_3$ group to this molecule would further enhance its properties through increased permeability and metabolic stability.[17-19]

### 3.2 Literature reports for the synthesis of 4-pyrrolin-2-one scaffold

Initial strategies for constructing 4-pyrrolin-2-one scaffolds rely heavily on transition metal catalysts such as Ru,[20-23] Ir,[24] Pd,[25] Rh,[26] and Cu[27-29] complexes (**Scheme 3.1**). However, these methods have serious disadvantages, including the use of noble transition metal salts, high reaction temperature, and other challenging reaction conditions.

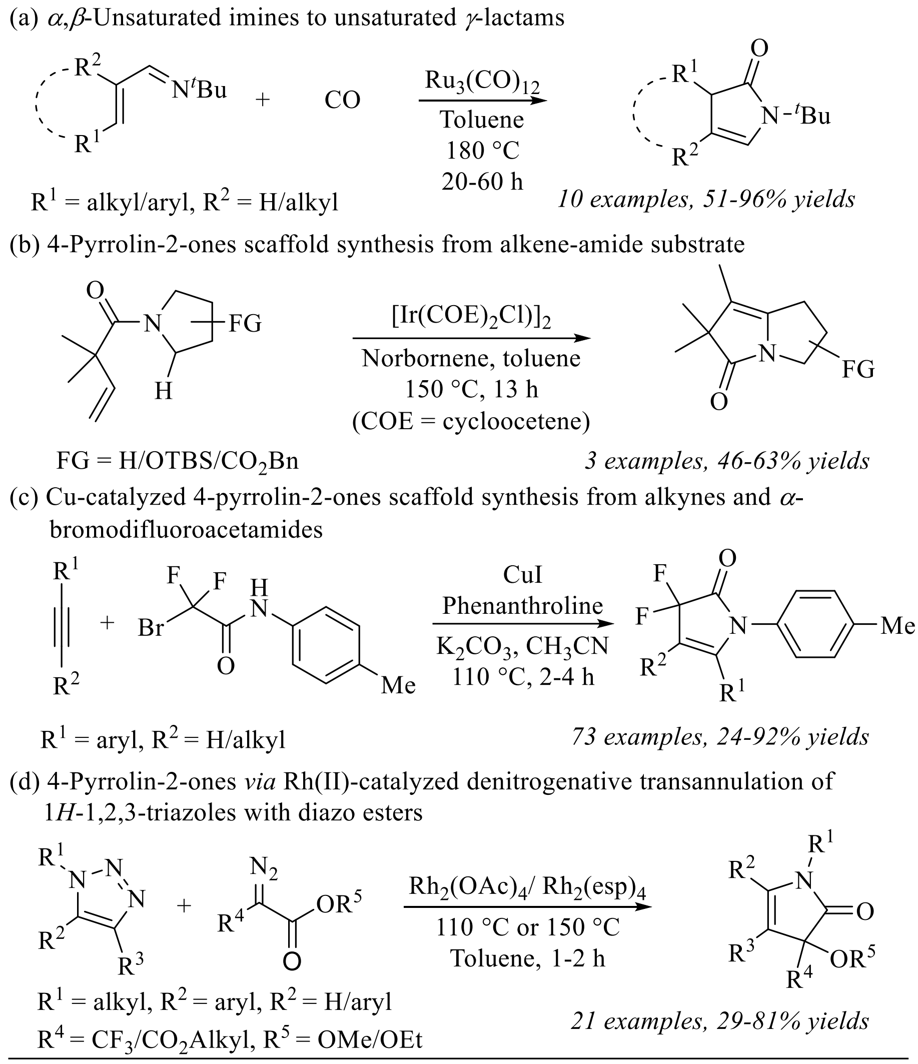


**Scheme 3.1** Selected examples for the construction of 4-pyrrolin-2-one using transition metal catalysts

Recent studies have demonstrated that the 3-aza-1,5-dienes serve as suitable substrates for efficiently constructing functionalized 4-pyrrolin-2-ones *via* regioselective radical addition followed by cascade cyclization. Using sulfonyl chloride as a radical precursor under thermal conditions, Wang and coworkers in 2021 demonstrated the copper-catalyzed regioselective sulfonylation-cyclization of 3-aza-1,5-dienes to produce 3-sulfonyl-1,3-dihydropyrrol-2-ones. The method was well tolerated for a wide range of substituents, yielding moderate to good yields (**Scheme 3.2a**).*[30]* Soon after, the Chen and Wu group collectively developed a transition metal-free synthesis of sulfonylated pyrrolidinones *via* a regioselective radical-relay sulfonylation/cascade cyclization protocol (**Scheme 3.2b**).[31-32] Subsequently, Wu and co-workers developed copper-catalyzed cascade reaction of cyclobutanone oxime ester-derived radicals with 1,5-dienes for the synthesis of 1,5-dihydro-2*H*-pyrrol-2-ones under thermal conditions (**Scheme 3.2c**).[33]

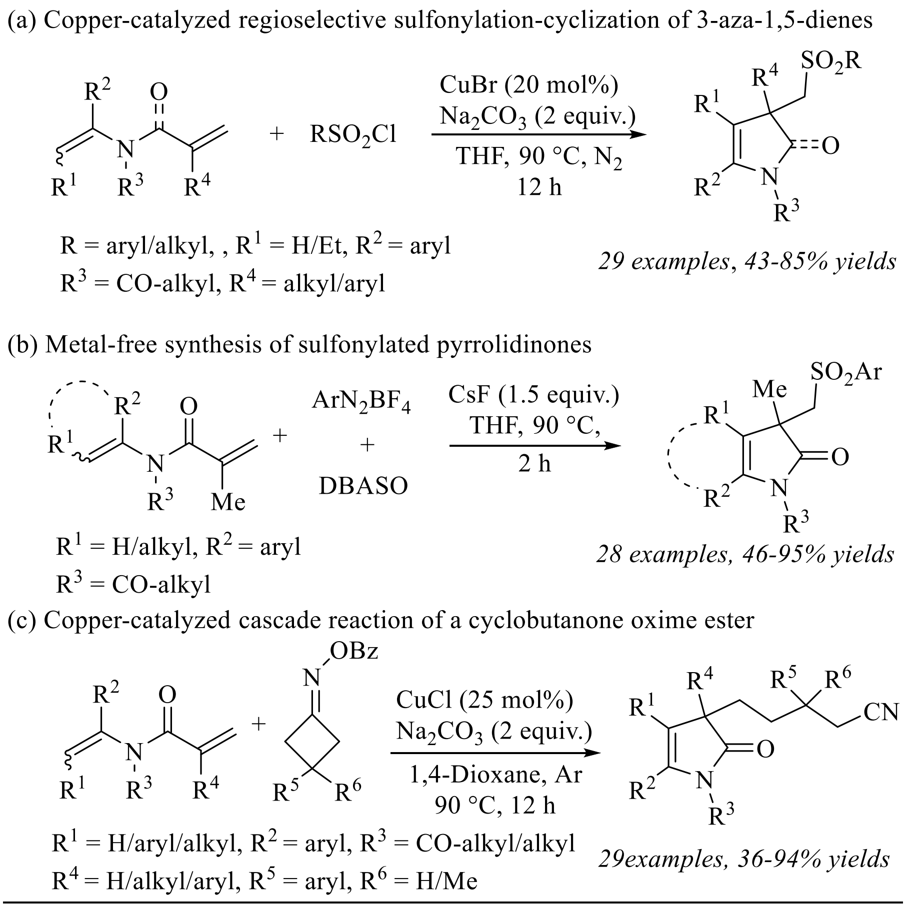


**Scheme 3.2** Radical addition/cascade cyclization of 3-aza-1,5-dienes under thermal conditions

Furthermore, the Liang group explored the photochemical regioselective addition/cyclization of alkyl radicals,[34] cyanoalkyl radicals[35] and perfluoroalkyl radicals[36] with 3-aza-1,5-dienes (**Scheme 3.3**). The electro-photochemical methods for alkenylpolyfluoroalkylative, selenylative, alkylative and thiocyanative cascade cyclization of 3-aza-1,5-dienes were developed by Sun and coworkers (**Scheme 3.4a-c**).[37-39] Similarly, the Liang group developed an electrochemical protocol to construct 4-pyrrolin-2-one (**Scheme 3.4d-e**).[40-41]

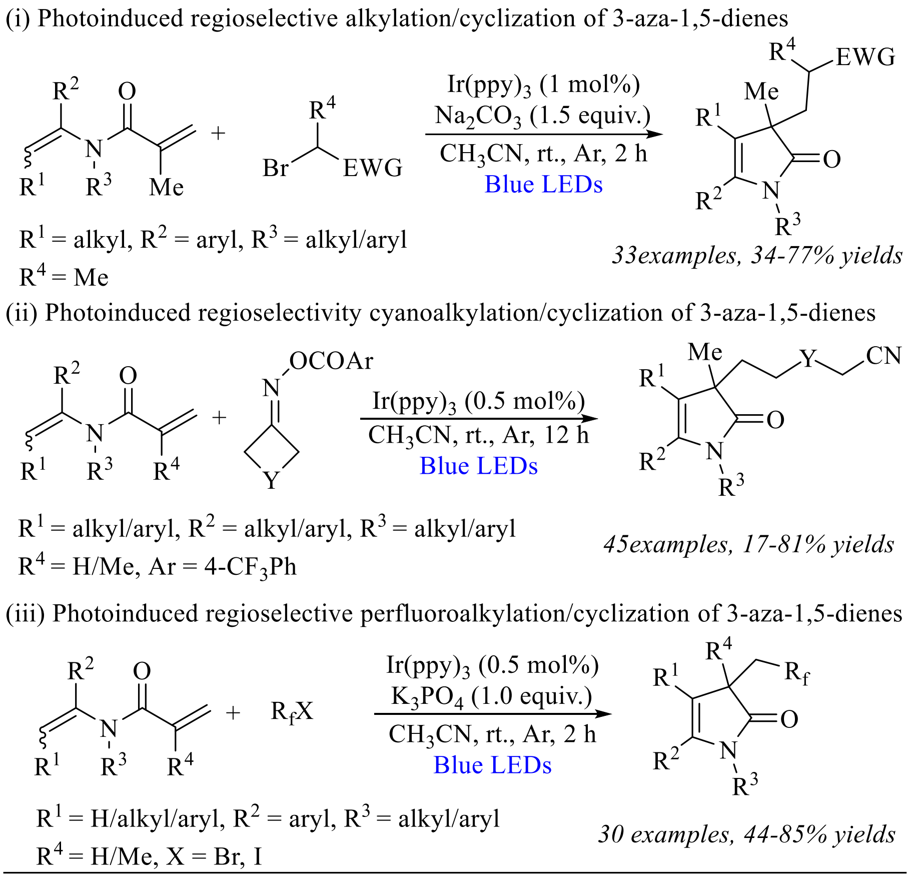


**Scheme 3.3** Photochemical regioselective addition/cyclization of 3-aza-1,5-dienes

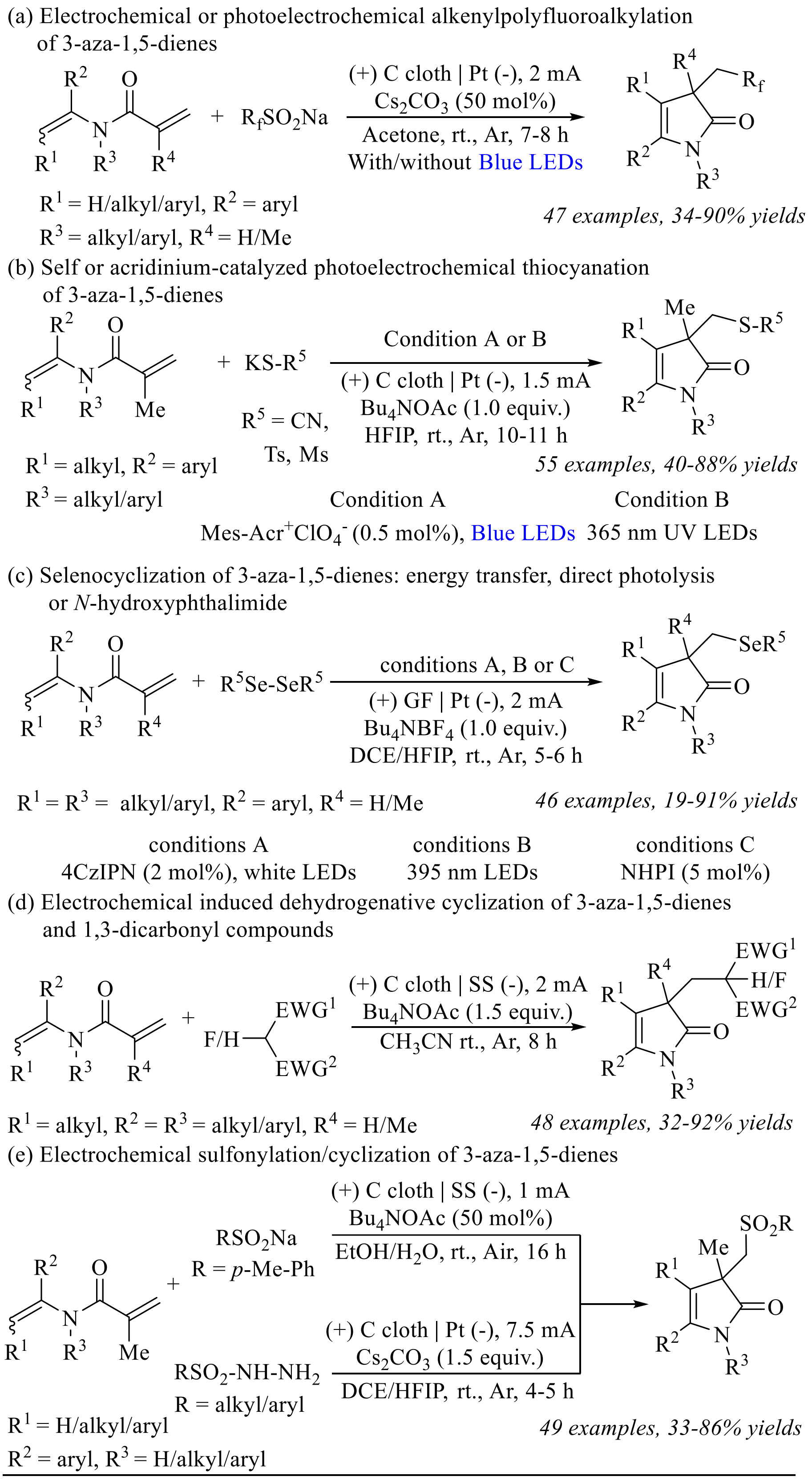


**Scheme 3.4** Photo-electrochemical and electrochemical radical addition/cascade cyclization of 3-aza-1,5-dienes

### 3.3 Objective

Although a number of methods have been developed to synthesize 4-pyrrolin-2-one derivatives from 3-aza-1,5-dienes through radical addition followed by cascade cyclization but they are limited with the type of radicals utilized. In this context, the development of an efficient protocol employing other radical species for the synthesis of densely functionalized 4-pyrrolin-2-one scaffolds is highly desirable. As part of our continued interest in the development of photocatalyzed organosilicon and organogermanium compounds from hydrosilane and hydrogermanes through *N*-centered sulfamidyl radical-assisted hydrogen atom transfer process*[42-43]*, we were fascinated by the prospect of investigating hydrosilanes/hydrogermanes as radical surrogates to introduce silyl/germyl functionalities onto the 4-pyrrolin-2-one scaffolds.

### 3.4 3-Aza-1,5-dienes in radical addition-cascade cyclization

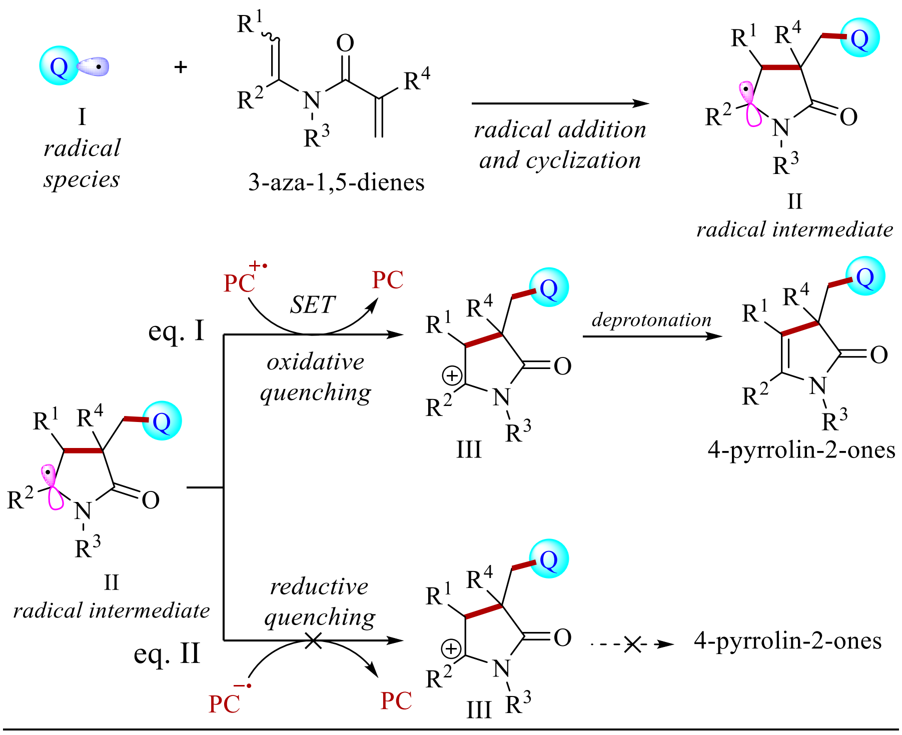


**Scheme 3.5** Tentative mechanism for the synthesis of 4-pyrrolin-2-ones from 3-aza-1,5-dienes *via* radical/cascade cyclization

Based on the literature reports, we evaluate the tentative mechanism for the synthesis of the 4-pyrolin-2-one scaffold from 3-aza-1,5-dienes. The regioselective addition of a radical to 3-aza-1,5-diene, followed by radical cascade cyclization, as illustrated in **Scheme 3.5**, yields the radical intermediate **II**, which would undergoes oxidation *via* SET with oxidized photocatalyst (**Scheme 3.5 eq. I**) to give cationic intermediate **III**, followed by deprotonation of intermediate **III** could give rise to 4-pyrrolin-2-ones. Therefore, the oxidized photocatalyst is crucial for the generation of cation intermediate **III**.

In our previous study*[42]*, the sulfamidyl radical facilitates, hydrogen-atom-transfer process and it was generated from the corresponding sulfonamide *via* a reductive quenching pathway with the generation of reduced photocatalyst (**Scheme 3.6, eq I**). Since the cationic intermediate **III** cannot be generated by the reduced photocatalyst (**Scheme 3.5, eq II**), the previously developed protocol is not suitable for accomplishing the proposed transformation. Consequently, this limitation necessitated the development of an alternative strategy for the generation of the sulfamidyl radical.

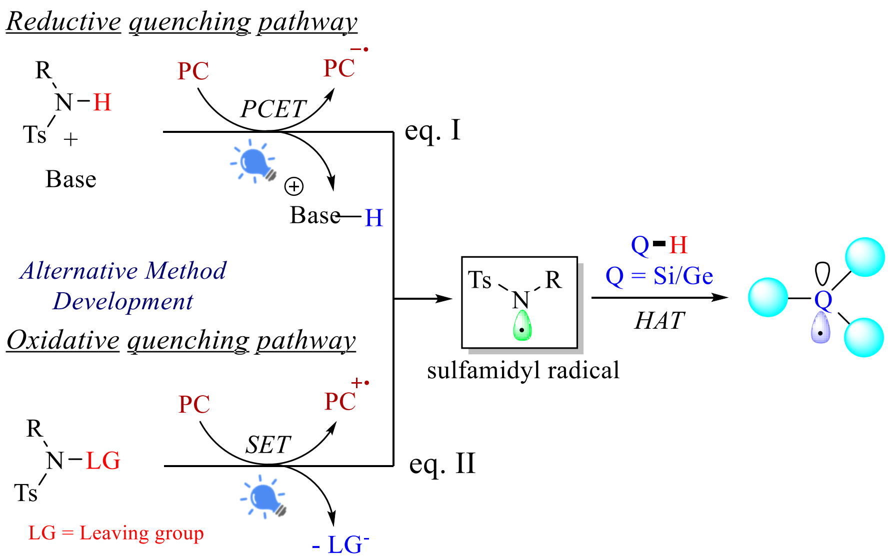


**Scheme 3.6** Development of an alternative approach for the generation of *N*-sulfamidyl radical

In this context, we hypothesized to replace the N-H hydrogen of the sulfonamide with a leaving group, and that would enable the resulting precursor to generate a sulfamidyl radical upon single-electron reduction by the excited photocatalyst, while simultaneously generating the oxidized photocatalyst *via* an oxidative quenching pathway (**Scheme 3.6 eq. II**).

In our search for an appropriate precursor to be used as an hydrogen atom transfer catalyst/reagent, we realized that *N*-aminopyridinium salt proved to be suitable for providing the necessary sulfamidyl radical through an oxidative quenching pathway (**Scheme 3.7**). This process enables the concurrent generation of sulfamidyl radical and oxidized photocatalyst with the extrusion of the leaving group. In 2015, Studer and coworkers amidated arenes and heteroarenes using *N*-aminopyridinium salt under photoredox catalysis.[44] Other groups have also utilized this salt in the amidation of enones,[45] C-H acylation,[46] alkene difunctionalization,[47-48] and amination of $\pi$-nucleophiles.[49]

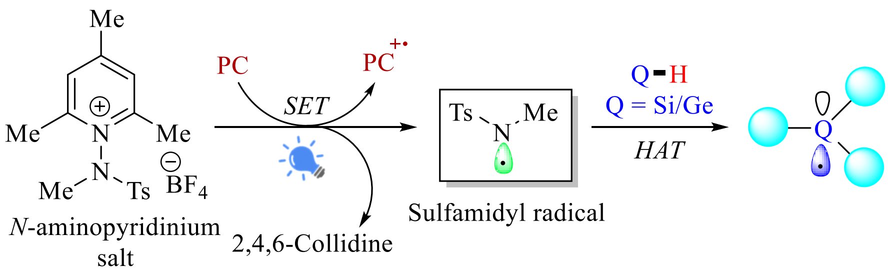


**Scheme 3.7** *N*-Aminopyridinium salt as hydrogen atom transfer reagent

## 3.5 Present work

### 3.5.1 Selection of model reaction

To evaluate our strategy, we chose *N*-benzyl-*N*-(1-phenylprop-1-en-1-yl)-2-(trifluoromethyl)acrylamide **1a** as a model starting material and $^{t}BuMe_2SiH$ **2a** as a silyl precursor under the photocatalytic oxidative quenching condition. The addition of the $CF_3$ group $\alpha$ to the acryloyl olefin in 3-aza-1,5-diene increases its reactivity and serves as a handle to alter the regioselectivity during the radical addition (**Scheme 3.8**).

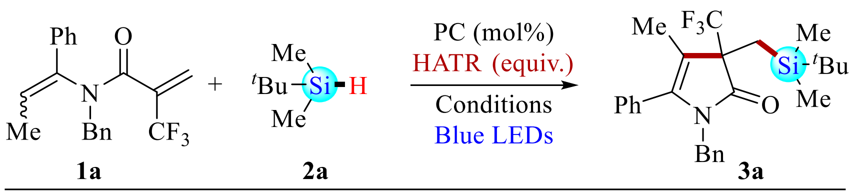

**Scheme 3.8** Selected model reaction for screening of reaction optimization

### 3.5.2 Optimization of reaction conditions

The optimization of reaction conditions is described in **Table 3.1**. Started our investigation with *fac*-Ir(ppy)$_3$ as photocatalyst, *N*-aminopyridinium salts as hydrogen atom transfer reagent (HATR) and acetonitrile as solvent, under 455 nm blue LEDs irradiation for 1 hour (entry 1), which provides the desired product **3a** in 32% yield, along with 5-hydroxy-pyrrolidin-one derivative **3a'**. We anticipated that the formation of the hydroxy derivative could arised from the moisture present in the reaction mixture. On performing the reaction with 4Å molecular sieves, to our surprise yield of the desired product increased to 42% (entry 2). Further screening of other Ir-photocatalysts, such as *fac*-Ir(dFppy)$_3$ gives 53% yield (entry 3), while in the case of [Ir(dF(CF$_3$)ppy)$_2$(dtbbpy)]PF$_6$ the desired product formation was not observed (entry 4). However, [Ir(ppy)$_2$(dtbbpy)]PF$_6$ provides the highest yield among the Ir-photocatalysts screened (entry 5). With other commonly used Ru-photocatalyst such as Ru(bpy)$_3$Cl$_2$·6H$_2$O, only a trace amount of the desired product was observed (entry 7). Among the organic photocatalysts screened, 4CzIPN was initially evaluated which afforded inferior results (entry 8). In contrast, 3DPAFIPN delivered the silylated 4-pyrrolin-2-one product in only 25% yield. Notably, 4DPAIPN exhibited a significant increase in product formation and provided 59% yield of silylated 4-pyrrolin-2-one, comparable to that obtained with the Ir-based photocatalyst (entry 10 vs. entry 5). To avoid using precious transition metal catalysts and make the protocol environmentally benign, the organic photocatalyst 4DPAIPN was selected for further screenings. Lowering the loading of 4DPAIPN from

5 mol% to 3 mol% exhibits a slight increase in the yield of silylated 4-pyrrolin-2-ones (entry 11).

**Table 3.1** Optimization of reaction conditions

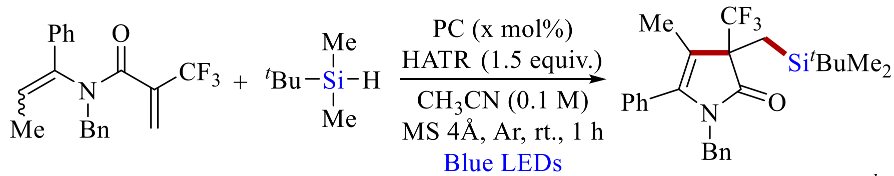


**1a** **2a** **3a**, Yield (%)$^b$

| Entry | PC (mol%) | 4ÅMS | Yield (%)$^b$ |
|---|---|---|---|
| 1.$^c$ | *fac*-Ir(ppy)$_3$ (1) | - | 32 |
| 2. | *fac*-Ir(ppy)$_3$ (1) | 50 mg | 42 |
| 3. | *fac*-Ir(dFppy)$_3$ (1) | 50 mg | 53 |
| 4. | [Ir(dF(CF$_3$)ppy)$_2$(dtbbpy)]PF$_6$ (1) | 50 mg | n.d. |
| 5. | [Ir(ppy)$_2$(dtbbpy)]PF$_6$ (1) | 50 mg | 59 |
| 6. | [Ir(dtbppy)$_2$(dtbbpy)]PF$_6$ (1) | 50 mg | 8 |
| 7. | Ru(bpy)$_3$Cl$_2$.6H$_2$O (5) | 50 mg | trace |
| 8. | 4CzIPN (5) | 50 mg | 10 |
| 9. | 3DPAFIPN (5) | 50 mg | 25 |
| 10. | 4DPAIPN (5) | 50 mg | 59 |
| 11. | 4DPAIPN (3) | 50 mg | 64 |
| 12.$^d$ | 4DPAIPN (3) | 100 mg | 69 |
| 13.$^e$ | 4DPAIPN (3) | 100 mg | 74 |
| **14.$^e$** | **4DPAIPN (1)** | **100 mg** | **78** |
| 15.$^e$ | Without Photocatalyst | 100 mg | n.r. |
| 16.$^{e,f}$ | 4DPAIPN (1) | 100 mg | n.r. |

$^a$Reaction Conditions: **1a** (0.2 mmol), **2a** (0.6 mmol), HATR (0.3 mmol), PC (x mol%), dry $CH_3CN$ (2 mL), molecular sieves 4Å, under blue LEDs irradiation. $^b$isolated yield. $^c$moisture trapped derivative **3a'** detected. $^d$dry $CH_3CN$ (1 mL). $^e$dry $PhCF_3$ (1 mL). $^f$without light. n.d. = not detected. n.r. = no reaction.

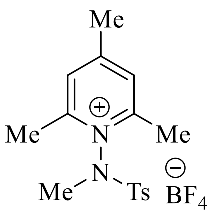

**HATR**

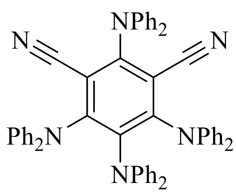

**4DPAIPN**

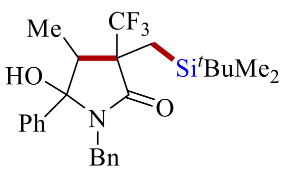

**3a'**

Meanwhile, increasing the concentration along with the amount of molecular sieves leads to a 69% yield of the desired product (entry 12). Then change in the solvent from acetonitrile to *α,α,α*-trifluorotoluene (entry 13) along with lowering in loading of photocatalyst, provides the optimum yield for silylated 4-pyrrolin-2-one **3a** (78%) (entry 14). No reaction observed either in the absence of photocatalyst or in the absence of light (entries 15-16). Additionally, the screening of other solvents like acetone, dichloroethane, dimethylsulfoxide, and toluene provided lower yield of silylated 4-pyrrolin-2-one **3a**.

### 3.5.3 Substrate scope for silylation of 3-aza-1,5-dienes

After establishing the optimal reaction conditions, we proceeded to investigate the substrate scope of 3-aza-1,5-dienes **1** (**Scheme 3.9**). Screening of different substituents such as ethyl (**1b**), propyl (**1c**), and phenyl (**1d**) groups at the 2-position of the enamide gave the desired products **3b**-**3d** (70−85%) in good to excellent yields. However, without any substituent at the *β*-position of enamide, the yield of product **3e** was slightly reduced. The screening of *N*-substituents on the dienes reveals compatibility with both aryl and alkyl groups. Phenyl (**1f)**, *n*-propyl (**1g)**, and cyclohexyl (**1h**) substituents provided product **3f-3h** in moderate to good yield (35-82%). *N*-unsubstituted 3-aza-1,5-diene **1i** failed to give the desired product. In the case of substrate containing *meta*-substituents like fluoro (**1j**) and chloro (**1k**) on the aryl ring *α* to the enamide gave desired product **3j**-**3k** in 67% and 61% yield respectively. When substitution at the *para*-position of the aryl ring *α* to the enamide are electron-donating like methyl (**1l**) and methoxy (**1m**) provided the corresponding product **3l** and **3m** in excellent yields of 84% and 81% respectively. Similarly, with electron-withdrawing groups such as fluoro (**1n**), chloro (**1o**), and trifluoromethyl (**1p**), provided desired products **3n**-**3p** in good to excellent yields. Furthermore, under the optimized reaction conditions, the substrate with an alcohol group protected as an acetate (**1q**), a flexible synthetic handle was well tolerated and provided the desired product **3q** in a 58% yield.

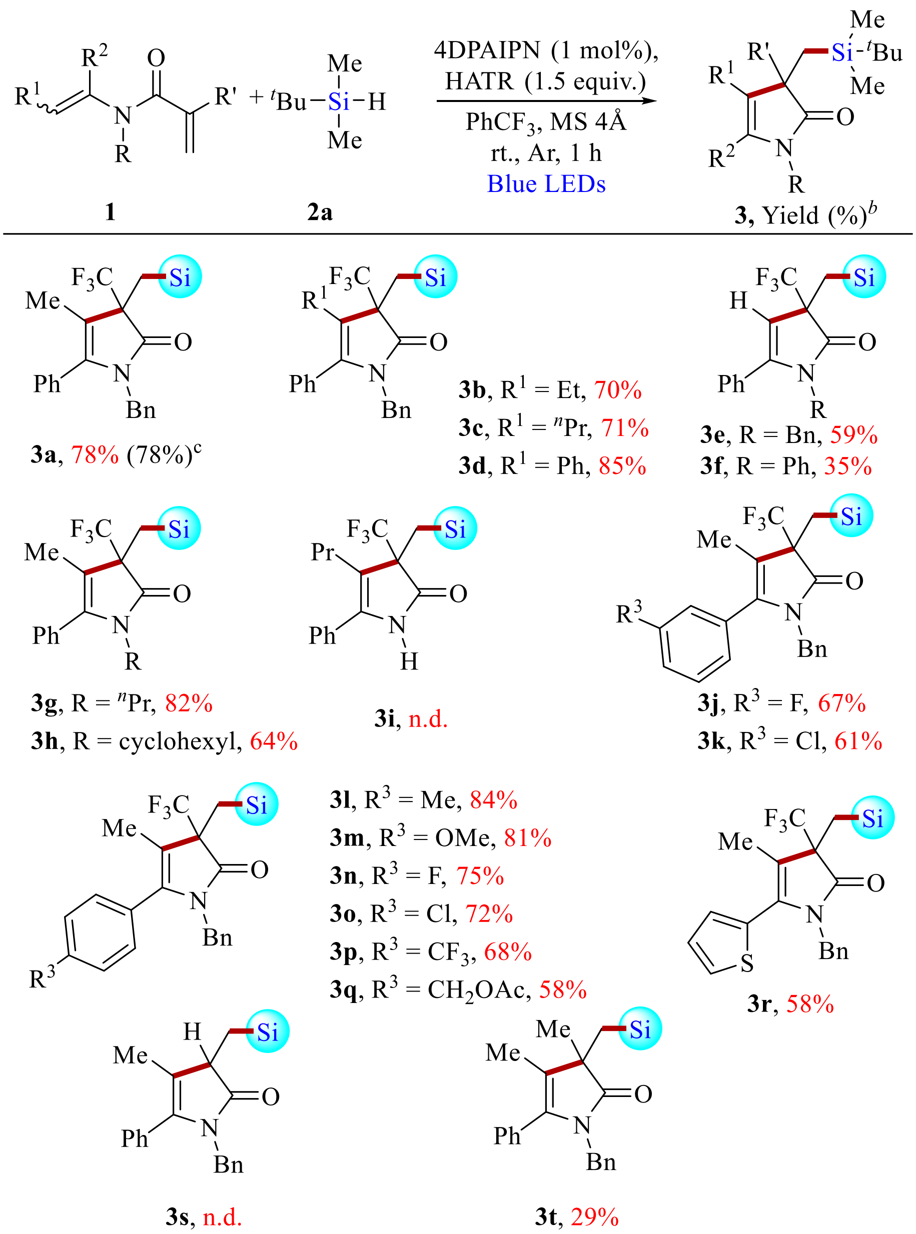


[a]Reaction Condition: **1** (0.2 mmol), **2a** (0.6 mmol), HATR (0.3 mmol), 4DPAIPN (1 mol%), dry $PhCF_3$ (1 mL), dry molecular sieves 4Å (100 mg), under blue LEDs irradiation. [b]isolated yield. [c]yield for 2 mmol scale reaction for 3 h. n.d. = not detected.

**Scheme 3.9** Scope of 3-aza-1,5-dienes in synthesis of silylated 4-pyrrolin-2-ones

Gratifyingly, 2-thienyl ring $\alpha$ to the enamide provides the desired product **3r** in 58% yield under optimized reaction conditions. The reactivity of the diene is greatly impacted when the $\alpha$-$CF_3$ group is replaced with H (**1s**) or methyl (**1t**). When it is H, no desired product formation was detected, while with methyl the desired product **3t** was obtained in 29% yield.

### 3.5.4 Scope of hydrosilanes

Then, we move towards investigating the scope of hydrosilanes under optimized reaction conditions (**Scheme 3.10**).

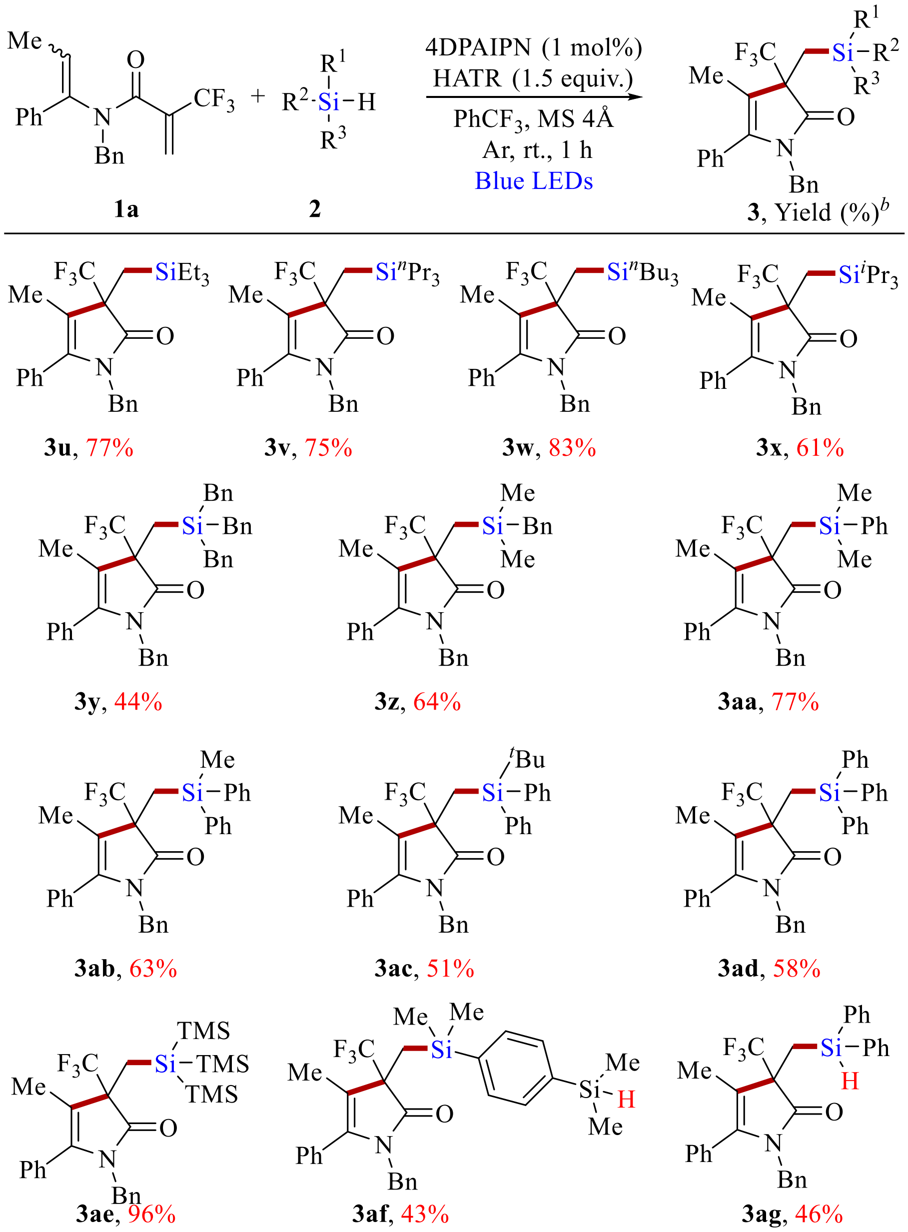


[a]Reaction Conditions: **1a** (0.2 mmol), **2** (0.6 mmol), HATR (0.3 mmol), 4DPAIPN (1 mol%), dry $PhCF_3$ (1 mL), dry molecular sieves 4Å (100 mg), under blue LEDs irradiation. [b]isolated yield.

**Scheme 3.10** Scope of hydrosilanes with **1a** as 3-aza-1,5-diene

The screening began with different alkylsilanes, such as triethylsilane (**2b**), tri-*n*-propylsilane (**2c**), tri-*n*-butylsilane (**2d**), and triisopropylsilane (**2e**), which furnished the desired products **3u**-**3x** in good to excellent yields (61-83%). The tribenzylsilane (**2f**) and dimethylbenzylsilane (**2g**) yielded the desired products **3y**-**3z** in 44% and 64% respectively. Subsequently, aryl silanes were investigated and found to be compatible under the optimized reaction conditions. Dimethylphenylsilane (**2h**), methyldiphenylsilane (**2i**), *tert*-butyldiphenylsilane (**2j**), and triphenylsilane (**2k**) smoothly underwent cyclization to afford the desired products **3aa-3ad** in moderate to good yields (51-77%). The supersilane tris(trimethylsilyl)silane afforded the desired product **3ae** in excellent yield (96%). In addition, the *para*-phenylenebis(dimethylsilane) (**2m**) as a silicon source, produced only the monosilylated product **3af** in 43% yield. Surprisingly, diphenylsilane (**2n**) was also compatible under optimized reaction conditions to give desired product **3ag** in 46% yield.

### 3.5.5 Synthesis of germylated 4-pyrrolin-2-ones

Motivated by these results, we expanded our protocol to synthesize germylated 4-pyrrolin-2-ones (**Scheme 3.11**). To evaluate the scope of 3-aza-1,5-dienes, hydrogermane $Ph_3GeH$ (**4a**) was used as a source of germylating agent. Only 1.5 equivalents of $Ph_3GeH$ were sufficient with **1a** as diene, to provide germylated 3-(trifluoromethyl)-1,3-dihydro-2*H*-pyrrol-2-one (**5a**) in 98% yield under the optimized reaction conditions. The dienes with methyl and halogen substituents (F, Cl, Br) on the aryl ring $\alpha$ to enamide underwent smooth cyclization and delivered the corresponding products **5b**-**5e** in moderate to good yields (60-88%). The diene (**1d**) bearing phenyl groups at both the $\alpha$- and $\beta$-positions of enamide afforded product **5f** in 92% yield. Also, triethyl (**4b**) and tributyl (**4c**) hydrogermanes were tolerated under the reaction conditions and provided the corresponding products **5g** and **5h** in excellent yields (89% and 88%). Notably, the thiophene-substituted enamide (**1r**) proved to be compatible with the reaction conditions and delivering germylated 5-(thiophen-2-yl)-4-pyrrolin-2-one (**5i**) in 76% yield.

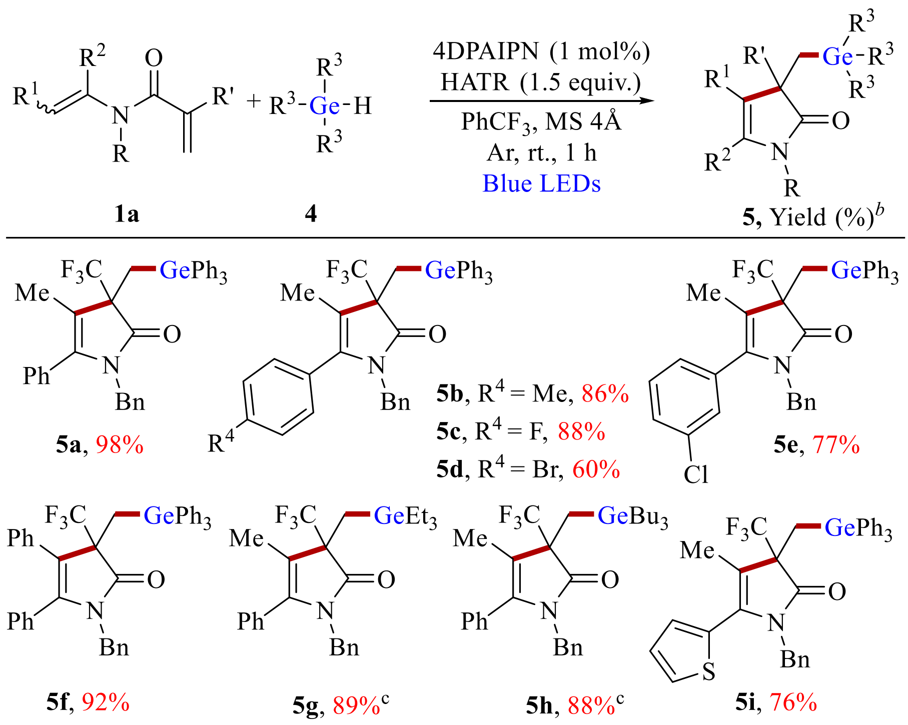


$^a$Reaction Conditions: **1a** (0.2 mmol), **4** (0.3 mmol), HATR (0.3 mmol), 4DPAIPN (1 mol%), dry $PhCF_3$ (1 mL), dry molecular sieves 4Å (100 mg), under blue LEDs irradiation. $^b$isolated yield. $^c$using 2 equiv. of **4**.

**Scheme 3.11** Scope for germylation in synthesis of germylated 4-pyrrolin-2-ones

### 3.5.6 Late-stage functionalization of natural products and drug molecules tethered 3-aza-1,5-dienes

The mild characteristics and robustness of this method was further demonstrated by testing substrates tethered to complex molecules derived from natural products and drugs (**Scheme 3.12**). The natural product (+)-*α*-tocopherol tethered diene smoothly cyclized with *tert*-butyldimethylsilane (**2a**) under optimized conditions, provided **3ah** in 37% yield. Additionally, (*S*)-ibuprofen, oxaprozin, isoxepac, gemfibrozil, and (*S*)-naproxen were easily attached to the dienes *via* a straightforward coupling reaction. These dienes subsequently underwent cascade cyclization under optimized conditions to produce the desired products **3ai-3am** in moderate to good yields (40-65%).

Notably, the germyl derivative of 4-pyrrolin-2-one with (*S*)-naproxen tethered **5j** was also synthesized in good yield (63%).

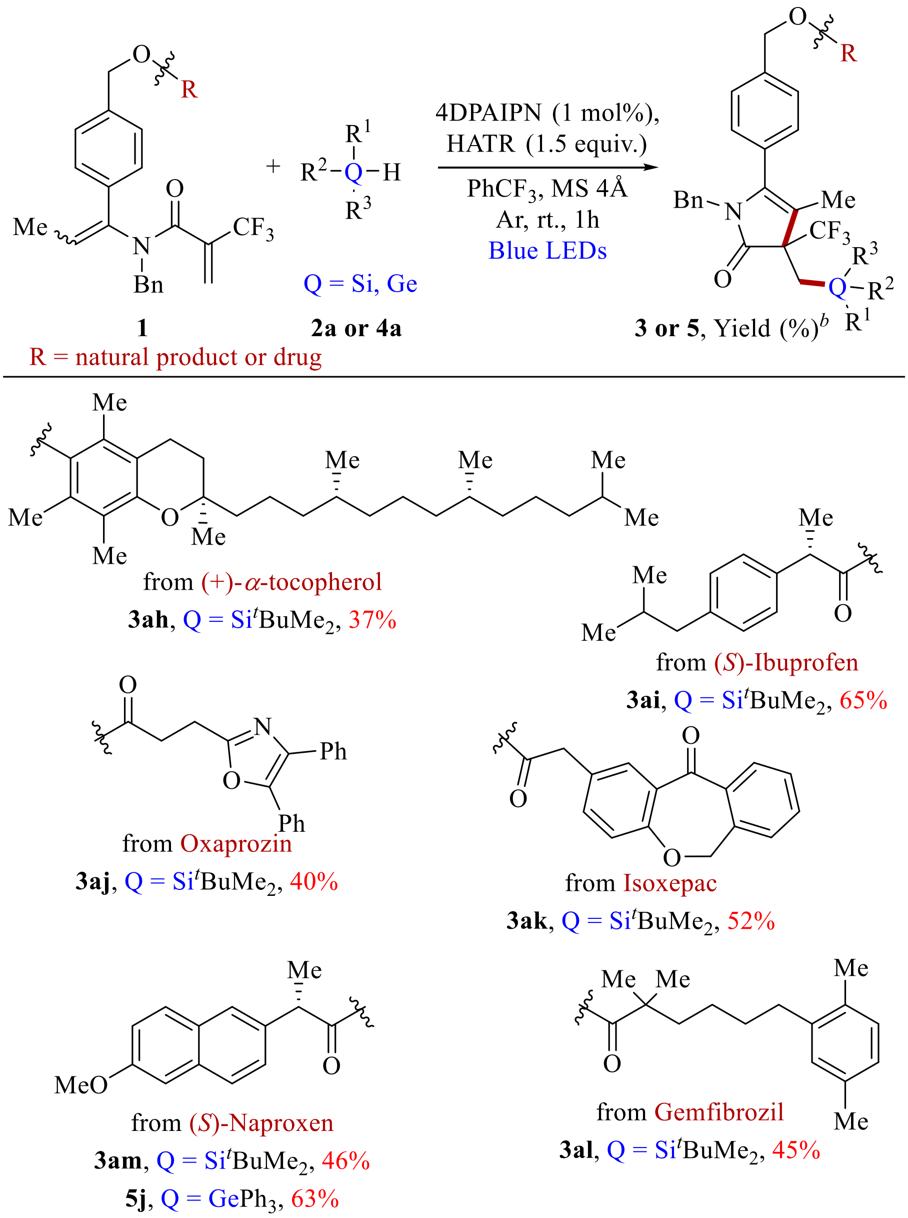


[a]Reaction Conditions: **1** (0.2 mmol), **2a** (0.6 mmol) or **4a** (0.3 mmol), HATR (0.3 mmol), 4DPAIPN (1 mol%), dry $PhCF_3$ (1 mL), dry molecular sieves 4Å (100 mg), under blue LEDs irradiation. [b]isolated yield.

**Scheme 3.12** Late-stage functionalization of natural product and drug tethered with 3-aza-1,5-dienes

### 3.5.7 Large-scale synthesis of silylated 4-pyrrolin-2-one

The practicality of the developed protocol was further demonstrated by 2 mmol scale reaction of diene **1a**, which provided silylated 4-pyrrolin-2-one **3a** in 78% yield (**Scheme 3.13**).

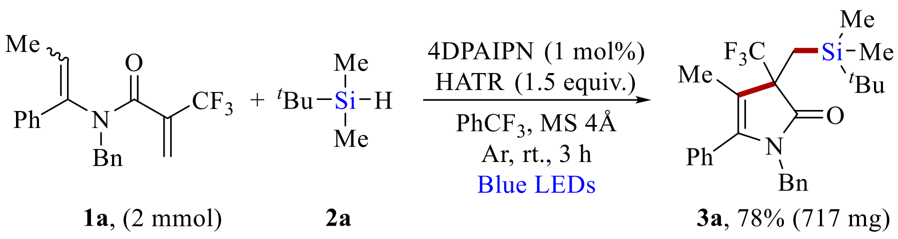


**Scheme 3.13** Scale-up of silylated 4-pyrrolin-2-one **3a**

### 3.6 Mechanistic investigations

To gain insight into the reaction mechanism, radical trapping experiments, fluorescence quenching studies, and quantum yield calculation were performed.

#### 3.6.1 Radical inhibition and trapping experiments

The involvement of radical species in the reaction mechanism was determined by performing the reaction with radical scavengers, such as TEMPO and 1,1-diphenylethylene using diene **1a** and hydrosilane (**2h** )/hydrogermane (**4a**) under standard reaction conditions (**Scheme 3.14 (i-ii)**).

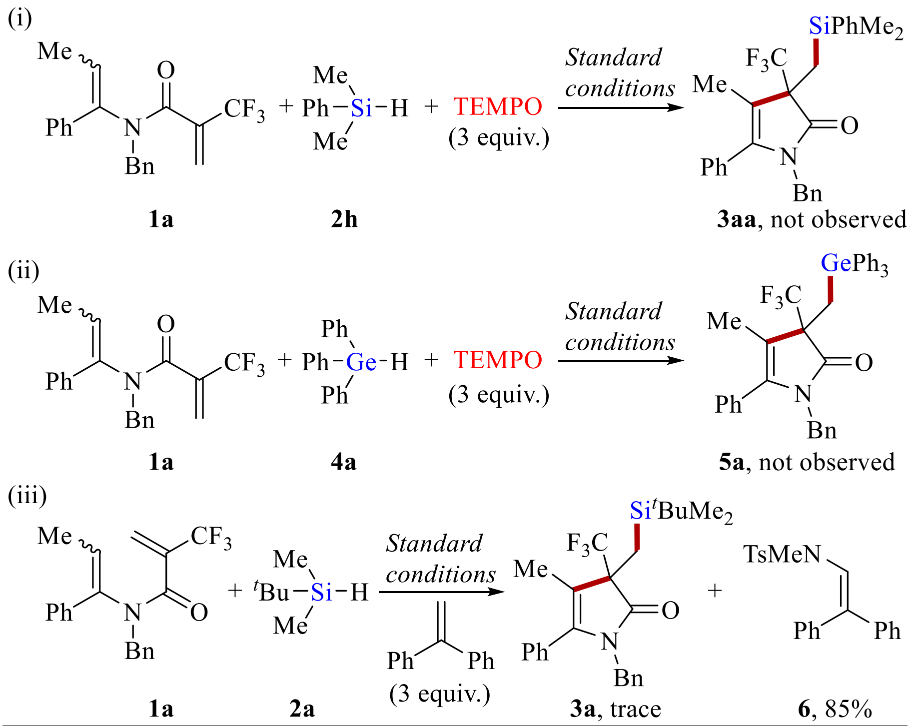


**Scheme 3.14** Radical inhibition and trapping experiments

In all these conditions, the formation of photoproducts (**3aa**/**5a**) was completely suppressed, while an 85% yield of sulfamidyl radical-trapped product **6** was observed with 1,1-diphenylethylene (**Scheme 3.14** (**iii**)). These findings provide compelling evidence that a sulfamidyl radical intermediate was involved in this cascade reaction.

### 3.6.2 Stern-Volmer quenching studies

To identify the species that quenches the excited state photocatalyst during the reaction, Stern-Volmer quenching studies have been performed. The quenching study was conducted between the photocatalyst 4DPAIPN and other reaction components, including the diene **1a**, hydrosilane **2a**, hydrogermane **4a**, and *N*-aminopyridinium salt (HATR). Stern-Volmer studies demonstrated that 4DPAIPN fluorescence emission was quenched only by *N*-aminopyridinium salts (**Figure 3.2**) and not by 3-aza-1,5-diene (**1a**) or hydrosilanes (**2a**)/hydrogermanes (**4a**).

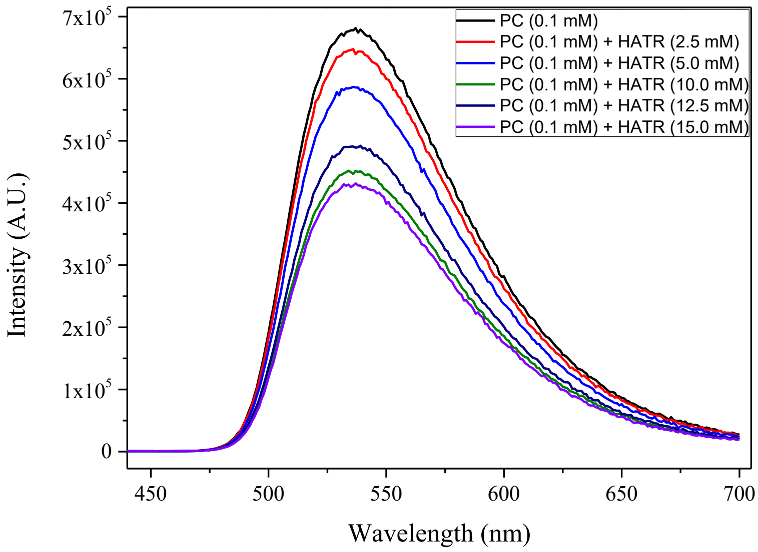

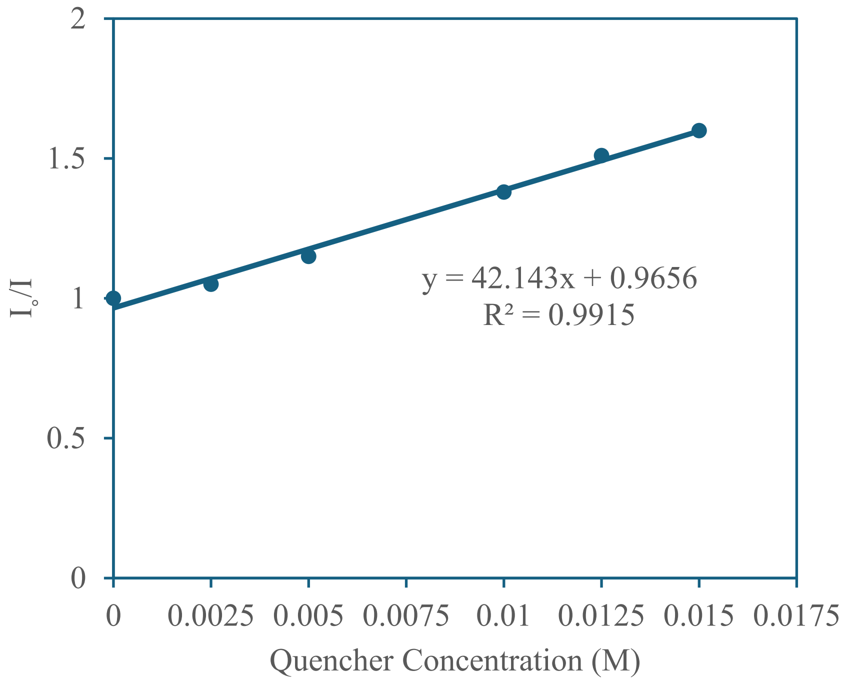


**Figure 3.2** Fluorescence quenching and Stern-Volmer plot of 4DPAIPN *vs N*-aminopyridinium salt

### 3.6.3 Quantum yield calculation

The quantum yield of the standard reaction was calculated to determine the involvement of a radical chain pathway in the product formation. The calculated quantum yield ($\phi$ = 25.23) suggests the possible involvement of a radical chain process in the reaction (**Scheme 3.15**).

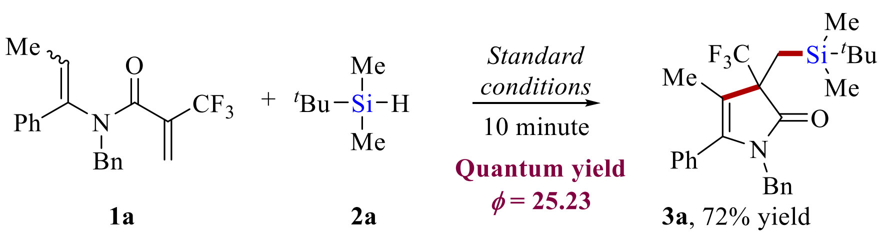


**Scheme 3.15** Quantum yield calculation of standard reaction

### 3.7 Possible mechanism

A possible reaction mechanism is proposed based on mechanistic investigations and literature reports (**Scheme 3.16**).[43-49] Upon irradiation with light, the photocatalyst 4DPAIPN gets excited, and the excited photocatalyst 4DPAIPN* undergoes SET with *N*-

aminopyridinium salt to generate *N*-centered sulfamidyl radical **I** and oxidized photocatalyst 4DPAIPN$^{\bullet+}$ with the extrusion of 2,4,6-collidine. The sulfamidyl radical **I,** activate the Si-H/Ge-H bond of hydrosilanes/hydrogermanes through hydrogen atom transfer (HAT) to produce silyl/germy radical **II**. Following the regioselective addition and cascade cyclization of silyl/germyl radical **II** to 3-aza-1,5-diene **1a** leads to the formation of transient $\alpha$-amino radical **III**. The transient $\alpha$-amino radical **III** gets oxidized *via* SET by the oxidized photocatalyst 4DPAIPN$^{\bullet+}$ with the regeneration of the photocatalyst and formation of a cationic species **IV**. The involvement of cationic species **IV** was further confirmed by the formation of 5-hydroxy-pyrrolidin-one derivative **3a'** on performing the reaction in the absence of 4Å molecular sieves.

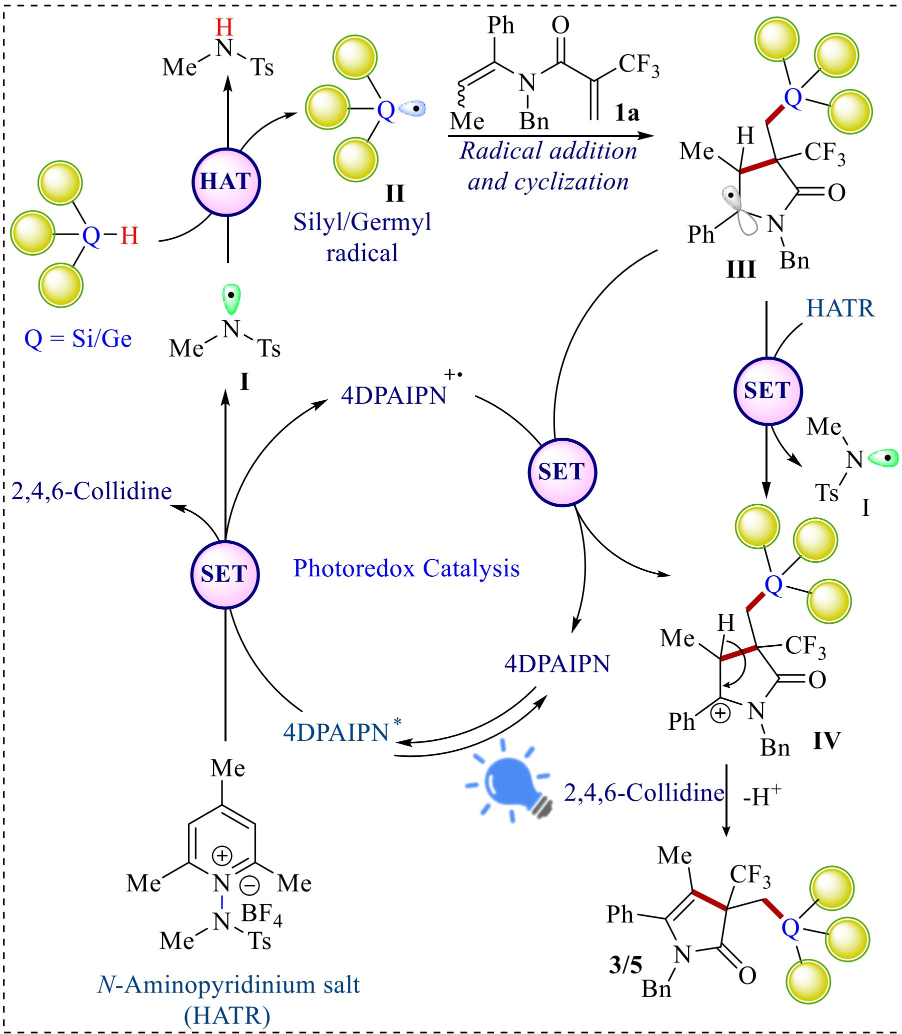


**Scheme 3.16** Possible mechanism

The cationic species **IV** gets deprotonated with the assistance of 2,4,6-collidine to give the desired silylated/germylated 4-pyrrolin-2-one derivative **3/5**. The observed high quantum yield suggests the involvement of a radical chain pathway in the reaction. The $\alpha$-amino radical **III** could undergo SET with *N*-aminopyridinium salt and leads to the formation of cationic species **IV** along with *N*-centered sulfamidyl radical **I**. Thus, the *N*-centered sulfamidyl radical **I** can be generated without the involvement of the photocatalytic cycle. The subsequent HAT process between sulfamidyl radical **I** and hydrosilanes or hydrogermanes can provide silyl or germyl radical, followed by radical addition and cascade cyclization with 3-aza-1,5-diene, leads to the formation of the desired product **3/5**.

### 3.8 Conclusion

In conclusion, we developed a complementary protocol for the generation of *N*-centered sulfamidyl radical by employing *N*-aminopyridinium salts as hydrogen atom transfer reagent for Si-H/Ge-H bond functionalization *via* an oxidative quenching pathway under visible-light irradiation. This strategy was successfully applied to the synthesis of silylated and germylated 4-pyrrolin-2-ones from 3-aza-1,5-dienes through regioselective radical addition and cascade cyclization of silyl and germyl radicals derived from hydrosilanes and hydrogermanes. The developed protocol is operationally simple, exhibits mild reaction conditions. The scope of dienes was thoroughly investigated by introducing different substituents on alkenes, aryl rings $\alpha$ to enamide, and substitutions at nitrogen of 3-aza-1,5-dienes. The scope of hydrosilanes demonstrated the tolerance of both alkyl and aryl hydrosilanes. The developed protocol was successfully applied to the synthesis of germylated 4-pyrrolin-2-ones. In addition, natural product and drug molecules tethered dienes were also employed in the synthesis of silylated/germylated 4-pyrrolin-2-ones. Moreover, the proposed mechanism for the synthesis of silyl/germyl 4-pyrrolin-2-ones derivatives is supported by the results of the controlled experiments and photophysical studies.

### 3.9 Experimental section

#### 3.9.1 Synthesis of *N*-aminopyridinium salt

The *N*-aminopyridinium salt (HATR) was prepared according to the reported procedure.[44] To an oven-dried round-bottom flask, dry THF (11 mL) was taken, and cooled on an ice bath. 1.66 mL of methylhydrazine and 4.4 mL of $Et_3N$ were added sequentially to the above solution. Stir the mixture for 15 minutes at the same temperature. Separately, a solution of tosyl chloride (4 g) in THF (10 mL) was prepared and added slowly to the above solution. Stir for an additional 15 minutes, then transfer to room temperature. After the reaction was completed, the organic layer was separated using diethyl ether and washed with water. The combined organic layer was dried over $Na_2SO_4$ and filtered into a round-bottom flask. Seal the round-bottom flask with a stopper and keep it in the fridge. White crystals of *N*,4-dimethylbenzenesulfonohydrazide were then separated from the mother liquor, washed with diethyl ether, and dried under high vacuum to yield 2.5 g of *N*,4-dimethylbenzenesulfonohydrazide.

1.5 g of *N*,4-dimethylbenzenesulfonohydrazide was taken in an oven-dried round-bottom flask and dissolved in EtOH (25 mL). While stirring, 2,4,6-trimethylpyrylium tetrafluoroborate (1.2 g) was added portion-wise at room temperature, and the mixture was stirred overnight. After the reaction was completed, 20 mL of diethyl ether was added, and the mixture was kept in the fridge for crystallisation, yielding 1.2 g of 1-((*N*, *N*-dimethylphenyl)sulfonamido)-2,4,6-trimethylpyridin-1-ium tetrafluoroborate as a white solid.

**$^1$H NMR** (500 MHz, $CDCl_3$) δ 7.75 – 7.70 (m, 2H), 7.52 (s, 2H), 7.47 – 7.43 (m, 2H), 3.59 (s, 3H), 2.58 (s, 3H), 2.57 (s, 6H), 2.50 (s, 3H). **$^{13}$C NMR** (126 MHz, $CDCl_3$) δ 161.8, 158.8, 146.8, 134.3, 130.9, 129.2, 127.7, 37.9, 22.2, 21.9, 20.1.

### 3.9.2 Synthesis of 4DPAIPN

The organophotocatalyst 4DPAIPN was prepared according to the reported procedure.[50] To an oven-dried RB flask, diphenylamine (6 equiv.) was added and diluted with 20 mL of DMF. While stirring under an argon atmosphere, NaH (10 equiv., 60% suspension in mineral oil) was added portion-wise, and the reaction was transferred to an oil bath for heating at 60 °C for 1 h. The reaction was cooled to 40 °C, and 2,4,5,6-tetrafluoroisophthalonitrile (1 equiv., 400 mg) was added. The mixture was stirred overnight at the same temperature. After completion of the reaction, it was quenched by the addition of water and separated using dichloromethane as the organic solvent. The organic layer was then further washed with brine. The crude mixture was purified by column chromatography (DCM/hexane) and then by recrystallization (DCM/Hexane). Yellow crystals; yield: 38% (600 mg). **$^1$H NMR** (500 MHz, $CDCl_3$) δ 7.30 – 7.23 (m, 4H), 7.12 – 7.05 (m, 12H), 7.05 – 6.99 (m, 2H), 6.94 – 6.84 (m, 8H), 6.73 – 6.66 (m, 10H), 6.56 (d, $J$ = 8.0 Hz, 4H). **$^{13}$C NMR** (126 MHz, $CDCl_3$) δ 154.3, 151.8, 145.6, 144.8, 143.2, 140.4, 129.5, 128.7, 127.7, 124.3, 124.0, 123.0, 122.7, 122.7, 121.2, 113.2, 113.1.

### 3.9.3 Synthesis of starting material

List of starting materials

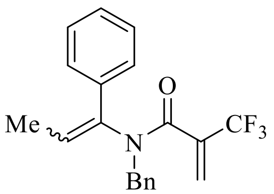

**1a**

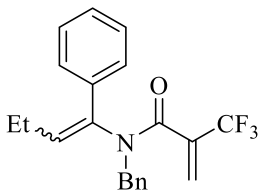

**1b**

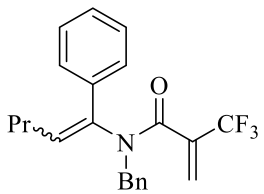

**1c**

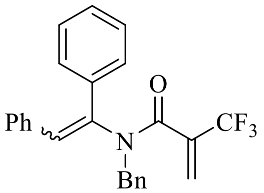

**1d**

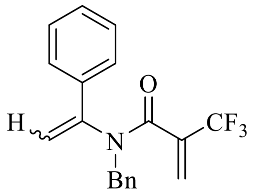

**1e**

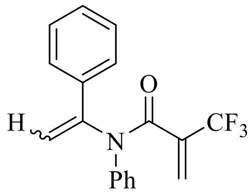

**1f**

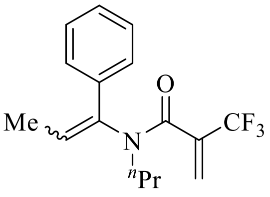
**1g**

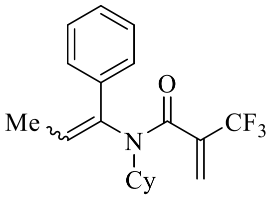
**1h**

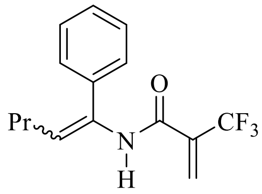
**1i**

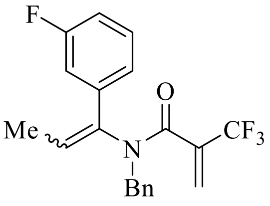
**1j**

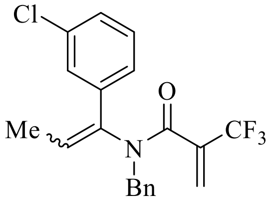
**1k**

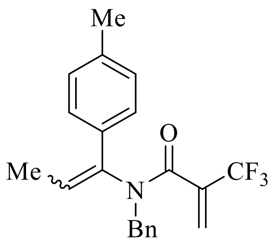
**1l**

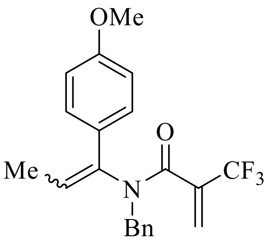
**1m**

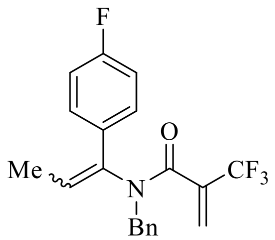
**1n**

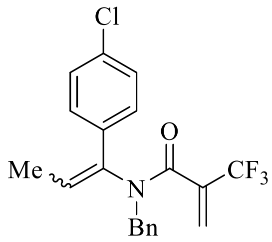
**1o**

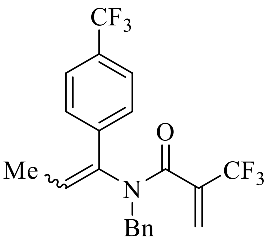
**1p**

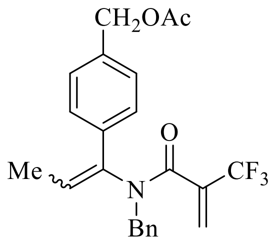
**1q**

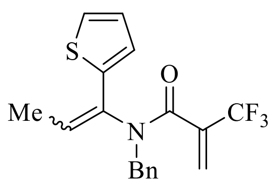
**1r**

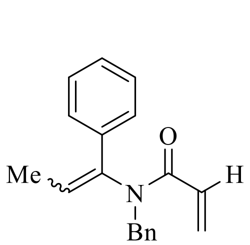
**1s**

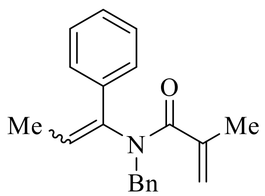
**1t**

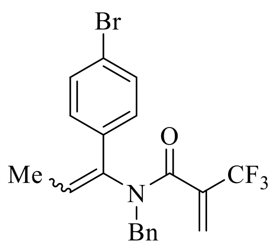
**1u**

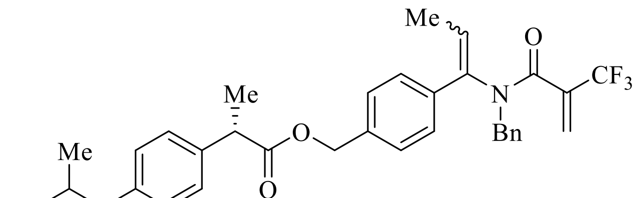
**1v**

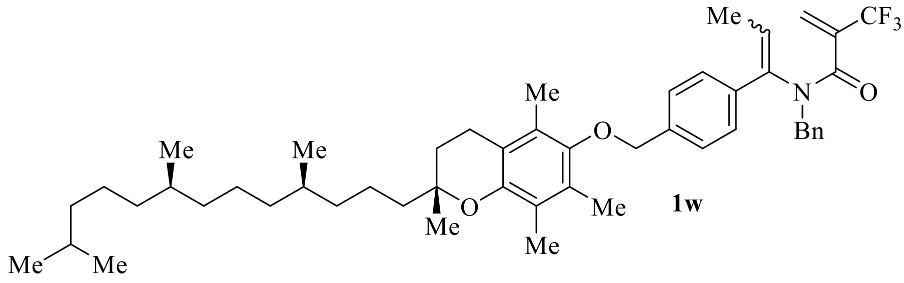

**1w**

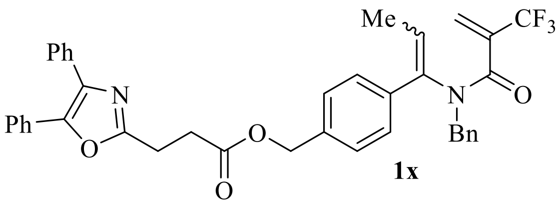

**1x**

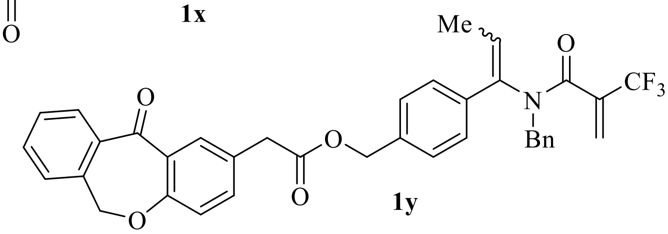

**1y**

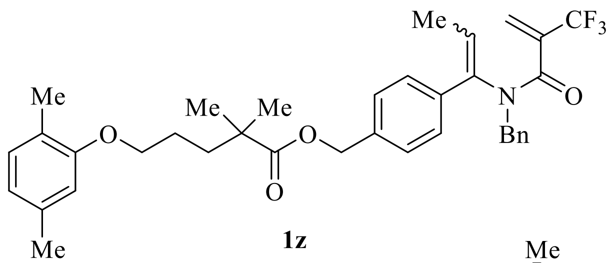

**1z**

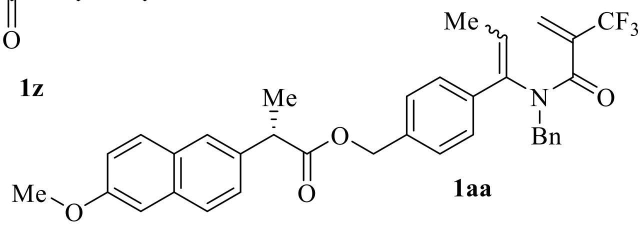

**1aa**

Different imines were synthesized according to the literature with slight modification in the procedure.[39] A mixture of primary amine (1 equiv.), ketone (1 equiv.), 10 mol% TsOH·$H_2O$ and 4Å molecular sieves (powder and heat gun dried with vacuum, 1gm/mmol) in toluene (1 mL/mmol) was taken in an oven-dried pressure tube and stirred at 120 °C for 24 h in an oil bath. After the reaction was completed, the mixture was cooled to room temperature and filtered through filter paper, then washed with toluene. The evaporation of the filtrate provides crude imine (confirmed with $^1$H-NMR). The residue of the crude imine was re-dissolved in DCM (5 mL/mmol), cooled on an ice bath, and then $Et_3N$ (2.0 equiv.) was added. Freshly prepared 2-(trifluoromethyl)acryloyl chloride was added dropwise at 0 °C for 10 minutes. Stir the reaction mixture overnight at room temperature. Quench the reaction mixture with a saturated solution of $NaHCO_3$ and then separate the organic layer using DCM. Dry the organic layer over $Na_2SO_4$, filter and the desired product is purified by column chromatography using EtOAc and hexane as eluent.

***N*-benzyl-*N*-(1-phenylprop-1-en-1-yl)-2-(trifluoromethyl)acrylamide (1a):** 5.0 mmol scale, (700 mg, 40%, over two steps). White solid. **M.P.**: 60-62 °C. **$^1$H NMR** (500 MHz, $CDCl_3$) δ 7.43 – 7.39 (m, 2H), 7.38 – 7.33 (m, 1H), 7.31 – 7.24 (m, 5H), 7.22 – 7.18 (m, 2H), 5.91 (s, 1H), 5.80 (s, 1H), 5.48 – 5.37 (m, 1H), 4.66 (s, 2H), 1.74 (d, *J* = 7.4 Hz, 3H). **$^{13}$C NMR** (126 MHz, $CDCl_3$) δ 164.6, 138.8, 136.8, 135.7 (q, *J* = 31.6 Hz), 134.5, 129.0, 128.9, 128.8, 128.7, 128.5, 127.6, 126.9, 122.5 (q, *J* = 5.2 Hz), 121.8 (q, *J* = 273.6 Hz), 50.3, 14.7. **$^{19}$F NMR** (471 MHz, $CDCl_3$) δ -63.81. **IR** (neat): 3066, 2938, 1659, 1628, 1396, 1165, 1119 cm$^{-1}$. **HRMS** (ESI+ve) m/z: $[M+Na]^+$ calcd for $C_{20}H_{18}F_3NONa$; 368.1233, found 368.1236.

***N*-benzyl-*N*-(1-phenylbut-1-en-1-yl)-2-(trifluoromethyl)acrylamide (1b):** 5.0 mmol scale, (468 mg, 26%, over two steps). White solid. **M.P.**: 67-69 °C. **$^1$H NMR** (500 MHz, $CDCl_3$) δ 7.45 – 7.34 (m, 3H), 7.31 – 7.23 (m, 5H), 7.21 – 7.17 (m, 2H), 5.91 (s, 1H), 5.82 (s, 1H), 5.31 – 5.24 (m, 1H), 4.65 (s, 2H), 2.21 – 2.12 (m, 2H), 0.87 (t, *J* = 7.5 Hz, 3H). **$^{13}$C NMR** (126 MHz, $CDCl_3$) δ 164.6, 137.5, 136.7, 135.5 (q, *J* = 31.5 Hz), 134.7, 134.3, 129.1, 128.9, 128.8, 128.7, 128.5, 127.6, 122.5 (q, *J* = 5.4 Hz), 121.8 (q, *J* = 275.5 Hz), 50.1, 22.2, 13.5. **$^{19}$F NMR** (471 MHz, $CDCl_3$) δ -63.88. **IR** (neat): 3061, 2956, 2872, 1657, 1626, 1369, 1338, 1163 cm$^{-1}$. **HRMS** (ESI+ve) m/z: $[M+Na]^+$ calcd for $C_{21}H_{20}F_3NONa$; 382.1389, found 382.1406.

***N*-benzyl-*N*-(1-phenylpent-1-en-1-yl)-2-(trifluoromethyl)acrylamide (1c):** 5.0 mmol scale, (561 mg, 30%, over two steps). White solid. **M.P.**: 53-55 °C. **$^1$H NMR** (500 MHz, $CDCl_3$) δ 7.44 – 7.33 (m, 3H), 7.32 – 7.23 (m, 5H), 7.22 – 7.17 (m, 2H), 5.91 (s, 1H), 5.82 (s, 1H), 5.36 – 5.24 (m, 1H), 4.65 (s, 2H), 2.12 (q, *J* = 7.6 Hz, 2H), 1.32 – 1.22 (m, 2H), 0.80 (t, *J* = 7.4 Hz, 3H). **$^{13}$C NMR** (126 MHz,

$CDCl_3$) δ 164.6, 137.8, 136.7, 135.5 (q, $J$ = 31.4 Hz), 134.8, 132.8, 129.1, 128.9, 128.8, 128.7, 128.5, 127.6, 122.6 (q, $J$ = 5.4 Hz), 121.8 (q, $J$ = 274.8 Hz), 50.2, 30.9, 22.5, 13.8. **$^{19}$F NMR** (471 MHz, $CDCl_3$) δ -63.93. **IR** (neat): 3036, 2960, 2878, 1662, 1627, 1398, 1183, 1134 $cm^{-1}$. **HRMS** (ESI+ve) m/z: $[M+Na]^+$ calcd for $C_{22}H_{22}F_3NONa$; 396.1545, found 396.1543.

***N*-benzyl-*N*-(1,2-diphenylvinyl)-2-(trifluoromethyl)acrylamide (1d):** 5.0 mmol scale, (815 mg, 37%, over two steps). Pale-yellow solid. **M.P.**: 104-106 °C. **$^1$H NMR** (500 MHz, $CDCl_3$) δ 7.37 – 7.23 (m, 8H), 7.23 – 7.19 (m, 2H), 7.16 – 7.09 (m, 3H), 6.94 – 6.89 (m, 2H), 6.17 (s, 1H), 6.00 (s, 1H), 5.99 (s, 1H), 4.69 (s, 2H). **$^{13}$C NMR** (126 MHz, $CDCl_3$) δ 164.6, 138.7, 136.4, 135.8 (q, $J$ = 31.7 Hz), 135.3, 134.2, 130.2, 129.9, 129.3, 129.2, 129.1, 128.9, 128.5, 128.4, 127.8, 127.7, 123.2 (q, $J$ = 5.3 Hz), 121.7 (q, $J$ = 275.1 Hz), 50.0. **$^{19}$F NMR** (471 MHz, $CDCl_3$) δ -63.93. **IR** (neat): 3031, 2925, 2855, 1685, 1662, 1407, 1250, 1145 $cm^{-1}$. **HRMS** (ESI+ve) m/z: $[M+Na]^+$ calcd for $C_{25}H_{20}F_3NONa$; 430.1389, found 430.1388.

***N*-benzyl-*N*-(1-phenylvinyl)-2-(trifluoromethyl)acrylamide (1e):** 5.0 mmol scale, (564 mg, 34%, over two steps). White solid. **M.P.**: 40-42 °C. **$^1$H NMR** (500 MHz, $CDCl_3$) δ 7.44 – 7.35 (m, 5H), 7.32 – 7.22 (m, 5H), 5.83 (s, 1H), 5.76 (s, 1H), 5.53 (s, 1H), 4.85 (s, 1H), 4.78 (s, 2H). **$^{13}$C NMR** (126 MHz, $CDCl_3$) δ 164.5, 145.8, 136.5, 135.3, 134.7 (q, $J$ = 31.7 Hz), 129.4, 129.2, 129.1, 128.5, 127.8, 126.1, 122.8 (q, $J$ = 5.3 Hz), 121.7 (q, $J$ = 273.9 Hz ), 114.7, 50.5. **$^{19}$F NMR** (471 MHz, $CDCl_3$) δ -64.22. **IR** (neat): 3071, 3036, 2932, 1661, 1626, 1393, 1277, 1166 $cm^{-1}$. **HRMS** (ESI+ve) m/z: $[M+Na]^+$ calcd for $C_{19}H_{16}F_3NONa$; 354.1076, found 354.1071.

***N*-phenyl-*N*-(1-phenylvinyl)-2-(trifluoromethyl)acrylamide (1f):** 5.0 mmol scale, (760 mg, 42%, over two steps). White solid. **M.P.**: 66-68 °C. $^1$H NMR (500 MHz, $CDCl_3$) δ 7.54 – 7.48 (m, 2H), 7.38 – 7.28 (m, 7H), 7.25 – 7.18 (m, 1H), 5.98 (s, 1H), 5.87 (s, 1H), 5.75 (s, 1H), 5.25 (s, 1H). **$^{13}$C NMR** (126 MHz, $CDCl_3$) δ 164.3, 147.8, 146.5, 136.0, 135.4

(d, $J$ = 31.3 Hz), 129.3, 129.1, 128.9, 128.6, 127.1, 126.1, 121.6 (d, $J$ = 274.1 Hz), 114.4. **$^{19}$F NMR** (471 MHz, $CDCl_3$) δ -64.18. **IR** (neat): 3115, 3096, 3027, 1664, 1632, 1593, 1367, 1294, 1157 $cm^{-1}$. **HRMS** (ESI+ve) m/z: $[M+Na]^+$ calcd for $C_{18}H_{14}F_3NONa$; 340.0920, found 340.0920.

***N*-(1-phenylprop-1-en-1-yl)-*N*-propyl-2-(trifluoromethyl)acrylamide (1g):** 5.0 mmol scale, (506 mg, 34%, over two steps). Yellow oil . **$^1$H NMR** (500 MHz, $CDCl_3$) δ 7.44 – 7.37 (m, 2H), 7.37 – 7.30 (m, 3H), 5.86 (s, 1H), 5.73 (s, 1H), 5.70 – 5.61 (m, 1H), 3.38 (s, 2H), 1.85 (d, $J$ = 7.4 Hz, 3H), 1.60 – 1.52 (m, 2H), 0.85 (t, $J$ = 7.4 Hz, 3H). **$^{13}$C NMR** (126 MHz, $CDCl_3$) δ 164.4, 139.3, 136.0 (q, $J$ = 31.6 Hz), 134.5, 128.9, 128.7, 128.6, 125.9, 121.9 (q, $J$ = 5.4 Hz), 121.80 (q, $J$ = 273.9 Hz), 48.2, 20.6, 14.7, 11.2. **$^{19}$F NMR** (471 MHz, $CDCl_3$) δ -63.83. **IR** (neat): 2967, 2876, 1659, 1630, 1398, 1333, 1169 $cm^{-1}$. **HRMS** (ESI+ve) m/z: $[M+Na]^+$ calcd for $C_{16}H_{18}F_3NONa$; 320.1233, found 320.1233.

***N*-cyclohexyl-*N*-(1-phenylprop-1-en-1-yl)-2-(trifluoromethyl)acrylamide (1h):** 5.0 mmol scale, (254 mg, 15%, over two steps). White solid. **M.P.**: 75-77 °C. **$^1$H NMR** (500 MHz, $CDCl_3$) δ 7.41 – 7.29 (m, 5H), 5.84 – 5.64 (m, 3H), 4.04 (s, 1H), 1.89 (d, $J$ = 7.3 Hz, 3H), 1.82 – 1.64 (m, 4H), 1.57 – 1.51 (m, 1H), 1.49 – 1.32 (m, 2H), 1.29 – 1.17 (m, 2H), 1.03 – 0.91 (m, 1H). **$^{13}$C NMR** (126 MHz, $CDCl_3$) δ 164.5, 138.2, 136.7 (q, $J$ = 31.5 Hz), 136.3 129.1, 128.3, 127.9, 125.9, 121.9 (q, $J$ = 273.3 Hz), 121.0 (q, $J$ = 5.4 Hz), 58.0, 30.7, 26.1, 25.4, 15.0. **$^{19}$F NMR** (471 MHz, $CDCl_3$) δ -63.42. **IR** (neat): 2940, 2859, 1655, 1628, 1398, 1369, 1290, 1165 $cm^{-1}$. **HRMS** (ESI+ve) m/z: $[M+Na]^+$ calcd for $C_{19}H_{22}F_3NONa$; 360.1546, found 360.1569.

***N*-benzyl-*N*-(1-(3-fluorophenyl)prop-1-en-1-yl)-2-(trifluoromethyl)acrylamide (1j):** 5.0 mmol scale, (330 mg, 18%, over two steps). White solid. **M.P.**: 56-58 °C.**$^1$H NMR** (500 MHz, $CDCl_3$) δ 7.42 – 7.34 (m, 1H), 7.34 – 7.26 (m, 3H), 7.22 – 7.18 (m, 2H), 7.09 – 7.00 (m, 3H), 6.96 – 6.90 (m, 1H), 5.93 (s, 1H), 5.78 (s, 1H), 5.54 – 5.42 (m, 1H), 4.67 (s, 2H), 1.75 (d, $J$ = 7.4 Hz, 3H). **$^{13}$C NMR** (126 MHz,

$CDCl_3$) δ 164.6, 162.98 (d, *J* = 247.0 Hz), 137.9, 137.0 (d, *J* = 7.4 Hz), 136.6, 135.8 (q, *J* = 31.7 Hz), 130.3 (d, *J* = 8.4 Hz), 129.0, 128.6, 128.1, 127.8, 124.7 (d, *J* = 3.0 Hz), 122.9 (q, *J* = 5.3 Hz), 121.7 (q, *J* = 274.3 Hz), 115.9 (d, *J* = 22.3 Hz), 115.7 (d, *J* = 21.1 Hz), 50.6, 14.7. **$^{19}$F NMR** (471 MHz, $CDCl_3$) δ -63.80, -111.99. **IR** (neat): 3034, 2982, 2856, 1657, 1630, 1395, 1270, 1165 cm$^{-1}$. **HRMS** (ESI+ve) m/z: $[M+Na]^+$ calcd for $C_{20}H_{17}F_4NONa$; 386.1138, found 386.1142.

***N*-benzyl-*N*-(1-(3-chlorophenyl)prop-1-en-1-yl)-2-(trifluoromethyl)acrylamide (1k):** 5.0 mmol scale, (685 mg, 36%, over two steps). White solid. **M.P.**: 88-90 °C. **$^1$H NMR** (500 MHz, $CDCl_3$) δ 7.29 – 7.17 (m, 5H), 7.15 – 7.09 (m, 3H), 7.07 – 7.01 (m, 1H), 5.86 (s, 1H), 5.69 (s, 1H), 5.43 (s, 0H), 4.59 (s, 2H), 1.66 (d, *J* = 7.4 Hz, 3H). **$^{13}$C NMR** (126 MHz, $CDCl_3$) δ 164.6, 138.0, 137.9, 136.5, 135.8 (q, *J* = 31.9 Hz), 134.5, 133.0, 130.3, 129.0, 128.9, 128.6, 127.7, 127.5, 126.9, 122.9 (q, *J* = 5.4 Hz), 121.7 (q, *J* = 274.7 Hz), 50.4, 14.7. **$^{19}$F NMR** (471 MHz, $CDCl_3$) δ -63.79. **IR** (neat): 3036, 2960, 2878, 1662, 1627, 1398, 1336, 1183 cm$^{-1}$. **HRMS** (ESI+ve) m/z: $[M+Na]^+$ calcd for $C_{20}H_{17}ClF_3NONa$; 402.0843, found 402.0835.

***N*-benzyl-*N*-(1-(*p*-tolyl)prop-1-en-1-yl)-2-(trifluoromethyl)acrylamide (1l):** 5.0 mmol scale, (760 mg, 42%, over two steps). White solid. **M.P.**: 62-64 °C. **$^1$H NMR** (500 MHz, $CDCl_3$) δ 7.24 – 7.16 (m, 4H), 7.15 – 7.07 (m, 5H), 5.82 (s, 1H), 5.72 (s, 1H), 5.32 – 5.24 (m, 1H), 4.56 (s, 2H), 2.31 (s, 3H), 1.65 (d, *J* = 7.4 Hz, 3H). **$^{13}$C NMR** (126 MHz, $CDCl_3$) δ 164.6, 138.7, 138.7, 136.8, 135.7 (q, *J* = 31.5 Hz), 131.5, 129.5, 129.0, 128.9, 128.5, 127.5, 126.4, 122.3 (q, *J* = 5.2 Hz), 121.8 (q, *J* = 274.7 Hz), 50.0, 21.3, 14.7. **$^{19}$F NMR** (471 MHz, $CDCl_3$) δ -63.79. **IR** (neat): 3031, 2925, 1659, 1627, 1400, 1274, 1158 cm$^{-1}$. **HRMS** (ESI+ve) m/z: $[M+Na]^+$ calcd for $C_{21}H_{20}F_3NONa$; 382.1389, found 382.1381.

***N*-benzyl-*N*-(1-(4-methoxyphenyl)prop-1-en-1-yl)-2-(trifluoromethyl)acrylamide (1m):** 5.0 mmol scale, (720 mg, 38%, over two steps). Yellowish oil. **$^1$H NMR** (500 MHz, $CDCl_3$) δ 7.32 – 7.22 (m, 3H), 7.21 – 7.16 (m, 4H), 6.95 – 6.90 (m, 2H), 5.90 (s, 1H), 5.79 (s, 1H), 5.37 – 5.27 (m, 1H), 4.64 (s, 2H), 3.85 (s, 3H), 1.71 (d, *J* =

7.4 Hz, 3H). **$^{13}$C NMR** (126 MHz, $CDCl_3$) δ 164.6, 159.7, 138.4, 136.8, 135.8 (q, $J$ = 31.6 Hz), 130.3, 129.0, 128.5, 127.6, 126.7, 125.5, 122.3 (q, $J$ = 5.3 Hz) 121.3 (q, $J$ = 274.3 Hz), 114.1, 55.4, 50.1, 14.6. **$^{19}$F NMR** (471 MHz, $CDCl_3$) δ -63.77. **IR** (neat): 3034, 2937, 1656, 1625, 1510, 1399, 1251, 1147 cm$^{-1}$. **HRMS** (ESI+ve) m/z: $[M+Na]^+$ calcd for $C_{21}H_{20}F_3NO_2Na$; 398.1338, found 398.1329.

***N*-benzyl-*N*-(1-(4-fluorophenyl)prop-1-en-1-yl)-2-(trifluoromethyl)acrylamide (1n):** 5.0 mmol scale, (804 mg, 44%, over two steps). White solid. **M.P.**: 60-62 °C. **$^1$H NMR** (500 MHz, $CDCl_3$) δ 7.31 – 7.24 (m, 3H), 7.23 – 7.15 (m, 4H), 7.11 – 7.05 (m, 2H), 5.93 (s, 1H), 5.77 (s, 1H), 5.44 (s, 1H), 4.66 (s, 2H), 1.71 (d, $J$ = 7.5 Hz, 3H). **$^{13}$C NMR** (126 MHz, $CDCl_3$) δ 164.6, 162.6 (d, $J$ = 249.3 Hz), 138.0, 136.6, 135.9 (q, $J$ = 31.7 Hz), 130.6 (2C), 128.9, 128.6, 127.7, 126.7, 122.8 (q, $J$ = 5.5 Hz), 121.7 (q, $J$ = 271.2 Hz), 115.8 (d, $J$ = 21.6 Hz), 50.5, 14.6. **$^{19}$F NMR** (471 MHz, $CDCl_3$) δ -63.78, -112.01. **IR** (neat): 3034, 2937, 1656, 1625, 1510, 1399, 1251, 1147 cm$^{-1}$. **HRMS** (ESI+ve) m/z: $[M+Na]^+$ calcd for $C_{20}H_{17}F_4NONa$; 386.1138, found 386.1122.

***N*-benzyl-*N*-(1-(4-chlorophenyl)prop-1-en-1-yl)-2-(trifluoromethyl)acrylamide (1o):** 5.0 mmol scale, (838 mg, 44%, over two steps). Yellowish oil. **$^1$H NMR** (500 MHz, $CDCl_3$) δ 7.29 (d, $J$ = 8.2 Hz, 2H), 7.24 – 7.17 (m, 3H), 7.13 – 7.06 (m, 4H), 5.85 (s, 1H), 5.69 (s, 1H), 5.39 (s, 1H), 4.58 (s, 2H), 1.64 (d, $J$ = 7.4 Hz, 3H). **$^{13}$C NMR** (126 MHz, $CDCl_3$) δ 164.6, 137.9, 136.5, 135.8 (q, $J$ = 32.1 Hz), 134.5, 133.0, 130.3, 129.0, 128.9, 128.6, 127.7, 127.5, 122.9 (q, $J$ = 5.3 Hz), 121.7 (q, $J$ = 274.2 Hz), 50.4, 14.7. **$^{19}$F NMR** (471 MHz, $CDCl_3$) δ -63.76. IR (neat): 3033, 2981, 1660, 1630, 1492, 1394, 1170, 1137 cm$^{-1}$. **HRMS** (ESI+ve) m/z: $[M+Na]^+$ calcd for $C_{20}H_{17}ClF_3NONa$; 402.0843, found 402.0842.

***N*-benzyl-2-(trifluoromethyl)-*N*-(1-(4-(trifluoromethyl)phenyl)prop-1-en-1yl)acrylamide (1p):** 5.0 mmol scale, (517 mg, 25%, over two steps). Yellowish oil. **$^1$H NMR** (500 MHz, $CDCl_3$) δ 7.65 – 7.58 (m, 2H), 7.34 – 7.21 (m, 6H), 7.19 – 7.12 (m, 2H), 5.92 (s, 1H), 5.75 (s, 1H), 5.55 (s, 1H), 4.65 (s, 2H), 1.73 (d, $J$

= 7.5 Hz, 3H). **$^{13}$C NMR** (126 MHz, $CDCl_3$) δ 164.6, 138.3, 137.8, 136.4, 135.8 (q, *J* = 31.5 Hz), 130.6 (q, *J* = 32.6 Hz), 129.3, 129.0, 128.9, 128.6, 127.8, 126.1 (274.17 Hz), 125.7 (q, *J* = 3.7 Hz), 123.2 (q, *J* = 5.2 Hz), 121.6 (q, *J* = 274.3 Hz), 50.7, 14.7. **$^{19}$F NMR** (471 MHz, $CDCl_3$) δ -62.77, -63.80. **IR** (neat): 3039, 2923, 1662, 1631, 1399, 1322, 1166, 1147 cm$^{-1}$. **HRMS** (ESI+ve) m/z: $[M+Na]^+$ calcd for $C_{21}H_{17}F_6NONa$; 436.1107, found 436.1105.

**4-(1-(*N*-benzyl-2-(trifluoromethyl)acrylamido)prop-1-en-1-yl)benzyl acetate (1q):** 5.0 mmol scale, (419 mg, 20%, over two steps). Clear oil. **$^1$H NMR** (500 MHz, $CDCl_3$) δ 7.42 – 7.37 (m, 2H), 7.30 – 7.23 (m, 5H), 7.21 – 7.16 (m, 2H), 5.91 (s, 1H), 5.79 (s, 1H), 5.49 – 5.38 (m, 1H), 5.14 (s, 2H), 4.64 (s, 2H), 2.14 (s, 3H), 1.73 (d, *J* = 7.4 Hz, 3H). **$^{13}$C NMR** (126 MHz, $CDCl_3$) δ 170.9, 164.6, 136.6, 134.4, 129.2, 129.0, 128.5 (2C), 128.2, 127.6, 127.5, 122.6 (q, *J* = 5.3 Hz), 121.8 (q, *J* = 274.8 Hz), 65.8, 50.2, 46.5, 29.8, 21.1, 14.7. **$^{19}$F NMR** (471 MHz, $CDCl_3$) δ -63.78. **IR** (neat): 3033, 2940, 2861, 1738, 1660, 1630, 1396, 1225, 1169 cm$^{-1}$. **HRMS** (ESI+ve) m/z: $[M+Na]^+$ calcd for $C_{23}H_{22}F_3NO_3Na$; 440.1444, found 440.1436.

***N*-benzyl-*N*-(1-(thiophen-2-yl)prop-1-en-1-yl)-2-(trifluoromethyl)acrylamide (1r):** 5.0 mmol scale, (510 mg, 29%, over two steps). White solid. **M.P.**: 53-55 °C. **$^1$H NMR** (500 MHz, $CDCl_3$) δ 7.43 – 7.38 (m, 1H), 7.32 – 7.21 (m, 5H), 7.12 – 7.06 (m, 2H), 5.82 (s, 1H), 5.81 (s, 1H), 5.33 – 5.25 (m, 1H), 4.74 (s, 2H), 1.82 (d, *J* = 7.5 Hz, 3H). **$^{13}$C NMR** (126 MHz, $CDCl_3$) δ 164.5, 138.3, 136.6, 135.3 (q, *J* = 31.7 Hz), 133.1, 129.3, 128.5, 128.3, 127.8, 127.7, 127.3, 126.8, 121.8 (q, *J* = 5.3 Hz), 121.8 (q, *J* = 275.1 Hz), 50.3, 14.6. **$^{19}$F NMR** (471 MHz, $CDCl_3$) δ -63.85. **IR** (neat): 3102, 3055, 2929, 1657, 1629, 1399, 1339, 1162 cm$^{-1}$. **HRMS** (ESI+ve) m/z: $[M+Na]^+$ calcd for $C_{18}H_{16}F_3NOSNa$; 374.0797, found 374.0805.

***N*-benzyl-*N*-(1-phenylprop-1-en-1-yl)acrylamide (1s):** 5.0 mmol scale, (652 mg, 47%, over two steps). Pale yellow oil. **$^1$H NMR** (500 MHz, $CDCl_3$) δ 7.42 – 7.32 (m, 3H), 7.29 – 7.18 (m, 7H), 6.73 – 6.64 (m, 1H), 6.53 – 6.45 (m, 1H), 5.67 (dd, *J* = 10.1, 2.1 Hz, 1H), 5.37 (q, *J* = 7.3 Hz, 1H), 4.49 (s, 2H), 1.76 (d, *J* = 7.3 Hz, 3H). **$^{13}$C NMR** (126

MHz, $CDCl_3$) δ 166.4, 138.0, 137.5, 134.8, 129.1, 128.9, 128.7 (2C), 128.3, 128.0, 127.8, 127.2, 49.1, 14.5. **IR** (neat): 3029, 2929, 2858, 1650, 1406, 1372, 1249 $cm^{-1}$. **HRMS** (ESI+ve) m/z: $[M+H]^+$ calcd for $C_{19}H_{20}NO$; 278.1539, found 278.1548.

***N*-benzyl-*N*-(1-(4-bromophenyl)prop-1-en-1-yl)-2-(trifluoromethyl)acrylamide (1u):** 5.0 mmol scale, (1190 mg, 56%, over two steps). Clear oil. **$^1$H NMR** (500 MHz, $CDCl_3$) δ 7.45 (d, *J* = 8.1 Hz, 2H), 7.24 – 7.17 (m, 3H), 7.13 – 7.08 (m, 2H), 7.02 (d, *J* = 8.1 Hz, 2H), 5.85 (s, 1H), 5.69 (s, 1H), 5.40 (s, 1H), 4.58 (s, 2H), 1.64 (d, *J* = 7.4 Hz, 3H). **$^{13}$C NMR** (126 MHz, $CDCl_3$) δ 164.6, 137.9, 136.5, 135.8 (q, *J* = 31.6 Hz), 133.5, 132.0, 130.5, 128.9, 128.6, 127.8, 127.7, 122.7, 122.9 (q, *J* = 5.3 Hz), 121.7 (q, *J* = 274.2 Hz), 50.4, 14.7. **$^{19}$F NMR** (471 MHz, $CDCl_3$) δ -63.75. **IR** (neat): 3032, 2981, 1660, 1630, 1487, 1393, 1169, 1120 $cm^{-1}$. **HRMS** (ESI+ve) m/z: $[M+Na]^+$ calcd for $C_{20}H_{17}BrF_3NONa$; 446.0338, found 446.0333.

***N*-benzyl-*N*-(1-(4-((((*R*)-2,5,7,8-tetramethyl-2-((4*R*,8*R*)-4,8,12-trimethyltridecyl)chroman-6-yl)oxy)methyl)phenyl)prop-1-en-1-yl)-2-(trifluoromethyl)acrylamide (1v):** 2.5 mmol scale, (573 mg, 27%, over two steps (BSMR)). Clear oil. **$^1$H NMR** (500 MHz, $CDCl_3$) δ 7.58 – 7.52 (m, 2H), 7.34 – 7.26 (m, 5H), 7.23 – 7.18 (m, 2H), 5.92 (s, 1H), 5.82 (s, 1H), 5.47 – 5.35 (m, 1H), 4.73 (s, 2H), 4.66 (s, 2H), 2.65 – 2.56 (m, 2H), 2.24 (s, 3H), 2.18 (s, 3H), 2.12 (s, 3H), 1.89 – 1.72 (m, 5H), 1.55 – 1.02 (m, 24H), 0.90 – 0.82 (m, 12H). **$^{13}$C NMR** (126 MHz, $CDCl_3$) δ 164.7, 148.2, 148.1, 138.7, 138.5, 136.7, 135.8 (q, *J* = 30.8 Hz), 133.9, 129.1, 129.0, 128.5, 128.0, 127.9, 127.6, 127.3, 126.0, 123.2, 122.4 (q, *J* = 5.1 Hz), 121.9 (q, *J* = 274.6 Hz), 117.8, 75.0, 74.2, 40.2, 39.5, 37.6 (2C), 37.5, 37.4, 32.9, 32.8, 31.4, 28.1, 24.9, 24.6, 24.0, 22.8, 22.7, 21.1, 20.8, 19.9, 19.8, 14.7, 13.0, 12.1, 11.9. **$^{19}$F NMR** (471 MHz, $CDCl_3$) δ -63.76. **IR** (neat): 2924, 2966, 1663, 1662, 1454, 1377, 1170 $cm^{-1}$. **HRMS** (ESI+ve) m/z: $[M+Na]^+$ calcd for $C_{50}H_{68}F_3NO_3Na$; 810.5043, found 810.5040.

**4-(1-(*N*-benzyl-2-(trifluoromethyl)acrylamido)prop-1-en-1-yl)benzyl (*S*)-2-(4-isobutylphenyl)propanoate (1w):** 2.8 mmol scale, (585 mg, 37%, over two steps (BSMR)). Clear oil. $^1$H NMR (500 MHz, $CDCl_3$) δ 7.33 – 7.18 (m, 11H), 7.16 – 7.11 (m, 2H), 5.93 (s, 1H), 5.79 (s, 1H), 5.50 – 5.38 (m, 1H), 5.17 (s, 2H), 4.66 (s, 2H), 3.81 (q, *J* = 7.2 Hz, 1H), 2.48 (d, *J* = 6.9 Hz, 2H), 1.88 (hept, *J* = 6.8 Hz, 1H), 1.75 (d, *J* = 7.3 Hz, 3H), 1.56 (d, *J* = 7.2 Hz, 3H), 0.93 (d, *J* = 6.6 Hz, 6H). **$^{13}$C NMR** (126 MHz, $CDCl_3$) δ 174.5, 164.6, 140.7, 138.3, 137.6, 136.7, 136.6, 135.7 (q, *J* = 31.7 Hz), 134.1, 129.4, 129.0, 128.9, 128.5, 127.9, 127.6, 127.3, 122.5 (q, *J* = 5.4 Hz), 121.7 (q, *J* = 274.1 Hz), 65.7, 50.2, 45.2, 45.1, 30.3, 22.4, 18.5, 14.7. **$^{19}$F NMR** (471 MHz, $CDCl_3$) δ -63.77. **IR** (neat): 2954, 2925, 1736, 1661, 1631, 1409, 1333, 1140 cm$^{-1}$. **HRMS** (ESI+ve) m/z: $[M+Na]^+$ calcd for $C_{34}H_{36}F_3NO_3Na$; 586.2539, found 586.2555.

**4-(1-(*N*-benzyl-2-(trifluoromethyl)acrylamido)prop-1-en-1-yl)benzyl 3-(4,5-diphenyloxazol-2-yl)propanoate (1x):** 2.5 mmol scale, (749 mg, 46%, over two steps (BSMR)). Glue Type. **$^1$H NMR** (500 MHz, $CDCl_3$) δ 7.68 – 7.63 (m, 2H), 7.62 – 7.56 (m, 2H), 7.41 – 7.26 (m, 11H), 7.20 (m, 4H), 5.91 (s, 1H), 5.76 (s, 1H), 5.43 (m, 1H), 5.24 (s, 2H), 4.63 (s, 2H), 3.26 (t, *J* = 7.3 Hz, 2H), 3.04 (t, *J* = 7.3 Hz, 2H), 1.72 (d, *J* = 7.3 Hz, 3H). **$^{13}$C NMR** (126 MHz, $CDCl_3$) δ 171.9, 164.5, 161.7, 145.5, 138.2, 136.6, 136.4, 135.6 (q, *J* = 31.5 Hz), 135.1, 134.2, 132.4, 129.1, 128.9 (3C), 128.7, 128.6 (2C), 128.5, 128.2 (2C), 127.9, 127.6, 127.4, 126.5, 122.5 (q, *J* = 5.5 Hz), 121.7 (q, *J* = 274.9 Hz), 65.9, 50.1, 31.1, 23.5, 14.6. **$^{19}$F NMR** (471 MHz, $CDCl_3$) δ -63.78. **IR** (neat): 3039, 2923, 1662, 1631, 1399, 1322, 1166, 1147 cm$^{-1}$. **HRMS** (ESI+ve) m/z: $[M+Na]^+$ calcd for $C_{39}H_{33}F_3N_2O_4Na$; 673.2285, found 673.2285.

**4-(1-(*N*-benzyl-2-(trifluoromethyl)acrylamido)prop-1-en-1-yl)benzyl 2-(11-oxo-6,11-dihydrodibenzo[*b,e*]oxepin-2-yl)acetate (1y):** 1.5 mmol scale, (273 mg, 29%, over two steps (BSMR)). Clear oil. **$^1$H NMR** (500 MHz, $CDCl_3$) δ 8.05 (s, 1H), 7.78 (d, *J* = 7.7 Hz, 1H), 7.46 (t, *J* = 7.5 Hz, 1H), 7.40 – 7.31 (m, 2H), 7.29 – 7.24 (m, 3H), 7.24 – 7.12 (m, 5H), 7.11 – 7.06 (m, 2H), 6.94 (d, *J* = 8.4 Hz, 1H), 5.80 (s, 1H), 5.68 (s, 1H), 5.37 – 5.29 (m, 1H), 5.08 (s, 2H), 5.07 (s, 2H), 4.54 (s, 2H), 3.62 (s, 2H), 1.63 (d, *J* = 7.4 Hz, 3H). **$^{13}$C NMR** (126 MHz,

$CDCl_3$) δ 190.9, 171.2, 164.6, 160.6, 140.4, 138.3, 136.6, 136.4, 136.3, 135.8, 135.6, 135.5, 134.4, 132.9, 132.6, 129.5, 129.3, 129.1, 128.9, 128.5, 128.4, 127.9, 127.6 (2C), 127.4, 125.2, 122.6 (q, *J* = 5.3 Hz), 121.7 (q, *J* = 274.49 Hz), 121.2, 73.7, 66.2, 40.2, 14.7. **$^{19}$F NMR** (471 MHz, $CDCl_3$) δ -63.75. **IR** (neat): 2953, 2928, 1716, 1649, 1600, 1375, 1284, 1138 $cm^{-1}$. **HRMS** (ESI+ve) m/z: $[M+Na]^+$ calcd for $C_{37}H_{30}F_3NO_5Na$; 648.1968, found 648.1959.

**4-(1-(*N*-benzyl-2-(trifluoromethyl)acrylamido)prop-1-en-1-yl)benzyl 5-(2,5-dimethylphenoxy)-2,2-dimethylpentanoate (1z):** 1.6 mmol scale, (360 mg, 37%, over two steps (BSMR)). Clear oil. **$^1$H NMR** (500 MHz, $CDCl_3$) δ 7.37 (d, *J* = 8.1 Hz, 2H), 7.29 – 7.26 (m, 2H), 7.24 (d, *J* = 8.2 Hz, 2H), 7.21 – 7.16 (m, 2H), 6.99 (d, *J* = 7.4 Hz, 1H), 6.66 (d, *J* = 7.4 Hz, 1H), 6.59 (s, 1H), 5.89 (s, 1H), 5.79 – 5.74 (m, 1H), 5.49 – 5.38 (m, 1H), 5.14 (s, 2H), 4.64 (s, 2H), 3.94 – 3.88 (m, 2H), 2.29 (s, 3H), 2.15 (s, 3H), 1.82 – 1.73 (m, 4H), 1.73 (s, 2H), 1.72 (s, 2H), 1.27 (s, 6H). **$^{13}$C NMR** (126 MHz, $CDCl_3$) δ 177.6, 164.6, 157.0, 138.4, 136.9, 136.7, 136.6, 135.7 (q, *J* = 32.0 Hz), 134.2, 130.4, 130.2, 129.1, 129.0, 128.5, 128.0, 127.6, 127.3, 125.8, 123.6, 122.6 (q, *J* = 5.4 Hz), 121.8 (q, *J* = 274.2 Hz), 120.8, 112.0, 67.9, 65.6, 50.3, 42.3, 37.2, 25.3 (2C), 21.5, 15.8, 14.7. **$^{19}$F NMR** (471 MHz, $CDCl_3$) δ -63.79. **IR** (neat): 2965, 2923, 1728, 1661, 1631, 1394, 1263, 1170, 1122 $cm^{-1}$. **HRMS** (ESI+ve) m/z: $[M+Na]^+$ calcd for $C_{36}H_{40}F_3NO_4Na$; 630.2802, found 630.2795.

**4-(1-(*N*-benzyl-2-(trifluoromethyl)acrylamido)prop-1-en-1-yl)benzyl (S)-2-(6-methoxynaphthalen-2-yl)propanoate (1aa):** 1.8 mmol scale, (286 mg, 27%, over two steps (BSMR)). Yellowish oil. **$^1$H NMR** (500 MHz, $CDCl_3$) δ 7.72 – 7.65 (m, 3H), 7.43 – 7.39 (m, 1H), 7.30 – 7.21 (m, 6H), 7.18 – 7.10 (m, 5H), 5.87 (s, 1H), 5.72 (s, 1H), 5.44 – 5.37 (m, 1H), 5.14 (s, 2H), 4.60 (s, 2H), 3.96 – 3.92 (m, 1H), 3.91 (s, 3H), 1.69 (d, *J* = 7.4 Hz, 3H), 1.62 (d, *J* = 7.1 Hz, 3H). **$^{13}$C NMR** (126 MHz, $CDCl_3$) δ 174.5, 164.6, 157.7, 138.2, 136.6, 136.5, 135.4, 135.6 (q, *J* = 31.4 Hz), 134.1, 133.8, 129.3, 129.0, 128.9 (2C), 128.5, 128.1, 127.6, 127.3, 127.2, 126.3, 126.1, 122.6 (q, *J* = 5.3 Hz), 121.7 (q, *J* =

274.3 Hz), 119.1, 105.6, 65.8, 55.3, 45.5, 18.5, 14.6. **$^{19}$F NMR** (471 MHz, $CDCl_3$) δ -63.78. **IR** (neat): 2937, 2844, 1733, 1660, 1394, 1263, 1170 cm$^{-1}$. **HRMS** (ESI+ve) m/z: $[M+Na]^+$ calcd for $C_{35}H_{32}F_3NO_4Na$; 610.2175, found 610.2158.

***N*-(1-phenylpent-1-en-1-yl)-2-(trifluoromethyl)acrylamide (1i):**

The 1-phenylpentan-1-imine[52] was synthesized as per available literature report. A round-bottom flask was charged with benzonitrile (2.0 equiv., 10 mmol) and THF (10 mL). The mixture was cooled to −78 °C, and $^n$BuLi (1.0 equiv., 5 mmol (3.12 mL of $^n$BuLi solution of 1.6 M in Hexane) was added dropwise. After addition, the resulting mixture was stirred for 2 h at -40 °C. The mixture was cooled to −78 °C and quenched with anhydrous MeOH (1.0 equiv., 5 mmol, 0.2 mL). The cooling bath was removed, and the reaction mixture was allowed to warm to r.t. for 1 hour. The resultant slurry was filtered through a 2 cm pad of Celite, and the filtrate was concentrated using a rotary evaporator and then dried under high vacuum. The resultant imine was then redissolved in anhydrous dichloromethane (10 mL) and cooled to 0 °C on an ice bath under an argon atmosphere. The freshly prepared 2-(trifluoromethyl)acryloyl chloride (1.2 equiv., 6 mmol) was separately dissolved in 5 mL dichloromethane and added dropwise to imine solution at 0 °C over 10 minutes. The reaction mixture was then transferred to room temperature and stirred overnight. After completion, the reaction was quenched with the addition of water. The organic layer was separated using dichloromethane, dried over sodium sulphate, and concentrated using a rotary evaporator. Purified by column chromatography using 230-400 mesh size silica gel and 5-10% EA/H. The obtained product was a white solid (128 mg, 9% yield). White solid. **$^1$H NMR** (500 MHz, $CDCl_3$) δ 7.41 – 7.36 (m, 2H), 7.36 – 7.31 (m, 2H), 7.31 – 7.27 (m, 1H), 7.07 (s, 1H), 6.68 (s, 1H), 6.34 (s, 1H), 5.93 (t, *J* = 7.2 Hz, 1H), 2.15 (q, *J* = 7.3 Hz, 2H), 1.57 – 1.48 (m, 2H), 0.97 (t, *J* = 7.4 Hz, 3H). **$^{13}$C NMR** (126 MHz, $CDCl_3$) δ 159.0, 137.4, 133.7 (q, *J* = 30.9 Hz), 132.7, 130.7 (q, *J* = 5.5 Hz), 128.6, 128.1, 127.5, 125.5, 122.5 (q, *J* = 272.9 Hz) 30.4, 22.2, 14.0. **$^{19}$F NMR** (471 MHz, $CDCl_3$) δ -

63.46. **IR** (neat): 3289, 2956, 2924, 2854, 1739, 1669, 1522, 1348 cm$^{-1}$. **HRMS** (ESI+ve) m/z: $[M+Na]^+$ calcd $C_{15}H_{16}F_3NONa$ 306.1076, found 306.1078.

### 3.9.4 List of hydrosilanes and hydrogermanes

All hydrosilanes and hydrogermanes were commercially available and used as received.

$^{t}BuMe_2SiH$ **2a**, $Et_3SiH$ **2b**, $^{n}Pr_3SiH$ **2c**, $^{n}Bu_3SiH$ **2d**, $^{i}Pr_3SiH$ **2e**, $Bn_3SiH$ **2f**, $BnMe_2SiH$ **2g**, $PhMe_2SiH$ **2h**

$Ph_2MeSiH$ **2i**, $^{t}BuPh_2SiH$ **2j**, $Ph_3SiH$ **2k**, $(TMS)_3SiH$ **2l**, 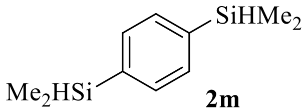 **2m**, $Ph_2SiH_2$ **2n**

$Ph_3GeH$ **4a**, $Et_3GeH$ **4b**, $^{n}Bu_3GeH$ **4c**

### 3.9.5 Blue LEDs source and temperature control

The visible light irradiation was performed using high power blue LEDs (make: Original Opulant America, power = 3 W, λmax = 455 nm, luminous flux/radiant flux = 687 mW at 700 mA) fitted in an aluminium block. The block contains 6 holes to hold vials and is fitted with water inlet-outlet nozzles. The vials are placed in holes on the block and irradiated from bottom at a distance of approximately 2 cm. The reaction temperature can be maintained by circulating water through the aluminium block through inlet-outlet nozzles.

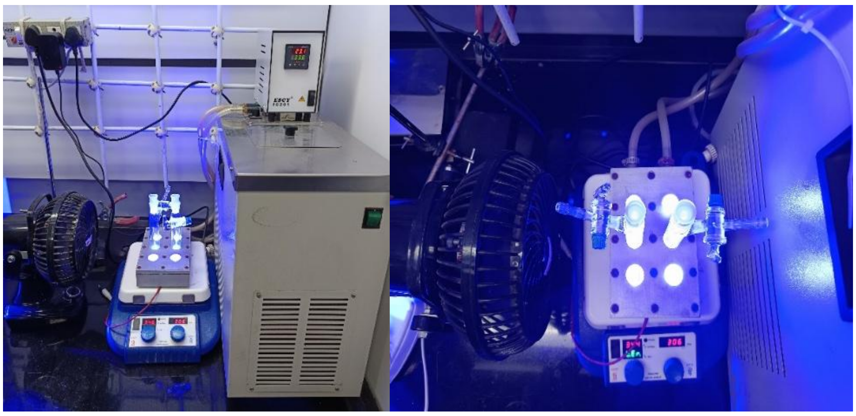

### 3.9.6 Procedure for optimization of reaction conditions

To an oven-dried 10 mL Schlenk tube equipped with a magnetic stir bar were added *N*-benzyl-*N*-(1-phenylprop-1-en-1-yl)-2-(trifluoromethyl)acrylamide **1a** (0.2 mmol, 69.1 mg), $^t$BuMe$_2$SiH **2a** (0.6 mmol, 0.1 mL), 1 mol% 4DPAIPN (1.6 mg, 0.002 mmol), 1.5 equivalent of hydrogen atom transfer reagent (HATR) (0.3 mmol, 117.7 mg) and 100 mg 4Å molecular sieves (powder and heat gun dried). The reaction tube was sealed and placed under an argon atmosphere, then 1 mL α,α,α-trifluorotoluene (dried over 4Å granules molecular sieves) was added *via* syringe, the reaction mixture was then degassed *via* freeze pump thaw (x 3 times) and refilled with argon. The sealed reaction tube was then placed inside the aluminium block, fitted with blue LEDs (λ = 455 nm), and irradiated for 1 hour. After the reaction was completed, the mixture was filtered using dichloromethane and then evaporated under reduced pressure. The crude product was then purified by flash column chromatography on silica gel (mesh 100-200) using a gradient elution with hexane/ethyl acetate (50:1 to 30:1), which yielded the silylation product **3a**.

### 3.9.7 General procedure for the silylation of 3-aza-1,5-dienes

To an oven-dried 10 mL Schlenk tube equipped with a magnetic stir bar were added 3-aza-1,5-dienes **1** (0.2 mmol), hydrosilane **2** (0.6 mmol, 3 equiv.), 1 mol% 4DPAIPN (1.6 mg, 0.002 mmol), 1.5 equivalent of hydrogen atom transfer reagent (HATR) (0.3 mmol, 117.7 mg) and 100 mg 4Å molecular sieves (powder and heat gun dried). The reaction tube was sealed and placed under an argon atmosphere, then 1 mL α,α,α-trifluorotoluene (dried over 4Å granules molecular sieves) was added *via* syringe, the reaction mixture was then degassed *via* freeze pump thaw (x 3 times) and refilled with argon. The sealed reaction tube was then placed inside the aluminium block fitted with blue LEDs (λ = 455 nm) and irradiated for 1 hour. After the reaction was completed, the mixture was filtered using dichloromethane and then evaporated under reduced pressure. The crude product was then purified by flash column chromatography on silica gel (mesh 100-200) using a gradient elution with hexane/ethyl acetate (50:1 to 5:1) to yield the silylation product **3**.

### 3.9.8 Characterization data of 3a-3am and 3a'

**1-benzyl-3-((*tert*-butyldimethylsilyl)methyl)-4-methyl-5-phenyl-3-(trifluoromethyl)-1,3-dihydro-2*H*-pyrrol-2-one (3a):** 0.2 mmol scale, ( 71.7 mg, 78%). White solid. Column chromatography: 1-3% EA/H. **M.P.**: 100-102 °C. **$^1$H NMR** (500 MHz, $CDCl_3$) δ 7.41 – 7.32 (m, 3H), 7.16 – 7.10 (m, 3H), 7.09 – 7.03 (m, 2H), 6.87 – 6.81 (m, 2H), 4.97 (d, *J* = 15.3 Hz, 1H), 4.13 (d, *J* = 15.3 Hz, 1H), 1.67 (s, 3H), 1.60 (d, *J* = 14.3 Hz, 1H), 1.29 (d, *J* = 14.3 Hz, 1H), 0.90 (s, 9H), 0.00 (s, 3H), -0.05 (s, 3H). **$^{13}$C NMR** (126 MHz, $CDCl_3$) δ 174.2, 141.3, 136.7, 129.6, 129.5, 129.2, 128.6, 128.3, 127.7, 127.3, 126.7 (q, *J* = 283.2 Hz), 112.8, 57.0 (q, *J* = 25.6 Hz), 44.6, 26.2, 16.7, 11.4, 10.7, -4.87, -5.68. **$^{19}$F NMR** (471 MHz, $CDCl_3$) δ -73.6. **IR** (neat): 2930, 2858, 1709, 1377, 1241, 1162 $cm^{-1}$. **HRMS** (ESI+ve) m/z: $[M+H]^+$ calcd for $C_{26}H_{33}F_3NOSi$; 460.2278, found 460.2284.

**1-benzyl-3-((*tert*-butyldimethylsilyl)methyl)-4-ethyl-5-phenyl-3-(trifluoromethyl)-1,3-dihydro-2*H*-pyrrol-2-one (3b):** 0.2 mmol scale, (66.4 mg, 70%). White solid. Column chromatography: 1-3% EA/H. **M.P.**: 84-86 °C. $^1$H NMR (500 MHz, $CDCl_3$) δ 7.43 – 7.36 (m, 1H), 7.35 – 7.29 (m, 2H), 7.19 – 7.13 (m, 3H), 7.11 – 7.03 (m, 2H), 6.87 – 6.82 (m, 2H), 4.91 (d, *J* = 15.3 Hz, 1H), 4.01 (d, *J* = 15.3 Hz, 1H), 2.19 – 2.08 (m, 1H), 2.01 – 1.92 (m, 1H), 1.64 – 1.58 (m, 1H), 1.32 – 1.26 (m, 1H), 0.92 – 0.82 (m, 12H), -0.03 (s, 6H). **$^{13}$C NMR** (126 MHz, $CDCl_3$) δ 173.9, 142.2, 136.8, 130.0, 129.6, 129.3, 128.6, 128.3, 127.6, 127.3, 125.8 (q, *J* = 284.3 Hz), 118.4, 57.0 (q, *J* = 25.8 Hz), 44.5, 26.3, 18.5, 16.7, 14.3, 11.9, -4.7, -5.7. **$^{19}$F NMR** (471 MHz, $CDCl_3$) δ -73.18. **IR** (neat): 2926, 2856, 1708, 1355, 1152 $cm^{-1}$. **HRMS** (ESI+ve) m/z: $[M+Na]^+$ calcd for $C_{27}H_{34}F_3NOSiNa$; 496.2254, found 496.2254.

**1-benzyl-3-((*tert*-butyldimethylsilyl)methyl)-5-phenyl-4-propyl-3-(trifluoromethyl)-1,3-dihydro-2*H*-pyrrol-2-one (3c):** 0.2 mmol scale, (69.3 mg, 71%). White solid. Column chromatography: 1-3% EA/H. **M.P.**: 72-74 °C. **$^{1}$H NMR** (500 MHz, $CDCl_3$) δ 7.42 – 7.35 (m, 1H), 7.36 – 7.29 (m, 2H), 7.19 – 7.12 (m, 3H), 7.08 – 7.02 (m, 2H), 6.88 – 6.82 (m, 2H), 4.90 (d, *J* = 15.3 Hz, 1H), 4.01 (d, *J* = 15.3 Hz, 1H), 2.09 – 1.99 (m, 1H), 1.90 – 1.81 (m, 1H), 1.64 – 1.58 (m, 1H), 1.45 – 1.34 (m, 1H), 1.33 – 1.26 (m, 1H), 1.1–1.06 (m, 1H), 0.90 (s, 9H), 0.70 (t, *J* = 7.4 Hz, 3H), -0.01 (s, 3H), -0.03 (s, 3H). **$^{13}$C NMR** (126 MHz, $CDCl_3$) δ 173.9, 142.3, 136.8, 130.0, 129.5, 129.3, 128.6, 128.3, 127.6, 127.3, 125.8 (q, *J* = 286.4 Hz), 117.3, 57.0 (q, *J* = 25.7 Hz), 44.5, 27.8, 26.3, 23.0, 16.7, 14.6, 11.9, -4.7, -5.7. **$^{19}$F NMR** (471 MHz, $CDCl_3$) δ -73.16. **IR** (neat): 2959, 2859, 1710, 1377, 1157 $cm^{-1}$. **HRMS** (ESI+ve) m/z: $[M+Na]^+$ calcd for $C_{28}H_{36}F_3NOSiNa$; 510.2410, found 510.2405.

**1-benzyl-3-((*tert*-butyldimethylsilyl)methyl)-4,5-diphenyl-3-(trifluoromethyl)-1,3-dihydro-2*H*-pyrrol-2-one (3d):** 0.2 mmol scale, (88.7 mg, 85%). Viscous gum. Column chromatography: 1-3% EA/H. $^{1}$H NMR (500 MHz, $CDCl_3$) δ 7.33 – 7.27 (m, 1H), 7.25 – 7.19 (m, 5H), 7.14 – 7.07 (m, 5H), 7.05 – 7.01 (m, 2H), 7.01 – 6.97 (m, 2H), 4.92 (d, *J* = 15.5 Hz, 1H), 4.31 (d, *J* = 15.5 Hz, 1H), 1.73 – 1.65 (m, 1H), 1.64 – 1.57 (m, 1H), 0.93 (s, 9H), 0.09 (s, 3H), 0.02 (s, 3H). **$^{13}$C NMR** (126 MHz, $CDCl_3$) δ 173.9, 144.1, 136.7, 133.1, 130.5, 129.9, 129.8, 129.3, 128.6 (2C), 127.9, 127.6, 127.5, 127.1, 125.4 (q, *J* = 285.8 Hz), 117.3, 58.4 (q, *J* = 25.2 Hz), 45.1, 26.3, 17.1, 12.3, -4.4, -5.0. **$^{19}$F NMR** (471 MHz, $CDCl_3$) δ -72.53. **IR** (neat): 2953, 2857, 1720, 1369, 1230, 1158 $cm^{-1}$. **HRMS** (ESI+ve) m/z: $[M+Na]^+$ calcd for $C_{31}H_{34}F_3NOSiNa$; 544.2253, found 544.2263.

**1-benzyl-3-((*tert*-butyldimethylsilyl)methyl)-5-phenyl-3-(trifluoromethyl)-1,3-dihydro-2*H*-pyrrol-2-one (3e):** 0.2 mmol scale, (52.6 mg, 59%). Clear oil. Column chromatography: 1-3% EA/H. **$^{1}$H NMR** (500 MHz, $CDCl_3$) δ 7.42 – 7.37 (m, 1H), 7.36 – 7.32 (m, 2H), 7.23 – 7.16 (m, 5H), 6.99 – 6.94 (m, 2H), 5.26 (s, 1H), 4.96 (d, *J* = 15.6 Hz, 1H), 4.32 (d, *J* = 15.6 Hz, 1H), 1.55 (d, *J* = 14.3 Hz, 1H), 1.29 (d, *J* = 14.3 Hz, 1H), 0.88 (s, 9H), 0.03 (s, 3H), -0.07 (s, 3H). **$^{13}$C NMR** (126

MHz, $CDCl_3$) δ 175.5, 148.1, 136.7, 130.5, 129.7, 128.7, 128.5, 128.2, 127.4, 127.3, 125.49 (q, *J* = 282.8 Hz), 105.6, 55.91 (q, *J* = 26.8 Hz), 44.9, 26.3, 16.6, 13.7, -4.0, -5.8. **$^{19}$F NMR** (471 MHz, $CDCl_3$) δ -74.18. **IR** (neat): 2927, 2856, 1721, 1345, 1247, 1158 $cm^{-1}$. **HRMS** (ESI+ve) m/z: $[M+Na]^+$ calcd for $C_{25}H_{30}F_3NOSiNa$; 468.1940, found 468.1956.

**3-((*tert*-butyldimethylsilyl)methyl)-1,5-diphenyl-3-(trifluoromethyl)-1,3-dihydro-2*H*-pyrrol-2-one (3f):** 0.2 mmol scale, (30.2 mg, 35%). Viscous oil. Column chromatography: 1-3% EA/H. **$^1$H NMR** (500 MHz, $CDCl_3$) δ 7.33 – 7.26 (m, 3H), 7.26 – 7.21 (m, 3H), 7.14 – 7.09 (m, 2H), 7.03 (d, *J* = 7.3 Hz, 2H), 5.46 (s, 1H), 1.63 (d, *J* = 14.4 Hz, 1H), 1.33 (d, *J* = 14.4 Hz, 1H), 0.89 (s, 9H), 0.06 (s, 3H), 0.01 (s, 3H). **$^{13}$C NMR** (126 MHz, $CDCl_3$) δ 174.2, 147.7, 134.9, 130.3, 129.4, 128.9, 128.5, 127.7, 127.4, 126.8, 125.4 (q, *J* = 283.1 Hz), 106.2, 56.2 (q, *J* = 26.9 Hz), 16.6, 13.7, -3.9, -5.5. **$^{19}$F NMR** (471 MHz, $CDCl_3$) δ -74.65. **IR** (neat): 2957, 2927, 1729, 1364, 1158 $cm^{-1}$. **HRMS** (ESI+ve) m/z: $[M+Na]^+$ calcd for $C_{24}H_{28}F_3NOSiNa$; 454.1784, found 454.1775.

**3-((*tert*-butyldimethylsilyl)methyl)-4-methyl-5-phenyl-1-propyl-3-(trifluoromethyl)-1,3-dihydro-2*H*-pyrrol-2-one (3g):** 0.2 mmol scale, (67.5 mg, 82%). Clear oil. Column chromatography: 1-3% EA/H. $^1$H NMR (500 MHz, $CDCl_3$) δ 7.53 – 7.43 (m, 3H), 7.31-7.26 (m, 2H), 3.61 – 3.51 (m, 1H), 3.13 – 3.04 (m, 1H), 1.68 (s, 3H), 1.62 – 1.56 (m, 1H), 1.41 – 1.28 (m, 2H), 1.27 – 1.21 (m, 1H), 0.90 (s, 9H), 0.70 (t, *J* = 7.5 Hz, 3H), 0.00 (s, 3H), -0.05 (s, 3H). **$^{13}$C NMR** (126 MHz, $CDCl_3$) δ 174.1, 141.4, 129.9, 129.3 (2C), 128.8, 126.7 (q, *J* = 285.5 Hz), 112.5, 56.9 (q, *J* = 25.5 Hz), 42.6, 26.2, 21.8, 16.7, 11.2, 11.04, 10.8, -4.9, -5.7. **$^{19}$F NMR** (471 MHz, $CDCl_3$) δ -73.97. **IR** (neat): 2930, 2860, 1717, 1347, 1158 $cm^{-1}$. **HRMS** (ESI+ve) m/z: $[M+Na]^+$ calcd for $C_{22}H_{32}F_3NOSiNa$; 434.2097, found 434.2099.

**3-((*tert*-butyldimethylsilyl)methyl)-1-cyclohexyl-4-methyl-5-phenyl-3-(trifluoromethyl)-1,3-dihydro-2*H*-pyrrol-2-one (3h):** 0.2 mmol scale, (57.9 mg, 64%). White Solid. Column chromatography: 1-

3% EA/H. **M.P.**: 128-130 °C. **$^1$H NMR** (500 MHz, $CDCl_3$) δ 7.51 – 7.41 (m, 3H), 7.30-7.15 (br, 2H), 3.20 – 3.10 (m, 1H), 2.27 – 2.15 (m, 1H), 2.11 – 1.99 (m, 1H), 1.76 – 1.63 (m, 3H), 1.60 (s, 3H), 1.59 – 1.54 (m, 1H), 1.54 – 1.45 (m, 2H), 1.18 (d, *J* = 14.4 Hz, 1H), 1.14 – 0.93 (m, 3H), 0.88 (s, 9H), 0.05 (s, 3H), -0.06 (s, 3H). **$^{13}$C NMR** (126 MHz, $CDCl_3$) δ 174.2, 142.6, 130.6, 130.4, 129.2, 128.9, 128.4, 125.7 (q, *J* = 285.3 Hz), 112.1, 57.2 (q, *J* = 25.2 Hz), 55.0, 29.9, 29.0, 26.2 (2C), 25.9, 25.1, 16.7, 11.0, 10.7, -4.9, -5.1. **$^{19}$F NMR** (471 MHz, $CDCl_3$) δ -74.50. **IR** (neat): 2930, 2858, 1710, 1337, 1150 $cm^{-1}$. **HRMS** (ESI+ve) m/z: $[M+Na]^+$ calcd for $C_{25}H_{36}F_3NOSiNa$; 474.2410, found 474.2400.

**1-benzyl-3-((*tert*-butyldimethylsilyl)methyl)-5-(3-fluorophenyl)-4-methyl-3-(trifluoromethyl)-1,3-dihydro-2*H*-pyrrol-2-one (3j):** 0.2 mmol scale, (64 mg, 67%). White solid. Column chromatography: 1-3% EA/H. **M.P.**: 102-104 °C. $^1$H NMR (500 MHz, $CDCl_3$) δ 7.35 – 7.29 (m, 1H), 7.19 – 7.11 (m, 3H), 7.11 – 7.04 (m, 1H), 6.87 – 6.82 (m, 3H), 6.73 (d, *J* = 9.2 Hz, 1H), 5.01 (d, *J* = 15.3 Hz, 1H), 4.10 (d, *J* = 15.3 Hz, 1H), 1.66 (s, 3H), 1.60 (d, *J* = 14.3 Hz, 1H), 1.31 – 1.24 (m, 1H), 0.89 (s, 9H), -0.01 (s, 3H), -0.06 (s, 3H). **$^{13}$C NMR** (126 MHz, $CDCl_3$) δ 174.0, 162.6 (d, *J* = 248.1 Hz), 140.0, 136.5, 131.6 (d, *J* = 7.9 Hz), 130.3 (d, *J* = 8.4 Hz), 128.4, 127.6, 127.4, 125.6 (q, *J* = 284.6 Hz), 125.3, 116.6 (d, *J* = 22.1 Hz), 116.3 (d, *J* = 20.9 Hz), 113.6, 57.1 (q, *J* = 25.6 Hz), 44.7, 26.2, 16.7, 11.4, 10.7, -4.8, -5.6. **$^{19}$F NMR** (471 MHz, $CDCl_3$) δ -73.58, -111.81 (m). **IR** (neat): 2926, 2856, 1710, 1358, 1158 $cm^{-1}$. **HRMS** (ESI+ve) m/z: $[M+Na]^+$ calcd for $C_{26}H_{31}F_4NOSiNa$; 500.2003, found 500.2017.

**1-benzyl-3-((*tert*-butyldimethylsilyl)methyl)-5-(3-chlorophenyl)-4-methyl-3-(trifluoromethyl)-1,3-dihydro-2*H*-pyrrol-2-one (3k):** 0.2 mmol scale, (60.3 mg, 61%). Clear oil. Column chromatography: 1-3% EA/H. **$^1$H NMR** (500 MHz, $CDCl_3$) δ 7.39 – 7.33 (m, 1H), 7.31 – 7.24 (m, 1H), 7.19 – 7.12 (m, 3H), 6.98 – 6.91 (m, 2H), 6.84 (dd, *J* = 6.5, 2.8 Hz, 2H), 5.01 (d, *J* = 15.4 Hz, 1H), 4.08 (d, *J* = 15.4 Hz, 1H), 1.66 (s, 3H), 1.64 – 1.57 (m, 1H), 1.28 (d, *J* = 14.4 Hz, 1H), 0.90 (s, 9H), 0.00

(s, 3H), -0.05 (s, 3H). **$^{13}$C NMR** (126 MHz, $CDCl_3$) δ 174.0 (2C), 140.0, 136.5, 134.6, 131.3, 129.9, 129.6, 129.5, 128.4, 127.6, 125.6 (q, *J* = 285.9 Hz), 127.5, 113.7, 57.1 (q, *J* = 25.6 Hz), 44.7, 26.2, 16.7, 11.4, 10.7, -4.8, -5.6. **$^{19}$F NMR** (471 MHz, $CDCl_3$) δ -73.56. **IR** (neat): 2927, 2857, 1709, 1382, 1162 cm$^{-1}$. **HRMS** (ESI+ve) m/z: $[M+Na]^+$ calcd for $C_{26}H_{31}F_3ClNOSiNa$; 516.1707, found 516.1711.

**1-benzyl-3-((*tert*-butyldimethylsilyl)methyl)-4-methyl-5-(p-tolyl)-3-(trifluoromethyl)-1,3-dihydro-2*H*-pyrrol-2-one (3l):** 0.2 mmol scale, (79.5 mg, 84%). White solid. Column chromatography: 1-3% EA/H. **M.P.**: 105-107 °C. **$^1$H NMR** (500 MHz, $CDCl_3$) δ 7.18 – 7.12 (m, 5H), 6.98 – 6.93 (m, 2H), 6.90 – 6.85 (m, 2H), 4.93 (d, *J* = 15.3 Hz, 1H), 4.14 (d, *J* = 15.3 Hz, 1H), 2.38 (s, 3H), 1.65 (s, 3H), 1.58 (d, *J* = 13.8 Hz, 1H), 1.27 (d, *J* = 13.8 Hz, 1H), 0.89 (s, 9H), -0.02 (s, 3H), -0.06 (s, 3H). **$^{13}$C NMR** (126 MHz, $CDCl_3$) δ 174.2, 141.4, 139.2, 136.9, 129.4, 129.3, 128.3, 127.6, 127.2, 126.6, 125.7 (q, *J* = 284.84 Hz), 112.6, 57.0 (q, *J* = 25.5 Hz), 44.5, 26.2, 21.4, 16.7, 11.4, 10.7, -4.9, -5.7. **$^{19}$F NM**R (471 MHz, $CDCl_3$) δ -73.60. **IR** (neat): 2928, 2858, 1712, 1510, 1356, 1150 cm$^{-1}$. **HRMS** (ESI+ve) m/z: $[M+Na]^+$ calcd for $C_{27}H_{34}F_3NOSiNa$; 496.2253, found 496.2253.

**1-benzyl-3-((*tert*-butyldimethylsilyl)methyl)-5-(4-methoxyphenyl)-4-methyl-3 (trifluoromethyl)-1,3-dihydro-2*H*-pyrrol-2-one (3m):** 0.2 mmol scale, (79.4 mg, 81%). White solid. Column chromatography: 1-3% EA/H. **M.P.**: 106-108 °C. **$^1$H NMR** (500 MHz, $CDCl_3$) δ 7.18 – 7.12 (m, 3H), 7.01 – 6.96 (m, 2H), 6.91 – 6.83 (m, 4H), 4.94 (d, *J* = 15.3 Hz, 1H), 4.12 (d, *J* = 15.3 Hz, 1H), 3.83 (s, 3H), 1.65 (s, 3H), 1.58 (d, *J* = 14.3 Hz, 1H), 1.27 (d, *J* = 14.3 Hz, 1H), 0.89 (s, 9H), -0.02 (s, 3H), -0.06 (s, 3H). **$^{13}$C NMR** (126 MHz, $CDCl_3$) δ 174.1, 160.1, 141.0, 136.8, 130.7, 128.2, 127.5, 127.1,125.6 (q, *J* = 285.46 Hz), 121.6, 113.9, 112.5, 56.9 (q, *J* = 25.6 Hz), 55.3, 44.4, 26.1, 16.6, 11.3, 10.6, -5.0, -5.8. **$^{19}$F NMR** (471 MHz, $CDCl_3$) δ -73.59. **IR** (neat): 2928, 2857, 1712, 1368, 1248, 1157 cm$^{-1}$. **HRMS** (ESI+ve) m/z: $[M+Na]^+$ calcd for $C_{27}H_{34}F_3NO_2SiNa$; 512.2203, found 512.2200.

**1-benzyl-3-((*tert*-butyldimethylsilyl)methyl)-5-(4-fluorophenyl)-4-methyl-3-(trifluoromethyl)-1,3-dihydro-2*H*-pyrrol-2-one (3n):** 0.2 mmol scale, (71.5 mg, 75%). White solid. Column chromatography: 1-3% EA/H. **M.P.**: 77-79 °C. $^1$H NMR (500 MHz, $CDCl_3$) δ 7.17 – 7.12 (m, 3H), 7.05 – 6.98 (m, 4H), 6.87 – 6.81 (m, 2H), 4.99 (d, *J* = 15.3 Hz, 1H), 4.07 (d, *J* = 15.3 Hz, 1H), 1.64 (s, 3H), 1.60 (d, *J* = 14.2 Hz, 1H), 1.27 (d, *J* = 14.2 Hz, 1H), 0.89 (s, 9H), -0.01 (s, 3H), -0.06 (s, 3H). **$^{13}$C NMR** (126 MHz, $CDCl_3$) δ 174.1, 163.1 (d, *J* = 249.8 Hz), 140.3, 136.6, 131.4 (d, *J* = 8.3 Hz), 128.4, 127.5, 127.4, 125.6 (q, *J* = 284.03 Hz), 125.6 (d, *J* = 3.5 Hz), 115.8 (d, *J* = 21.7 Hz), 113.3, 57.0 (q, *J* = 25.7 Hz), 44.6, 26.2, 16.7, 11.4, 10.6, -4.8, -5.6. **$^{19}$F NMR** (471 MHz, $CDCl_3$) δ -73.59, -111.15. **IR** (neat): 2924, 2859, 1709, 1358, 1252 cm$^{-1}$. **HRMS** (ESI+ve) m/z: $[M+Na]^+$ calcd for $C_{26}H_{31}F_4NOSiNa$; 500.2000, found 500.1990.

**1-benzyl-3-((*tert*-butyldimethylsilyl)methyl)-5-(4-chlorophenyl)-4-methyl-3-(trifluoromethyl)-1,3-dihydro-2*H*-pyrrol-2-one (3o):** 0.2 mmol scale, (71.2 mg, 72%). White solid. Column chromatography: 1-3% EA/H. **M.P.**: 84-86 °C. **$^1$H NMR** (500 MHz, $CDCl_3$) δ 7.31 (d, *J* = 8.0 Hz, 2H), 7.19 – 7.12 (m, 3H), 6.97 (d, *J* = 8.0 Hz, 2H), 6.88 – 6.82 (m, 2H), 4.99 (d, *J* = 15.4 Hz, 1H), 4.07 (d, *J* = 15.4 Hz, 1H), 1.64 (s, 3H), 1.59 (d, *J* = 14.3 Hz, 1H), 1.27 (d, *J* = 14.3 Hz, 1H), 0.89 (s, 9H), -0.01 (s, 3H), -0.07 (s, 3H). **$^{13}$C NMR** (126 MHz, $CDCl_3$) δ 174.1 (2C), 140.2, 136.5, 135.4, 130.8, 128.9, 128.4, 128.0, 127.5, 127.4, 125.6 (q, *J* = 287.68 Hz), 113.5, 57.1 (q, *J* = 25.6 Hz), 44.6, 26.2, 16.7, 11.4, 10.6, -4.8, -5.6. **$^{19}$F NMR** (471 MHz, $CDCl_3$) δ -73.56. **IR** (neat): 2928, 2858, 1716, 1361, 1151 cm$^{-1}$. **HRMS** (ESI+ve) m/z: $[M+Na]^+$ calcd for $C_{26}H_{31}ClF_3NOSiNa$; 516.1707, found 516.1699.

**1-benzyl-3-((*tert*-butyldimethylsilyl)methyl)-4-methyl-3-(trifluoromethyl)-5-(4-(trifluoromethyl)phenyl)-1,3-dihydro-2*H*-pyrrol-2-one (3p):** 0.2 mmol scale, (71.8 mg, 68%). White solid. Column chromatography: 1-3% EA/H. **M.P.**: 83-85 °C. $^1$H NMR (500 MHz, $CDCl_3$) δ 7.59 (d, *J* = 7.9 Hz, 2H), 7.18 – 7.09 (m, 5H), 6.83 –

6.78 (m, 2H), 5.04 (d, *J* = 15.4 Hz, 1H), 4.06 (d, *J* = 15.4 Hz, 1H), 1.66 (s, 3H), 1.65-1.58 (m, 1H), 1.32-1.26 (m, 1H), 0.90 (s, 9H), 0.01 (s, 3H), -0.06 (s, 3H). **$^{13}$C NMR** (126 MHz, $CDCl_3$) δ 174.0, 140.0, 136.3, 133.4, 131.3 (q, *J* = 32.7 Hz), 129.9, 128.5, 127.9 (d, *J* = 230.75 Hz), 127.5, 125.60 (d, *J* = 3.7 Hz), 125.60 (q, *J* = 286.1 Hz), 123.8 (q, *J* = 275.5 Hz), 114.1, 57.2 (q, *J* = 25.7 Hz), 44.7, 26.2, 16.7, 11.4, 10.6, -4.8, -5.5. **$^{19}$F NMR** (471 MHz, $CDCl_3$) δ -62.89, -73.53. **IR** (neat): 2931, 2860, 1709, 1374, 1160 $cm^{-1}$. **HRMS** (ESI+ve) m/z: $[M+Na]^+$ calcd for $C_{27}H_{31}F_6NOSiNa$; 550.1971, found 550.1971.

**4-(1-benzyl-4-((*tert*-butyldimethylsilyl)methyl)-3-methyl-5-oxo-4-(trifluoromethyl)-4,5-dihydro-1*H*-pyrrol-2-yl)benzyl acetate (3q):** 0.2 mmol scale, (70.1 mg, 58%). Clear oil. Column chromatography: 5-10% EA/H. **$^{1}$H NMR** (500 MHz, $CDCl_3$) δ 7.35 – 7.30 (m, 2H), 7.20 – 7.10 (m, 3H), 7.09 – 7.04 (m, 2H), 6.87 – 6.82 (m, 2H), 5.12 (s, 2H), 4.96 (d, *J* = 15.3 Hz, 1H), 4.11 (d, *J* = 15.3 Hz, 1H), 2.14 (s, 3H), 1.66 (s, 3H), 1.59 (d, *J* = 14.3 Hz, 1H), 1.28 (d, *J* = 14.3 Hz, 1H), 0.89 (s, 9H), -0.01 (s, 3H), -0.06 (s, 3H). **$^{13}$C NMR** (126 MHz, $CDCl_3$) δ 174.1, 170.8, 140.8, 137.2, 136.6, 129.7, 129.4, 128.3, 128.2, 127.5, 127.3, 125.6 (q, *J* = 286.4 Hz), 113.1, 65.7, 57.0 (q, *J* = 25.6 Hz), 44.6, 26.2, 21.0, 16.7, 11.4, 10.7, -4.8, -5.7. **$^{19}$F NMR** (471 MHz, $CDCl_3$) δ -73.56. **IR** (neat): 2930, 2859, 1730, 1717, 1374, 1160 $cm^{-1}$. **HRMS** (ESI+ve) m/z: $[M+Na]^+$ calcd for $C_{29}H_{36}F_3NO_3SiNa$; 554.2308, found 554.2311.

**1-benzyl-3-((*tert*-butyldimethylsilyl)methyl)-4-methyl-5-(thiophen-2-yl)-3-(trifluoromethyl)-1,3-dihydro-2*H*-pyrrol-2-one (3r):** 0.2 mmol scale, (54.1 mg, 58%). White solid. Column chromatography: 1-3% EA/H. **M.P.**: 104-106 °C. **$^{1}$H NMR** (500 MHz, $CDCl_3$) δ 7.43 – 7.39 (m, 1H), 7.21 – 7.14 (m, 3H), 7.05 – 6.99 (m, 1H), 6.97 – 6.91 (m, 2H), 6.81 – 6.77 (m, 1H), 5.03 (d, *J* = 15.5 Hz, 1H), 4.24 (d, *J* = 15.5 Hz, 1H), 1.76 (s, 3H), 1.59 (d, *J* = 14.3 Hz, 1H), 1.28 (d, *J* = 14.3 Hz, 1H), 0.88 (s, 9H), -0.04 (s, 3H), -0.05 (s, 3H). **$^{13}$C NM**R (126 MHz, $CDCl_3$) δ 173.6, 136.8, 134.7, 129.9, 129.0, 128.4, 128.0, 127.3 (2C), 125.5 (q, *J* = 285.76 Hz), 116.7, 57.2 (q, *J* = 25.7 Hz), 44.5, 26.2, 16.7, 11.7, 11.2,

-4.9, -5.7. **$^{19}$F NMR** (471 MHz, $CDCl_3$) δ -73.34. **IR** (neat): 2929, 2858, 1708, 1362, 1159 $cm^{-1}$. **HRMS** (ESI+ve) m/z: $[M+Na]^+$ calcd for $C_{24}H_{30}F_3NOSSiNa$; 488.1661, found 488.1667.

**1-benzyl-3-((*tert*-butyldimethylsilyl)methyl)-3,4-dimethyl-5-phenyl-1,3-dihydro-2*H*-pyrrol-2-one (3t):** 0.2 mmol scale, (23.6 mg, 29%). Clear oil. Column chromatography: 1-3% EA/H. **$^1$H NMR** (500 MHz, $CDCl_3$) δ 7.38 – 7.28 (m, 3H), 7.17 – 7.09 (m, 3H), 7.09 – 7.03 (m, 2H), 6.90 – 6.83 (m, 2H), 4.88 (d, *J* = 15.2 Hz, 1H), 4.20 (d, *J* = 15.2 Hz, 1H), 1.61 (s, 3H), 1.33 (s, 3H), 1.26 (d, *J* = 14.6 Hz, 1H), 0.94 (d, *J* = 14.6 Hz, 1H), 0.85 (s, 9H), -0.05 (s, 3H), -0.11 (s, 3H). **$^{13}$C NMR** (126 MHz, $CDCl_3$) δ 183.0, 138.0, 135.4, 130.8, 129.8, 128.5, 128.4, 128.2, 127.8, 127.0, 121.3, 49.4, 44.2, 27.6, 26.4, 19.3, 16.7, 9.4, -4.9, -5.5. **IR** (neat): 2953, 2880, 1703, 1367, 1340, 1247, 1137 $cm^{-1}$. **HRMS** (ESI+ve) m/z: $[M+H]^+$ calcd for $C_{26}H_{36}NOSi$; 406.2561, found 406.2558.

**1-benzyl-4-methyl-5-phenyl-3-((triethylsilyl)methyl)-3-(trifluoromethyl)-1,3-dihydro-2*H*-pyrrol-2-one (3u):** 0.2 mmol scale, (70.8 mg, 77%). Clear oil. Column chromatography: 1-3% EA/H. **$^1$H NMR** (500 MHz, $CDCl_3$) δ 7.42 – 7.31 (m, 3H), 7.17 – 7.09 (m, 3H), 7.08 – 7.01 (m, 2H), 6.87 – 6.80 (m, 2H), 4.94 (d, *J* = 15.5 Hz, 1H), 4.13 (d, *J* = 15.5 Hz, 1H), 1.66 (s, 3H), 1.61 – 1.55 (m, 1H), 1.29 (d, *J* = 14.9 Hz, 1H), 0.98 – 0.91 (m, 9H), 0.54 (m, 6H). **$^{13}$C NMR** (126 MHz, $CDCl_3$) δ 174.3, 141.1, 136.7, 129.6, 129.5, 129.2, 128.6, 128.3, 127.7, 127.2, 125.7 (q, *J* = 285.1 Hz), 113.1, 57.0 (q, *J* = 25.5 Hz), 44.6, 11.6, 10.6, 7.4, 3.9. **$^{19}$F NMR** (471 MHz, $CDCl_3$) δ -73.52. **IR (neat):** 2953, 2877, 1718, 1372, 1236, 1158 $cm^{-1}$. **HRMS** (ESI+ve) m/z: $[M+Na]^+$ calcd for $C_{26}H_{32}F_3NOSiNa$; 482.2097, found 482.2094.

**1-benzyl-4-methyl-5-phenyl-3-(trifluoromethyl)-3-((tripropylsilyl)methyl)-1,3-dihydro-*2H*-pyrrol-2-one (3v):** 0.2 mmol scale, ( 75.2 mg, 75%). Clear oil. Column chromatography: 1-3% EA/H. **$^1$H NMR** (500 MHz, $CDCl_3$) δ 7.42 – 7.29 (m, 3H), 7.16 – 7.09 (m, 3H), 7.08 – 7.03 (m, 2H), 6.86 – 6.81 (m, 2H), 4.95 (d, *J* = 15.2 Hz, 1H), 4.11 (d, *J* = 15.2 Hz, 1H), 1.65 (s, 3H), 1.60 – 1.56 (m, 1H), 1.42 –

1.26 (m, 7H), 0.94 (t, *J* = 7.2 Hz, 9H), 0.59 – 0.41 (m, 6H). **$^{13}$C NMR** (126 MHz, $CDCl_3$) δ 174.3, 141.0, 136.8, 129.7, 129.5, 129.2, 128.5, 128.3, 127.6, 127.2, 125.7 (q *J* = 284.68 Hz), 113.0, 57.1 (q, *J* = 25.4 Hz), 44.5, 18.7, 17.4, 15.8, 12.3, 10.6. **$^{19}$F NMR** (471 MHz, $CDCl_3$) δ -73.56. **IR** (neat): 2954, 2868, 1718, 1372, 1222, 1158 cm$^{-1}$. **HRMS** (ESI+ve) m/z: $[M+Na]^+$ calcd for $C_{29}H_{38}F_3NOSiNa$; 524.2566, found 524.2566.

**1-benzyl-4-methyl-5-phenyl-3-((tributylsilyl)methyl)-3-(trifluoromethyl)-1,3-dihydro-2*H*-pyrrol-2-one (3w):** 0.2 mmol scale, ( 88 mg, 83%). Clear oil. Column chromatography: 1-3% EA/H. **$^{1}$H NMR** (500 MHz, $CDCl_3$) δ 7.41 – 7.30 (m, 3H), 7.16 – 7.09 (m, 3H), 7.07 – 7.01 (m, 2H), 6.86 – 6.80 (m, 2H), 4.98 (d, *J* = 15.2 Hz, 1H), 4.08 (d, *J* = 15.2 Hz, 1H), 1.65 (s, 3H), 1.61 – 1.56 (m, 1H), 1.36 – 1.19 (m, 13H), 0.93 – 0.83 (m, 9H), 0.60 – 0.45 (m, 6H). **$^{13}$C NMR** (126 MHz, $CDCl_3$) δ 174.3, 141.0, 136.8, 129.6, 129.5, 129.2, 128.5, 128.3, 127.6, 127.2, 125.7 (q, *J* = 284.5 Hz), 113.0, 57.1 (q, *J* = 25.6 Hz), 44.5, 27.0, 26.9, 26.0, 13.8, 12.7, 12.4, 10.6. **$^{19}$F NMR** (471 MHz, $CDCl_3$) δ -73.50. **IR** (neat): 2923, 2871, 1719, 1373, 1225, 1162 cm$^{-1}$. **HRMS** (ESI+ve) m/z: $[M+Na]^+$ calcd for $C_{32}H_{44}F_3NOSiNa$; 566.3036, found 566.3029.

**1-benzyl-4-methyl-5-phenyl-3-(trifluoromethyl)-3-((triisopropylsilyl)methyl)-1,3-dihydro-2*H*-pyrrol-2-one (3x):** 0.2 mmol scale, (61.3 mg, 61%). Clear oil. Column chromatography: 1-3% EA/H. **$^{1}$H NMR** (500 MHz, $CDCl_3$) δ 7.41 – 7.30 (m, 3H), 7.16 – 7.10 (m, 3H), 7.07 – 7.02 (m, 2H), 6.87 – 6.82 (m, 2H), 4.93 (d, *J* = 15.2 Hz, 1H), 4.12 (d, *J* = 15.2 Hz, 1H), 1.72 (s, 3H), 1.67 (d, *J* = 14.9 Hz, 1H), 1.28 (d, *J* = 14.9 Hz, 1H), 1.12 – 1.05 (m, 21H). **$^{13}$C NMR** (126 MHz, $CDCl_3$) δ 174.4, 141.5, 136.8, 129.7, 129.6, 129.2, 128.6, 128.3, 127.7, 127.2, 127.1, 125.9 (q, *J* = 284.9 Hz), 112.9, 57.3 (q, *J* = 24.8 Hz), 44.7, 19.0 (2C), 11.8, 10.8, 8.9. **$^{19}$F NMR** (471 MHz, $CDCl_3$) δ -73.68. **IR** (neat): 2943, 2867, 1718, 1371, 1211, 1158 cm$^{-1}$. **HRMS** (ESI+ve) m/z: $[M+Na]^+$ calcd for $C_{29}H_{38}F_3NOSiNa$; 524.2566, found 524.2577.

**1-benzyl-4-methyl-5-phenyl-3-((tribenzylsilyl)methyl)-3-(trifluoromethyl)-1,3-dihydro-2*H*-pyrrol-2-one (3y):** 0.2 mmol scale, (56.9 mg, 44%). White solid. Column chromatography: 1-3% EA/H. **M.P.**: 70-72 °C. $^{1}$H NMR (500 MHz, $CDCl_3$) δ 7.41 – 7.36 (m, 1H), 7.36 – 7.31 (m, 2H), 7.23 (t, *J* = 7.5 Hz, 6H), 7.18 – 7.14 (m, 3H), 7.14 – 7.09 (m, 3H), 7.05 (d, *J* = 7.3 Hz, 2H), 6.99 (d, *J* = 7.5 Hz, 6H), 6.93 – 6.89 (m, 2H), 4.94 (d, *J* = 15.2 Hz, 1H), 4.33 (d, *J* = 15.2 Hz, 1H), 2.09 (s, 6H), 1.63 – 1.58 (m, 1H), 1.32 (s, 3H), 1.07 (d, *J* = 14.9 Hz, 1H). **$^{13}$C NMR** (126 MHz, $CDCl_3$) δ 174.5, 141.4, 138.4, 136.6, 129.4 (2C), 129.3, 129.0, 128.7, 128.5, 128.5, 127.9, 127.5, 125.4 (q, *J* = 285.8 Hz), 124.7, 113.0, 57.0 (q, *J* = 25.6 Hz), 44.8, 21.2, 9.7, 8.9. **$^{19}$F NMR** (471 MHz, $CDCl_3$) δ -73.77. **IR** (neat): 2918, 2899, 2247, 1706, 1667, 1207 $cm^{-1}$. **HRMS** (ESI+ve) m/z: $[M+Na]^+$ calcd for $C_{41}H_{38}F_3NOSiNa$; 668.2566, found 668.2565.

**1-benzyl-3-((benzyldimethylsilyl)methyl)-4-methyl-5-phenyl-3-(trifluoromethyl)-1,3-dihydro-2*H*-pyrrol-2-one (3z):** 0.2 mmol scale, ( 63.2 mg, 64%). Yellowish oil. Column chromatography: 1-3% EA/H. **$^{1}$H NMR** (500 MHz, $CDCl_3$) δ 7.42 – 7.32 (m, 3H), 7.26 – 7.19 (m, 2H), 7.16 – 7.04 (m, 6H), 6.99 (d, *J* = 7.4 Hz, 2H), 6.87 – 6.81 (m, 2H), 4.98 (d, *J* = 15.3 Hz, 1H), 4.15 (d, *J* = 15.3 Hz, 1H), 2.10 (dd, *J* = 21.5, 13.6 Hz, 2H), 1.70 – 1.61 (m, 4H, (1H, $CH_2$ & 3H,$CH_3$)), 1.34 (d, *J* = 14.3 Hz, 1H), 0.00 (s, 3H), -0.05 (s, 3H). **$^{13}$C NMR** (126 MHz, $CDCl_3$) δ 174.2 (2C), 141.3, 139.2, 136.6, 129.5, 129.4, 129.3, 128.9, 128.6, 128.4, 128.3 (2C), 127.6, 127.3, 125.5 (q, *J* = 285.1 Hz) 124.4, 112.9, 57.0 (q, *J* = 25.9 Hz), 44.6, 26.1, 15.1, 10.6, -2.5, -2.7. **$^{19}$F NMR** (471 MHz, $CDCl_3$) δ -73.54. **IR** (neat): 3057, 2924, 1715, 1513, 1372, 1160 $cm^{-1}$. **HRMS** (ESI+ve) m/z: $[M+Na]^+$ calcd for $C_{29}H_{30}F_3NOSiNa$; 516.1941, found 516.1934.

**1-benzyl-3-((dimethyl(phenyl)silyl)methyl)-4-methyl-5-phenyl-3-(trifluoromethyl)-1,3-dihydro-2*H*-pyrrol-2-one (3aa):** 0.2 mmol scale, ( 71.7 mg, 77%). Clear oil. Column chromatography: 1-3% EA/H. **$^{1}$H NMR** (500 MHz, $CDCl_3$) δ 7.56 – 7.48 (m, 2H), 7.40 – 7.28 (m, 6H), 7.16 – 7.08 (m, 3H), 6.99 (d, $J$ = 7.3 Hz, 2H), 6.83 – 6.76 (m, 2H), 4.79 (d, $J$ = 15.4 Hz, 1H), 3.89 (d, $J$ = 15.4 Hz, 1H), 1.85 (d, $J$ = 14.5 Hz, 1H), 1.54 (d, $J$ = 14.5 Hz, 1H), 1.48 (s, 3H), 0.34 (s, 3H), 0.32 (s, 3H). $^{13}$C NMR (126 MHz, $CDCl_3$) δ 173.9, 141.3, 137.7, 136.8, 133.8, 129.5, 129.5, 129.4, 129.1, 128.5, 128.3, 127.8, 127.5, 127.2, 125.6 (q, $J$ = 284.5 Hz), 112.6, 57.0 (q, $J$ = 25.9 Hz), 44.4, 16.2, 10.5, -1.8, -2.1. $^{19}$F NMR (471 MHz, $CDCl_3$) δ -73.54. **IR** (neat): 2955, 2925, 1715, 1373, 1160, 1112 cm$^{-1}$. **HRMS** (ESI+ve) m/z: $[M+Na]^+$ calcd for $C_{28}H_{28}F_3NOSiNa$; 502.1784, found 502.1782.

**1-benzyl-4-methyl-3-((methyldiphenylsilyl)methyl)-5-phenyl-3-(trifluoromethyl)-1,3-dihydro-2*H*-pyrrol-2-one (3ab):** 0.2 mmol scale, (68.3 mg, 63%). Yellowish oil. column Chromatography: 1-3% EA/H. **$^1$H NMR** (500 MHz, $CDCl_3$) δ 7.64 – 7.55 (m, 2H), 7.54 – 7.49 (m, 2H), 7.43 – 7.23 (m, 9H), 7.12 – 7.05 (m, 3H), 6.89 – 6.84 (m, 2H), 6.77 – 6.71 (m, 2H), 4.61 (d, $J$ = 15.5 Hz, 1H), 3.68 (d, $J$ = 15.5 Hz, 1H), 2.22 (d, $J$ = 14.5 Hz, 1H), 1.85 (d, $J$ = 14.5 Hz, 1H), 1.37 (s, 3H), 0.60 (s, 3H). **$^{13}$C NMR** (126 MHz, $CDCl_3$) δ 173.5, 141.4, 136.6, 136.2, 135.3, 134.7, 134.4, 129.6, 129.5, 129.3, 129.2, 129.0, 128.2, 128.1, 127.8, 127.7, 127.2, 127.0, 125.5 (q, $J$ = 283.5 Hz), 112.2, 56.8 (q, $J$ = 25.7 Hz), 44.1, 14.6, 10.4, -3.8. **$^{19}$F NMR** (471 MHz, $CDCl_3$) δ -73.46. **IR** (neat): 3068, 2924, 1715,1428, 1239, 1152 cm$^{-1}$. **HRMS** (ESI+ve) m/z: $[M+Na]^+$ calcd for $C_{33}H_{30}F_3NOSiNa$; 564.1941, found 564.1927.

**1-benzyl-3-((*tert*-butyldiphenylsilyl)methyl)-4-methyl-5-phenyl-3-(trifluoromethyl)-1,3-dihydro-2*H*-pyrrol-2-one (3ac):** 0.2 mmol scale, ( 59.6 mg, 51%). Yellowish oil. Column chromatography: 1-3% EA/H. **$^1$H NMR** (500 MHz, $CDCl_3$) δ 7.74 (d, $J$ = 7.1 Hz, 2H), 7.65 (d, $J$ = 7.1 Hz, 2H), 7.48 – 7.32 (m, 4H), 7.31 – 7.20 (m, 3H), 7.19 – 7.11 (m, 2H), 7.11 – 7.01 (m, 3H), 6.65 (d, $J$ = 7.1 Hz, 2H), 6.52 (d, $J$ = 7.3 Hz, 2H), 4.45 (d, $J$ = 15.6 Hz, 1H), 3.34 (d, $J$ = 15.6 Hz, 1H), 2.27 (d, $J$ = 14.9 Hz, 1H), 1.92 (d, $J$ = 14.9 Hz, 1H), 1.27 (s, 3H), 1.02 (s, 9H). **$^{13}$C NMR** (126 MHz, $CDCl_3$) δ 173.9, 141.6, 137.3, 137.1, 136.7, 134.9, 133.6, 132.2, 129.6, 129.6, 129.5, 129.2, 128.8, 128.2, 127.9, 127.5, 127.3, 127.2, 126.9,125.8 (q, $J$ = 286.0 Hz), 111.8, 57.3 (q, $J$ = 24.9 Hz), 44.3, 27.7, 18.7, 10.6, 8.9. **$^{19}$F NMR** (471 MHz, $CDCl_3$) δ -73.69. **IR** (neat): 3058, 2929, 1714, 1373, 1243, 1158 cm$^{-1}$. **HRMS** (ESI+ve) m/z: $[M+Na]^+$ calcd for $C_{36}H_{36}F_3NOSiNa$; 606.2409, found 606.2409.

**1-benzyl-4-methyl-5-phenyl-3-(trifluoromethyl)-3-((triphenylsilyl)methyl)-1,3-dihydro-2*H*-pyrrol-2-one (3ad):** 0.2 mmol scale, ( 70.1 mg, 58%). White solid. Column chromatography: 1-3% EA/H. **M.P.**: 107-109 °C. **$^1$H NMR** (500 MHz, $CDCl_3$) δ 7.64 – 7.57 (m, 6H), 7.42 – 7.37 (m, 3H), 7.36 – 7.28 (m, 6H), 7.27 – 7.20 (m, 3H), 7.11 – 7.01 (m, 3H), 6.77 – 6.70 (m, 2H), 6.68 – 6.60 (m, 2H), 4.36 (d, $J$ = 15.7 Hz, 1H), 3.41 (d, $J$ = 15.7 Hz, 1H), 2.58 (d, $J$ = 14.8 Hz, 1H), 2.16 (d, $J$ = 14.8 Hz, 1H), 1.33 (s, 3H). **$^{13}$C NMR** (126 MHz, $CDCl_3$) δ 173.6, 141.8, 136.9, 136.2, 133.8, 129.8, 129.5, 129.3, 129.0, 128.3, 128.2, 127.9, 127.2, 127.0, 126.9, 125.7 (q, $J$ = 285.3 Hz), 124.6, 112.1, 57.5, 57.3, 57.2 (q, $J$ = 25.3 Hz), 57.1, 56.9, 44.2, 13.2, 10.9. **$^{19}$F NMR** (471 MHz, $CDCl_3$) δ -73.59. **IR** (neat): 2924, 2859, 1709, 1428, 1371, 1158 cm$^{-1}$. **HRMS** (ESI+ve) m/z: $[M+Na]^+$ calcd for $C_{38}H_{32}F_3NOSiNa$; 626.2097, found 626.2108.

**1-benzyl-3-((1,1,1,3,3,3-hexamethyl-2-(trimethylsilyl)trisilan-2-yl)methyl)-4-methyl-5-phenyl-3-(trifluoromethyl)-1,3-dihydro-2*H*-pyrrol-2-one (3ae):** 0.2 mmol scale, ( 113.7 mg, 96%). Clear oil. Column chromatography: 1-3% EA/H. **$^1$H NMR** (500 MHz, $CDCl_3$) δ 7.40 – 7.27 (m, 3H), 7.16 – 7.02 (m, 5H), 6.86 – 6.73 (m, 2H), 5.06 (d, $J$ = 15.3 Hz, 1H), 4.07 (d, $J$ = 15.3 Hz, 1H), 1.85 (d, $J$ = 14.6 Hz, 1H), 1.70 (s, 3H), 1.42 (d, $J$ = 14.6 Hz, 1H). **$^{13}$C NMR** (126 MHz, $CDCl_3$) δ 174.0, 141.6, 136.8, 129.9, 129.5, 129.1, 128.4, 128.2, 127.5, 127.2, 125.7 (q, $J$ = 283.3 Hz), 112.9, 58.4 (q, $J$ = 24.1 Hz), 44.7, 10.7, 8.5, 1.7. **$^{19}$F NMR** (471 MHz, $CDCl_3$) δ -72.38. **IR** (neat): 2948, 2893, 1718, 1372, 1177 cm$^{-1}$. **HRMS** (ESI+ve) m/z: $[M-SiMe_3]^+$ calcd for $C_{26}H_{35}F_3NOSi_3$; 518.1973, found 518.1975.

**1-benzyl-3-(((4-(dimethylsilyl)phenyl)dimethylsilyl)methyl)-4-methyl-5-phenyl-3-(trifluoromethyl)-1,3-dihydro-2*H*-pyrrol-2-one**

**(3af):** 0.2 mmol scale, (46.2 mg, 43%). Clear oil. Column chromatography: 1-3% EA/H. $^{1}$H NMR (500 MHz, $CDCl_3$) δ 7.57 – 7.47 (m, 4H), 7.40 – 7.29 (m, 3H), 7.16 – 7.08 (m, 3H), 6.97 (d, *J* = 7.4 Hz, 2H), 6.83 – 6.75 (m, 2H), 4.76 (d, *J* = 15.5 Hz, 1H), 4.46 – 4.38 (m, 1H), 3.87 (d, *J* = 15.5 Hz, 1H), 1.85 (d, *J* = 14.5 Hz, 1H), 1.58 – 1.47 (m, 4H), 0.38 – 0.28 (m, 12H). **$^{13}$C NMR** (126 MHz, $CDCl_3$) δ 173.8, 141.3, 138.9, 138.7, 136.7, 133.4, 133.2, 129.5, 129.4, 129.2, 128.5, 128.3, 127.4, 127.2, 125.6 (q, *J* = 285.6), 112.6, 57.0 (q, *J* = 25.7 Hz), 44.4, 16.1, 10.6, -1.9, -2.1, -3.7. **$^{19}$F NMR** (471 MHz, $CDCl_3$) δ -73.54. **IR** (neat): 2957, 2954, 1717, 1379, 1240, 1158 cm$^{-1}$. **HRMS** (ESI+ve) m/z: $[M+Na]^+$ calcd for $C_{30}H_{34}F_3NOSi_2Na$; 560.2023, found 560.2017.

**1-benzyl-3-((diphenylsilyl)methyl)-4-methyl-5-phenyl-3-(trifluoromethyl)-1,3-dihydro-2*H*-pyrrol-2-one (3ag):** 0.2 mmol scale, (49.5 mg, 46%). Viscous oil. Column chromatography: 1-3% EA/H. **$^{1}$H NMR** (500 MHz, $CDCl_3$) δ 7.67 – 7.61 (m, 2H), 7.53 (d, *J* = 7.1 Hz, 2H), 7.46 – 7.38 (m, 4H), 7.37 – 7.32 (m, 3H), 7.32 – 7.27 (m, 2H), 7.16 – 7.08 (m, 3H), 6.89 (d, *J* = 7.4 Hz, 2H), 6.82 – 6.76 (m, 2H), 4.82 – 4.76 (m, 1H), 4.47 (d, *J* = 15.6 Hz, 1H), 3.74 (d, *J* = 15.6 Hz, 1H), 2.24 (dd, *J* = 14.6, 4.4 Hz, 1H), 1.90 (dd, *J* = 14.6, 4.4 Hz, 1H), 1.55 (s, 3H). **$^{13}$C NMR** (126 MHz, $CDCl_3$) δ 173.5, 142.0, 136.9, 135.6, 135.0, 133.4, 132.3, 130.2, 130.1, 129.7, 129.3, 129.1, 128.3 (2C), 128.2, 128.1, 127.5, 127.1, 125.5 (d, *J* = 284.1 Hz), 111.8, 56.8 (q, *J* = 26.2 Hz), 44.1, 13.3, 10.5. **$^{19}$F NMR** (471 MHz, $CDCl_3$) δ -73.15. **IR** (neat): 2925, 2854, 1710, 1427, 1189, 1152 cm$^{-1}$. **HRMS** (ESI+ve) m/z: $[M+Na]^+$ calcd for $C_{32}H_{28}F_3NOSiNa$; 550.1784, found 550.1779.

**1-benzyl-3-((*tert*-butyldimethylsilyl)methyl)-4-methyl-5-(4-((((*R*)-2,5,7,8-tetramethyl-2-((4*R*,8*R*)-4,8,12-trimethyltridecyl)chroman-6-yl)oxy)methyl)phenyl)-3-(trifluoromethyl)-1,3-dihydro-2*H*-pyrrol-2-one (3ah):** 0.2 mmol scale, (33.4 mg, 37%). Clear oil. Column chromatography: 1-3% EA/H. **$^{1}$H NMR** (500 MHz, $CDCl_3$) δ 7.50 – 7.44 (m, 2H), 7.18 – 7.13 (m, 3H), 7.13 – 7.08 (m, 2H), 6.92 – 6.87 (m, 2H), 4.96 (d, *J* = 15.4 Hz, 1H), 4.72 (s, 2H), 4.16 (d, *J* = 15.4 Hz, 1H), 2.63 – 2.56 (m, 2H), 2.21 (s, 3H), 2.18 – 2.14 (m, 3H), 2.11 (s, 3H), 1.88

– 1.73 (m, 2H), 1.68 (s, 3H), 1.63 – 1.00 (m, 26H), 0.92 – 0.80 (m, 21H), -0.01 (s, 3H), -0.05 (s, 3H). **$^{13}$C NMR** (126 MHz, $CDCl_3$) δ 174.2, 148.2, 148.0, 141.1, 139.3, 136.8, 129.6, 128.9, 128.4, 127.9, 127.8, 127.6, 127.3, 125.9, 125.7 (q, *J* = 285.9 Hz), 123.2, 117.8, 113.0, 75.0, 74.2, 57.0 (q, *J* = 25.7 Hz), 44.6, 40.1, 39.5, 37.6 (2C), 37.5, 37.4, 32.9, 32.8, 31.4, 29.8, 28.1, 26.3, 24.9, 24.5, 24.0, 22.8, 22.7, 21.1, 20.8, 19.9, 19.8, 16.7, 13.0, 12.1, 11.9, 11.4, 10.7, -4.8, -5.6. **$^{19}$F NMR** (471 MHz, $CDCl_3$) δ -73.55. **IR** (neat): 2951, 2857, 1721, 1456, 1368, 1162 cm$^{-1}$. **HRMS** (ESI+ve) m/z: [M+Na]$^+$ calcd for $C_{56}H_{82}F_3NO_3SiNa$; 924.5908, found 924.5906.

**4-(1-benzyl-4-((*tert*-butyldimethylsilyl)methyl)-3-methyl-5-oxo-4-(trifluoromethyl)-4,5-dihydro-1*H*-pyrrol-2-yl)benzyl (2*S*)-2-(4-isobutylphenyl)propanoate (3ai):** 0.2 mmol scale, (88.2 mg, 65%). Clear oil. Column chromatography: 5-10% EA/H. **$^1$H NMR** (500 MHz, $CDCl_3$) δ 7.23 – 7.19 (m, 2H), 7.18 – 7.06 (m, 7H), 6.99 – 6.94 (m, 2H), 6.83 – 6.78 (m, 2H), 5.17 – 5.07 (m, 2H), 4.94 (d, *J* = 15.3 Hz, 1H), 4.07 (d, *J* = 15.3 Hz, 1H), 3.78 (q, *J* = 7.2 Hz, 1H), 2.44 (d, *J* = 7.2 Hz, 2H), 1.89 – 1.79 (m, 1H), 1.64 (s, 3H), 1.61 – 1.57 (m, 1H), 1.53 (d, *J* = 7.2 Hz, 3H), 1.30 – 1.25 (m, 1H), 0.92 – 0.87 (m, 15H), -0.02 (s, 3H), -0.07 (s, 3H). **$^{13}$C NMR** (126 MHz, $CDCl_3$) δ 174.5, 174.1, 140.9, 140.8, 137.6, 137.5, 137.4, 136.6, 129.5 (2C), 129.2, 128.3, 127.6 (3C), 127.3, 127.3, 125.6 (q, *J* = 286.2 Hz), 113.0, 65.6, 57.0 (q, *J* = 25.5 Hz), 45.2, 45.2, 45.1, 44.6, 30.3, 26.2, 22.4, 18.5, 18.4, 16.7, 11.4, 10.7, -4.8, -5.6. **$^{19}$F NMR** (471 MHz, $CDCl_3$) δ -73.59. **IR** (neat): 2928, 2860, 1719, 1668, 1464, 1373, 1160 cm$^{-1}$. **HRMS** (ESI+ve) m/z: [M+Na]$^+$ calcd for $C_{40}H_{50}F_3NO_3SiNa$ [M+Na]$^+$ : 700.3404, found 700.3399.

**4-(1-benzyl-4-((*tert*-butyldimethylsilyl)methyl)-3-methyl-5-oxo-4-(trifluoromethyl)-4,5-dihydro-1*H*-pyrrol-2-yl)benzyl 3-(4,5-diphenyloxazol-2-yl)propanoate (3aj):** 0 .2 mmol scale, (61.3 mg, 40%). Clear oil. Column chromatography: 10-20% EA/H. **$^1$H NMR** (500 MHz, $CDCl_3$) δ 7.65 – 7.60 (m, 2H), 7.58 – 7.53 (m, 2H), 7.38 – 7.27 (m, 8H), 7.15 – 7.10 (m, 3H), 7.01 – 6.95 (m, 2H), 6.86 – 6.79 (m, 2H), 5.20 (s, 2H), 4.93 (d, $J$ = 15.4 Hz, 1H), 4.06 (d, $J$ = 15.4 Hz, 1H), 3.23 (t, $J$ = 7.4 Hz, 2H), 3.02 (t, $J$ = 7.4 Hz, 2H), 1.65 – 1.56 (m, 4H), 1.30 – 1.26 (m, 1H), 0.89 (s, 9H), -0.02 (s, 3H), -0.08 (s, 3H). **$^{13}$C NMR** (126 MHz, $CDCl_3$) δ 176.1, 174.1, 172.5 (2C), 171.9, 161.7, 145.6, 140.8, 137.0, 136.6, 135.2, 133.8, 133.4, 132.5, 129.7, 129.5, 129.4, 129.0, 129.0, 128.8, 128.7, 128.6, 128.3 (2C), 128.2, 127.9 (2C), 127.6, 127.3, 126.5, 125.6 (q, $J$ = 285.0 Hz), 113.1, 65.9, 57.0 (q, $J$ = 25.6 Hz), 44.6, 31.2, 26.2, 23.6, 16.7, 11.4, 10.7, -4.8, -5.6. $^{19}$F NMR (471 MHz, $CDCl_3$) δ -73.56. **IR** (neat): 2926, 2858, 1715, 1672, 1374, 1206, 1157 cm$^{-1}$. **HRMS** (ESI+ve) m/z: $[M+Na]^+$ calcd for $C_{45}H_{47}F_3N_2O_4SiNa$; 787.3149, found 787.3149.

**4-(1-benzyl-4-((*tert*-butyldimethylsilyl)methyl)-3-methyl-5-oxo-4-(trifluoromethyl)-4,5-dihydro-1*H*-pyrrol-2-yl)benzyl 2-(11-oxo-6,11-dihydrodibenzo[*b,e*]oxepin-2-yl)acetate (3ak):** 0 .2 mmol scale, (77 mg, 52%). Viscous gum. Column chromatography: 10-20% EA/H. **$^1$H NMR** (500 MHz, $CDCl_3$) δ 8.17 (s, 1H), 7.92 – 7.87 (m, 1H), 7.62 – 7.55 (m, 1H), 7.53 – 7.42 (m, 2H), 7.41 – 7.36 (m, 1H), 7.34 – 7.28 (m, 2H), 7.17 – 7.08 (m, 3H), 7.08 – 7.03 (m, 3H), 6.85 – 6.80 (m, 2H), 5.19 (s, 2H), 5.18 (s, 2H), 4.96 (d, $J$ = 15.3 Hz, 1H), 4.11 (d, $J$ = 15.3 Hz, 1H), 3.74 (s, 2H), 1.66 (s, 3H), 1.64 – 1.60 (m, 1H), 1.32 – 1.25 (m, 1H), 0.90 (s, 9H), 0.00 (s, 3H), -0.05 (s, 3H). **$^{13}$C NMR** (126 MHz, $CDCl_3$) δ 190.8, 174.1, 171.2, 160.6, 140.8, 140.4, 137.0, 136.6, 136.4, 135.6, 132.9, 132.6, 129.7, 129.5 (2C), 129.40 128.3, 128.1, 127.9, 127.6, 127.3, 125.6 (q, $J$ = 285.0 Hz), 125.3, 121.2, 113.1, 73.7, 66.1, 57.0 (q, $J$ = 25.4 Hz), 44.6, 40.3, 26.2, 16.7, 11.4, 10.7, -4.8, -5.6. **$^{19}$F NMR** (471 MHz, $CDCl_3$) δ -73.57. **IR** (neat): 3065, 2953, 2857, 1716, 1649, 1375, 1284, 1138 cm$^{-1}$. **HRMS** (ESI+ve) m/z: $[M+Na]^+$ calcd for $C_{43}H_{44}F_3NO_5SiNa$; 762.2833, found 762.2817.

**4-(1-benzyl-4-((*tert*-butyldimethylsilyl)methyl)-3-methyl-5-oxo-4-(trifluoromethyl)-4,5-dihydro-1*H*-pyrrol-2-yl)benzyl 5-(2,5-dimethylphenoxy)-2,2-dimethylpentanoate (3al):** 0.2 mmol scale, (65 mg, 45%). Clear oil. Column chromatography: 5-10% EA/H. **$^1$H NMR**

(500 MHz, $CDCl_3$) δ 7.31 (d, *J* = 7.8 Hz, 2H), 7.16 – 7.09 (m, 3H), 7.04 (d, *J* = 7.8 Hz, 2H), 7.02 – 6.97 (m, 1H), 6.86 – 6.80 (m, 2H), 6.69 – 6.63 (m, 1H), 6.59 (s, 1H), 5.13 (s, 2H), 4.96 (d, *J* = 15.3 Hz, 1H), 4.09 (d, *J* = 15.3 Hz, 1H), 3.94 – 3.87 (m, 2H), 2.30 (s, 3H), 2.15 (s, 3H), 1.82 – 1.71 (m, 4H), 1.65 (s, 3H), 1.63 – 1.56 (m, 1H), 1.31 – 1.24 (m, 7H), 0.89 (s, 9H), -0.01 (s, 3H), -0.06 (s, 3H). **$^{13}$C NMR** (126 MHz, $CDCl_3$) δ 177.5, 174.1, 157.0, 140.8, 137.6, 136.6 (2C), 130.4, 129.6, 129.3, 128.3, 127.8, 127.6, 127.3, 125.6 (q, *J* = 284.5 Hz), 123.6, 120.9, 113.1, 112.0, 67.9, 65.6, 57.0 (q, *J* = 25.6 Hz), 44.6, 42.3, 37.2, 26.2, 25.3, 25.2, 21.5, 16.7, 15.8, 11.4, 10.7, -4.8, -5.6. **$^{19}$F NMR** (471 MHz, $CDCl_3$) δ -73.57. **IR** (neat): 2926, 2859, 1720, 1373, 1264, 1160 cm$^{-1}$. **HRMS** (ESI+ve) m/z: $[M+Na]^+$ calcd for $C_{42}H_{54}F_3NO_4SiNa$; 744.3666, found 744.3669.

**4-(1-benzyl-4-((*tert*-butyldimethylsilyl)methyl)-3-methyl-5-oxo-4-(trifluoromethyl)-4,5-dihydro-1*H*-pyrrol-2-yl)benzyl (2*S*)-2-(6-methoxynaphthalen-2-yl)propanoate (3am):** 0.2 mmol scale, (64.6 mg, 46%). Viscous gum. Column chromatography: 5-10% EA/H. **$^1$H NMR** (500 MHz, $CDCl_3$) δ 7.71 – 7.65 (m, 3H), 7.43 – 7.37 (m, 1H), 7.20 – 7.05 (m, 7H), 6.98 – 6.92 (m, 2H), 6.80 – 6.75 (m, 2H), 5.13 (s, 2H), 4.92 (d, *J* = 15.4 Hz, 1H), 4.04 (d, *J* = 15.4 Hz, 1H), 3.98 – 3.89 (m, 4H), 1.64 – 1.57 (m, 7H), 1.29 – 1.25 (m, 1H), 0.89 (s, 9H), -0.03 (s, 3H), -0.08 (s, 3H). **$^{13}$C NMR** (126 MHz, $CDCl_3$) δ 174.4, 174.1, 157.8, 140.8, 137.2, 136.6, 135.4, 135.4, 133.8, 129.5, 129.3, 129.2, 129.0, 128.3, 127.8 (2C), 127.6 (2C), 127.2, 126.3, 126.1, 125.6 (q, *J* = 283.3 Hz), 119.2, 113.0, 105.6, 65.8, 57.0 (q, *J* = 25.6 Hz), 55.3, 45.5 (2C), 44.5, 26.2, 18.6, 18.5, 16.7, 11.4, 10.6, -4.9, -5.7. **$^{19}$F NMR** (471 MHz, $CDCl_3$) δ -73.59. **IR** (neat): 2928, 2859, 1709, 1373, 1219, 1159 cm$^{-1}$. **HRMS** (ESI+ve) m/z: $[M+Na]^+$ calcd for $C_{41}H_{46}F_3NO_4SiNa$; 724.3040, found 724.3039.

**1-benzyl-3-((*tert*-butyldimethylsilyl)methyl)-5-hydroxy-4-methyl-5-phenyl-3-(trifluoromethyl)pyrrolidin-2-one (3a'):** 0.2 mmol scale, (55.4 mg, 58 %). Viscous oil. Column chromatography: 1-5% EA/H. **$^1$H**

**NMR** (500 MHz, $CDCl_3$) δ 7.45 – 7.35 (m, 3H), 7.32 – 7.26 (m, 2H), 7.26 – 7.17 (m, 3H), 7.00 – 6.94 (m, 2H), 4.95 (d, *J* = 14.7 Hz, 1H), 3.83 (d, *J* = 14.6 Hz, 1H), 2.67 (q, *J* = 7.0 Hz, 1H), 1.95 (d, *J* = 1.2 Hz, 1H), 1.30 (d, *J* = 15.4 Hz, 1H), 1.10 (d, *J* = 15.4 Hz, 1H), 0.94 (d, *J* = 7.0 Hz, 3H), 0.87 (s, 9H), 0.21 (s, 3H), 0.15 (s, 3H). **$^{13}$C NMR** (126 MHz, $CDCl_3$) δ 172.6, 140.4, 137.0, 129.0 (2C), 128.9, 128.8, 128.2, 126.5, 124.8 (q, *J* = 282.6 Hz), 92.6, 53.43 (q, *J* = 24.9 Hz), 47.7, 43.9, 26.5, 17.3, 12.6, 7.52, -4.73 (2C), -4.80 (2C). **$^{19}$F NMR** (471 MHz, $CDCl_3$) δ -71.90. **IR** (neat): 3419, 2953, 2856, 1682, 1408, 1359, 1215, 1175 $cm^{-1}$. **HRMS** (ESI+ve) m/z: $[M+Na]^+$ calcd for $C_{26}H_{34}F_3NO_2SiNa$; 500.2203, found 500.2185.

### 3.9.9 General procedure for the germylation of 3-aza-1,5-dienes

To an oven-dried 10 mL Schlenk tube equipped with a magnetic stir bar were added 3-aza-1,5-dienes **1** (0.2 mmol), hydrogermane **4** (0.3 mmol, 1.5 equiv. for **4a**, or 0.4 mmol, 2 equiv. for **4b**/**4c**), 1 mol% 4DPAIPN (1.6 mg, 0.002 mmol), 1.5 equivalent of hydrogen atom transfer reagent (HATR) (0.3 mmol, 117.7 mg) and 100 mg 4Å molecular sieves (powder and heat gun dried). The reaction tube was sealed and placed under an argon atmosphere, then 1 mL *α*,*α*,*α*-trifluorotoluene (dried over 4Å granules molecular sieves) was added *via* syringe, the reaction mixture was then degassed *via* freeze pump thaw (x 3 times) and refilled with argon. The sealed reaction tube was then placed inside the aluminium block fitted with blue LEDs (λ = 455 nm) and irradiated for 1 hour. After the reaction was completed, the mixture was filtered using dichloromethane and then evaporated under reduced pressure. The crude product was then purified by flash column chromatography on silica gel (mesh 100-200) using a gradient elution with hexane/ethyl acetate (50:1 to 5:1), which yielded the germylation product 5.

### 3.9.10 Characterization data of 5a-5aj and 6

**1-benzyl-4-methyl-5-phenyl-3-(trifluoromethyl)-3-((triphenylgermyl)methyl)-1,3-dihydro-2*H*-pyrrol-2-one (5a):** 0.2 mmol scale, (127.1 mg, 98%). White Solid. Column Chromatography: 1-5% EA/H. **M.P.**: 120-122 °C. **$^{1}$H NMR** (500 MHz, $CDCl_3$) δ 7.57 – 7.50 (m, 6H), 7.40 – 7.18 (m, 12H), 7.09 – 6.99 (m, 3H), 6.70 – 6.62 (m, 4H), 4.39 (d, $J$ = 15.6 Hz, 1H), 3.31 (d, $J$ = 15.6 Hz, 1H), 2.61 (d, $J$ = 13.7 Hz, 1H), 2.23 (d, $J$ = 13.7 Hz, 1H), 1.43 (s, 3H). **$^{13}$C NMR** (126 MHz, $CDCl_3$) δ 173.6, 141.9, 136.9, 136.0, 135.3, 129.5, 129.2 (2C), 129.0, 128.3, 128.2, 128.1, 127.2, 127.0, 125.7 (q, $J$ = 285.6 Hz), 112.0, 57.5 (q, $J$ = 25.3 Hz), 44.1, 13.8, 10.8. **$^{19}$F NMR** (471 MHz, $CDCl_3$) δ -73.2. **IR** (neat): 2922, 2858, 1704, 1432, 1377, 1152 $cm^{-1}$. **HRMS** (ESI+ve) m/z: $[M+Na]^+$ calcd for $C_{38}H_{32}F_3NOGeNa$; 672.1539, found 672.1541.

**1-benzyl-4-methyl-5-(*p*-tolyl)-3-(trifluoromethyl)-3-((triphenylgermyl)methyl)-1,3-dihydro-2*H*-pyrrol-2-one (5b):** 0.2 mmol scale, (114 mg, 86%). White solid. Column chromatography: 1-5% EA/H. **M.P.**: 141-143 °C. **$^{1}$H NMR** (500 MHz, $CDCl_3$) δ 7.57 – 7.51 (m, 6H), 7.42 – 7.31 (m, 9H), 7.12 – 7.01 (m, 5H), 6.72 – 6.67 (m, 2H), 6.58 (d, $J$ = 7.7 Hz, 2H), 4.32 (d, $J$ = 15.7 Hz, 1H), 3.33 (d, $J$ = 15.7 Hz, 1H), 2.60 (d, $J$ = 13.8 Hz, 1H), 2.34 (s, 3H), 2.23 (d, $J$ = 13.8 Hz, 1H), 1.44 (s, 3H). **$^{13}$C NMR** (126 MHz, $CDCl_3$) δ 173.6, 142.0, 138.9, 137.0, 136.0, 135.3, 129.4, 129.2, 128.8, 128.2 (2C), 127.1, 126.9, 126.1, 125.7 (q, $J$ = 286.2 Hz), 111.6, 57.4 (q, $J$ = 25.2 Hz), 44.0, 21.4, 13.8, 10.8. **$^{19}$F NMR** (471 MHz, $CDCl_3$) δ -73.23. **IR** (neat): 2924, 2859, 1718, 1430, 1351, 1160 $cm^{-1}$. **HRMS** (ESI+ve) m/z: $[M+Na]^+$ calcd for $C_{39}H_{34}F_3NOGeNa$; 686.1696, found 686.1697.

**1-benzyl-5-(4-fluorophenyl)-4-methyl-3-(trifluoromethyl)-3-((triphenylgermyl)methyl)-1,3-dihydro-2*H*-pyrrol-2-one (5c):** 0.2 mmol scale, (117.3 mg, 88%). White solid. Column chromatography: 1-5% EA/H. **M.P.**: 152-154 °C. **$^{1}$H NMR** (500 MHz, $CDCl_3$) δ 7.56 – 7.51 (m, 6H), 7.43 – 7.32 (m, 9H), 7.13 – 7.03 (m, 3H), 6.90 (t, $J$ = 8.6 Hz, 2H), 6.69 – 6.63 (m, 2H), 6.63 – 6.57 (m, 2H), 4.45 (d, $J$ = 15.7 Hz, 1H), 3.25 (d, $J$ = 15.7 Hz, 1H), 2.61 (d, $J$ = 13.8 Hz, 1H), 2.23 (d, $J$ = 13.8 Hz, 1H), 1.42 (s, 3H). **$^{13}$C NMR** (126 MHz, $CDCl_3$) δ 173.5, 162.9 (d, $J$ = 249.7 Hz), 140.9, 136.7, 136.0, 135.2, 131.5 (d, $J$ = 8.3 Hz), 129.3, 128.3 (2C), 127.1 (2C), 125.6 (q, $J$ = 286.38 Hz), 125.1 (d, $J$ = 3.5 Hz), 115.3 (d, $J$ = 21.7 Hz), 112.4, 57.5 (q, $J$ = 25.3 Hz), 44.1, 13.7, 10.8. **$^{19}$F NMR** (471 MHz, $CDCl_3$) δ -73.23, -111.44. **IR** (neat): 2945, 2862, 1706, 1433, 1221, 1153 cm$^{-1}$. **HRMS** (ESI+ve) m/z: $[M+Na]^+$ calcd for $C_{38}H_{31}F_4NOGeNa$; 690.1445, found 690.1445.

**1-benzyl-5-(4-bromophenyl)-4-methyl-3-(trifluoromethyl)-3-((triphenylgermyl)methyl)-1,3-dihydro-2*H*-pyrrol-2-one (5d):** 0.2 mmol scale, (87.3 mg, 60%). White solid. Column chromatography: 1-5% EA/H. **M.P.**: 152-154 °C. **$^1$H NMR** (500 MHz, $CDCl_3$) δ 7.56 – 7.49 (m, 6H), 7.41 – 7.31 (m, 9H), 7.18 (d, $J$ = 8.1 Hz, 1H), 7.13 – 7.03 (m, 3H), 6.67 (d, $J$ = 7.1 Hz, 2H), 6.55 (d, $J$ = 8.1 Hz, 1H), 6.48 (d, $J$ = 8.1 Hz, 1H), 4.44 (d, $J$ = 15.8 Hz, 1H), 3.25 (d, $J$ = 15.8 Hz, 1H), 2.61 (d, $J$ = 13.9 Hz, 1H), 2.23 (d, $J$ = 13.9 Hz, 1H), 1.43 (s, 3H). **$^{13}$C NMR** (126 MHz, $CDCl_3$) δ 173.5, 140.9, 136.6, 136.0, 135.2, 131.4, 131.1, 130.9, 129.3, 128.4, 128.3, 127.2, 127.1, 125.6 (q, $J$ = 285.4 Hz), 123.3, 112.6, 57.6 (q, $J$ = 25.3 Hz), 44.2, 13.6, 10.8. **$^{19}$F NMR** (471 MHz, $CDCl_3$) δ -73.22. **IR** (neat): 2922, 2865, 2360, 1709, 1430, 1158, 1056 cm$^{-1}$. **HRMS** (ESI+ve) m/z: $[M+Na]^+$ calcd for $C_{38}H_{31}BrF_3NOGeNa$; 750.0645, found 750.0634.

**1-benzyl-5-(3-chlorophenyl)-4-methyl-3-(trifluoromethyl)-3-((triphenylgermyl)methyl)-1,3-dihydro-2*H*-pyrrol-2-one (5e):** 0.2 mmol scale, (105.2 mg, 77%). White solid. Column chromatography: 1-5% EA/H. **M.P.**: 136-138 °C. **$^1$H NMR** (500 MHz, $CDCl_3$) δ 7.56 – 7.51 (m, 6H), 7.41 – 7.32 (m, 9H), 7.21 – 7.16 (m, 2H), 7.13 – 7.04 (m, 3H), 6.70 – 6.65 (m, 2H), 6.57 – 6.53 (m, 2H), 4.44 (d, $J$ = 15.7 Hz, 1H), 3.25 (d, $J$ = 15.7 Hz, 1H), 2.61 (d, $J$ = 13.8 Hz, 1H), 2.23 (d, $J$ = 13.9 Hz, 1H), 1.43 (s, 3H). **$^{13}$C NMR** (126 MHz, $CDCl_3$) δ 173.5, 140.8, 136.7, 136.0, 135.2, 135.1, 130.9, 129.3, 128.4, 128.3 (2C), 127.6, 127.2, 127.1, 125.6 (q, $J$ = 286.4 Hz), 112.6, 57.6 (q, $J$ = 25.3 Hz), 44.2, 13.6, 10.8. $^{19}$**F NMR** (471 MHz, $CDCl_3$) δ -73.22. **IR** (neat): 2922, 2858, 1709, 1430, 1377, 1162 $cm^{-1}$. **HRMS** (ESI+ve) m/z: $[M+Na]^+$ calcd for $C_{38}H_{31}ClF_3NOGeNa$; 706.1150, found 706.1146.

**1-benzyl-4,5-diphenyl-3-(trifluoromethyl)-3-((triphenylgermyl)methyl)-1,3-dihydro-2*H*-pyrrol-2-one (5f):** 0.2 mmol scale, (130.7 mg, 92%). White solid. Column chromatography: 1-5% EA/H. **M.P.**: 189-191 °C. $^{1}$**H NMR** (500 MHz, $CDCl_3$) δ 7.67 – 7.59 (m, 6H), 7.43 – 7.33 (m, 9H), 7.26 – 7.13 (m, 4H), 7.14 – 7.07 (m, 1H), 7.08 – 7.01 (m, 2H), 7.02 – 6.95 (m, 2H), 6.93 – 6.87 (m, 4H), 6.71 – 6.65 (m, 2H), 4.15 (d, $J$ = 15.9 Hz, 1H), 3.11 (d, $J$ = 15.9 Hz, 1H), 2.62 (d, $J$ = 14.0 Hz, 1H), 2.39 (d, $J$ = 14.0 Hz, 1H). $^{13}$**C NMR** (126 MHz, $CDCl_3$) δ 174.3, 145.2, 137.1, 136.1, 135.6, 132.9, 130.9, 129.8, 129.3, 128.9 (2C), 128.6, 128.3, 128.1, 127.9, 127.3, 127.1, 126.6, 125.3 (q, $J$ = 286.5 Hz), 116.1, 59.3 (q, $J$ = 24.7 Hz), 44.5, 13.0. $^{19}$**F NMR** (471 MHz, $CDCl_3$) δ -72.67. **IR** (neat): 2925, 2862, 1712, 1426, 1374, 1156 $cm^{-1}$. **HRMS** (ESI+ve) m/z: $[M+Na]^+$ calcd for $C_{43}H_{34}F_3NOGeNa$; 734.1696, found 734.1691.

**1-benzyl-4-methyl-5-phenyl-3-((triethylgermyl)methyl)-3-(trifluoromethyl)-1,3-dihydro-2*H*-pyrrol-2-one (5g):** 0.2 mmol scale, (89.8 mg, 89%). Clear oil. Column chromatography: 1-5% EA/H. $^{1}$**H NMR** (500 MHz, $CDCl_3$) δ 7.40 – 7.31 (m, 3H), 7.15 – 7.10 (m, 3H), 7.07 – 7.02 (m, 2H), 6.85 – 6.80 (m, 2H), 4.97 (d, $J$ = 15.3 Hz, 1H), 4.11 (d, $J$ = 15.3 Hz, 1H), 1.69 (d, $J$ = 13.5 Hz, 1H), 1.66 (s, 3H), 1.40 (d, $J$ = 13.5 Hz, 1H), 1.02 (t, $J$ = 7.9 Hz, 9H), 0.82 – 0.69 (m, 6H). $^{13}$**C NMR** (126 MHz, $CDCl_3$) δ 174.4, 141.0, 136.7, 129.6, 129.5, 129.2, 128.6, 128.3, 127.6, 127.2, 125.7 (q, $J$ = 284.8 Hz), 113.1, 57.5 (q, $J$ = 25.5 Hz), 44.5, 11.6, 10.5, 8.9, 4.7. $^{19}$**F NMR** (471 MHz, $CDCl_3$) δ -73.16. **IR** (neat): 2949, 2872, 1717, 1428, 1372, 1160 $cm^{-1}$. **HRMS** (ESI+ve) m/z: $[M+Na]^+$ calcd for $C_{26}H_{32}F_3NOGeNa$; 528.1539, found 528.1539.

**1-benzyl-4-methyl-5-phenyl-3-((tributylgermyl)methyl)-3-(trifluoromethyl)-1,3-dihydro-2*H*-pyrrol-2-one (5h):** 0.2 mmol scale, (88.6 mg, 88%). Clear oil. Column chromatography: 1-5% EA/H. $^{1}$**H**

**NMR** (500 MHz, $CDCl_3$) δ 7.39 – 7.30 (m, 3H), 7.15 – 7.09 (m, 3H), 7.07 – 7.02 (m, 2H), 6.85 – 6.80 (m, 2H), 4.98 (d, *J* = 15.3 Hz, 1H), 4.08 (d, *J* = 15.3 Hz, 1H), 1.69 (d, *J* = 13.5 Hz, 1H), 1.65 (s, 3H), 1.39 (d, *J* = 13.5 Hz, 1H), 1.36 – 1.27 (m, 12H), 0.92 – 0.85 (m, 9H), 0.79 – 0.67 (m, 6H). **$^{13}$C NMR** (126 MHz, $CDCl_3$) δ 174.3, 141.0, 136.8, 129.6, 129.5, 129.2, 128.5, 128.3, 127.6, 127.2, 125.8 (q, *J* = 284.7 Hz), 113.1, 57.6 (q, *J* = 25.5 Hz), 44.5, 27.3, 26.7, 13.8, 13.2, 12.4, 10.5. **$^{19}$F NMR**(471 MHz, $CDCl_3$) δ -73.16. **IR** (neat): 2923, 2870, 1719, 1430, 1372, 1161 $cm^{-1}$. **HRMS** (ESI+ve) m/z: $[M+Na]^+$ calcd for $C_{32}H_{44}F_3NOGeNa$; 612.2478 found 612.2475.

**1-benzyl-4-methyl-5-(thiophen-2-yl)-3-(trifluoromethyl)-3-((triphenylgermyl)methyl)-1,3-dihydro-2*H*-pyrrol-2-one (5i):** 0.2 mmol scale, (99.5 mg, 76%). White solid. Column chromatography: 1-5% EA/H. **M.P.**: 162-164 °C. **$^{1}$H NMR** (500 MHz, $CDCl_3$) δ 7.57 – 7.52 (m, 6H), 7.42 – 7.31 (m, 10H), 7.12 – 7.06 (m, 3H), 6.95 – 6.90 (m, 1H), 6.77 – 6.70 (m, 2H), 6.56 – 6.51 (m, 1H), 4.33 (d, *J* = 15.9 Hz, 1H), 3.36 (d, *J* = 15.9 Hz, 1H), 2.57 (d, *J* = 13.8 Hz, 1H), 2.23 (d, *J* = 13.8 Hz, 1H), 1.54 (s, 3H). **$^{13}$C NMR** (126 MHz, $CDCl_3$) δ 172.9, 136.9, 135.8, 135.5, 135.3, 130.0, 129.3, 128.8, 128.3 (2C), 127.8, 127.0, 126.9, 126.8, 125.5 (q, *J* = 285.7 Hz), 115.3, 57.7 (q, *J* = 25.4 Hz), 43.8, 13.8, 11.3. **$^{19}$F NMR** (471 MHz, $CDCl_3$) δ -73.09. **IR** (neat): 2923, 2857, 1712, 1430, 1216, 1156 $cm^{-1}$. **HRMS** (ESI+ve) m/z: $[M+Na]^+$ calcd for $C_{36}H_{30}F_3NOSGeNa$; 678.1104 found 678.1086.

**4-(1-benzyl-4-((*tert*-butyldimethylsilyl)methyl)-3-methyl-5-oxo-4-(trifluoromethyl)-4,5-dihydro-1*H*-pyrrol-2-yl)benzyl (2*S*)-2-(6-methoxynaphthalen-2-yl)propanoate (5j):** 0.2 mmol scale, (112.3 mg, 63%).Viscous gum. Column chromatography: 5-10% EA/H. **$^{1}$H NMR** (500 MHz, $CDCl_3$) δ 7.73 – 7.66 (m, 3H), 7.54 – 7.49 (m, 6H), 7.44 – 7.37 (m, 1H), 7.40 – 7.29 (m, 9H), 7.17 – 7.08 (m, 2H), 7.08 – 6.97 (m, 5H), 6.63 – 6.57 (m, 2H), 6.59 – 6.53 (m, 2H), 5.14 – 5.05 (m, 2H), 4.36 (d, *J* = 15.7 Hz, 1H), 3.94 (q, *J* = 7.3 Hz, 1H), 3.90 (d, *J* = 3.4 Hz, 3H), 3.24 (dd, *J* = 15.7, 4.2 Hz, 1H), 2.59 (d, *J* = 13.8 Hz, 1H), 2.22 (d, *J* =

13.8 Hz, 1H), 1.62 (d, $J$ = 7.3 Hz, 3H), 1.40 (s, 3H). **$^{13}$C NMR** (126 MHz, $CDCl_3$) δ 174.4, 173.5, 157.8, 141.4, 137.0, 136.7, 136.0, 135.5 (2C), 135.3, 133.8, 129.6, 129.3, 129.3, 129.0, 128.8, 128.3, 128.2, 127.3 (2C), 127.2, 127.0, 126.3, 126.1 (2C), 125.6 (q, $J$ = 285.6 Hz), 119.2, 112.2, 105.7, 65.8, 57.54 (q, $J$ = 25.3 Hz), 55.4, 45.6 (2C), 44.0, 18.66 (2C), 13.79, 10.85. **$^{19}$F NMR** (471 MHz, $CDCl_3$) δ -73.21. **IR** (neat): 2934, 2859, 1715, 1606, 1485, 1376, 1265 $cm^{-1}$. **HRMS** (ESI+ve) m/z: $[M+Na]^+$ calcd for $C_{53}H_{46}F_3NO_4GeNa$; 914.2482 found 914.2469.

***N*-(2,2-diphenylvinyl)-N,4-dimethylbenzenesulfonamide (6):**[48] White solid (92.9 mg, 85% yield); 15-20% EA/H. **$^1$H NMR** (500 MHz, $CDCl_3$) δ 7.71 (d, J = 8.3 Hz, 2H), 7.37 (d, J = 7.9 Hz, 2H), 7.28–7.16 (m, 6H), 7.13–7.08 (m, 2H), 6.87-6.82 (m, 3H), 2.56 (s, 3H), 2.48 (s, 3H); **$^{13}$C NMR** (126 MHz, CDCl3) δ 144.0, 141.3, 138.4, 134.9, 132.6, 130.3, 130.0, 128.3, 128.3, 128.0, 127.8, 127.6, 127.4, 126.0, 36.6, 21.8; **IR** (neat): 2921, 2362, 1612, 1345, 2257 $cm^{-1}$.

### 3.9.11 Procedure for scale-up silylation of 3-aza-1,5-dienes

To an oven-dried 10 mL Schlenk tube equipped with a magnetic stir bar were added *N*-benzyl-*N*-(1-phenylprop-1-en-1-yl)-2-(trifluoromethyl)acrylamide **1a** (2 mmol, 690.7 mg), $^t$BuMe$_2$SiH **2a** (6 mmol, 1 mL), 1 mol% 4DPAIPN (15.9 mg, 0.02 mmol), 1.5 equivalent of hydrogen atom transfer reagent (HATR) (3 mmol, 1.1767 g) and 1 g 4Å molecular sieves (powder and heat gun dried). The reaction tube was sealed and placed under an argon atmosphere. Then, 10 mL of *α*,*α*,*α*-trifluorotoluene (dried over 4 Å granules of molecular sieves) was added *via* syringe. The reaction mixture was then degassed *via* freeze-pump-thaw (three times) and refilled with argon. The sealed reaction tube was then placed inside the aluminium block, fitted with blue LEDs (λ = 455 nm), and irradiated for 3 hours. After the reaction was completed, the mixture was filtered using dichloromethane and then evaporated under reduced pressure. The crude product was then purified by flash column chromatography on silica gel (mesh 100-200) using a gradient elution with hexane/ethyl acetate (50:1 to 30:1), which gave the silylation product **3a** as a white solid in 78% yield (717.3 mg).

### 3.9.12 Stern-Volmer fluorescence quenching experiments

A $2.0\times10^{-4}$ M stock solution was prepared by dissolving 2.4 mg 4DPAIPN photocatalyst in 15 mL of spectroscopic grade acetonitrile. The quenching experiment was performed by taking an appropriate volume of 4DPAIPN photocatalyst from the stock solution, along with different concentrations of the quencher. The Emission intensity was observed at 536 nm with an excitation wavelength of 360 nm.

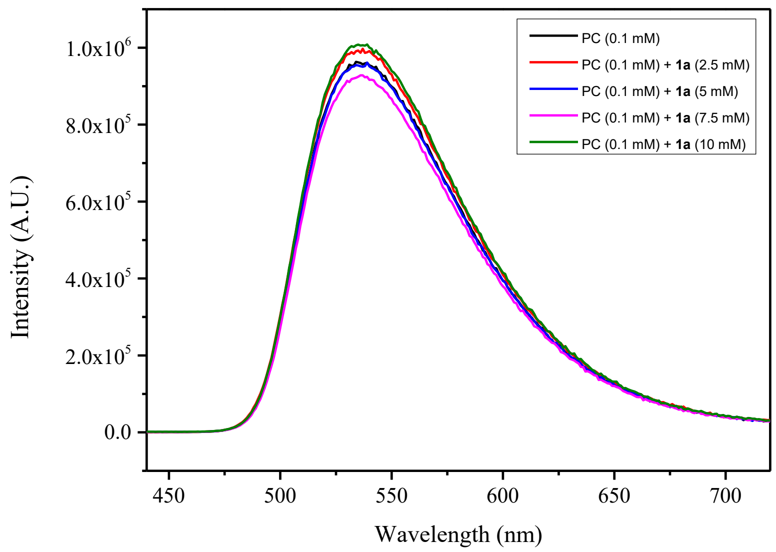

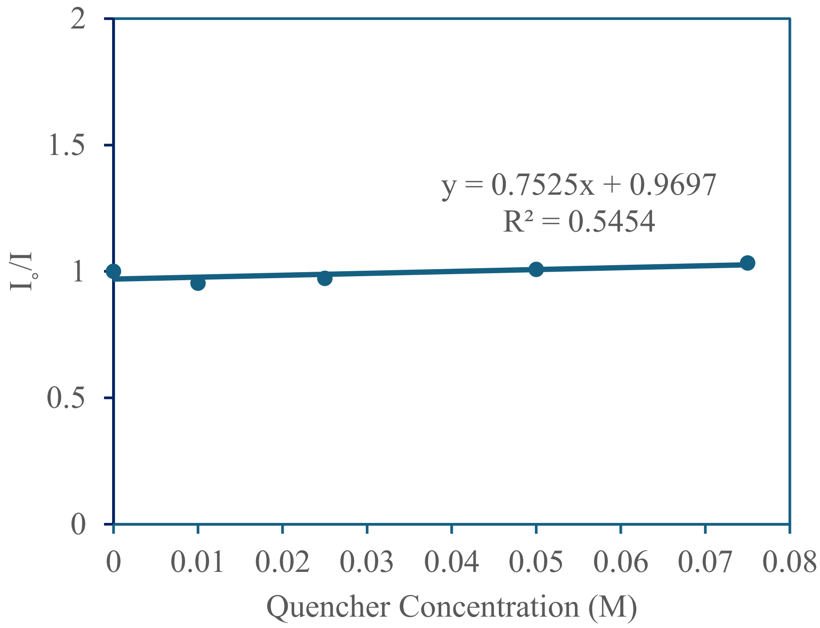


**Figure 3.3** Fluorescence quenching and Stern-Volmer plot of 4DPAIPN *vs* **1a**

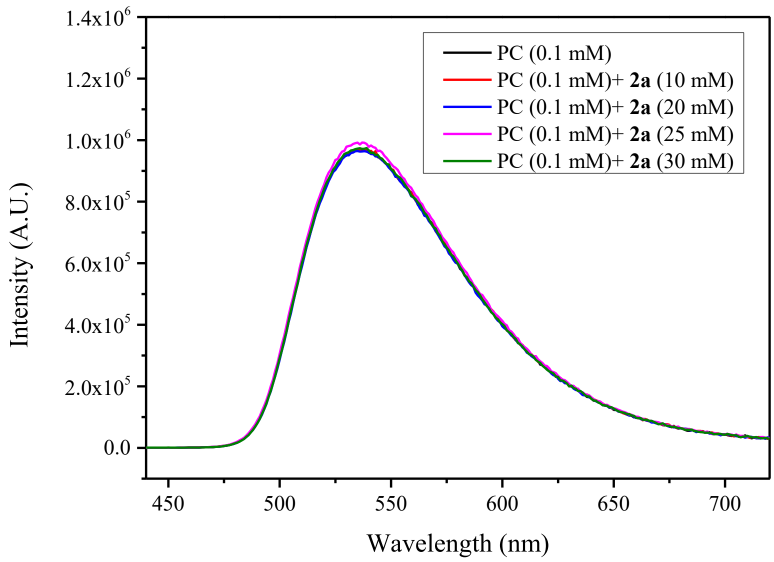

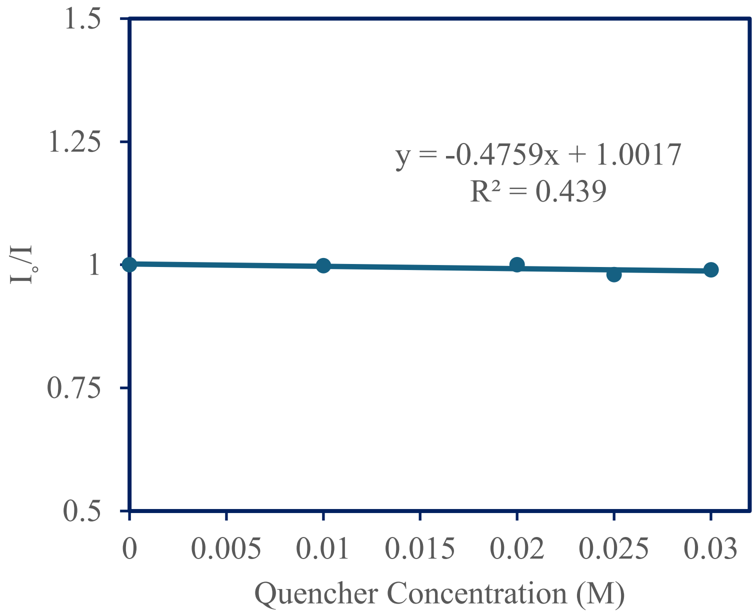


**Figure 3.4** Fluorescence quenching and Stern-Volmer plot of 4DPAIPN *vs* **2a**

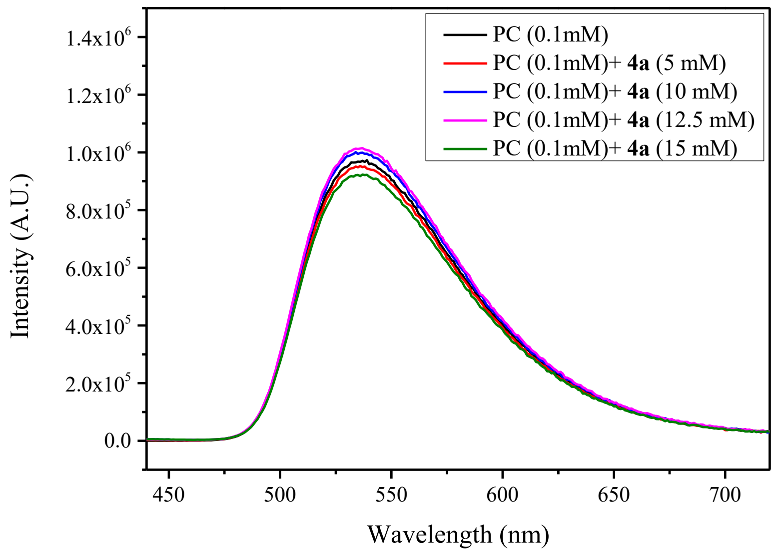

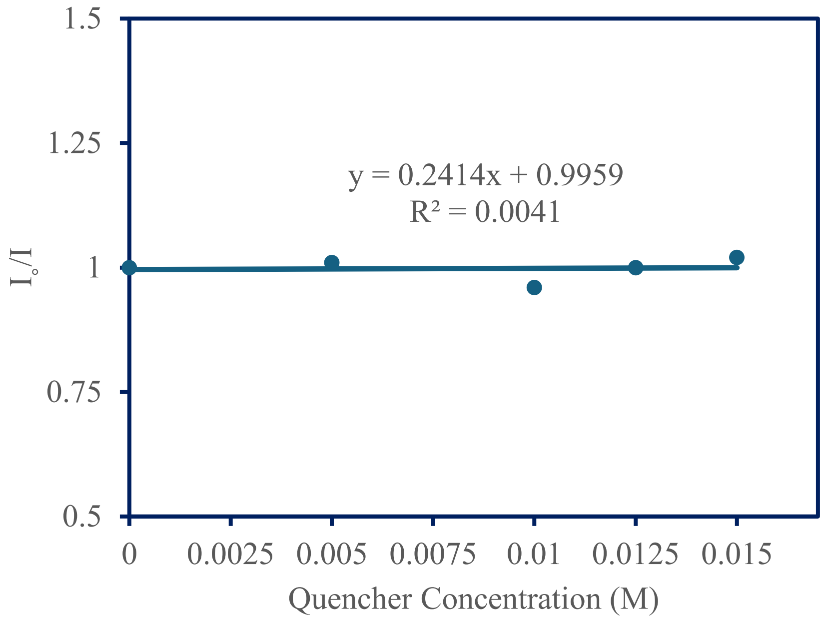


**Figure 3.5** Fluorescence quenching and Stern-Volmer plot of 4DPAIPN *vs* **4a**

### 3.9.13 Determination of quantum yield[54,55]

Sample preparation: Following previously reported procedures. A potassium ferrioxalate solution (0.15 M) was prepared by dissolving 2.21 g of potassium ferrioxalate trihydrate in 30 mL $H_2SO_4$ (0.05 M). A buffer solution was prepared by dissolving 50 mg of phenanthroline and 11.25 g sodium acetate in 50 mL $H_2SO_4$ (0.5 M). Both solutions were stored in the dark and wrapped with aluminium foil.

A 10 mL reaction tube was covered with black electric tape and wrapped with aluminium foil except for a small window at the bottom for irradiation. Then the reaction tube was charged with 5 mL ferrioxalate solution and irradiated for 10 seconds. This solution was treated with 0.875 mL buffered phenanthroline solution. After irradiation, the reaction tube was completely covered with aluminium foil and kept on stirring for 1 hour in dark conditions so that the ferrous ion could completely coordinate with phenanthroline. The absorbance of resulting solutions was measured on HORIBA FLUOROMAX_PLUS_C modal at 510 nm. A non-irradiated solution was also prepared, and absorbance was measured at 510 nm.

The conversion of ferrioxalate was calculated as:

Mol $Fe^{2+} = \frac{V \times \Delta A}{l \times \varepsilon} = \frac{0.005875\ L \times (2.145301 - 1.960492)}{1\ cm \times 11100\ L\ mol^{-1} cm^{-1}} = 9.59101694 \times 10^{-8}\ mol$

Where $V$ is the total volume (0.005875 L) of the solution after the addition of phenanthroline solution, $\Delta A$ is the difference in absorbance between irradiated and non-irradiated solutions at 510 nm, $l$ is the path length (1.0 cm) and $\varepsilon$ is the molar absorptivity at 510 nm.

The photo-flux was calculated as:

Photon flux $= \frac{molFe^{2+}}{\Phi \times t \times f} = \frac{9.59101694 \times 10^{-8}}{1.01 \times 10 \times 0.9985} = 9.50955596 \times 10^{-9}\ einstein\ sec^{-1}$

Where $\phi$ is the quantum yield for the ferrioxalate actinometer (1.01 for 0.15 M solution), t is the time, 10 seconds and *f* is the fraction of light absorbed by the ferrioxalate actinometer solution at λ = 450 nm. Absorbance at λ = 436 nm by ferrioxalate actinometer is A = 2.847874.

So, the fraction of light absorbed (*f*) by the ferrioxalate actinometer at 436 nm is as:

$$f = 1 - 10^{-A} = 1 - 10^{-2.847874} = 0.9985$$

The quantum yield was calculated as:

The parent reaction was performed in a 10 mL reaction tube with the standard reaction condition at 0.2 mmol scale for 10 minutes, which gave 72% yield of **3a**.

$$\phi = \frac{mol\ product}{flux \times t \times f} = \frac{0.2 \times 0.72 \times 10^{-3}}{9.50955596 \times 10^{-9} \times 600 \times 1} = 25.23$$

Where $\phi$ is the quantum yield of the reaction, t is the reaction time (600 seconds).

### 3.10 Selected NMR spectra

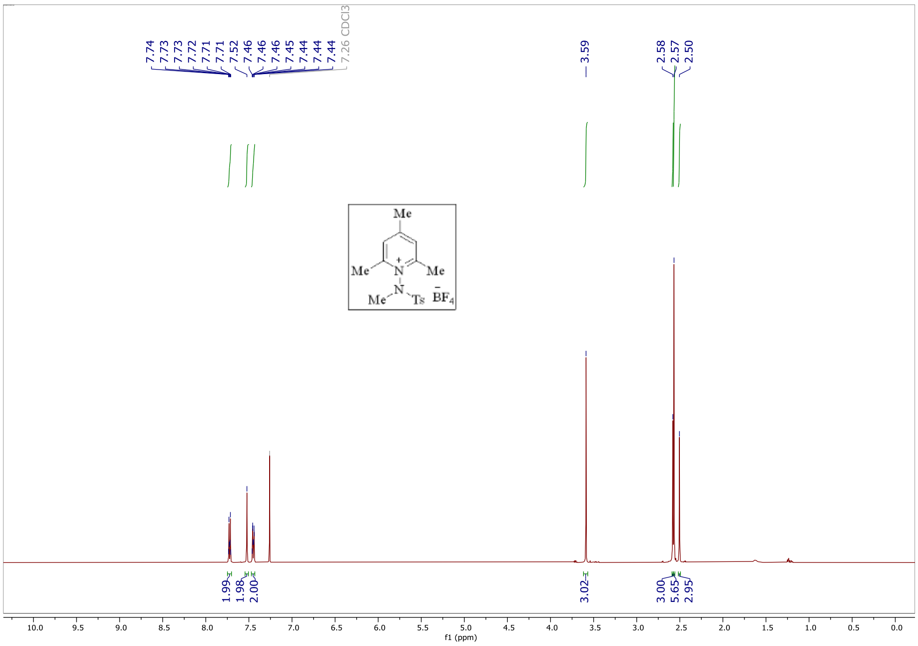

**Figure 3.10.1** $^{1}$H NMR of *N*-aminopyridinium salt (HATR) in [$CDCl_3$, 500 MHz]

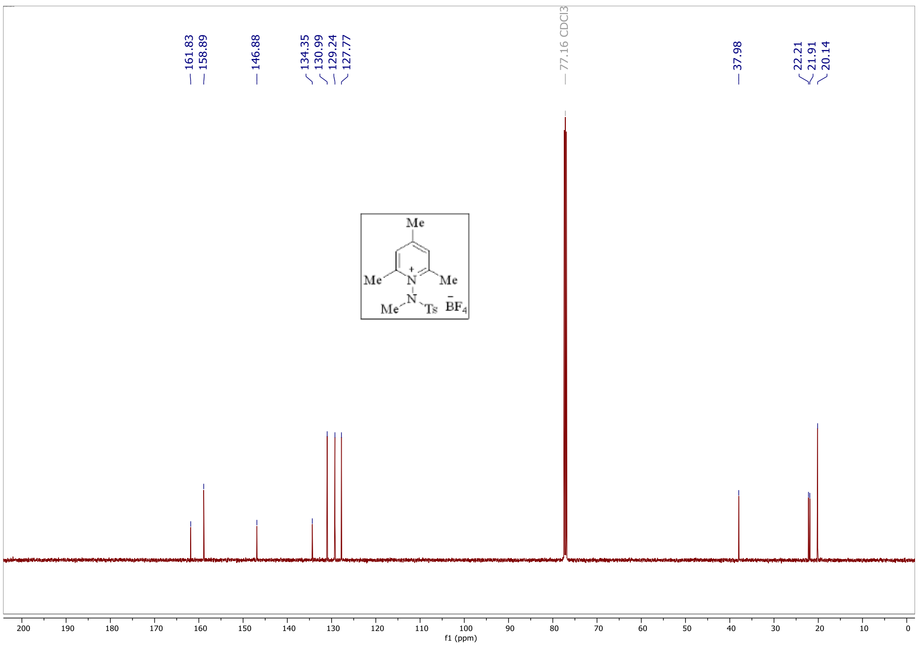

**Figure 3.10.2** $^{13}$C NMR of *N*-aminopyridinium salt (HATR) in [$CDCl_3$, 126 MHz]

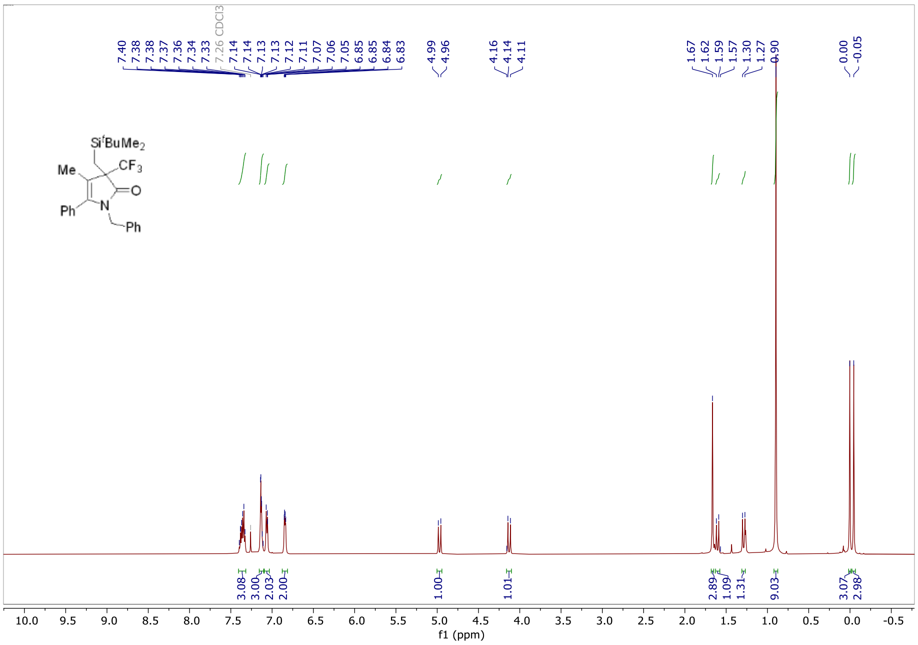

**Figure 3.10.3** $^{1}H$ NMR spectra of **3a** [$CDCl_3$, 500 MHz]

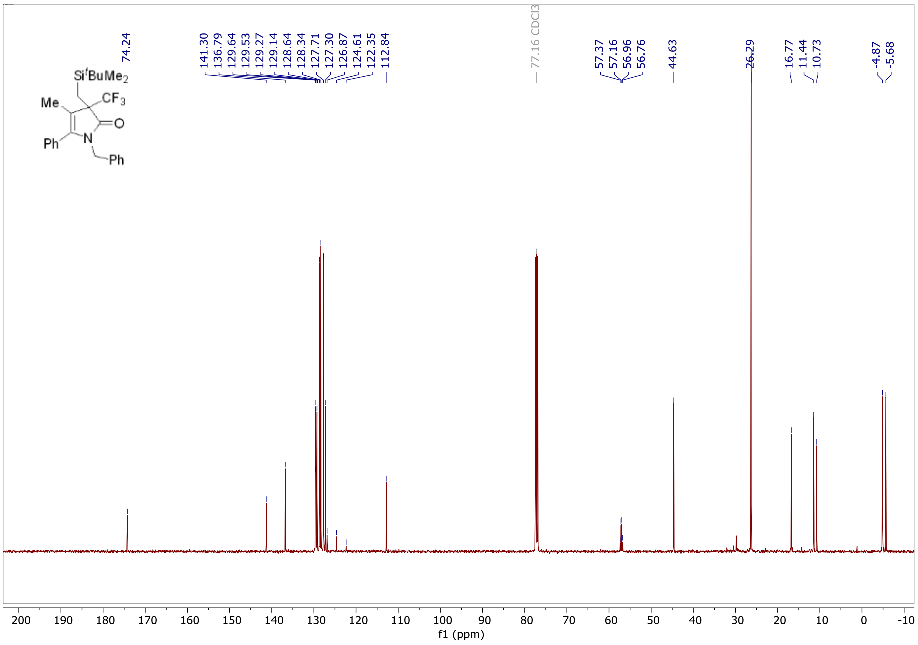

**Figure 3.10.4** $^{13}C$ NMR spectra of **3a** [$CDCl_3$, 126 MHz]

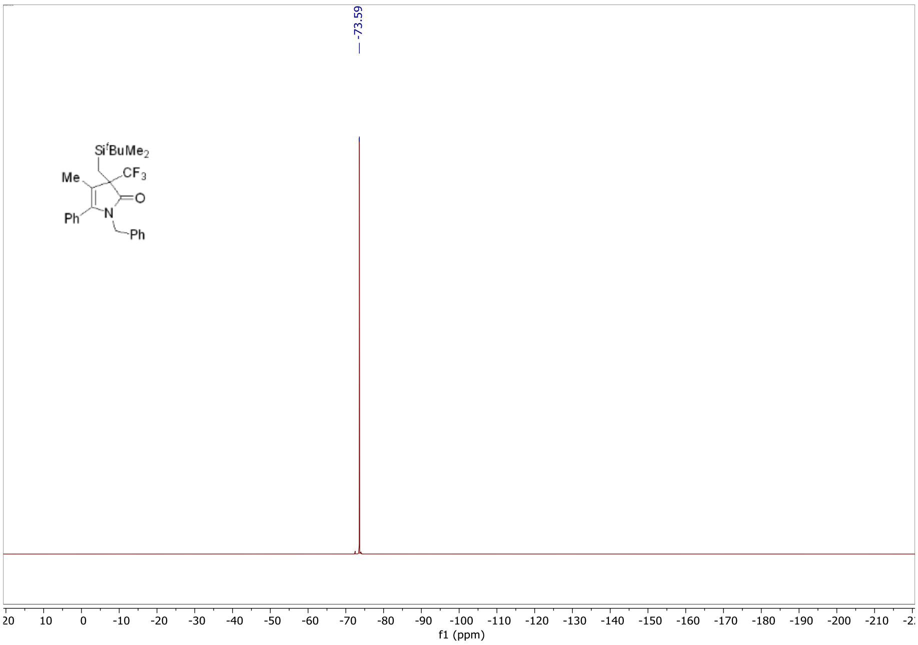

**Figure 3.10.5** $^{19}$F NMR spectra of **3a** [$CDCl_3$, 471 MHz]

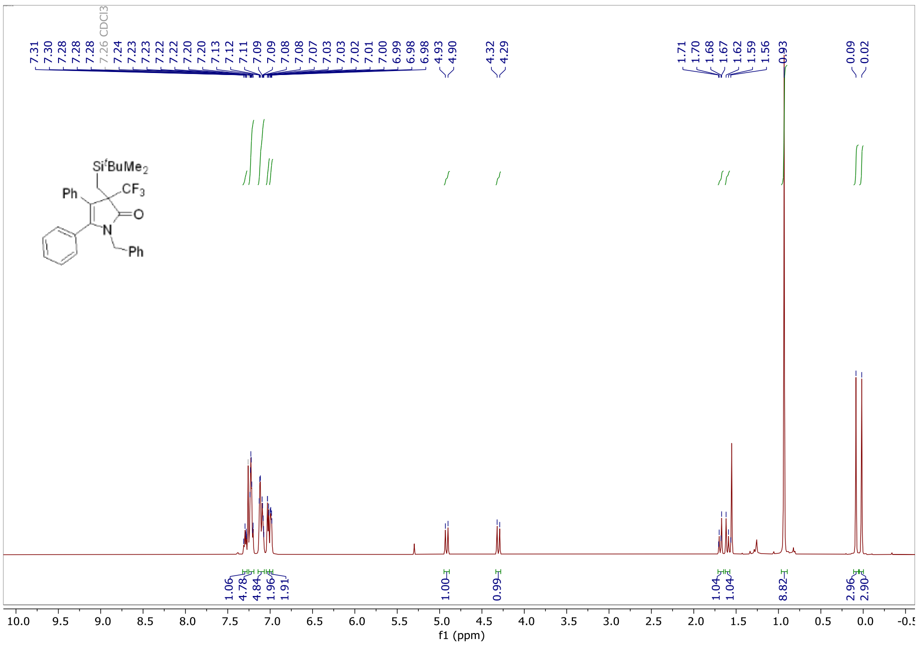

**Figure 3.10.6** $^{1}$H NMR spectra of **3d** [$CDCl_3$, 500 MHz]

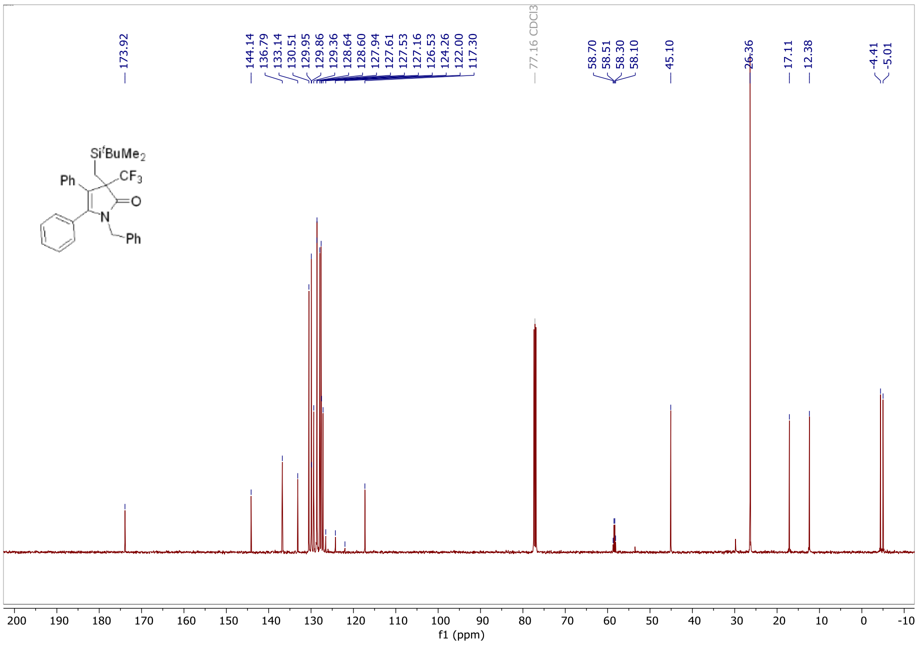

**Figure 3.10.7** $^{13}C$ NMR spectra of **3d** [$CDCl_3$, 126 MHz]

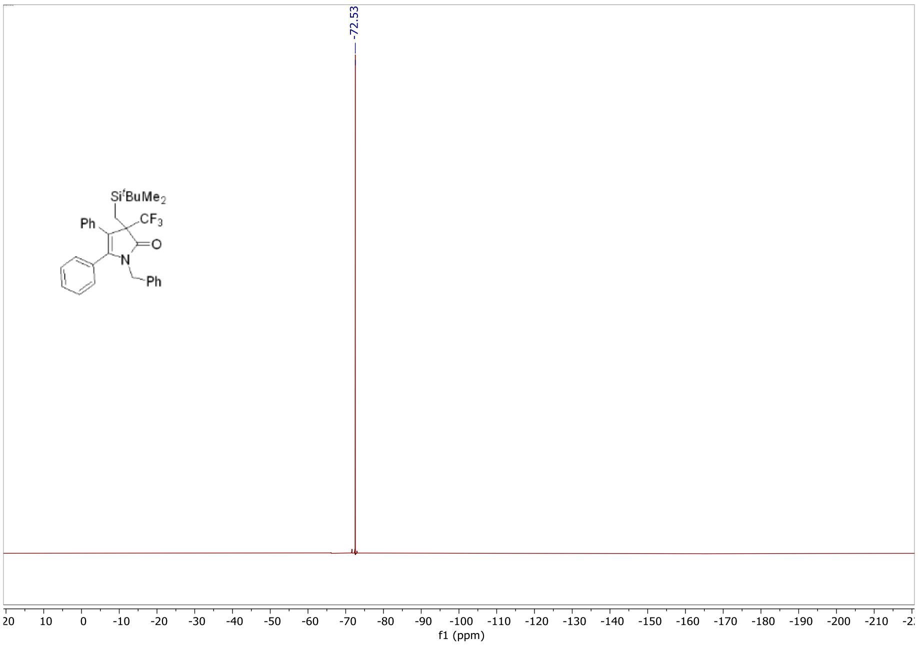

**Figure 3.10.8** $^{19}F$ NMR spectra of **3d** [$CDCl_3$, 471 MHz]

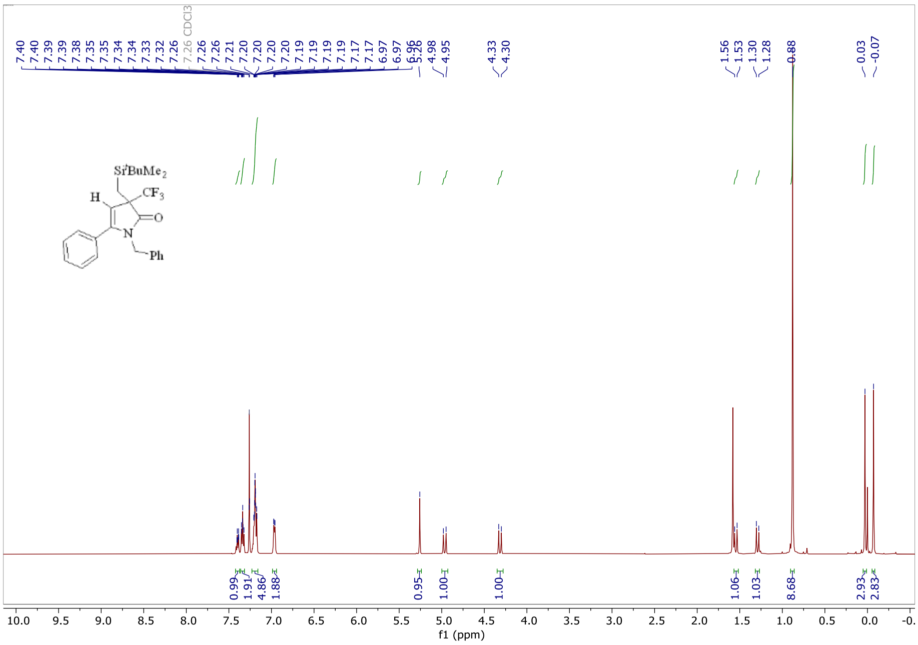

**Figure 3.10.9** $^{1}$H NMR spectra of **3e** [$CDCl_3$, 500 MHz]

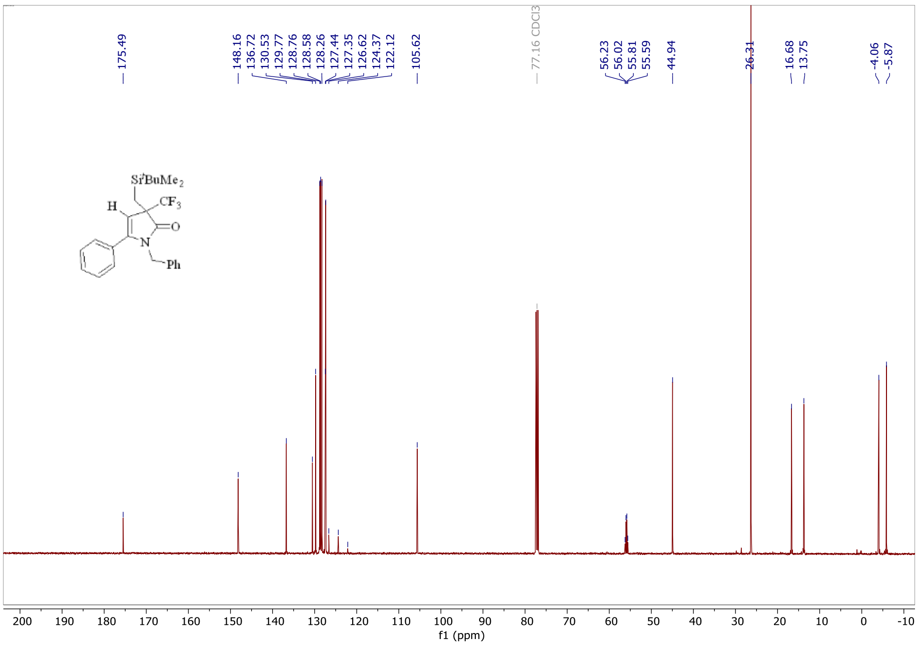

**Figure 3.10.10** $^{13}$C NMR spectra of **3e** [$CDCl_3$, 126 MHz]

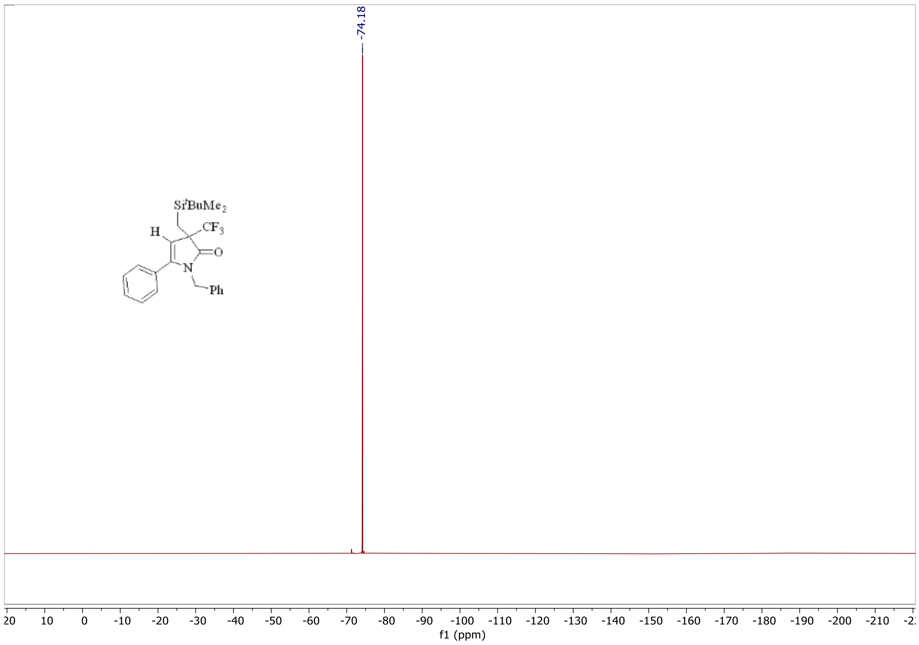

**Figure 3.10.11** $^{19}F$ NMR spectra of **3e** [$CDCl_3$, 471 MHz]

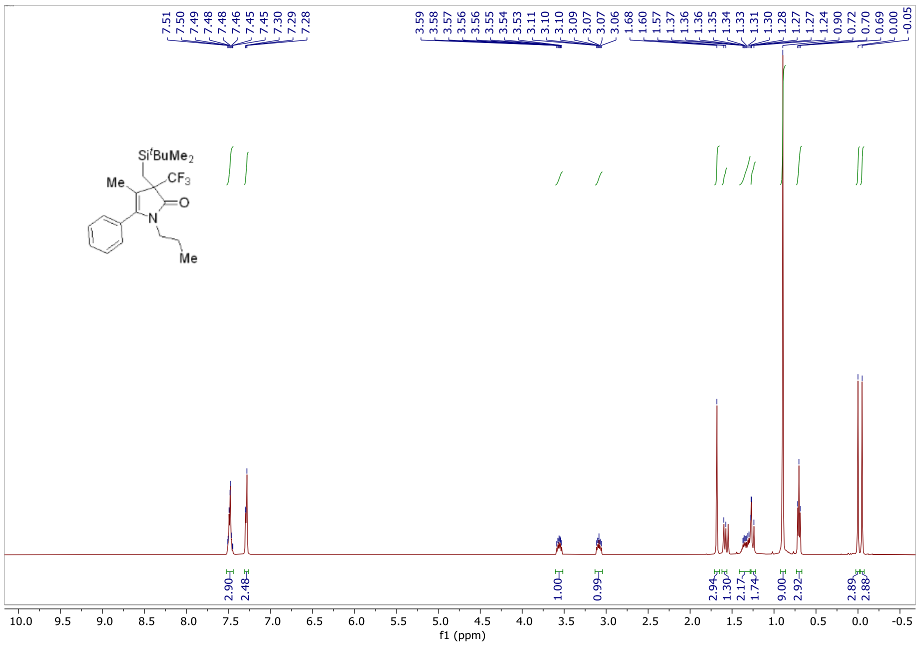

**Figure 3.10.12** $^{1}H$ NMR spectra of **3g** [$CDCl_3$, 500 MHz]

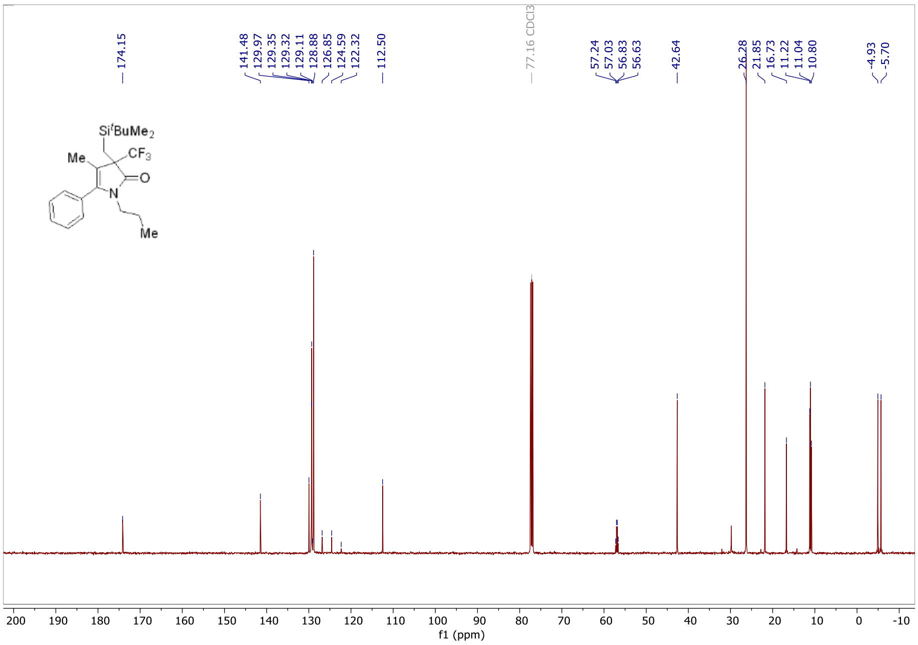


**Figure 3.10.13** $^{13}C$ NMR spectra of **3g** [$CDCl_3$, 126 MHz]

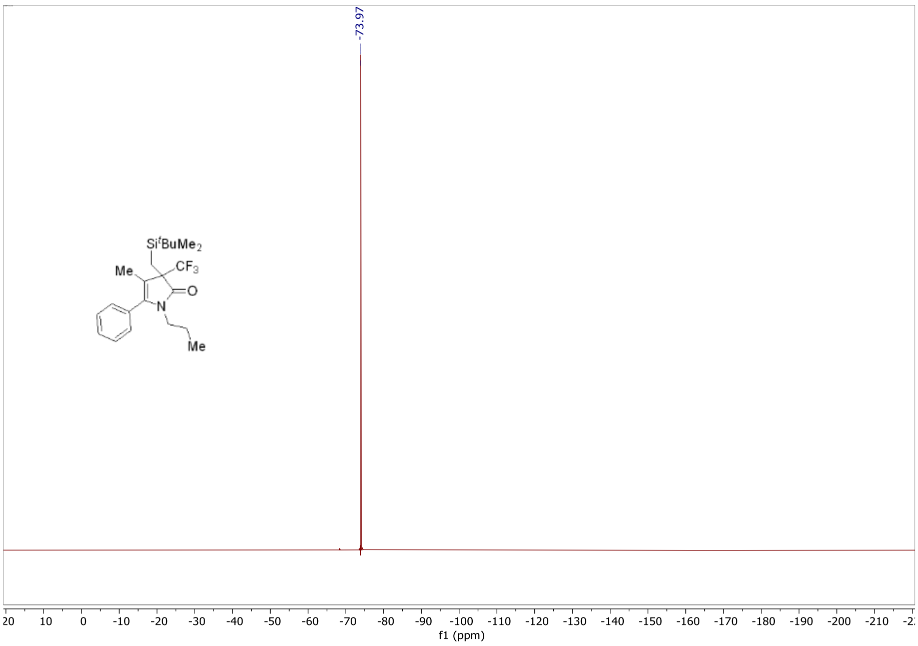


**Figure 3.10.14** $^{19}F$ NMR spectra of **3g** [$CDCl_3$, 471 MHz]

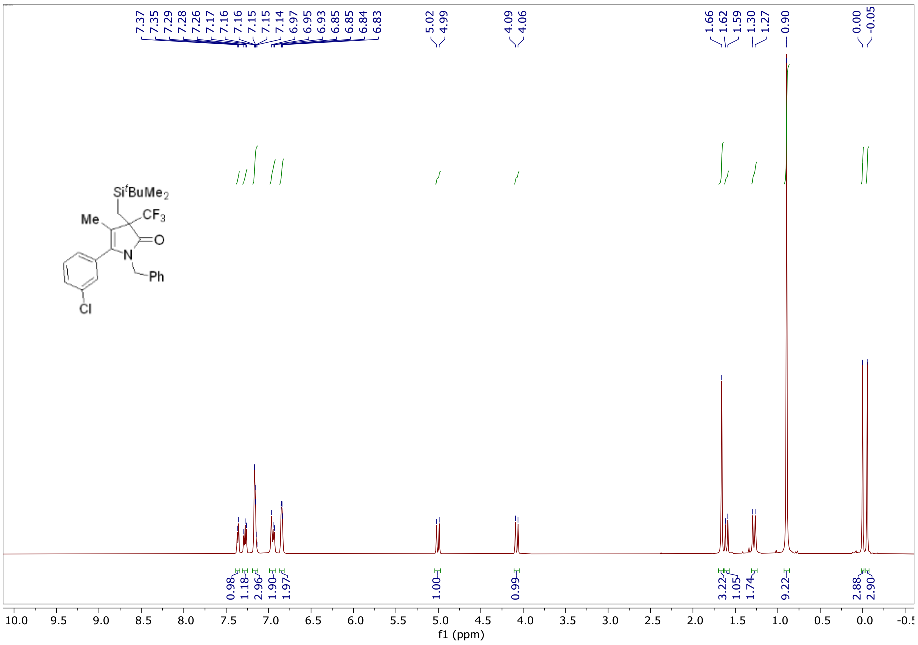

**Figure 3.10.15** $^{1}H$ NMR spectra of **3k** [$CDCl_3$, 500 MHz]

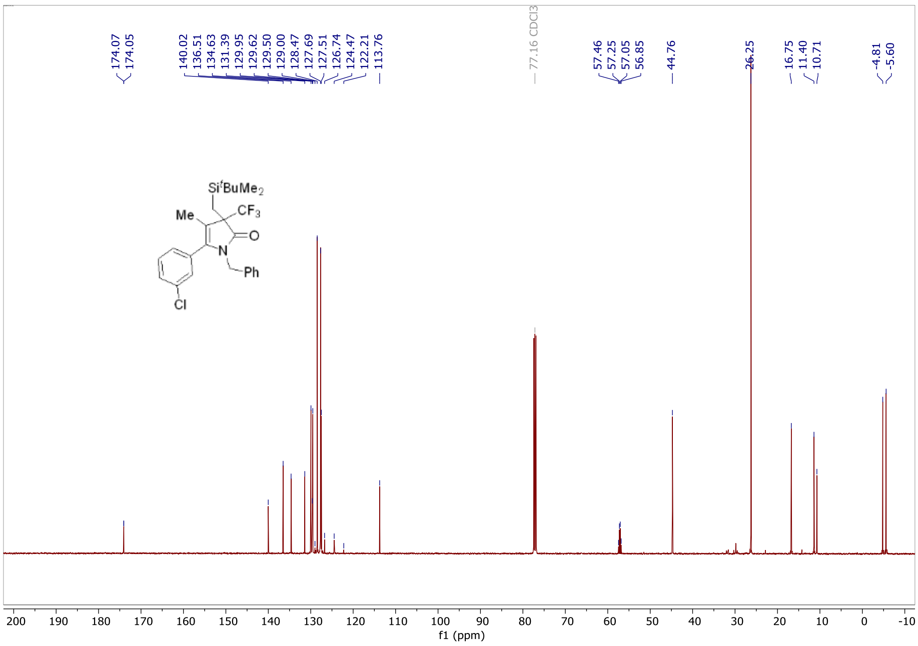

**Figure 3.10.16** $^{13}C$ NMR spectra of **3k** [$CDCl_3$, 126 MHz]

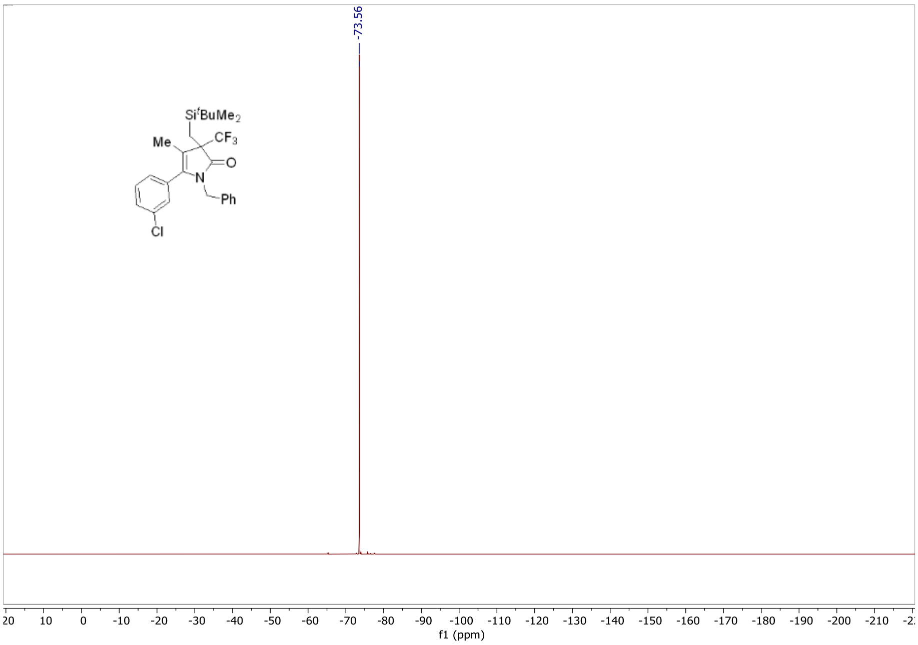

**Figure 3.10.17** $^{19}F$ NMR spectra of **3k** [$CDCl_3$, 471 MHz]

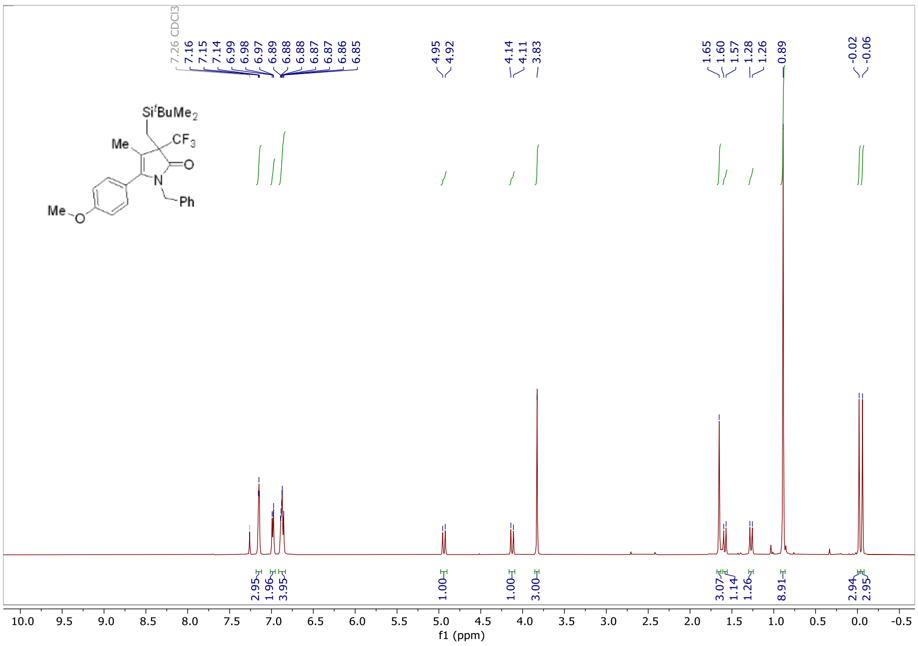

**Figure 3.10.18** $^{1}H$ NMR spectra of **3m** [$CDCl_3$, 500 MHz]

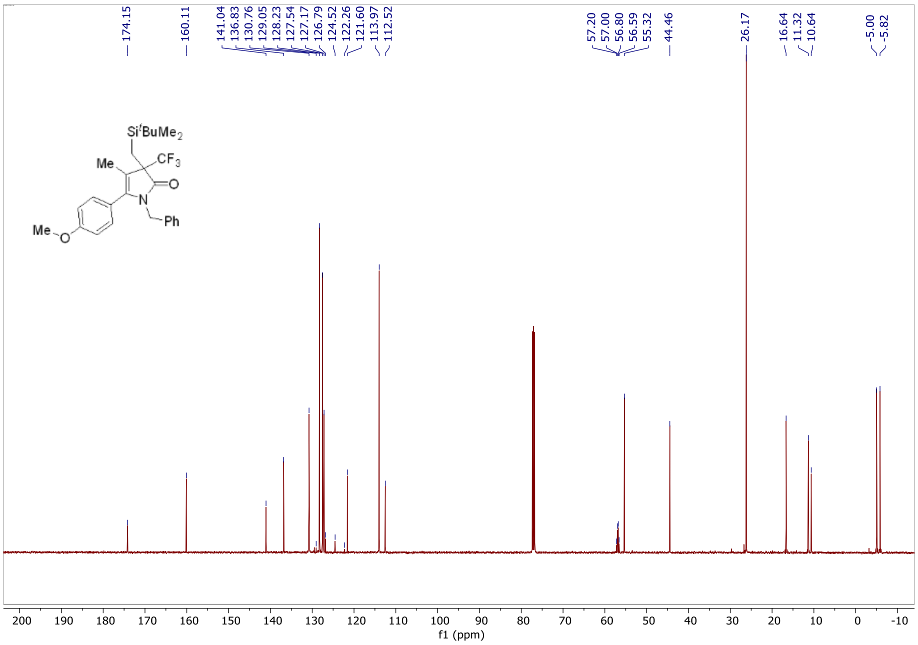

**Figure 3.10.19** $^{13}$C NMR spectra of **3m** [$CDCl_3$, 126 MHz]

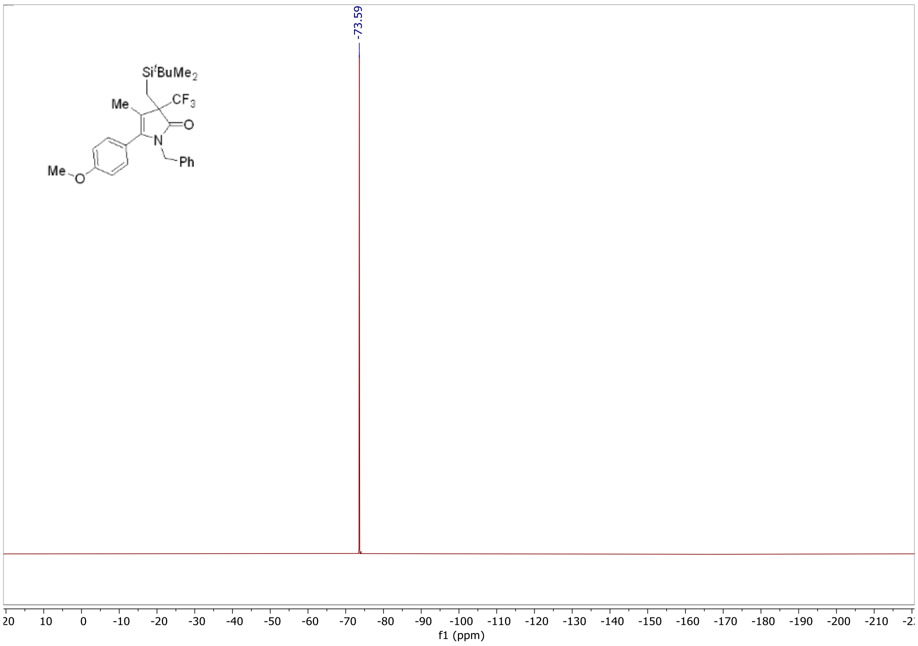

**Figure 3.10.20** $^{19}$F NMR spectra of **3m** [$CDCl_3$, 471 MHz]

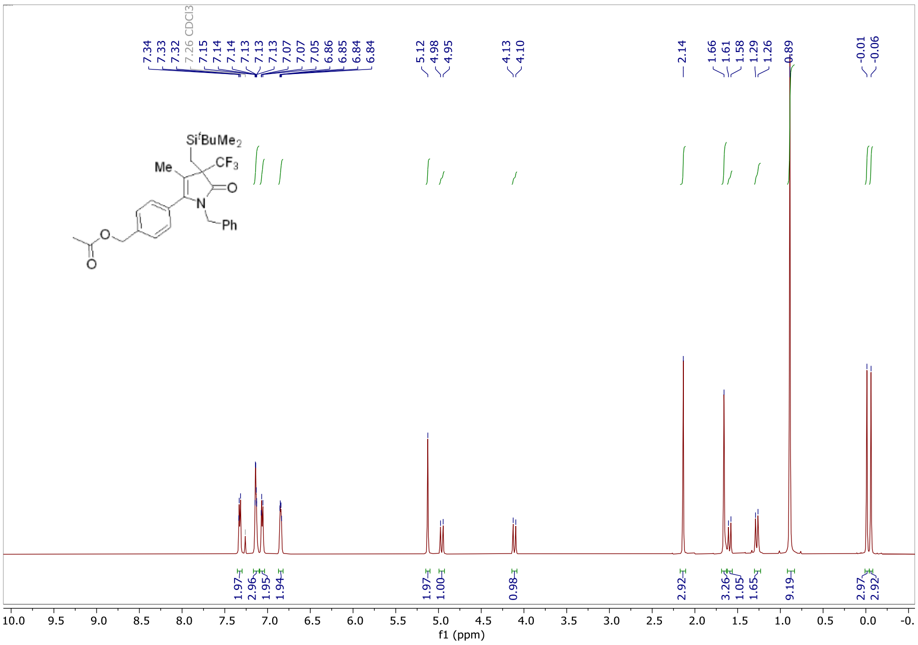

**Figure 3.10.21** $^{1}H$ NMR spectra of **3q** [$CDCl_3$, 500 MHz]

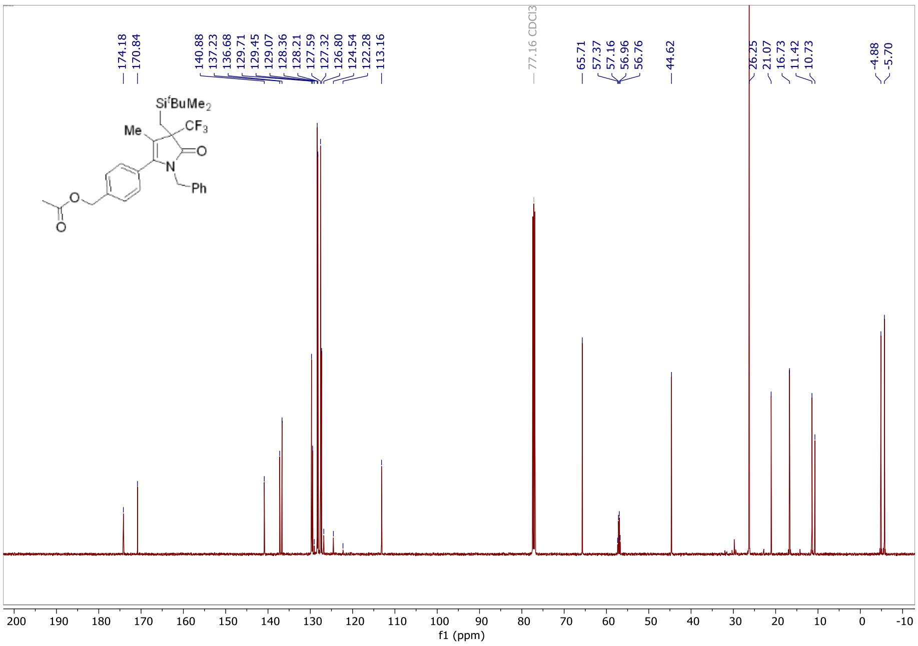

**Figure 3.10.22** $^{13}C$ NMR spectra of **3q** [$CDCl_3$, 126 MHz]

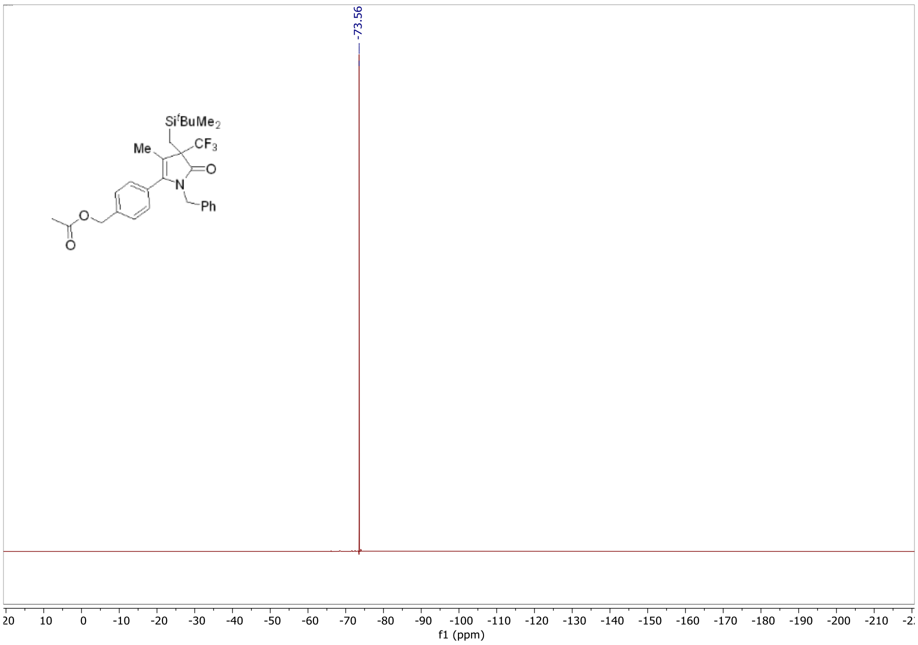

**Figure 3.10.23** $^{19}$F NMR spectra of **3q** [$CDCl_3$, 471 MHz]

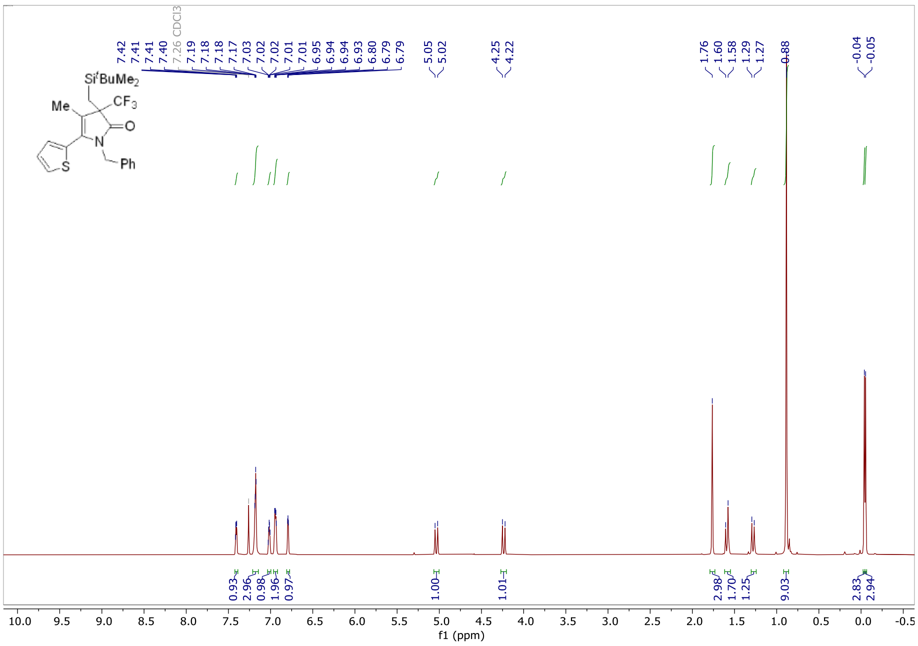

**Figure 3.10.24** $^{1}$H NMR spectra of **3r** [$CDCl_3$, 500 MHz]

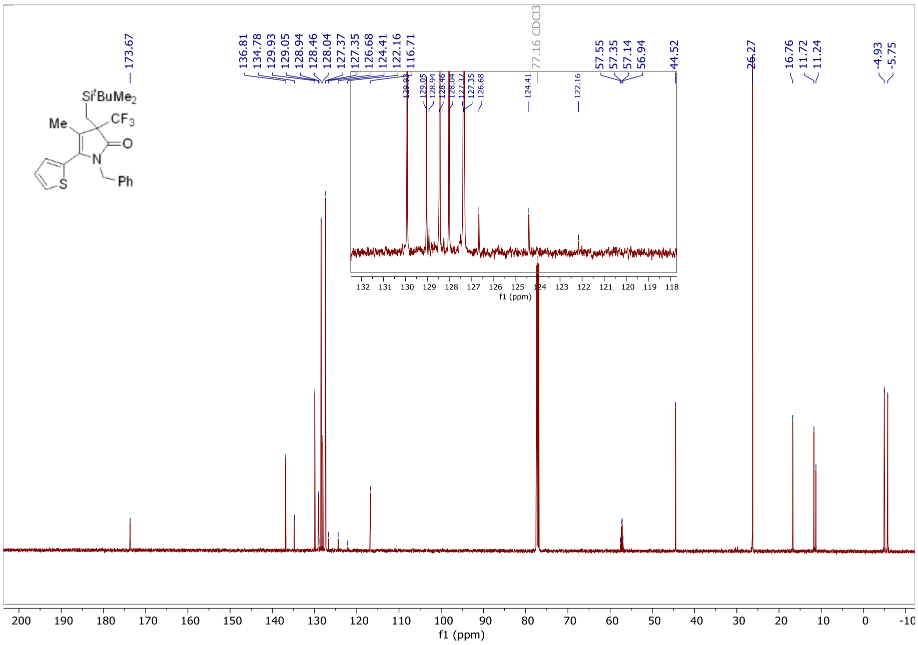

**Figure 3.10.25** $^{13}C$ NMR spectra of **3r** [$CDCl_3$, 126 MHz]

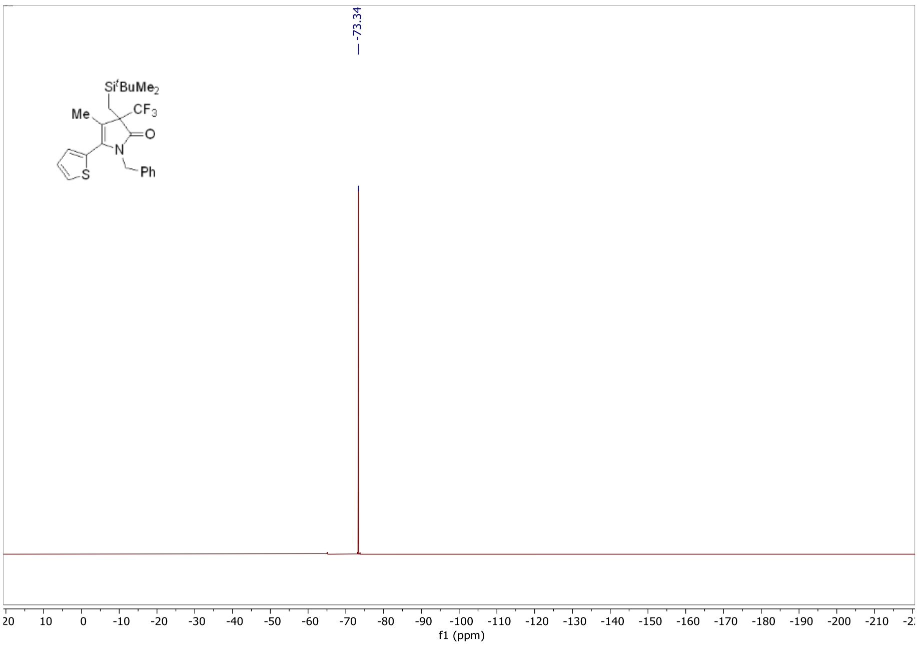

**Figure 3.10.26** $^{19}F$ NMR spectra of **3r** [$CDCl_3$, 471 MHz]

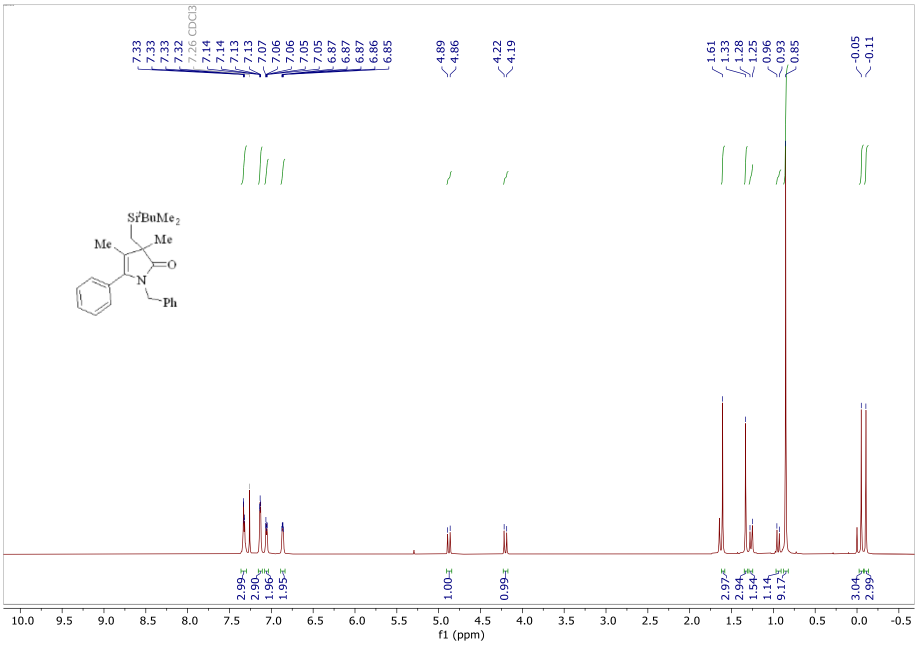

**Figure 3.10.27** $^{1}$H NMR spectra of **3t** [$CDCl_3$, 500 MHz]

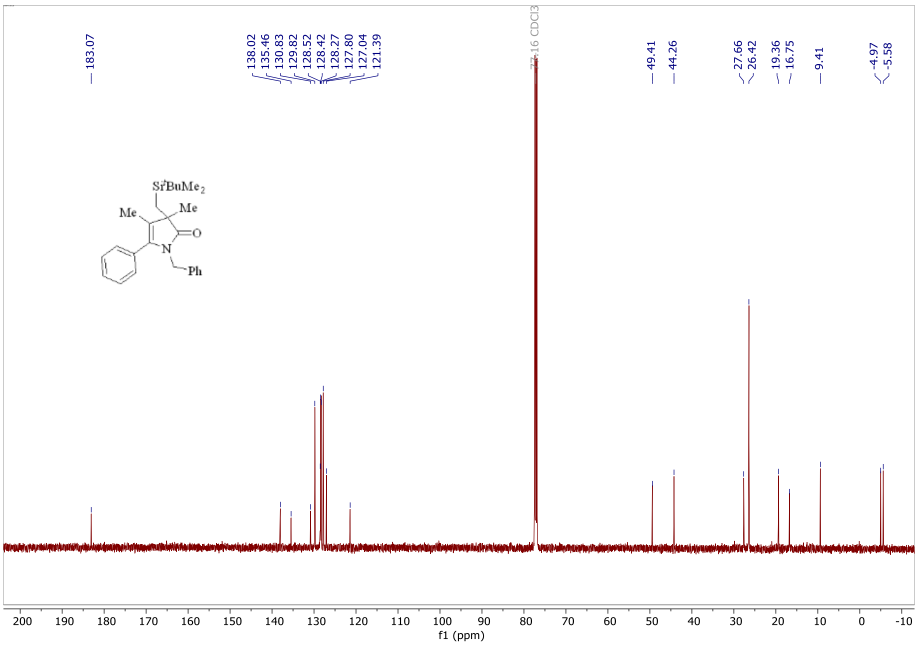

**Figure 3.10.28** $^{13}$C NMR spectra of **3t** [$CDCl_3$, 126 MHz]

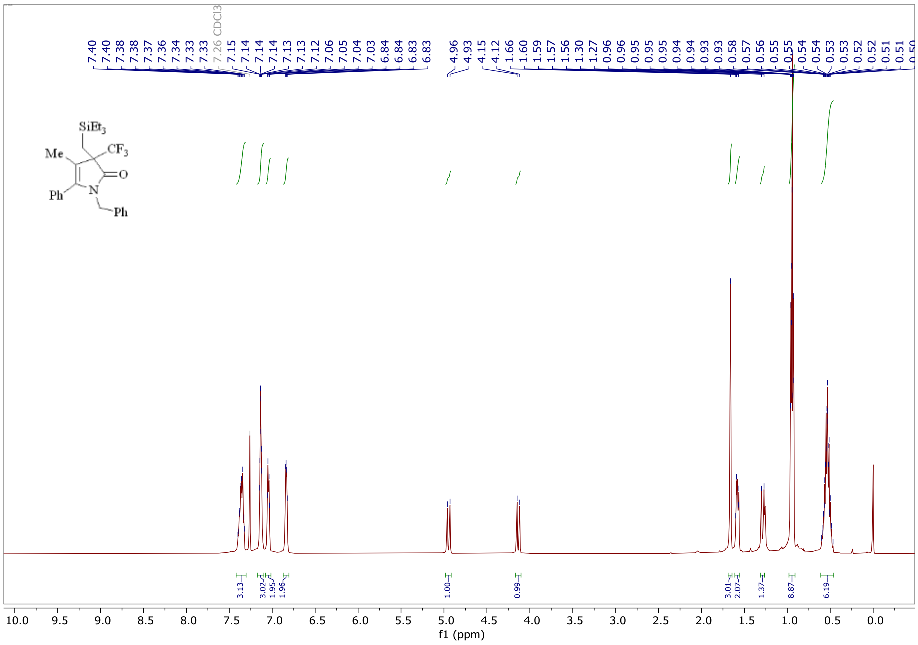

**Figure 3.10.29** $^{1}$H NMR spectra of **3u** [$CDCl_3$, 500 MHz]

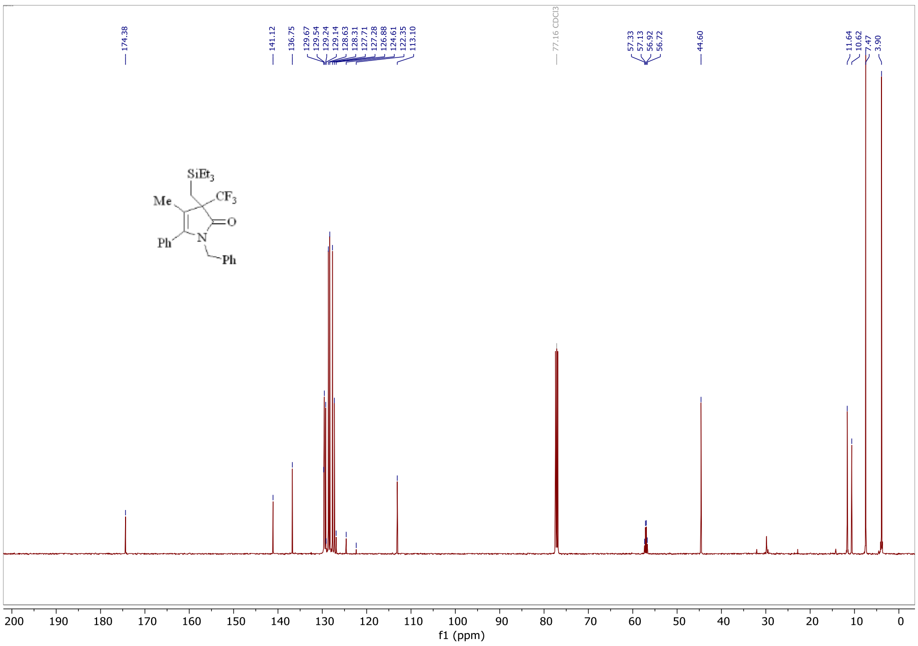

**Figure 3.10.30** $^{13}$C NMR spectra of **3u** [$CDCl_3$, 126 MHz]

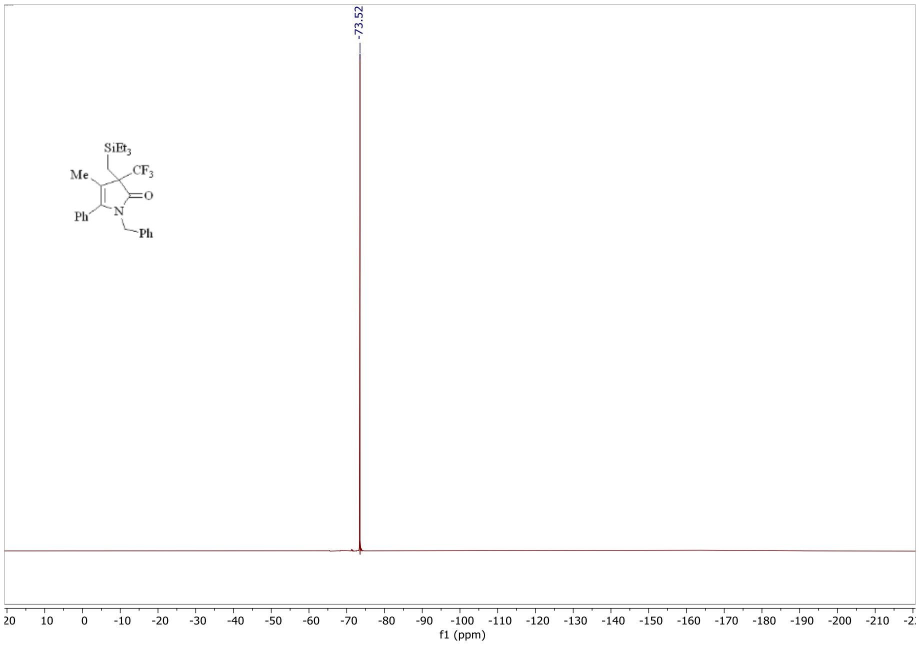

**Figure 3.10.31** $^{19}F$ NMR spectra of **3u** [$CDCl_3$, 471 MHz]

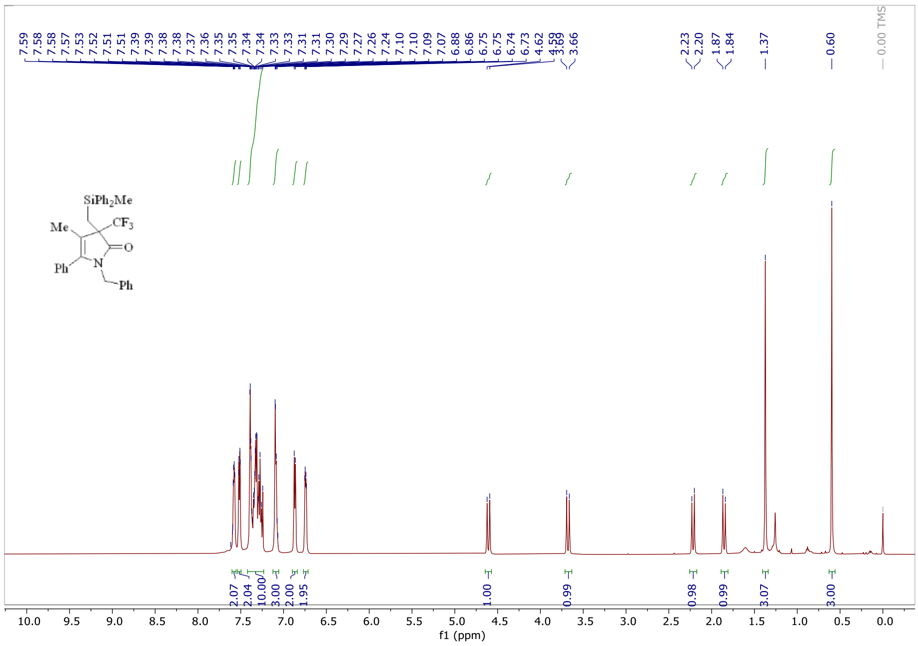

**Figure 3.10.32** $^{1}H$ NMR spectra of **3ab** [$CDCl_3$, 500 MHz]

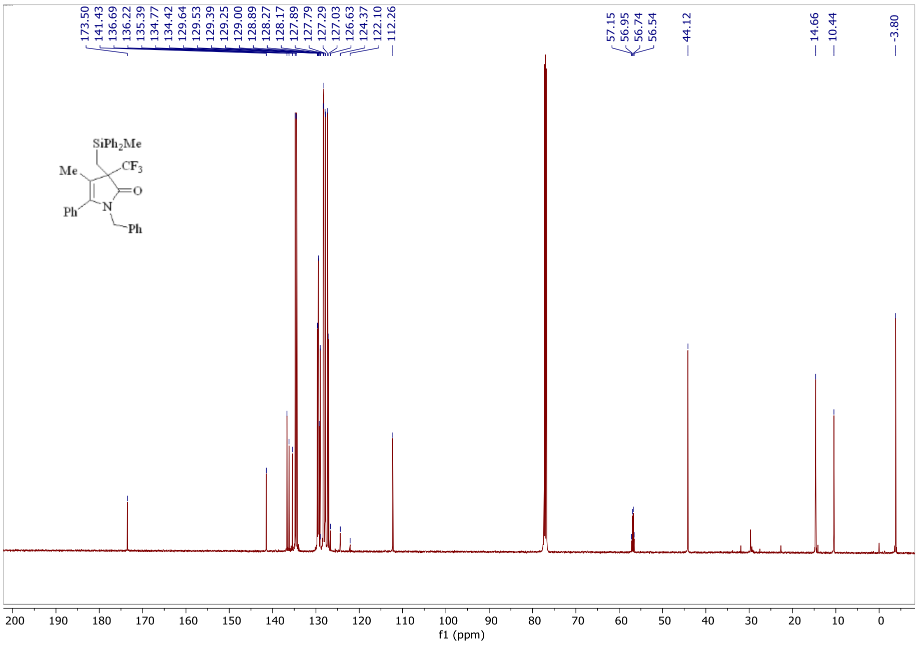


**Figure 3.10.33** $^{13}$C NMR spectra of **3ab** [$CDCl_3$, 126 MHz]

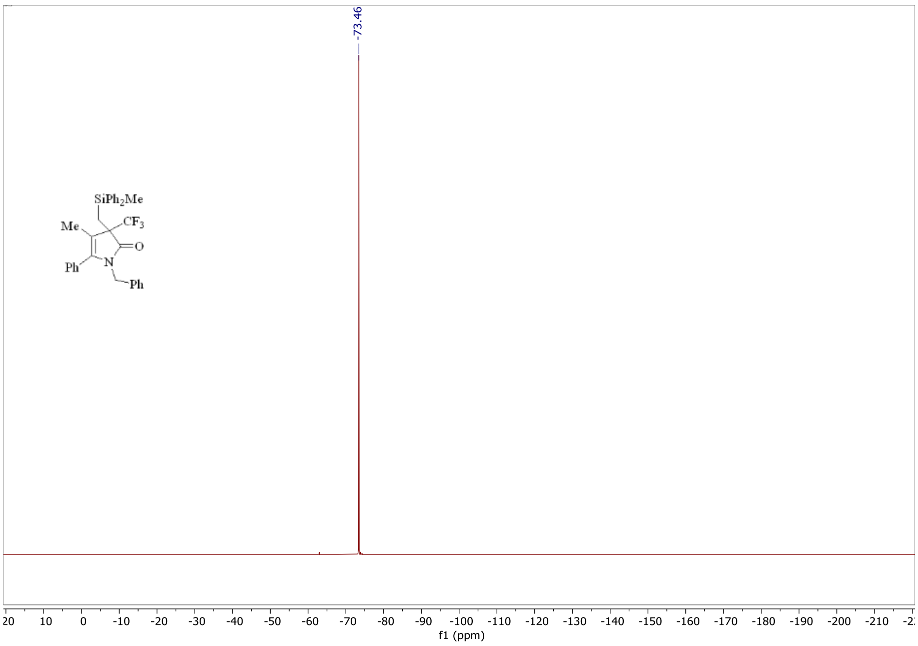


**Figure 3.10.34** $^{19}$F NMR spectra of **3ab** [$CDCl_3$, 471 MHz]

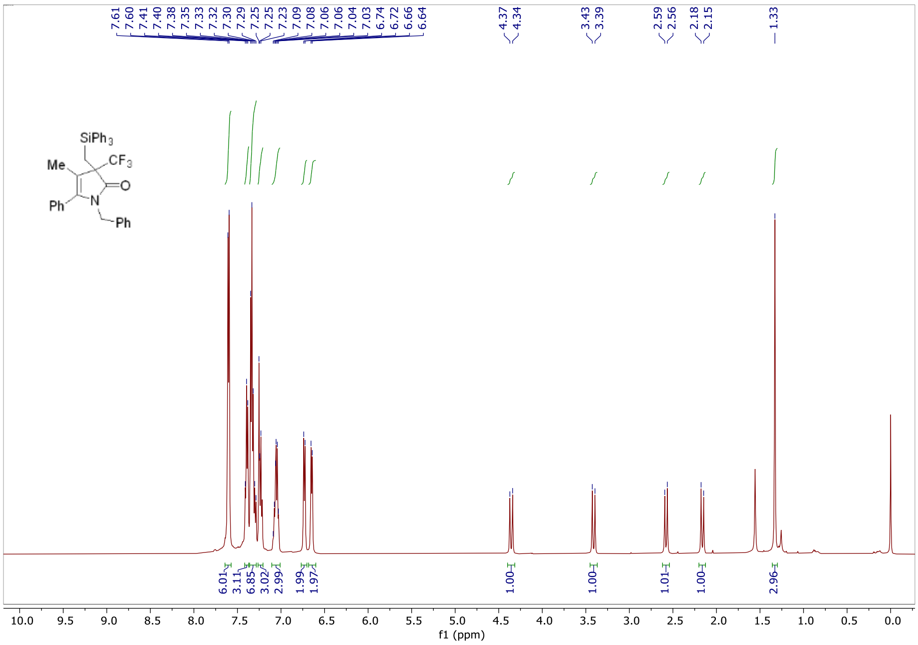

**Figure 3.10.35** $^{1}H$ NMR spectra of **3ad** [$CDCl_3$, 500 MHz]

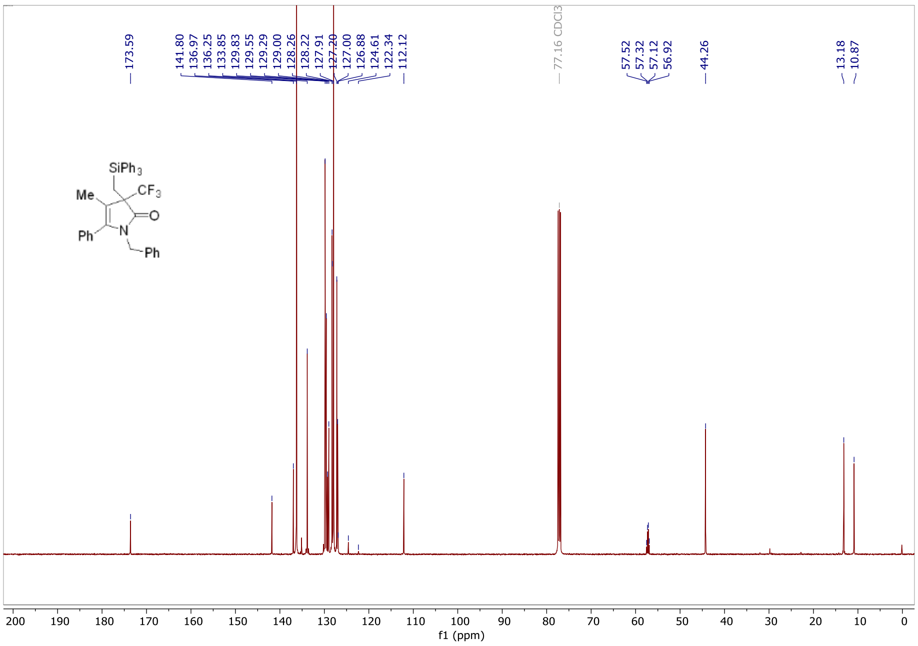

**Figure 3.10.36** $^{13}C$ NMR spectra of **3ad** [$CDCl_3$, 126 MHz]

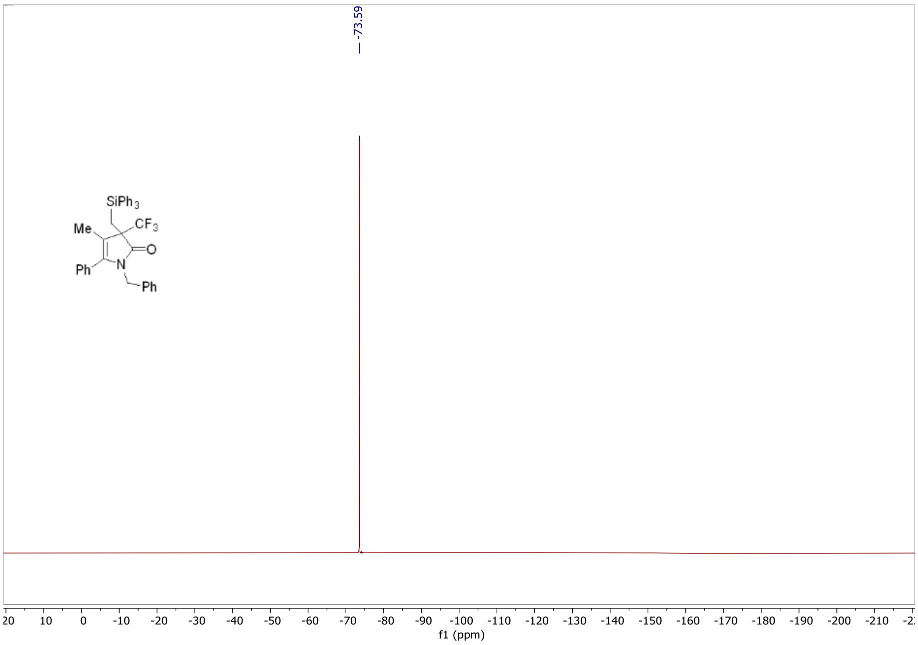

**Figure 3.10.37** $^{19}$F NMR spectra of **3ad** [$CDCl_3$, 471 MHz]

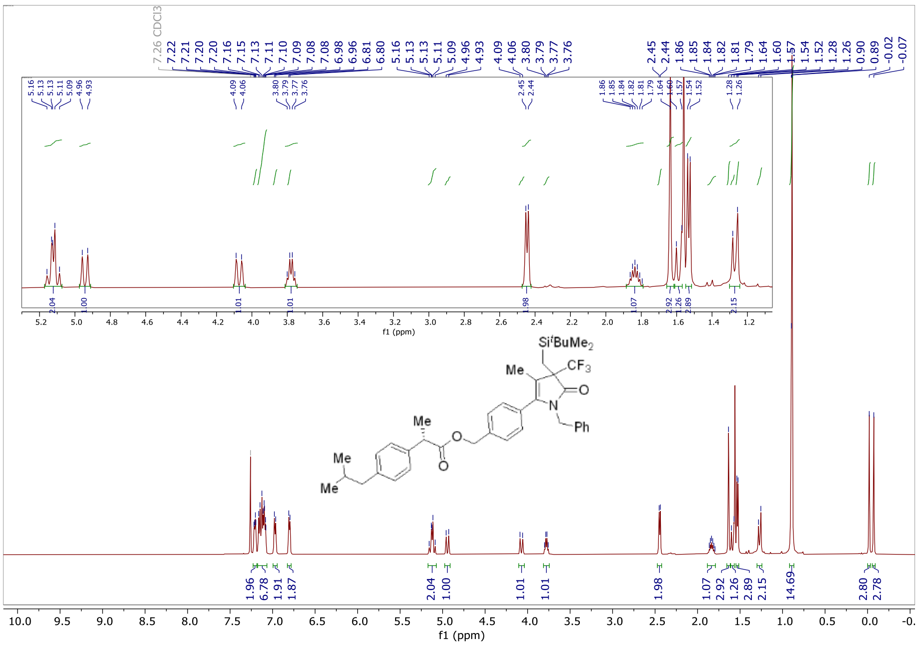

**Figure 3.10.38** $^{1}$H NMR spectra of **3ai** [$CDCl_3$, 500 MHz]

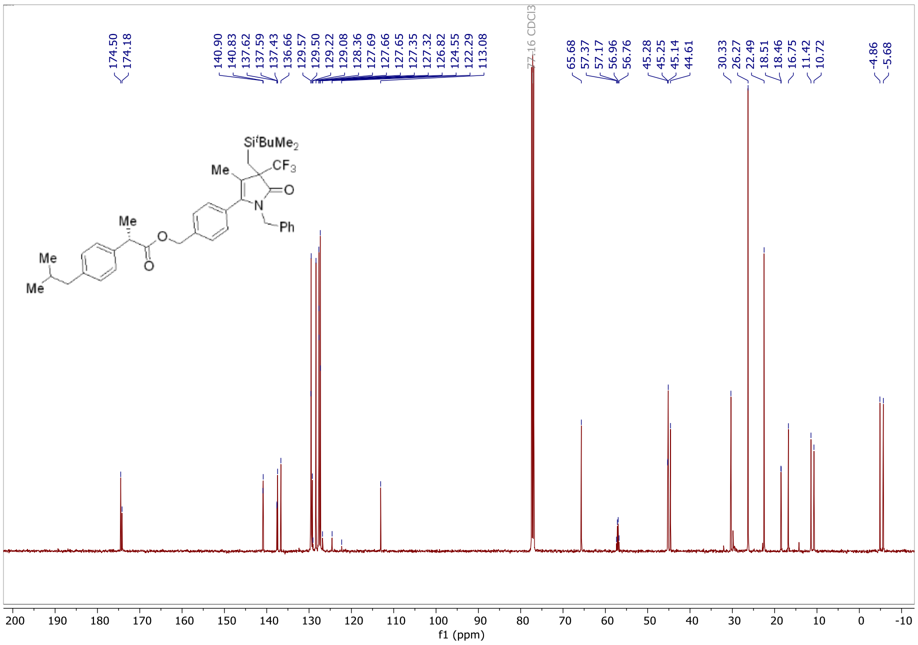

**Figure 3.10.39** $^{13}C$ NMR spectra of **3ai** [$CDCl_3$, 126 MHz]

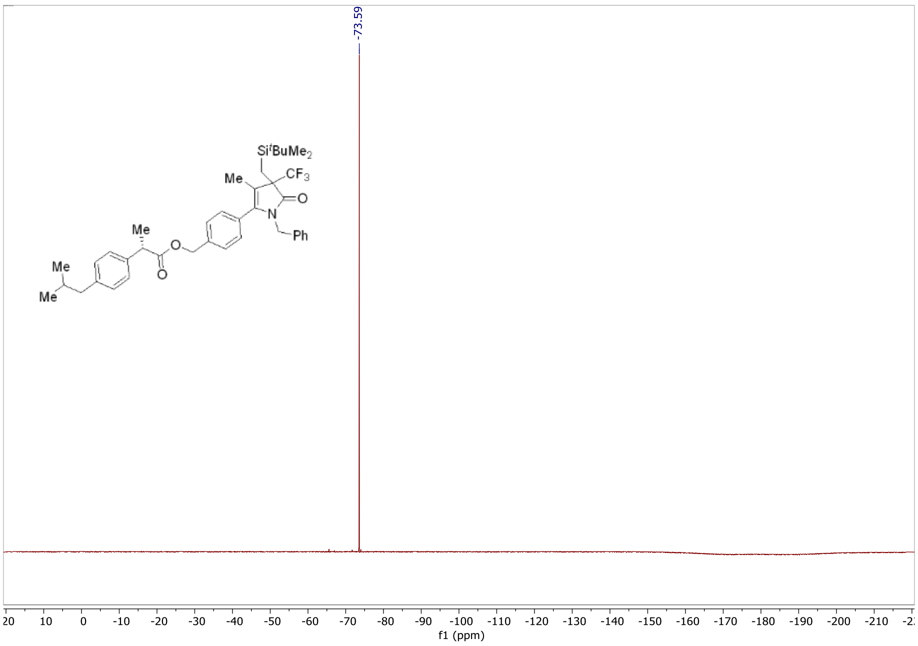

**Figure 3.10.40** $^{19}F$ NMR spectra of **3ai** [$CDCl_3$, 471 MHz]

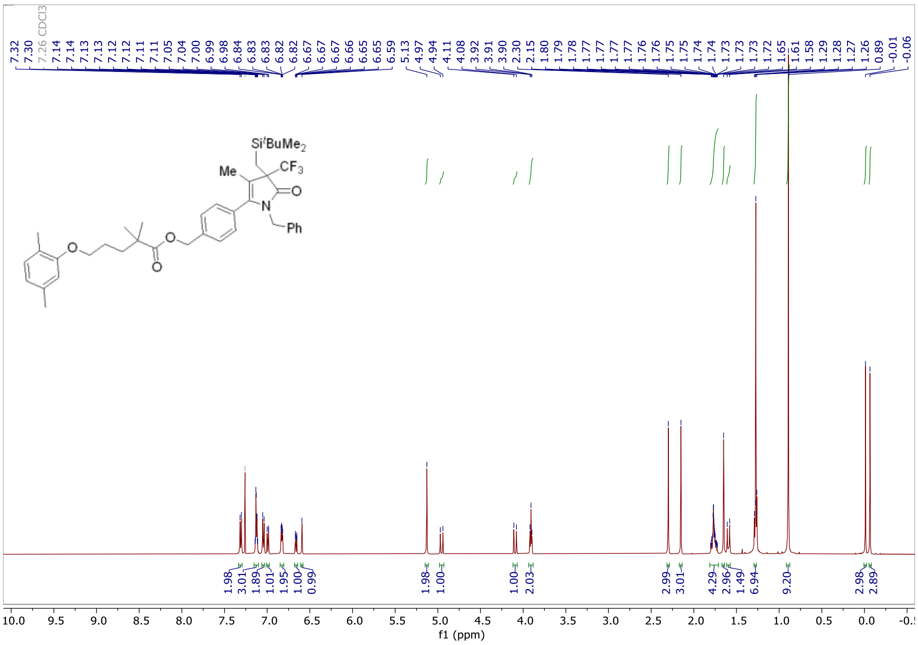

**Figure 93.10.41** $^{1}H$ NMR spectra of **3al** [$CDCl_3$, 500 MHz]

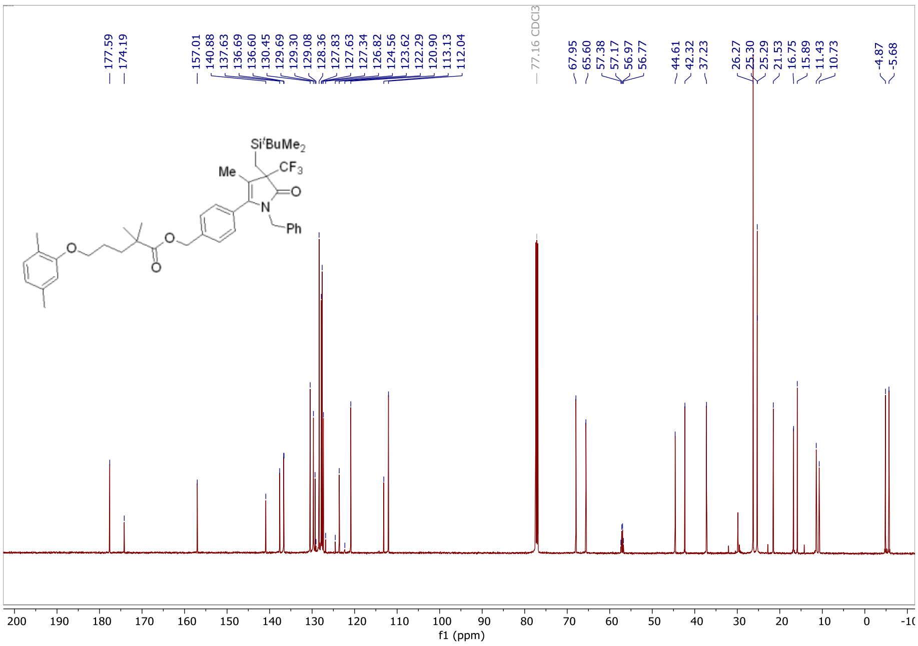

**Figure 3.10.42** $^{13}C$ NMR spectra of **3al** [$CDCl_3$, 126 MHz]

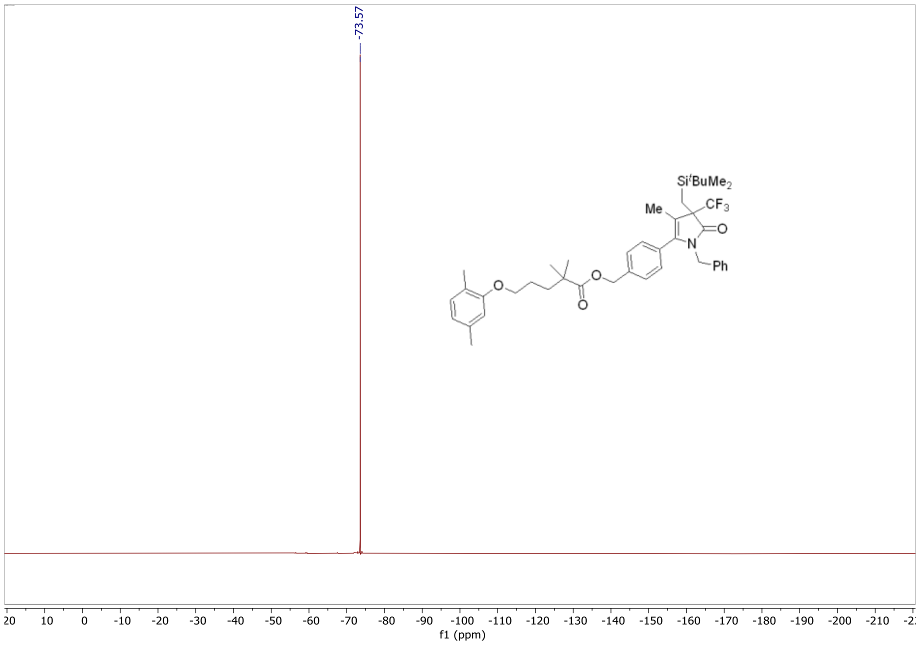


**Figure 3.10.43** $^{19}$F NMR spectra of **3al** [$CDCl_3$, 471 MHz]

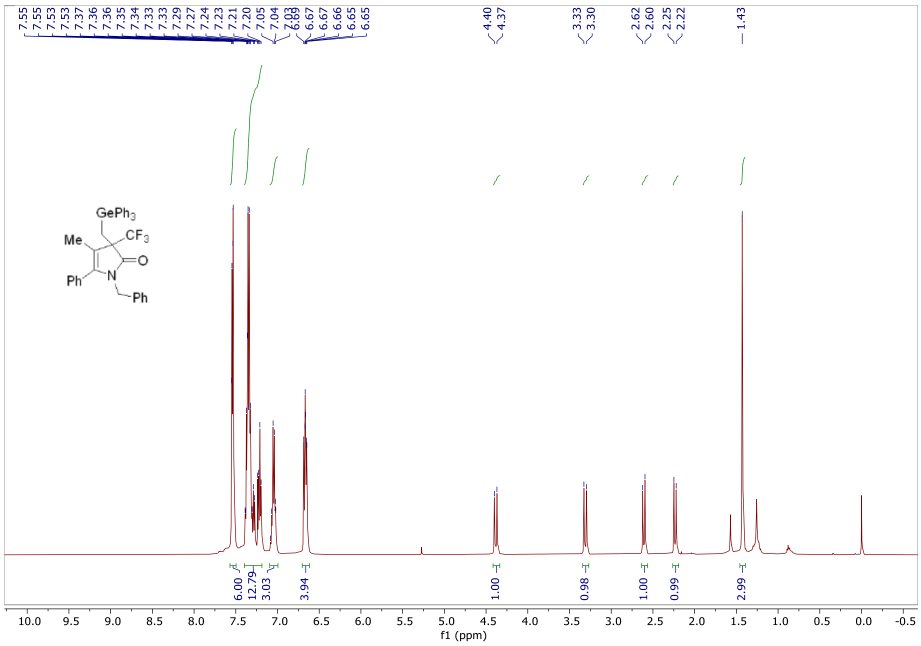


**Figure 3.10.44** $^{1}$H NMR spectra of **5a** [$CDCl_3$, 500 MHz]

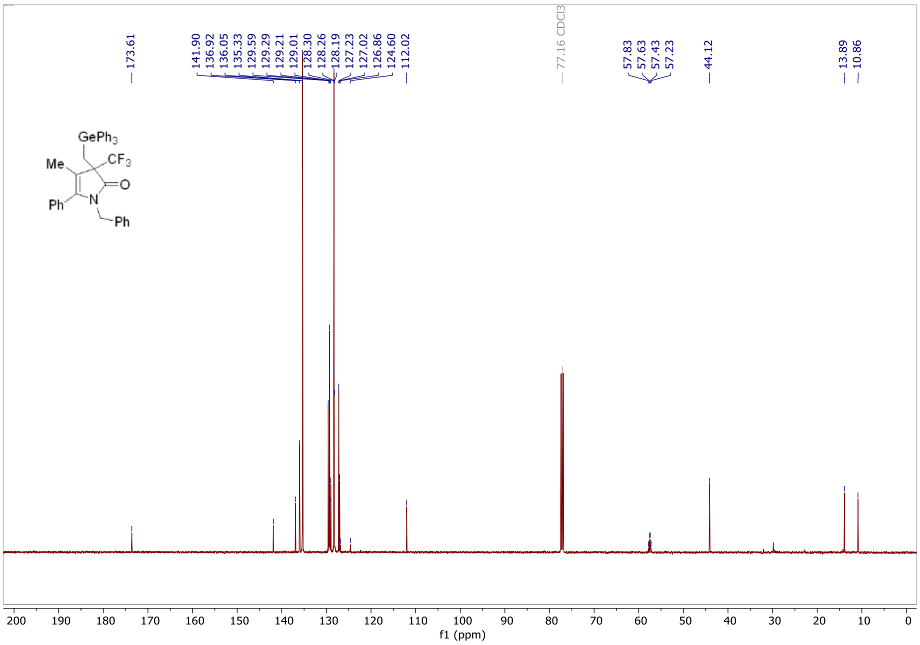


**Figure 3.10.45** $^{13}$C NMR spectra of **5a** [$CDCl_3$, 126 MHz]

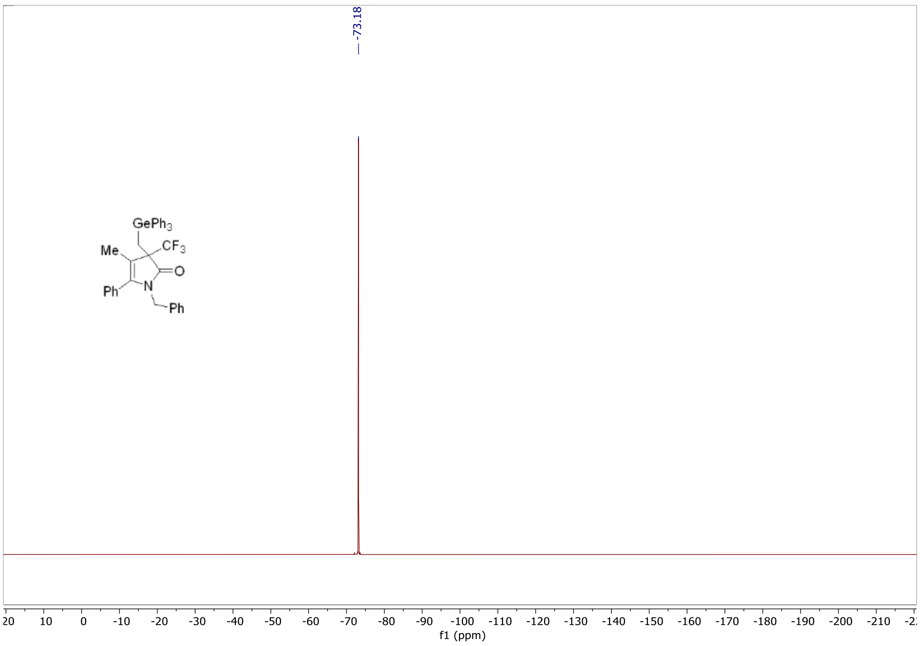


**Figure 3.10.46** $^{19}$F NMR spectra of **5a** [$CDCl_3$, 471 MHz]

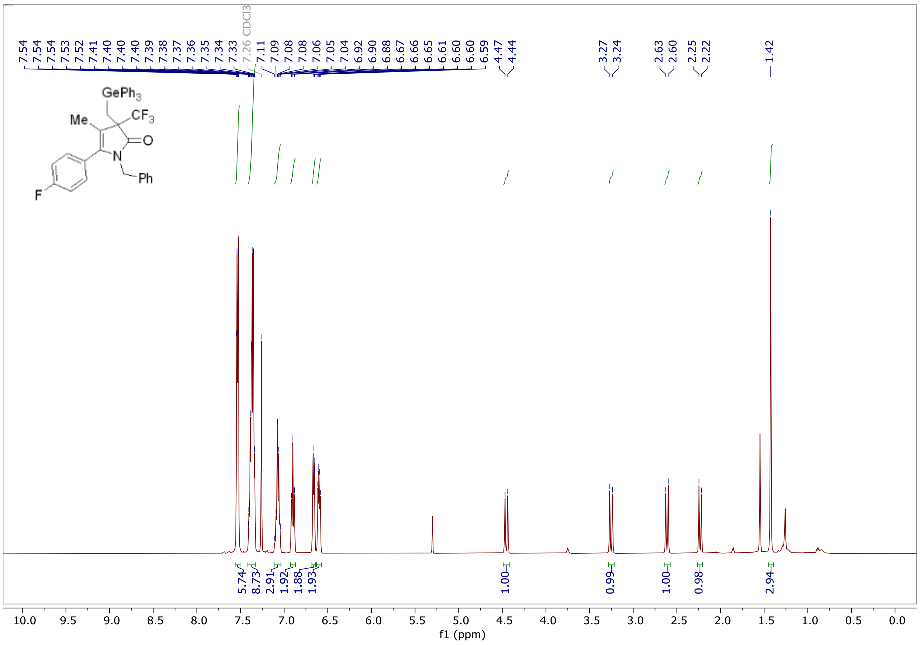

**Figure 3.10.47** $^{1}H$ NMR spectra of **5c** [$CDCl_3$, 500 MHz]

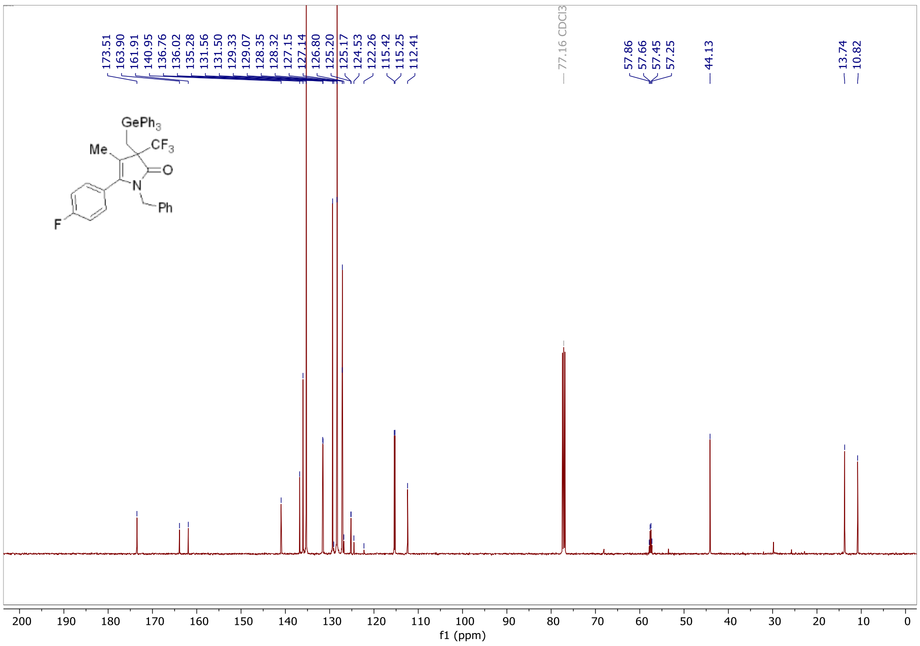

**Figure 3.10.48** $^{13}C$ NMR spectra of **5c** [$CDCl_3$, 126 MHz]

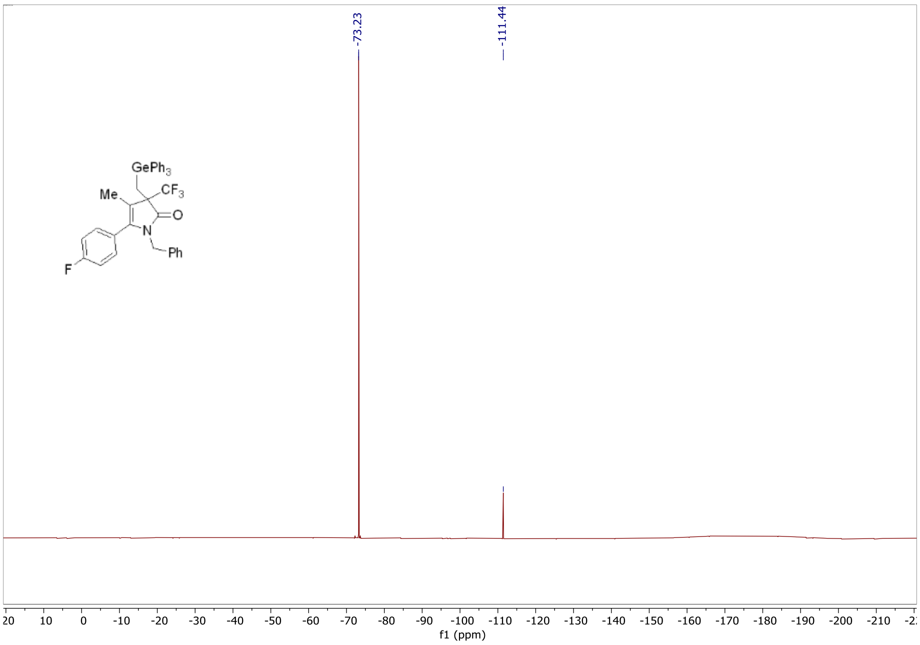

**Figure 3.10.49** [19]F NMR spectra of **5c** [$CDCl_3$, 471 MHz]

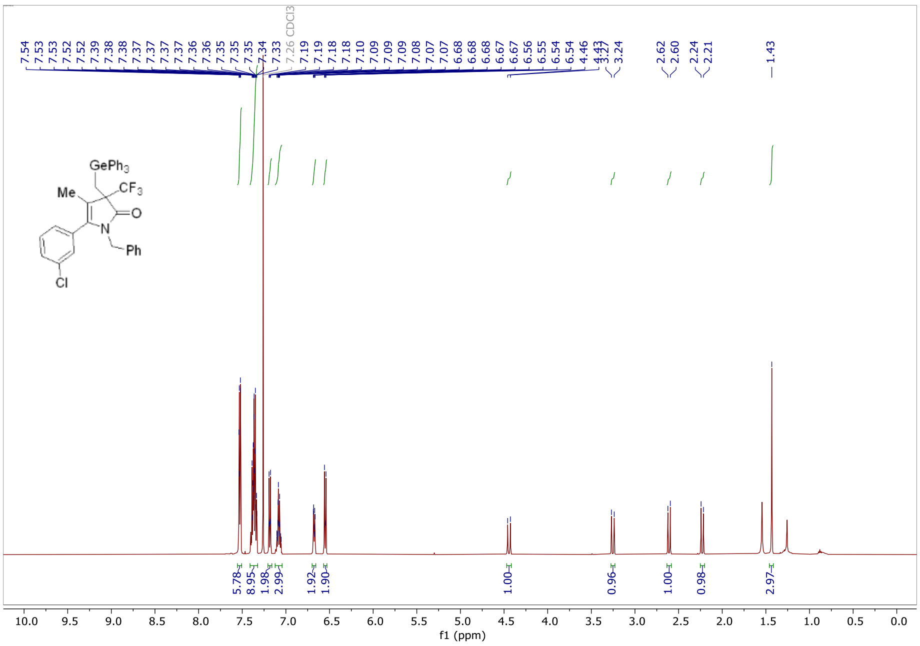

**Figure 3.10.50** [1]H NMR spectra of **5e** [$CDCl_3$, 500 MHz]

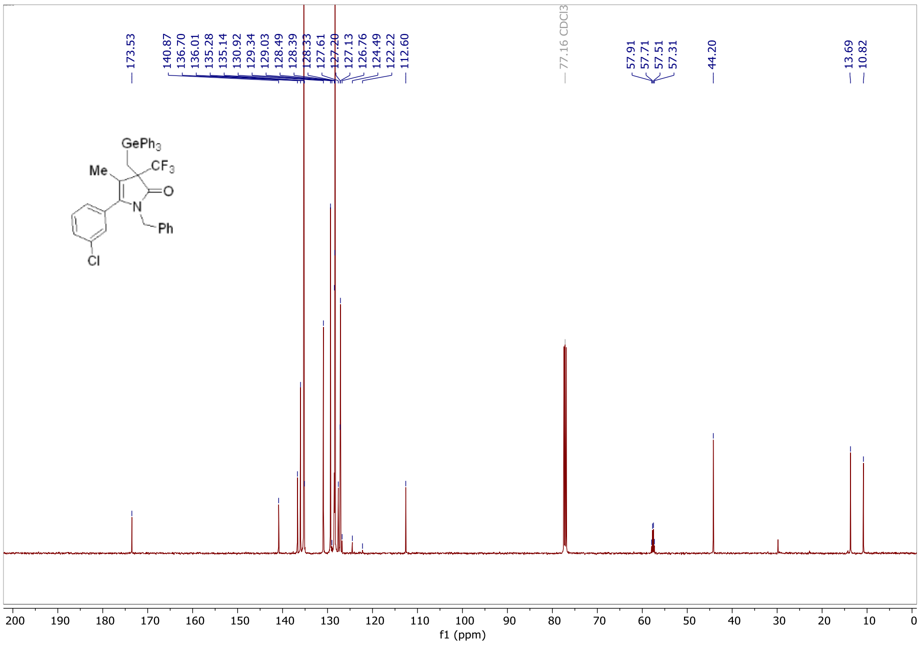

**Figure 3.10.51** $^{13}C$ NMR spectra of **5e** [$CDCl_3$, 126 MHz]

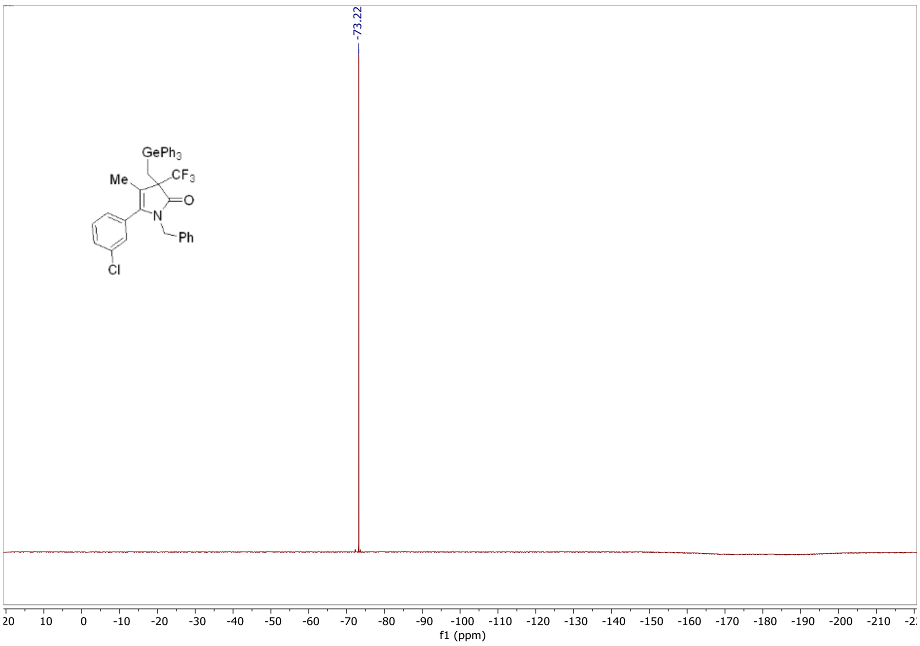

**Figure 3.10.52** $^{19}F$ NMR spectra of **5e** [$CDCl_3$, 471 MHz]

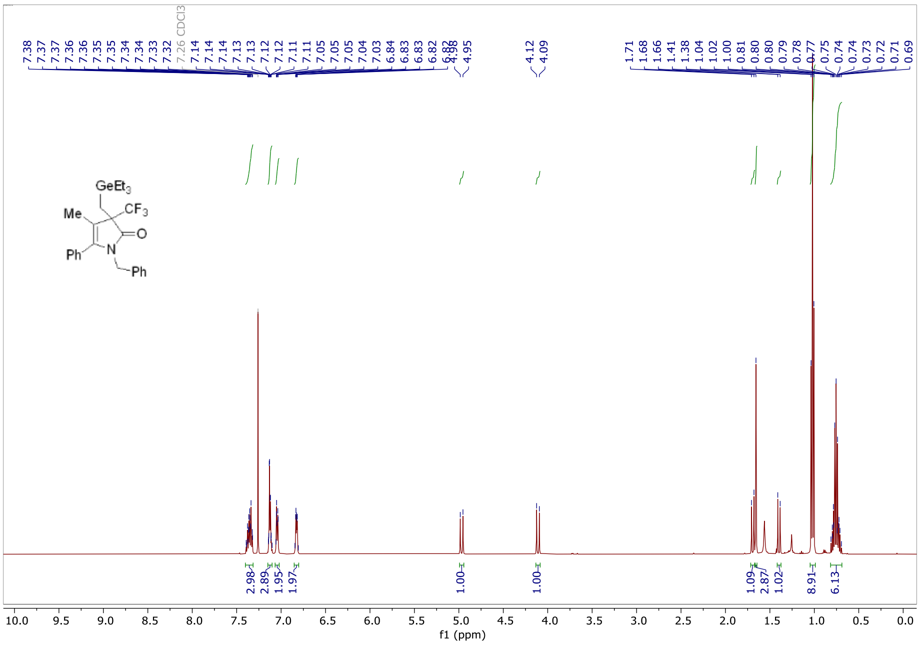

**Figure 3.10.53** $^{1}H$ NMR spectra of **5g** [$CDCl_3$, 500 MHz]

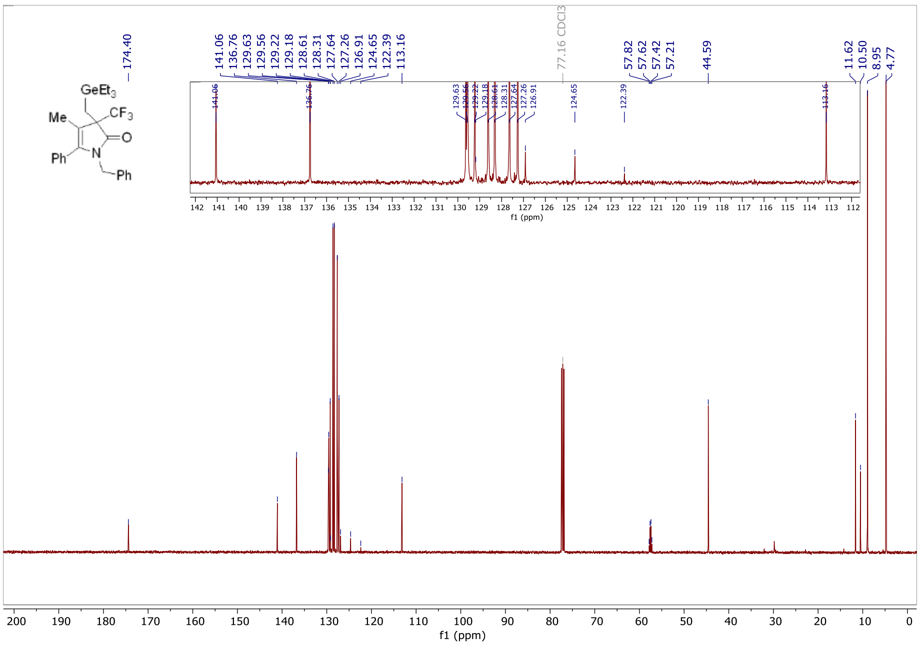

**Figure 3.10.54** $^{13}C$ NMR spectra of **5g** [$CDCl_3$, 126 MHz]

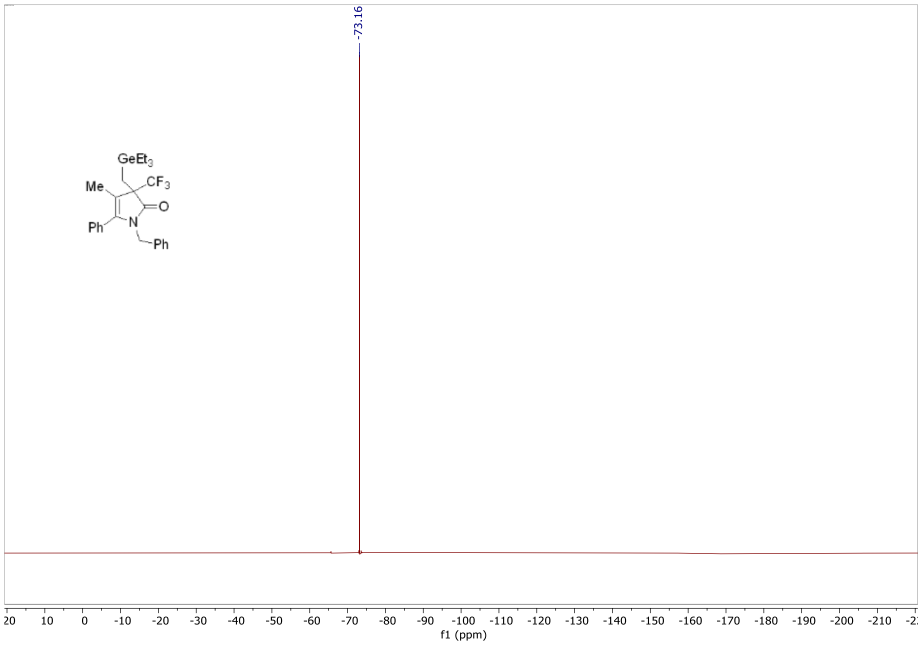

**Figure 3.10.55** $^{19}$F NMR spectra of **5g** [$CDCl_3$, 471 MHz]

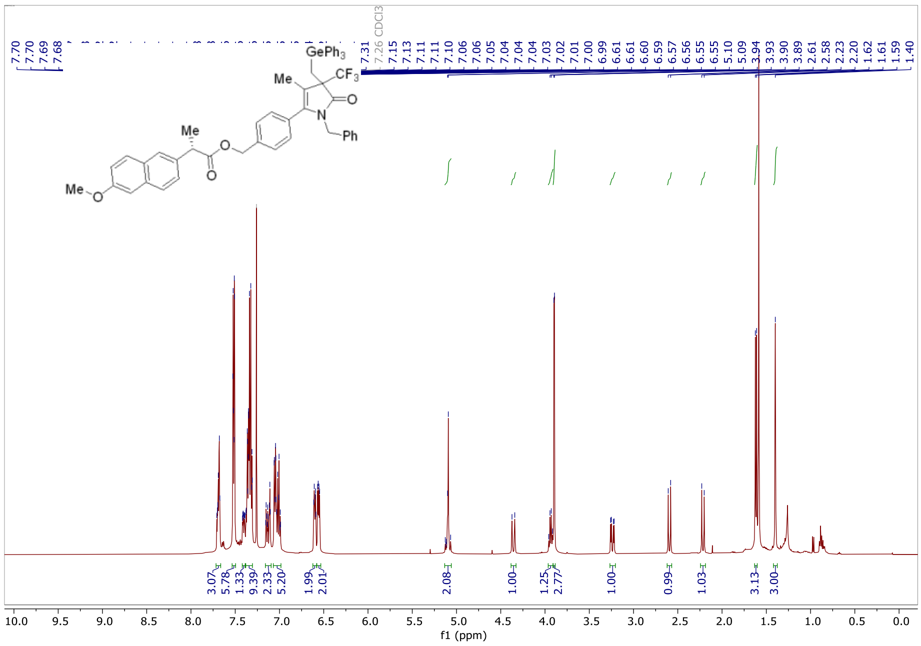

**Figure 3.10.56** $^{1}$H NMR spectra of **5j** [$CDCl_3$, 500 MHz]

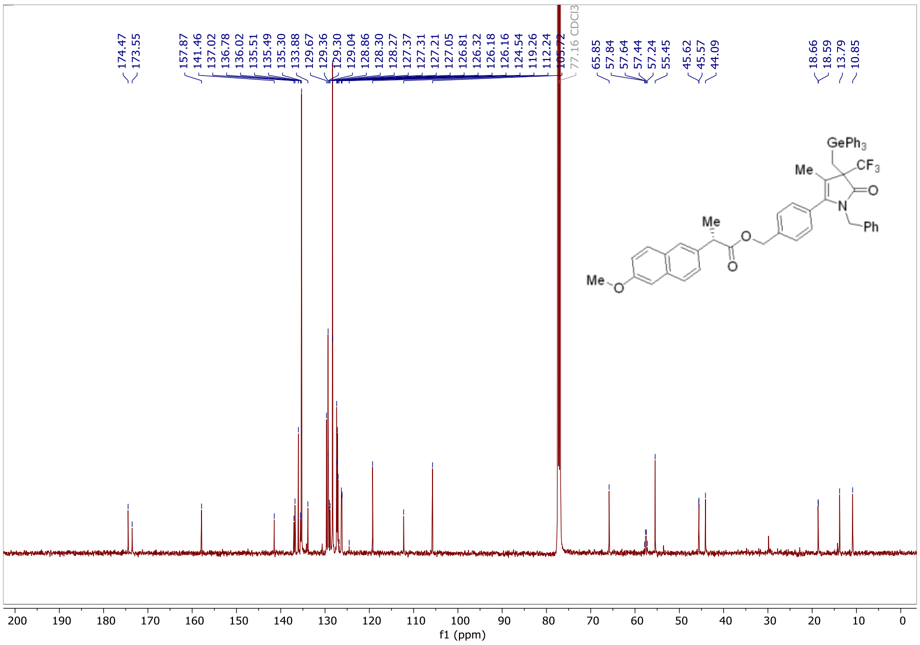

**Figure 3.10.57** $^{13}C$ NMR spectra of **5j** [$CDCl_3$, 126 MHz]

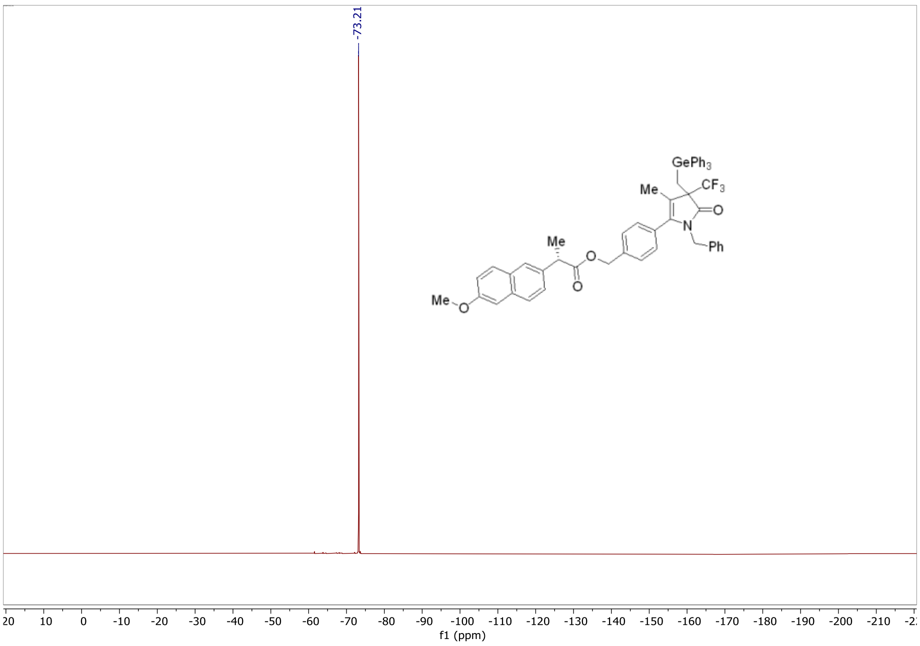

**Figure 3.10.58** $^{19}F$ NMR spectra of **5j** [$CDCl_3$, 471 MHz]

## 3.11 References


1. Huang, H.-M., Garduno-Castro, M. H., Morrill, C., Procter, D.J. (2019). Catalytic cascade reactions by radical relay. *Chem. Soc. Rev. 48*, 4626-4638. (DOI: 10.1039/C8CS00947C).

2. Nicolaou, K. C., Edmonds, D. J., Bulger, P. G. (2006). Cascade reactions in total synthesis. *Angew. Chem. Int. Ed. 45*, 7134-7186. (DOI:10.1002/anie.200601872).
3. Ardkhean, R., Caputo, D. F. J., Morrow, S. M., Shi, H., Xiong, Y., Anderson, E. A. (2016). Cascade polycyclizations in natural product synthesis. *Chem. Soc. Rev. 45*, 1557-1569. (DOI:10.1039/C5CS00105F).
4. Xuan, J., Studer, A. (2017). Radical cascade cyclization of 1,*n*-enynes and diynes for the synthesis of carbocycles and heterocycles. *Chem. Soc. Rev. 46*, 4329-4346. (DOI:10.1039/C6CS00912C).
5. Liao, J., Yang, X., Ouyang, L., Lai, Y., Huang, J., Luo, R. (2021). Recent advances in cascade radical cyclization of radical acceptors for the synthesis of carbo- and heterocycles. *Org. Chem. Front. 8*, 1345-1363. (DOI:10.1039/D0QO01453B).
6. Arora, P., Arora, V., Lamba, H., Wadhwa, D. (2012). Importance of heterocyclic chemistry: A review. *Int. J. Pharma Sci. Res*. *3*, 2947–2954. (DOI:10.13040/IJPSR.0975-8232.3(9).2947-54).
7. Heravi, M. M., Zadsirjan, V. (2020). Prescribed drugs containing nitrogen heterocycles: An overview. *RSC Adv. 10*, 44247-44311. (DOI:10.1039/d0ra09198g).
8. Kaushik, N. K., Kaushik, N., Attri, P., Kumar, N., Kim, C. H., Verma, A. K., Choi, E. H. (2013). Biomedical importance of indoles. *Molecules 18*, 6620-6662. (DOI: 10.3390/molecules18066620).
9. Saini, M. S., Kumar, A., Dwivedi, J., Singh, R. (2013). A review: Biological significances of heterocyclic compounds. *Int. J. Pharma. Sci. Res 4*, 66-77. (DOI:IJPSR13-04-03-005).
10. Taylor, R. D., Maccoss, M., Lawson, A. D. (2014). Rings in drugs. *J. Med. Chem. 57*, 5845-5859. (DOI: 10.1021/jm4017625).

11. Vitaku, E., Smith, D. T., Njardarson, J. T. (2014). Analysis of the structural diversity, substitution patterns, and frequency of nitrogen heterocycles among U.S. FDA-approved pharmaceuticals. *J. Med. Chem. 57*, 10257-10274. (DOI: 10.1021/jm501100b).
12. Marshall, C. M., Federice, J. G., Bell, C. N., Cox, P. B., Njardarson, J. T. (2024). An update on the nitrogen heterocycle compositions and properties of U.S. FDA-approved pharmaceuticals (2013-2023). *J. Med. Chem. 67*, 11622-11655. (DOI:10.1021/acs.jmedchem.4c011220).
13. Nozaki, H., Fukuoka, Y., Matsuo, A., Soga, O., Nakayama, M. (1980). Structure of sargassumlactam, a new *β*, *γ*-unsaturated-*γ*-lactam, from the marine alga Sargassum kjellmanianum. *Chem. Lett.* 1453-1454. (DOI:10.1246/cl.1980.1453).
14. Fu, P., Kong, F., Li, X., Wang, Y., Zhu, W. (2014). Cyanogramide with a new spiro [indolinone-pyrroloimidazole] skeleton from Actinoalloteichus cyanogriseus. *Org. Lett. 16*, 3708-3711. (DOI:10.1021/ol501523d).
15. Kang, U., Cartner, L. K., Wang, D. *et al.* (2020). Denigrins and dactylpyrroles, arylpyrrole alkaloids from a Dactylia sp. marine sponge. *J. Nat. Prod. 83*, 3464-3470. (DOI:10.1021/acs.jnatprod.0c01103).
16. Khamthong, N., Rukachaisirikul, V., Phongpaichit, S., Preedanon, S., Sakayaroj, J. (2014). An antibacterial cytochalasin derivative from the marine-derived fungus Diaporthaceae sp. PSU-SP2/4. *Phytochem. Lett. 10*, 5-9. (DOI: 10.1016/j.phytol.2014.06.014).
17. Merino, E., Nevado, C. (2014). Addition of $CF_3$ across unsaturated moieties: A powerful functionalization tool. *Chem. Soc. Rev. 43*, 6598-6608. (DOI:10.1039/C4CS00025K).
18. Wang, S., Wang, W. (2020). Recent advances of the construction of trifluoromethylated quaternary carbon center. *Chin. J. Org. Chem. 40*, 1901-1911. (DOI: 10.6023/cjoc202001012).

19. Charvillat, T., Bernardelli, P., Daumas, M., Pannecoucke, X., Ferey, V., Besset, T. (2021). Hydrogenation of fluorinated molecules: An overview. *Chem. Soc. Rev. 50*, 8178-8192. (DOI: 10.1039/D0CS00736F).
20. Berger, D., Imhof, W. (1999). One-pot synthesis of *γ*-lactams in a reaction cascade from *α*,*β*-unsaturated imines, CO and ethylene catalyzed by $Ru_3(CO)_{12}$. *Chem. Commun.* 1457- 1458. (DOI: 10.1039/a903266e).
21. Morimoto, T., Chatani, N., Murai, S. (1999). The first catalytic carbonylative [4+1] cycloaddition using a 1,3-conjugated system: A new transformation of *α*,*β*-unsaturated imines to unsaturated *γ*-lactams catalyzed by $Ru_3(CO)_{12}$. *J. Am. Chem. Soc. 121*, 1758-1959. (DOI: 10.1021/ja983546i).
22. Imhof, W., Berger, D., Kotteritzsch, M., Rost, M., Schonecker, B. (2001). The stereoselective $Ru_3(CO)_{12}$-catalyzed synthesis of steroidal 1,3-dihydropyrrol-2-one derivatives from *α*,*β*-unsaturated imines, carbon monoxide and ethylene. *Adv. Synth. Catal. 343*, 795-801.
(DOI:10.1002/16154169(20011231)343:8<795::AID-ADSC795>3.0.CO;2-M).
23. Chatani, N., Kamitani, A., Murai, S. (2002). Ruthenium-catalyzed reaction of *α*,*β*-unsaturated imines with carbon monoxide and alkenes leading to *β*,*γ*-unsaturated *γ*-butyrolactams: Involvement of direct carbonylation at olefinic C-H bonds as a key step. *J. Org. Chem. 67*, 7014-7018. (DOI: 10.1021/jo026001m).
24. DeBoef, B., Pastine, S. J., Sames, D. (2004). Cross-coupling of $sp^3$ C-H bonds and alkenes: Catalytic cyclization of alkene-amide substrates. *J. Am. Chem. Soc. 126*, 6556-6557. (DOI: 10.1021/ja049111e).
25. Song, T., Arseniyadis, S., Cossy, J. (2019). Asymmetric synthesis of *α*-quaternary *γ*-lactams through palladium-catalyzed asymmetric allylic alkylation. *Org. Lett. 21*, 603-607. (DOI: 10.1021/acs.orglett.8b03613).

26. Koronatov, A. N., Rostovskii, N. V., Khlebnikov, A. F., Novikov, M. S. (2020). Synthesis of 3-alkoxy-4-pyrrolin-2-ones *via* Rhodium-(II)-catalyzed denitrogenative transannulation of 1*H*-1,2,3-triazoles with diazo esters. *Org. Lett. 22*, 7958-7963. (DOI:10.1021/acs.orglett.0c02893).
27. Lv, Y., Pu, W., Chen, Q., Wang, Q., Niu, J., Zhang, Q. (2017). Cu-Catalyzed aminodifluoroalkylation of alkynes and *α*-bromodifluoroacetamides. *J. Org. Chem. 82*, 8282-8289. (DOI:10.1021/acs.joc.7b01313).
28. Liu, Y., Song, H., Zhang, C., Liu, Y., Shi, B. (2020). Copper-catalyzed modular access to *N*-fused polycyclic indoles and 5-aroyl-pyrrol-2-ones *via* intramolecular N-H/C-H annulation with alkynes: Scope and mechanism probes. *Chin. J. Chem. 38*, 1545-1552. (DOI:10.1002/cjoc.202000246).
29. Hu, R., Tao, Y., Zhang, X., Su, W. (2021). 1,2-Aryl migration induced by amide C-N bond-formation: Reaction of alkyl aryl ketones with primary amines towards *α,α*-diaryl *β,γ*-unsaturated *γ*-lactams. *Angew. Chem., Int. Ed. 60*, 8425-8430. (DOI:10.1002/anie.202014900).
30. Ding, R., Liu, Y.-L., Hao, H., Chen, C.-Y., Liu, L., Chen, N.-S., Guo, Y., Wang, P.-L. (2021). Regioselective, copper(I)-catalyzed, tandem sulfonylation-cyclization of 1,5-dienes with sulfonyl chlorides. *Org. Chem. Front. 8*, 3123-3127. (DOI:10.1039/D1QO00460C).
31. Liu, F., Huang, J., Wu, X., Du, F., Zeng, L., Wu, J., Chen, Z. (2022). Regioselective radical-relay sulfonylation/cyclization protocol to sulfonylated pyrrolidones under transition metal-free conditions. *J. Org. Chem. 87*, 6137-6145. (DOI:10.1021/acs.joc.2c00381).
32. Li, W., Wang, C., Zhu, T., Liu, G., Wu, J. (2024). Metal- and additive-free β-C($sp^2$)-H decarboxylative alkylsulfonylation of enamides from phenyliodine(III) dicarboxylates and sulfur dioxide. *Chem. Commun. 60*, 8212-8215. (DOI: 10.1039/D4CC02865A).

33. Wang, P., Leng, Y., Wu, Y. (2020). Copper(I)-catalyzed regioselective tandem cyanoalkylative cyclization of 1,5-dienes with cyclobutanone oxime esters. *Eur. J. Org. Chem.* e202201091. (DOI:10.1002/ejoc.202201091).
34. Hu, X., Tao, M., Ma, Z., Zhang, Y., Li, Y., Liang, D. (2022). Regioselective photocatalytic dialkylation/cyclization sequence of 3-aza-1,5-dienes: access to 3,4-dialkylated 4-pyrrolin-2-ones. *Adv. Synth. Catal. 364*, 2163-2168. (DOI: 10.1002/adsc.202200183).
35. He, J.-Q., Yang, Z.-X., Zhou, X.-L., Li, Y., Gao, S., Shi, L., Liang, D. (2022). Exploring the regioselectivity of the cyanoalkylation of 3-aza-1,5-dienes: Photoinduced synthesis of 3-cyanoalkyl-4-pyrrolin-2-ones. *Org. Chem. Front. 9*, 4575-4582. (DOI:10.1039/D2QO00918H).
36. Yang, R., Chen, D., Lin, S., Yang, X., Shi, L., Chang, Q., Liang, D. (2023). Photoinduced regioselective perfluoroalkylation/cyclization cascade of 3-aza-1,5-dienes: Access to pentasubstituted 3-perfluoroalkyl-1,3-dihydropyrrol-2-ones. *Eur. J. Org. Chem. 26*, e202300528. (DOI: 10.1002/ejoc.202300528).
37. Hu, X., Tao, M., Gong, K., Feng, Q., Hu, X., Li, Y., Sun, S., Liang, D. (2023). Electrochemical or photoelectrochemical alkenylpolyfluoroalkylation of 3-aza-1,5-dienes: Regioselective entry to polyfluoroalkylated 4-pyrrolin-2-ones. *J. Org. Chem. 88*, 12935-12948. (DOI:10.1021/acs.joc.3c00790).
38. Wang, D., Zeng, L., Shi, J., Gao, S., Shi, L., Sun, S., Liang, D. (2024). Electrophotocatalysis versus indirect electrolysis: electrochemical selenocyclization of 3-aza-1,5-dienes facilitated by energy transfer, direct photolysis or *N*-hydroxyphthalimide. *Chem. Eur. J. 30*, e202400280. (DOI:10.1002/chem.202400280).
39. Gong, K., Ma, Y., Yu, P., Gao, S., Li, Y., Liang, D., Sun, S., Wang, B. (2024). Self- or acridinium-catalyzed electrophotosynthesis of thiocyanato heterocycles from

activated alkenes. *Adv. Synth. Catal*. *366*, 2352-2362. (DOI:10.1002/adsc.202400153).

40. Ji, X., He, R., Shi, L., Sun, S., Liang, D. (2024). Synthesis of diverse 4-pyrrolin-2-ones by electrochemically induced dehydrogenative regioselective cyclization of 3-aza-1,5-dienes and 1,3-dicarbonyl compounds. *Eur. J. Org. Chem. 27*, e202301246. (DOI:10.1002/ejoc.202301246).
41. Yang, Z.-X., Ding, L.-C., Yang, G.-H., Wang, D., Shi, L., Li, Y., Liang, D. (2024). Electrochemical sulfonylation/cyclization of *N*-alkenylacrylamides with sodium sulfinates or sulfonyl hydrazides. *J. Org. Chem. 89*, 10660-10677. (DOI:10.1021/acs.joc.4c00892).
42. Bajya, K. R., Kumar, M., Ansari, A., Selvakumar, S. (2023). Sulfonamide as photoinduced hydrogen atom transfer catalyst for organophotoredox hydrosilylation and hydrogermylation of activated alkenes. *Adv. Synth. Catal. 365*, 976-982. (DOI:10.1002/adsc.202300040).
43. Ladumor, R., Samanta, S., Selvakumar, S. (2024). Photocatalytic silylation of aryl alkynoates: Synthesis of silylated coumarins. *Adv. Synth. Catal. 367,* e202401007. (DOI:10.1002/adsc.202401007).
44. Greulich, T. W., Daniliuc, C. G., Studer, A. (2015). *N*-Aminopyridinium salts as precursors for *N*-centered radicals: Direct amidation of arenes and heteroarenes. *Org. Lett. 17,* 254-257. (DOI:10.1021/ol503338b).
45. Szabo, K. F., Goliszewska, K. Szurmak, J., Jasinska, K. R., Gryko, D. (2022). Site-selective, photocatalytic vinylogous amidation of enones. *Org. Lett. 24*, 8120-8124. (DOI:10.1021/acs.orglett.2c03161).
46. Jung, S., Lee, H., Moon, Y., Jung,H.-Y., Hong, S. (2019). Site-selective C−H acylation of pyridinium derivatives by photoredox catalysis. *ACS Catal. 9*, 9891-9896. (DOI:10.1021/acscatal.9b03367).

47. Guo, W., Wang, Q., Zhu, J. (2021). Selective 1,2-aminoisothiocyanation of 1,3-dienes under visible-Light photoredox catalysis. *Angew. Chem. Int. Ed. 60*, 4085-4089. (DOI:10.1002/anie.202014518).
48. Forster, D., Guo, W., Wang, Q., Zhu, J. (2021). Photoredox catalytic three-component amidoazidation of 1,3-dienes. *ACS Catal. 11*, 10871-10877. (DOI:10.1021/acscatal.1c03545).
49. Goliszewska, K., Jasinska, K. R., Szurmak, J., Gryko, D. (2019). Visible-light-mediated amination of $\pi$-nucleophiles with *N*-aminopyridinium salts. *J. Org. Chem. 84*, 15834-15844. (DOI:10.1021/acs.joc.9b02073).
50. M. Garreau, F. Le Vaillant, J. Waser (2019). C-Terminal bioconjugation of peptides through photoredox catalyzed decarboxylative alkynylation. *Angew. Chem. Int. Ed. 58*, 8182-8186. (DOI: 10.1002/anie.201901922).
51. Liang Y., Luo J., Diskin-Posner Y., Milstein D. (2023). Designing new magnesium pincer complexes for catalytic hydrogenation of imines and *N*-heteroarenes: $H_2$ and N-H activation by metal-ligand cooperation as key steps. *J. Am. Chem. Soc. 145*, 9164-9175. (DOI:10.1021/jacs.3c01091).
52. Zhou M., Lin Y., Chen Xiao-X., Xu G., Chung L.W., Tang W., (2023). Asymmetric synthesis of vicinal tetrasubstituted diamines *via* reductive coupling of ketimines templated by chiral diborons. *Angew. Chem. Int. Ed. 62*, e202300334. (DOI:10.1002/anie.202300334).
53. Gao, Y., Chen, S., Lu, W., Gu, W., Liu, P., Sun, P. (2017). Visible light-induced C3-sulfonamidation of imidazopyridines with sulfamides. *Org. Biomol. Chem. 15*, 8102-8109. (DOI:10.1039/C7OB02029E).
54. Hatchard, C. G., Parker, C. A. (1956). A new sensitive chemical actinometer-II. Potassium ferrioxalate as a standard chemical actinometer. *Proc. Roy. Soc. (London) A235*, 518-536. (DOI:10.1098/rspa.1956.0102).

55. Cismesia, M.A., Yoon, T. P. (2015). Characterization chain processes in visible light photoredox catalysis. *Chem. Sci. 6*, 5426-5434. (DOI:10.1039/C5SC02185E).

## Chapter 4

## Organophotocatalytic Regioselective Silylation/Germylation and Cascade Cyclization of 1,7-Dienes: Access to Silylated/Germylated Benzazepine Derivatives

### 4.1 Introduction

Benzazepine, a notable class of seven-membered heterocycles and it is a privileged structural motif in numerous natural bioactive molecules which exhibits different medicinal properties (e.g., benazepril, varenicline, and fenoldopam).[1-4] The selected examples (**Figure 4.1**) of benzazepines demonstrate distinctive bioactive and pharmacological characteristics, including antitumor, anticancer, and enzyme inhibitory effects, among others.[5-12] Consequently, the effective synthesis of benzazepine scaffolds has garnered significant interest from organic chemists and pharmacologists.[13-15]

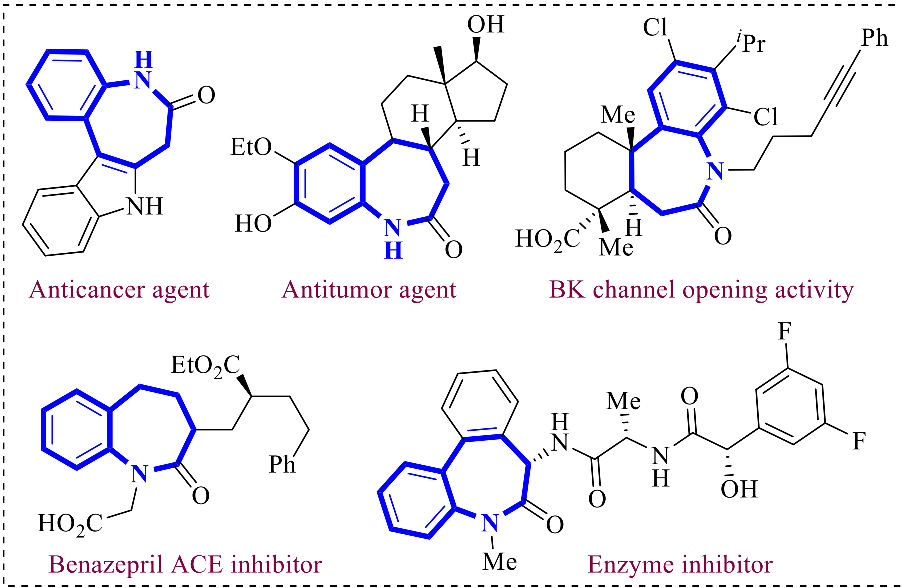


**Figure 4.1** Representative examples of bioactive molecules containing a benzazepine scaffold

Owing to the distinct physicochemical characteristics of the silyl and germyl functionalities,[16-22] the integration of these functionalities into heterocycles, such as the benzazepine scaffold, could offer the advantage of their combined inherent properties to the final compound, which would provide an ideal design for investigating its pharmacological activity.

### 4.2 Literature reports on construction of benzazepine scaffolds

The benzazepine scaffold can be constructed using several strategies, including rearrangements,*[23-27]* transition metal-mediated coupling reactions,*[25,28-30]* ring-closing metathesis,*[31-33]* radical additions,*[34-40]* and others.*[41-42]* Among these methods, benzazepines are most effectively synthesized *via* radical cascade reaction because of its efficiency and practicality. In 2015 Shi's group disclosed an efficient approach for the synthesis of trifluoromethyl-containing polycyclic benzazepine derivatives from acrylamides tethered to alkylidenecyclopropanes using copper or iron salts as catalysts under thermal conditions (**Scheme 4.1a**).*[34]*

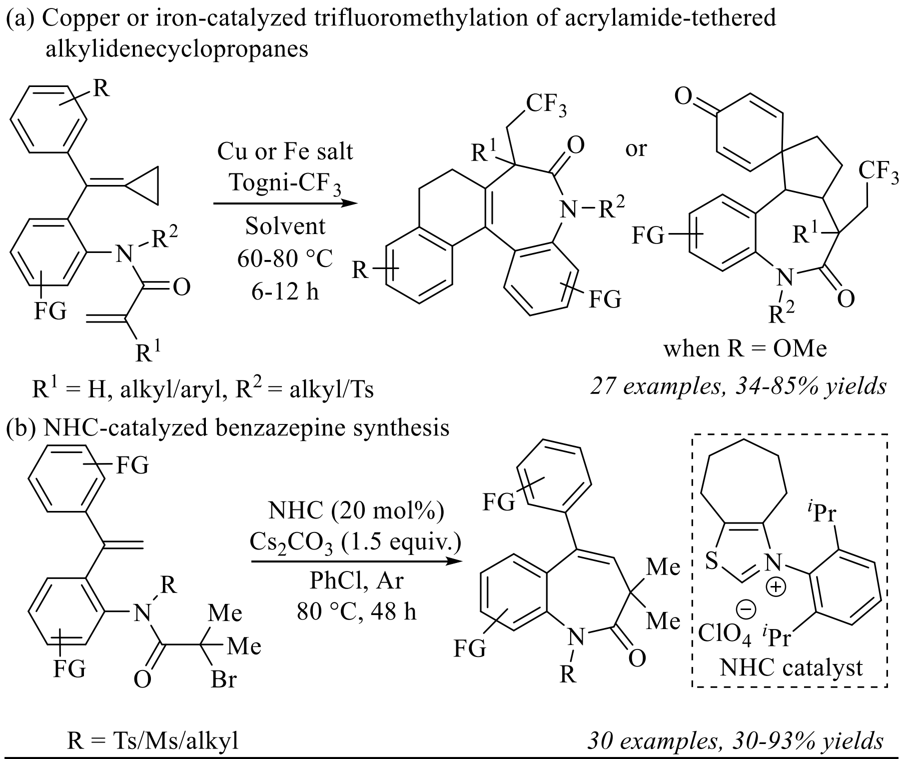


**Scheme 4.1** Metal and NHC-catalyzed benzazepine synthesis under thermal conditions

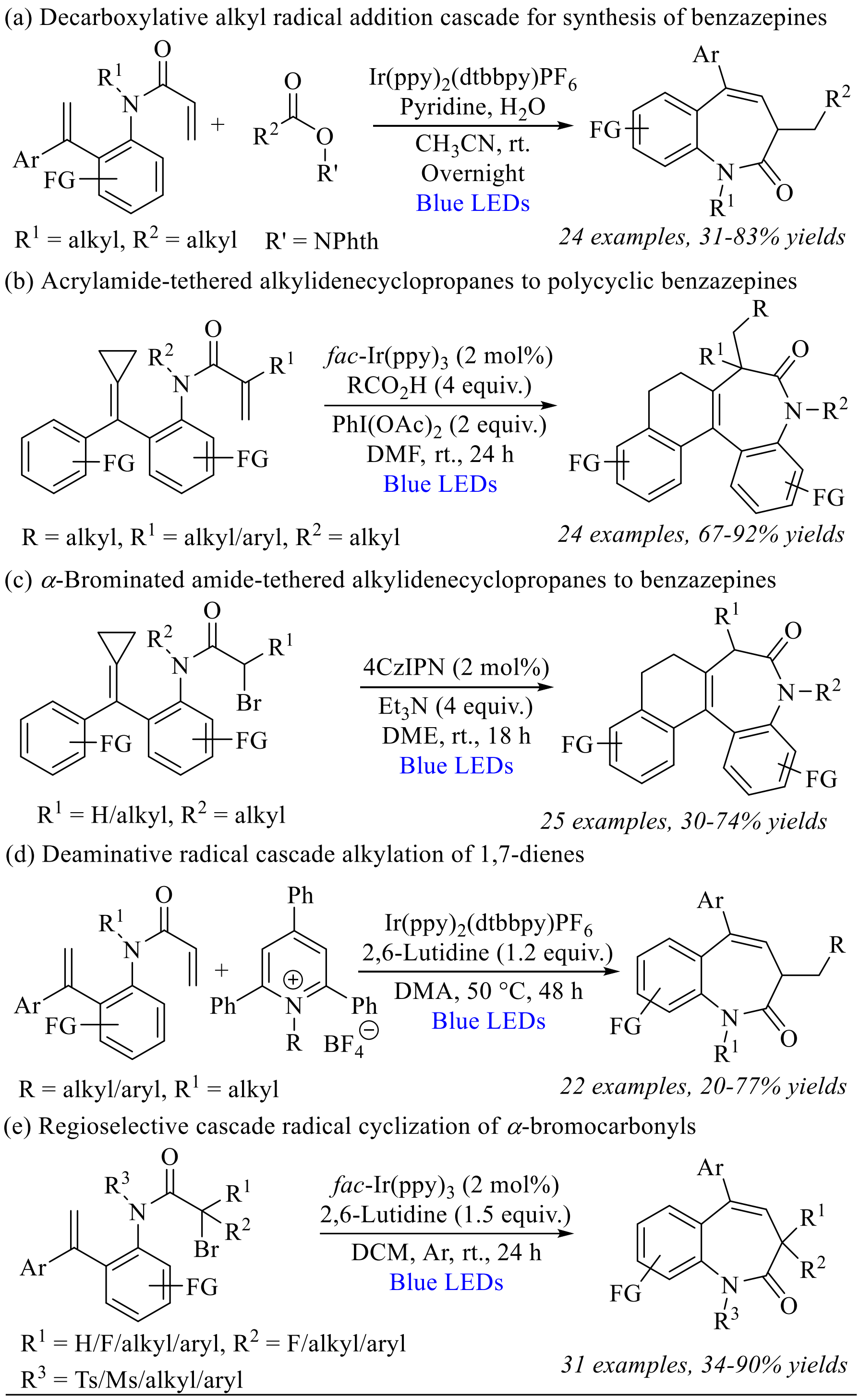


**Scheme 4.2** Photocatalytic method for the synthesis of benzazepine scaffold

Recently, the Zang[43] and Wang[44] group developed metal-free, *N*-heterocyclic carbene-catalyzed synthesis of benzazepines and polycyclic benzazepines under thermal conditions using *α*-bromo arylamide-tethered styrene and alkylidenecyclopropanes as starting material (**scheme 4.1b**). Among the photochemical methods, the Xiao group disclosed an Ir-catalyzed decarboxylative radical cascade reaction between a redox-active ester and acrylamide-tethered styrene (**Scheme 4.2a**).[45] Soon after, Shi's group developed tetracyclic benzazepine derivatives *via* decarboxylative tandem carbocyclization of acrylamide-tethered alkylidenecyclopropanes with $PhI(OAc)_2$ and other aliphatic acids (**Scheme 4.2b**).[46] In 2022, the same group reported the organophotocatalyzed halogen atom-transfer radical cascade cyclization of $\alpha$-brominated amide-tethered alkylidenecyclopropanes (**Scheme 4.2c**).[47] The Katritzky salt-derived alkyl radical addition to 1,7-dienes were also reported to provide benzazepine derivatives (**Scheme 4.2d**).[48] Recently, the Zhou group reported access to benzazepine derivatives *via* regioselective radical cascade cyclization of $\alpha$-bromocarbonyls, under visible light photoredox catalytic condition (**Scheme 4.2e**).[49]

### 4.3 Synthesis of silylated benzazepine

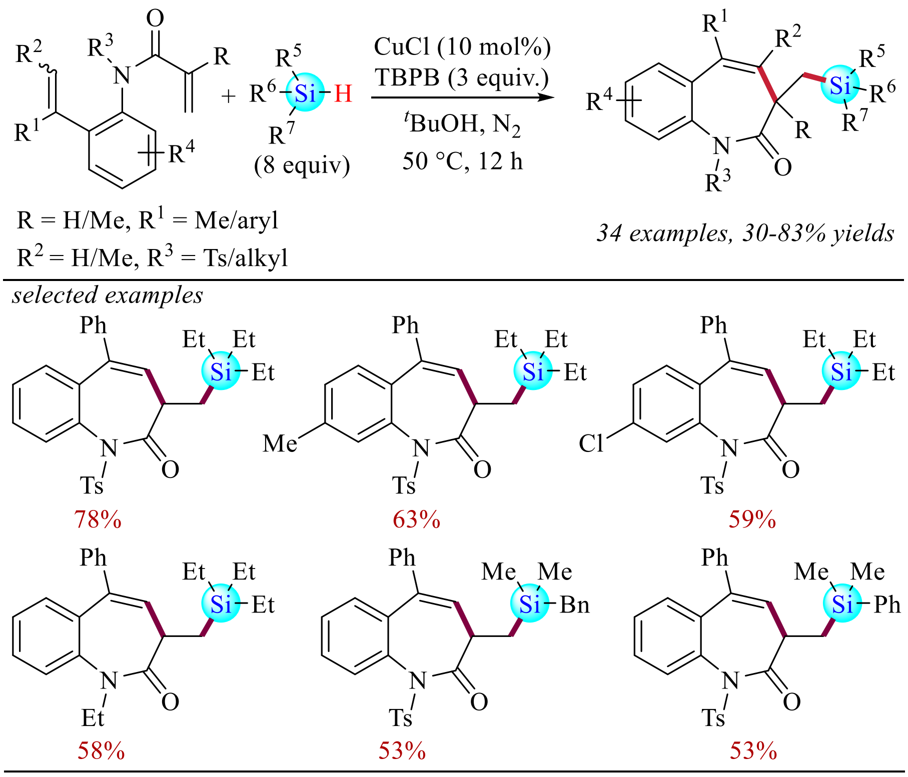


**Scheme 4.3** Transition metal-catalyzed radical cascade silylation of 1,7-dienes

The synthesis of silylated benzazepine was reported by Sun and coworkers *via* copper-catalyzed protocol using 1,7-diene as a starting material and a stoichiometric amount of *tert*-butyl peroxybenzoate (TBPB) as oxidant, to generate the silyl radical from hydrosilanes under thermal conditions. The triarylhydrosilanes and dihydrosilanes were not compatible in this reaction conditions, and high loading of hydrosilanes was required (**Scheme 4.3**).[50]

## 4.4 Objective

A survey of the literature revealed that, although the aforementioned strategies have been successfully employed for the synthesis of benzazepine scaffolds bearing diverse functionalities, only a single protocol has been reported for the synthesis of silyl benzazepines.[50] These reported methods have several shortcomings in the synthesis of benzazepine, as they rely on metal catalysts or salts and often require specific ligands. Moreover, the synthesis of silylated benzazepines typically necessitates high loading of both hydrosilanes and oxidants, which reduces the overall efficiency and practicality of the process. Since the available reports suffer from these drawbacks, exploration of mild, efficient, and metal-free silylation protocol is highly desirable for the synthesis of silylated benzazepine derivatives. As a part of our ongoing interest in the development of photoinduced silylation/ germylation protocols through *in situ* generated sulfamidyl radical.[51-53] We anticipated the generation of silyl/germyl radical from hydrosilanes/hydrogermanes as radical surrogate *via* hydrogen atom transfer and the chemoselective addition of silyl/germyl radical to 1,7-dienes followed by cascade cyclization could leads to the formation of silylated/germylated benzazepines.

## 4.5 Present work

### 4.5.1 Selection of model reaction

To evaluate our hypothesis, *N*-(2-(1-phenylvinyl)phenyl)-*N*-tosylacrylamide **1a** was selected as a model starting material and $Et_3SiH$ **2a** as a silyl source under photochemical condition (**Scheme 4.4**).

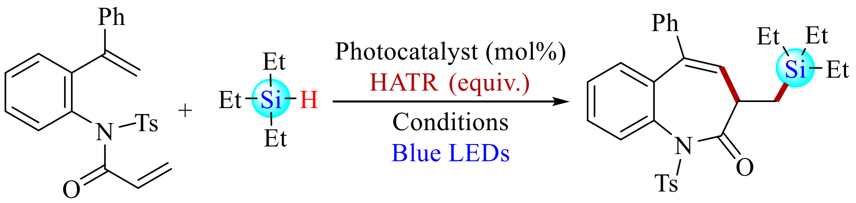


**1a** **2a** **3a**

**Scheme 4.4** Representative model reaction

### 4.5.2 Reaction optimization

The optimization of reaction conditions is described in **Table 4.1**. Started our investigation with *fac*-Ir(ppy)$_3$ as photocatalyst, *N*-aminopyridinium salts as hydrogen atom transfer reagents (HATR), and acetonitrile as solvent under blue LEDs irradiation for 30 minutes (entry 1) afforded the desired product **3a** in 45% yield. To further evaluate the reaction conditions, we tested a series of Iridium-based photocatalysts. A slight increase in the yield was observed upon using [Ir(ppy)$_2$(dtbbpy)]PF$_6$ (entry 2). The iridium photocatalyst bearing additional *tert*-butyl substituents resulted in a significant increase in product formation**,** affording the desired product in 63% yield (entry 3). In contrast, using [Ir(dF(CF$_3$)ppy)$_2$(dtbbpy)]PF$_6$ a drastic decrease in yield of **3a** was observed (entry 4). In pursuit of a metal-free protocol for the synthesis of silylated benzazepines, we turned our attention towards screening of organophotocatalysts such as 4CzIPN, 4DPAIPN, 3DPAFIPN, and Eosin-Y. Employing 4CzIPN as an organophotocatalyst afforded inferior results with 36% yield of silylated benzazepine (entry 5). Surprisingly, 4DPAIPN with a 3 mol% loading exhibits an excellent increment in the formation of silylated benzazepine, resulted in 72% yield of the desired product (entry 6). The screening of 3DPAFIPN and Eosin-Y shows inferior results (entries 7 and 8). Furthermore, reduction in loading of organophotocatalyst 4DPAIPN from 3 mol% to 1 mol% doesn't affect the reaction efficiency (entry 9). Next, we sought to reduce the equivalents of hydrosilane and HAT reagent and this resulted in a drastic decrease in product formation (entry 10).

**Table 4.1** Optimization table

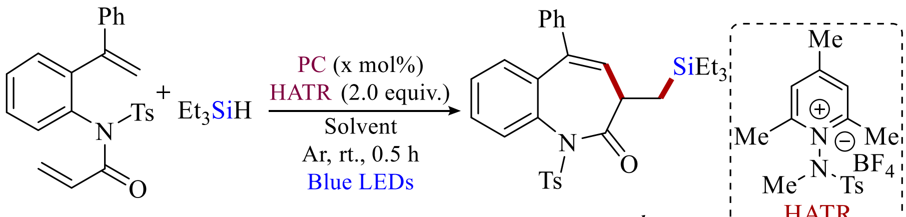


**1a** **2a** **3a, yield**[b]

| Entry | Photocatalyst (x mol%) | Solvent | Yield (%)[b] |
|---|---|---|---|
| 1 | *fac*-Ir(ppy)$_3$ (1) | $CH_3CN$ | 45 |
| 2 | [Ir(ppy)$_2$(dtbbpy)]PF$_6$ (1) | $CH_3CN$ | 48 |
| 3 | [Ir(dtbppy)$_2$(dtbbpy)]PF$_6$ (1) | $CH_3CN$ | 63 |
| 4 | [Ir(dF(CF$_3$)ppy)$_2$(dtbbpy)]PF$_6$ (1) | $CH_3CN$ | 12 |
| 5 | 4CzIPN (3) | $CH_3CN$ | 36 |
| 6 | 4DPAIPN (3) | $CH_3CN$ | 72 |
| 7 | 3DPAFIPN (3) | $CH_3CN$ | 46 |
| 8[c] | Eosin-Y (5) | $CH_3CN$ | trace |
| **9** | **4DPAIPN (1)** | **$CH_3CN$** | **72** |
| 10[d] | 4DPAIPN (1) | $CH_3CN$ | 48 |
| 11 | 4DPAIPN (1) | $PhCF_3$ | 28 |
| 12 | 4DPAIPN (1) | DCE | 40 |
| 13 | 4DPAIPN (1) | Acetone | 55 |
| 14 | 4DPAIPN (1) | DMSO | 59 |
| 15[e] | 4DPAIPN (1) | $CH_3CN$ | 64 |
| 16[f] | 4DPAIPN (1) | $CH_3CN$ | 64 |
| 17 | none | $CH_3CN$ | n.r. |
| 18[g] | 4DPAIPN (1) | $CH_3CN$ | n.r. |
| 19[h] | 4DPAIPN (1) | $CH_3CN$ | n.r. |

[a]Reaction conditions: **1a** (0.1 mmol), **2a** (0.5 mmol), PC (x mol%), HATR (0.2 mmol) and acetonitrile (1 mL) were irradiated under blue LEDs for 0.5 h. [b]isolated yield. [c]525 nm kessil was used. [d]using 3.0 equiv. of **2a** and 1.5 equvi. HATR. [e]solvent conc. 0.05 M. [f]solvent conc. 0.2 M. [g]without HATR. [h]without light. n.r = no reaction. PC = photocatalyst.

After identifying the ideal photocatalyst and establishing the appropriate equivalents of the hydrosilane and HAT reagent, we turned our attention to solvent screening. The systematic screening of different solvents such as *α*-*α*-*α*-trifluorotoluene, dichloroethane, acetone, and dimethylsulfoxide revealed acetonitrile as the most suitable solvent for this transformation (entries 11-14). To further improve the yield of the silylated benzazepine, variations in reaction concentration were tried, however inferior outcomes were observed on both decreasing (entry 15) and increasing (entry 16) the reaction concentration. Control experiments established that the photocatalyst, HAT reagent, and light irradiation were all essential for this radical cascade cyclization, as no product formation was observed in the absence of any of these components (entries 17-19).

### 4.5.3 Scope of 1,7-dienes in the synthesis of silylated benzazepines

After establishing the optimal reaction conditions, the scope of 1,7-dienes **1** was systematically investigated, as shown in **Scheme 4.5**. Starting with the effect of substituents on the benzene ring tethered to the alkene. The methyl (**1b**) and chloro (**1c**) substituents at the *para*-position afforded the desired products **3b** and **3c** in 51% and 60% yield respectively. Additionally, chloro (**1d**) substituent at the *meta*-position also provided corresponding silylated benzazepine **3d** in 64% yield. Similarly, methyl group (**1e**) at *ortho*-position gives **3e** in good yield (72%). Meanwhile, dichloro-substituents (**1f**) at *ortho* and *para*-positions afforded the desired product **3f** in a slightly lower yield (47%). In case of substrate with strong electron-withdrawing cyano-substituent (**1g**) at the *para*-position, undergoes smooth radical cascade cyclization and provided **3g** in 63% yield. The substrate with a 2-thienyl ring (**1h**) attached to the alkene was found to be compatible. However, it was more reactive towards the addition of the silyl radical and provided the desired silylated benzazepine product **3h** with 25% yield. Employing the 1,1-phenylmethyl alkene (**1i**) tethered to acrylamide as a substrate, the desired product **3i** was not detected. Next, we turned our attention to examine the influence of substituents on the benzene ring of aryl amines.

Introduction of a methyl substituent (**1j**) at the *ortho*-position led to a significant decrease in yield, affording **3j** in 37% yield.

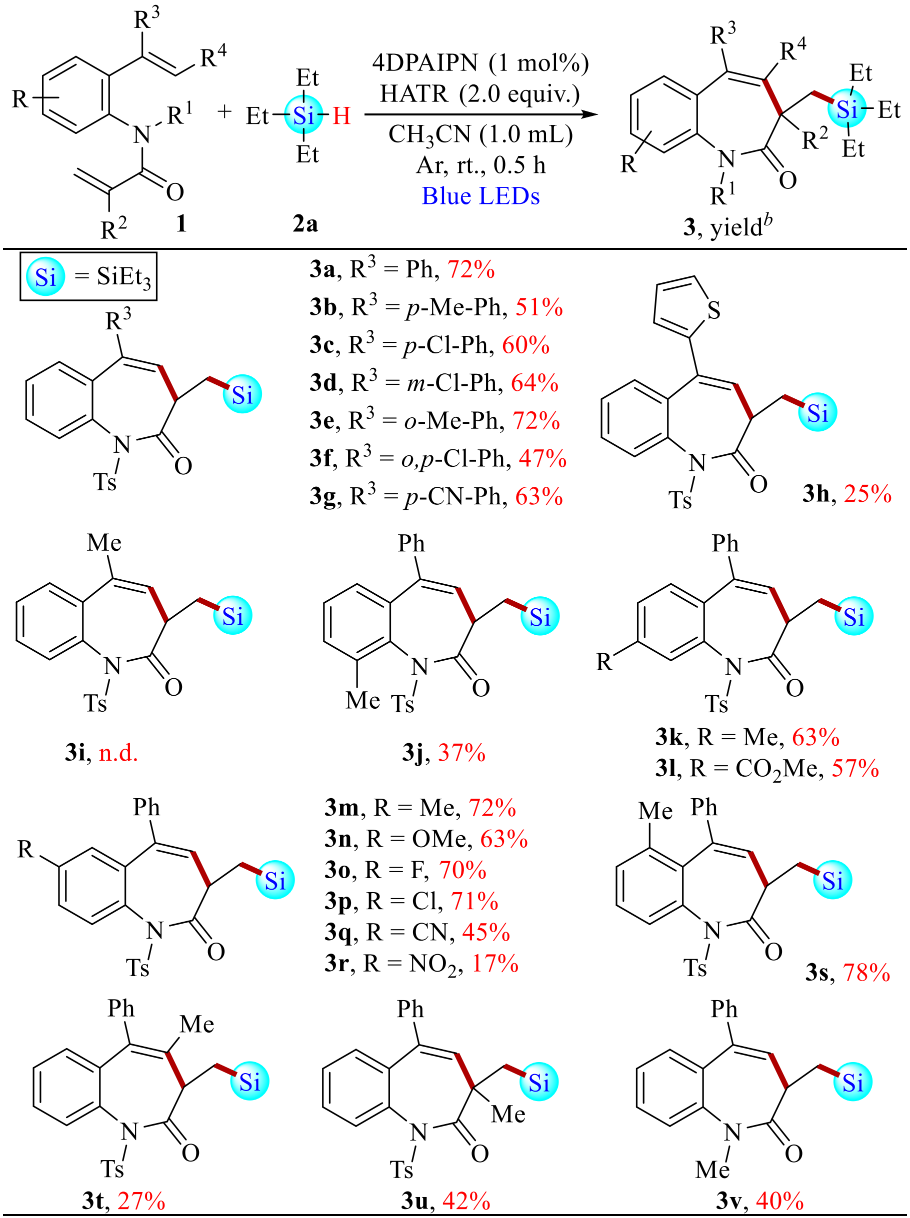


[a]Reaction conditions: **1** (0.1 mmol), **2a** (0.5 mmol), HATR (0.2 mmol), 4DPAIPN (1 mol%), and dry acetonitrile (1.0 mL) were irradiated under blue LEDs. [b]isolated yield. n.d. = not detected.

**Scheme 4.5** Scope of 1,7-dienes in the synthesis of silylated benzazepines

In contrast, substrates bearing methyl (**1k**) or electron-withdrawing ester (**1l**) substituents at the *meta*-position relative to the *N*-Ts group exhibited no significant impact on reactivity and afforded desired products **3k** and **3l** in 63% and 57% yield respectively. Whereas, for substitution at the *para*-position both electron-donating groups (Me, OMe) and electron-withdrawing groups (F, Cl, CN) was well tolerated under the optimized reaction conditions and afforded corresponding products **3m**-**3q** in good yield (45-72%). In contrast, a *para*-nitro substituent (**1r**) exhibited low reactivity, delivered the silylated benzazepine **3r** in 17% yield. One of the reason for the lower reactivity of substrate **1r** could be destabilization towards the formation of carbocation by the nitro substituent. The methyl substitution (**1s**) at the *ortho*-position of the alkene in arylamine ring provided the desired product **3s** in excellent yield (78%). Notably, the insertion of a methyl group (**1t**) at the terminal position of the tethered alkene lowers its reactivity to give product **3t** in 27% yield. The reduced reactivity of this substrate may have resulted from the steric effects induced by the addition of a terminal methyl group. Similarly, the *α*-methacryloyl-derived substrate (**1u**) was also compatible and afforded the photoproduct **3u** in 42% yield. This method is also compatible with *N*-methyl-substituted 1,7-dienes (**1v**) and provided the desired product **3v** in 40% yield.

#### 4.5.4 Scope of hydrosilanes in the synthesis of silylated benzazepines

We next investigated the scope of different hydrosilanes with 1,7-dienes **1a** under the standard reaction conditions (**Scheme 4.6**). A variety of trialkylhydrosilanes underwent the cyclization efficiently and smoothly. The linear tri-*n*-propylsilane (**2b**) and branched triisopropylsilane (**2c**) provide the desired products **3w** and **3x** in 63% and 43% yield respectively. Other alkyl silanes, such as benzyldimethylsilane (**2d**) and *tert*-butyldimethylsilane (**2e**), provided the silylated benzazepine **3y** and **3z** in good to excellent yields (64-77%). Additionally, aryl silanes bearing one or two alkyl substituents (**2f**-**2h**) were well tolerated under the optimized reaction conditions and afforded the corresponding products **3aa-3ac** in good to moderate yield (39-63%). Notably, both triphenyl (**2i**) and diphenylhydrosilane (**2j**) proved compatible under the optimized conditions, afforded the silylated benzazepine derivatives **3ad** and **3ae** in 44% and 46% yield respectively. The super silane *tris*-

(trimethylsilyl)silane (**2k**) yielded the desired product **3af** in excellent yield (91%). In addition, *para*-phenylenebis(dimethylsilane) (**2l**) undergoes cyclization to give only the monosilylated product **3ag** in 70% yield.

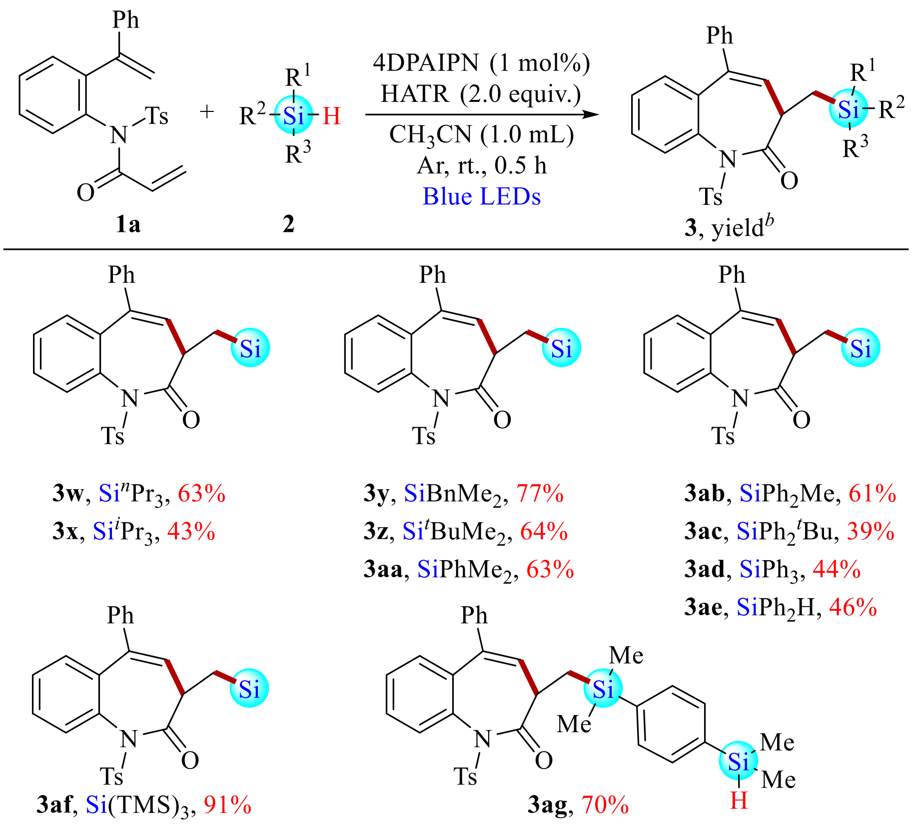


[a]Reaction conditions: **1a** (0.1 mmol), **2** (0.5 mmol), HATR (0.2 mmol), 4DPAIPN (1 mol%), and dry acetonitrile (1.0 mL) were irradiated under blue LEDs. [b]isolated yield.

**Scheme 4.6** Scope of hydrosilanes in the synthesis of silylated benzazepine

### 4.5.5 Substrate scope for the germylation of 1,7-dienes

Motivated by these findings, we extended this strategy to synthesize germylated benzazepines. The optimized reaction conditions for the synthesis of silylated benzazepine were well-suited for the synthesis of germylated benzazepine, even with the lesser equivalent of hydrogermanes (**Scheme 4.7**). As the hydrogermane source, both alkyl hydrogermane ($Et_3GeH$, **4a**; $^nBu_3GeH$, **4b**) and aryl hydrogermane ($Ph_3GeH$, **4c**) were well tolerated under the optimized reaction conditions. Started the screening of 1,7 dienes in the synthesis of germylated benzazepines, and the basic substrate **1a** provided the desired product **5a** in 84%. The screening of substituents on the benzene ring tethered to the alkene, provided a series of germylated benzazepine derivatives **5b-5d** with a range of substituents, such as *p*-Me, *p*-CN, and *m*-Cl on aryl rings in good to excellent yields (57-77%) under the optimized reaction conditions.

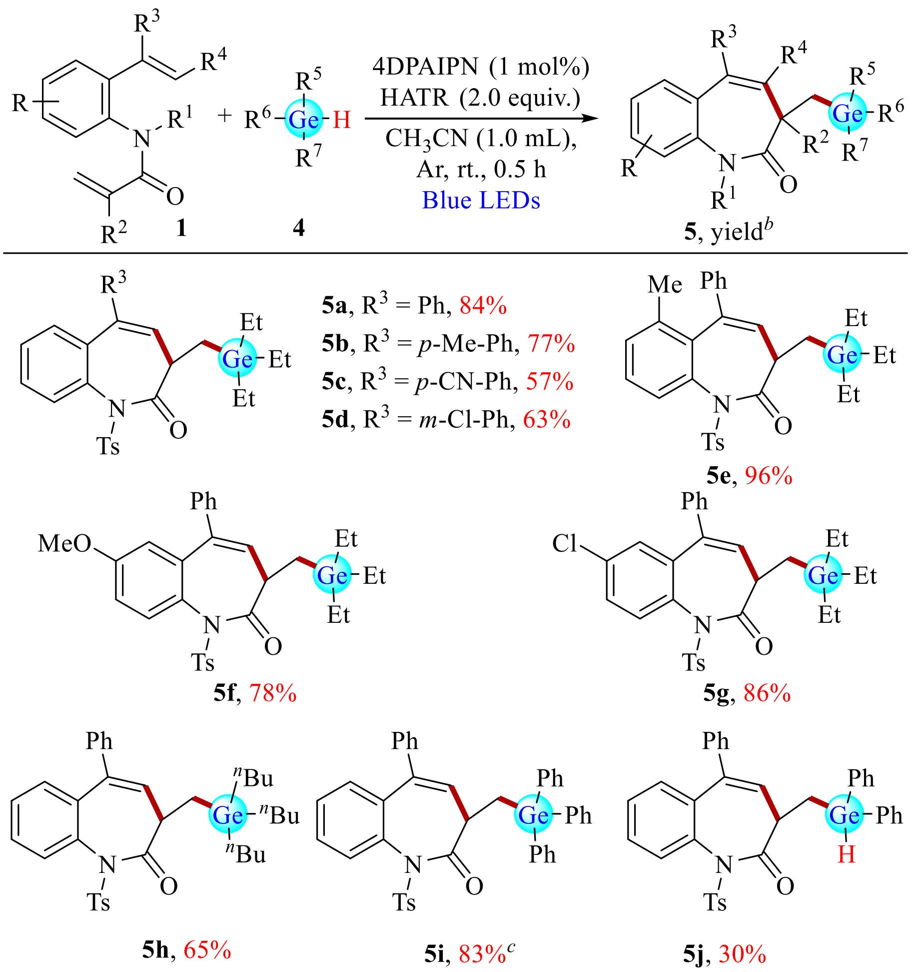

[a]Reaction conditions: **1** (0.1 mmol), **4** (0.3 mmol), HATR (0.2 mmol), 4DPAIPN (1 mol%), and dry acetonitrile (1.0 mL) were irradiated under blue LEDs. [b]isolated yield. [c]using **4** equiv. of $Ph_3GeH$.

**Scheme 4.7** Scope in the synthesis of the germylated benzazepines

Next, we turned our attention to examine the influence of substituents on the benzene ring of aryl amines in the synthesis of germylated benzazepines. The methyl group at the *ortho*-position of the alkene in arylamine ring delivered the desired product **5e** in excellent yield (96%).

Both methoxy- and chloro- substituents at the *para*-position also tolerated under the reaction conditions and provided **5f** and **5g** in 78% and 86% yield respectively. Screening of alkyl and aryl hydrogermanes afforded the desired products **5h**-**5i** in moderate to excellent yields (65-83%). To our surprise, diphenyldihydrogermane ($Ph_2GeH_2$, **4d**) was also found to be compatible under the standard reaction conditions and afforded the germylated benzazepine **5j** in 30% yield.

### 4.5.6 Late-stage functionalization of natural products and drug molecules tethered to 1,7-dienes

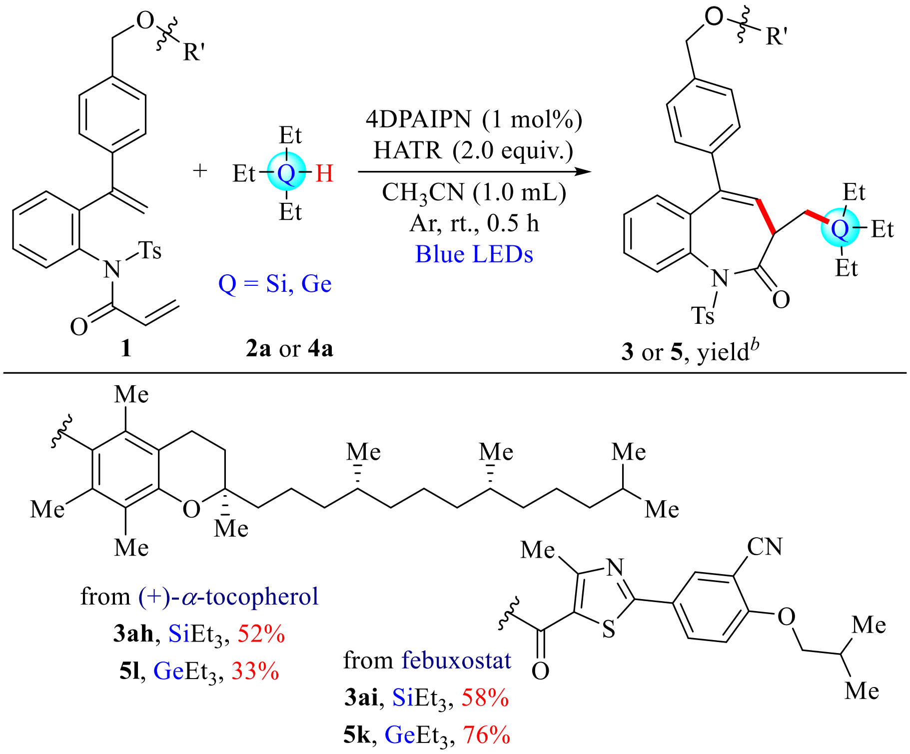


[a]Reaction conditions: **1** (0.1 mmol), **2a** (0.5 mmol) or **4a** (0.3 mmol), HATR (0.2 mmol), 4DPAIPN (1 mol%), and dry acetonitrile (1.0 mL) were irradiated under blue LEDs. [b]isolated yield.

**Scheme 4.8** Late-stage functionalization of natural product and drug tethered 1,7-dienes

The mildness and robustness of the protocol were further demonstrated using substrates tethered to natural product and drug-derived molecules (**Scheme 4.8**). Natural product (+)-$\alpha$-tocopherol-tethered dienes (**1w**) underwent smooth cyclization with triethylsilane (**2a**) and triethylgermane (**4a**) under the optimized conditions, afforded the corresponding silylated and germylated benzazepines **3ah** and **5l** in 52% and 33% yield respectively. Likewise, a drug molecule febuxostat-tethered substrate (**1x**) successfully cyclized with hydrosilane (**2a**) and hydrogermane (**4a**) to deliver the desired products **3ai** and **5k** in 58% and 76% yield respectively.

### 4.5.7 Scale-up synthesis of silylated benzazepine

The practicality of the developed protocol was further demonstrated by a 2 mmol scale reaction of 1,7-diene **1a**, which provided silylated benzazepine **3a** in 61% yield (**Scheme 4.9**).


**Scheme 4.9** Scale-up synthesis of silylated benzazepine

## 4.6 Mechanistic investigation

To gain insight into the reaction mechanism, radical trapping experiments, kinetic isotope effect (KIE) study, carbocation trapping, fluorescence quenching experiments, and quantum yield calculation were performed.

### 4.6.1 Radical inhibition experiments

The involvement of radical species in the reaction was evaluated using the radical scavenger TEMPO in reaction of **1a** with hydrosilane or hydrogermane (**2a**/**4a**) under standard reaction conditions. In both cases, the formation of corresponding products **3a** and **5a** was completely suppressed (**Scheme 4.10**), providing strong evidence for the involvement of radical intermediates in the reaction.

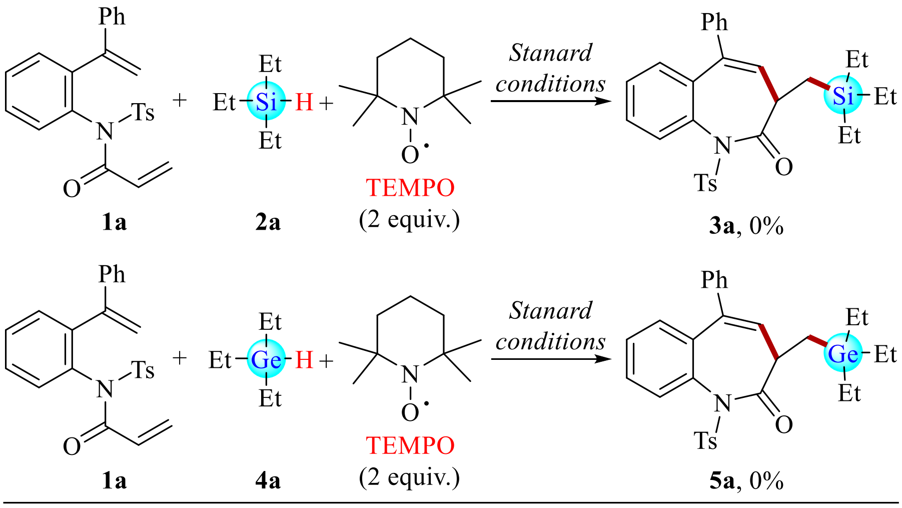


**Scheme 4.10** Radical inhibition experiment with TEMPO

### 4.6.2 Kinetic isotope effect (KIE) study

The kinetic isotope effect (KIE) study was conducted to assess the involvement of C-H bond cleavage in the rate-determining step. A low KIE value ($k_H/k_D$ = 1.12) was obtained from parallel photoreaction, indicating the cleavage of the C-H bond is unlikely to be part of the rate-determining step (**Scheme 4.11** and **Figure 4.2**).

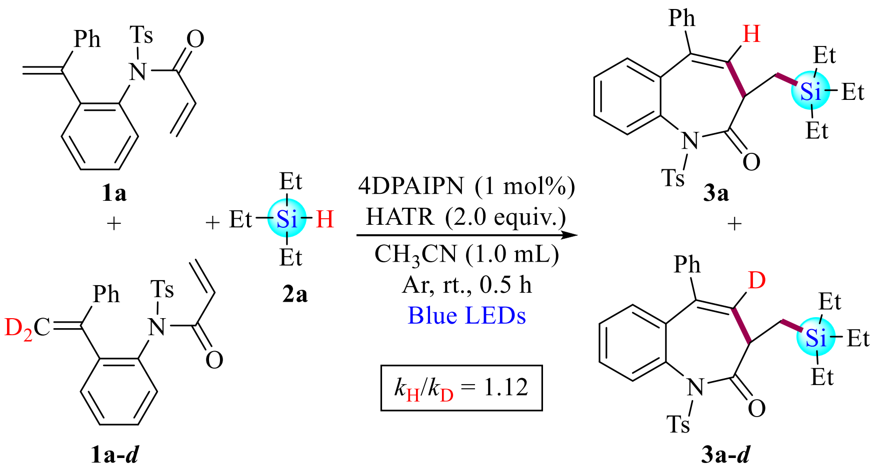


**Scheme 4.11** Kinetic isotope effect study by parallel photoreaction

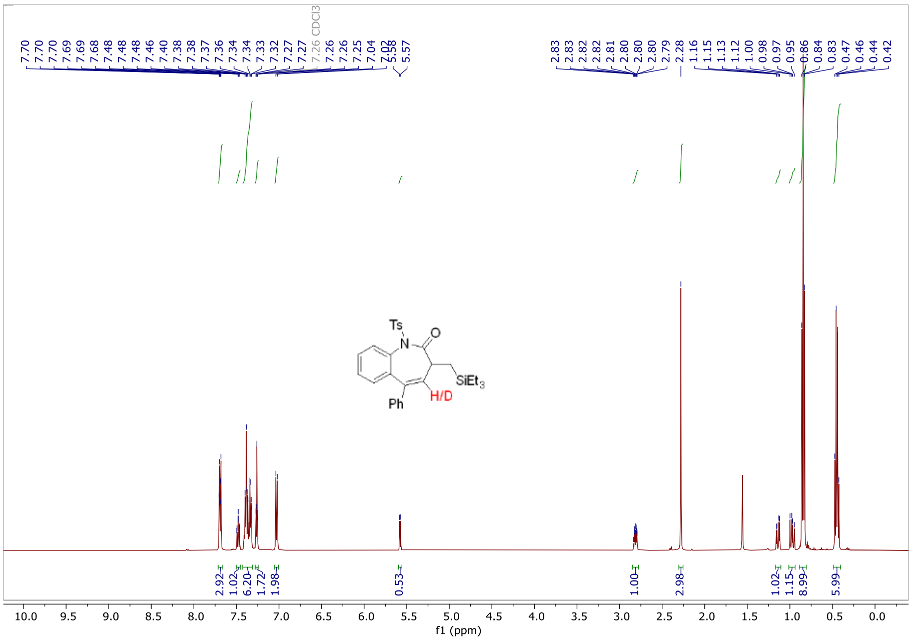

**Figure 4.2** $^1$H NMR for kinetic isotope effect study

### 4.6.3 Trapping of carbocation intermediate

A carbocation-trapping experiment was carried out to confirm the formation of cationic intermediate in the reaction pathway leading to the product formation. When the standard reaction was performed in the presence of 10 equiv. of water, the desired product **3a** was obtained in 65% yield, along with the formation of water trapped hydroxybenzazepine derivative (**3a'**), which was detected by HRMS analysis (**Scheme 4.12**).

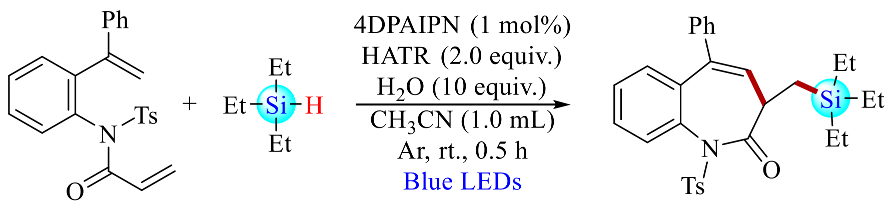


**1a** **2a** **3a**, 65%

HRMS (ESI +ve) m/z:
[M+Na]$^+$ Calcd $C_{30}H_{37}NO_4SSiNa$ 558.2110;
found 558.2108.

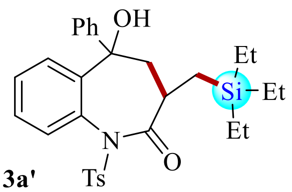

**3a'**

**Scheme 4.12** Carbocation trapping experiment

### 4.6.4 Stern-Volmer quenching studies

To identify the active species responsible for the quenching of the excited-state photocatalyst, fluorescence quenching studies were conducted. The studies were performed between the photocatalyst 4DPAIPN solution and other reaction components, including the 1,7-diene **1a**, triethylsilane **2a**, triethylgermane **4a**, and *N*-aminopyridinium salt (HATR). Stern-Volmer studies revealed that the excited-state photocatalyst 4DPAIPN$^*$ was quenched exclusively by the hydrogen atom transfer reagent *N*-aminopyridinium salt (**Figure 4.3**), no fluorescence quenching was observed between photocatalyst and 1,7-diene **1a**, or hydrosilane **2a**, or hydrogermane **4a**.

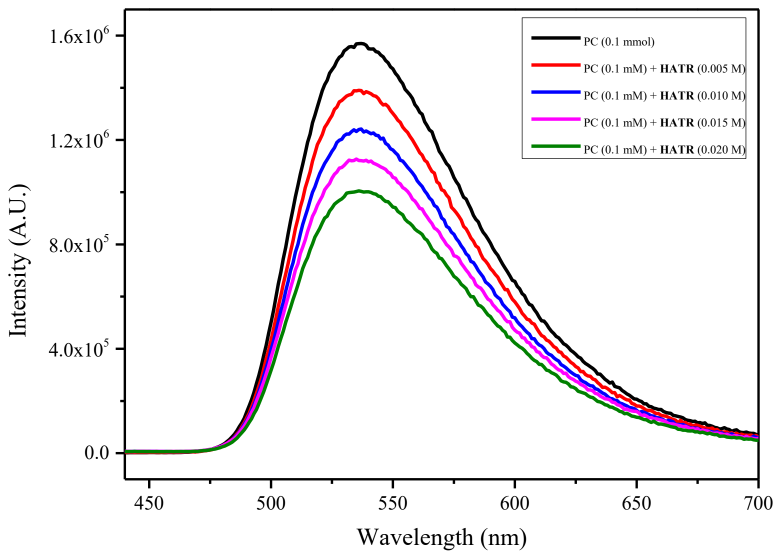

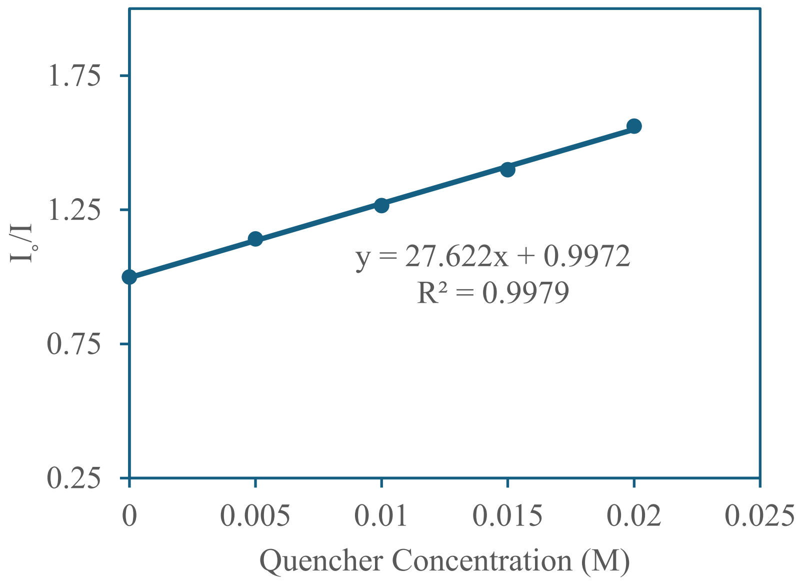


**Figure 4.3** Fluorescence quenching and Stern-Volmer plot of 4DPAIPN vs *N*-aminopyridinium salt

### 4.6.5 Quantum yield calculation

The quantum yield for the standard reaction was calculated to determine the involvement of a radical chain pathway in the reaction. The calculated quantum yield ($\phi$ = 1.59) suggests the possible involvement of a short-chain radical process in the reaction (**Scheme 4.13**).

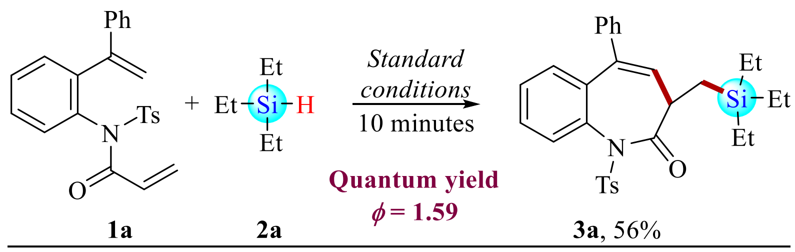


**Scheme 4.13** Quantum yield calculation of standard reaction

### 4.7 Possible mechanism

A possible reaction mechanism is proposed based on the mechanistic investigations and literature reports (**Scheme 4.14**).[52-57]

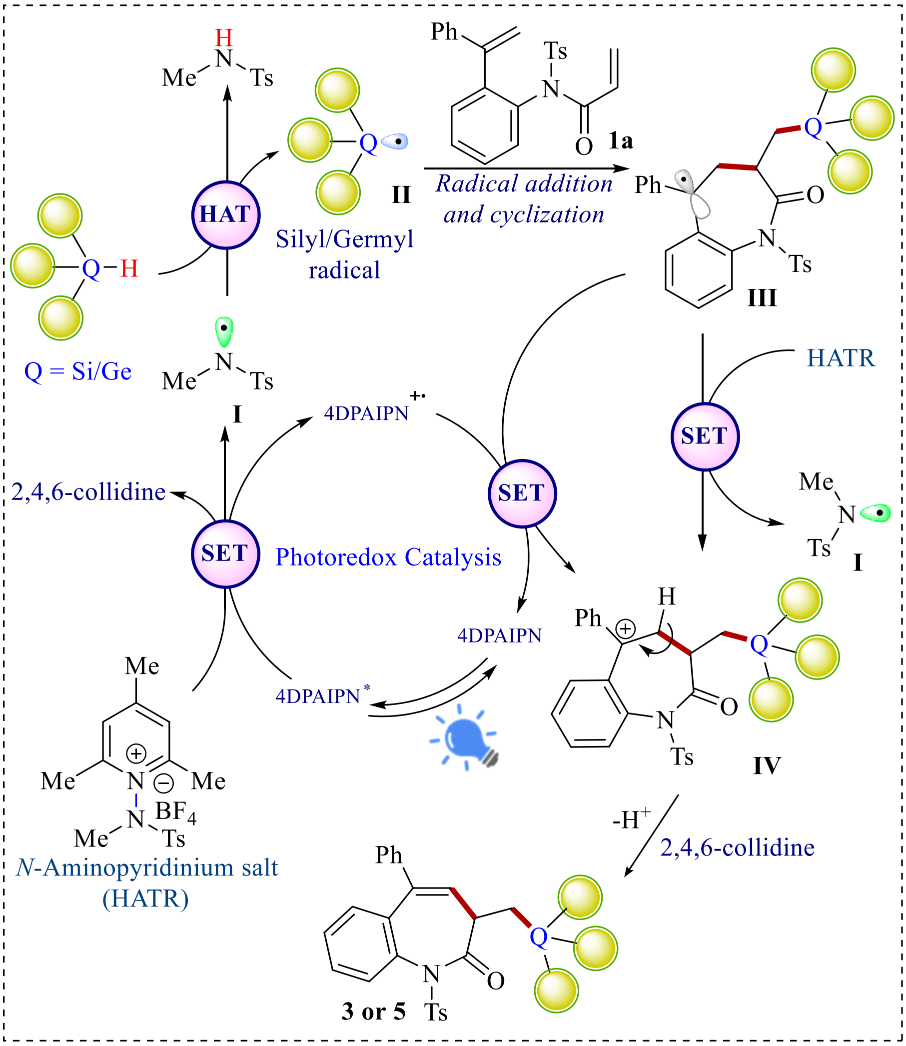


**Scheme 4.14** Possible mechanism

Upon visible-light irradiation, the photocatalyst 4DPAIPN gets excited, and the excited-state photocatalyst 4DPAIPN* undergoes single-electron transfer with the *N*-aminopyridinium salt (HATR) to form the oxidized photocatalyst 4DPAIPN$^{\bullet+}$ and generate the *N*-centered sulfamidyl radical **I**, followed by extrusion of 2,4,6-collidine. The resulting sulfamidyl radical **I**, activates Si-H/Ge-H bond of hydrosilanes (**2**) or hydrogermanes (**4**) *via* hydrogen atom transfer to generate the corresponding silyl or germyl radical **II**. Addition of the silyl or germyl radical **II** to the 1,7-diene **1a**, followed by cascade cyclization affords a benzylic radical **III** which is subsequently oxidized by 4DPAIPN$^{\bullet+}$ *via* single-electron transfer to generate the benzylic cation **IV** with concomitant regeneration of 4DPAIPN. The cationic species **IV** gets deprotonated with the assistance of 2,4,6-collidine to give the desired silylated/germylated benzazepine derivatives **3 or 5**. The possibility of radical chain involvement in the reaction, could arise through SET from radical intermediate **III** with the HATR and generate the cationic intermediate **IV** with the formation of sulfamidyl radical **I**. This sulfamidyl radical can further functionalize the Si-H or Ge-H bond of hydrosilanes or hydrogermanes and lead to the formation of desired benzazepine derivatives.

### 4.8 Further transformation of silylated benzazepine

Further synthetic transformations of the silylated benzazepine **3a** were also explored. When silylated benzazepine **3a** was treated with Mg and trimethylsilyl chloride,[58] a detosylated product **6a** was obtained in 92% yield (**Scheme 4.15a-I**). Upon treatment of **6a** with Lawesson's reagent,[59] thioamide derivative **6b** was obtained in 51% yield (**Scheme 4.15a-II**). Furthermore, the bromination of **3a** using NBS led to the formation of **7** in 87% yield (**Scheme 4.15b**).

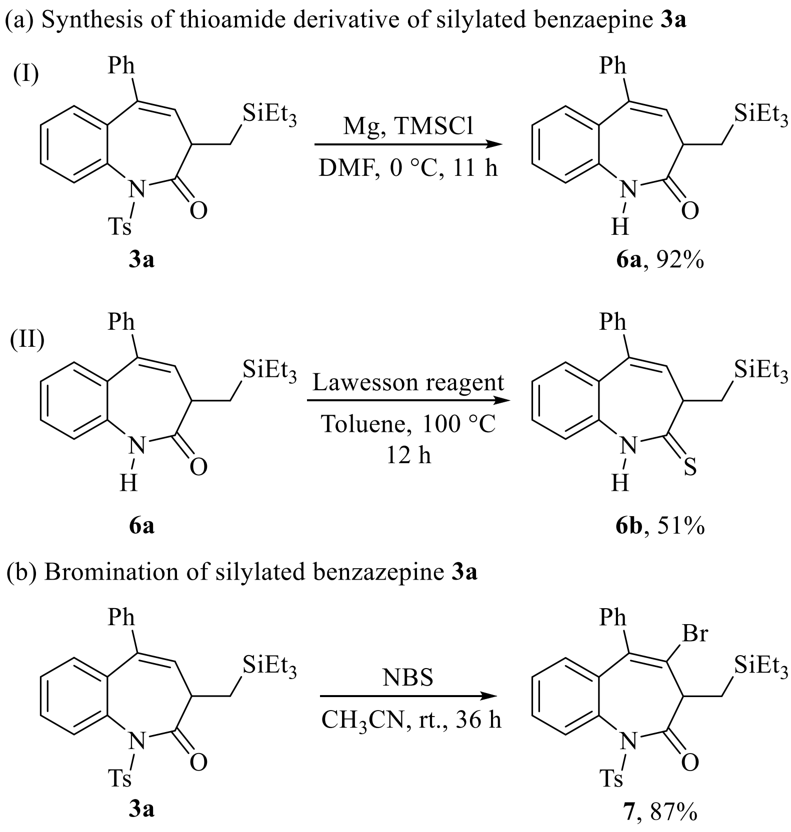

**Scheme 4.15** Further transformation of silylated benzazepine **3a**

### 4.9 Conclusion

In conclusion, we have developed an efficient method to synthesize silylated/germylated benzazepine derivatives under metal-free, environmentally benign reaction conditions, using an *N*-aminopyridinium salt as a hydrogen atom transfer reagent along with hydrosilanes and hydrogermanes as silicon and germanium surrogates in a shorter reaction time. The generality of the method was tested by screening a variety of substituents on the arene ring tethered to alkene, substituents on the alkene and nitrogen, as well as the benzene ring of aryl amine. Different alkyl, aryl and diphenyldihydrosilane were found to be compatible under the reaction conditions. The developed protocol was extended to the synthesis of germylated benzazepine, and both alkyl and aryl hydrogermanes were found to be well tolerated under the reaction conditions. The robustness and practical utility of the protocol were established by the smooth radical addition and cyclization of natural product/drug molecule tethered 1,7-dienes late-stage functionalization, and performing the reaction on a scale 20 times that of the optimized reaction condition. The silylated benzazepine was further transformed into synthetically valuable derivatives. Moreover, the proposed mechanism for the synthesis of silylated and germylated benzazepines was well supported by the results of the control experiments and photophysical studies.

### 4.10 Experimental section

#### 4.10.1 General procedure for the synthesis of starting materials

List of substrates

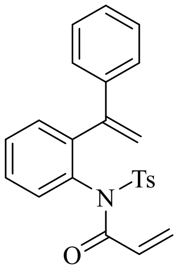
**1a**

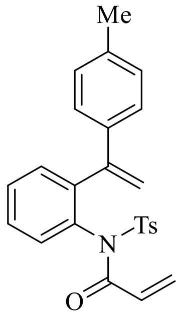
**1b**

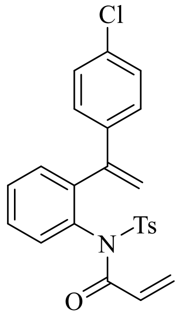
**1c**

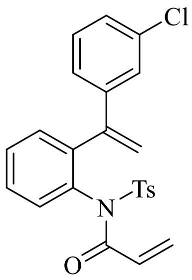
**1d**

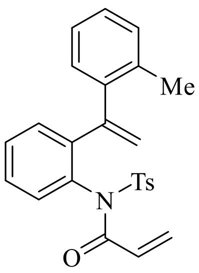
**1e**

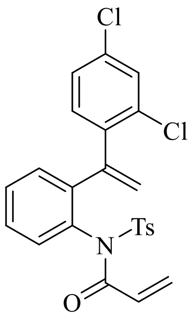
**1f**

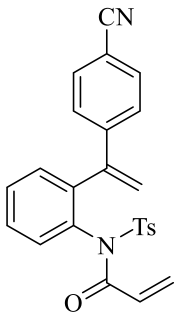
**1g**

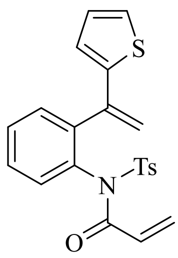
**1h**

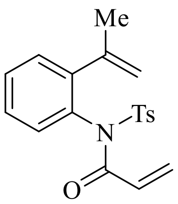
**1i**

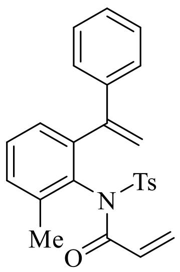
**1j**

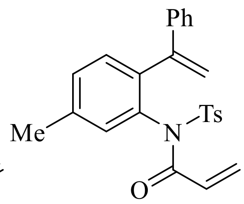
**1k**

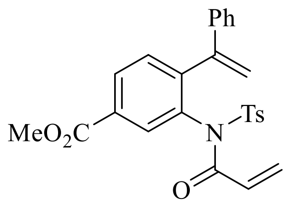
**1l**

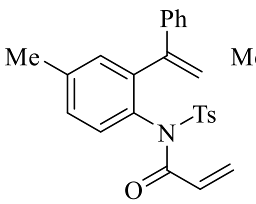
**1m**

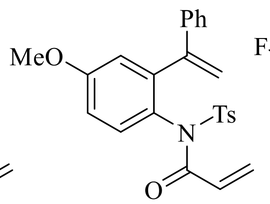
**1n**

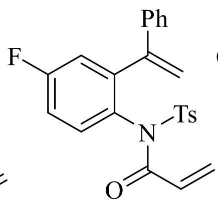
**1o**

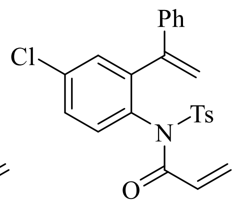
**1p**

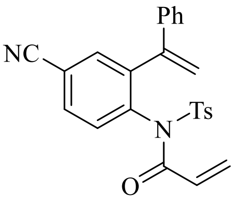 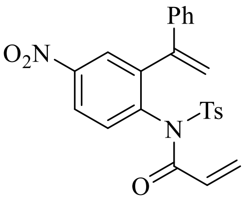 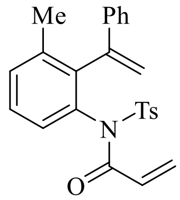 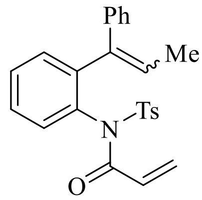

**1q** **1r** **1s** **1t**

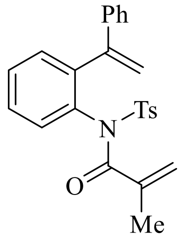 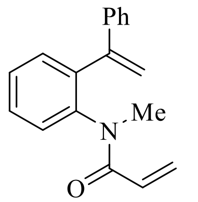

**1u** **1v**

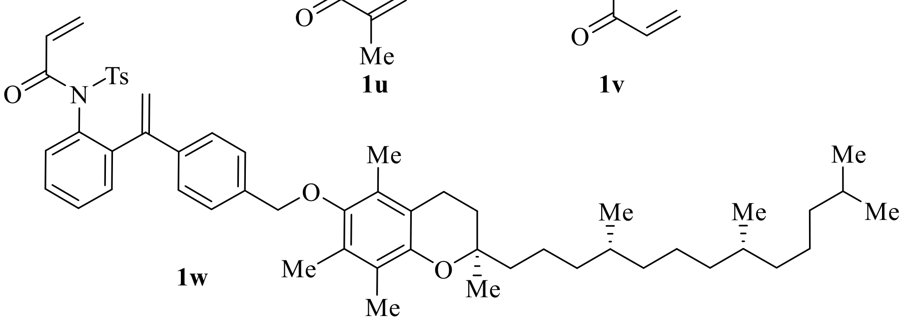

**1w**

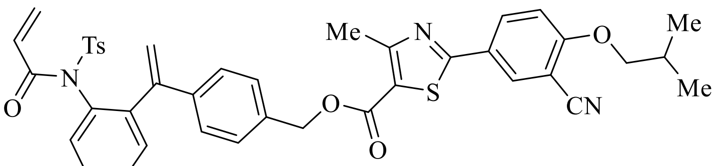

**1x**

All starting materials were synthesized according to literature reports.[60] The derivatives of *N*-tosylated phenyl vinyl aniline were dissolved in DCM (3 mL/mmol), cooled on an ice bath, and then $Et_3N$ (2.0 equiv.) was added. Freshly prepared acryloyl chloride (1.2 eq.) was added dropwise over 10 minutes at 0 °C. The reaction mixture was stirred overnight at room temperature. The reaction mixture was then quenched with a saturated solution of $NaHCO_3$, and the organic layer was separated by DCM. The combined organic layer was dried over $Na_2SO_4$, filtered, and the desired product was purified by column chromatography using a mixture of ethyl acetate and hexane as the eluent.

**Characterization data for selected substrates**

***N*-(2-(1-phenylvinyl)phenyl)-*N*-tosylacrylamide (1a):**[60] Column chromatography 10-15% EA/H; white solid; reaction scale 3 mmol, Yield: 64% (827 mg). **$^{1}$H NMR** (500 MHz, $CDCl_3$) δ 7.88 (d, *J* = 8.1 Hz, 2H), 7.56 – 7.50 (m, 1H), 7.50 – 7.40 (m, 2H), 7.30 – 7.20 (m, 7H), 7.20 – 7.14 (m, 1H), 6.11 (dd, *J* = 16.7, 1.6 Hz, 1H), 5.73 (s, 1H), 5.61 (dd, *J* = 16.7, 10.3 Hz, 1H), 5.38 (s, 1H), 5.32 (dd, *J* = 10.3, 1.6 Hz, 1H), 2.42 (s, 3H). **$^{13}$C NMR** (126 MHz, $CDCl_3$) δ 164.6, 146.1, 144.8, 143.6, 140.6, 136.7, 134.3, 132.2, 130.7 (2C), 130.2, 129.7, 129.2, 129.0, 128.3, 127.9, 127.8, 127.6, 118.9, 21.8.

***N*-(2-(1-(4-chlorophenyl)vinyl)phenyl)-*N*-tosylacrylamide (1c):** Column chromatography 10-15% EA/H; Yellow oil; reaction scale 1 mmol, Yield: 52% (228 mg). **$^{1}$H NMR** (500 MHz, $CDCl_3$) δ 7.91 (d, *J* = 8.4 Hz, 2H), 7.60 – 7.53 (m, 1H), 7.52 – 7.45 (m, 2H), 7.34 – 7.28 (m, 3H), 7.26 (s, 3H), 7.22 – 7.16 (m, 1H), 6.21 (dd, *J* = 16.7, 1.6 Hz, 1H), 5.76 (s, 1H), 5.69 (dd, *J* = 16.7, 10.3 Hz, 1H), 5.47 – 5.40 (m, 2H), 2.46 (s, 3H). **$^{13}$C NMR** (126 MHz, $CDCl_3$) δ 164.4, 145.0, 145.0, 143.1, 139.1, 136.6, 134.4, 133.9, 132.1, 131.2, 130.7, 130.3, 129.6, 129.3, 129.2, 128.5, 127.6, 119.4, 21.8. **IR** (neat): 2923, 1687, 1616, 1595, 1488, 1444, 1392, 1360, 1243 $cm^{-1}$. **HRMS** (ESI +ve) m/z: $[M+Na]^+$ Calcd for $C_{24}H_{20}ClNO_3SNa$ 460.0750; found 460.0740.

***N*-(2-(1-(3-chlorophenyl)vinyl)phenyl)-*N*-tosylacrylamide (1d):** Column chromatography 10-15% EA/H; White solid; reaction scale 1 mmol, Yield: 58% (254 mg). **M.P.**: 153-155 °C. **$^{1}$H NMR** (500 MHz, $CDCl_3$) δ 7.89 (d, *J* = 8.4 Hz, 2H), 7.59 – 7.52 (m, 1H), 7.50 – 7.43 (m, 2H), 7.29 (d, *J* = 8.1 Hz, 2H), 7.26 – 7.14 (m, 4H), 7.12 – 7.08 (m, 1H), 6.12 (dd, *J* = 16.7, 1.6 Hz, 1H), 5.75 (s, 1H), 5.64 (dd, *J* = 16.7, 10.3 Hz, 1H), 5.45 (s, 1H), 5.41 (dd, *J* = 10.3, 1.6 Hz, 1H), 2.43 (s, 3H). **$^{13}$C NMR** (126 MHz, $CDCl_3$) δ 164.3, 145.1, 145.0, 143.0, 142.4, 136.5, 134.4, 134.0, 132.2, 130.9, 130.7, 130.4, 129.8, 129.7, 129.3 (2C), 127.9, 127.8, 127.5, 126.2, 120.2, 21.8. **IR** (neat): 2924, 1687, 1617, 1595, 1487, 1400, 1367, 1241 $cm^{-1}$. **HRMS** (ESI +ve) m/z: $[M+H]^+$ Calcd for $C_{24}H_{21}ClNO_3S$ 438.0931; found 438.0927.

***N*-(2-(1-(2,4-dichlorophenyl)vinyl)phenyl)-*N*-tosylacrylamide (1f):** Column chromatography 10-15% EA/H; White solid; reaction scale 1 mmol, Yield: 67% (317 mg). **M.P.**: 136-138 °C. **$^1$H NMR** (500 MHz, $CDCl_3$) δ 7.91 (d, *J* = 8.5 Hz, 2H), 7.68 (dd, *J* = 7.7, 1.6 Hz, 1H), 7.60 – 7.50 (m, 2H), 7.42 – 7.35 (m, 1H), 7.32 (d, *J* = 8.1 Hz, 2H), 7.28 – 7.22 (m, 1H), 7.17 (d, *J* = 2.1 Hz, 1H), 6.89 (dd, *J* = 7.8, 1.3 Hz, 1H), 6.05 (dd, *J* = 16.7, 1.6 Hz, 1H), 5.71 (d, *J* = 1.1 Hz, 1H), 5.61 (d, *J* = 1.2 Hz, 1H), 5.47 (dd, *J* = 16.7, 10.3 Hz, 1H), 5.28 (dd, *J* = 10.3, 1.6 Hz, 1H), 2.44 (s, 3H). **$^{13}$C NMR** (126 MHz, $CDCl_3$) δ 164.2, 145.1, 145.0, 143.0, 138.2, 136.3, 134.5, 134.0, 133.8, 133.7 (2C), 130.9, 130.3, 129.8, 129.8, 129.4, 129.2 (2C), 127.5, 126.9, 124.6, 21.8. **IR** (neat): 2923, 1693, 1618, 1549, 1483, 1399, 1303 $cm^{-1}$. **HRMS** (ESI +ve) m/z: $[M+H]^+$ Calcd for $C_{24}H_{20}Cl_2NO_3S$ 472.0541; found 472.0525.

***N*-(2-(1-(4-cyanophenyl)vinyl)phenyl)-*N*-tosylacrylamide (1g):** Column chromatography 20-25% EA/H; White solid; reaction scale 1 mmol, Yield: 62% (266 mg). **M.P.**: 154-156 °C. **$^1$H NMR** (500 MHz, $CDCl_3$) δ 7.86 (d, *J* = 8.4 Hz, 2H), 7.56 – 7.52 (m, 2H), 7.51 – 7.39 (m, 5H), 7.32 – 7.27 (m, 2H), 7.15 – 7.10 (m, 1H), 6.17 (dd, *J* = 16.7, 1.5 Hz, 1H), 5.84 (s, 1H), 5.66 (dd, *J* = 16.7, 10.3 Hz, 1H), 5.53 (s, 1H), 5.42 (dd, *J* = 10.3, 1.5 Hz, 1H), 2.43 (s, 3H). **$^{13}$C NMR** (126 MHz, $CDCl_3$) δ 164.2, 145.2, 145.1, 144.9, 142.5, 136.4, 134.5, 132.2, 132.0, 131.6, 130.6, 130.5, 129.6, 129.5, 129.4, 128.5, 127.4, 121.7, 111.5, 21.8. **IR** (neat): 2923, 2277, 1690, 1602, 1492, 1465, 1366, 1164 $cm^{-1}$. **HRMS** (ESI +ve) m/z: $[M+H]^+$ Calcd for $C_{25}H_{21}N_2O_3S$ 429.1273; found 429.1266.

***N*-(2-(1-(thiophen-2-yl)vinyl)phenyl)-*N*-tosylacrylamide (1h):** Column chromatography 10-15% EA/H; White solid; reaction scale 1 mmol, Yield: 55% (225 mg). **M.P.**: 125-127 °C.**$^1$H NMR** (500 MHz, $CDCl_3$) δ 7.85 (d, *J* = 8.4 Hz, 2H), 7.56 – 7.50 (m, 2H), 7.50 – 7.45 (m, 1H), 7.32 – 7.28 (m, 1H), 7.26 – 7.23 (m, 2H), 7.22 – 7.18 (m, 1H), 6.90 (dd, *J* = 5.1, 3.6 Hz, 1H), 6.75 (dd, *J* = 3.6, 1.2 Hz, 1H), 6.28 (dd, *J* = 16.7, 1.6 Hz, 1H), 5.82 (dd, *J* = 16.7, 10.3 Hz, 1H), 5.74 (s, 1H), 5.49 (dd, *J* = 10.3, 1.6 Hz, 1H), 5.17 (s, 1H), 2.41 (s, 3H). **$^{13}$C NMR** (126 MHz, $CDCl_3$) δ 164.7, 144.8, 144.4, 142.2, 138.9, 136.5, 134.1, 131.9, 131.4, 131.0, 130.1, 129.7, 129.3, 129.2, 127.8, 127.5, 127.4, 125.4, 116.8, 21.8. **IR** (neat): 2927, 1690, 1595, 1489, 1397, 1361, 1300, 1242, 1230 cm$^{-1}$. **HRMS** (ESI +ve) m/z: $[M+H]^+$ Calcd for $C_{22}H_{20}NO_3S_2$ 410.0885; found 410.0875.

***N*-(2-(prop-1-en-2-yl)phenyl)-*N*-tosylacrylamide (1i):** Column chromatography 10-15% EA/H; White solid; reaction scale 1 mmol, Yield: 59% (202 mg). **M.P.**: 93-95 °C.**$^1$H NMR** (500 MHz, $CDCl_3$) δ 8.00 (d, *J* = 8.4 Hz, 2H), 7.51 – 7.44 (m, 1H), 7.45 – 7.39 (m, 1H), 7.38 – 7.31 (m, 3H), 7.07 (dd, *J* = 7.9, 1.3 Hz, 1H), 6.41 (dd, *J* = 16.8, 1.6 Hz, 1H), 5.87 (dd, *J* = 16.8, 10.3 Hz, 1H), 5.60 (dd, *J* = 10.3, 1.6 Hz, 1H), 5.33 – 5.28 (m, 1H), 5.06 – 5.02 (m, 1H), 2.45 (s, 3H), 2.13 (s, 3H). **$^{13}$C NMR** (126 MHz, $CDCl_3$) δ 164.8, 145.1, 145.0, 142.1, 136.4, 133.1, 131.7, 130.3 (2C), 129.7, 129.4, 129.3, 128.4, 128.2, 118.0, 24.0, 21.8. **IR** (neat): 2925, 1691, 1613, 1594, 1489, 1399, 1360, 1163 cm$^{-1}$. **HRMS** (ESI +ve) m/z: $[M+Na]^+$ Calcd for $C_{19}H_{19}NO_3SNa$ 364.0983; found 364.0972.

***N*-(2-methyl-6-(1-phenylvinyl)phenyl)-*N*-tosylacrylamide (1j):** Column chromatography 5-10% EA/H; White solid; reaction scale 1 mmol, Yield: 27% (113 mg). **M.P.**: 133-35 °C. **$^1$H NMR** (500 MHz, $CDCl_3$) δ 7.96 (d, *J* = 8.4 Hz, 2H), 7.40 (t, *J* = 7.5 Hz, 1H), 7.35 – 7.30 (m, 1H), 7.26 – 7.23 (m, 1H), 7.23 – 7.18 (m, 5H), 7.17 – 7.12 (m, 2H), 6.19 (dd, *J* = 16.7, 1.7 Hz, 1H), 5.61 – 5.54 (m, 1H), 5.54 (s, 1H), 5.35 (dd, *J* = 10.3, 1.7 Hz, 1H), 5.27 – 5.23 (m, 1H), 2.41 (s, 3H), 2.24 (s, 3H). **$^{13}$C NMR** (126 MHz, $CDCl_3$) δ 164.7, 146.4, 144.9, 143.3, 140.7, 139.4, 136.4, 133.5, 131.2, 130.9, 130.5, 129.8, 129.8, 128.8, 128.2, 127.9, 127.7, 127.1, 118.5 21.7, 19.2. **IR** (neat): 2922, 1686, 1618, 1596, 1399, 1360, 1299, 1234, 1165 cm$^{-1}$. **HRMS** (ESI +ve) m/z: $[M+Na]^+$ Calcd for $C_{25}H_{23}NO_3SNa$ 440.1296; found 440.1306.

**methyl 4-(1-phenylvinyl)-3-(*N*-tosylacrylamido)benzoate (1l):** Column chromatography 15-20% EA/H; White solid; reaction scale 1 mmol, Yield: 49% (227 mg). **M.P.**: 149-151 °C. **$^1$H NMR** (500 MHz, $CDCl_3$) δ 8.18 (dd, *J* = 8.0, 1.7 Hz, 1H), 7.88 (d, *J* = 8.4 Hz, 2H), 7.83

(d, $J$ = 1.7 Hz, 1H), 7.56 (d, $J$ = 7.9 Hz, 1H), 7.32 – 7.26 (m, 2H), 7.28 – 7.22 (m, 5H), 6.12 (dd, $J$ = 16.7, 1.5 Hz, 1H), 5.78 (s, 1H), 5.60 (dd, $J$ = 16.7, 10.3 Hz, 1H), 5.44 (s, 1H), 5.35 (dd, $J$ = 10.3, 1.5 Hz, 1H), 3.95 (s, 3H), 2.43 (s, 3H). **$^{13}$C NMR** (126 MHz, $CDCl_3$) δ 165.7, 164.2, 148.2, 145.5, 145.1, 140.0, 136.4, 134.8, 132.3, 131.8, 131.3, 131.0, 129.7, 129.4, 128.4, 128.2, 127.8, 127.3, 119.7, 52.6, 21.8. **IR** (neat): 2927, 1724, 1690, 1598, 1441, 1399, 1361, 1245, 1165 $cm^{-1}$. **HRMS** (ESI +ve) m/z: $[M+H]^+$ Calcd for $C_{26}H_{24}NO_5S$ 462.1375; found 462.1376.

***N*-(4-cyano-2-(1-phenylvinyl)phenyl)-*N*-tosylacrylamide (1q):** Column chromatography 15-20% EA/H; White solid; reaction scale 1 mmol, Yield: 62% (266 mg). **M.P.**: 134-136 °C. $^1$H NMR (500 MHz, $CDCl_3$) δ 7.83 (d, $J$ = 8.2 Hz, 2H), 7.78 (d, $J$ = 1.9 Hz, 1H), 7.72 (dd, $J$ = 8.1, 2.0 Hz, 1H), 7.32 – 7.19 (m, 8H), 6.14 (d, $J$ = 16.7 Hz, 1H), 5.79 (s, 1H), 5.62 (dd, $J$ = 16.7, 10.3 Hz, 1H), 5.45 – 5.36 (m, 2H), 2.43 (s, 3H). **$^{13}$C NMR** (126 MHz, $CDCl_3$) δ 163.9, 145.5, 145.1, 144.6, 139.5, 138.6, 136.1, 135.6, 132.3, 131.9, 131.8, 129.6, 129.5, 128.6, 128.4, 127.8, 127.0, 120.5, 117.6, 114.3, 21.8. **IR** (neat): 2929, 2232, 1692, 1484, 1619, 1596, 1399, 1371, 1167 $cm^{-1}$. **HRMS** (ESI +ve) m/z: $[M+Na]^+$ Calcd for $C_{25}H_{20}N_2O_3SNa$ 451.1092; found 451.1110.

***N*-(3-methyl-2-(1-phenylvinyl)phenyl)-*N*-tosylacrylamide (1s):** Column chromatography 5-10% EA/H; White solid; reaction scale 1 mmol, Yield: 31% (130 mg). **M.P.**: 163-165 °C. (Rotamers observed) **$^1$H NMR** (500 MHz, $CDCl_3$) δ 7.97 (d, $J$ = 8.0 Hz, 1.42 H), 7.63 (d, $J$ = 8.0 Hz, 0.66 H), 7.49 (d, $J$ = 7.7 Hz, 0.75 H), 7.43 – 7.37 (m, 1.35 H), 7.37 – 7.27 (m, 3.56 H), 7.21 – 7.15 (m, 3.06 H), 7.11 (d, $J$ = 7.9 Hz, 0.86 H), 6.96 (d, $J$ = 7.8 Hz, 0.73 H), 6.42 (d, $J$ = 16.7 Hz, 0.35 H), 5.98 (s, 0.75 H), 5.96 – 5.85 (m, 0.68 H), 5.77 (d, $J$ = 16.7 Hz, 0.72 H), 5.63 (d, $J$ = 10.3 Hz, 0.35 H), 5.56 (s, 0.72 H), 5.21 (dd, $J$ = 16.7, 10.3 Hz, 0.71 H), 4.99 (s, 0.34 H), 4.95 (d, $J$ = 10.3 Hz, 0.71 H), 2.52 (s, 2.05 H), 2.43 (s, 2.04 H), 2.36 (s, 0.95 H), 2.16 (s, 0.95 H). **$^{13}$C NMR** (126 MHz, $CDCl_3$) δ 165.18, 164.29, 144.77, 143.86, 143.65, 143.49, 141.83, 139.84, 139.07, 138.39, 137.06, 136.69, 134.91, 134.63, 132.22, 131.60, 129.70, 129.47, 129.31, 129.03, 128.68, 128.43, 128.40, 127.75, 127.39, 127.22, 126.84, 120.79, 115.82, 77.41, 77.36, 77.16, 76.91, 21.80, 20.70. **IR** (neat): 2924, 1687, 1621, 1491, 1444, 1360, 1300, 1196 $cm^{-1}$. **HRMS** (ESI +ve) m/z: $[M+Na]^+$ Calcd for $C_{25}H_{23}NO_3SNa$ 440.1296; found 440.1292.

***N*-(2-(1-phenylprop-1-en-1-yl)phenyl)-*N*-tosylacrylamide (1t):** Column chromatography 10-15% EA/H; White solid; reaction scale 1 mmol, Yield: 43% (180 mg). **M.P.**: 171-173 °C. **$^1$H NMR** (500 MHz, $CDCl_3$) δ 7.99 – 7.91 (m, 2H), 7.63 – 7.54 (m, 2H), 7.48 – 7.41 (m, 1H), 7.31 (d, *J* = 7.9 Hz, 2H), 7.10 (q, *J* = 8.3, 7.4 Hz, 6H), 6.12 (q, *J* = 6.9 Hz, 1H), 5.75 (d, *J* = 16.6 Hz, 1H), 5.18 – 5.03 (m, 1H), 4.99 – 4.89 (m, 1H), 2.43 (s, 3H), 1.86 – 1.79 (m, 3H). **$^{13}$C NMR** (126 MHz, $CDCl_3$) δ 164.2, 144.7, 142.4, 142.0, 139.4, 137.1, 135.3, 132.6, 130.7, 130.4, 130.1, 129.6, 129.3, 129.2, 128.8, 128.1, 128.0, 126.8, 126.6, 21.8, 16.1. **IR** (neat): 2924, 1686, 1618, 1596, 1399, 1360, 1234, 1135 $cm^{-1}$. **HRMS** (ESI +ve) m/z: $[M+Na]^+$ Calcd for $C_{25}H_{23}NO_3SNa$ 440.1296; found 440.1288.

***N*-(2-(1-(4-((((*R*)-2,5,7,8-tetramethyl-2-((4*R*,8*R*)-4,8,12-trimethyltridecyl)chroman-6-yl)oxy)methyl)phenyl)vinyl)phenyl)-*N*-tosylacrylamide (1w):** Column chromatography 10-15% EA/H; Clear thick oil; reaction scale 1 mmol, Yield: 39% (331 mg). **$^1$H NMR** (500 MHz, $CDCl_3$) δ 7.92 – 7.87 (m, 2H), 7.55 – 7.51 (m, 1H), 7.49 – 7.46 (m, 1H), 7.46 – 7.42 (m, 1H), 7.41 – 7.38 (m, 2H), 7.35 – 7.30 (m, 2H), 7.29 – 7.26 (m, 2H), 7.22 – 7.17 (m, 1H), 6.16 (dd, *J* = 16.7, 1.6 Hz, 1H), 5.76 (s, 1H), 5.66 (dd, *J* = 16.7, 10.3 Hz, 1H), 5.39 (s, 1H), 5.37 (dd, *J* = 10.3, 1.6 Hz, 1H), 4.65 (q, *J* = 11.5 Hz, 2H), 2.58 (t, *J* = 6.8 Hz, 2H), 2.42 (s, 3H), 2.20 (s, 3H), 2.15 (s, 3H), 2.10 (s, 3H), 1.87 – 1.72 (m, 2H), 1.57 – 1.23 (m, 15H), 1.25 – 1.00 (m, 9H), 0.89 – 0.82 (m, 12H). **$^{13}$C NMR** (126 MHz, $CDCl_3$) δ 164.6, 148.2, 148.0, 145.8, 144.8, 143.5, 140.2, 137.9, 136.6, 134.3, 132.2, 131.0, 130.7, 130.2, 129.7, 129.2, 129.0, 128.0, 127.6, 127.5, 126.0, 123.0, 118.8, 117.7, 74.9, 74.4, 40.1, 39.5, 37.6, 37.6, 37.5, 37.4, 32.9, 32.8, 31.4, 28.1, 24.9, 24.5, 24.0, 22.8, 22.7, 21.8, 21.1, 20.8, 19.9, 19.8, 12.9, 12.1, 11.9. **IR** (neat): 2948,2865, 1695, 1456, 1399, 1365, 1304, 1256, 1164, 1080 $cm^{-1}$. **HRMS** (ESI +ve) m/z: $[M+Na]^+$ Calcd for $C_{54}H_{71}NO_5SNa$ 868.4951; found 868.4991.

**4-(1-(2-(*N*-tosylacrylamido)phenyl)vinyl)benzyl 2-(3-cyano-4-isobutoxyphenyl)-4-methylthiazole-5-carboxylate (1x):** Column chromatography 25-30% EA/H; White solid; reaction scale 1 mmol, Yield: 54% (395 mg). **M.P.**: 106-108 °C. **$^1$H NMR** (500 MHz, $CDCl_3$) δ 8.16 (d, $J$ = 2.3 Hz, 1H), 8.08 (dd, $J$ = 8.8, 2.4 Hz, 1H), 7.88 (d, $J$ = 8.4 Hz, 2H), 7.57 – 7.50 (m, 1H), 7.49 – 7.41 (m, 2H), 7.36 – 7.29 (m, 4H), 7.30 – 7.24 (m, 2H), 7.18 – 7.13 (m, 1H), 7.00 (d, $J$ = 8.8 Hz, 1H), 6.10 (dd, $J$ = 16.7, 1.6 Hz, 1H), 5.76 (s, 1H), 5.62 (dd, $J$ = 16.7, 10.3 Hz, 1H), 5.41 (s, 1H), 5.32 (dd, $J$ = 10.3, 1.6 Hz, 1H), 5.28 (d, $J$ = 2.4 Hz, 2H), 3.89 (d, $J$ = 6.4 Hz, 2H), 2.76 (s, 3H), 2.41 (s, 3H), 2.26 – 2.14 (m, 1H), 1.09 (d, $J$ = 6.7 Hz, 6H). **$^{13}$C NMR** (126 MHz, $CDCl_3$) δ 167.6, 164.5, 162.6, 161.8, 161.6, 145.6, 144.9, 143.4, 140.9, 136.6, 135.2, 134.4, 132.7, 132.2, 132.1, 130.9, 130.6, 130.3, 129.6, 129.3, 129.1, 128.2, 128.2, 127.6, 125.9, 121.5, 119.4, 115.4, 112.7, 103.1, 75.8, 66.7, 28.2, 21.8, 19.1, 17.6. **IR** (neat): 2962, 2927, 2228, 1693, 1604, 1507, 1432, 1398, 1256, 1164 $cm^{-1}$. **HRMS** (ESI +ve) m/z: $[M+Na]^+$ Calcd for $C_{41}H_{31}N_3O_6S_2Na$ 754.2021; found 754.2042.

### 4.10.2 List of hydrosilanes and hydrogermanes

All hydrosilanes and hydrogermanes were commercially available and used as received.

$Et_3SiH$ **2a**, $^nPr_3SiH$ **2b**, $^iPr_3SiH$ **2c**, $BnMe_2SiH$ **2d**, $^tBuMe_2SiH$ **2e**, $PhMe_2SiH$ **2f**, $Ph_2MeSiH$ **2g**

$^tBuPh_2SiH$ **2h**, $Ph_3SiH$ **2i**, $Ph_2SiH_2$ **2j**, $(TMS)_3SiH$ **2k**

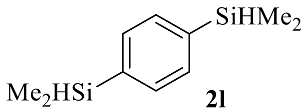

**2l**

$Et_3GeH$ **4a**, $^nBu_3GeH$ **4b**, $Ph_3GeH$ **4c**, $Ph_2GeH_2$ **4d**

### 4.10.3 Light source

All the photoreactions were performed using a blue LEDs Kessil® PR-160 lamp (λ = 456 nm) lamp with a fan kit for maintaining the ambient temperature.

### 4.10.4 General procedure for silylation of 1,7-dienes

To an oven-dried 10 mL Schlenk tube equipped with a magnetic stir bar 1,7-diene **1** (0.1 mmol), hydrosilane **2** (0.5 mmol, 5 equiv.), 1 mol% 4DPAIPN (0.8 mg, 0.001 mmol), and 2.0 equivalents of hydrogen atom transfer reagent (HATR) (0.2 mmol, 78.5 mg) were added. The reaction tube was sealed and placed under an argon atmosphere, then 1 mL acetonitrile was added *via* syringe. The reaction mixture was then degassed *via* freeze-pump-thaw (three times) and refilled with argon. The sealed reaction tube was then placed in blue LEDs Kessil® PR-160 lamp (λ = 456 nm) and irradiated for 30 minutes. After the reaction was completed, the mixture was transferred to a round-bottom flask and evaporated under reduced pressure. The crude product was then purified by column chromatography on silica gel (mesh 100-200) using a gradient eluent hexane/ethyl acetate (50:1 to 5:1), which provided the silylated benzazepines **3**.

**Characterization data of 3a-3ai**

**5-phenyl-1-tosyl-3-((triethylsilyl)methyl)-1,3-dihydro-2*H*-benzo[*b*]azepin-2-one (3a):** Column chromatography 3-5% EA/H; White solid; Yield: 72% (37.3 mg); **M.P.**: 125-126 °C. **$^1$H NMR** (500 MHz, $CDCl_3$) δ 7.72 – 7.66 (m, 3H), 7.50 – 7.45 (m, 1H), 7.42 – 7.36 (m, 4H), 7.36 – 7.32 (m, 1H), 7.28 – 7.25 (m, 2H), 7.03 (d, *J* = 8.1 Hz, 2H), 5.58 (d, *J* = 6.1 Hz, 1H), 2.85 – 2.78 (m, 1H), 2.28 (s, 3H), 1.14 (dd, *J* = 15.1, 4.1 Hz, 1H), 0.97 (dd, *J* = 15.1, 10.5 Hz, 1H), 0.84 (t, *J* = 7.9 Hz, 9H), 0.45 (q, *J* = 7.9 Hz, 6H). **$^{13}$C NMR** (126 MHz, $CDCl_3$) δ 172.9, 144.7, 140.4, 139.2, 136.0, 135.3, 134.8, 130.2, 129.7, 129.5, 129.1, 128.8, 128.7, 128.3, 128.3, 128.2, 128.1, 42.3, 21.7, 11.0, 7.3, 3.7. **IR** (neat): 2923, 2870, 1709, 1596, 1445, 1358, 1172 $cm^{-1}$.

**5-(*p*-tolyl)-1-tosyl-3-((triethylsilyl)methyl)-1,3-dihydro-2*H*-benzo[*b*]azepin-2-one (3b):** Column chromatography 3-5% EA/H; White solid; Yield: 51% (27.5 mg); **M.P.**:166-168 °C.**$^1$H NMR** (400 MHz, $CDCl_3$) δ 7.73 (d, *J* = 8.0 Hz, 3H), 7.56 – 7.47 (m, 1H), 7.44 – 7.36 (m, 1H), 7.35 – 7.21 (m, 5H), 7.08 (d, *J* = 8.0 Hz, 2H), 5.58 (d, *J* = 6.2 Hz, 1H), 2.89 – 2.79 (m, 1H), 2.45 (s, 3H), 2.33 (s, 3H), 1.18 (dd, *J* = 15.1, 4.2 Hz, 1H), 1.01 (dd, *J* = 15.1, 10.4 Hz, 1H), 0.89 (t, *J* = 7.9 Hz, 9H), 0.49 (q, *J* = 7.9 Hz, 6H). **$^{13}$C NMR** (101 MHz, $CDCl_3$) δ 172.9, 144.7, 140.3, 138.2, 136.4, 136.0, 135.4, 134.7, 129.7, 129.4, 129.4, 129.1, 128.8, 128.2, 128.0, 42.2, 21.7, 21.3, 11.0, 7.3, 3.7. **IR** (neat): 2957, 2873, 1715, 1596, 1447, 1355, 1237, 1173 $cm^{-1}$.

**5-(4-chlorophenyl)-1-tosyl-3-((triethylsilyl)methyl)-1,3-dihydro-2*H*-benzo[*b*]azepin-2-one (3c):** Column chromatography 5-10% EA/H; White solid; Yield: 60% (33.2 mg); **M.P.**: 144-146 °C. **$^1$H NMR** (500 MHz, $CDCl_3$) δ 7.65 – 7.58 (m, 3H), 7.45 – 7.38 (m, 1H), 7.33 – 7.26 (m, 3H), 7.21 – 7.16 (m, 2H), 7.15 (dd, *J* = 7.9, 1.6 Hz, 1H), 7.02 – 6.96 (m, 2H), 5.50 (d, *J* = 6.3 Hz, 1H), 2.76 – 2.68 (m, 1H), 2.23 (s, 3H), 1.07 (dd, *J* = 15.1, 4.3 Hz, 1H), 0.88 (dd, *J* = 15.1, 10.2 Hz, 1H), 0.76 (t, *J* = 7.9 Hz, 9H), 0.36 (q, *J* = 7.9 Hz, 6H). **$^{13}$C NMR** (126 MHz, $CDCl_3$) δ 172.7, 144.9, 139.3, 137.7, 136.0, 134.9, 134.8, 134.3, 130.7, 129.5, 129.5, 129.4, 129.1, 129.0, 128.8, 128.5, 128.2, 42.4, 21.7, 11.0, 7.3, 3.7. **IR** (neat): 2951, 2873, 1711, 1596, 1486, 1359, 1237, 1172 $cm^{-1}$.

**5-(3-chlorophenyl)-1-tosyl-3-((triethylsilyl)methyl)-1,3-dihydro-2*H*-benzo[*b*]azepin-2-one (3d):** Column chromatography 5-10% EA/H; White solid; Yield: 64% (35.4 mg); **M.P.**: 135-137 °C. **$^1$H NMR** (500 MHz, $CDCl_3$) δ 7.73 – 7.66 (m, 3H), 7.53 – 7.46 (m, 1H), 7.41 – 7.37 (m, 1H), 7.36 – 7.30 (m, 2H), 7.30 – 7.27 (m, 1H), 7.25 – 7.18 (m, 2H), 7.08 (d, *J* = 8.1 Hz, 2H), 5.59 (d, *J* = 6.1 Hz, 1H), 2.84 – 2.76 (m, 1H), 2.30 (s, 3H), 1.16 (dd, *J* = 15.1, 4.4 Hz, 1H), 0.97 (dd, *J* = 15.1, 10.1 Hz, 1H), 0.84 (t, *J* = 8.0 Hz, 9H), 0.44 (q, *J* = 7.9 Hz, 6H). **$^{13}$C NMR** (126 MHz, $CDCl_3$) δ 172.5, 144.9, 141.0, 139.2, 135.8, 134.8, 134.7, 134.6, 131.5, 130.0, 129.6, 129.5, 129.1, 128.8, 128.6, 128.4, 128.3, 128.2, 126.4, 42.4, 21.7, 11.1, 7.3, 3.7. **IR** (neat): 2949, 2873, 1714, 1593, 1444, 1353, 1281, 1155 $cm^{-1}$. **HRMS** (ESI +ve) m/z: $[M+Na]^+$ Calcd for $C_{30}H_{34}ClNO_3SSiNa$ 574.1615; found 574.1620.

**5-(*o*-tolyl)-1-tosyl-3-((triethylsilyl)methyl)-1,3-dihydro-2*H*-benzo[*b*]azepin-2-one (3e):** Column chromatography 3-5% EA/H; White solid; Yield: 72% (38.3 mg); **M.P.**: 102-104 °C. **$^1$H NMR** (500 MHz, $CDCl_3$) δ 8.04 (d, $J$ = 8.4 Hz, 2H), 7.68 – 7.62 (m, 1H), 7.45 – 7.39 (m, 1H), 7.34 – 7.31 (m, 2H), 7.31 – 7.18 (m, 5H), 7.05 (dd, $J$ = 7.9, 1.6 Hz, 1H), 5.60 (d, $J$ = 5.7 Hz, 1H), 2.85 – 2.77 (m, 1H), 2.43 (s, 3H), 2.11 (s, 3H), 1.18 (dd, $J$ = 15.1, 4.4 Hz, 1H), 1.01 (dd, $J$ = 15.1, 10.2 Hz, 1H), 0.84 (t, $J$ = 7.9 Hz, 9H), 0.45 (q, $J$ = 7.9 Hz, 6H). **$^{13}$C NMR** (126 MHz, $CDCl_3$) δ 174.3, 145.0, 141.4, 139.2, 136.8, 136.8, 136.6, 133.7, 133.0, 130.7, 130.4, 129.4, 129.3, 128.4, 128.3, 128.0, 127.9, 126.0, 42.1, 21.8, 21.0, 11.0, 7.4, 3.8. **IR** (neat): 29571 2874, 1717, 1597, 1482, 1361, 1238, 1132 $cm^{-1}$.

**5-(2,4-dichlorophenyl)-1-tosyl-3-((triethylsilyl)methyl)-1,3-dihydro-2*H*-benzo[*b*]azepin-2-one (3f):** Column chromatography 3-5% EA/H; Clear oil; Yield: 47% (27.5 mg). **$^1$H NMR** (500 MHz, $CDCl_3$) δ 8.02 – 7.96 (m, 2H), 7.72 – 7.67 (m, 1H), 7.49 – 7.42 (m, 2H), 7.34 – 7.26 (m, 4H), 7.23 (d, $J$ = 8.2 Hz, 1H), 7.06 – 7.01 (m, 1H), 5.65 (d, $J$ = 5.8 Hz, 1H), 2.85 – 2.77 (m, 1H), 2.41 (s, 3H), 1.18 (dd, $J$ = 15.2, 4.3 Hz, 1H), 0.96 (dd, $J$ = 15.2, 10.2 Hz, 1H), 0.83 (t, $J$ = 7.9 Hz, 9H), 0.44 (q, $J$ = 7.9 Hz, 6H). **$^{13}$C NMR** (126 MHz, $CDCl_3$) δ 173.7, 144.9, 138.1, 136.8, 136.6, 135.2, 134.9, 134.8, 134.4, 133.8, 132.6, 130.2, 129.3 (2C), 128.6, 128.2, 128.0, 127.9, 127.4, 42.2, 21.8, 11.0, 7.3, 3.7. **IR** (neat): 2952, 2873, 1717, 1597, 1468, 1357, 1234, 1165 $cm^{-1}$. **HRMS** (ESI +ve) m/z: $[M+Na]^+$ Calcd for $C_{30}H_{33}Cl_2NO_3SSiNa$ 608.1225; found 608.1229.

**4-(2-oxo-1-tosyl-3-((triethylsilyl)methyl)-2,3-dihydro-1*H*-benzo[*b*]azepin-5-yl)benzonitrile (3g):** Column chromatography 15-20% EA/H; White solid; Yield: 63% (34.8 mg); **M.P.**: 153-155 °C. **$^1$H NMR** (500 MHz, $CDCl_3$) δ 7.72 – 7.67 (m, 5H), 7.54 – 7.49 (m, 1H), 7.46 – 7.42 (m, 2H), 7.42 – 7.37 (m, 1H), 7.20 – 7.16 (m, 1H), 7.08 (d, *J* = 8.1 Hz, 2H), 5.72 (d, *J* = 6.2 Hz, 1H), 2.87 – 2.79 (m, 1H), 2.32 (s, 3H), 1.17 (dd, *J* = 15.1, 4.4 Hz, 1H), 0.98 (dd, *J* = 15.1, 10.1 Hz, 1H), 0.84 (t, *J* = 7.9 Hz, 9H), 0.44 (q, *J* = 7.9 Hz, 6H). **$^{13}$C NMR** (126 MHz, $CDCl_3$) δ 172.4, 145.1, 143.6, 139.0, 135.9, 134.9, 134.2, 133.2, 132.6, 129.6, 129.3, 129.2, 128.9, 128.8, 128.7, 128.4, 118.6, 112.0, 42.7, 21.7, 11.0, 7.3, 3.7. **IR** (neat): 2954, 2924, 2128, 1713, 1596, 1442, 1352, 1247, 1174 cm$^{-1}$. **HRMS** (ESI +ve) m/z: $[M+Na]^+$ Calcd for $C_{31}H_{34}N_2O_3SSiNa$: 563.1957; found 563.1960.

**5-(thiophen-2-yl)-1-tosyl-3-((triethylsilyl)methyl)-1,3-dihydro-2*H*-benzo[*b*]azepin-2-one (3h)**: Column chromatography 3-5% EA/H; White solid; Yield: 25% (13.1 mg); **M.P.**: 167-169 °C. **$^{1}$H NMR** (500 MHz, $CDCl_3$) δ 7.71 – 7.66 (m, 1H), 7.62 (d, *J* = 8.3 Hz, 2H), 7.57 (dd, *J* = 7.8, 1.6 Hz, 1H), 7.51 (td, *J* = 7.7, 1.7 Hz, 1H), 7.46 – 7.39 (m, 1H), 7.31 – 7.28 (m, 1H), 7.09 – 7.04 (m, 1H), 7.05 – 7.01 (m, 1H), 6.99 (d, *J* = 8.1 Hz, 2H), 5.57 (d, *J* = 6.4 Hz, 1H), 2.83 – 2.75 (m, 1H), 2.29 (s, 3H), 1.08 (dd, *J* = 15.1, 4.2 Hz, 1H), 0.95 (dd, *J* = 15.1, 10.5 Hz, 1H), 0.82 (t, *J* = 7.9 Hz, 9H), 0.42 (q, *J* = 7.9 Hz, 6H). **$^{13}$C NMR** (126 MHz, $CDCl_3$) δ 172.4, 144.8, 142.6, 135.7, 134.5, 134.3, 133.7, 129.9, 129.5, 129.1, 129.0, 128.8, 128.7, 128.3, 127.7, 126.8, 125.7, 42.2, 21.7, 10.8, 7.3, 3.7. **IR** (neat): 2948, 2872, 1978, 1718, 1595, 1445, 1356, 1157, 1087 cm$^{-1}$. **HRMS** (ESI +ve) m/z: $[M+Na]^+$ Calcd for $C_{28}H_{33}NO_3S_2SiNa$ 546.1569, found 546.1576.

**9-methyl-5-phenyl-1-tosyl-3-((triethylsilyl)methyl)-1,3-dihydro-2*H*-benzo[*b*]azepin-2-one (3j):** Column chromatography 3-5% EA/H; White solid; Yield: 37% (19.7 mg); **M.P.**: 134-136 °C. **$^{1}$H NMR** (500 MHz, $CDCl_3$) δ 7.63 (d, *J* = 8.1 Hz, 2H), 7.43 – 7.36 (m, 6H), 7.30 – 7.26 (m, 1H), 7.15 – 7.09 (m, 1H), 6.85 (d, *J* = 8.1 Hz, 2H), 5.46 (d, *J* = 6.1 Hz, 1H), 2.86 – 2.78 (m, 1H), 2.70 (s, 3H), 2.22 (s, 3H), 1.14 (dd, *J* = 15.0, 5.2 Hz, 1H), 0.91 – 0.86 (m, 1H), 0.83 (t, *J* = 8.0 Hz, 9H), 0.44 (q, *J* = 7.9 Hz, 6H). **$^{13}$C NMR** (126 MHz, $CDCl_3$) δ 172.9, 144.7, 140.8, 139.1, 139.0, 136.0, 135.4, 135.0, 131.2, 129.5, 129.3, 128.7, 128.6, 128.3, 128.1, 128.0, 127.5, 42.4, 21.6, 20.6, 11.0, 7.4, 3.7. **IR** (neat):

2950, 2872, 1702, 1594, 1454, 1359, 1165, 1131 cm$^{-1}$. **HRMS** (ESI +ve) m/z: $[M+Na]^+$ Calcd for $C_{31}H_{37}NO_3SSiNa$ 554.2161; found 554.2165.

**8-methyl-5-phenyl-1-tosyl-3-((triethylsilyl)methyl)-1,3-dihydro-2*H*-benzo[*b*]azepin-2-one (3k):** Column chromatography 3-5% EA/H; White solid; Yield: 63% (33.5 mg); **M.P.**: 140-142 °C. **$^1$H NMR** (500 MHz, $CDCl_3$) δ 7.67 (d, *J* = 8.3 Hz, 2H), 7.52 – 7.48 (m, 1H), 7.41 – 7.36 (m, 3H), 7.35 – 7.31 (m, 2H), 7.20 – 7.11 (m, 2H), 7.01 (d, *J* = 8.1 Hz, 2H), 5.51 (d, *J* = 6.1 Hz, 1H), 2.86 – 2.78 (m, 1H), 2.48 (s, 3H), 2.27 (s, 3H), 1.12 (dd, *J* = 15.1, 4.0 Hz, 1H), 0.96 (dd, *J* = 15.2, 10.6 Hz, 1H), 0.85 (t, *J* = 7.9 Hz, 9H), 0.45 (q, *J* = 7.9 Hz, 6H). **$^{13}$C NMR** (126 MHz, $CDCl_3$) δ 172.9, 144.6, 140.4, 139.3, 138.5, 136.0, 134.6, 132.4, 129.8, 129.4, 129.5, 129.2, 129.0, 128.8, 128.7, 128.2, 42.3, 21.6, 21.4, 11.0, 7.4, 3.7. **IR** (neat): 2949, 2872, 1713, 1614, 1455, 1358, 1170, 1141 cm$^{-1}$.

**methyl 2-oxo-5-phenyl-1-tosyl-3-((triethylsilyl)methyl)-2,3-dihydro-1*H*-benzo[*b*]azepine-8-carboxylate (3l):** Column chromatography 5-10% EA/H; White solid; Yield: 57% (32.9 mg); **M.P.**: 179-181 °C. **$^1$H NMR** (500 MHz, $CDCl_3$) δ 8.36 (d, *J* = 1.7 Hz, 1H), 8.01 (dd, *J* = 8.2, 1.7 Hz, 1H), 7.72 (d, *J* = 8.4 Hz, 2H), 7.44 – 7.38 (m, 3H), 7.34 (d, *J* = 8.2 Hz, 1H), 7.32 – 7.28 (m, 2H), 7.07 (d, *J* = 8.1 Hz, 2H), 5.67 (d, *J* = 6.1 Hz, 1H), 3.98 (s, 3H), 2.80 – 2.73 (m, 1H), 2.30 (s, 3H), 1.15 (dd, *J* = 15.1, 4.2 Hz, 1H), 0.99 (dd, *J* = 15.1, 10.4 Hz, 1H), 0.84 (t, *J* = 7.9 Hz, 9H), 0.45 (q, *J* = 7.9 Hz, 6H). **$^{13}$C NMR** (126 MHz, $CDCl_3$) δ 172.4, 165.9, 145.0, 140.0, 139.4, 138.7, 135.8, 134.8, 131.8, 130.6, 130.1, 129.9, 129.2, 128.9, 128.9, 128.8, 128.6, 128.2, 52.6, 42.4, 21.7, 11.1, 7.3, 3.7. **IR** (neat): 2955, 287, 1716, 1595, 1433, 1353, 1254, 1176 cm$^{-1}$. **HRMS** (ESI +ve) m/z: $[M+Na]^+$ Calcd for $C_{32}H_{37}NO_5SSiNa$ 598.2059; found 598.2061.

**7-methyl-5-phenyl-1-tosyl-3-((triethylsilyl)methyl)-1,3-dihydro-2*H*-benzo[*b*]azepin-2-one (3m):** Column chromatography 3-5% EA/H; White solid; Yield: 72% (38.3 mg); **M.P.**: 112-114 °C. **$^1$H NMR** (500 MHz, $CDCl_3$) δ 7.68 (d, *J* = 8.0 Hz, 2H), 7.57 (d, *J* = 8.2 Hz, 1H), 7.42

– 7.36 (m, 3H), 7.35 – 7.32 (m, 2H), 7.30 – 7.26 (m, 1H), 7.05 – 7.00 (m, 3H), 5.53 (d, $J$ = 6.1 Hz, 1H), 2.86 – 2.79 (m, 1H), 2.35 (s, 3H), 2.27 (s, 3H), 1.14 (dd, $J$ = 15.1, 4.2 Hz, 1H), 0.95 (dd, $J$ = 15.1, 10.4 Hz, 1H), 0.85 (t, $J$ = 7.9 Hz, 9H), 0.45 (q, $J$ = 7.9 Hz, 6H). **$^{13}$C NMR** (126 MHz, $CDCl_3$) δ 172.9, 144.6, 140.4, 139.4, 138.2, 136.0, 135.0, 132.4, 130.2, 129.9, 129.3, 129.2, 129.0, 128.8, 128.7, 128.3, 128.2, 42.3, 21.7, 21.3, 11.0, 7.4, 3.7. **IR** (neat): 2923, 2870, 1707, 1596, 1445, 1356, 1233, 1171 cm$^{-1}$.

**7-methoxy-5-phenyl-1-tosyl-3-((triethylsilyl)methyl)-1,3-dihydro-2*H*-benzo[*b*]azepin-2-one (3n):** Column chromatography 5-10% EA/H; White solid; Yield: 63% (34.6 mg); **M.P.**: 135-137 °C. **$^{1}$H NMR** (500 MHz, $CDCl_3$) δ 7.67 (d, $J$ = 8.4 Hz, 2H), 7.61 (d, $J$ = 8.9 Hz, 1H), 7.42 – 7.33 (m, 5H), 7.04 – 6.99 (m, 3H), 6.72 (d, $J$ = 3.0 Hz, 1H), 5.54 (d, $J$ = 6.1 Hz, 1H), 3.77 (s, 3H), 2.91 – 2.83 (m, 1H), 2.27 (s, 3H), 1.14 (dd, $J$ = 15.1, 4.1 Hz, 1H), 0.96 (dd, $J$ = 15.1, 10.4 Hz, 1H), 0.86 (t, $J$ = 7.9 Hz, 9H), 0.46 (q, $J$ = 7.9 Hz, 6H). **$^{13}$C NMR** (126 MHz, $CDCl_3$) δ 172.92, 158.8, 144.6, 140.4, 139.1, 136.4, 135.9, 130.7, 130.4, 129.0, 128.8, 128.7, 128.3, 128.2, 128.0, 114.3, 114.2, 55.7, 42.3, 21.7, 11.0, 7.4, 3.7. **IR** (neat): 2951, 2874, 1978, 1709, 1597, 1465, 1355, 1225, 1172 cm$^{-1}$.

**7-fluoro-5-phenyl-1-tosyl-3-((triethylsilyl)methyl)-1,3-dihydro-2*H*-benzo[*b*]azepin-2-one (3o):** Column chromatography 3-5% EA/H; White solid; Yield: 70% (37.5 mg); **M.P.**: 162-164 °C. **$^{1}$H NMR** (500 MHz, $CDCl_3$) δ 7.70 – 7.66 (m, 3H), 7.43 – 7.37 (m, 3H), 7.34 – 7.29 (m, 2H), 7.22 – 7.16 (m, 1H), 7.04 (d, $J$ = 8.0 Hz, 2H), 6.95 (dd, $J$ = 9.2, 2.9 Hz, 1H), 5.60 (d, $J$ = 6.1 Hz, 1H), 2.84 – 2.77 (m, 1H), 2.28 (s, 3H), 1.15 (dd, $J$ = 15.1, 4.2 Hz, 1H), 0.97 (dd, $J$ = 15.1, 10.3 Hz, 1H), 0.86 (t, $J$ = 7.9 Hz, 9H), 0.46 (q, $J$ = 7.9 Hz, 6H). **$^{19}$F NMR** (471 MHz, $CDCl_3$) δ (-111.86) to (-111.95) (m). **$^{13}$C NMR** (126 MHz, $CDCl_3$) δ 172.6, 161.4 (d, $J$ = 250.0 Hz), 144.9, 139.8 (2C), 138.6, 137.3 (d, $J$ = 8.3 Hz), 135.7, 131.4 (d, $J$ = 8.8 Hz), 131.1, 130.9 (d, $J$ = 3.1 Hz), 129.1, 128.9, 128.8, 128.6, 128.1, 115.9 (dd, $J$ = 23.1, 13.2 Hz), 42.4, 21.7, 11.0, 7.4, 3.7. **IR** (neat): 2922, 2853, 1706, 1577, 1487, 1355, 1264, 1197 cm$^{-1}$.

**7-chloro-5-phenyl-1-tosyl-3-((triethylsilyl)methyl)-1,3-dihydro-2*H*-benzo[*b*]azepin-2-one (3p):** Column chromatography 3-5% EA/H; White solid; Yield: 71% (39.3 mg); **M.P.**: 146-148 °C. **$^{1}$H NMR** (400 MHz, $CDCl_3$) δ 7.68 (d, *J* = 8.1 Hz, 2H), 7.64 (d, *J* = 8.6 Hz, 1H), 7.47 – 7.38 (m, 4H), 7.33 – 7.28 (m, 2H), 7.25 – 7.22 (m, 1H), 7.04 (d, *J* = 8.1 Hz, 2H), 5.60 (d, *J* = 6.1 Hz, 1H), 2.83 – 2.74 (m, 1H), 2.29 (s, 3H), 1.16 (dd, *J* = 15.1, 4.3 Hz, 1H), 0.97 (dd, *J* = 15.2, 10.2 Hz, 1H), 0.86 (t, *J* = 7.9 Hz, 9H), 0.46 (q, *J* = 7.9 Hz, 6H). **$^{13}$C NMR** (126 MHz, $CDCl_3$) δ 172.4, 145.0, 139.6, 138.6, 136.7, 135.6, 134.0, 133.2, 131.3, 130.8, 129.3, 129.2, 128.9, 128.8, 128.6, 128.5, 128.2, 42.4, 21.7, 11.1, 7.4, 3.7. **IR** (neat): 2949, 2883, 1708, 1596, 1481, 1356, 1276, 1172 $cm^{-1}$.

**2-oxo-5-phenyl-1-tosyl-3-((triethylsilyl)methyl)-2,3-dihydro-1*H*-benzo[*b*]azepine-7-carbonitrile (3q):** Column chromatography 10-15% EA/H; White solid; Yield: 45% (24.5 mg); **M.P.**: 163-165 °C. **$^{1}$H NMR** (500 MHz, $CDCl_3$) δ 7.83 (d, *J* = 8.4 Hz, 1H), 7.74 (dd, *J* = 8.4, 2.0 Hz, 1H), 7.68 (d, *J* = 8.1 Hz, 2H), 7.60 – 7.56 (m, 1H), 7.46 – 7.41 (m, 3H), 7.29 – 7.26 (m, 2H), 7.08 (d, *J* = 8.1 Hz, 2H), 5.68 (d, *J* = 6.2 Hz, 1H), 2.72 – 2.64 (m, 1H), 2.30 (s, 3H), 1.17 (dd, *J* = 15.1, 4.3 Hz, 1H), 0.99 (dd, *J* = 15.1, 10.2 Hz, 1H), 0.86 (t, *J* = 7.9 Hz, 9H), 0.46 (q, *J* = 7.9 Hz, 6H). **$^{13}$C NMR** (126 MHz, $CDCl_3$) δ 171.9, 145.4, 139.1, 138.2, 138.0, 136.4, 135.4, 133.9, 132.1, 131.0, 130.5, 129.3, 129.1, 129.0, 128.9, 128.2, 117.8, 112.1, 42.5, 21.7, 11.1, 7.4, 3.7. **IR** (neat): 2951, 2874, 1978, 1709, 1597, 1491, 1355, 1225, 1172 $cm^{-1}$. **HRMS** (ESI +ve) m/z: $[M+Na]^+$ Calcd for $C_{31}H_{34}N_2O_3SSiNa$ 565.1957; found 565.1970.

**7-nitro-5-phenyl-1-tosyl-3-((triethylsilyl)methyl)-1,3-dihydro-2*H*-benzo[*b*]azepin-2-one (3r):** Column chromatography 10-15% EA/H; White solid; Yield: 17% (9.6 mg); **M.P.**: 194-196 °C. **$^{1}$H NMR** (500 MHz, $CDCl_3$) δ 8.31 (dd, *J* = 8.9, 2.7 Hz, 1H), 8.14 (d, *J* = 2.6 Hz, 1H), 7.89 (d, *J* = 8.9 Hz, 1H), 7.69 (d, *J* = 8.3 Hz, 2H), 7.48 – 7.40 (m, 3H), 7.32 – 7.27 (m, 2H), 7.08 (d, *J* = 8.1 Hz, 2H), 5.71 (d, *J* = 6.2 Hz, 1H), 2.73 – 2.65 (m, 1H), 2.31 (s, 3H), 1.18 (dd, *J* = 15.1, 4.2 Hz, 1H), 1.00 (dd, *J* = 15.1, 10.2 Hz, 1H), 0.86 (t, *J* = 7.9 Hz, 9H), 0.46 (q, *J* = 7.9 Hz, 6H). **$^{13}$C NMR** (126 MHz, $CDCl_3$) δ 171.8, 146.7, 145.5, 139.4, 139.4, 138.1, 136.4, 135.3, 132.3, 130.6, 129.3, 129.2, 129.1, 128.9, 128.1, 125.0, 122.7, 42.6, 21.7, 11.1, 7.4, 3.7. **IR** (neat): 2950, 2873, 1714, 1596, 1456, 1342, 1277, 1171 $cm^{-1}$.

**6-methyl-5-phenyl-1-tosyl-3-((triethylsilyl)methyl)-1,3-dihydro-2*H*-benzo[*b*]azepin-2-one (3s):** Column chromatography 3-5% EA/H; White solid; Yield: 78% (41.5 mg); **M.P.**: 148-150 °C. **$^{1}$H NMR** (500 MHz, $CDCl_3$) δ 7.67 (d, $J$ = 8.4 Hz, 2H), 7.54 (d, $J$ = 8.0 Hz, 1H), 7.42 – 7.30 (m, 4H), 7.29 – 7.21 (m, 3H), 6.95 (d, $J$ = 8.2 Hz, 2H), 5.68 (d, $J$ = 6.9 Hz, 1H), 2.92 – 2.84 (m, 1H), 2.27 (s, 3H), 1.89 (s, 3H), 1.06 (dd, $J$ = 15.1, 3.6 Hz, 1H), 0.95 (dd, $J$ = 15.1, 11.1 Hz, 1H), 0.84 (t, $J$ = 7.9 Hz, 9H), 0.45 (q, $J$ = 7.9 Hz, 6H). **$^{13}$C NMR** (126 MHz, $CDCl_3$) δ 173.8, 144.6, 140.0, 139.7, 137.8, 135.9, 135.5, 133.8, 132.4, 131.2, 129.0, 128.9, 128.1, 127.9, 126.7, 126.5, 42.6, 21.7, 21.6, 10.6, 7.3, 3.8. **IR** (neat): 2951, 2879, 1713, 1596, 1458, 1356, 1270, 1171 $cm^{-1}$. **HRMS** (ESI +ve) m/z: $[M+Na]^+$ Calcd for $C_{31}H_{37}NO_3SSiNa$ 554.2161; found 554.2142.

**4-methyl-5-phenyl-1-tosyl-3-((triethylsilyl)methyl)-1,3-dihydro-2*H*-benzo[*b*]azepin-2-one (3t):** Column chromatography 3-5% EA/H; White solid; Yield: 27% (14.4 mg); **M.P.**: 131-132 °C. **$^{1}$H NMR** (500 MHz, $CDCl_3$) δ 7.79 (d, $J$ = 8.4 Hz, 2H), 7.66 (d, $J$ = 8.0 Hz, 1H), 7.43 – 7.35 (m, 3H), 7.37 – 7.30 (m, 1H), 7.30 – 7.23 (m, 1H), 7.19 – 7.11 (m, 4H), 7.01 (dd, $J$ = 7.8, 1.6 Hz, 1H), 3.03 (dd, $J$ = 8.6, 5.8 Hz, 1H), 2.33 (s, 3H), 1.55 (s, 3H), 1.20 (dd, $J$ = 14.8, 8.6 Hz, 1H), 0.83 – 0.77 (m, 10H), 0.39 (q, $J$ = 7.9 Hz, 6H). **$^{13}$C NMR** (126 MHz, $CDCl_3$) δ 170.88, 144.60, 140.18, 137.28, 136.27, 136.18, 135.43, 134.64, 130.82, 130.41, 129.08, 128.67, 128.58, 128.37, 127.89, 127.57, 45.14, 21.71, 16.82, 8.54, 7.37, 3.61. **IR** (neat): 2949, 2872, 1708, 1594, 1440, 1355, 1237, 1158 $cm^{-1}$. **HRMS** (ESI +ve) m/z: $[M+Na]^+$ Calcd for $C_{31}H_{37}NO_3SSiNa$ 554.2161; found 554.2151.

**3-methyl-5-phenyl-1-tosyl-3-((triethylsilyl)methyl)-1,3-dihydro-2*H*-benzo[*b*]azepin-2-one (3u):** Column chromatography 3-5% EA/H;

White solid; Yield: 42% (22.4 mg); **M.P.**: 129-131 °C. $^{1}$**H NMR** (500 MHz, $CDCl_3$) δ 7.75 (d, *J* = 8.2 Hz, 2H), 7.66 – 7.61 (m, 1H), 7.48 – 7.42 (m, 1H), 7.42 – 7.33 (m, 5H), 7.32 – 7.27 (m, 1H), 7.20 – 7.14 (m, 1H), 7.11 (d, *J* = 8.1 Hz, 2H), 5.74 (s, 1H), 2.32 (s, 3H), 1.35 (s, 3H), 0.71 (t, *J* = 7.9 Hz, 9H), 0.58 – 0.52 (m, 1H), 0.48 – 0.43 (m, 1H), 0.42 – 0.32 (m, 6H). $^{13}$**C NMR** (126 MHz, $CDCl_3$) δ 175.9, 144.5, 140.8, 140.2, 136.6, 135.7, 135.1, 134.8, 129.9, 129.1, 128.9, 128.8, 128.7, 128.4, 128.3, 128.1, 127.7, 47.0, 27.6, 21.7, 15.9, 7.4, 4.6. **IR** (neat): 2951, 2872, 1707, 1577, 1421, 1356, 1198, 1170 $cm^{-1}$.

**1-methyl-5-phenyl-3-((triethylsilyl)methyl)-1,3-dihydro-2*H*-benzo[*b*]azepin-2-one (3v):** Column chromatography 3-5% EA/H; Clear oil; Yield: 40% (15.2 mg). $^{1}$**H NMR** (500 MHz, $CDCl_3$) δ 7.42 – 7.28 (m, 6H), 7.25 – 7.23 (m, 1H), 7.22 – 7.19 (m, 1H), 7.14 – 7.09 (m, 1H), 5.84 (d, *J* = 6.3 Hz, 1H), 3.44 (s, 3H), 2.64 – 2.56 (m, 1H), 1.33 (dd, *J* = 15.0, 4.8 Hz, 1H), 1.18 (dd, *J* = 15.0, 10.0 Hz, 1H), 0.91 (t, *J* = 7.9 Hz, 9H), 0.53 (q, *J* = 7.9 Hz, 6H). $^{13}$**C NMR** (126 MHz, $CDCl_3$) δ 173.9, 142.9, 140.6, 139.2, 133.2, 133.2, 130.1, 128.7, 128.6, 128.4, 127.7, 124.2, 122.5, 40.1, 36.9, 11.8, 7.5, 3.9. **IR** (neat): 2927, 2869, 1665, 1598, 1445, 1362, 1237, 1113 $cm^{-1}$.

**5-phenyl-1-tosyl-3-((tripropylsilyl)methyl)-1,3-dihydro-2*H*-benzo[*b*]azepin-2-one (3w):** Column chromatography 3-5% EA/H; White solid; Yield: 63% (35.3 mg); **M.P.**: 135-137 °C. $^{1}$**H NMR** (500 MHz, $CDCl_3$) δ 7.72 – 7.66 (m, 3H), 7.52 – 7.45 (m, 1H), 7.43 – 7.32 (m, 6H), 7.29 – 7.26 (m, 1H), 7.03 (d, *J* = 8.1 Hz, 2H), 5.58 (d, *J* = 6.2 Hz, 1H), 2.84 – 2.76 (m, 1H), 2.28 (s, 3H), 1.25 – 1.15 (m, 6H), 1.13 (dd, *J* = 15.1, 4.0 Hz, 1H), 0.96 (dd, *J* = 15.1, 10.5 Hz, 1H), 0.86 (t, *J* = 7.2 Hz, 9H), 0.47 – 0.39 (m, 6H). $^{13}$**C NMR** (126 MHz, $CDCl_3$) δ 172.8, 144.6, 140.2, 139.1, 135.9, 135.2, 134.7, 130.1, 129.6, 129.3, 128.9, 128.7, 128.6, 128.2, 128.1, 128.1, 127.9, 42.3, 21.5, 18.5, 17.3, 15.6, 11.8. **IR** (neat): 2956, 2862, 1717, 1597, 1446, 1356, 1232, 1172 $cm^{-1}$. **HRMS** (ESI +ve) m/z: $[M+H]^+$ Calcd for $C_{33}H_{42}NO_3SSi$ 560.2654; found 560.2632.

**5-phenyl-1-tosyl-3-((triisopropylsilyl)methyl)-1,3-dihydro-2*H*-benzo[*b*]azepin-2-one (3x):** Column chromatography 3-5% EA/H; White solid; Yield: 43% (24.1 mg); **M.P.**: 143-145 °C . **$^{1}$H NMR** (500 MHz, $CDCl_3$) δ 7.71 – 7.66 (m, 3H), 7.50 – 7.45 (m, 1H), 7.42 – 7.31 (m, 6H), 7.26 – 7.23 (m, 1H), 7.02 (d, $J$ = 8.1 Hz, 2H), 5.64 (d, $J$ = 6.3 Hz, 1H), 2.95 – 2.88 (m, 1H), 2.28 (s, 3H), 1.31 (dd, $J$ = 15.4, 3.6 Hz, 1H), 0.99 (dd, $J$ = 15.4, 10.1 Hz, 1H), 0.96 – 0.86 (m, 21H). **$^{13}$C NMR** (126 MHz, $CDCl_3$) δ 172.9, 144.8, 140.4, 139.1, 135.9, 135.2, 134.9, 130.5, 129.6, 129.4, 129.1, 128.8, 128.7, 128.3, 128.3, 128.2, 128.1, 42.3, 21.7, 18.7, 18.7, 11.1, 8.4. **IR** (neat): 2922, 2857, 1712, 1597, 1447, 1360, 1173, 1139 cm$^{-1}$.

**3-((benzyldimethylsilyl)methyl)-5-phenyl-1-tosyl-1,3-dihydro-2*H*-benzo[*b*]azepin-2-one (3y):** Column chromatography 5-10% EA/H; White solid; Yield: 77% (42.5 mg); **M.P.**: 120-122 °C. **$^{1}$H NMR** (500 MHz, $CDCl_3$) δ 7.67 (d, $J$ = 8.1 Hz, 3H), 7.51 – 7.46 (m, 1H), 7.42 – 7.35 (m, 4H), 7.33 – 7.29 (m, 2H), 7.26 – 7.22 (m, 1H), 7.08 (t, $J$ = 7.4 Hz, 2H), 7.02 (d, $J$ = 8.1 Hz, 2H), 6.97 (t, $J$ = 7.4 Hz, 1H), 6.89 – 6.84 (m, 2H), 5.52 (d, $J$ = 6.2 Hz, 1H), 2.71 – 2.64 (m, 1H), 2.28 (s, 3H), 2.02 (s, 2H), 1.17 (dd, $J$ = 15.1, 5.0 Hz, 1H), 0.97 (dd, $J$ = 15.1, 9.7 Hz, 1H), -0.03 (s, 3H), -0.07 (s, 3H). **$^{13}$C NMR** (126 MHz, $CDCl_3$) δ 172.5, 144.7, 140.4, 139.5, 139.2, 135.9, 135.2, 134.7, 129.9, 129.8, 129.5, 129.1, 128.8, 128.7, 128.3, 128.3, 128.2, 128.1, 128.0, 124.3, 42.2, 26.0, 21.7, 14.3, -2.3, -2.6. **IR** (neat): 2956, 2923, 1716, 1598, 1492, 1355, 1253, 1166 cm$^{-1}$.

**3-((*tert*-butyldimethylsilyl)methyl)-5-phenyl-1-tosyl-1,3-dihydro-2*H*-benzo[*b*]azepin-2-one (3z):** Column chromatography 3-5% EA/H; White solid; Yield: 64% (33.2 mg); **M.P.**: 111-113 °C. **$^{1}$H NMR** (500 MHz, $CDCl_3$) δ 7.73 – 7.66 (m, 3H), 7.51 – 7.45 (m, 1H), 7.42 – 7.33 (m, 6H), 7.28 – 7.26 (m, 1H), 7.03 (d, $J$ = 8.1 Hz, 2H), 5.58 (d, $J$ = 6.2 Hz, 1H), 2.84 – 2.77 (m, 1H), 2.28 (s, 3H), 1.18 (dd, $J$ = 15.1, 4.2 Hz, 1H), 0.95 (dd, $J$ = 15.1, 10.4 Hz, 1H), 0.81 (s, 9H), -0.05 (s, 3H), -0.20 (s, 3H). **$^{13}$C NMR** (126 MHz, $CDCl_3$) δ 172.8, 144.7, 140.3, 139.2, 136.0, 135.3, 134.8, 130.3, 129.7, 129.5, 129.1, 128.8, 128.7, 128.3, 128.3, 128.2, 128.1, 42.6, 26.4, 21.7, 16.5, 11.5, -4.7, -5.9. **IR** (neat): 2951, 2857, 1711, 1596, 1446, 1361, 1283, 1172 $cm^{-1}$.

**3-((dimethyl(phenyl)silyl)methyl)-5-phenyl-1-tosyl-1,3-dihydro-2*H*-benzo[*b*]azepin-2-one (3aa):** Column chromatography 5-10% EA/H; White solid; Yield: 63% (33.9 mg); **M.P.**: 186-188 °C. **$^1$H NMR** (500 MHz, $CDCl_3$) δ 7.66 (d, $J$ = 8.0 Hz, 2H), 7.61 (d, $J$ = 8.1 Hz, 1H), 7.47 – 7.41 (m, 1H), 7.39 – 7.36 (m, 2H), 7.36 – 7.26 (m, 7H), 7.24 – 7.18 (m, 1H), 7.11 – 7.05 (m, 2H), 7.01 (d, $J$ = 8.1 Hz, 2H), 5.42 (d, $J$ = 6.2 Hz, 1H), 2.81 – 2.73 (m, 1H), 2.27 (s, 3H), 1.31 (dd, $J$ = 15.1, 4.5 Hz, 1H), 1.22 (dd, $J$ = 15.1, 10.2 Hz, 1H), 0.25 (s, 3H), 0.23 (s, 3H). **$^{13}$C NMR** (126 MHz, $CDCl_3$) δ 172.7, 144.7, 140.3, 139.1, 138.3, 136.0, 135.2, 134.7, 133.6, 129.8, 129.7, 129.5, 129.2, 129.1, 128.8, 128.5, 128.2 (2C), 128.1, 128.0 (2C), 42.5, 21.7, 15.3, -1.8, -2.9. **IR** (neat): 2954, 2873, 1718, 1597, 1445, 1352, 1237, 1172 $cm^{-1}$.

**3-((methyldiphenylsilyl)methyl)-5-phenyl-1-tosyl-1,3-dihydro-2*H*-benzo[*b*]azepin-2-one (3ab):** Column chromatography 5-10% EA/H; White solid; Yield: 61% (36.6 mg); **M.P.**: 202-204 °C. **$^1$H NMR** (500 MHz, $CDCl_3$) δ 7.66 (d, $J$ = 8.0 Hz, 2H), 7.60 – 7.56 (m, 1H), 7.45 – 7.38 (m, 5H), 7.37 – 7.32 (m, 3H), 7.31 – 7.24 (m, 7H), 7.22 – 7.18 (m, 1H), 7.02 (d, $J$ = 8.1 Hz, 2H), 6.93 – 6.88 (m, 2H), 5.41 (d, $J$ = 6.1 Hz, 1H), 2.88 – 2.80 (m, 1H), 2.28 (s, 3H), 1.61 – 1.53 (m, 2H), 0.49 (s, 3H). **$^{13}$C NMR** (126 MHz, $CDCl_3$) δ 172.7, 144.7, 140.3, 139.0, 136.5, 136.0, 135.8, 135.2, 134.7 (2C), 134.5, 129.6 (2C), 129.5 (2C), 129.4, 129.1, 128.8, 128.4, 128.2, 128.1 (2C), 128.0 (2C), 42.5, 21.7, 13.7, -3.4. **IR** (neat): 2949, 2921, 1720, 1596, 1484, 1357, 1173, 1158 $cm^{-1}$.

**3-((*tert*-butyldiphenylsilyl)methyl)-5-phenyl-1-tosyl-1,3-dihydro-2*H*-benzo[*b*]azepin-2-one (3ac):** Column chromatography 5-10% EA/H; White solid; Yield: 39% (25.1 mg); **M.P.**: 183-185 °C. **$^1$H NMR** (500 MHz, $CDCl_3$) δ 7.69 – 7.64 (m, 2H), 7.57 – 7.49 (m, 3H), 7.48 – 7.41 (m, 1H), 7.42 – 7.32 (m, 5H), 7.32 – 7.24 (m, 2H), 7.26 – 7.19 (m, 3H), 7.18 – 7.11 (m, 2H), 7.09 – 7.02 (m, 3H), 6.74 – 6.69 (m, 2H), 5.41 (d, $J$ = 6.2 Hz, 1H), 2.72 – 2.64 (m, 1H), 2.31 (s, 3H), 1.71 (dd, $J$ = 15.4, 3.2 Hz, 1H), 1.62 (dd, *J* = 15.4, 11.1 Hz, 1H), 1.04 (s, 9H). **$^{13}$C NMR** (126 MHz, $CDCl_3$) δ 173.1, 144.7, 140.0, 139.0, 136.4, 136.0, 135.9, 135.0, 134.7, 134.5, 133.3, 129.8, 129.6, 129.3 (2C), 129.2, 129.1, 128.7, 128.3, 128.2, 128.0, 127.8, 127.7, 42.8, 27.7, 21.7, 18.0, 9.3. **IR** (neat): 2928, 2855, 1715, 1596, 1487, 1356, 1173, 1149 cm$^{-1}$. **HRMS** (ESI +ve) m/z: [M+Na]$^+$ Calcd for $C_{40}H_{39}NO_3SSiNa$ 664.2318; found 664.2332.

**5-phenyl-1-tosyl-3-((triphenylsilyl)methyl)-1,3-dihydro-2*H*-benzo[*b*]azepin-2-one (3ad):** Column chromatography 5-10% EA/H; White solid; Yield: 44% (29.2 mg); **M.P.**:241-244 °C. **$^1$H NMR** (500 MHz, $CDCl_3$) δ 7.64 (d, *J* = 8.3 Hz, 2H), 7.54 – 7.49 (m, 1H), 7.40 – 7.31 (m, 12H), 7.25 – 7.22 (m, 6H), 7.22 – 7.15 (m, 3H), 7.01 (d, *J* = 8.0 Hz, 2H), 6.67 – 6.62 (m, 2H), 5.43 (d, *J* = 6.3 Hz, 1H), 2.94 – 2.86 (m, 1H), 2.26 (s, 3H), 1.92 – 1.79 (m, 2H). **$^{13}$C NMR** (126 MHz, $CDCl_3$) δ 172.9, 144.7, 140.4, 138.9, 136.0, 135.7, 135.2, 134.8, 134.0, 129.7, 129.6, 129.5 (2C), 129.1, 128.8, 128.4, 128.2 (2C), 128.1 (2C), 127.9, 42.6, 21.7, 12.5. **IR**(neat): 2923, 2852, 1710, 1596, 1428, 1367, 1173, 1106 cm$^{-1}$. **HRMS** (ESI +ve) m/z: [M+Na]$^+$ Calcd for $C_{42}H_{35}NO_3SSiNa$ 684.2004; found 684.2017.

**3-((diphenylsilyl)methyl)-5-phenyl-1-tosyl-1,3-dihydro-2*H*-benzo[*b*]azepin-2-one (3ae):** Column chromatography 5-10% EA/H; White solid; Yield: 46% (27.0 mg); **M.P.**: 62-64 °C. **$^1$H NMR** (500 MHz, $CDCl_3$) δ 7.69 – 7.65 (m, 2H), 7.59 – 7.56 (m, 1H), 7.52 – 7.49 (m, 2H), 7.44 – 7.38 (m, 4H), 7.36 – 7.24 (m, 9H), 7.21 – 7.18 (m, 1H), 7.05 – 6.98 (m, 4H), 5.50 (d, *J* = 6.2 Hz, 1H), 4.88 (t, *J* = 3.7 Hz, 1H), 2.92 – 2.85 (m, 1H), 2.28 (s, 3H), 1.67 – 1.62 (m, 2H). **$^{13}$C NMR** (126 MHz, $CDCl_3$) δ 172.5, 144.8, 140.7, 139.0, 135.9, 135.4, 135.2, 135.1, 134.6, 134.2 (2C), 133.3, 130.0, 129.9, 129.7, 129.5, 129.2, 129.1 (2C), 128.8 (2C), 128.5, 128.3 (3C), 128.2 (3C), 128.1 (4C), 128.0, 42.7, 21.7, 11.9. **IR** (neat): 2922, 2852, 1714, 1596, 1445, 1358, 1281, 1156 cm$^{-1}$**.** **HRMS** (ESI +ve) m/z: [M+Na]$^+$ Calcd for $C_{36}H_{31}NO_3SSiNa$ 608.1692; found 608.1701.

**3-((1,1,1,3,3,3-hexamethyl-2-(trimethylsilyl)trisilan-2-yl)methyl)-5-phenyl-1-tosyl-1,3-dihydro-2*H*-benzo[*b*]azepin-2-one (3af):** Column chromatography 3-5% EA/H; White solid; Yield: 91% (59.2 mg); **M.P.**: 178-180 °C. **$^1$H NMR** (500 MHz, $CDCl_3$) δ 7.72 – 7.64 (m, 3H), 7.50 – 7.43 (m, 1H), 7.42 – 7.33 (m, 6H), 7.30 – 7.25 (m, 1H), 7.02 – 6.97 (m, 2H), 5.64 (d, $J$ = 6.3 Hz, 1H), 2.89 – 2.82 (m, 1H), 2.27 (s, 3H), 1.66 (dd, $J$ = 15.0, 4.8 Hz, 1H), 1.02 (dd, $J$ = 15.0, 7.8 Hz, 1H), 0.03 (s, 27H). **$^{13}$C NMR** (126 MHz, $CDCl_3$) δ 172.3, 144.8, 140.6, 138.7, 135.8, 135.4, 135.0, 130.7, 129.8, 129.6, 129.1, 128.8, 128.7, 128.3, 128.1 (2C), 45.8, 21.7, 6.7, 1.1. **IR** (neat): 2950, 2895, 1719, 1596, 1445, 1365, 1244, 1173 $cm^{-1}$.

**3-(((4-(dimethylsilyl)phenyl)dimethylsilyl)methyl)-5-phenyl-1-tosyl-1,3-dihydro-2*H*-benzo[*b*]azepin-2-one (3ag):** Column chromatography 5-10% EA/H; White solid; Yield: 70% (41.9 mg); **M.P.**: 166-168 °C. **$^1$H NMR** (500 MHz, $CDCl_3$) δ 7.66 (d, $J$ = 8.5 Hz, 2H), 7.62 – 7.57 (m, 1H), 7.47 – 7.40 (m, 3H), 7.39 – 7.32 (m, 3H), 7.35 – 7.29 (m, 3H), 7.23 – 7.18 (m, 1H), 7.12 – 7.04 (m, 2H), 7.01 (d, $J$ = 8.1 Hz, 2H), 5.41 (d, $J$ = 6.2 Hz, 1H), 4.41 (hept, $J$ = 3.7 Hz, 1H), 2.79 – 2.71 (m, 1H), 2.27 (s, 3H), 1.30 (dd, $J$ = 15.0, 4.5 Hz, 1H), 1.21 (dd, $J$ = 15.0, 10.2 Hz, 1H), 0.33 (d, $J$ = 3.7 Hz, 6H), 0.25 (s, 3H), 0.23 (s, 3H). **$^{13}$C NMR** (126 MHz, $CDCl_3$) δ 172.7, 144.7, 140.2, 139.3, 139.0, 138.5, 136.0, 135.3, 134.7, 133.5, 133.0, 129.8, 129.7, 129.4, 129.1, 128.8, 128.5, 128.2, 128.1, 128.0, 42.6, 21.7, 15.2, -1.9, -3.0, -3.7, -3.7. **IR** (neat): 2954, 2897, 2128, 1714, 1696, 1443, 1352, 1248, 1172 $cm^{-1}$. **HRMS** (ESI +ve) m/z: $[M+Na]^+$ Calcd for $C_{34}H_{37}NO_3SSi_2Na$ 618.1931; found 618.1935.

**5-(4-((((*R*)-2,5,7,8-tetramethyl-2-((4*R*,8*R*)-4,8,12-trimethyltridecyl)chroman-6-yl)oxy)methyl)phenyl)-1-tosyl-3-((triethylsilyl)methyl)-1,3-dihydro-2*H*-benzo[*b*]azepin-2-one (3ah):** Column chromatography 5-10% EA/H; Clear oil; Yield: 52% (50.0 mg). **$^1$H NMR** (500 MHz, $CDCl_3$) δ 7.74 – 7.68 (m, 3H), 7.54 (d, $J$ = 7.9 Hz, 2H), 7.53 – 7.46 (m, 1H), 7.41 – 7.34 (m, 3H), 7.31 – 7.25 (m, 1H), 7.07 (d, $J$ = 8.1 Hz, 2H), 5.61 (d, $J$ = 6.0 Hz, 1H), 4.75 (s, 2H), 2.87 – 2.79

(m, 1H), 2.62 (t, $J$ = 6.8 Hz, 2H), 2.30 (s, 3H), 2.26 (s, 3H), 2.22 (s, 3H), 2.13 (s, 3H), 1.90 – 1.74 (m, 2H), 1.63 – 1.28 (m, 15H), 1.24 – 1.04 (m, 10H), 0.99 (dd, $J$ = 15.1, 10.5 Hz, 1H), 0.90 – 0.82 (m, 21H), 0.46 (q, $J$ = 7.9 Hz, 6H). **$^{13}$C NMR** (126 MHz, $CDCl_3$) δ 172.9, 148.1, 144.8, 140.2, 138.8, 138.2, 136.0, 135.3, 134.8, 130.2, 129.7, 129.5, 129.1, 128.8, 128.4, 128.3, 128.1, 127.9, 126.0, 123.1, 117.8, 75.0, 74.4, 42.3, 40.2, 39.5, 37.6 (2C), 37.5, 37.4, 32.9, 32.8, 32.0, 31.4, 29.8, 29.5, 28.1, 24.9, 24.5, 24.0, 22.8 (2C), 22.7, 21.7, 21.1, 20.8, 19.9, 19.8, 14.2, 13.0, 12.1, 11.9, 11.0, 7.3, 3.7. **IR** (neat): 2950, 2871, 1718, 1597, 1458, 1410, 1358, 1255, 1173 cm$^{-1}$. **HRMS** (ESI +ve) m/z: $[M+H]^+$ Calcd for $C_{60}H_{86}NO_5SSi$ 960.5996; found 960.6026.

**4-(2-oxo-1-tosyl-3-((triethylsilyl)methyl)-2,3-dihydro-1*H*-benzo[*b*]azepin-5-yl)benzyl 2-(3-cyano-4-isobutoxyphenyl)-4-methylthiazole-5-carboxylate (3ai):** Column chromatography 15-20% EA/H; yellowish solid; Yield: 58% (48.3 mg); **M.P.**: 76-78 °C. **$^1$H NMR** (500 MHz, $CDCl_3$) δ 8.20 – 8.16 (m, 1H), 8.10 (dd, $J$ = 8.9, 2.4 Hz, 1H), 7.72 – 7.66 (m, 3H), 7.52 – 7.43 (m, 3H), 7.39 – 7.34 (m, 3H), 7.28 – 7.23 (m, 1H), 7.05 (d, $J$ = 8.1 Hz, 2H), 7.01 (d, $J$ = 8.9 Hz, 1H), 5.61 (d, $J$ = 6.1 Hz, 1H), 5.39 (s, 2H), 3.90 (d, $J$ = 6.5 Hz, 2H), 2.84 – 2.81 (m, 1H), 2.80 (s, 3H), 2.28 (s, 3H), 2.24 – 2.15 (m, 1H), 1.14 (dd, $J$ = 15.1, 4.2 Hz, 1H), 1.09 (d, $J$ = 6.7 Hz, 6H), 0.97 (dd, $J$ = 15.1, 10.4 Hz, 1H), 0.84 (t, $J$ = 7.9 Hz, 9H), 0.44 (q, $J$ = 7.9 Hz, 6H). **$^{13}$C NMR** (126 MHz, $CDCl_3$) δ 172.9, 167.7, 162.7, 161.9 (2C), 144.8, 139.9, 139.4, 136.0, 135.7, 135.1, 134.8, 132.7, 132.3, 130.7, 129.8, 129.6, 129.4, 129.1, 128.8, 128.5, 128.4 (2C), 128.2, 127.4, 126.0, 121.4, 115.4, 112.7, 103.1, 75.8, 66.6, 42.4, 28.3, 21.7, 19.1, 17.7, 11.0, 7.3, 3.7. **IR** (neat): 2951, 2873, 2227, 1711, 1604, 1432, 1369, 1256, 1162 cm$^{-1}$. **HRMS** (ESI +ve) m/z: $[M+Na]^+$ Calcd for $C_{47}H_{51}N_3O_6S_2SiNa$ 868.2886; found 868.2914.

### 4.10.5 General procedure for Germylation of 1,7-dienes

To an oven-dried 10 mL Schlenk tube equipped with a magnetic stir bar 1,7-diene **1** (0.1 mmol), hydrogermane **4** (0.3 mmol, 3 equiv.), 1 mol%

4DPAIPN (0.8 mg, 0.001 mmol), and 2.0 equivalents of hydrogen atom transfer reagent (HATR) (0.2 mmol, 78.5 mg)were added. The reaction tube was sealed and placed under an argon atmosphere, then 1 mL of acetonitrile was added *via* syringe. The reaction mixture was then degassed *via* freeze-pump-thaw (three times) and refilled with argon. The sealed reaction tube was then placed in a blue LEDs Kessil lamp (λ = 456 nm) and irradiated for 30 minutes. After the completion of the reaction, the mixture was transferred to an RB flask and evaporated under reduced pressure. The crude product was purified by column chromatography on silica gel (mesh 100-200) using gradient eluent hexane/ethyl acetate (50:1 to 5:1) to give the germylated benzazepine product **5**.

**Characterization data of 5a-5l**

**5-phenyl-1-tosyl-3-((triethylgermyl)methyl)-1,3-dihydro-2*H*-benzo[*b*]azepin-2-one (5a):** Column chromatography 3-5% EA/H; White solid; Yield: 84% (47.3 mg); **M.P.**: 117-119 °C. **$^1$H NMR** (500 MHz, $CDCl_3$) δ 7.73 – 7.66 (m, 3H), 7.51 – 7.45 (m, 1H), 7.42 – 7.32 (m, 6H), 7.27 – 7.24 (m, 1H), 7.03 (d, *J* = 8.1 Hz, 2H), 5.57 (d, *J* = 6.2 Hz, 1H), 2.88 – 2.80 (m, 1H), 2.28 (s, 3H), 1.26 (dd, *J* = 14.0, 4.8 Hz, 1H), 1.12 (dd, *J* = 14.0, 10.1 Hz, 1H), 0.92 (t, *J* = 7.9 Hz, 9H), 0.65 (q, *J* = 7.9 Hz, 6H). **$^{13}$C NMR** (126 MHz, $CDCl_3$) δ 172.9, 144.7, 140.5, 139.2, 136.0, 135.3, 134.8, 130.2, 129.7, 129.5, 129.1, 128.8, 128.7, 128.3 (2C), 128.2, 128.1, 43.3, 21.7, 11.2, 8.9, 4.5. **IR** (neat): 2947, 2888, 1704, 1595, 1444, 1358, 1254, 117 cm$^{-1}$. **HRMS** (ESI +ve) m/z: $[M+Na]^+$ Calcd for $C_{30}H_{35}NO_3SGeNa$ 586.1453; found 586.1465.

**5-(*p*-tolyl)-1-tosyl-3-((triethylgermyl)methyl)-1,3-dihydro-2*H*-benzo[*b*]azepin-2-one (5b):** Column chromatography 3-5% EA/H; White solid; Yield: 77% (44.4 mg); **M.P.**: 154-156 °C. **$^1$H NMR** (500 MHz, $CDCl_3$) δ 7.71 – 7.66 (m, 3H), 7.49 – 7.43 (m, 1H), 7.37 – 7.32 (m, 1H), 7.25 – 7.18 (m, 5H), 7.04 (d, *J* = 8.1 Hz, 2H), 5.53 (d, *J* = 6.1 Hz, 1H), 2.86 – 2.78 (m, 1H), 2.41 (s, 3H), 2.29 (s, 3H), 1.24 (dd, *J* = 14.1, 4.7 Hz, 1H), 1.11 (dd, *J* = 14.1, 10.1 Hz, 1H), 0.92 (t, *J* = 7.9 Hz, 9H), 0.65 (q, $J$ = 7.9 Hz, 6H). $^{13}$**C NMR** (126 MHz, $CDCl_3$) δ 173.0, 144.7, 140.4, 138.2, 136.4, 136.0, 135.5, 134.7, 129.7, 129.4 (2C), 129.1, 128.8, 128.1, 128.0, 43.2, 21.7, 21.3, 11.2, 8.9, 4.5. **IR** (neat): 2925, 2869, 1715, 1596, 1447, 1355, 1284, 1172 cm$^{-1}$. **HRMS** (ESI +ve) m/z: [M+Na]$^+$ Calcd for $C_{31}H_{37}NO_3SGeNa$ 600.1609, found 600.1620.

**4-(2-oxo-1-tosyl-3-((triethylgermyl)methyl)-2,3-dihydro-1*H*-benzo[*b*]azepin-5-yl)benzonitrile (5c):** Column chromatography 15-20% EA/H; White solid; Yield: 57% (33.5 mg); **M.P.**: 146-148 °C. $^{1}$**H NMR** (500 MHz, $CDCl_3$) δ 7.73 – 7.66 (m, 5H), 7.55 – 7.48 (m, 1H), 7.47 – 7.42 (m, 2H), 7.42 – 7.36 (m, 1H), 7.17 (dd, $J$ = 7.8, 1.6 Hz, 1H), 7.08 (d, $J$ = 8.1 Hz, 2H), 5.71 (d, $J$ = 6.2 Hz, 1H), 2.90 – 2.82 (m, 1H), 2.32 (s, 3H), 1.28 (dd, $J$ = 14.1, 5.1 Hz, 1H), 1.12 (dd, $J$ = 14.1, 9.7 Hz, 1H), 0.92 (t, $J$ = 7.9 Hz, 9H), 0.64 (q, $J$ = 7.9 Hz, 6H). $^{13}$**C NMR** (126 MHz, $CDCl_3$) δ 172.5, 145.1, 143.6, 139.0, 135.9, 134.9, 134.2, 133.2, 132.6, 129.6, 129.3, 129.2, 128.9, 128.8, 128.7, 128.4, 118.7, 112.0, 43.6, 21.7, 11.2, 8.9, 4.5. **IR** (neat): 2929, 2870, 2228, 1720, 1598, 1446, 1357, 1285, 1171 cm$^{-1}$. **HRMS** (ESI +ve) m/z: [M+Na]$^+$ Calcd for $C_{31}H_{34}N_2O_3SGeNa$: 611.1406; found 611.1415.

**5-(3-chlorophenyl)-1-tosyl-3-((triethylgermyl)methyl)-1,3-dihydro-2*H*-benzo[*b*]azepin-2-one (5d):** Column chromatography 3-5% EA/H; White solid; Yield: 63% (37.6 mg); **M.P.**: 132-134 °C. $^{1}$**H NMR** (500 MHz, $CDCl_3$) δ 7.70 (d, $J$ = 8.3 Hz, 3H), 7.53 – 7.46 (m, 1H), 7.42 – 7.27 (m, 4H), 7.24 – 7.18 (m, 2H), 7.08 (d, $J$ = 8.1 Hz, 2H), 5.59 (d, $J$ = 6.2 Hz, 1H), 2.87 – 2.79 (m, 1H), 2.30 (s, 3H), 1.28 (dd, $J$ = 14.1, 5.2 Hz, 1H), 1.12 (dd, $J$ = 14.1, 9.8 Hz, 1H), 0.92 (t, $J$ = 7.9 Hz, 9H), 0.65 (q, $J$ = 7.9 Hz, 6H). $^{13}$**C NMR** (126 MHz, $CDCl_3$) δ 172.6, 144.9, 141.0, 139.2, 135.8, 134.7, 134.7, 131.5, 130.0, 129.6, 129.5, 129.1, 128.8, 128.6, 128.3 (2C), 128.2, 126.4, 43.4, 21.7, 11.2, 8.9, 4.5. **IR** (neat): 2946, 2868, 1714, 1593, 1444, 1355, 1242, 1176 cm$^{-1}$. **HRMS** (ESI +ve) m/z: [M+Na]$^+$ Calcd for $C_{30}H_{34}ClNO_3SGeNa$ 620.1059; found 620.1072.

**6-methyl-5-phenyl-1-tosyl-3-((triethylgermyl)methyl)-1,3-dihydro-2*H*-benzo[*b*]azepin-2-one (5e):** Column chromatography 3-5% EA/H; White solid; Yield: 96% (55.4 mg); **M.P.**: 159-161 °C. **$^{1}$H NMR**(500 MHz, $CDCl_3$) δ 7.67 (d, $J$ = 8.1 Hz, 2H), 7.53 (d, $J$ = 8.0 Hz, 1H), 7.42 – 7.31 (m, 4H), 7.28 – 7.25 (m, 2H), 7.25 – 7.21 (m, 1H), 6.95 (d, $J$ = 8.1 Hz, 2H), 5.67 (d, $J$ = 6.9 Hz, 1H), 2.95 – 2.87 (m, 1H), 2.27 (s, 3H), 1.89 (s, 3H), 1.17 (dd, $J$ = 14.2, 4.3 Hz, 1H), 1.10 (dd, $J$ = 14.2, 10.7 Hz, 1H), 0.92 (t, $J$ = 7.9 Hz, 9H), 0.65 (q, $J$ = 7.9 Hz, 6H). **$^{13}$C NMR** (126 MHz, $CDCl_3$) δ 173.8, 144.6, 140.1, 139.7, 137.8, 135.9, 135.5, 133.8, 132.3, 131.2, 129.0, 128.9, 128.1, 127.9, 126.7, 126.5, 43.5, 21.7 (2C), 10.7, 8.9, 4.5. **IR** (neat): 2949, 2869, 1706, 1596, 1459, 1358, 1266, 1171 $cm^{-1}$. **HRMS** (ESI +ve) m/z: $[M+Na]^+$ Calcd for $C_{31}H_{37}NO_3SGeNa$ 600.1609; found 600.1620.

**7-methoxy-5-phenyl-1-tosyl-3-((triethylgermyl)methyl)-1,3-dihydro-2*H*-benzo[*b*]azepin-2-one (5f):** Column chromatography 5-10% EA/H; White solid; Yield: 78% (46.2 mg); **M.P.**: 127-129 °C. **$^{1}$H NMR** (500 MHz, $CDCl_3$) δ 7.68 (d, $J$ = 8.4 Hz, 2H), 7.60 (d, $J$ = 8.9 Hz, 1H), 7.43 – 7.32 (m, 5H), 7.05 – 6.99 (m, 3H), 6.72 (d, $J$ = 3.0 Hz, 1H), 5.54 (d, $J$ = 6.2 Hz, 1H), 3.77 (s, 3H), 2.94 – 2.86 (m, 1H), 2.27 (s, 3H), 1.25 (dd, $J$ = 14.1, 4.9 Hz, 1H), 1.11 (dd, $J$ = 14.1, 10.1 Hz, 1H), 0.93 (t, $J$ = 7.9 Hz, 9H), 0.66 (q, $J$ = 7.9 Hz, 6H). **$^{13}$C NMR** (126 MHz, $CDCl_3$) δ 172.9, 158.8, 144.6, 140.4, 139.1, 136.5, 135.9, 130.7, 130.4, 129.0, 128.8, 128.7, 128.3, 128.2, 128.0, 114.3, 114.1, 55.7, 43.3, 21.7, 11.2, 8.9, 4.5. **IR** (neat): 2949, 2870, 1708, 1597, 1492, 1356, 1225, 1171 $cm^{-1}$. **HRMS** (ESI +ve) m/z: $[M+H]^+$ Calcd for $C_{31}H_{38}NO_4SGe$: 594.1739; found 594.1755.

**7-chloro-5-phenyl-1-tosyl-3-((triethylgermyl)methyl)-1,3-dihydro-2*H*-benzo[*b*]azepin-2-one (5g):** Column chromatography 3-5% EA/H; White solid; Yield: 86% (51.4 mg); **M.P.**: 142-144 °C. **$^{1}$H NMR** (500 MHz, $CDCl_3$) δ 7.68 (d, $J$ = 8.1 Hz, 2H), 7.63 (d, $J$ = 8.7 Hz, 1H), 7.47 – 7.37 (m, 4H), 7.34 – 7.28 (m, 2H), 7.23 (d, $J$ = 2.4 Hz, 1H), 7.05 (d, $J$ = 8.1 Hz, 2H), 5.60 (d, $J$ = 6.1 Hz, 1H), 2.85 – 2.77 (m, 1H), 2.29 (s, 3H), 1.26 (dd, $J$ = 14.1, 4.9 Hz, 1H), 1.11 (dd, $J$ = 14.1, 9.9 Hz, 1H), 0.94 (t, $J$ = 7.9 Hz, 9H), 0.66 (q, $J$ = 7.9 Hz, 6H). **$^{13}$C NMR** (126 MHz, $CDCl_3$) δ 172.4, 145.0, 139.7, 138.6, 136.8, 135.7, 134.0, 133.2, 131.3, 130.7, 129.3, 129.2, 128.9, 128.8, 128.6, 128.5, 128.2, 43.3, 21.7, 11.2, 8.9, 4.5. **IR** (neat): 2926, 2901, 2867, 1704, 1598, 1480, 1357, 1279, 1170 cm$^{-1}$. **HRMS** (ESI +ve) m/z: Calcd for $[M+Na]^+$ $C_{30}H_{34}ClNO_3SGeNa$ 620.1059; found 620.1071.

**5-phenyl-1-tosyl-3-((tributylgermyl)methyl)-1,3-dihydro-2*H*-benzo[*b*]azepin-2-one (5h):** Column chromatography 3-5% EA/H; White solid; Yield: 65% (42.1 mg); **M.P.**: 129-131 °C. **$^1$H NMR** (500 MHz, $CDCl_3$) δ 7.73 – 7.66 (m, 3H), 7.51 – 7.44 (m, 1H), 7.41 – 7.32 (m, 6H), 7.28 – 7.23 (m, 1H), 7.04 (d, $J$ = 8.2 Hz, 2H), 5.58 (d, $J$ = 6.2 Hz, 1H), 2.88 – 2.80 (m, 1H), 2.29 (s, 3H), 1.28 – 1.16 (m, 13H), 1.12 (dd, $J$ = 14.1, 10.5 Hz, 1H), 0.86 – 0.75 (m, 9H), 0.69 – 0.59 (m, 6H). **$^{13}$C NMR** (126 MHz, $CDCl_3$) δ 173.0, 144.7, 140.5, 139.2, 136.0, 135.4, 134.8, 130.3, 129.7, 129.4, 129.1, 128.8, 128.7, 128.3, 128.2, 128.0, 43.4, 27.4, 26.6, 21.7, 13.8, 13.1, 12.1. **IR** (neat): 2955, 2850, 1712, 1596, 1443, 1354, 1174, 1158 cm$^{-1}$. **HRMS** (ESI +ve) m/z: $[M+Na]^+$ Calcd for $C_{36}H_{47}NO_3SGeNa$ 670.2393; found 670.2408.

**5-phenyl-1-tosyl-3-((triphenylgermyl)methyl)-1,3-dihydro-2*H*-benzo[*b*]azepin-2-one (5i):** Column chromatography 5-10% EA/H; White solid; Yield: 83% (58.7 mg); **M.P.**: 239-242 °C. **$^1$H NMR** (500 MHz, $CDCl_3$) δ 7.67 (d, $J$ = 8.4 Hz, 2H), 7.53 – 7.47 (m, 1H), 7.42 – 7.37 (m, 1H), 7.37 – 7.32 (m, 10H), 7.31 – 7.25 (m, 7H), 7.24 – 7.18 (m, 3H), 7.04 (d, $J$ = 8.1 Hz, 2H), 6.75 – 6.69 (m, 2H), 5.50 (d, $J$ = 6.3 Hz, 1H), 2.98 – 2.90 (m, 1H), 2.29 (s, 3H), 2.03 – 1.94 (m, 2H). **$^{13}$C NMR** (126 MHz, $CDCl_3$) δ 172.8, 144.7, 140.7, 138.9, 136.0, 135.2, 134.9, 134.7, 129.6, 129.5 (2C), 129.2, 129.1, 128.8, 128.4 (2C), 128.2 (2C), 128.1, 127.9, 43.1, 21.7, 13.4. **IR** (neat): 2921, 2851, 1709, 1582, 1429, 1363, 1174, 1159 cm$^{-1}$. **HRMS** (ESI +ve) m/z: $[M+Na]^+$ Calcd for $C_{42}H_{35}NO_3SGeNa$ 730.1456; found 730.1483.

**3-((diphenylgermyl)methyl)-5-phenyl-1-tosyl-1,3-dihydro-2*H*-benzo[*b*]azepin-2-one (5j):** Column chromatography 5-10% EA/H;

White solid; Yield: 30% (19.1 mg); **M.P.**: 181-183 °C. **$^1$H NMR** (500 MHz, $CDCl_3$) δ 7.71 – 7.65 (m, 2H), 7.56 – 7.51 (m, 1H), 7.46 – 7.39 (m, 3H), 7.42 – 7.34 (m, 3H), 7.37 – 7.25 (m, 9H), 7.22 – 7.17 (m, 1H), 7.06 – 6.99 (m, 4H), 5.52 (d, *J* = 6.1 Hz, 1H), 5.07 (t, *J* = 3.1 Hz, 1H), 2.95 – 2.87 (m, 1H), 2.29 (s, 3H), 1.85 – 1.72 (m, 2H). **$^{13}$C NMR** (126 MHz, $CDCl_3$) δ 172.5, 144.8, 140.8, 139.0, 135.9, 135.8, 135.5, 135.1, 135.0, 134.6, 129.7, 129.5, 129.2 (2C), 129.1 (2C), 128.8, 128.5, 128.4, 128.3, 128.2, 128.1, 128.0, 43.6, 21.7, 12.9. **IR** (neat): 2922, 2863, 2062, 1704, 1596, 1433, 1360, 1164, 1133 cm$^{-1}$. **HRMS** (ESI +ve) m/z: $[M+Na]^+$ Calcd for $C_{36}H_{31}NO_3SGeNa$ 654.1141; found 654.1146.

**4-(2-oxo-1-tosyl-3-((triethylgermyl)methyl)-2,3-dihydro-1*H*-benzo[*b*]azepin-5-yl)benzyl 2-(3-cyano-4-isobutoxyphenyl)-4-methylthiazole-5-carboxylate (5k):** Column chromatography 15-20% EA/H; White solid; Yield: 76% (67.8 mg); **M.P.**: 72-74 °C. **$^1$H NMR** (500 MHz, $CDCl_3$) δ 8.18 (d, *J* = 2.3 Hz, 1H), 8.10 (dd, *J* = 8.8, 2.3 Hz, 1H), 7.73 – 7.65 (m, 3H), 7.50 – 7.43 (m, 3H), 7.40 – 7.33 (m, 3H), 7.28 – 7.22 (m, 1H), 7.05 (d, *J* = 8.1 Hz, 2H), 7.01 (d, *J* = 8.9 Hz, 1H), 5.61 (d, *J* = 6.2 Hz, 1H), 5.39 (s, 2H), 3.90 (d, *J* = 6.5 Hz, 2H), 2.88 – 2.80 (m, 1H), 2.80 (s, 3H), 2.28 (s, 3H), 2.20 (hept, *J* = 6.7 Hz, 1H), 1.16 – 1.11 (m, 1H), 1.09 (d, *J* = 6.7 Hz, 6H), 0.91 (t, *J* = 7.9 Hz, 9H), 0.90 – 0.83 (m, 1H), 0.65 (q, *J* = 7.9 Hz, 6H). **$^{13}$C NMR** (126 MHz, $CDCl_3$) δ 172.9, 167.7, 162.7, 161.9 (2C), 144.7, 139.9, 139.3, 136.0, 135.7, 135.2, 134.8, 132.7, 132.2, 130.7, 129.6, 129.4, 129.1, 128.8, 128.5, 128.4 (2C), 128.1, 126.0, 121.4, 115.4, 112.7, 103.1, 75.8, 66.6, 43.3, 28.2, 21.7, 19.1, 17.7, 11.2, 8.9, 4.5. **IR** (neat): 2923, 2870, 1714, 1605, 1433, 1369, 1257, 1171 cm$^{-1}$. **HRMS** (APCI +ve) m/z: $[M+H]^+$ Calcd for $C_{47}H_{52}N_3O_6S_2Ge$ 892.2520; found 892.2546.

**5-(4-((((*R*)-2,5,7,8-tetramethyl-2-((4*R*,8*R*)-4,8,12-trimethyltridecyl)chroman-6-yl)oxy)methyl)phenyl)-1-tosyl-3-((triethylgermyl)methyl)-1,3-dihydro-2*H*-benzo[*b*]azepin-2-one (5l):** Column chromatography 5-10% EA/H; Clear gum-oil; Yield: 33% (33.2 mg). **$^1$H NMR** (500 MHz, $CDCl_3$) δ 7.73 – 7.68 (m, 3H), 7.56 – 7.51 (m, 2H), 7.51 – 7.46 (m, 1H), 7.40 – 7.34 (m, 3H), 7.28 – 7.26 (m, 1H), 7.07 (d, *J* = 8.1 Hz, 2H), 5.60 (d, *J* = 6.1 Hz, 1H), 4.74 (s, 2H), 2.89– 2.81 (m, 1H), 2.61 (t, *J* = 6.9 Hz, 2H), 2.30 (s, 3H), 2.25 (s, 3H), 2.21 (s, 3H), 2.12 (s, 3H), 1.88 – 1.75 (m, 2H), 1.58 – 1.30 (m, 15H), 1.22 – 1.03 (m, 10H), 0.93 (t, *J* = 7.9 Hz, 9H), 0.89 – 0.83 (m, 13H), 0.66 (q, *J* = 7.9 Hz, 6H). **$^{13}$C NMR** (126 MHz, $CDCl_3$) δ 173.0, 148.1, 144.8, 140.3, 138.8, 138.2, 136.0, 135.3, 134.8, 130.2, 129.7, 129.5, 129.1, 128.8, 128.4, 128.3, 128.1, 127.9, 126.0, 123.1, 117.8, 75.0, 74.4, 43.3, 40.2, 39.5, 37.6 (2C), 37.5, 37.4, 32.9, 32.8, 32.0, 31.4, 29.8, 28.1, 24.9, 24.6, 24.0, 22.8, 22.7, 21.7, 21.1, 20.8, 19.9, 19.8, 14.2, 13.0, 12.2, 12.0, 11.2, 8.9, 4.5. **IR** (neat): 2924, 2868, 1718, 1597, 1458, 1366, 1255, 1172 cm$^{-1}$. **HRMS** (ESI +ve) m/z: $[M+H]^+$ Calcd for $C_{60}H_{86}NO_5SGe$ 1006.5454; found 1006.5516.

### 4.10.6 Procedure for further transformation of silylated benzazepines 3a

4.10.6.1 Procedure for synthesis of the thioamide derivative of silylated benzazepine **3a**

Step I: To a 10 mL oven-dried Schlenk tube with a magnetic stir bar, **3a** (0.1 mmol, 51.7 mg), Mg (0.6 mmol, 14.6 mg) and DMF (1 mL) were added. The Schlenk tube was then sealed and placed at 0 °C, and TMSCl (0.5 mmol, 65 μL) was added dropwise. The reaction mixture was stirred at 0 °C for 11 h. After the reaction was completed, $H_2O$ was added to the reaction mixture and extracted with ethyl acetate three times (20 mL each). The combined organic layer was dried over anhydrous $Na_2SO_4$, filtered, and evaporated. The crude residue was purified by silica gel column chromatography (100-200 mesh) using ethyl acetate-hexane to afford the desired product **6a**.

Step II: To a 10 mL oven-dried Schlenk tube with a magnetic stir bar, **6a** (0.1 mmol, 36.3 mg), and Lawesson's reagent (0.05 mmol, 20.2 mg) were dissolved in toluene (0.34 mL) and placed in an oil bath at 80 °C for heating. After completion of the reaction, diluted with ethylacetate, filtered through a small pad of celite, washed with ethylacetate and evaporated. The crude residue was purified by silica gel (100-200 mesh) column chromatography using ethyl acetate-hexane to afford the desired product **6b**.

**5-phenyl-3-((triethylsilyl)methyl)-1,3-dihydro-2*H*-benzo[*b*]azepin-2-one (6a):** Column chromatography 10-15% EA/H; White solid; Yield: 92% (33.5 mg). **M.P.**: 153-155 °C **$^1$H NMR** (500 MHz, $CDCl_3$) δ 8.16 (brs, 1H), 7.37 – 7.28 (m, 4H), 7.23 – 7.18 (m, 3H), 7.15 – 7.06 (m, 2H), 5.78 (d, $J$ = 6.3 Hz, 1H), 2.71 – 2.58 (m, 1H), 1.38 – 1.31 (m, 1H), 1.13 (dd, $J$ = 15.0, 10.3 Hz, 1H), 0.94 (t, $J$ = 7.9 Hz, 9H), 0.57 (q, $J$ = 7.9 Hz, 6H). **$^{13}$C NMR** (126 MHz, $CDCl_3$) δ 175.1, 141.3, 140.4, 136.7, 131.5, 131.4, 130.9, 128.9 (2C), 128.4, 127.8, 123.8, 121.6, 39.8, 11.1, 7.5, 3.9. **IR** (neat): 3197, 2949, 2873, 1668, 1601, 1572, 1480, 1380, 1296 $cm^{-1}$.

**5-phenyl-3-((triethylsilyl)methyl)-1,3-dihydro-2*H*-benzo[*b*]azepine-2-thione (6b):** Column chromatography 5-10% EA/H; Clear oil; Yield: 51% (19.4 mg). **$^1$H NMR** (500 MHz, $CDCl_3$) δ 8.21 – 8.15 (m, 1H), 7.39 – 7.28 (m, 4H), 7.24 – 7.17 (m, 3H), 7.15 – 7.06 (m, 2H), 5.78 (d, $J$ = 6.3 Hz, 1H), 2.64 (s, 1H), 1.38 – 1.31 (m, 1H), 1.13 (dd, $J$ = 15.0, 10.4 Hz, 1H), 0.94 (t, $J$ = 7.9 Hz, 9H), 0.57 (d, $J$ = 7.9 Hz, 6H). **$^{13}$C NMR** (126 MHz, $CDCl_3$) δ 175.1, 141.3, 140.4, 136.6, 131.4 (2C), 130.9, 128.9 (2C), 128.4, 127.8, 123.9, 121.6, 39.7, 11.1, 7.5, 3.9. **IR** (neat): 3170, 2950, 2873, 1656, 1612, 1534, 1448, 1381, 1133 $cm^{-1}$. **HRMS** (ESI +ve) m/z: $[M+H]^+$ Calcd for $C_{23}H_{30}NSSi$ 380.1868; found 380.1885.

4.10.6.2 Procedure for bromination of Silylated Benzazepine **3a**

To an oven-dried 10 mL Schlenk tube with a magnetic stir bar, **3a** (0.1 mmol, 51.7 mg), NBS (0.5 mmol, 89 mg), and 1 mL of acetonitrile were added and sealed, then stirred for 36 h at room temperature. After the reaction was completed, it was quenched with sodium thiosulfate and washed with sodium bicarbonate using ethyl acetate as the organic solvent. The organic layer was collected, dried over sodium sulphate, filtered, and evaporated. Purified by silica gel column chromatography using ethyl acetate/hexane as eluent to afford the desired product **7**.

**4-bromo-5-phenyl-1-tosyl-3-((triethylsilyl)methyl)-1,3-dihydro-2*H*-benzo[*b*]azepin-2-one (7):** Column chromatography 5-10% EA/H; White solid; yield: 87% (52.0 mg). **M.P.**: 134-136 °C. **$^1$H NMR** (500 MHz, $CDCl_3$) δ 7.82 (d, *J* = 8.4 Hz, 2H), 7.72 – 7.67 (m, 1H), 7.49 – 7.44 (m, 1H), 7.44 – 7.37 (m, 3H), 7.33 – 7.28 (m, 3H), 7.19 (d, *J* = 8.1 Hz, 2H), 7.06 (dd, *J* = 7.9, 1.5 Hz, 1H), 3.26 (t, *J* = 7.1 Hz, 1H), 2.34 (s, 3H), 1.25 (dd, *J* = 15.0, 7.5 Hz, 1H), 1.07 (dd, *J* = 15.0, 6.7 Hz, 1H), 0.81 (t, *J* = 7.9 Hz, 9H), 0.43 (q, *J* = 7.9 Hz, 6H). **$^{13}$C NMR** (126 MHz, $CDCl_3$) δ 170.2, 145.0, 140.3 (2C), 136.3, 135.7, 134.3, 130.4, 130.2, 129.4, 128.9, 128.7 (2C), 128.4, 128.3, 124.3, 46.4, 21.7, 12.2, 7.3, 3.6. **IR** (neat): 2950, 2873, 1717, 1595, 1442, 1357, 1175, 1128 cm$^{-1}$. **HRMS** (ESI +ve) m/z: $[M+Na]^+$ Calcd for $C_{30}H_{34}BrNO_3SSiNa$ 620.1093; found 620.1110.

### 4.10.7 Procedure for the kinetic isotope effect experiment

To an oven-dried 10 mL Schlenk tube equipped with a magnetic stir bar 1,7-diene **1a** (18.7 mg, 0.0465 mmol), **1a-*d*** (21.7 mg, 0.0535 mmol), $Et_3SiH$ (80 μL, 0.5 mmol, 5 equiv.), 1 mol% 4DPAIPN (0.8 mg, 0.001 mmol), and 2.0 equivalent of hydrogen atom transfer reagent (HATR) (0.2 mmol, 78.5 mg) were added. The reaction tube was sealed and placed under an argon atmosphere, then 1 mL of acetonitrile was added *via* syringe. The reaction mixture was then degassed *via* freeze-pump-thaw (three times) and refilled with argon. The sealed reaction tube was placed in a blue LEDs Kessil® PR-160 lamp (λ = 456 nm) and irradiated for 30 minutes. After completion of the reaction, the mixture was transferred to a round-bottom flask and evaporated under reduced pressure. The crude product was then purified by column chromatography on silica gel (mesh 100-200) using a gradient eluent hexane/ethyl acetate (50:1 to 5:1), which provided the silylation product **3a/3a-*d***.

### 4.10.8 Stern-Volmer fluorescence quenching studies

All fluorescence quenching experiments were recorded on the HORIBA SCIENTIFIC FLUOROMAX_PLUS_C model. A $2.0\times10^{-4}$ M stock solution was prepared by dissolving 2.4 mg 4DPAIPN photocatalyst in 15 mL of spectroscopic grade acetonitrile. The quenching experiment was performed by taking an appropriate volume of 4DPAIPN photocatalyst from the stock solution, along with different concentrations of the quencher. The Emission intensity was observed at 536 nm with an excitation wavelength of 360 nm.

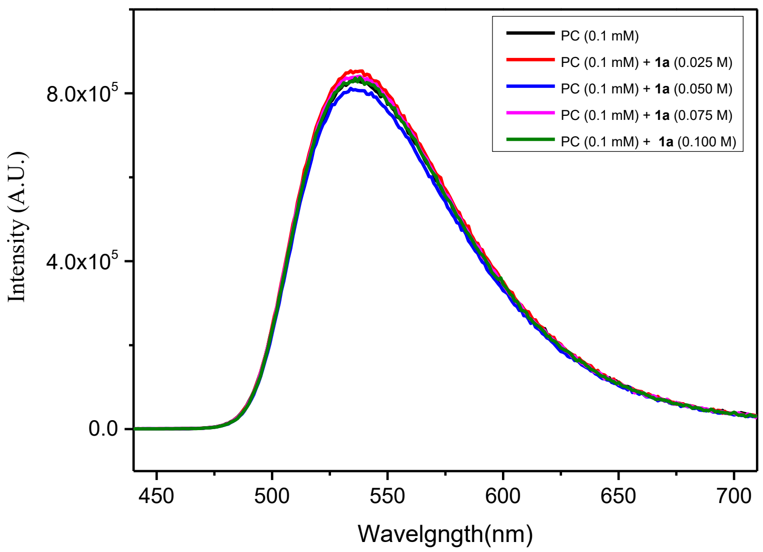

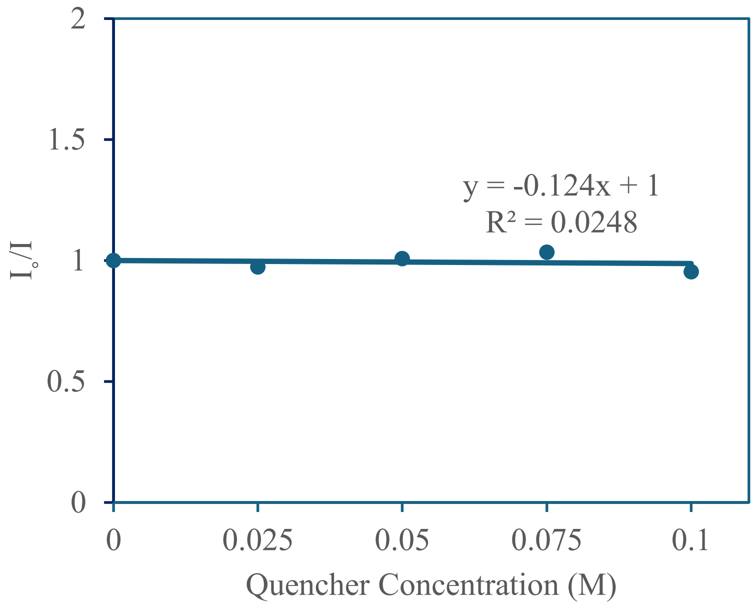


**Figure 4.4** Fluorescence quenching and Stern-Volmer plot of 4DPAIPN vs **1a**

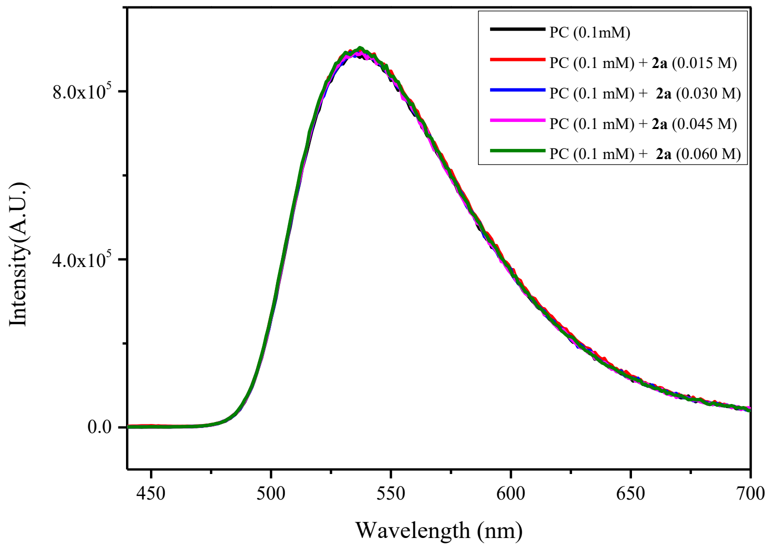

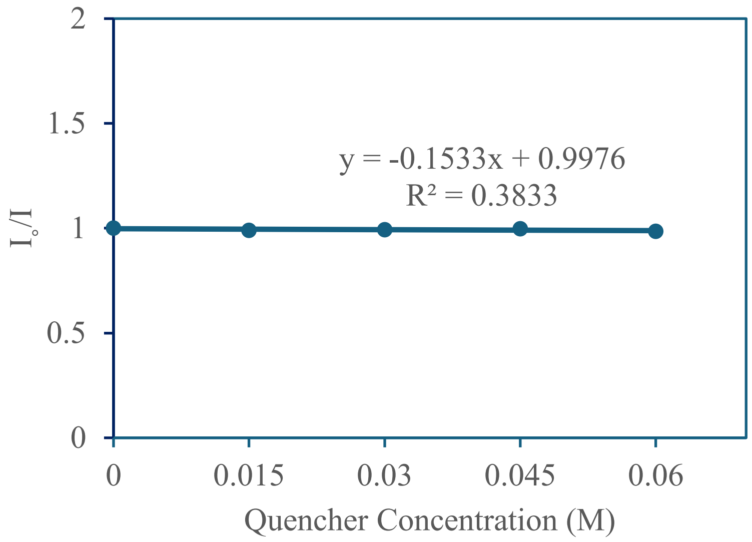


**Figure 4.5** Fluorescence quenching and Stern-Volmer plot of 4DPAIPN vs **2a**

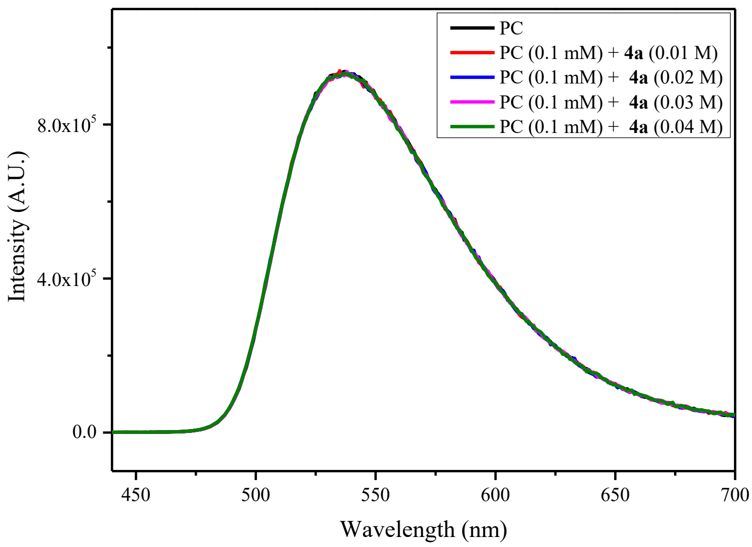

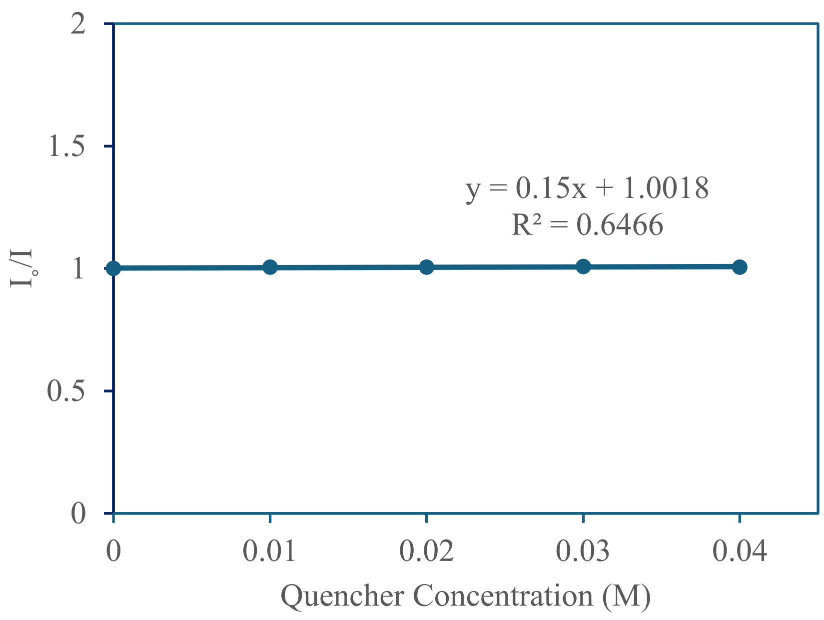


**Figure 4.6** Fluorescence quenching and Stern-Volmer plot of **4DPAIPN** vs **4a**

### 4.10.9 Quantum yield calculation[61,62]

Following the literature-reported procedure. A potassium ferrioxalate solution (0.15 M) was prepared by dissolving 2.21 g of potassium ferrioxalate trihydrate in 30 mL $H_2SO_4$ (0.05 M). A buffer solution was prepared by dissolving 50 mg of phenanthroline and 11.25 g of sodium acetate in 50 mL $H_2SO_4$ (0.5 M). Both solutions were stored in dark and wrapped with aluminium foil.

A 10 mL reaction tube was covered with black electrical tape and wrapped in aluminium foil, except for a small window at the bottom for irradiation. Then, the reaction tube was charged with 5 mL of ferrioxalate solution and irradiated for 10 seconds. This solution was treated with 0.875 mL of buffered phenanthroline solution. After irradiation, the reaction tube was completely covered with aluminium foil and stirred for 1 hour in a dark condition, allowing the ferrous ion to coordinate with phenanthroline completely. The absorbance of resulting solutions was measured on HORIBA

FLUOROMAX_PLUS_C modal at 510 nm. A non-irradiated solution was also prepared, and absorbance was measured at 510 nm.

The conversion of ferrioxalate was calculated as:

$$\text{Mole Fe}^{2+} = \frac{V \times \Delta A}{l \times \varepsilon}$$

$$= \frac{0.005875\ L \times (2.595114946 - 1.483394504)}{1\ cm \times 11100\ L\ mol^{-1} cm^{-1}}$$

$$= 5.88410594 \times 10^{-7}\ mole$$

Where $V$ is the total volume (0.005875 L) of the solution after the addition of phenanthroline solution, $\Delta A$ is the difference in absorbance between irradiated and non-irradiated solutions at 510 nm (2.595114946-1.483394504 = 1.111720442), $l$ is the path length (1.0 cm), and $\varepsilon$ is the molar absorptivity at 510 nm.

The photo-flux was calculated as:

$$\text{Photon flux} = \frac{mole\ Fe^{2+}}{\phi \times t \times f}$$

$$= \frac{5.88410594 \times 10^{-7}}{1.01 \times 10 \times 0.9985} = 5.8345993 \times 10^{-8}\ einstein\ sec^{-1}$$

Where $\phi$ is the quantum yield for the ferrioxalate actinometer (1.01 for 0.15 M solution), $t$ is the time, 10 seconds, and $f$ is the fraction of light absorbed by the ferrioxalate actinometer solution at $\lambda$ = 436 nm.

Absorbance at $\lambda$ = 436 nm by ferrioxalate actinometer is A = 2.847874.

So, the fraction of light absorbed (*f*) by the ferrioxalate actinometer at 436 nm is:

$$f = 1 - 10^{-A} = 1 - 10^{-2.847874} = 0.9985$$

**Quantum yield for silylation of 1,7-diene 1a**

The parent reaction was performed in a 10 mL reaction tube under optimal conditions at a 0.1 mmol scale for 10 minutes, and the isolated yield was 56%.

The quantum yield is determined as:

$$\phi = \frac{mole\ product}{flux \times t \times f} = \frac{0.1 \times 0.56 \times 10^{-3}}{5.8345993 \times 10^{-8} \times 600 \times 1} = 1.59$$

Where $\phi$ is the quantum yield of the reaction, *t* is the reaction time (600 seconds).

## 4.11 Selected NMR spectra

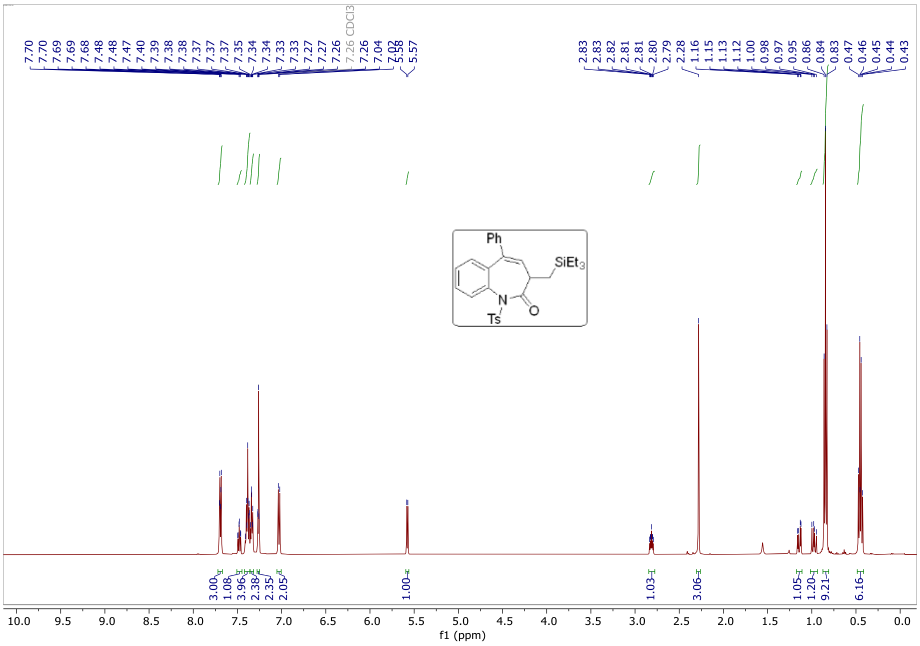

**Figure 4.11.1** $^1$H NMR spectrum of **3a** in $CDCl_3$ [500 MHz]

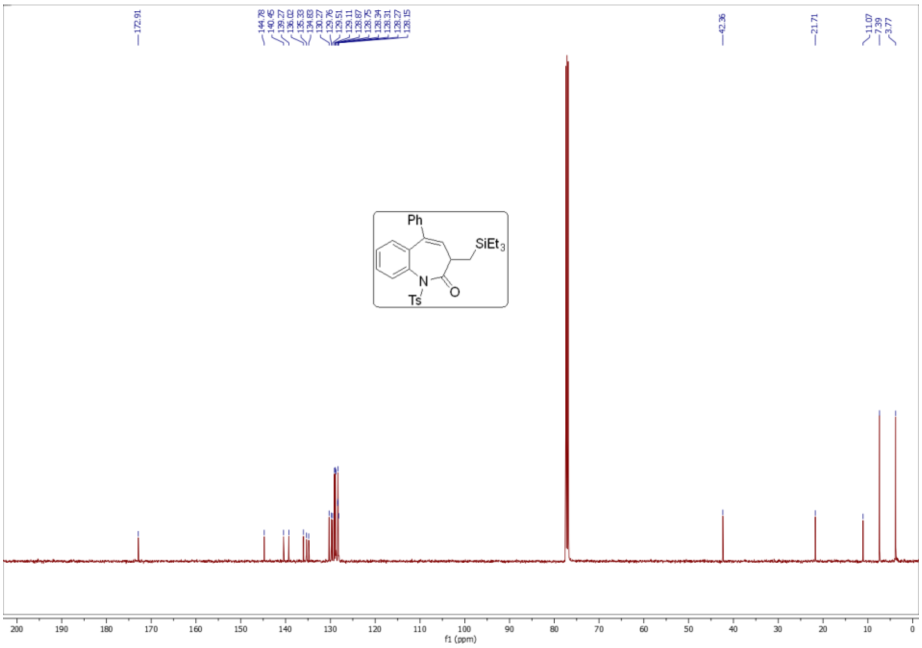

**Figure 4.11.2** $^{13}$C NMR spectrum of **3a** in $CDCl_3$ [126 MHz]

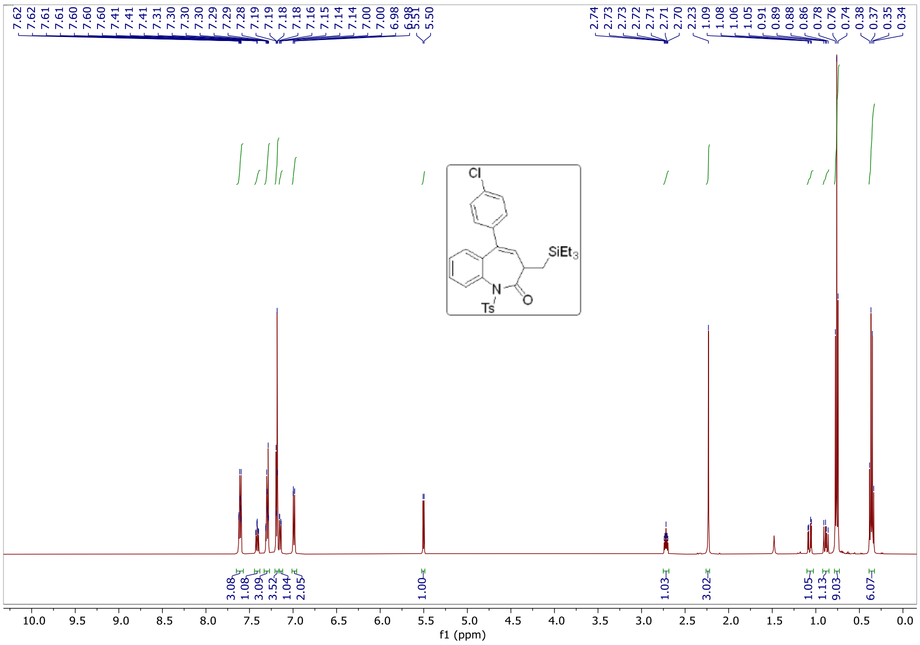

**Figure 4.11.3** $^{1}$H NMR spectrum of **3c** in $CDCl_3$ [500 MHz]

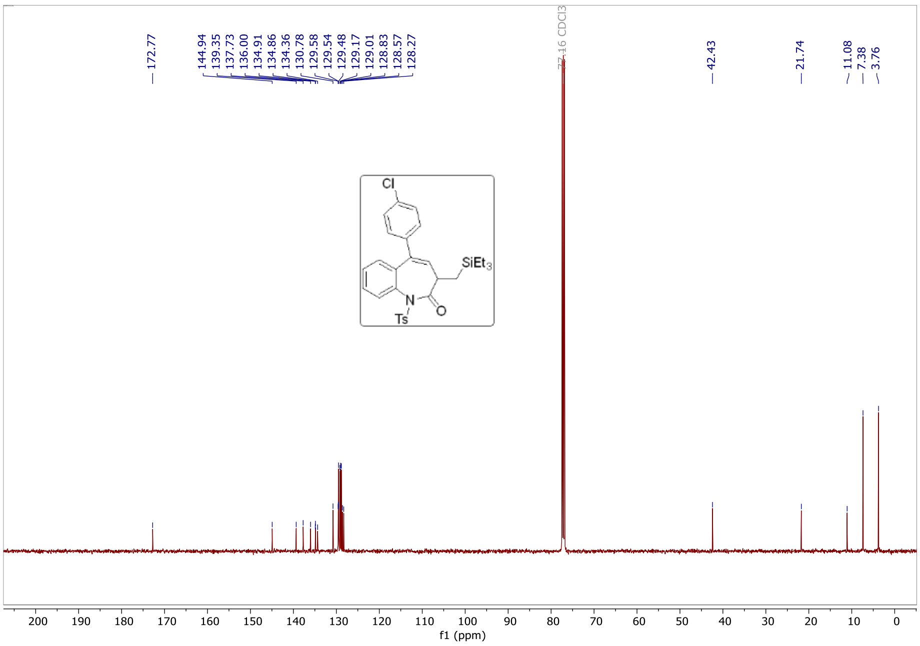

**Figure 4.11.4** $^{13}$C NMR spectrum of **3c** in $CDCl_3$ [126 MHz]

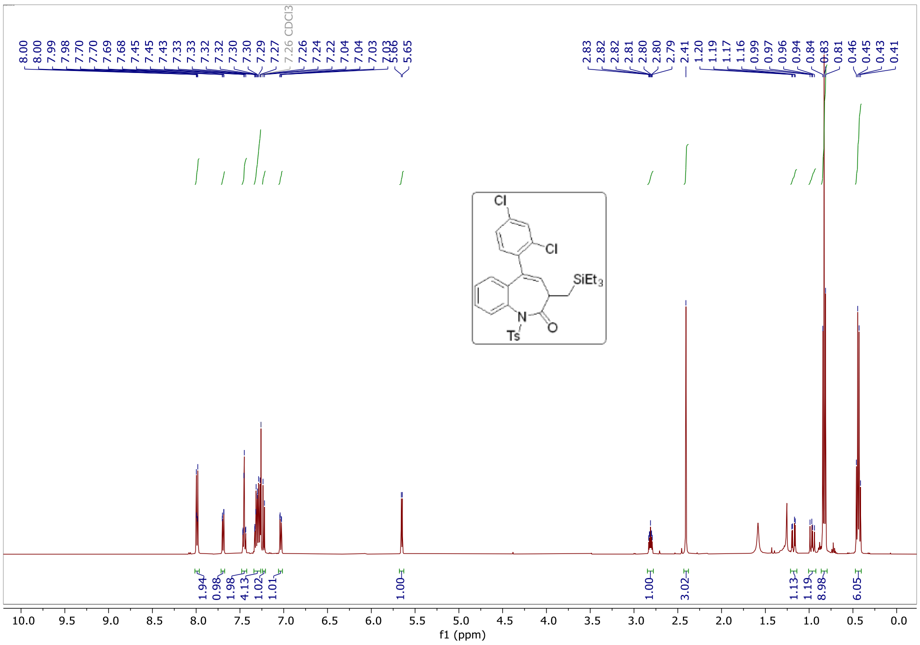

**Figure 4.11.5** $^{1}H$ NMR spectrum of **3f** in $CDCl_3$ [500 MHz]

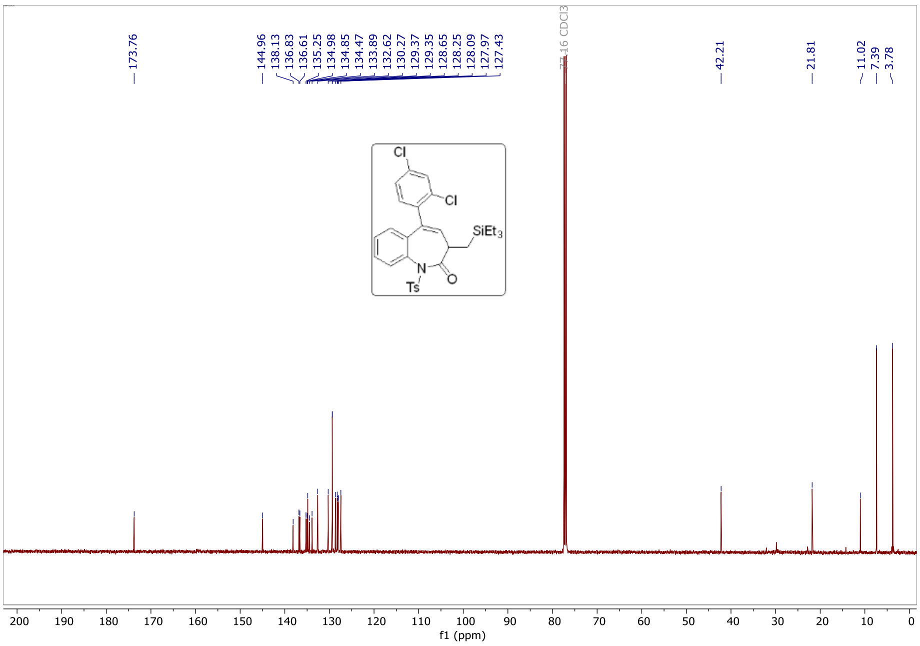

**Figure 4.11.6** $^{13}C$ NMR spectrum of **3f** in $CDCl_3$ [126 MHz]

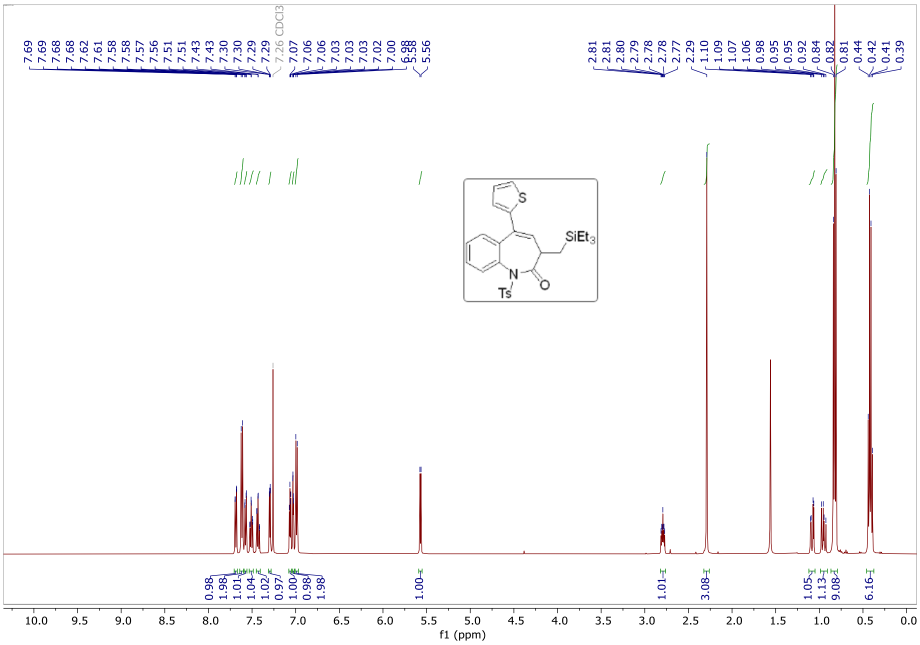

**Figure 4.11.7** $^{1}$H NMR spectrum of **3h** in $CDCl_3$ [500 MHz]

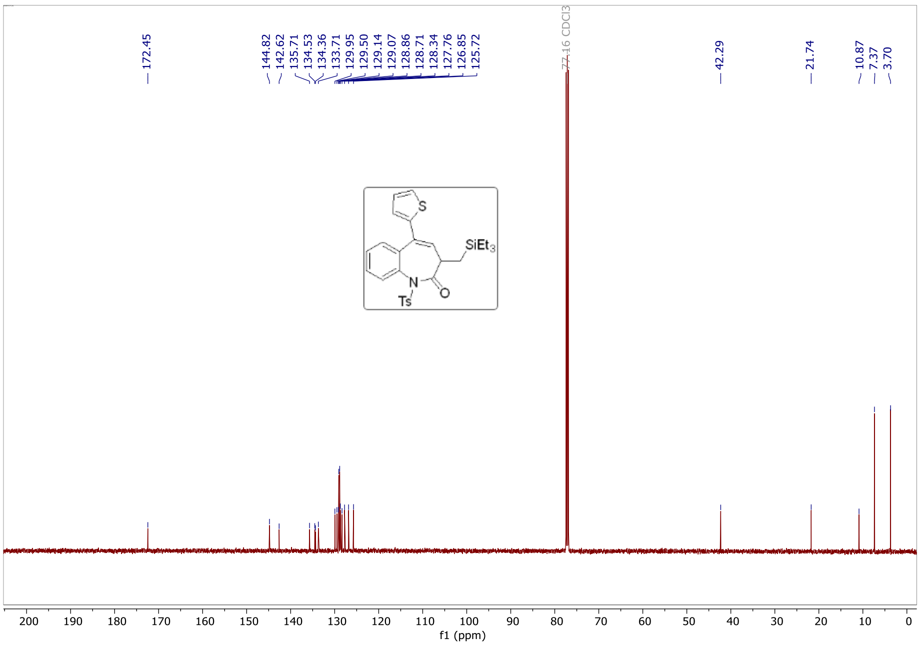

**Figure 4.11.8** $^{13}$C NMR spectrum of **3h** in $CDCl_3$ [126 MHz]

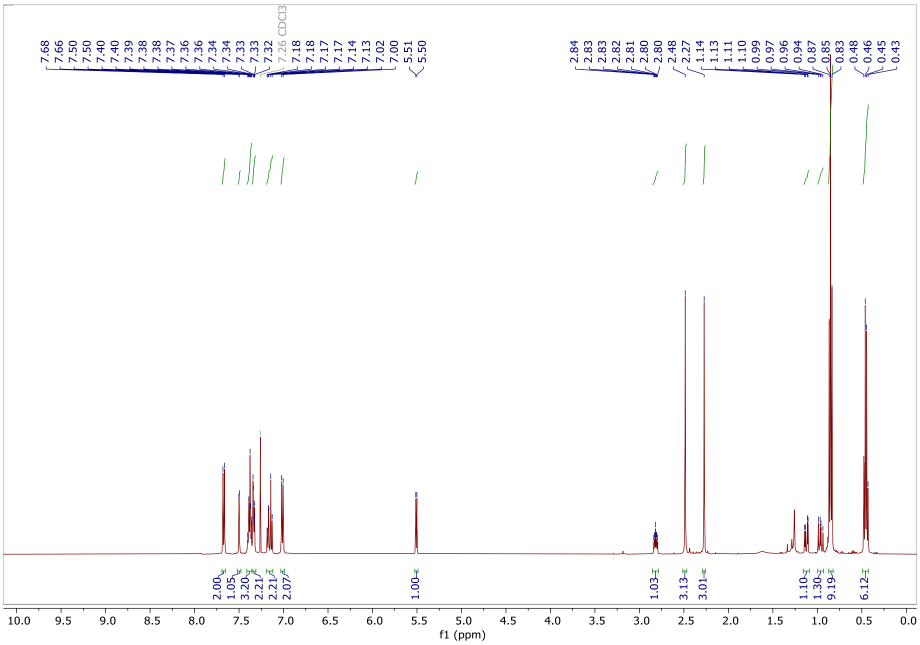

**Figure 4.11.9** $^{1}$H NMR spectrum of **3k** in $CDCl_3$ [500 MHz]

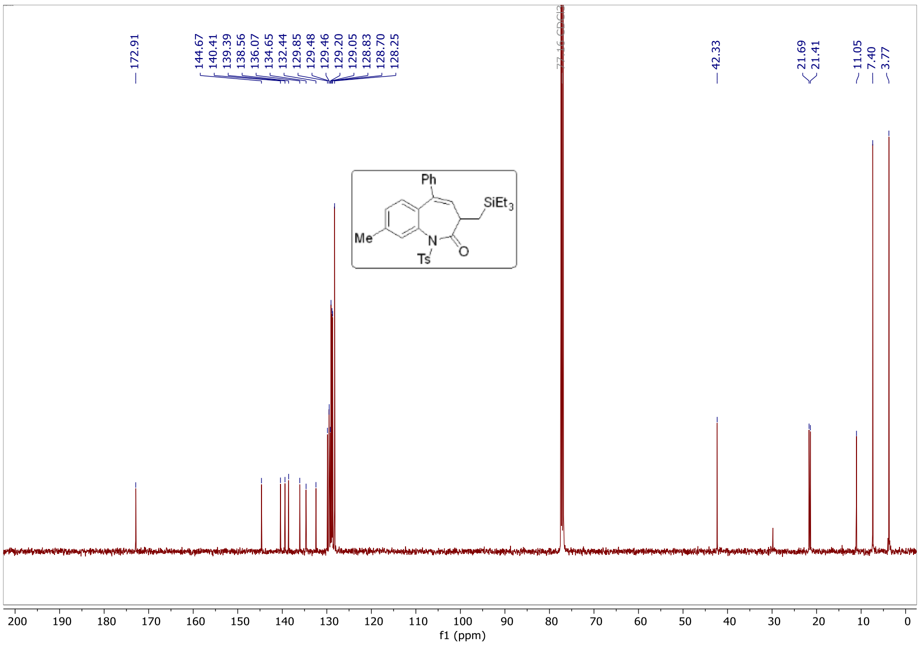

**Figure 4.11.10** $^{13}$C NMR spectrum of **3k** in $CDCl_3$ [126 MHz]

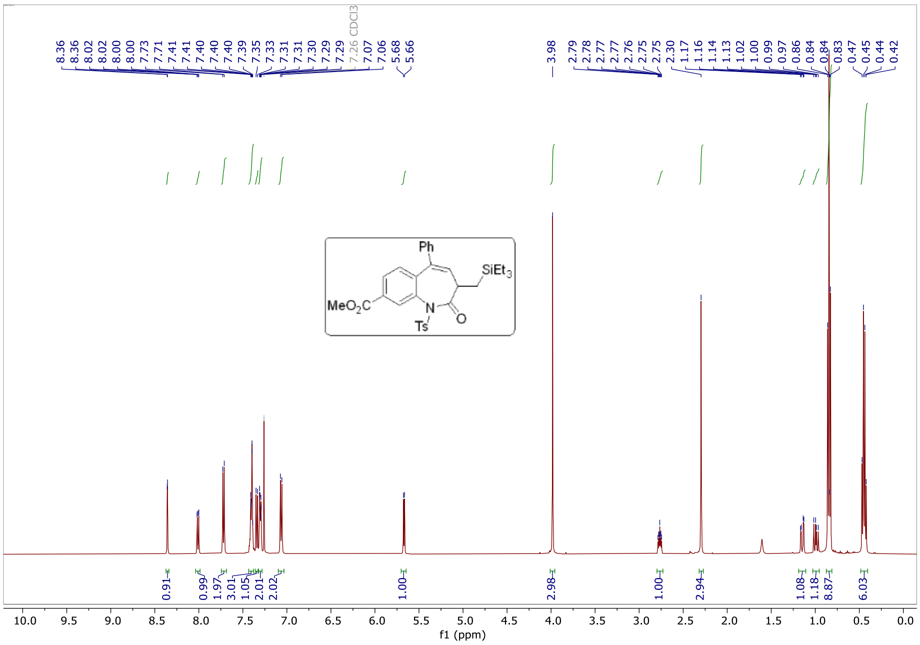

**Figure 4.11.11** $^{1}$H NMR spectrum of **3l** in $CDCl_3$ [500 MHz]

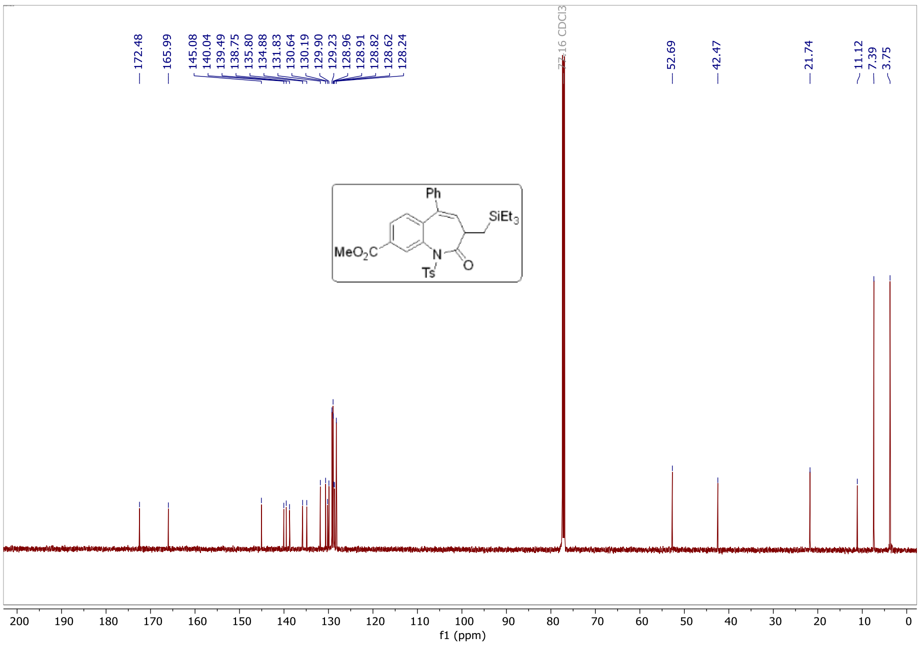

**Figure 4.11.12** $^{13}$C NMR spectrum of **3l** in $CDCl_3$ [126 MHz]

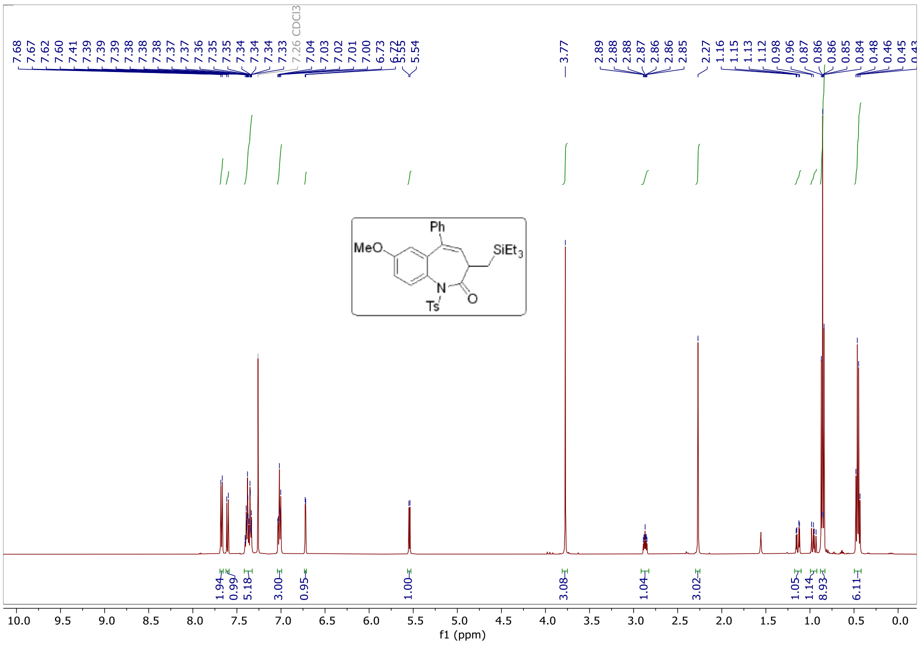

**Figure 4.11.13** $^{1}$H NMR spectrum of **3n** in $CDCl_3$ [500 MHz]

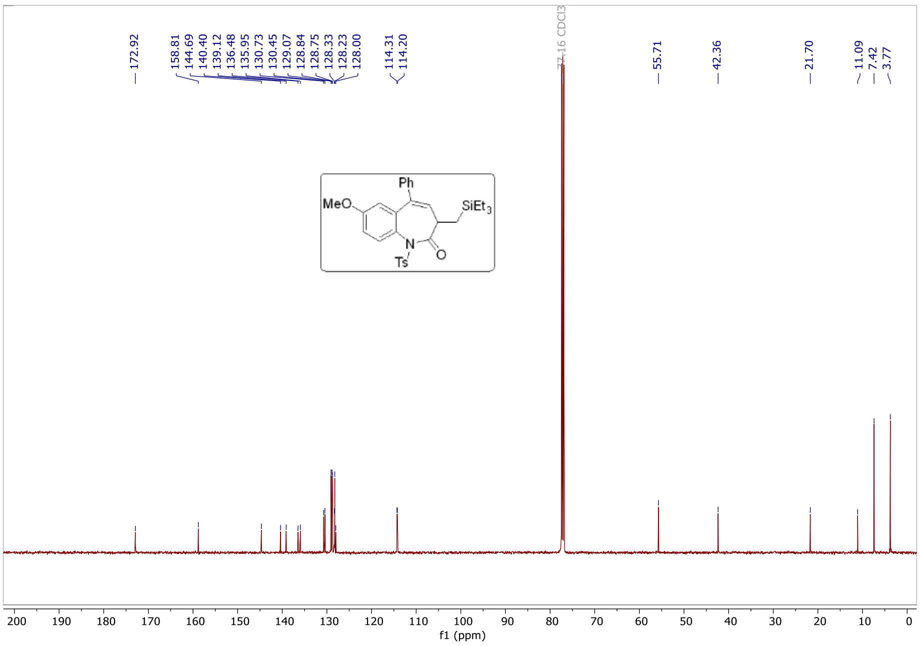

**Figure 4.11.14** $^{13}$C NMR spectrum of **3n** in $CDCl_3$ [126 MHz]

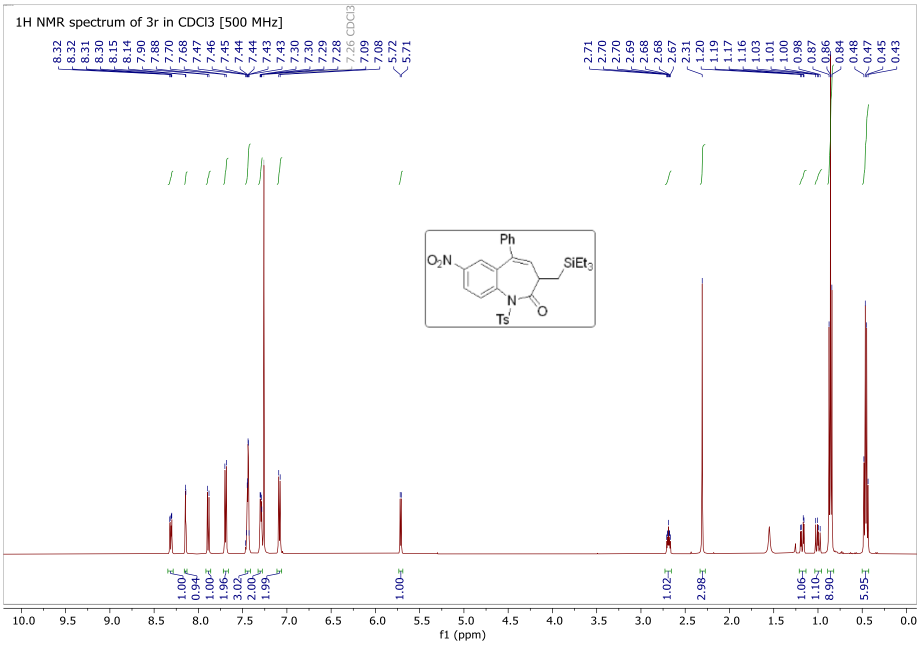

**Figure 4.11.15** $^{1}H$ NMR spectrum of **3r** in $CDCl_3$ [500 MHz]

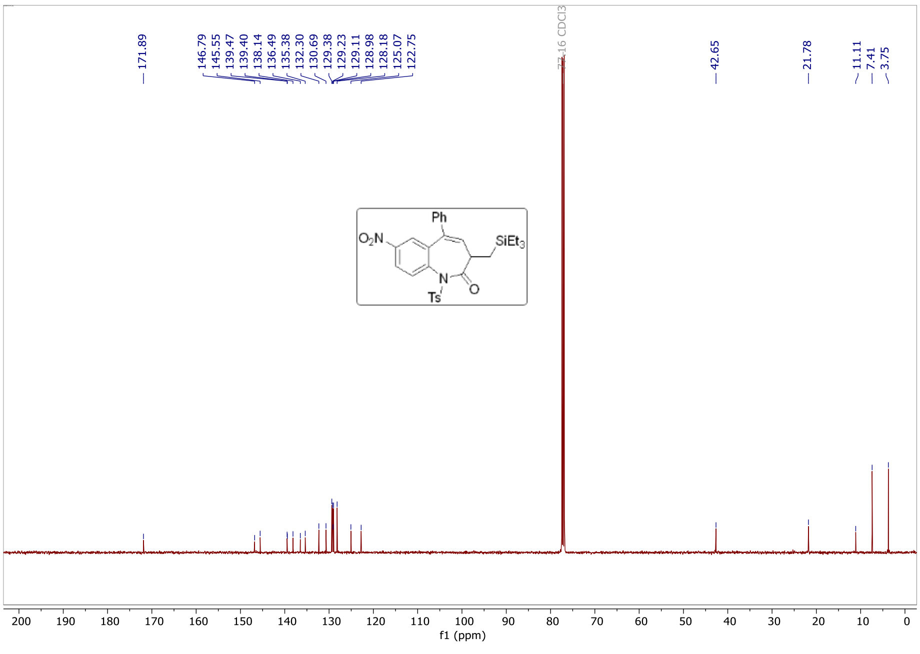

**Figure 4.11.16** $^{13}C$ NMR spectrum of **3r** in $CDCl_3$ [126 MHz]

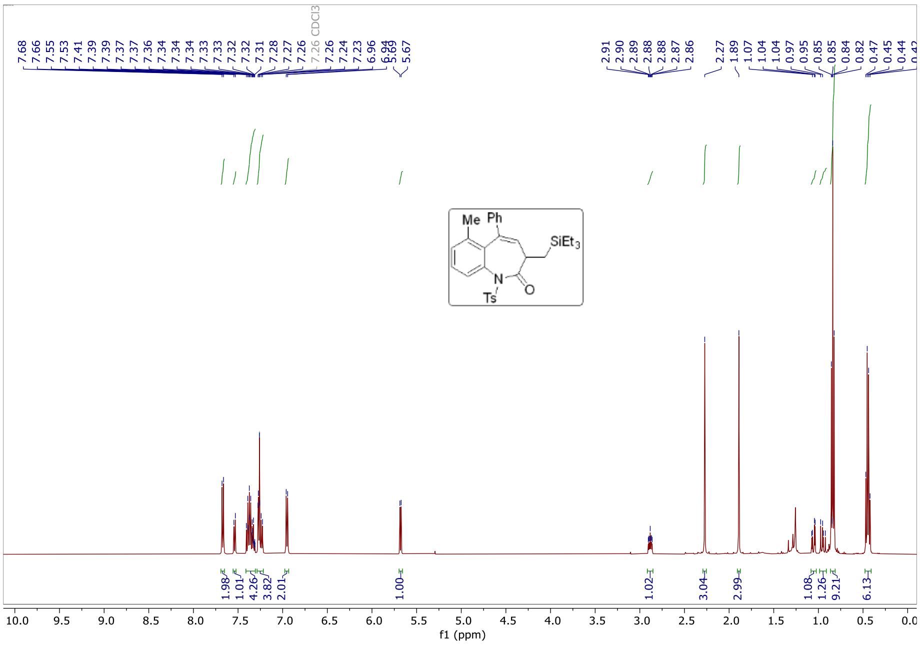

**Figure 4.11.17** $^{1}$H NMR spectrum of **3s** in $CDCl_3$ [500 MHz]

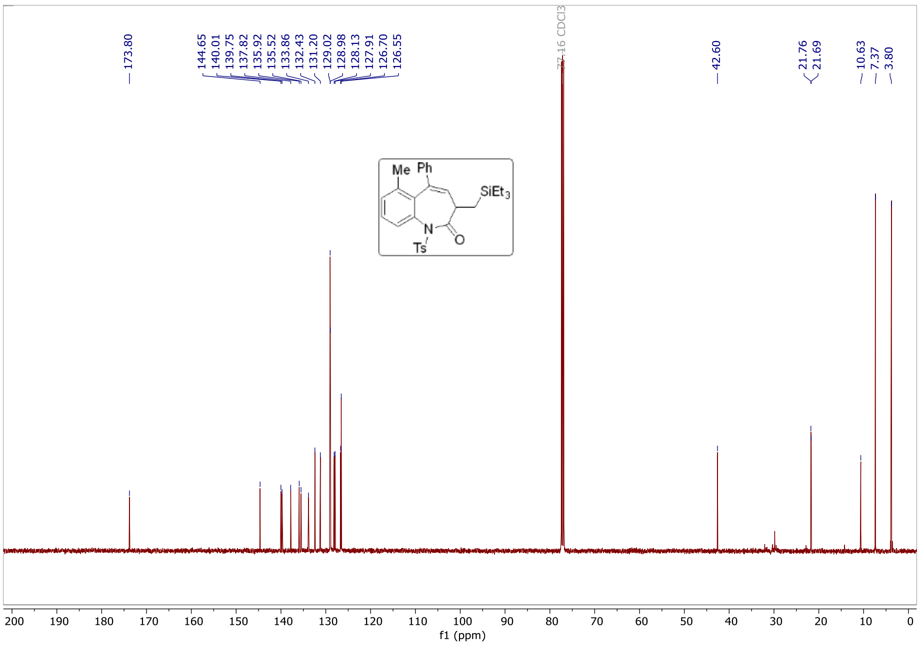

**Figure 4.11.18** $^{13}$C NMR spectrum of **3s** in $CDCl_3$ [126 MHz]

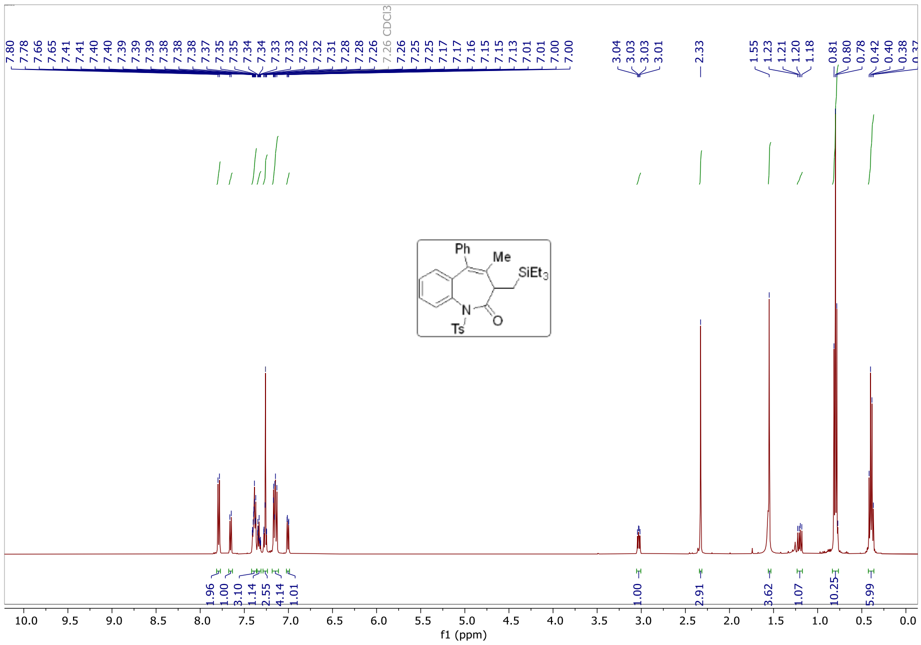

**Figure 4.11.19** $^{1}$H NMR spectrum of **3t** in $CDCl_3$ [500 MHz]

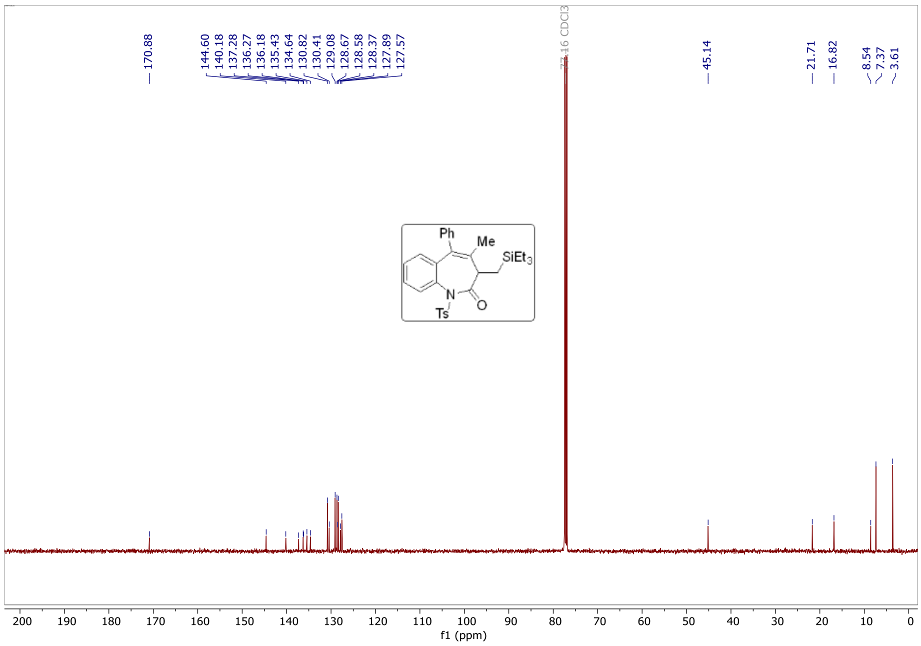

**Figure 4.11.20** $^{13}$C NMR spectrum of **3t** in $CDCl_3$ [126 MHz]

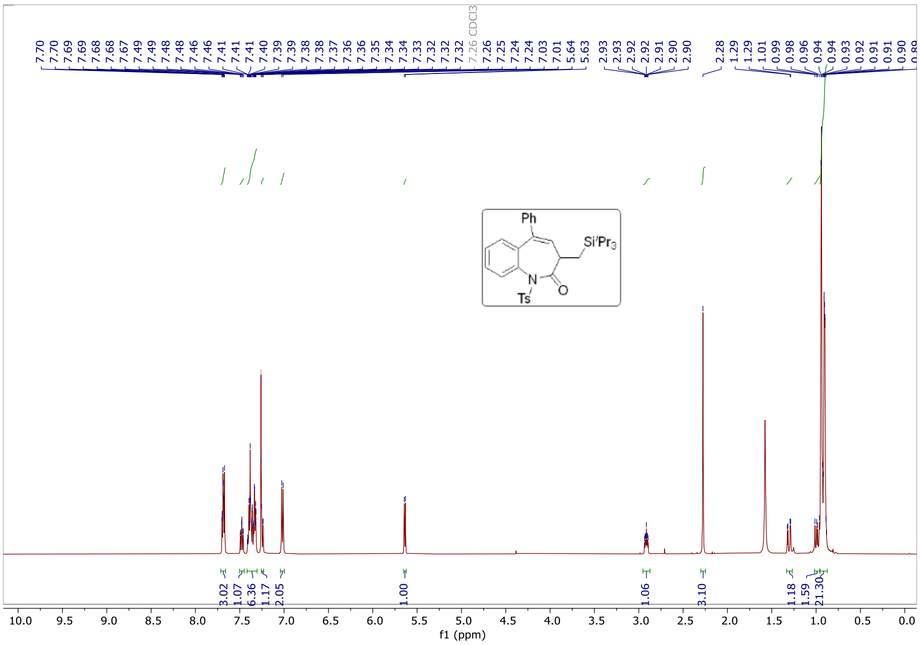

**Figure 4.11.21** $^{1}H$ NMR spectrum of **3x** in $CDCl_3$ [500 MHz]

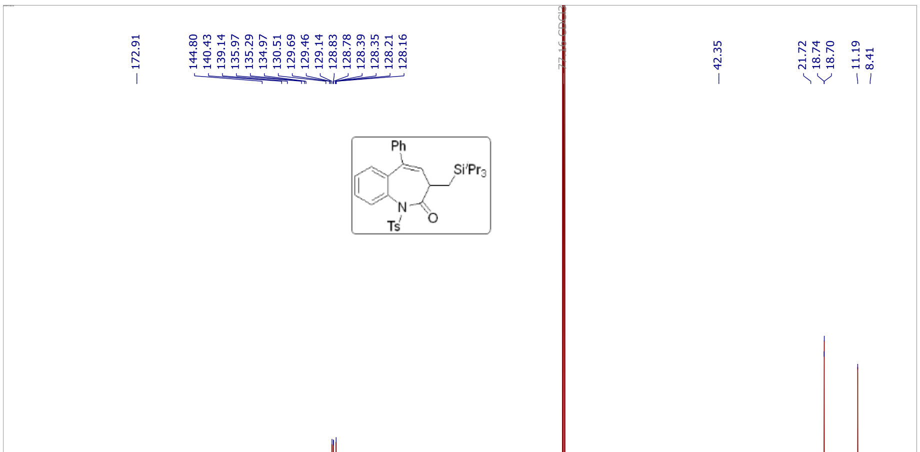

**Figure 4.11.22** $^{13}C$ NMR spectrum of **3x** in $CDCl_3$ [126 MHz]

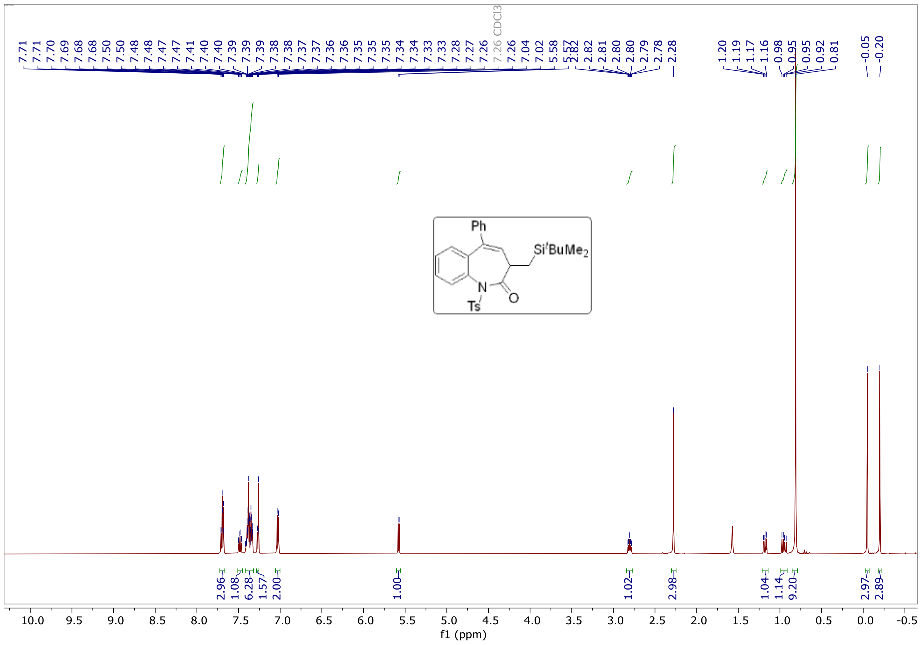

**Figure 4.11.23** $^{1}$H NMR spectrum of **3z** in $CDCl_3$ [500 MHz]

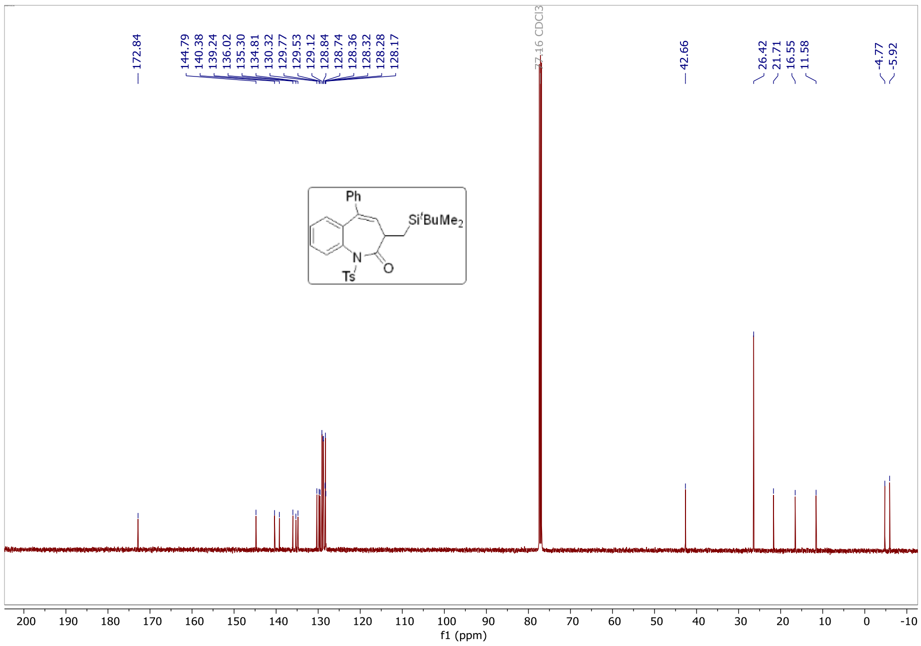

**Figure 4.11.24** $^{13}$C NMR spectrum of **3z** in $CDCl_3$ [126 MHz]

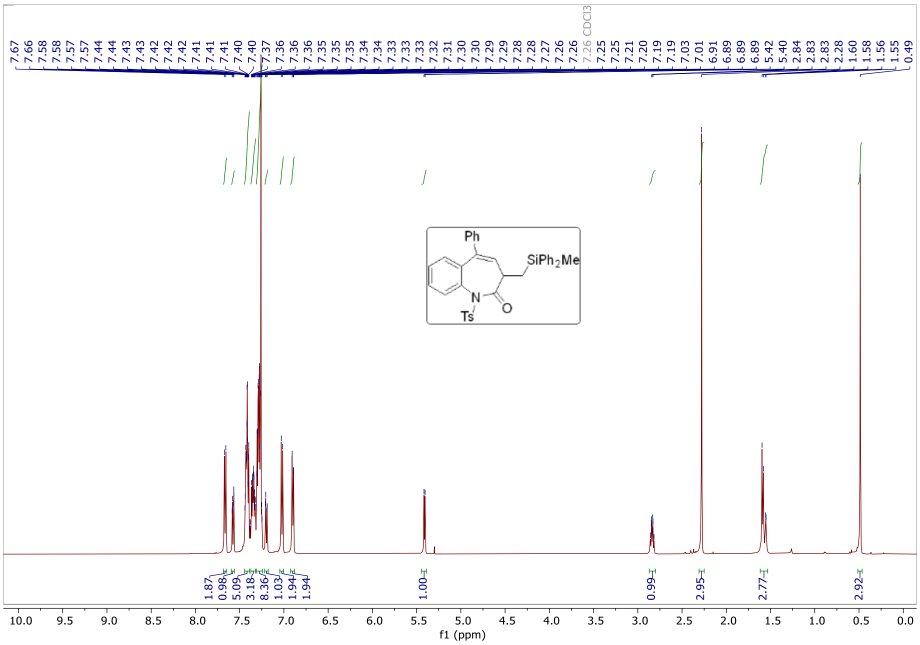

**Figure 4.11.25** $^1H$ NMR spectrum of **3ab** in $CDCl_3$ [500 MHz]

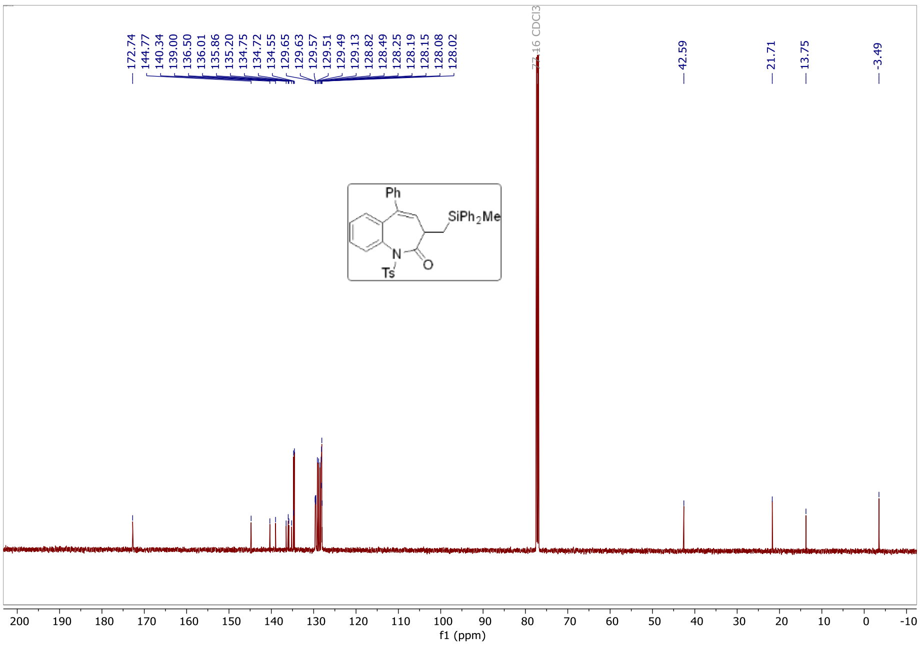

**Figure 4.11.26** $^{13}C$ NMR spectrum of **3ab** in $CDCl_3$ [126 MHz]

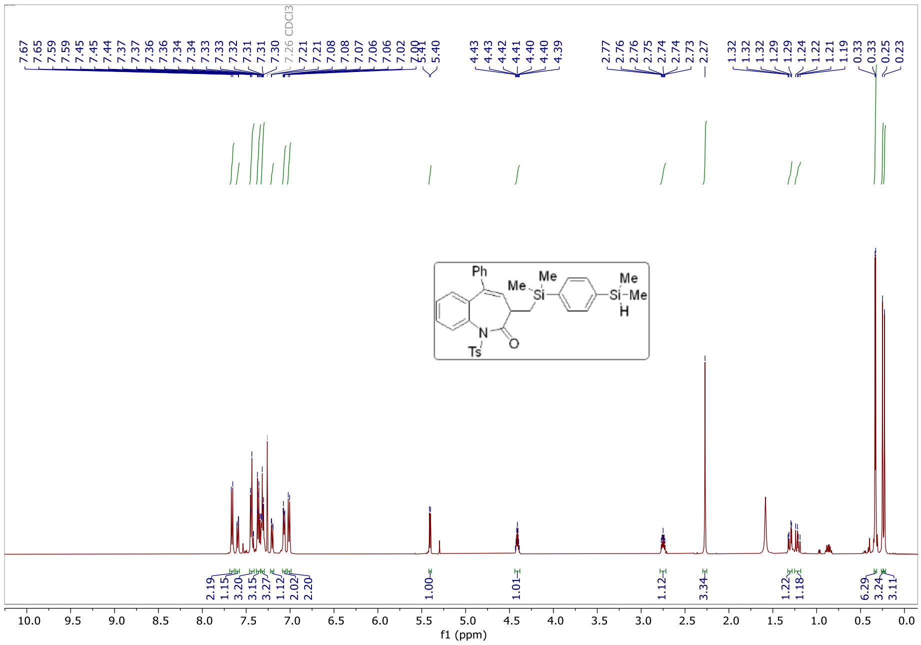

**Figure 4.11.27** $^{1}$H NMR spectrum of **3ag** in $CDCl_3$ [500 MHz]

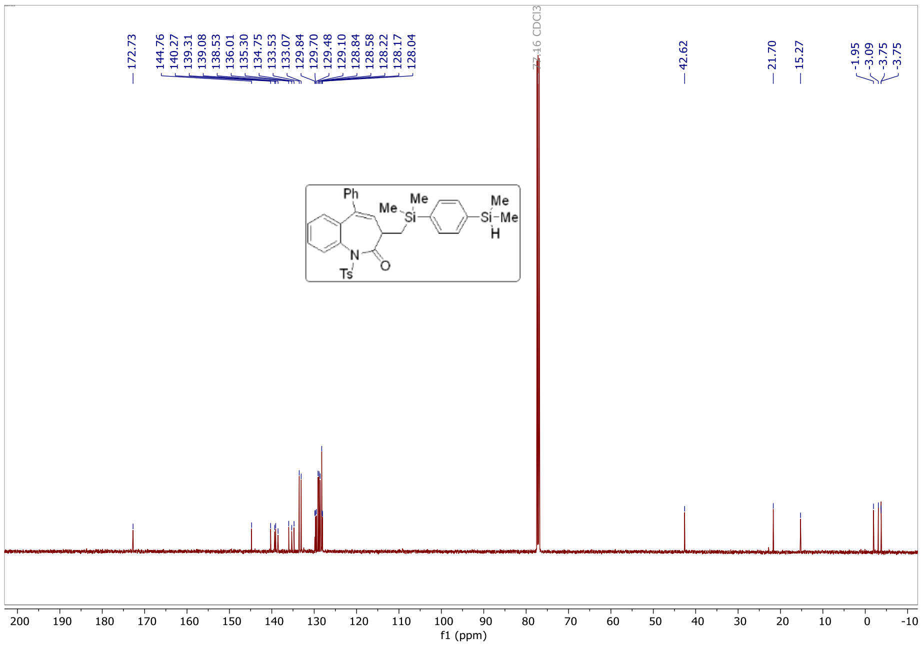

**Figure 4.11.28** $^{13}$C NMR spectrum of **3ag** in $CDCl_3$ [126 MHz]

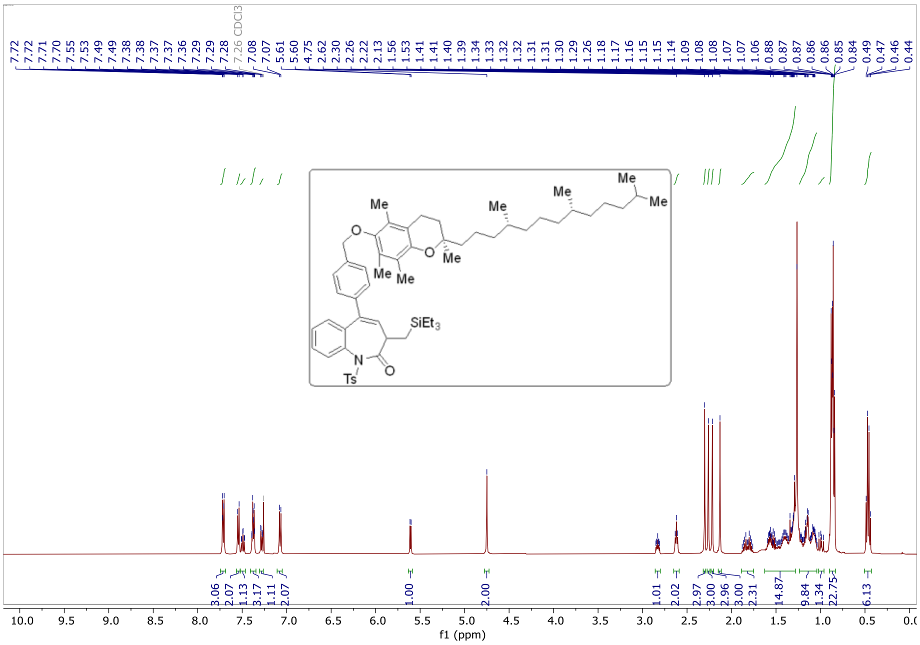

**Figure 4.11.29** $^{1}$H NMR spectrum of **3ah** in $CDCl_3$ [500 MHz]

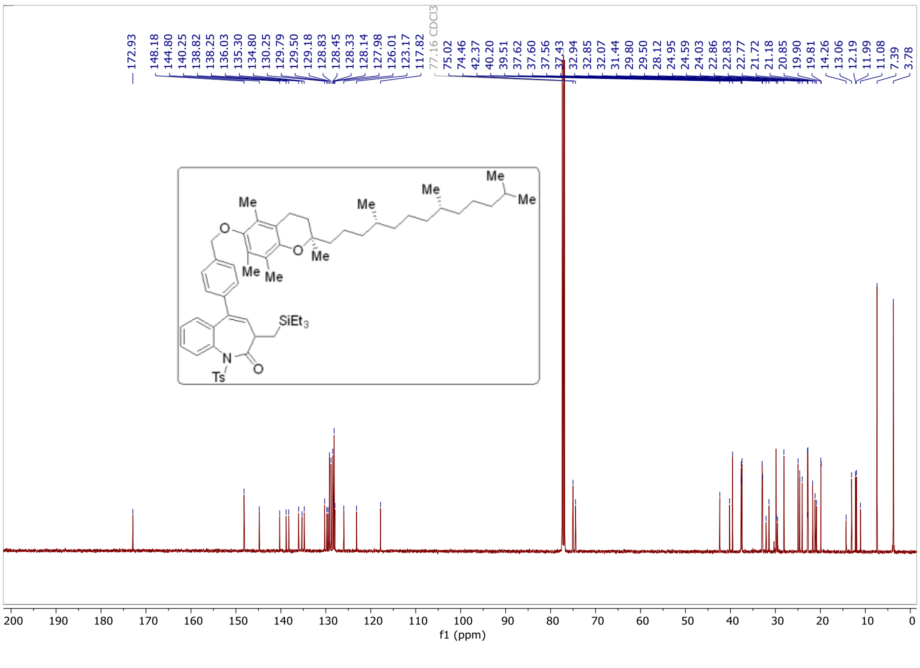

**Figure 4.11.30** $^{13}$C NMR spectrum of **3ah** in $CDCl_3$ [126 MHz]

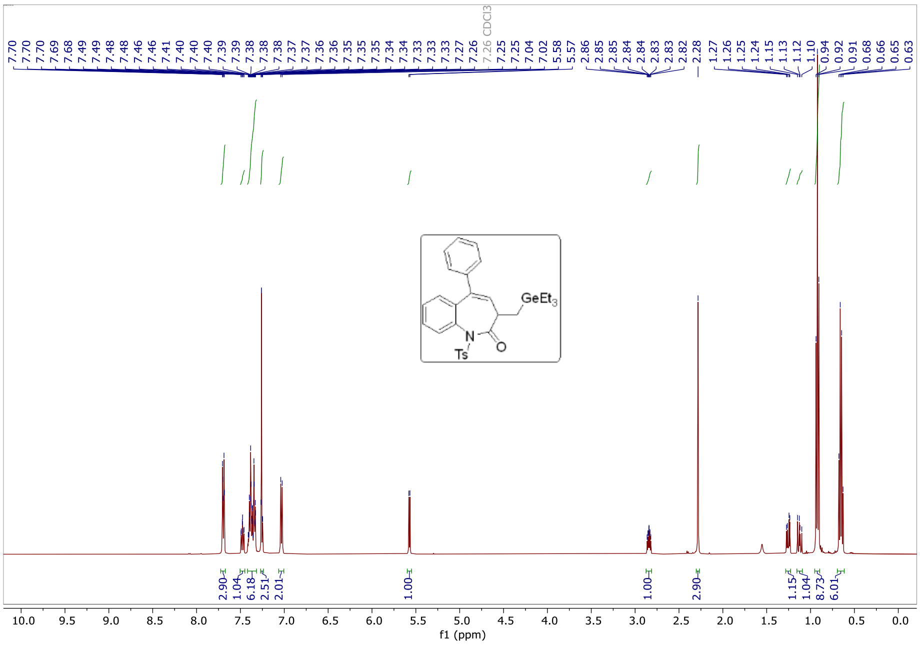

**Figure 4.11.31** $^{1}$H NMR spectrum of **5a** in $CDCl_3$ [500 MHz]

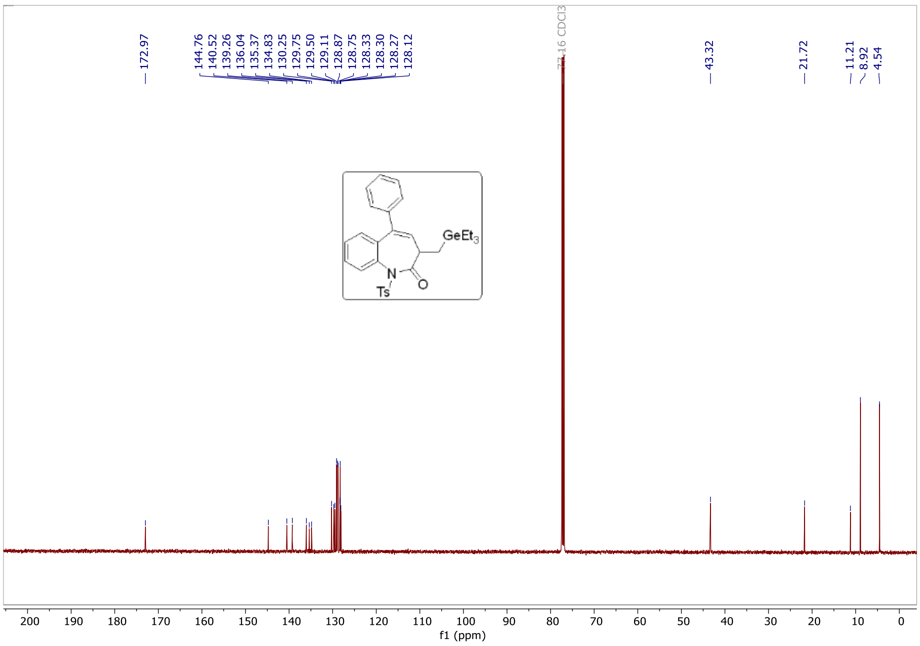

**Figure 4.11.32** $^{13}$C NMR spectrum of **5a** in $CDCl_3$ [126 MHz]

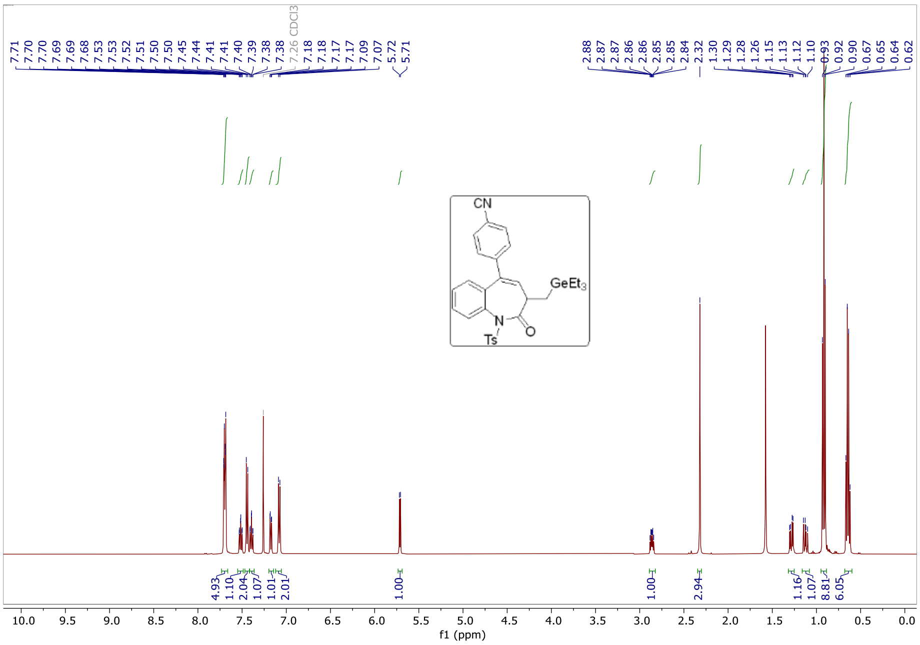

**Figure 4.11.33** $^{1}$H NMR spectrum of **5c** in $CDCl_3$ [500 MHz]

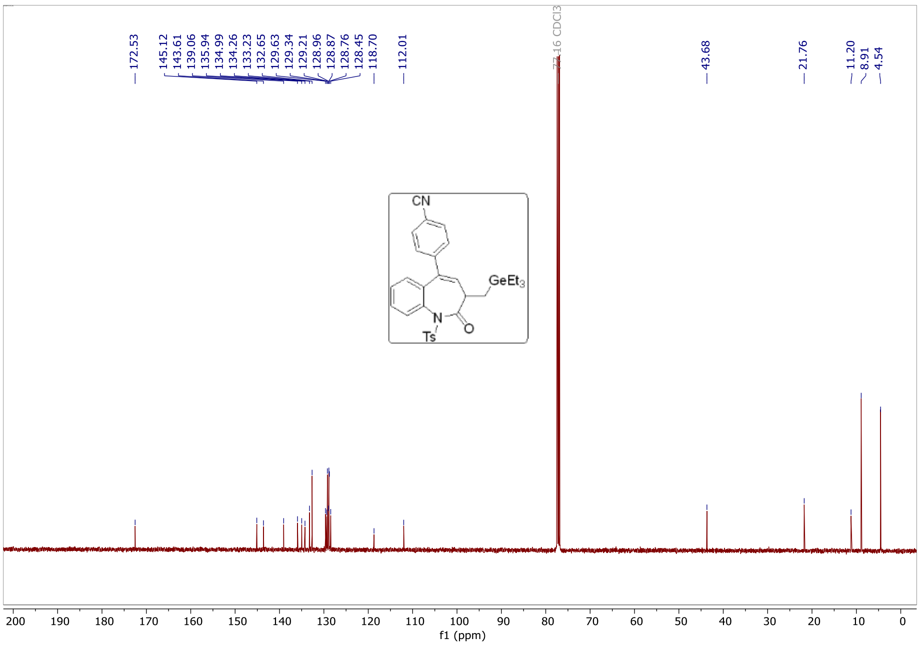

**Figure 4.11.34** $^{13}$C NMR spectrum of **5c** in $CDCl_3$ [126 MHz]

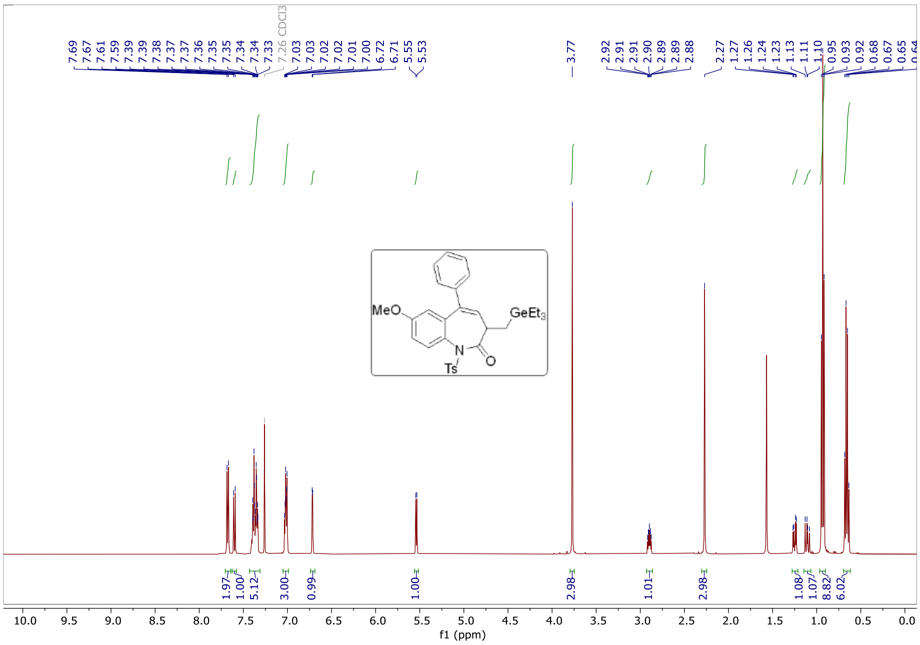

**Figure 4.11.35** $^{1}H$ NMR spectrum of **5f** in $CDCl_3$ [500 MHz]

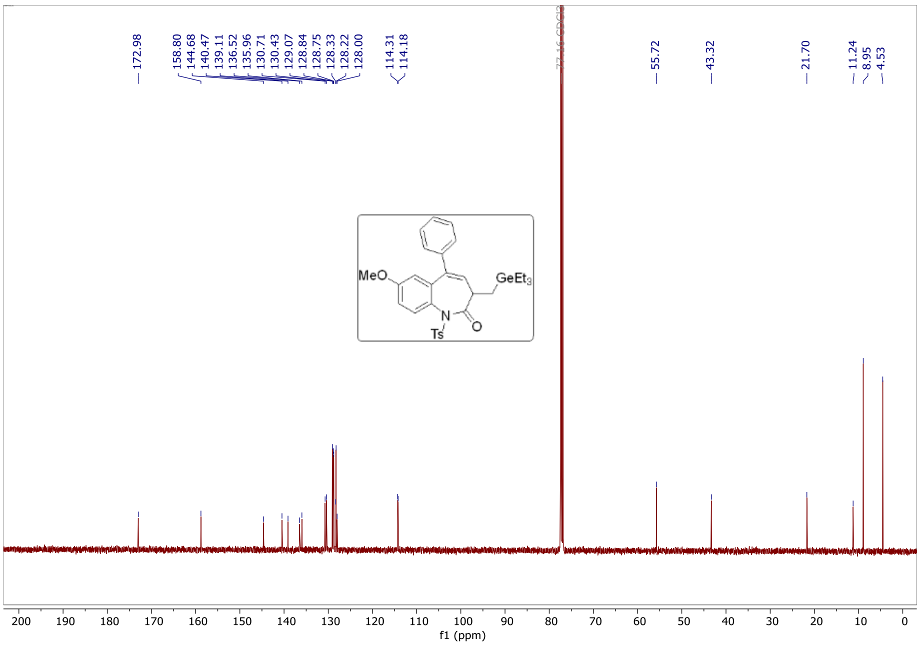

**Figure 4.11.36** $^{13}C$ NMR spectrum of **5f** in $CDCl_3$ [126 MHz]

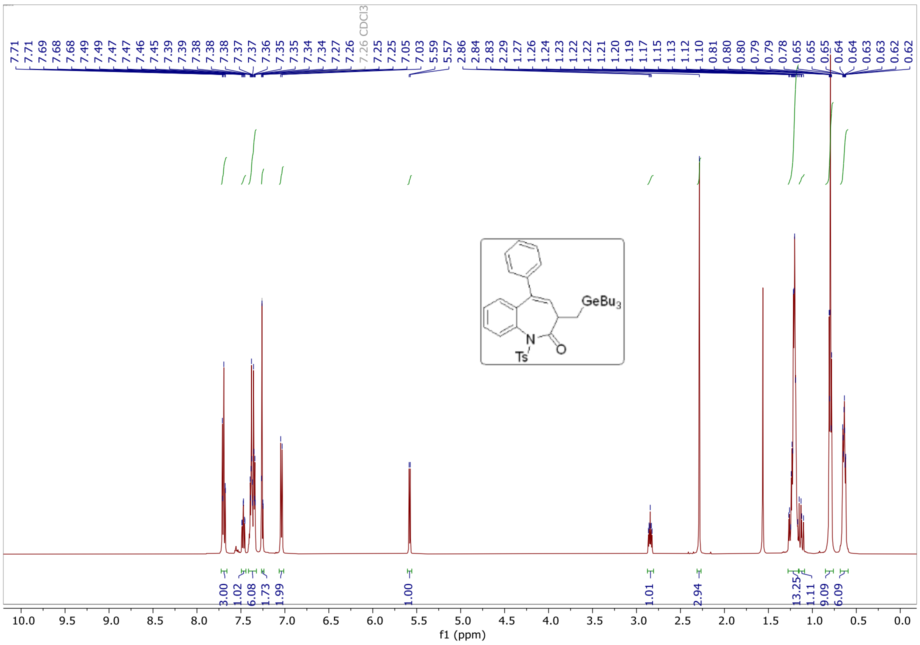

**Figure 4.11.37** $^{1}H$ NMR spectrum of **5h** in $CDCl_3$ [500 MHz]

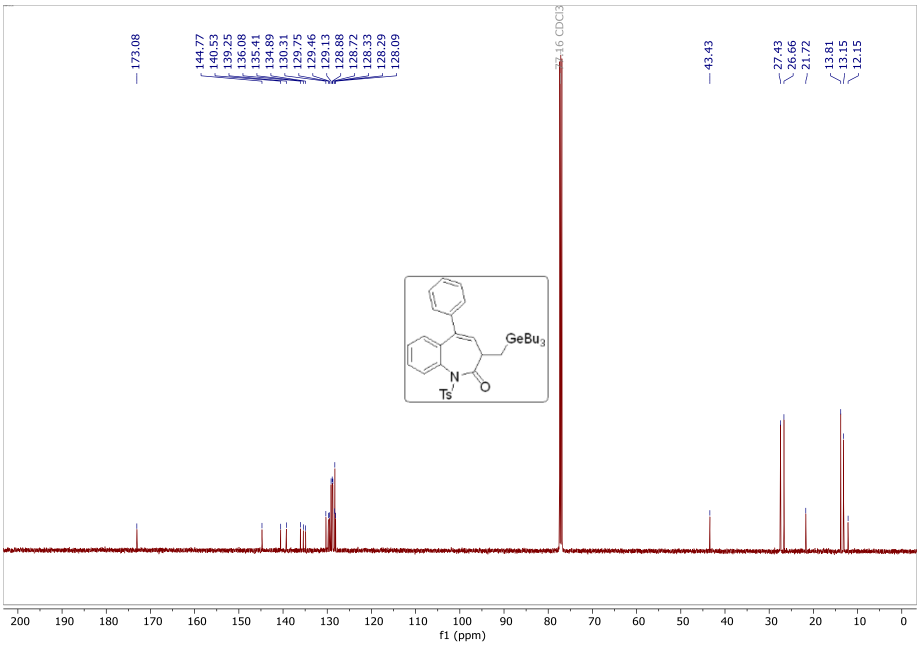

**Figure 4.11.38** $^{13}C$ NMR spectrum of **5h** in $CDCl_3$ [126 MHz]

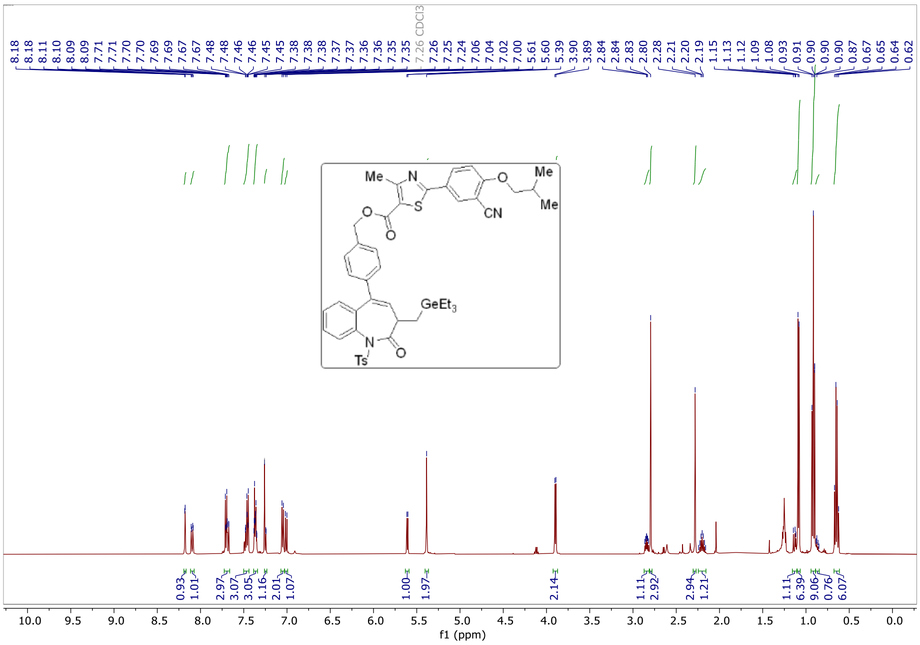

**Figure 4.11.39** $^{1}$H NMR spectrum of **5k** in $CDCl_3$ [500 MHz]

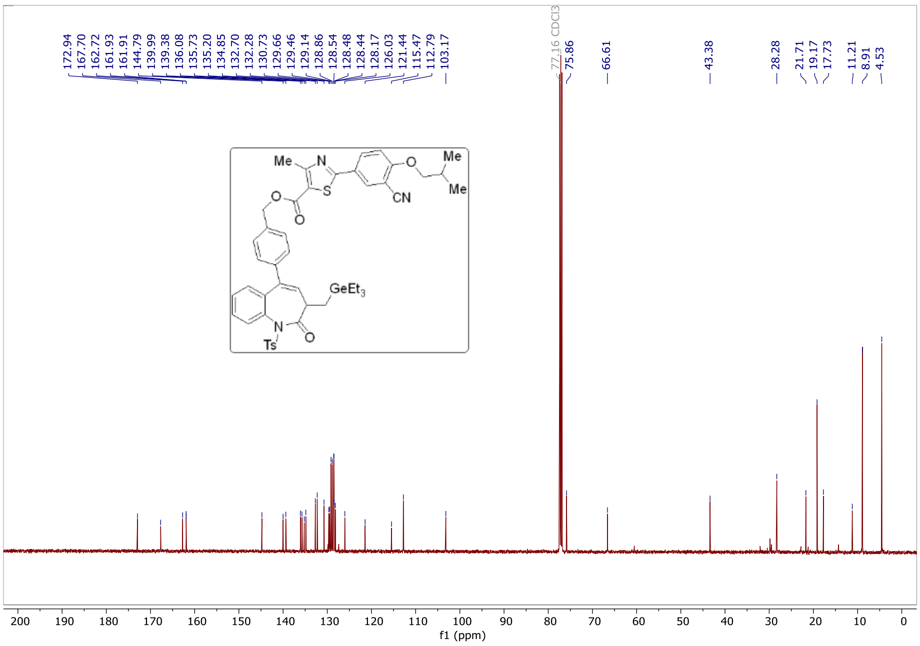

**Figure 4.11.40** $^{13}$C NMR spectrum of **5k** in $CDCl_3$ [126 MHz]

## 4.12 References


1. Murphy, M. B., Murray, C., Shorten, G. D. N. (2001). Fenoldopam: A selective peripheral dopamine-receptor agonist for the treatment of severe hypertension. *Engl. J. Med. 345*, 1548-1557. (DOI:10.1056/NEJMra010253).

2. Hou, F., Zhang, X., Zhang, G., Xie, D., Chen, P., Zhang, W., Jiang, J., Liang, M., Wang, G., Liu, Z., Geng, R. N. (2006). Efficacy and safety of benazepril for advanced chronic renal insufficiency. *Engl. J. Med. 354*, 131-140. (DOI:10.1056/NEJMoa053107).
3. Ryan, J. H., Hyland, C., Meyer, A. G., Smith, J. A., Yin, J.-X. (2012). Chapter: Seven-membered rings. *Prog. Heterocycl. Chem. 24*, 493-536. (DOI:10.1016/B978-0-08-096807-0.00016-6).
4. Ramig, K. (2013). Stereodynamic properties of medium-ring benzo-fused nitrogenous heterocycles: Benzodiazepines, benzazepines, benzazocines, and benzazonines. *Tetrahedron 69*, 10783-10795. (DOI: 10.1016/j.tet.2013.10.023).
5. Watthey, J. W. H., Stanton, J. L., Desai, M., Babiarz, J. E., Finn, B. M. (1985). Synthesis and biological properties of (carboxyalkyl)amino-substituted bicyclic lactam inhibitors of angiotensin converting enzyme. *J. Med. Chem. 28*, 1511-1516. (DOI:10.1021/jm00148a023).
6. O'Grady, M. R., O'Sullivan, M. L., Minors, S. L., Horne, R. (2009). Efficacy of Benazepril Hydrochloride to delay the progression of occult dilated cardiomyopathy in Doberman Pinschers. *J. Vet. Int. Med. 23*, 977-983. (DOI:10.1111/j.1939-1676.2009.0346.x).
7. Sozio, P., Marinelli, L., Cacciatore, I., Fontana, A., Türkez, H., Giorgioni, G., Ambrosini, D., Barbato, F., Grumetto, L., Pacella, S., Cataldi, A., Di Stefano, A. (2013). New flurbiprofen derivatives: Synthesis, membrane affinity and evaluation of in vitro effect on *β*-amyloid levels. *Molecules 18*, 10747-10767. (DOI: 10.3390/molecules180910747).
8. Denis, J. G., Franci, G., Altucci, L., Aurrecoechea, J. M., de Lera, A. R., Alvarez, R. (2015). Synthesis of 7-alkylidene-7,12-dihydroindolo[3,2-*d*]benzazepine-6-(5*H*)-ones (7-alkylidene-

paullones) by *N*-cyclization-oxidative Heck cascade and characterization as sirtuin modulators. *Org. Biomol. Chem. 13*, 2800-2810. (DOI:10.1039/C4OB02493A).

9. Hughes, R. A., Harris, T., Altmann, E., McAllister, D., Vlahos, R., Robertson, A., Cushman, M., Wang, Z., Stewart, A. G. (2002). 2-Methoxyestradiol and analogs as novel antiproliferative agents: analysis of three-dimensional quantitative structure-activity relationships for DNA synthesis inhibition and estrogen receptor binding. *Mol. Pharmacol. 61*, 1053-1069. (DOI:10.1016/S0026-895X(24)12200-6).
10. Tashima, T., Toriumi, Y., Mochizuki, Y., Nonomura, T., Nagaoka, S., Furukawa, K., Tsuru, H., Adachi-Akahane, S., Ohwada, T. (2006). Design synthesis, and BK channel-opening activity of hexahydrodibenzazepinone derivatives. *Bioorg. Med. Chem. 14*, 8014-8031. (DOI:10.1016/j.bmc.2006.07.042).
11. McGrath, N. A., Brichacek, M., Njardarson, J. T. (2010). A graphical journey of innovative organic architectures that have improved our lives. *J. Chem. Educ. 87*, 1348-1349. (DOI:10.1021/ed1003806).
12. Methot, J. L., Fischer, C., Li, C., Rivkin, A. *et al.* (2015). Potent benzoazepinone *γ*-secretase modulators with improved bioavailability. *Bioorg. Med. Chem. Lett. 25*, 3495-3500. (DOI:10.1016/j.bmcl.2015.06.032).
13. Johnson, P. D., Aristoff, P. A., Zurenko, G. E., Schaadt, R. D., Yagi, B. H., Ford, C. W., Hamel, J. C., Stapert, D., Moerman, J. K. (2003). Synthesis and biological evaluation of benzazepine oxazolidinone antibacterials. *Bioorg. Med. Chem. Lett. 13*, 4197-4200. (DOI:10.1016/j.bmcl.2003.07.017).
14. So, M., Kotake, T., Matsuura, K., Inui, M., Kamimura, A. (2012). Concise synthesis of 2-benzazepine derivatives and their biological activity. *J. Org. Chem. 77*, 4017-4028. (DOI:10.1021/jo300380z).

15. Shi, Q., Liao, Z., Liu, Z., Wen, J., Li, C., He, J., Deng, J., Cen, S., Cao, T., Zhou, J., Zhu, S. (2022). Divergent synthesis of benzazepines and bridged polycycloalkanones *via* dearomative rearrangement. *Nat. Commun. 13*, 4402. (DOI:10.1038/s41467-022-31920-1).
16. Showell, G. A., Mills, J. S. (2003). Chemistry challenges in lead optimization: silicon isosteres in drug discovery. *Drug discovery Today, 8*, 551-556. (DOI:10.1016/S1359-6446(03)02726-0).
17. Pooni, P. K., Showell, G. A. (2006). Silicon switches of marketed drugs. *Mini.-Rev. Med. Chem. 6*, 1169-1177. (DOI:10.2174/138955706778560120).
18. Franz, A. K., Wilson, S. O. (2013). Organosilicon molecules with medicinal applications. *J. Med. Chem. 56*, 388-405. (DOI: 10.1021/jm3010114).
19. Fujii, S., Miyajima, Y., Masuno, H., Kagechika, H. (2013). Increased hydrophobicity and estrogenic activity of simple phenols with silicon and germanium containing substituents. *J. Med. Chem. 56*, 160-116. (DOI:10.1021/jm3013757).
20. Fujii, S., Hashimoto, Y. (2017). Progress in the medicinal chemistry of silicon: C/Si exchange and beyond. *Future Med. Chem. 9*, 485-505. (DOI:10.4155/fmc-2016-0193).
21. Ramesh, R., Reddy, D. S. (2018). Quest for novel chemical entities through incorporation of silicon in drug scaffolds. *J. Med. Chem.* 2018, 61, 9, 3779-3798. (DOI:10.1021/acs.jmedchem.7b00718).
22. Xu, M. Y., Xiao, B. (2021). Germatranes and carbagermatranes: (Hetero)aryl and alkyl coupling partners in Pd-catalyzed crosscoupling reactions. *Chem. Commun. 57*, 11764-11775. (DOI:10.1039/D1CC04373K).
23. Horning, E. C., Stromberg, V. L., Lloyd, H. A. (1952). Beckmann rearrangements. an investigation of special Cases. *J. Am. Chem. Soc. 74*, 5153-5155. (DOI:10.1021/ja01140a048).
24. Armstrong, J. D., Eng, K., Keller, J. L., Purick, R. M., Hartner, F. W., Choi, W. B., Askin, D., Volante, R. P. (1994). An

efficient asymmetric synthesis of (*R*)-3-amino-2,3,4,5-tetrahydro-1*H*-[1]benzazepin-2-one. *Tetrahedron Lett. 35*, 3239-3242. (DOI:10.1016/S0040-4039(00)76874-2).

25. Sharif, S. A., Calder, E. D., Delolo, F. G., Sutherland, A. (2016). Synthesis of 5-amino-2,5-dihydro-1*H*-benzo[*b*]azepines using a one-pot multibond forming process. *J. Org. Chem. 81*, 6697-6706. (DOI:10.1021/acs.joc.6b01357).
26. Samineni, R., Bandi, C. R., Srihari, P., Mehta, G. (2016). Multiple aryne insertions into oxindoles: Synthesis of bioactive 3,3-diarylated oxindoles and dibenzo[*b,e*]azepin-6-ones. *Org. Lett. 18*, 6184-6187. (DOI:10.1021/acs.orglett.6b03224).
27. Gini, A.; Bamberger, J.; Luis-Barrera, J.; Zurro, M.; Mas-Balleste, R., Aleman, J., Mancheno, O. G. (2016). Synthesis of 3-benzazepines by metal-free oxidative C-H bond functionalization-ring expansion tandem reaction. *Adv. Synth. Catal. 358*, 4049-4056. (DOI:10.1002/adsc.201600985).
28. Pan, X., Wilcox, C. S. (2010). Synthesis of dibenzazepinones by palladium-catalyzed intramolecular arylation of *o*-(2-bromophenyl)anilide enolates. *J. Org. Chem. 75*, 6445-6451. (DOI:10.1021/jo101137r).
29. Cao, H., Vieira, T. O., Alper, H. (2011). Synthesis of unsaturated seven-membered ring lactams through palladium-catalyzed amination and intramolecular cyclocarbonylation reactions of amines and Baylis-Hillman acetates. *Org. Lett. 13*, 11-13 (DOI:10.1021/ol102699a).
30. Saget, T., Cramer, N. (2013). Enantioselective C-H arylation strategy for functionalized dibenzazepinones with quaternary stereocenters. *Angew. Chem. Int. Ed. 52*, 7865-7868. (DOI:10.1002/anie.201303816).
31. Sunderhaus, J. D., Dockendorff, C., Martin, S. F. (2009). Synthesis of diverse heterocyclic scaffolds *via* tandem additions to imine derivatives and ring-forming reactions. *Tetrahedron 65*, 6454-6469. (DOI: 10.1016/j.tet.2009.05.009).

32. Chang, M.-Y. Chan, C.-K., Lin, S.-Y. (2013). Synthesis of dihydro-1-benzazepines. *Heterocycles 87*, 1519-1536. (DOI:10.3987/COM-13-12729).
33. Grubbs, R. H. (2004). Olefin metathesis. *Tetrahedron 60*, 7117-7140. (DOI:10.1016/j.tet.2004.05.124).
34. Yu, L.-Z., Xu, Q., Tang, X.-Y., Shi, M. (2016). Iron- or copper-catalyzed trifluoromethylation of acrylamide-tethered alkylidenecyclopropanes: facile synthesis of $CF_3$-containing polycyclic benzazepine derivatives. *ACS Catal. 6*, 526-531. (DOI:10.1021/acscatal.5b02400).
35. Bhakuni, B. S., Kumar, A., Balkrishna, S. J., Sheikh, J. A., Konar, S., Kumar, S. (2012). KO$^t$Bu mediated synthesis of phenanthridinones and dibenzoazepinones. *Org. Lett. 14*, 2838-2841. (DOI:10.1021/ol301077y).
36. Li, Y., Hu, M., Li, J.-H. (2017). Silver-catalyzed intermolecular [3+2]/[5+2] annulation of *N*-arylpropiolamides with vinyl acids: Facile synthesis of fused 2*H*-Benzo[*b*]azepin-2-ones. *ACS Catal. 7*, 6757-6761. (DOI:10.1021/acscatal.7b02061).
37. Zhao, Y., Chen, J.-R., Xiao, W.-J. (2018). Visible-light photocatalytic decarboxylative alkyl radical addition cascade for synthesis of benzazepine derivatives. *Org. Lett. 20*, 224-227. (DOI:10.1021/acs.orglett.7b03588).
38. Zhang, Z., Tan, P., Wang, S., Wang, H., Xie, L., Chen, Y., Han, L., Yang, S., Sun, K. (2023). Visible-light-promoted selective sulfonylation and selenylation of dienes to access sulfonyl-/seleno-benzazepine derivatives. *Org. Lett. 25*, 4208-4213. (DOI:10.1021/acs.orglett.3c01550).
39. Tan, P., Wang, S., Li, G., Wang, H., Zhao, Z., Jiang, H., Xie, L., Yang, L., Chen, J., Zhang, Z. (2024). Oxidative cascade iodocyclization of 1,*n*-dienes: Synthesis of iodinated benzo[*b*]azepine and benzo[*b*]azocine derivatives. *J. Org. Chem. 89*, 6405-6415. (DOI:10.1021/acs.joc.4c00438).
40. Shi, T., Tian, M., Sun, Z., Zou, R., Zhang, Z., Xie, N., Hao, E., Xu, X., Sun, K. (2025). Photochemical aerobic

sulfonylation-cyclization-selenylation to indole-fused medium-sized *N*-heterocycles in 2-Me-THF. *Chem. Commun. 61*, 4066-4069. (DOI:10.1039/D4CC06686C).

41. Jackson, R. F. W., Moore, R. J., Dexter, C. S., Elliott, J., Mowbray, C. E. (1998). Concise synthesis of enantiomerically pure phenylalanine, homophenylalanine, and bishomophenylalanine derivatives using organozinc chemistry: NMR studies of amino acid-derived organozinc reagents. *J. Org. Chem. 63*, 7875-7884. (DOI:10.1021/jo981133u).
42. Fujita, K., Takahashi, Y.; Owaki, M., Yamamoto, K., Yamaguchi, R. (2004). Synthesis of five-, six-, and seven-membered ring lactams by Cp*Rh complex-catalyzed oxidative *N*-heterocyclization of amino alcohols. *Org. Lett. 6*, 2785-2788. (DOI:10.1021/ol0489954).
43. Zhou, N., Zhao, F., Wang, L., Gao, X., Zhao, X., Zhang, M. (2023). NHC-catalyzed regioselective intramolecular cyclization reaction for the synthesis of benzazepine derivatives. *Org. Lett. 25*, 6072-6076. (DOI: 10.1021/acs.orglett.3c02323).
44. Feng, Z., Wu, L., Zhou, C.-Y., Wang, C. (2024). *N*-Heterocyclic carbene catalysis for polycyclic benzazepines assembly: Regioselective intramolecular tandem radical cyclization. *Org. Lett. 26*, 9068-9072. (DOI:10.1021/acs.orglett.4c03303).
45. Zhao, Y., Chen, J.-R., Xiao, W.-J. (2018). Visible-light photocatalytic decarboxylative alkyl radical addition cascade for synthesis of benzazepine derivatives. *Org. Lett. 20*, 224-227. (DOI:10.1021/acs.orglett.7b03588).
46. Zhang, X.-Y., Ning, C., Long, Y.-J., Wei, Y., Shi, M. (2020). Visible-light mediated decarboxylative tandem carbocyclization of acrylamide-attached alkylidenecyclopropanes: access to polycyclic benzazepine derivatives. *Org. Lett. 22*, 5212-5216. (DOI:10.1021/acs.orglett.0c01856).

47. Mao, B., Zhang, X.-Y., Wei, Y., Shi, M. (2022). Visible-light mediated intramolecular radical cyclization of $\alpha$-brominated amide-tethered alkylidenecyclopropanes. *Chem. Commun. 58*, 3653-3656. (DOI:10.1039/D1CC07136J).
48. de Souza, W. C., Lima, R. N., de Jesus, I. S., Correia, J. T. M., Paixão, M. W. (2023). Synthesis of benzoazepinone derivatives *via* photoredox deaminative radical cascade alkylation of 1,7-dienes and 1,7-enynes. *Synthesis 55*, 967-976. (DOI:10.1055/a-1953-1849).
49. Zhou, N., Zhao, F., Wang, L., Gao, X., Zhao, X., Zhang, M. (2024). Visible-light induced regioselective cascade radical cyclization of $\alpha$-bromocarbonyls: access to benzazepine derivatives. *J. Org. Chem. 89*, 2238-2246. (DOI:10.1021/acs.joc.3c02184).
50. Zhang, Z., Lu, L., Li, G., Sheng, X., Zhang, Y., Yang, L., Zhao, J., Xie, L., Li, J., Sun, K. (2024). Radical cascade silylation/cyclization of 1,7-dienes to access silyl-substituted benzo[*b*]azepin-2-ones. *Chem. Commun. 60*, 4206-4209. (DOI:10.1039/D4CC00499J).
51. Bajya, K. R., Kumar, M., Ansari, A., Selvakumar, S. (2023). Sulfonamide as photoinduced hydrogen atom transfer catalyst for organophotoredox hydrosilylation and hydrogermylation of activated alkenes. *Adv. Synth. Catal. 365*, 976-982. (DOI:10.1002/adsc.202300040).
52. Bajya, K. R., Maurya, S. K., Selvakumar, S. (2024). Organophotocatalytic regioselective silylation/germylation and cascade cyclization of *N*-alkenyl α-$CF_3$ acrylamides: Access to densely functionalized 4-pyrrolin-2-ones. *Org. Lett. 26*, 9269-9275. (DOI:10.1021/acs.orglett.4c03427).
53. Ladumor, R., Samanta, S., Selvakumar, S. (2025). Photocatalytic silylation of aryl alkynoates: Synthesis of silylated coumarins. *Adv. Synth. Catal. 367*, e202401007. (DOI:10.1002/adsc.202401007).

54. Greulich, T. W., Daniliuc, C. G., Studer, A. (2015). *N*-aminopyridinium salts as precursors for *N*-centered radicals-direct amidation of arenes and heteroarenes. *Org. Lett. 17,* 254-257. (DOI:10.1021/ol503338b).
55. Goliszewska, K., Jasinska, K. R., Szurmak, J., Gryko, D. (2019). visible-light-mediated amination of *π*-nucleophiles with *N*-aminopyridinium salts. *J. Org. Chem. 84*, 15834-15844. (DOI:10.1021/acs.joc.9b02073).
56. Guo, W., Wang, Q., Zhu, J. (2021). Selective 1,2-aminoisothiocyanation of 1,3-dienes under visible-light photoredox catalysis *Angew. Chem. Int. Ed. 60*, 4085-4089. (DOI:10.1002/anie.202014518).
57. Forster, D., Guo, W., Wang, Q., Zhu, J. (2021). Photoredox catalytic three-component amidoazidation of 1,3-dienes. *ACS Catal. 11*, 10871-10877. (DOI:10.1021/acscatal.1c03545).
58. Nishiguchi, I., Matsumoto, T., Kuwahara, T., Kyoda, M., Maekawa, H. (2022). Mg-promoted stereoselective desulfonation of *β*-arylvinyl sulfone derivatives. *Chem. Lett. 31*, 478-479. (DOI:10.1246/cl.2002.478).
59. Link, A.; Kunick, C. (1998). *δ*-Fused benzazepines with selective in vitro antitumor activity: synthesis and structure-activity relationships. *J. Med. Chem. 41*, 1299-1305. (DOI:10.1021/jm970675l).
60. Li, D., Zeng, F. (2017). Palladium-catalyzed domino alkenylation/amination/pyridination reactions of 2-vinylanilines with alkynes: Access to cyclopentaquinolines. *Org. Lett. 19*, 6498-6501. (DOI: 10.1021/acs.orglett.7b03164).
61. Hatchard, C. G., Parker, C. A. (1956). A new sensitive chemical actinometer - II. Potassium ferrioxalate as a standard chemical actinometer. *Proc. Roy. Soc. (London) A235*, 518-536. (DOI:10.1098/rspa.1956.0102).
62. Cismesia, M.A., Yoon, T. P. (2015). Characterization chain processes in visible light photoredox catalysis. *Chem. Sci. 6*, 5426-5434. (DOI:10.1039/C5SC02185E).

## Summary

The focus of this thesis is to harness the potential of sulfamidyl radical for the functionalization of Si-H/Ge-H bonds of hydrosilanes/hydrogermanes through hydrogen atom transfer for the photocatalytic synthesis of organosilicon and organogermanium compounds. Firstly, the sulfamidyl radical was generated under visible light-assisted photocatalytic reductive quenching condition by using simple sulfonamide as a precursor for sulfamidyl radical and achieved selective functionalization of Si-H/Ge-H bond over C-H bond of hydrosilanes/hydrogermanes. Moreover, sulfonamides are readily accessible from inexpensive and commercially available sulfonyl chlorides and amines, rendering them cost-effective HAT catalyst. The steric and electronic properties of sulfonamide can be systematically tuned, enabling optimal matching with the varying bond dissociation energies of the Si-H and Ge-H bond of hydrosilanes and hydrogermanes respectively.

In addition, a complementary protocol was also developed for the generation of sulfamidyl radical under photocatalytic oxidative quenching condition using *N*-aminopyridinium salt, enabling the synthesis of organosilicon and organogermanium compounds.

In **Chapter 1**, we discussed an overview of silicon and germanium, describing their fundamental physicochemical properties and the distinctive features that differentiate them from carbon. It then surveys the established synthetic strategies for organosilicon and organogermanium compounds, using different silyl and germyl sources. Furthermore, the applications of organosilicon and organogermanium compounds are discussed, including their use in daily life, medicinal and agrochemical applications, as well as the role of silicon as a bioisosteres in bioactive molecules. With our interest in the photocatalytic synthesis of organosilicon and organogermanium compounds, a brief overview of photoredox catalysis is also provided, including the fundamental

photophysical properties of photocatalyst and the mechanistic pathways like oxidative and reductive quenching cycles. Lastly, we discuss our approach for the synthesis of organosilicon and organogermanium compounds *via* functionalization of Si-H and Ge-H bonds of hydrosilanes and hydrogermanes with the help of an electrophilic radical.

In **Chapter 2**, we describe the development of sulfonamide as a photoinduced hydrogen atom transfer catalyst for hydrosilylation and hydrogermylation of activated alkenes under visible light-assisted photocatalytic condition. A series of sulfonamides, photocatalysts, bases and solvents were screened to obtain optimized condition. The optimized condition were tested with a wide variety of activated alkenes, including acrylates, maleate esters, *α*-methylene-*γ*-butyrolactone, cyclopentenone, acrylamides, vinyl phosphine oxide, and vinyl sulfone, which were shown to undergo smooth hydrosilylation and hydrogermylation. The protocol proved compatible with both alkyl and aryl hydrosilanes and hydrogermanes. Also, a scale-up experiment demonstrates the practicality and robustness of the developed methodology. Theoretical studies further validate the selective functionalization of Si-H and Ge-H bonds of hydrosilanes and hydrogermanes.

In **Chapter 3**, we presented the development of a complementary approach to generate sulfamidyl radical using *N*-aminopyridinium salt as hydrogen atom transfer reagent for functionalization of Si-H/Ge-H bond of hydrosilanes and hydrogermanes and employed in radical cascade cyclization reactions for the synthesis of silylated and germylated 4-pyrrolin-2-ones. The developed protocol exhibits mild reaction conditions, broad substrate scope and tolerates a wide range of functional groups. The method demonstrates synthetic and practical utility by showing the compatibility with natural products and drug scaffolds-tethered to the starting material, as well as with scale-up reaction.

In, **Chapter 4**, we described the access to silylated and germylated benzazepines *via* regioselective addition of silyl/germyl radicals to 1,7-dienes, followed by cascade cyclization under metal-free photocatalytic condition using *N*-aminopyridinium salt as a hydrogen atom transfer reagent through Si-H/Ge-H bond functionalization of hydrosilanes and hydrogermanes. This method tolerates a wide range of functional groups and extended to late-stage functionalization. Further transformation of photoproduct is also described in this chapter for converting silylated benzazepine into other synthetically valuable products. The proposed mechanism has been validated through various control experiments, including radical quenching, intermediate trapping, kinetic isotope effect, fluorescence quenching, and quantum yield calculation.

## Future scope

The development of modern and mild methodologies for the synthesis of organosilicon and organogermanium compounds is an area of great interest for synthetic chemists, as these compounds have widespread applications in materials science, medicinal chemistry, and agrochemicals. The methodologies developed in this thesis offer versatile routes for the generation of silyl/germyl radical under metal-free condition, and the integration of these functionalities into heterocycles could offer the advantage of their combined inherent properties to the final molecule, which would provide an ideal design for investigating its pharmacological activity. Organosilicons are highly lipophilic in nature, and the incorporation of the silyl group in bioactive carbon analogues can enhance cell and tissue penetration, as well as modulate the potency and selectivity. The developed protocols offer suitable routes for the late-stage functionalization of bioactive compounds through silyl/germyl group incorporation, which would alter the pharmacological properties of bioactive molecules. By streamlining the synthetic routes, these approaches would significantly reduce the number of steps and deliver complex target molecules in an efficient and economical manner through radical cascade cyclization reactions.